The University of Sydney
Faculty of Engineering
School of Chemical & Biomolecular Engineering

Multiscale Modelling of Non-Thermal Plasma Tar Cracking for Waste Gasification

Eric Sanjaya

A thesis submitted in fulfilment of the requirements for the degree of Doctor of Philosophy.

April 2024

Abstract

Waste generation is a persistent environmental challenge for the modern society. Despite its potential, waste gasification has been hindered by tar by-product generation. Both Thermal Plasma and Non-Thermal Plasma (NTP) have shown promise for tar cracking. However, NTP tar cracking is in the early development stage, necessitating further research. This work explores the viability of plasma for tar cracking for waste gasification and its environmental impact using diverse modelling techniques. The work begins with an investigation into NTP tar cracking kinetics, where the developed model is applied for process simulation and environmental impact investigation.

A comprehensive reaction kinetic model for NTP tar cracking is developed and exhibits agreement with experimental data from external works, particularly within the 600-800 K. The resulting mechanism highlights the significance of radical collisions for tar cracking. Tar ring-opening reactions occur when a reactive functional group attacks aromatic double bonds, producing cyclopentane and smaller gases. In the syngas environment, tar degradation results in an abundance of acetylene at the output. The comprehensive reaction kinetic model is applied to a waste gasification process modelling via reduced order correlations, showcasing R^2 up to 94.7%. The waste gasification-NTP tar cracking model is employed for various energy and mass recovery scenarios. For energy recovery, the data suggests that NTP's high energy requirement necessitates advanced syngas energy recovery (e.g., fuel cells). Alternatively, the tar-free syngas may be used for chemical synthesis, yielding 0.94 kg of methanol per kg of waste. The methanol-and-power co-production scenario is unfavourable, as both processes compete for syngas. For comprehensiveness, a meta-analysis of 25 LCA works shows that thermal plasma gasification is environmentally cleaner than waste incineration, yet it is inconclusive for conventional gasification. Cleaner thermal conversion and high energy recovery are the key factors. The NTP waste gasification's environmental impact is estimated and compared with other technologies via Life Cycle Assessment (LCA). The result disfavours thermal plasma gasification due to its high-power consumption. NTP waste gasification for methanol production is the most favourable scenario due to its ability to replace conventional methanol production. This highlights the importance of valuable product generation and avoiding fossil fuel-based power. The primary contribution lies in establishing a "proof-of-concept" for NTP tar cracking for waste gasification, substantiated by the numerical validity of the modelling work provided, which has not been demonstrated for this technology.

Statement of Originality

This is to certify that to the best of my knowledge; the content of this thesis is my own work. This thesis has not been submitted for any degree or other purposes.

I certify that the intellectual content of this thesis is the product of my own work and that all the assistance received in preparing this thesis and sources have been acknowledged.

Eric Sanjaya

Date

Contents

Authorship Attribution Statement

Chapter 5 of this thesis have been published as: Sanjaya, E. and Abbas, A., 2023. Plasma gasification as an alternative energy-from-waste (EFW) technology for the circular economy: An environmental review. Resources, Conservation and Recycling, 189, p.106730.

Chapter 3 of this thesis have been published as: Sanjaya, E., Fimbres Weihs, G., Manaf, N.A. and Abbas, A., 2024. Reaction kinetic modelling of tar cracking in a non-thermal plasma reactor: Model evaluation and reaction mechanism investigation. Chemical Engineering Journal, 479, p.147649.

Chapter 4 of this thesis is currently under preparation for submissions as: E. Sanjaya, G. Fimbres Weihs, and A. Abbas (2024) Process simulation of waste gasification with Non-Thermal Plasma (NTP) tar cracking unit for material and energy recovery.

Chapter 6 of this thesis currently under the preparation of submission as: E. Sanjaya, G Fimbres Weihs, and A. Abbas (2024) Environmental impact of potential NTP tar cracking implementation for waste gasification.

For the aforementioned manuscripts, I designed the study, analysed the data, and wrote the draft of the manuscripts, with the help of the mentioned authors in methodology guidance and feedback. In addition to the previous statements, in case where I am not the corresponding authors of a published item, permission to include the published material has been granted by the corresponding author.

Eric Sanjaya

Date

As the supervisor for the candidature upon which this thesis is based, I can confirm that the authors attribution statements above are correct.

Ali Abbas

Date

Acknowledgment

First and foremost, I would like to express my deepest gratitude to my primary supervisor, Professor Ali Abbas. His wisdom, persistence, and support have made the completion of this thesis possible. Secondly, I would like to thank my secondary supervisor, Dr. Gustavo Fimbres Weihs for his expert input and technical understanding of this field. His support gave me the confidence and skills I needed to finalise this thesis.

During the early stage of the project, I discussed my research project with Dr. Behnam Akhavan, Professor Marcela Bilek, Dr. Renwu Zhou, Dr. Tianqi Zhang, and Professor PJ Cullen. I would like to thank them for the discussion I had, which may or may not shape the direction of this thesis. I also would like to thank Dr Xinying Liu, Dr Jasleen Kaur Daljit Singh, and Dr Jungmi Hong, for their assistance in setting up the simulation programs required for this project.

I would like to acknowledge the scholarship funding from the University of Sydney International Strategic Tuition Fee Scholarship.

Finally, to my friends and family. Their patience, support, and their faith in me are irreplaceable.

List of Figures

List of Tables

Nomenclature

List of Symbols

Symbol	Definition	Unit
A	Pre-exponential factor	-
b	Linear regression coefficient	-
c_{ve}	Electron constant specific heat capacity	
c_{pe}	Electron constant pressure specific heat capacity	
ΔT	Temperature difference	K
E	Activation energy	J mol^{-1}, eV mol^{-1}
$_e$	Physical properties for electron	-
F-stat	Significant variance in the model	-
$_g$	Physical properties for gas	-
H	Enthalpy	J kg^{-1}
HV	Heating Value	MJ/kg
HHV	Higher Heating Value	MJ/kg
$_k$	Physical properties for species k	-
k	Reaction rate kinetic	M s^{-1}
$k_{b,r}$	Reverse reaction rate kinetic	M s^{-1}
$k_{f,r}$	Forward reaction rate kinetic	M s^{-1}
LHV	Higher Heating Value	MJ/kg
M	Molar flowrate	mol s^{-1}
m	Mass flowrate	kg s^{-1}
n	Number of reactions	-
p-value	Probability of null hypothesis effect	
Q	Heat (Chapter 4)	J
Q_{source}	Power/Energy deposition	W
Q_{loss}^{elas}	Energy loss from elastic collision	W
Q_{loss}^{inel}	Energy loss from inelastic collision	W
q	Progress reaction rate	-
R	Gas constant	-
R^2	Dependent variable relation to the independent variable	%
RMSE	Root Mean Square Error	-
RMSD	Root Mean Square Derivation	-
$_r$	Properties for reaction rate r	-
SEI	Specific Energy Input	kWh m^{-3}

Symbol	Definition	Unit
T	Temperature	K
t	Time	s
V	Volume	m^{-3}
v_{ek}	Momentum transfer collision frequency between electron and species k	s^{-1}
v'_{kr}	Stoichiometric coefficient for forward reactions	-
v''_{kr}	Stoichiometric coefficient for reverse reactions	-
W	Molecular weight (Chapter 3)	g mol^{-1}
W	Power (Chapter 4)	kW
X_{tar}	Tar degradation	mol mol^{-1} (%)
X_{CO_2}	CO_2 Conversion	mol mol^{-1} (%)
X	Conversion	mol mol^{-1} (%)
$[X_k]$	Molar concentration for species k	
Y	Mass fraction	mol mol^{-1}
y	Yield	mol mol^{-1} (%)
β	Dimensionless constant	-
ρ	Density	kg m^{-3}
ω	Molar rate	mol m^{-3} s^{-1}

List of Abbreviations

Abbreviation	Meaning
AC	Alternating Current
AD	Abiotic Depletion Potential
AGG	Aggregates
ALC	Agriculture Land Occupation
AP	Acidification Potential
APC	Air Pollution Control
APP	Advanced Plasma Process
ASR	Automotive Shredded Residue
AU	Australia
AU-G	Australian Grid
B	Benzene
C2	C_2 Formation
CCE	Carbon Conversion Efficiency
CCHH	Climate Change on Human Health
CE	Circular Economy
CFD	Computational Fluid Dynamic
CGE	Cold Gas Efficiency
CRL	Commercial Readiness Leve
DBD	Dielectric Barrier Discharge

Abbreviation	Meaning
DC	Direct Current
DE	Decomposition
DR	Drying
EEDF	Electron Energy Distribution Function,
EFW	Energy-from-Waste
EP	Eutrophication potential
ER	Equivalence Ratio
FC	Fixed Carbon
FM	Ferrous metal
FPG	Fuel Gas Production
G	Gasification (Reduction)
GAD	Gliding Arc Discharge
GAS	Conventional Gasification
GHG	Greenhouse Gases
GWP	Global Warming Potential
HGE	Hot Gas Efficiency
HT	High temperature
HTP	Human Toxicity Potential
HV	Heating Value
IC	Impact Category
IMRG	The Integrated Multifuel Recuperative Gasification
INC	Incineration (INC-A and INC-B)
IR	Ionising Radiation
JRC	Joint Research Centre
LCA	Life Cycle Assessment
LF	Landfilling
LHC	Lower Hydrocarbon
LHS	Latin Hypercube Square
MCA	Multi-Criteria Analysis
ME	Marine Ecotoxicity
MeOH	Methanol
MGE	Mechanical Gas Efficiency
MLR	Multilinear regression
MSW	Municipal Solid Waste
N	Naphthalene
NASA	The National Aeronautics and Space Administration
NFM	Non-ferrous metal
NTP	Non-Thermal Plasma
NTP-E	Gasification with NTP tar cracking for energy recovery
NTP-M	Gasification with NTP tar cracking for methanol synthesis

Abbreviation	Meaning
O	Oxidation
ODP	Ozone Depletion Potential
OLGA	Oil based washer scrubber
P	Pyrolysis
P	Phenol
PAH	Polycyclic aromatic hydrocarbons
PAHs	polycyclic aromatic hydrocarbons
PED	Primary Energy Demand
PEGS ®	Plasma-enhanced gasification
PG	Thermal Plasma Gasification
PGM	Plasma Global Model
Ph	Phenanthrene
PIC	Particle in Cells
PM	Particulate Matter
PMFP	Particulate Matter Formation Potential
POCP	Photochemical ozone creation potential
POPs	Persistent Organic Pollutants
PRRS	Pyrogenesis Plasma Resource Recovery System
PSC	Phoenix Solution Company
PSR	Perfectly Stirred Reactor
PTRD	Plasma Thermal Destruction and Recovery
PYRO	Pyrolysis
RDF	Refuse Derived Fuel
RXN	Reactions (Chapter 4 gasification reactions)
Sc	Scenario
SG	Syngas
SGG	Simulated Gasification Gas
STP	Standard Temperature and Pressure
T	Toluene
TE	Terrestrial ecotoxicity
TF	Tar Formation
TP	Thermal Plasma
tpd	Tonne per day
tph	Tonne per hour
TRC	Thermal Residence Chamber
TRL	Technological Readiness Level
UK	United Kingdom
UK-G	United Kingdom Grid
ULC	Urban Land Occupation
VM	Volatile Matter

Abbreviation	Meaning
VOC	Volatile Organic Compound
WE	Freshwater ecotoxicity
WGS	Water Gas Shift
WPC	Westinghouse Plasma Company

List of Chemicals

Formula	Chemical
1,4-DCB	1,4-Dichlorobenzene
Al_2O_3	Aluminium Oxide (Alumina)
Ar	Argon
Ar^+	Excited argon
C	Elemental carbon
$C_{10}H_{14}$	n-butylbenzene
$C_{10}H_8$	Naphthalene (Nap or N)
$C_{11}H_{10}$	Methylnaphthalene
$C_{14}H_{14}$	Bi-benzyl
C_2	Two carbon hydrocarbons
C_2H_2	Acetylene
C_2H_3	Ethylenyl
C_2H_4	Ethene (Ethylene)
C_2H_5	Ethyl
C_2H_6	Ethane
C_3	Three carbon hydrocarbons
C_3H_3	Cyclopropenyl
C_3H_3	Propyne
C_3H_4	Propadiene
C_3H_6	Propane
C_3H_6	Propene (Propylene)
C_3H_8	Propane
C_4	Four carbon hydrocarbons
C_4H_2	But-1-en-3-yne
C_4H_4	Butadiene
C_4H_5	But-1-en-3-yl
C_5	Five carbon hydrocarbons
C_5H_5	Cyclopentadiene anion
C_6H_2	Hexa-1,3,5-triyne
C_6H_4	Benzyne
$C_6H_5C_2H_3$	Styrene
$C_6H_5C_2H_5$	Ethylbenzene

Formula	Chemical
$C_6H_5CH_2$	Benzyl cation
$C_6H_5CH_3$	Toluene
C_6H_5O	Phenolate
C_6H_5OH	Phenol
C_6H_6	Benzene
C_7H_{16}	Heptane
C_9H_6O	Ethynlbenzaldehyde
C_9H_7	Indenide
C_9H_8	Indene
C_aH_b	General hydrocarbon gas empirical formula
CH_2	Methylene radical
CH_2CO	Acetaldehyde
CH_2O	Formaldehyde
CH_3	Methyl radical
CH_3^+ CH_4^+	Ionised methane
CH_3OH	Methanol
CH_4	Methane
$CH_4(v)$	Excited methane
Char	Charcoal
Cl_2	Chlorine
C_nH_m	Polymer
CO	Carbon monoxide
Co	Cobalt
CO_2	Carbon dioxide
COS	Carbonyl sulphide
Cr	Chromium
CS_2	Carbon Disulphide
C_xH_y	Tar
$C_xH_yO_z$	General tar empirical formula
DME	Dimethyl ether
E (or e^-)	Electron
Fe	Iron
H_2	Hydrogen
H_2O	Water
H_2S	Hydrogen sulphide
HCN	Hydrogen cyanide
N_2	Nitrogen
N_2 ($A3\ \Sigma_u^+$)	Excited nitrogen
NH_3	Ammonia
NH_4Cl	Ammonium chloride

Formula	Chemical
Ni	Nickel
NMVOC	Non-Methane Volatile Organic Compounds
NOx	Nitrogen oxides
O	Oxygen radical
O_2	Oxygen
OH	Hydroxyl radical
P	Phosphorous
PCDD/Fs	Polychlorinated Dibenzo-p-dioxins and Dibenzofurans
PM_{10}	Particulate Matter less than 10 micron
Pt	Platinum
PVC	Polyvinyl Chloride
SO_2	Sulphur dioxide
SOx	Sulphur Oxides
TiO_2	Titanium Dioxide
Zn	Zinc

Chapter 1

Introduction

Since the creation of society, humanity has consumed materials from the extracted Earth's biosphere to produce goods, improving lives, and supporting society. The era of industrialisation and rapid population expansion have further intensified our consumerism [1]. Whilst society's proficiency in manufacturing has flourished, our efforts in harvesting commodities from waste have not equated to our production counterparts. To this day, there is a heavy reliance on landfilling to manage the generated Municipal Solid Waste (MSW), resulting in a pressing environmental and social concern [2]. The National Aeronautics and Space Administration (NASA) reported that 20% of methane produced by humans is originated from landfill [3]. Their detrimental impacts are pervasive, encompassing both environmental and socio-economic spheres, disproportionately affecting lower-income communities to burden its negative impact [4].

In financially capable regions such as Japan and the European Union, incineration has been widely embraced [5, 6]. Incineration has evolved from simple combustion into a highly efficient moving grate reactor [7], operating at impressive capacity and equipped with advanced Air Pollution Control (APC). However, incineration conversion into energy destroys materials, which eliminates the recovery potential while releasing CO_2 as emissions. Incineration has traditionally been the go-to method for managing waste, but it has been criticised for its negative environmental impact and the production of harmful pollutants. Incineration demands complicated APC that operates at mammoth capacity with a centralised operation [8].

1.1 MSW Gasification

Alternatively, waste gasification is a thermal process that converts waste into syngas. Waste gasification converts solid waste into a gaseous fuel (syngas) by heating the waste in a restrictive oxidant environment. Syngas are composed mainly of hydrogen, carbon monoxide, and methane, which can be used as fuels for power generation or as feedstock to produce chemicals. However, gasification development has been hampered by tar production, a by-product of the gasification process that may clog the reactor and reduce the efficiency of the process.

The presence of tar in syngas can cause equipment fouling, leading to reduced efficiency and increased maintenance costs [9]. It can also cause corrosion in the downstream equipment, which can ultimately result in system failure. In addition, tar may cause environmental pollution when released into the atmosphere, along with health risks to workers handling syngas-containing tar [10]. Tom Reed shows his insight into his expertise, quoted [11]:

> *"While a great deal of time and money has been spent on … gasification … there are very few truly commercial gasifiers, operating without government support or subsidies, day in, day out, generating useful (syn)-gas… Then it is found that the gas contains 0.1-10% tars. The rest of the time and money is spent trying to solve this problem. Most of the gasifier projects then quietly disappear. In some cases, the cost of cleaning up the experimental site exceeds the cost of the project! Thus 'tars' can be considered the Achilles heel of … gasification."*

Therefore, tar removal has been a critical step in gasification advancement. Researchers have been exploring an innovative way to effectively remove tar from syngas. Early research focused on the utilisation of physical removal that is filter, scrubber, cyclone, or introduction of bed filter [12]; however, it was found to be inadequate.

1.2 Plasma Tar Cracking

Although there is a diverse tar abatement strategy, the challenge lies in developing an efficient and cost-friendly process that avoids secondary pollution and maintains syngas's quality [13]. Physical tar removal is sparsely applied due to its reduction in efficiency and secondary pollutant creation [14].

Thermal plasma can be directly injected into a gasifier for tar cracking, while supporting cleaner gasification reactions [15]. Although thermal plasma gasification has been demonstrated by some organisations, its implementation has been plagued with high energy consumption. In contrast, Non-thermal Plasma (NTP) tar cracking is an emerging research direction, supported by its initial, yet promising, laboratory scale finding. NTP's direct approach simultaneously destroys tar and improves syngas quality.

NTP offers the advantage of catalyst coupling, operation at lower temperatures, and lower energy requirement. The utilisation of NTP for tar cracking has progressed in tandem with the advancement of NTP reactors [16]. Initial investigations centred around corona discharge [17] and later demonstrated Gliding Arc Discharge (GAD) and Dielectric Barrier Discharge (DBD). GAD is favoured due to its capacity to generate robust arc flames, rendering it akin to warm plasma within a

tubular reactor [18]. Conversely, DBD distinguishes itself through its straightforward design, promising facile scalability and examination [19]. Nonetheless, due to its early days, NTP tar cracking necessitates future evidence before implementation.

1.3 Research Novelty and Contribution

NTP tar cracking has been an active research field; concurrently, the advancement of NTP modelling has allowed interpretation for this technique to be applied for tar cracking [20]. As the fourth state of matter, plasma's complexity resulted in various mathematical approaches to describe its properties. NTP modelling is an active research field of its own, with various modelling approaches often tailored to specific plasma's properties aligning them with the study's objective. For tar cracking purposes, there is a high interest in fundamentally understanding the reactive chemistry interaction between NTP's chemical species and tar. Understanding this mechanism may further actualise the technology for implementation [18, 21]. Furthermore, there is a minimal study that investigates NTP tar cracking coupled with waste gasification, along with its potential environmental impact.

Therefore, the novelty of this thesis resides in its approach of plasma characterisation through a comprehensive reaction kinetic model to investigate tar cracking efficiency and its potential mechanism. The model is later employed for waste gasification, delving into its operational unit through process simulation. The result is investigated for its potential environmental impact in comparison to other waste management, along with an investigation of the current environmental studies on thermal plasma gasification.

The thesis' findings offer a distinctive "proof-of-evidence" that holds relevance for the prospective integration of tar cracking into gasification practices. Furthermore, it provides valuable insights into the trajectory of research required to actualise the practical application of NTP tar cracking for waste gasification.

1.4 Thesis structure

Chapter 2 presents a comprehensive literature review on the field of waste gasification and the role of plasma in tar cracking for both thermal and non-thermal plasma. The literature review identifies key research gaps in the field, emphasising the critical role of modelling research in advancing gasification technology. Currently, there is a lack of studies that investigate NTP from a modelling perspective due to plasma complexity. This resulted in the absence of studies demonstrating NTP as an operational unit for waste gasification, which subsequently led to a lack of environmental impact validation. Both

process modelling and environmental impact assessment are crucial for verifying NTP efficacy as a tar-cracking unit for waste gasification. Therefore, this thesis's main aim is to investigate the validity of NTP tar cracking for waste gasification and its implications to the environment.

Chapters 3, 4, 5, and 6 are the body chapters, with the scope of each chapter outlined in Figure 1-1, which illustrates a waste gasification process. Figure 1-2 illustrates the flow of this thesis. Given the multiscale modelling approach adopted in this work, each chapter employs a distinct modelling methodology designed for the respective chapter's objectives. Hence, the simulation methodology, data inventory, and assumptions are explained in depth in the respective chapters.

Chapter 3 delves into the fundamental aspects of NTP tar cracking, focusing on gas-phase reaction kinetics and elucidating its reaction mechanism and product generation. The proposed methodology simplifies the complex plasma modelling as gas species, identifying reaction pathways and the possibility of by-product generation.

Chapter 4 investigates the process engineering aspects of NTP tar cracking, applying the model developed in Chapter 3 as a unit operation for waste gasification. The cleaned produced syngas are assessed through energy recovery and chemical synthesis. The chapter result shows the ideal operating conditions and syngas recovery method for waste gasification with NTP tar cracking.

Chapters 5 and 6 explore the environmental implications of thermal and non-thermal plasma-aided waste gasification. As the premise of this thesis revolves around adopting advanced gasification techniques for waste management, it is imperative to comprehend the full extent of the processes' environmental impacts.

Chapter 5 delves into the environmental impacts of thermal plasma gasification versus alternative waste management approaches. Various the Life Cycle Assessment (LCA) work have been done for thermal plasma gasification, this chapter meticulously examines existing studies to unveil commonalities and trends. It introduces a novel comparison method not previously employed in gasification technology evaluations. For inclusivity, conventional gasification's environmental impacts are also evaluated. In comparison to other chapters, this chapter diverge as it examines thermal plasma gasification; in addition, this meta-analysis work does not employ traditional modelling methodology. Nevertheless, the niche review method and findings of this works merits it to be a standalone chapter.

Chapter 6 assesses the environmental impact of NTP tar cracking through LCA. The study aims to compare the environmental impact of waste gasification-NTP tar cracking to other waste management techniques, namely, landfilling, incineration, gasification, and thermal plasma gasification.

Chapter 7 provides the thesis' conclusion, detailed research contribution, and the perspective on plasma tar cracking and its implication for waste gasification.

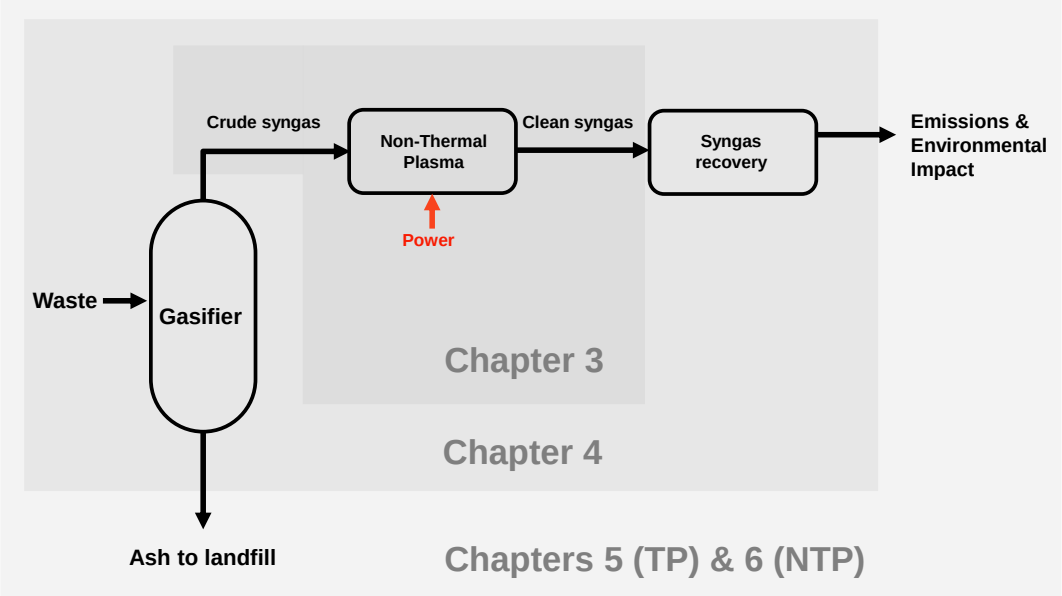

Figure 1-1: The scope for each chapter in this thesis (TP: Thermal Plasma and NTP: Non-Thermal Plasma).

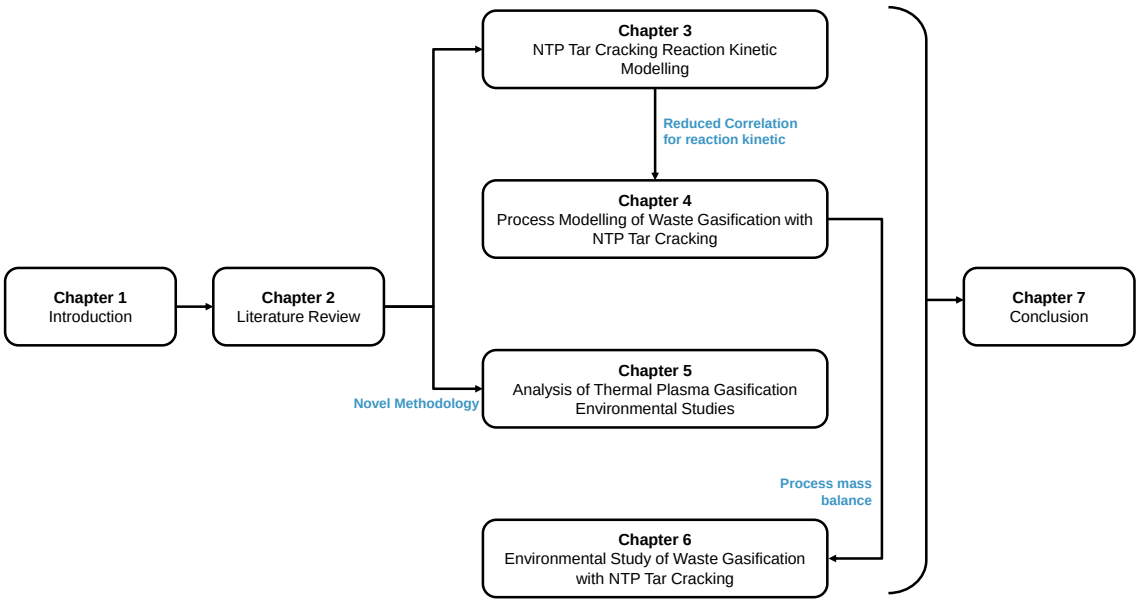

Figure 1-2: The thesis chapter's flow.

Chapter 2

Literature Review: Research Direction for Plasma Gasification

Parts of this chapter have been used as content for the following manuscripts:

Sanjaya, E. and Abbas, A., 2023. Plasma gasification as an alternative energy-from-waste (EFW) technology for the circular economy: An environmental review. Resources, Conservation and Recycling, 189, p.106730.

Sanjaya, E., Weihs, G.F., Manaf, N.A. and Abbas, A., 2024. Reaction kinetic modelling of tar cracking in a non-thermal plasma reactor: Model evaluation and reaction mechanism investigation. Chemical Engineering Journal, 479, p.147649.

With growing populations and shifting economies, the pressure to adopt adequate end-of-life waste resources strategies has never been greater [22]. Countries like Australia, despite having good success in recycling, continue to rely on landfilling and the export of waste, but such practices are not environmentally sustainable, and have recently faced international pressures from the China Sword Policy, and local pressures from the Australian Government's ban on export of certain wastes [23]. Local waste management strategies are therefore being sought for swift expansions of recycling capability [24]. From a technical angle, recycling is not a silver bullet solution, mainly because materials cannot be looped around infinitely due to quality degradation and contamination [25]. Moreover, waste sorting and recycling logistics are energy-intensive processes that often detract from feasible economics or viable business case [26, 27]. Sustainable, practical, and clean technology options that present alternatives to landfilling may therefore address the rapid momentum of waste generation currently present in the economy. Circular Economy (CE) is a novel model that minimises waste production by maximising waste recovery.

2.1 Energy-from-Waste

Energy-from-Waste (EFW) is a resource recovery option that lies between recycling and disposal (landfilling) in the traditional waste hierarchy. It is the final waste treatment option before landfilling [28]. Although EFW is popular in Europe, Japan, and China [29], it has been predominantly absent in

countries such as Australia due to constant regulatory hesitation and social backlash against EFW [30, 31]. In the late 1800s, incineration as a process technology had the sole objective of volume reduction, and neither Air Pollution Control (APC) nor energy recovery were employed [7]. Nowadays, incineration is a clean technology equipped with advanced APC, effective energy recovery, and is typically accompanied by strict air emission regulations [7]. Despite these advances in incineration technology and the technology's energy recovery value, the material destruction feature of incineration through thermal oxidation has rendered incineration to conflict with the circular economy principle of "keeping materials in use for as long as possible".

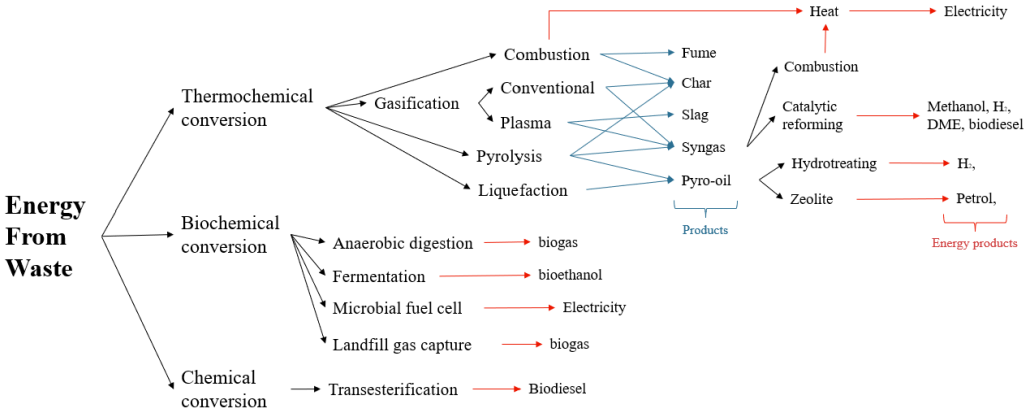

Figure 2-1: Various energy-from-waste conversion pathways (Modified from [32])

Research effort continues to seek and identify EFW technologies as an alternative to incineration [33]. Figure 2-1 shows the different potential EFW pathways and Table 2-1 shows the different methods of thermal EFW. However, incineration remains as the workhorse of the EFW industry due to its efficiency and suitability for integration with electricity grid systems. Gasification, an alternative EFW technology, partially oxidises waste into synthetic gas (syngas) that can be combusted for energy, synthesised for fuel [34], or refined for hydrogen [35] and other chemicals [36]. In this way, gasification aligns with the circular economy principle by keeping materials cycling in the economy. The production of tar as a gasification by-product has however hampered the progress of this technology Therefore, tar in syngas confines the application and use of syngas to combustion, rather than advanced fuel and chemical production, and this will therefore restrict its progression as a circular economy technology.

In a broader perspective, EFW can be used as a transitional tool for the Circular Economy [37], it complements recycling by removing unfit non-recyclable materials from circulation, provides value from discarded material, and destroys toxin and pollutant build-up [38]. In the future, possible scenarios for EFW in the CE are [39]:

1. *In a sustainable consumption model*, common products will have a long-life span and customised design. Targeted EFW will be in place to recover metal and energy to avoid landfilling.
2. *In a deep recycling model*, companies' product ownership supports an effective return and recycling process. EFW will be integrated with a recycling facility, i.e., in an integrated eco-industrial park[40].

With the rise of CE, 'mega' incineration popularity may diminish in favour of alternative EFW [41], such as gasification. The modular gasification design is appropriate for smaller scales or retrofitting, evading future 'lock-in' investment risk. Its compatibility aligns with EFW decentralisation business strategies [42].

Table 2-1: Comparison of various thermochemical EFW conversions.

Parameter	**Pyrolysis**	**Gasification**	**Incineration**	**Ref**
Principal	Thermal degradation of organic material	Partial oxidation of feedstock.	Oxidative combustion	[43-46]
Temperature (^oC)	400-800	800-1600	850-1200	[47, 48]
Reaction in plant	Endothermic	Exothermic	Exothermic	[49]
Oxidant stochiometric	Absence, 0	Controlled, between 0-1	Sufficient, 1	[49]
Pre-treatment	Required (MSW to RDF)	Required (MSW to RDF)	Not required	[47]
Solid Product	Char, ash	Ash	Bottom and fly ash	[50] [46]
Liquid product	Oil, wax, tar	-	-	[51, 52]
Gas product	Syngas (low quality)	Syngas (low quality)	CO_2, H_2O, N_2	[43, 50]
Energy product	Chemical, fuel, electricity.	Fuel, electricity, chemical	Heat and electricity	[47, 53]
Problematic compounds	Coke formation, tar, POPs, emissions	Tar, POPs, emissions	POPs, emissions	[52]
Advantages	- High calorific value oil product	- High syngas yield - Small scale feasibility - Versatile	- Mature technology - Fuel flexibility	[42, 49, 54]
Drawbacks	- Tar clogging - For biomass or polymeric waste only (plastic, tyre etc.) - Auxiliary energy requirement	- Tar clogging - Require pretreatment	- Centralised EFW - Lengthy APC units - Only feasible in large-scale - Product is limited to heat or grid energy.	[49]

POPs: Persistent Organic Pollutants, EFW: Energy-from-waste, APC: Air Pollution control; RDF: Refuse Derived Fuel.

2.2 Gasification

Gasification is a partial oxidation of solid feedstock into gas products in the presence of oxidant (gasifying agent) and heat. Gasification offers a versatile waste transformation, producing versatile syngas for various applications [55]. Although gasification appears to be the solution for an advanced EFW, significant challenges continue to hinder its implementation. Gasification still requires optimisation and sensible evidence before a wide-scale implementation. The process is plagued with several technical challenges that require further research, in particular, tar by-product.

2.2.1 Gasification Reaction

In a gasifier, various reactions occur under the 'gasification process'. Fabry et al. [56] explained that gasification occurred after pyrolysis, where solids partially oxidised in complex chemical reactions at gas-solid and gas-gas phases. These reactions are summarised in Table 2-2. The reaction begins with drying, heating, devolatilization (pyrolysis), and gasification reactions [54]. The objective of waste gasification is to produce syngas that can be used to produce energy or intermediate product, various variables influence the final syngas quality, namely [54]:

1. *Equivalence ratio (ER)* – the ratio of oxygen content in the oxidant supply and the required oxidant to complete the stoichiometric, where ER = 0 is pyrolysis and ER = 1 is combustion. Generally, lower ER will generate less gas product with higher CO and H_2 content [57]
2. *Residence time* **–** This controls the heat transfer between gas and solid material. However, this will also be controlled by other variables, such as the air velocity and reactor design.
3. *Reactor Type and design* – The design will influence the overall performance, where it will influence the heat transfer, gas flow (counter or co-current), and product recovery.
4. *Gasifying medium* - or oxidant, is the gas supply into the gasifier. The most widely utilised medium is air; however, this yields high N_2 syngas. This also controls which reaction will be favoured, such as the hydrogen production from steam addition.
5. *Gasifier temperature profile* – Different temperature zones may induce different reactions, yielding a certain product over the other. e.g. the top section of the gasifier that receives less heat will favour pyrolysis reaction, if the output nozzle is at the top, the product may contain high tar content [58].
6. *Waste Physical properties* – influence the effectiveness of the gasification reaction, properties include particle size, heating value, moisture content, ash content, volatile matter content, and elemental composition.

Table 2-2: The main gasification reactions, excluding pollutant formation [54]

Oxidation			**Reaction**
1	$C + {}^{1}/_{2}\,O_2 \rightarrow CO$	-111 MJ/kmol	Carbon Partial oxidation
2	$CO + {}^{1}/_{2}\,O_2 \rightarrow CO_2$	-283 MJ/kmol	Carbon monoxide oxidation
3	$C + O_2 \rightarrow CO_2$	-394 MJ/kmol	Carbon oxidation
4	$H_2 + {}^{1}/_{2}\,O_2 \rightarrow H_2O$	-242 MJ/kmol	Hydrogen oxidation
5	$C_nH_m + {}^{n}/_{2}\,O_2 \leftrightarrow nCO + {}^{m}/_{2}\,H_2$	Exothermic	Polymer partial oxidation
Gasification reaction involving steam			
6	$C + H_2O \leftrightarrow CO + H_2$	+131 MJ/kmol	Water-gas reaction
7	$CO + H_2O \leftrightarrow CO_2 + H_2$	-41 MJ/kmol	Water-gas shift reaction
8	$CH_4 + H_2O \leftrightarrow CO + 3H_2$	+206 MJ/kmol	Steam methane reforming
9	$C_nH_m + nH_2O \leftrightarrow nCO + (n + {}^{m}/_{2})H_2$	Endothermic	Steam reforming
Gasification reaction involving hydrogen			
10	$C + 2H_2 \leftrightarrow CH_4$	-75 MJ/kmol	Hydrogasification
11	$CO + 3H_2 \leftrightarrow CH_4 + H_2O$	-227 MJ/kmol	Methanation
Gasification reaction involving carbon dioxide			
12	$C + CO_2 \leftrightarrow 2CO$	+172 MJ/kmol	Boudouard reaction
13	$C_nH_m + nCO_2 \leftrightarrow 2nCO + {}^{m}/_{2}\,H_2$	Endothermic	Dry reforming
Decomposition reactions of tars and hydrocarbon			
14	$(tar)pC_xH_y \rightarrow qC_nH_m + rH_2$	Endothermic	Dehydrogenation
15	$C_nH_m \rightarrow nC + {}^{m}/_{2}\,H_2$	Endothermic	Carbonization

Table 2-3 summarises some gasifier reactor designs. Out of this, the fluidised bed is the most widely utilised design, the design allows high thermal contact and a rapid gasification process, producing high Heating Value (HV) syngas compared to other processes.

Because of the wide range of gasification variables, the simple combustion efficiency index is irrelevant for gasification**.** Some indications that can be used to quantify the performance are summarised in Table 2-4.

Table 2-3: Comparison of various widely utilised gasifier designs (Summarised from [54, 59, 60])

	Downdraft fixed bed	**Circulating fluidised bed**	**Rotary Kiln**	**Moving grate**
Feed particle size	<100 mm	< 100mm	No problem	<200 mm
Moisture	<20%	<55%	No problem	No problem
Temperature and profile	>1250°C, large gradient	>1000°C, small gradient	Large gradient	>1200°C, large gradient
Residence	Long	In a loop	Long (1-2 hr)	Long (>1 hr)
Conversion	High	High	Medium-high	>90%
Catalytic usage	Yes	Yes	No	No
Main drawbacks	Not flexible, feed specification requirement	Not flexible, feed specification requirement	Scaling up is not feasible, limited operating conditions, poor heat exchange	Very poor heat exchange, expensive operation
Example	Nippon steel (Kasuza, Kapan)	Ebara TwinRec (Kawaguchi, Japan)	Mitsui R21 (Toyohashi, Japan)	Energos Averoy (Norway)
Input	MSW, IW	MSW, IW	MSW, ASR	MSW
Gasifying agent	Oxygen	Oxygen	Air	Air
Capacity (tpd)	200	420	400	100
Power generated	2.3 MWe	5.5 MWe	8.7 MWe	10.2 MWe

Table 2-4: Summary of gasification performance indicator [54, 56, 61, 62]

Indicators	**Definition**
Fuel Gas Production (FPG)	Produced syngas mixture by gasification per kg of feedstock. The formula varies depending on oxidants and products.
Cold Gas Efficiency (CGE)	The ratio of syngas' chemical energy to feedstock embodied energy. The term cold signifies that the indicators only measure the gas heating value without its sensible energy.
Hot Gas Efficiency (HGE)	The ratio of syngas' chemical and sensible energy (exiting gasifier) to feedstock embodied energy.
Mechanical Gas Efficiency (MGE)	The ratio of syngas' chemical energy to feedstock embodied energy, without considering auxiliary energy requirement.
Carbon Conversion Efficiency (CCE)	The ratio of carbon in syngas product to carbon available in the feedstock
CO Yield	Carbon converted into CO, CO should be used to provide information for mass balance and conversion.
H_2 Yield	H_2 product, mainly controlled by oxidising agent and moisture content.
Pollutant concentration	Includes tar, dust, halogen, sulphur, nitrogen, heavy metals, and alkali salts. The contaminant causes corrosion and limits the application [63].

2.2.2 Gasification Process Simulation

Due to gasification complexity, process simulation is an integral part of gasification development, it is an effective method for gathering evidence and mechanistic investigation [64]. Gasification process simulation may be done through (1) equilibrium modelling and (2) kinetic modelling [65].

The equilibrium model predicts the composition of syngas from gasification in a fully mixed condition. Meanwhile, kinetic modelling predicts the non-equilibrium product distribution and gas composition across temperature profiles using various reactions [65]. The equilibrium model is a simplified representation of the gasification process, assuming ideal conditions and neglecting kinetic effects and non-equilibrium behaviour. Although equilibrium modelling provides valuable insights into the thermodynamic behaviour of the system, it may not accurately capture the actual behaviour of the gasification process. Moreover, the equilibrium model is unable to consider competing reactions and side reactions. Table 2-5 shows each modelling approach and limitation.

Table 2-5: Features and drawbacks for each modelling approach (Summarised from [65]).

Model	**Advantages**	**Disadvantages**
Equilibrium	- Simpler - No chemical reaction is required. - Predict maximum theoretical yield. - Independent to reactor design	- Assumption of well-mixed reactions and 0D reactor - Tar and heat loss are not considered. - Accuracy is limited to operating conditions
Kinetic	- Accurate detailed result - Inclusion of various reaction zones in the gasifier	- Computationally sensitive and intensive - Limited applicability across retrofitting and plant consideration

Table 2-6 shows the summary of recent modelling work on gasification process simulation. In general, most studies employed a mixed method of equilibrium and kinetic model, tailoring their methodology to their research question and objective. A common practice involves the utilisation of equilibrium correlation yield to predict the pyrolysis correlation followed by the gas phase reactions. The inclusion of the reactions and gas species varies across studies. Gasification process simulation is an active research field, with novel advancements such as adding correction factors [66] or using machine learning [67].

Despite the wide range of studies, significant works omit the inclusion of tar due to its complexity or lack of data. Mutlu and Zeng [91] have reviewed various Aspen-plus gasification modelling and analysed their assumptions, they argued that various studies neglect tar in favour of model simplicity. Meanwhile, Srinivas et al. [92] point out that although significant work has been done to model

gasification work, there is limited tar elimination modelling work, limited study has been done on (1) steam reforming, (2) partial oxidation, and (3) Adsorption.

Table 2-6: Recent gasification modelling studies.

Study	Gasifier & Feedstock	Gasification flowsheet (Simplified)	Comment
[68]	MSW	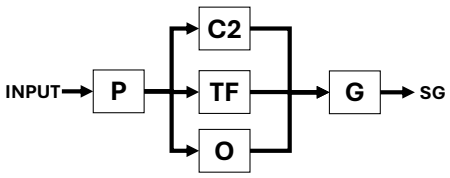	Comprehensive formation of tar and acidic gases through calculator block. Comparison with [69] and [70] for validation
[71]	Solid waste	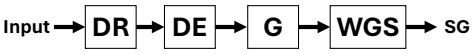	The reactions were unspecified. No tar formation. The model result is compared with [72]
[73]	Updraft gasifier MSW		Do not include tar formation, modelled through 5 reactions. The model result is validated with [74] experimental data across changing temperature
[75]	N/A Hazardous medical waste		Do not include tar formation but include acidic gases, modelled through 5 reactions. Validated with [76].
[77]	N/A MSW		Do not include tar formation, modelled through 5 reactions, including carbonation CO_2 trap. No validation.
[64]	Fluidised bed Biomass (wood)	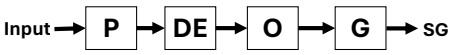	Comprehensive tar inclusion with gas phase kinetic (13 reactions). The gas phase kinetic data is compared with other studies. The model is validated with internal experiments
[78]	N/A MSW and biomass		Consider tar formation and tar cracking of naphthalene, including 9 gas phase reaction kinetics. The model result was validated with [79]
[80]	Entrained flow gasifier Biomass and Coal	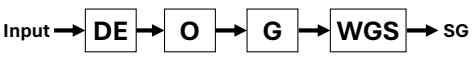	No tar modelling includes 10 gas formation reactions. No validation despite intending to model a real-life gasifier

Study	Gasifier & Feedstock	Gasification flowsheet (Simplified)	Comment
[81]	N/A Microalgae gasification	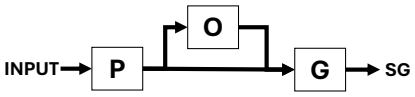	Consider the formation of methyl acetate and glycolaldehyde but not true tar. Gas phase reaction of 13 reactions. Validated with [82]
[83]	N/A Solid animal waste/manure	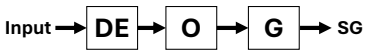	Do not include tar formation modelled through 11 reactions. Validated with [76]
[84]	Bubbling fluidised bed gasifier Biomass	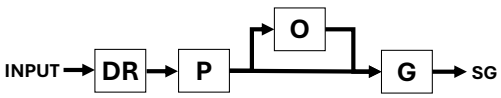	Include generalised tar formation. Validated with [85] The study also considers bed hydrodynamic, that is the bubbling reaction regime.
[86]	Entrained flow gasifier Coal and Biomass	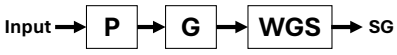	The simplified three-stage model did not include tar formation. The model was compared tabularly with [87]
[88]	N/A Biomass		The model only consists of one reactor to simulate the conversion of feedstock into syngas using the FORTRAN subroutine to simulate the fluidised bed reactions. Model validated with [89]
[90]	Dual Fluidised Bed Reactors Biomass	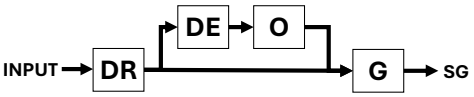	Consider 4 type of tars, the tar formation. The model is validated against internal experiments. Model configuration is designed to mimic different stages of a fluidised bed.

P: Pyrolysis, G: Gasification (Reduction), SG: Syngas, O: Oxidation, C2: C_2 Production, TF: Tar formation, DR: Drying, DE: Decomposition, WGS: Water Gas Shift

2.3 Tar Issues and Challenges

Tar is a complex, high-molecular-weight mixture of organic compounds that condenses on the gasification reactor walls and downstream equipment, leading to fouling, corrosion, and operational issues. Tar also blocks piping and catalysts, hindering syngas application [93]. Tar may contain toxic compounds, such as dioxins and polycyclic aromatic hydrocarbons (PAHs). Table 2-9 and Table 2-10 summarise the pollutants in syngas required for process advancement.

Tar generation is a byproduct of partial oxidation. Since the process does not reach thermodynamic equilibrium, the incoming feedstock polymer does not convert fully into smaller gasses, which is the

same reason for tar absence in waste combustion [12]. Moreover, tar formation is a complex process that is dictated by various variables. Materazzi et al. [94] hypothesised the formation to be temperature dependent, where increasing the temperature would improve the degradation into smaller hydrocarbon compounds (Table 2-8) Meanwhile, Palma et al. [95] argue that tar formation is the product of the polymer recombination that was present in the feedstock.

Furthermore, another challenge associated with tar is its quantifications and forensics. Table 2-7 shows the classification of various types of tars according to Lateh et al. [93]. Although there is a protocol to quantify tar (CEN BT/TF 143) [96], tar is an umbrella term that is used to define any byproduct hydrocarbon. The diversity in tar characterisation resulted in various in approaches to solving the tar issue.

Hence, tar complexity makes it the most challenging contaminant. The compound complexity resulted in difficult characterisation; consequently, describing its physical properties. Further research is also required to understand tar formation and its potential degradation mechanism [92], which may assist in designing an effective tar abatement strategy. Tar cleaning can be done physically by removing it from the syngas stream, or directly destroying the tar into smaller gases in syngas.

Table 2-7: Summary of tar classification, adopted from Lateh et al. [93].

Tar Class	Classification and properties	Example
I	Heavy tars that cannot be detected in chromatography	Gravimetric tar
II	Heterocyclic elements that are polar and water-soluble	Phenol, benzene, and pyridine
III	Single-ring aromatic compounds that do not condense easily but are not fully water-soluble.	Toluene and styrene
IV	Light PAHs (2-3 rings), condense at high concentrations and moderate temperature	Naphthalene, methylnaphthalene, and fluorene
V	Heavy PAHs (>3 rings), condense at low concentrations and high temperature	Fluoranthene and pyrene

Table 2-8: Tar production from gasification process (Summarised from [93]).

Gasification Temperature (ºC)	Tar productions	Yield (wt%)	Component
400-550	Primary	25-40	Class I
550-800	Secondary	40-25	Class IV-V
>800	Tertiary	<25%	Class II-III

Table 2-9: Contaminants and control method in syngas (summarised from [54, 63, 97])

Contaminant	Origins	Problems	Control
Dust/Particulate	Fine solid inorganic ash exiting the gasifier due to pressure differences	Fouling, corrosion, and erosion.	Removed from the stream from various filtration technologies: cyclone, Fabric filter, ESP, and wet scrubber
Tar Droplets	A mixture of condensable organic compounds, defined as all hydrocarbons with molecular weight greater than benzene.	Fouling, clogging, and heavier hydrocarbon will compete in catalytic upgrading units.	Tar cracking through plasma or catalyst. Scrubbing with oil or water. Downstream processing operates at temperatures higher than above tar's dew point.
Halogen compounds	Incoming waste contains halogen, commonly from PVC or e-waste.	Extremely corrosive to steel, react with other compound causing fouling (Salt, NH_4Cl)	Wet scrubbing with alkali solvent. Activated carbon injection.
Sulphur compounds	Combustion of sulphur leads to generation SO_2, while gasification often produces H_2S, COS, and CS_2	Condensation into sulphuric acid, corrosive to metal, and catalyst poisoning	Acid gas removal through scrubbing, various solvents exist, Plasma can assist in reducing the complex sulphur into SO_2
Nitrogen compounds	When air is used, N_2 is converted into NO_x during combustion, while in gasification, NH_3 HCN is produced	Reduces Lower heating value (LHV), lead to NO_x pollution, catalyst poisoning, and disturbing acid gas removal.	Ammonia and cyanide can be reduced into N_2 at gasification temperature, or into NOx during combustion. Selective and non-selective catalytic reduction.
Heavy metal	Less volatile heavy metals (Cr, Zn, etc.) will remain ash or slag. More volatile elements will be in syngas either at elemental or salt. Originated from e-waste, plastic stabiliser, medicine, paints, etc.	Soften metal, corrosive, deposit in downstream processing, and catalyst poisoning.	Activated carbon adsorption. Slag production to lock the me
Alkali salts/mineral	Typically, alkali salt will be deposited as inorganic material, however at temperatures higher than 800^{o}C, alkali salt can become molten or vaporised	Redeposited further down the stream, slagging ash in the boiler. Difficult to be removed. Catalyst poisoning.	Condensation or via solid adsorption

Table 2-10: Syngas quality requirement for downstream processing summarised from [63, 97, 98]

Contaminant	Combustion (boiler)	Gas engine	Gas turbine	Fuel Cells	Methanol synthesis	FT Synthesis
Dust	Removal of dust >10μm	< 5 mg/Nm^3	< 1.2 mg/Nm^3 (for 10-20 μm)	< 0.02 mg/Nm^3	< 0.02 mg/Nm^3	0 mg/Nm^3
Tars	Not required, operate a higher than tar dew point.	< 30 mg/Nm^3	< 5 mg/Nm^3	<0.1 mg/Nm^3	<0.1 mg/Nm^3	<0.01 μL/L
Halogen	Will be removed after	< 10 mg/Nm^3	<1 mg/Nm^3	0 mg/Nm^3	<0.1 mg/Nm^3	<0.01 μL/L
Sulphur	Will be removed after	< 100 mg/Nm^3	<1.5 mg/Nm^3	0 mg/Nm^3	<1 mg/Nm^3	<1 μL/L
Nitrogen	Will be removed after	(NO_x) < 50 mg/Nm^3	NH_3 removal	N/R	<0.1 mg/Nm^3	<0.02 μL/L
Heavy metal	Will be removed after	N/R	< 1 ppm	N/R	10 ppb	N/R
Alkali	Will be removed after	<1 mg/Nm^3	<0.1-0.2 mg/Nm^3	0 mg/Nm^3	N/R	<0.01 μL/L

At STP, N/R: not reported, 0 mg/Nm^3: Non detectable.

2.3.1 Tar Cleaning: Physical

Physical cleaning involves separating the tar from syngas. This is achieved via two main approaches: (1) when tar condenses into particles (dry gas cleaning) or (2) when tar remains as vapour as it exits the gasifier (wet gas cleaning).

Dry gas cleaning methods include cyclones, filters, separators, and absorbers. Their effectiveness varies depending on syngas quality and the presence of other contaminants [99]. Adding catalysts to filters may create a dual filter-cracking system to enhance efficiency [100]. Wet gas cleaning employs wet electrostatic precipitators or wet scrubbers. However, water as a medium is less favourable due to limited hydrocarbon solubility and potential byproduct formation. Despite the availability of various physical tar removal techniques, their implementation remains hindered by higher operational costs and efficiency reduction [14].

2.3.2 Tar Cleaning: Cracking

Tar cracking refers to the method that breaks down tar molecules into simpler and more valuable gases. Tar cracking can be done by (1) thermal decomposition, (2) catalytic cracking, and (3) plasma treatment. Direct tar cracking also improves the syngas quality by releasing more hydrocarbons into the syngas streams.

Thermal decomposition is done by elevating the temperature alone, ergo no addition of plasma into the system. Increasing temperature has been shown to produce less tar; however, this process often does not meet the tar concentration required for advanced downstream processing [14]. In contrast, catalytic cracking has been demonstrated in nickel [101], iron [102], and dolomite [103]. However, catalytic cracking has significant drawbacks, such as fouling, carbon deposition, and fast deactivation [16]. Lastly, plasma may be employed to assist tar cracking [104].

Utilising plasma for tar cleaning (plasma gasification) has been widely demonstrated in thermal plasma [105]. Although effective, thermal plasma comes with several drawbacks such as high energy consumption, material fusing, and uncontrollable reaction kinetics. Recently, there has been an emerging method to use Non-Thermal Plasma (NTP) for tar cracking. This approach allows researchers to utilise surrogate compounds, enabling them to investigate the efficacy of plasma and the reaction selectivity. The niche NTP operating conditions converts tar at atmospheric conditions with lower energy consumption, showing promising results at the laboratory scale [14].

2.4 Plasma

Plasma, the fourth state of matter, is a partial or fully ionised gas consisting of various species, namely electrons, ions (positive and negative), atoms, metastable, molecules, free radicals, and photons [106]. The temperature of these species is the basis of plasma classification. High-temperature plasma is when plasma temperature ranges from 10^6 K to 10^8 K, which is usually found in stars or laser fusion [107]. In temperatures lower than 10^6 K, plasma can be categorised into thermal plasma and non-thermal plasma (NTP) according to its degree of ionisation, defined as the temperature of electrons relative to ionisation energy. Plasma classification is provided in Figure 2-2.

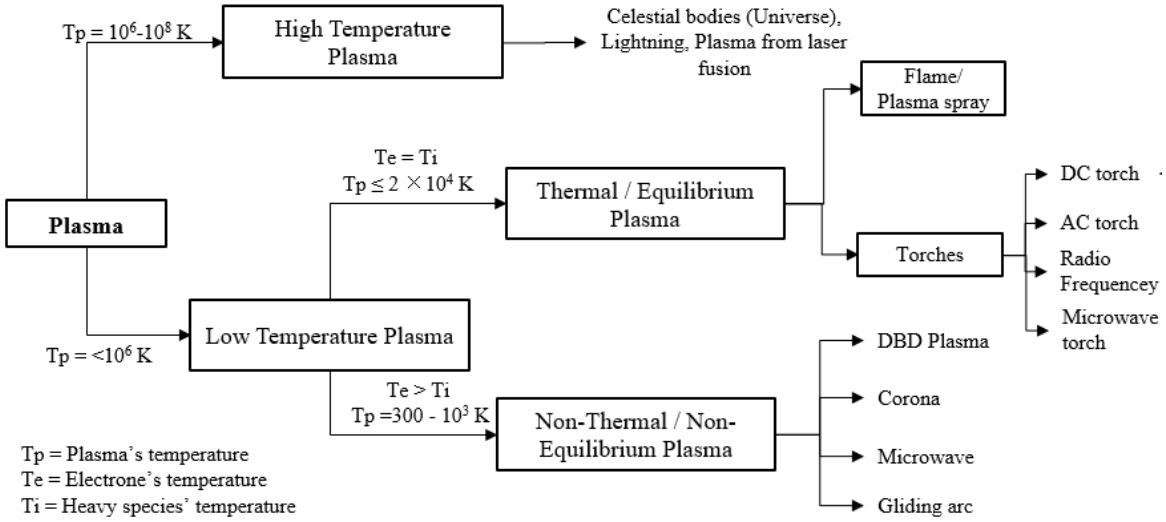

Figure 2-2: Plasma classification according to Gutsol adopted from [107-111]

Similarly, thermal plasma and NTP can be categorised by the temperature differences between electrons and heavier particles [48]. Non-thermal plasma's electron temperature is higher than ion and other heavier species. NTP electrons may exist as high as 10,000 ^oC while heavier species exist at lower or even at room temperature, resulting in the overall plasma temperature to relatively low. Meanwhile, if all plasma species are at the same temperature, the plasma is categorised as thermal or equilibrium plasma, which can only exist at higher temperatures.

2.4.1 Plasma Modelling

Plasma modelling research has existed since the mid-1900s. The earliest record of this approach is by Ruark in 1944, writing to the American Physical Society, showing its findings around "charged gas"

behaviour [112]. Later, Spitzer mathematically assessed plasma behaviour in his book and represented it as an "ideal charged gas", altering the ideal gas law to fit plasma [113]. Since then, various mathematical equation has risen to evaluate plasma behaviour, from treating it as electrically conducting fluid [114] to relating plasma behaviour using quantum theory [115]. Table 2-11 describe the various approach to mathematically model plasma behaviours [116].

Table 2-11: Summary of various approaches to describe plasma through a mathematical model.

Approach	**Plasma** as	**Description**	**Relevant theories**	**Example studies/ application**
Charged ideal gas	Fluid	Representing plasma as an ideal gas law but with charges [113].	Ideal gas law, Planck black body radiation, etc.	Energy and radiation distribution in gaseous plasma [117].
Computational Fluid Dynamic	Fluid	Representing plasma as a fluid	Navier-stokes, Lorentz force, Maxwell equation	Simulation of plasma torch jet nozzle [118]
Magneto-hydrodynamics	Fluid	Representing plasma as electrically conducting fluid [119]	Navier-stokes, Lorentz force, Maxwell equation	Low current DC plasma arc bath reactor at high-pressure modelling [120]
Two fluids	Fluids	Represent system as two gas systems of ion and electron [121].	Navier-stokes, Lorentz force, Maxwell equation	Turbulence modelling of plasma jet [122].
Gyrokinetic	Gas	A quantum framework to assess plasma's ion and electron motion that impacts the fluids [123].	Vlasov-Maxwell expansion equation, Gyro-Bohm model, Lorentz force	Electrostatic turbulence modelling of magnetised plasma [124].
Particle in Cell (PIC) kinetic	Gas	Plasma gas species are represented as "superparticles" and tracked via different cells [125].	Langrian frame, Lorentz force,	Development of code for astrophysical plasma dynamics [126]
Chemical kinetic	Gas	Represent plasma as a chemical species that contributes to chemical reactions. [127].	Boltzmann equation, Planck black body radiation, Electron energy equations, species conservation.	Methane reforming with DBD reactor. [128]
Quantum plasma	Fluid & wave	Focusing on the quantum effect due to the wave characteristic of plasma [115].	Degeneracy effect, de Broglie wavelength, Maxwell–Boltzmann distribution.	In assessing the model for fluid properties, most studies are still theoretical [129].

The challenge in plasma modelling is to derive a mathematical model that encapsulates all of the plasma's properties, ranging from its species behaviours [130] to its convergence impact, such as radiation [131], electromagnetic waves [132], surface interactions [133], Thomson scattering [134], etc. Because of its complexity, model usefulness relies significantly on the study's objective, influenced by the specific plasma application. For example, representing plasma as chemical kinetic

would not be fitting to represent a plasma gasification reactor that focuses on plasma thermal flow properties, and vice-versa [135]. Early plasma modelling often focuses on thermal plasma [131], with a few concepts that have been applied to NTP [136]. Moreover, Gleizes [131] argues the need to introduce a comprehensive databank for plasma modelling that may enable collaboration and stronger experimental validation.

2.5 Thermal Plasma Gasification

Thermal plasma can assist gasification through (1) Plasma gasifier (one-stage) or (2) Gasification and plasma tar cleaning (two-stage). In a one-stage plasma gasifier, thermal plasma is directly injected into the gasification reactor to sustain high temperature, assisting material decomposition and tar cracking simultaneously. The extreme temperature enables reactions that are unattainable in conventional gasification [54]. Figure 2-3 shows the different plasma gasifier configurations. Direct plasma contacts vitrify ash into slag, locking hazardous material into a solidified matrix [15].

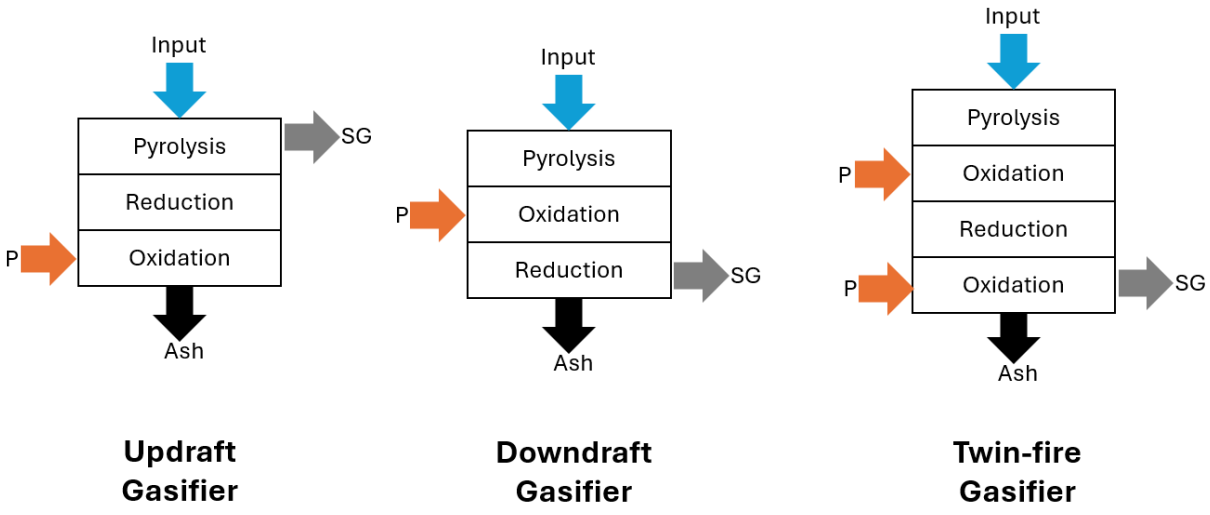

Figure 2-3: Designs of Plasma gasifiers (Selected from[58]).

Alternatively, the process can adopt a more targeted approach by using thermal plasma in the syngas streams to purify the tar in syngas (plasma cleaning unit). The modular process allows independent control of the gasification and tar cracking to produce a more consistent syngas quality, Meanwhile, a single-stage plasma gasifier's syngas quality is directly influenced by the gasification reaction [137], which fluctuates significantly in the face of waste inconsistency. While various method exists to generate thermal plasma, the industry prefer to utilise DC torch due to its reliability.

2.5.1 Plasma Gasification Implementation

For plasma gasification applications, two key sectors come into play: the plasma suppliers responsible for designing plasma torches, and the Energy-from-Waste (EFW) companies that employ these torches within their gasification processes. Four primary plasma torch suppliers for EFW are Westinghouse (WPC), Europlasma, Tetronics, and Phoenix Solution Company (PSC), [56]. Meanwhile, academic institutions such as PERSEE-MINES ParisTech and the Russian Academy of Science have gained recognition for their contributions to thermal plasma research, particularly in the advancement of AC torch designs for plasma gasification. Collaborative work between academic institutions and EFW companies have also driven progress, such as partnerships such as Pohang University's collaboration with GS Platech, or University College London's partnership with Advanced Plasma Power Ltd.

Table 2-12 shows the summary of plasma gasification industrial implementation. Despite various companies demonstrating pilot-scale operations, thermal plasma gasification is still riddled with challenges, that is:

(1) Technical challenges - It is widely accepted that high temperature, radiation, and ionisation affect the gasification reaction; however, the true reaction mechanism remains unexplored. Conventional attempt to optimise gasification departs with some unanswered question, especially in plasma discharge behaviour inside the gasifier, including plasma's impacts on reaction [48] and the overall thermodynamic [138]. In general, plasma gasification is desperate for critical optimisation. From the engineering standpoint: the torche sputtering effect lowers the electrode lifespan and consumes material [63, 139] while the intense heat requires an auxiliary cooling system [107]. This causes downstream corrosion and refractory material fusing, which need to be removed from the gasifier periodically [140]. Collectively, these constraints led to difficulties in scaling up and implementation [63].

***(**2) Economical challenges* – technical difficulties during scaling up constrict plasma gasification to be an uncertain investment [63]. Since capital investment cannot be reduced, a cost-effective operation is crucial [138]. The high electricity demands for plasma generation, coupled with the relatively short lifespan of plasma torches (300-500 hours [56]), along with auxiliary utility requirements, resulted in diminished energy commodities [15]. Furthermore, the motivation behind plasma gasification development is to produce a renewable bioenergy (biomass portion), sustainable waste management, and emission reduction. These incentives compete the conventional landfilling and incineration. In comparison to them, plasma gasification is an unlucrative business option. Adding tipping fees or

advanced products slightly helps the economic incentive (such as fuel or hydrogen production [138, 140]). Therefore, a technical advancement that supports techno-economic analysis in terms of profitability and energy balance is equally important as the technical improvements.

(3) Indirect challenges – The heterogeneous nature of waste continues to be the inherent problem in the waste management industry. Theoretically, plasma should be able to treat all types of waste. However, for a steady process, incoming waste has to be converted into fuel (RDF) by shredding and drying [140]. Separation based on size, calorific value, and ash content is also ideal [63]. In addition, feedstock competition may arise with other waste management '*giants'* (i.e., recycling and incineration) [141], this limitation can be overcome by working closely with the recycling company and the public [138].

2.5.2 Thermal Plasma Gasification Modelling

Thermal plasma gasification experiments are often carried out in a pilot-scale reactor, requiring high capital investment in designing and maintaining the reactor. This resulted in centralised innovation controlled by accessibility. Additionally, the high energy requirement makes repetition and variable manipulation to be limited. Hence, similar to conventional gasification, modelling is often the selected methodology for cost-effective proof of evidence.

Modelling approach may investigate (1) Process simulation and/or (2) Internal mechanism. In a process simulation, the modelling demonstrates the high-quality syngas utilisation, such as methane production [137], hydrogen-from-biomass [142], gas engine [143] and Solid Oxide Fuel Cell [144]. Meanwhile, the internal mechanism investigates the plasma reactor's reactions and or physical profile. This can be done by studying the gas phase reaction kinetic [145-151], including tar compound [152, 153], or internal fluid motion through Computational Fluid Dynamic (CFD) [135]. Table 2-13 shows some modelling work for thermal plasma gasification.

Nonetheless, there are various shortcomings with utilising modelling work for plasma gasification. Modelling studies are often lacking in validation [148, 150, 152], or validated with another modelling work [154]. Moreover, the modelling assumption may omit critical compounds from the model (e.g. tar and acidic gases) [155] [142]. An accurate model demands a large data set [154] [146]. Thus, a highly accurate model is still limited to the research facility that has access to large or pilot-scale plasma gasification. Furthermore, representing plasma as fluid motion often comes with streamlined assumptions of plasma flow inside the reactor that may be inaccurate.

Table 2-12: Thermal plasma gasification industrial implementation

Company and Process	Summary	Industrial implementation
Alter NRG Corp Downdraft plasma gasifier	Downdraft shaft plasma gasifier where plasma and waste are injected at the bottom and middle of the gasifier respectively. This creates freeboard, gasification, and melting zone throughout the reactor, overall rector temperature [63]. The company collaborate with WPC for its plasma torch.	The first that launched large-scale waste plasma gasification, operated for 10 years at 300 tpd [156]. Since then, the company predominantly supplied technology for hazardous waste management and biofuel production [157]. EFW attempts challenged feedstock scarcity and competition with incineration [158].
CHO Power Moving grate gasifier with syngas cleaning unit	Waste is gasified in a moving grate reactor where syngas is collected and treated with Euro plasma torch at 850^{o}C for tar cracking. Similarly, bottom ash is treated with an independent plasma chamber to produce slag The clean syngas is combusted for energy [159]	There is currently only one operating EFW plant at 137 tpd and producing 12 MWe. The facility also treats biomass and wood waste. The plasma supplier also experienced in hazardous waste and asbestos treatment [159].
Advanced Plasma Power (APP) Fluidised gasifier bed with syngas polishing unit	Pre-treated waste (RDF) is fed into a fluidised bed gasifier (~750^{o}C), and the produced syngas and ash are passed into a plasma chamber (~1500^{o}C) to crack tar and produce slag. The plasma chamber contains twin graphite DC electrodes. [153]. APP use Tetronic's DC torch	The company constructed a pilot-scale plasma gasifier for demonstration (10 kg/h), since then, the company expanded to syngas and natural gas production. Studies on MSW, RDF [145], biomass [137], syngas' pollutants [153, 160-162], and thermodynamic study [163]. This project has been abandoned [164] and expects future production[165].
Enersol Technologies	The feedstock is fed into a staged gasifier. The produced syngas is further refined with plasma and cleaned, while the as is melted with plasma to produce slag. Syngas is clean and synthesised into the desired product [166]	The company demonstrated two plants of fixed and mobile systems, with capacities of 10 and 5 tpd respectively. They also claim the possibility of syngas-to-alcohol synthesis. [167].
Environmental Energy Resource (ERR) Plasma Gasification and Melting (PGM) technology	The reactor has a built-in feeding system and melting chamber. The feedstock is gasified in a downdraft reactor, followed by a bottom melting chamber that transfers the heat from the melting chamber to assist the gasification reaction. Syngas is collected from the top of the reactor. [168]. The reactor has been studied through aspen modelling [169], steam injection [168], and represented as Eulerian Model [170].	The company built a pilot scale (20 tpd). Nevertheless, it was reported that further evidence is required in terms of efficacy in producing high-quality syngas and industrial tests before commercial implementation. [171]

Company and Process	Summary	Industrial implementation
OMNI Conversion Technology Gasification and plasma refining system (GPRS).	The feedstock is fed into a moving grate gasifier (drying and pyrolysis) and followed by a vertical fixed bed gasifier (gasification). The produced syngas is refined with two plasma electrodes to degrade tar and other pollutants [172].	There is only one operating system in the third phase trial. The second demonstration plant processes 135 tpd of waste[173], with a future waste-to-hydrogen facility expected[174].
Bellwether Gasification Technologies Ltd.	The feedstock is fed into a multistage gasification process. The first part of the chamber dried, while the second chamber gasified the feedstock into syngas which was later treated with a plasma reactor for clean syngas [175]	While the company stated some involvement in designing gasification projects (30-100 tpa), it is unclear whether it is plasma gasification or traditional gasification [175]
PEAT International	Waste is fed into high high-temperature gasifier (~1000^{o}C), prevents the formation of tar whilst vitrifying the ash content. The process is claimed to be able to process any type of feedstock without producing secondary waste for landfill [176].	The company designed different reactor sizes up to 250 tpd. PEAT successfully launched a plasma gasification system 8 tpd) for the defence department treating agricultural blast media and medical waste. [176, 177]
InEnTec Plasma Enhanced Melter (PEM)	InEnTec designed a process that involves three independent chambers. Waste is fed into a downdraft gasifier (up to 1,200^{o}C) converting it into syngas and inorganic ash. The Ash portion is vitrified in the plasma chamber (up to 1,500^{o}C with plasma plume reaching up to 5,000^{o}C). Syngas from both chambers were flown into the Thermal Residence Chamber (TRC) to further crack hydrocarbons [178]	InEnTec deployed its technology around the world and treated different waste types, such as Industrial, municipal, medical, electronic, and hazardous waste. However, there is a lack of information on capacity and energy product generation [178]
Pyrogenesis Plasma Resource Recovery System (PRRS)	RDF is fed into a gasifier equipped with graphite arc plasma. The inorganic ash is simultaneously vitrified while the crude syngas is treated with an air plasma torch to minimise the reformation of dioxins, furans, and tar. The syngas is cleaned to remove heavy metals, particulate matter, and acidic gases use [179].	The pilot PRRS (2 tpd) while a transportable plasma EFW system designed for the US Air Force processes up to 8.5 tpd of MSW. The system produces 420 kW through an internal combustion engine. The company has extensive expertise in waste destruction including vitrification and hazardous waste treatment [180]
GS Platech	Waste is fed into a thermal plasma gasification furnace equipped with two non-transferred thermal plasma torches. The waste is a gasifier with hot air (produced by heat exchange with syngas) molten slag. molten slag is quenched. Syngas is passed through a heat exchanger and into the cleaning unit before energy recovery [48]	The company built a 10 tpd pilot scale that converts MSW into syngas and slag (7/8% w/w). The hot syngas is used to generate steam at 1.2 tph while the syngas is combusted before stacking. Pilot has no energy recovery, planning to expand to 100 tpd [48]. While there is no update on the large-scale construction, the company reported its involvement on fuel cells (50 kW) through hydrogen-from-syngas [181] [182].

Table 2-13: Summary of selected thermal plasma gasification modelling work

Study	Approach	Validation	Aim and findings
[183]	Theoretical plasma gasifier and develop GasifEq model	Validated by using GasifEq model [184]	The study aimed to develop a plasma gasification process of sewage sludge and demonstrate the energy recovery feasibility through a thermodynamic model. For energy production, the study found that it best for the sludge to be dried prior to plasma gasification (moisture of 26.7%), with the possibility of processing 250 tpd of sewage sludge and producing 28.5 MW
[150]	Reaction modelling of plasma gasification	No reported validation attempt	The study aimed to evaluate the efficiency of RDF plasma gasification considering the reaction enthalpy, energy, and exergy analysis. The study found that the efficiency falls between 27-34%.
[135]	Fluid dynamic simulation on downdraft plasma gasifier	No reported validation attempt	The study aimed to simulate the internal profile of a novel 10 kW microwave plasms integrated down-draft coal gasifier design. From the model, the design emphasises the swirl effect of feedstock inside the reactor, where the interaction of the gas phase is done through the Eulerian-Lagrangian approach, and the finite Rate Chemistry/Eddy Dissipation model for gasification reaction. The model shows CGE of 55.3% and 18.4% and 37.2% yield for H_2 and CO respectively.
[146]	Artificial neural network to predict plasma gasification products	Compared with Experimental data on a pilot plant gasification process.	The thesis utilised a feedforward backpropagation black box artificial neural network to predict the syngas yield and temperature of the plasma gasification. The ANN was trained using the Levenberg-Marquardt nonlinear regression technique and overfitting was diminished through Bayesian regularisation.
[144]	Process simulation of plasma gasifier and downstream processing	Syngas comparison with [185]	The study aimed to demonstrate plasma gasification, cleaning unit, SOFC, and post-combustion process to be a feasible energy production system. The model demonstrated that microwave-induced plasma gasification shows the best efficiency when the moisture is around 21%, allowing 34% energy efficiency, and CHP efficiency of >70%
[155]	Computational Fluid Dynamic simulation on plasma gasifier	Syngas comparison with modelling of [135]	The study aims to investigate the plasma reaction and syngas produced from MSW plasma gasification. The turbulence reactor is simulated through the Euler-Lagrangian approach, where the result is validated with another model and in the face of changing feedstock.
[186]	Process simulation of plasma gasifier and various downstream processing	Syngas comparison with Experiment of [183]	The study aims to provide a computational tool for the analysis of plasma gasification combined cycle power. The study found that moisture content in MSW can impact the torch power consumption reduction by >50% and the process achieved the best result at high plasma temperature and low gasification temperature.

2.6 Non-Thermal Plasma Tar Cracking

Although thermal plasma gasification is a highly efficient process, it has several drawbacks such as high energy consumption, reactor sputtering, and uncontrollable reaction kinetics. Non-thermal plasma (NTP) (or cold plasma) has recently been demonstrated for tar cracking. While the overall plasma temperature is lower, energetic electrons' extreme temperature (~10,000 ºC) cleave the hydrocarbon bonds in the tar into simpler molecules. Compared to thermal plasma, the low temperature limits the occurrence of unfavourable reactions [187]. Furthermore, NTP can be coupled with catalysts which may lead to a superior tar cracking.

2.6.1 Bench Scale Evidence

NTP tar cracking allows researchers to utilise surrogate tar, allowing reaction selectivity and efficiency investigation. The niche operating conditions of NTP convert tar at atmospheric pressure with lower energy consumption [15]. Table 2-14 summarises the experimental work that has been done on demonstrating tar removal with an NTP plasma reactor. From the table, it appears that most researchers utilised GAD and DBD reactor tubes for tar cracking using surrogates (model) tar compound. The use of tar compound allows researchers to investigate the tar removal efficiency in detail along with a hypothetical degradation pathway. For example, Xiao et al. [188] demonstrate a synergistic effect between Mn-base catalyst and plasma power. The study claims that the catalyst acts as an oxygen storage for the oxidative degradation of tar in the presence of CO_2.

Mechanistically, some studies have hypothesised the potential pathway for tar cracking. According to Wang et al. [192], naphthalene tar cracking in air plasma involves four main pathways: the formation of indene, conversion into benzaldehyde, conversion into toluene, and ring-opening reactions. Meanwhile Saleem et al. [193] suggested that benzene tar cracking involves the formation of phenyl radicals, which eventually attack the double bond (or recombine into larger tar), and conduct ring-opening reactions. Liang et al. [194] hypothesised that toluene tar cracking requires OH radicals or electron to attack the toluene's alcohol function to form benzyl radical or phenyl radicals, which are unstable and degrade through ring-opening reactions. There is a trend among researchers that tar degradation involves the formation of radicals from incoming reactive plasma species, forming either (1) larger tar or (2) phenyl radicals that will degrade through ring-opening reactions. It is important to note that these pathways are hypothesised, and further investigation is required to affirm the validity of these theories.

Furthermore, NTP tar cracking has only been demonstrated on a bench scale with a few studies that utilise real tar from the gasification process ([189-191]). Most studies focus on the utilisation of model tar compound (usually up to Class IV, Table 2-7) at temperatures around 400-500ºC. Although there is industrial implementation of GAD for waste gasification operating at a non-equilibrium plasma phase [18], the high power suggests that this plasma is better labelled as warm plasma instead of NTP. Furthermore, most studies focus on the degradation of tar without the consideration of by-product generation, along with potential syngas reforming.

Table 2-14: NTP tar cracking experimental studies.

Study	Tar	Gas carrier	Catalyst	Reactor	Flowrate (ml/min)	Operating conditions	Tar removal
[189]	From biomass gasification	-	Zr Cr	DBD	-	Ambient temperature 30 kV	88%
[190]	From rice hull gasification	N_2 CO_2	-	DBD	40	Ambient temperature 225 V	-
[195]	T	N_2 CO_2 CO H_2	-	DBD	65-120	Ambient – 400ºC, 20 kV, 40W tar: 33 g/m^3	96.7%
[196]	T	N_2 SGG	Fe, Cu, Co, Ni-Al_2O_3	GAD	6,000	400ºC, 60 kV, 40W tar: 12% v/v	94.3%
[193]	B	CH_4	-	DBD	40.6 - 120	Ambient – 400ºC, 20 kV, tar: 20-82 g/m^3	82.9%
[197]	T and N	N_2 H_2O	Ni/Al_2O_3	GAC	3,500	Ambient – 300ºC, 56 W, tar: 1.1 and 15 g/m^3	86.3% 75.5%
[198]	N	H_2 N_2	-	Reverse vortex GAD	20,000–60,000	Ambient temperature 50–220 V, 300–460 W, tar: 610 mg/m^3	85%
[199]	B	Air H_2O	-	DBD	100	Ambient – 250ºC, 20 kV, 40W tar: 350 ppm	93.7%
[200]	B	H_2 CO_2 N_2	-	DBD	40.6 - 120	Ambient – 400ºC, tar: 201-120 g/m^3	96%
[188]	T	Ar CO_2	Mn	DBD	500	Ambient temperature, 30 kV, 2.637 g/m^3	98.5%
[191]	Real tar from cellulose gasification	Ar	Co-Al_2O_3	DBD	50	Ambient temperature, 10 kV	-

Study	Tar	Gas carrier	Catalyst	Reactor	Flowrate (ml/min)	Operating conditions	Tar removal
[201]	T	Air	Nickle-ZSM	DBD	100	500°C, 30 kV, tar: 259 g/m^3	87.9%
[202]	T	H_2 SGG N_2	Ni-K-Al_2O_3	DBD	1000	500°C, 30 kV, tar: 259 g/m^3	98%
[203]	T	Air	Nano film MnO_2	DBD	250	Ambient temperature, 0.97 g/m^3	93%
[204]	T, N, P (10:1:1)	N_2 and CO_2	-	GAD	6000	160–400 °C, tar: 8.8-19.3 g/m^3	85.8%, 76.4%, 93.4%
[205]	heptane	Air	Zeolite	DBD	1000	Ambient temperature, 12-16 kV, 12.2 g/m^3	-
[206]	real tar from plastic pyrolysis	Ar N_2	Fe Ni Co Cu Al_2O_3	DBD	-	250°C, 20 kV,	-
[207]	T	N_2 CO_2 CO H_2 SGG	Ni – Al_2O_3	DBD	1000	400°C, 30 kV, tar: 2.2 g/m^3	50.5% 90% with catalyst
[208]	T	H_2	-	DBD	40.6 - 120	Ambient – 400°C, 20 kV, tar: 20-82 g/m^3	99.5%
[209]	Real tar from coal gasification	Air	-	DBD	-	Ambient temperature, 10-20 kV	-
[210]	T	N_2 CO CO_2 H_2	Ni- Al_2O_3	GAD	16,667	500 °C	89%
[211]	n-dodecane	N_2	-	GAD	2750 - 3750	Tar: 3.3-97.5 g/m^3	68.1%
[212]	T	Air	-	DBD	100	200 – 500°C, 20 kV, tar: 261 g/m^3	90%
[213]	M	Air O_2 N_2	Al_2O_3 Pt/ Al_2O_3 TiO_2	DBD	500	121°C, 11 kV, tar: 0.5% v/v	100%
[214]	T, N, and Ph	N_2 and CO_2	Ni/Cr-Al_2O_3	GAD	6000	110°C, Tar: 12 g/m^3	95.2% to 83.9%
[215]	T	N_2	$Ni/(NO_3)_2$ $Fe/(NO_3)_2$	DBD	1000	300°C, 30 kV, tar: 30.8 g/m^3	86.5%
[216]	T	Ar	-	DBD	150	Ambient, 30 kV, 19.3 g/m^3	52%
[217]	N	N_2	-	GAD	20,000	tar: 0.6 – 1.3 %	79%
[218]	N	O_2 Air N_2 Ar	-	GAD	6800	Tar: 1.32 g/m^3	92.3%

B: Benzene, T: Toluene; N: Naphthalene, P: Phenol, Ph: phenanthrene, DBD: Dielectric barrier discharged, GAD: Gliding arc discharged. SGG: Simulated gasifier gas (syngas), Ambient: Ambient temperature

2.6.2 Modelling advancement

NTP's lower temperature enables easier species identification and diagnosis when compared to thermal plasma. This approach represents plasma as a chemical species, which enables reaction investigation, rather than a thermodynamic representation observed in thermal plasma modelling. Inside a plasma system, the species are [219]:

- *Electron (e-),* is generated through gas activation, where the naturally occurring free electron collides with the larger gases, resulting in the creation of ions and additional electrons.
- *Ion (CH_3^+, CH_4^+, H^-, etc.),* charged particles coming from the direct result of electron-induced reactions, their density may vary throughout the reactor depending on their charge.
- *Molecule (CH_4, C_2H_4, N_2, etc.),* input reactant that reacts with electrons and gases, often enough gas of interest that can be observed experimentally.
- *Radicals (O, OH, CH_3, CH_2, etc.)* are highly reactive neutral species, contributing to chain reactions and overall plasma system kinetic reactions.
- *Excited species (N_2 ($A3\ \Sigma_u^+$), Argon (Ar^+), etc.)* collision from electron can result in the colliding species higher electron energy. For NTP, there are three common excitations, that is rotational excitation, vibrational excitation, and electronical excitation.

These NTP species react with each other and their surroundings, which contributes to the overall plasma's bulk properties. Some possible reactions are shown in Table 2-15, where it is noticeable that the driving force of the reactions are the electron species. This importance led many kinetic modelling studies to focus their efforts on the prediction of electron properties, especially its energy distribution (Electron Energy distribution function, EEDF) [219].

If a study focuses predominantly on plasma's reaction capabilities, such approach may reduce the complex plasma modelling into focusing on predicting the production and/or loss of different species, calculated through a set of reaction rate equations. This approach eliminates the need to model the transport properties of each species or the bulk plasma properties. This modelling approach is described as the Plasma Global Model [220]

In the Plasma Global Model (PGM), the high-energy-electron impacted the gas in its path, which generates radicals, ions, excited species, and photons [128]. This electron impact reaction can be presented as the Arrhenius equation in terms of gas and electron temperature. Plasma global models have been deemed as an attractive first step in analysing plasma chemistry and identifying key reaction rates in a non-thermal plasma without excessive computational time [221]. To achieve the reaction rate kinetic, the electron collision reaction rate is estimated by solving EEDF whether it is through Maxwellwian or Boltzmann distribution, and multiplying it with its cross section and drift velocity

[219]. Various online solvers can be adapted to assist in the creation of the reaction kinetics, EEDF solvers such as BOLSIG+, EEDF [222], and LoKi [220] can be used to estimate the electron's energy density, that later translated into reaction rate kinetic.

Table 2-15: Summary of possible reactions within NTP Summarised from [219]

Type of reactions	**Subtype**	**Code**	**Example reactions**
Electron collision	Elastic collision	E1	$e^- + CH_4 \rightarrow e^- + CH_4$
	Excitation collision	E2	$e^- + CH_4 \rightarrow e^- + CH_4 (v_{24})$
	Ionisation (Non-Dissociative)	E3	$e^- + CH_4 \rightarrow 2e^- + CH_4^+$
	Ionisation (Dissociative)	E4	$e^- + CH_4 \rightarrow e^- + CH_3 + H$
	Dissociation	E5	$e^- + CH_4 \rightarrow e^- + C + 2H_2$
	Attachment reactions	E6	$e^- + CH_4 \rightarrow H_2 + CH_2^-$
	Dissociative recombination	E7	$e^- + CH_4^+ \rightarrow CH_3 + H$
Chemical reactions	Neutral-Neutral	C1	$H_2 + CH_2 \rightarrow CH_3 + H$
	Neutral-Neutral (Radical)	C2	$C_2H_5 + H \rightarrow CH_3 + CH_3$
	Neutral-Neutral (Third body)	C3	$CH_3 + CH_3 + M \rightarrow C_2H_6 + M$
	Ion-Neutral	C4	$CH_3^+ + CH_4 \rightarrow CH_4^+ + CH_3$
	Excited stated	C5	$CH_4(v) + M \rightarrow CH_4 + M + E_v$
	Energy relaxation	C6	$CH_4(v_3) + CH_4 \rightarrow CH_4(v_4) + CH_4(v_4)$

Table 2-16 reviews various NTP gas kinetic modelling. From this review, it can be said that there is a lack of higher hydrocarbon (tar) modelling in a plasma environment, with most studies focusing on the lower and simpler gases. Additionally, it can be observed that various modelling works reduce plasma's complexity by selecting a certain reaction type. PGM of these studies often disregards ionisation, excitation, and surface chemistry [128, 223]. This assumption may be adopted due to computer power limitation, and the possibly of the reactions minimal contribution. For example, Machrafi et al, [224] reduce 85% of its reaction sets when the model simulation is improved from 2D into 3D fluid simulation.

Table 2-16: Summary of plasma reaction kinetic modelling, focusing on global plasma model or similar approach.

Study	Gas	Simulation tool - modelling methodology	No of rxn and type	Result	Validation
[225]	CH_4 H_2O	Chemkin Ansys- Electron temperature is estimated by observing plasma reactor intensity. The electron collision rate is estimated by solving the Boltzmann equation through the Quantemol DB database.	166 rxn for 29 species E1 C1 C2	The study found that in the methane steam reforming model, hydrogen and radical H are the key species that convert methane into other products. The model also considers the production of C and formaldehyde formation.	Validated with internal experiment
[226]	C_7H_{16} CO_2	Chemkin Ansys - Electron temperature is estimated by observing plasma reactor intensity. The electron collision rate is estimated by solving the Boltzmann equation through the Quantemol DB database.	157 rxn E1 C1 C2	Heptane cracking is predominantly controlled by radical impact instead of electron. The model is tested through various oxidant-to-carbon ratios.	Validated with internal experiment
[227]	CH_4 O_2	Chemkin Ansys- Boltzmann equation is used to estimate the generation of radical species from electron impact collision, added with GRI-MECH Methane combustion database	372 rxn E5 C1 C2 C3	The model includes the production of acetic acid and formaldehyde. The author argues that electron impact is the driving force of the methane conversion, not atomic oxygen	Unclear
[228]	CH_4 O_2	Ansys Chemkin-Electron collision reaction rate is estimated by solving the Boltzmann equation, using the result from database LXCat. The dynamic behaviour is modelled through flux density, and rxn is complemented with GRI MECH 3.0	193 rxn with 87 Species E2-6 C1-6	Model the combustion of methane in plasma-assisted planar shear flow, demonstrating at higher voltage, more conversion is happening with O to be the most active species, and plasma assists the generation of H	Claiming that previous study has validated this model
[229]	CH_4 N_2	ZDPlaskin - 0D reaction model solved via electron density in the plasma reactor.	2174 rxn E1-7 C1-6	Comprehensive simulation of methane reforming that also accounts for charged species, radicals, and excited species	Compared with experimental data by [230]
[231]	C_3H_6 CO O_2	COMSOL MATLAB- Non-ideal compressible gas, Continuity equation and Navier Stokes equation for gas, while using electron collision for gas dissociation and depletion balance for equation	21 rxn E4 C1-3 C5	The model simulates the two-stage reduction by corona wire plasma and catalyst to reduce common pollutants in the exhaust gas. Plasma is more efficient in reducing C_3H_8 while catalyst is more efficient for NOx.	Validated with different experiment results [232]

Study	Gas	Simulation tool - modelling methodology	No of rxn and type	Result	Validation
[233]	CH_4 N_2	Chemkin Ansys Electron impact reaction is estimated using BOLSIG+ while the neutral rxn is collected from the NIST database. metastable rxn were collected from various references.	286 rxn for 32 species E1-5 C1-C4	Metastable nitrogen species are the driving force of methane conversion, while H radical plays an important role in ensuring the production of H2	Compared with an internal experiment
[234]	CH_4 O_2	Chemkin-Rxn databases were collected from LXCat database, while electron transport rxn was estimated using BOLSIG+	E1-4 C1-3	The model considers the plasma combustion of propane, ethylene and ethane in the presence of argon gas, consider the argon's excited state and its contribution to the gas products	Compared with external experimental data [235] [236]
[237]	C_2H_4 H_2O	Unspecified- Poisson's equation is used to estimate the electric potential, to be used to estimate the electron charge and the drift-diffusion equation to estimate the electron mobility transport. The electron reaction rate is estimated by integrating the electron collision cross-section with the isotropic part.	317 rxn with 42 chemical species E1-6 C1-6	The study evaluates the CO_2 dissociation in dielectric barrier discharged. Where the conversion of CO_2 into CO is evaluated through the reactor, the study identifies key pathways and the universal energy conversion rate.	Unspecified
[238]	C_3H_8 N_2	Fortran- The rxn is described using Arrhenius equations, while the equation of the electron continuity is described by solving Poisson's equation	20 rxn E1 E4-6 C1 C2 C4	The model evaluates the behaviour of CF4 in a DBD tube reactor, especially during reactor start-up. the model	No validation
[239]	CO_2 O_2 H_2O	Unclear-Theoretical simulation of excited species in plasma gas, estimated by Relativistic Binary Encounter Bethe to estimate electron energy distribution, coupled with conservation equation of electron energy.	157 rxn for 26 species E1-7	Estimate the plasma formation from X-ray flash of highly energetic photons. The study argues that the Compton electron beam is directly responsible for plasma creation	Unspecified
[240]	C_7H_{16} CF_4 N_2	Unspecified0Electron transport rxn was estimated using BOLSIG+, while neutral rxn was selected from GRIMECH database.	166 species and 611 rxn E1-7C1-4	The study focuses on the pulsed plasma discharged and how it impacted the heptane combustion.	Unclear
[128]	CH_4 Ar O_2	Chemkin Ansys-Mass balance equation, Momentum conservation equation. Arrhenius equation for rxn, estimated from Poisson's equation for electric field and Boltzmann equation.	175 rxn with 39 species E1 E4 E5 C1 C2	Model over-predicts H_2 and underpredicts CO The model accurately predicts the CH_4 conversion The model does not represent higher hydrocarbon conversion, which might contributed to the error	Validated with internal experiment
[241]	C_7H_{16}	FORTRAN-Continuity equation, followed by drift-diffusion of different particles, which is used for electron estimated via electron energy conservation equation with its electron flux density.	36 rxn E1 E2 E3	The rxn also include the generation of photon from ionised or excited species. The study focuses on modelling excited argon and nitrogen species throughout the reactor and different voltage	Claim to be in "good agreement" but it is unclear

Study	Gas	Simulation tool - modelling methodology	No of rxn and type	Result	Validation
[242]	CH_4	Globalkin-0D reaction model solved via electron density in the plasma reactor.	21 rxn E1-7 C1-4	Consider excited and oxygenated radical species. Despite the low number of rxn, the model is able to predict good results.	Experimental data compared with [230, 243, 244]
[245]	N_2	Chemkin Ansys-The study uses kinetic reactions collected from the STANJAN library and GRI MECH database.	Unspecified	The thermodynamic model is used as an experimental guide to reform light hydrocarbon with gliding arc plasma to produce rich hydrogen syngas	Unspecified
[246]	CH_4 CO_2 O_2	Unclear-The study collected rate coefficients of various rxn from [247] to simulate a DBD reactor.	17 Rxn E1 E3 C4	The study focused on modelling Helium DBD plasma in the face of Nitrogen impurities, which found the effect on the plasma's current density.	No Validation
[248]	C_2H_6 N_2	PLASIMO-Production of chemical species through energy balance solved through electron collision estimated with electron energy flux and density. Feed into Poisson's equation to obtain an electric field. The electron impact reaction rate is calculated with the Boltzmann equation.	More than 789 rxn with 69 chemical species E1 E2 E3 E4 C1 C2	The model includes the conversion of methane to higher hydrocarbon. The model simulates the conversion of methane into hydrocarbon, formaldehyde, methanol, and syngas. The effect of CO_2 and O_2 as oxidants is evaluated.	Not validated
[224]	C_3H_8 N_2	COMSOL, MATLAB - Diffusion model for C deposit, followed Nonlinear equation for conservation of ions and Poisson's equation of electric potential for active species distribution	29 rxn for 2D, 4 rxn for 3D E4 C1 C2	The model simulates carbon reforming in a flat-gap DBD reactor, along with the fluid simulation of the reactor.	No Validation
[249]	CH_4 H_2O	Chemkin Ansys- Electron impact cross section is estimated with Boltzmann equation, complemented with combustion kinetic from GRI MECH database.	>164 Rxn E2 E3 E5 E6 C1-6	The model is used to estimate methane combustion and found to be in good agreement with experimental data. The model contains elaborate species of ion and excited gases.	Compared with external experiment

Rxn: Reactions, type see Table 2-15.

Nonetheless, PGM has its limitations, ultimately, it is impossible to model every possible kinetic interaction as a reaction rate kinetic. Selectively choosing which reactions may produce a biased result. Reactions such as charged surface [131], ionisation [226], and exaction [128] are often disregarded. Furthermore, there is also an argument on whether the assumption around EEDF methodology is a valid approach in simulating reaction rate kinetics [221], questioning the methodology at its fundamental approach. Despite these disadvantages, the plasma global model is still an appealing first step in understanding plasma reaction rate kinetic.

2.7 Potential Environmental Impact

Furthermore, as an emerging technology. A comprehensive understanding of technological & commercial readiness levels (TRL and CRL), environmental impact, and public perception needs to be adequately understood before implementation and related policy development. Whilst a lot of researchers argue plasma gasification produces lower emissions. There is a limited number of environmental studies that attest to this claim [143].

Concurrently, LCA has emerged to become the preferred and standardised method to address waste management's footprint [250]. LCA's popularity rose with cumulative studies on thermal EFW jumped from 11 to 244 from 2001 to 2013 [251]. The assessment can include direct and indirect emissions within their system boundary [252]. LCA appears to be a holistic tool that provides quantified environmental impact that is useful for decision-making purposes.

Although ISO14040/44 exists to govern the transparency and accountability of LCA studies, the principle still allows room for interpretation [251, 253] or perhaps misinterpretations. Laurent et al. [254] reported that malpractices exist across different LCA studies arising from not following the standard properly, such as omitting the system boundary, impact coverage, and sensitivity analysis [255]. Even within an appropriate framework, significant differences can still occur from identical data when processed by different models, eventually arriving at different conclusions [256]. Hence, transparency in LCA assumptions and scope is important to provide confidence in the result [251, 252]. This means reviewers have a crucial role in the assessment of whether certain LCA is suitable and follows ISO14040/44 [255].

2.8 Summary

2.8.1 Current research status

Gasification has emerged as a viable alternative to incineration, offering a promising route through syngas production. However, the potential of syngas utilisation is hindered by the tar presence. Tar elimination via tar cracking simultaneously destroys tar and improves syngas quality. Tar cracking can be achieved by catalytic, thermal plasma, and non-thermal plasma (NTP) methods. Catalyst-based tar cracking, while effective, is hampered by fouling and deactivation challenges. Table 2-17 shows the comparisons between physical and tar cracking method, highlighting the novelty of NTP as tar cracking technology.

Thermal plasma gasification stands as a compelling option due to its capability to achieve high temperatures, ensuring efficient tar cracking and clean synthesis. Despite its promise, this approach has been plagued by technical, and consequently, economic obstacles. While pilot-scale demonstrations have been conducted by various organisations. Thermal plasma gasification research advancement can be said to achieve its maximum potential. This does not mean that plasma gasification does not have a place in waste management. Plasma gasification is still the best contender for hazardous waste management [105]. However, translating them for MSW remains a challenge.

Recent advancements in NTP offer promising results in its early lab-scale research. Exploration of surrogate compounds has enabled in-depth mechanistic studies and detailed efficiency. Concurrently, advancements in plasma modelling techniques enable researchers to apply plasma simulation techniques for tar cracking.

Furthermore, process simulation has emerged as a valuable tool in plasma gasification research and development. Researchers have demonstrated the utility of process simulation in evaluating environmental impact, assessing technology readiness as well and conducting comprehensive techno-economic analyses. As an emerging technology, it is essential to assess the environmental impact of plasma gasification with other waste management, whether it is thermal or the potential NTP-waste gasification.

Table 2-17: Summary of common tar removal method and their implementation stages.

Removal	Methodology	Demonstrated	Advantages	Disadvantages	Ref
Physical	Wet scrubber	In industrial level, can remove tar up to 90%. The crude syngas is contacted with water and the tar molecule dissolve and absorb into the water phase. The tar-contaminated water is later treated and cleaned.	Simple design, low operating cost, handling high temperature,	Small tar removal, create secondary pollutants from wastewater, high water consumption. Efficiency is limited to tar solubility in water.	[257]
	Wet electrostatic precipitator (ESP)	In industrial level, can remove tar up to 62%. Removes tar from gas streams by charging particles with a high-voltage electric field, attracting them to collection electrodes, and flushing them out for disposal or recovery.	Reduced water usage, compact design, removal of particulate matter and tar.	Complex maintenance, highly effective for particulate matter but not tar. More expensive than scrubber and sensitive to gas composition.	[258]
	OLGA wet scrubber	Oil based gas scrubber that removes tar by 99%. The scrubbing oil condensed and clean tar with higher efficiency than water.	Higher removal rate, straightforward design, easy maintenance	create secondary pollutants, high adsorbent consumption. Expensive	[259]
	Sand bed filter	Filtration system used to remove tar and solid contaminants by trapping them in sand bed. Reported up to 90% removal rate	Simple design and low cost	Tar condensation and blockage, no control, periodic filter removal, blockage	[260]
Cracking	Catalyst	Breaks down tar into simpler compounds using a catalyst. Demonstrate up to 99% removal on lab scale using surrogate compound. Demonstrated in pilot scale	Simple reactor design, can be imbedded into fluidised bed material.	Tar blockage, fouling, carbon deposition, and fast deactivation	[16]
	HT thermal chamber	Increasing temperature in secondary chamber to provide enough residence time for tar cracking, demonstrated in pilot scale	Simple design, low cost,	Not sufficient tar cracking, additional heating cost	[14] [261]
	Thermal plasma	Using thermal plasma directly into gasifier or as a cleaning unit, demonstrated in pilot scale	High tar cracking, clean production	Extremely high operating cost, material fusing, and difficult control	[105]
	Non-thermal plasma	Using NTP to target tar in syngas and break it down into simpler gases, demonstrated in bench scale	Low energy requirement, can be coupled with catalyst	Novel technology, require further research	[16]

OLGA: Open Loop Gas Absorption, HT: High temperature.

2.8.2 Research Gaps and Thesis Aims

Despite the wide range of experimental investigations of NTP tar cracking, there is a minimal body of work that attests its efficacy in terms of mathematical modelling. Some researchers argue the need to study the kinetic model for tar degradation, especially the synergic effect of different gases and tar compounds [262]. The kinetic reaction rate for NTP tar cracking is not a widely explored research field when compared to the experimental work. Since plasma reaction kinetic modelling is still an evolving subject, interpreting it for tar cracking chemistry can be challenging.

Understanding this, various studies have come up with simpler lumped models that represent the tar concentration changes at input at output [208]. However, this methodology fails to represent the real phenomenon behind the plasma kinetic degradation. In the pursuit of effective tar cracking, the development of a robust NTP modelling is paramount. Such model will play a pivotal role in driving advancements in tar cracking research [13, 21].

Furthermore, there is also a lack of study that conjugates the NTP tar cracking for waste gasification process, specifically, in terms of tar cracking and syngas utilisation. This absence further translates into the environmental impact studies. Thermal plasma gasification environmental impact studies require further analysis to verify its validity. Meanwhile, NTP tar cracking potential has not been investigated.

Therefore, this thesis main aims to investigate NTP tar cracking validity for waste gasification. To achieve this, a computational simulation approach was adopted where the result is validated with external experimental data collected from literatures. Understanding the wide scope of the thesis's aim, the detailed objectives for each chapter are:

- Chapter 3 - Investigating the tar cracking reaction mechanism in a NTP reactor.
- Chapter 4 - Conjugate and examine NTP tar cracking in a waste gasification process.
- Chapter 5 - Analyse the environmental impact studies on thermal plasma gasification.
- Chapter 6 - Assess the environmental impact on potential waste gasification with NTP tar cracking.

The finding of this thesis may act as a "proof-of-evidence" to shape the research direction for NTP tar cracking for waste gasification. The evidence is provided through numerical validity provided in the modelling result.

Chapter 3

Reaction Kinetic Modelling of Tar Cracking in a Non-Thermal Plasma Reactor

The bulk of this chapter have been published as: Sanjaya, E., Weihs, G.F., Manaf, N.A. and Abbas, A., 2024. Reaction kinetic modelling of tar cracking in a non-thermal plasma reactor: Model evaluation and reaction mechanism investigation. Chemical Engineering Journal, 479, p.147649.

3.1 Introduction

Gasification is a thermochemical process that converts waste into syngas. This process involves heating the waste in an oxygen-restricted environment to temperatures between 700 and 1500 °C, producing a syngas mixture of hydrogen (H_2), carbon monoxide (CO), carbon dioxide (CO_2), methane (CH_4) and impurities such as tars, nitrogen, and sulphur compounds [263]. Syngas can be combusted for energy, refined for hydrogen [35], synthesised into fuel [34] and other chemicals [36]. These pathways are unobtainable in incineration [8].

However, one of the major challenge with gasification is the formation of tars in the syngas [264]. Tar is a complex, high-molecular-weight mixture of organic compounds that condenses on the gasification reactor walls and downstream equipment, leading to fouling, corrosion, and operational issues [93], and may contain toxic compounds, such as dioxins and polycyclic aromatic hydrocarbons (PAHs).

Several approaches have been proposed to solve the tar problem, including thermal, catalytic [103], and plasma-based tar removal methods [104]. Utilising plasma for tar cleaning (plasma gasification) has been widely demonstrated in thermal plasma [105]. Although effective, thermal plasma comes with several drawbacks such as high energy consumption, and uncontrollable reaction kinetics. Recently, there has been an emerging method to use Non-Thermal Plasma (NTP) for tar cracking. This approach allows researchers to utilise surrogate compounds, enabling them to investigate the efficacy of plasma and the reaction selectivity. The niche operating conditions of NTP convert tar at atmospheric pressure with lower energy consumption, showing promising results at the laboratory scale [14] [265]. Direct reforming also improves the syngas quality by releasing more hydrocarbons

into the syngas streams. However, research is still required to demonstrate its viability, particularly in terms of its upscaling, reaction predictability, and energy efficiency.

Concurrently, the research field of plasma modelling has evolved from a simple charged ideal gas model [113] into various modelling approaches, including the complex fluid and wave plasma models [115]. One modelling approach is to represent NTP as a set of reaction kinetics, highlighting the chemical reactions and their behaviour in the NTP system [219]. This modelling approach allows researchers to focus on the reaction capabilities of plasma, simplifying complex plasma modelling into the prediction of the production and losses of various species in a set of reaction rate equations. This approach eliminates the need to model the bulk properties of plasma and is generally referred to as the Plasma Global Model (PGM) [220].

The simplicity of PGM makes it an attractive first step in analysing plasma chemistry and identifying key reaction rates in NTP tar cracking without excessive computational power [221]. In PGM, electrons are the driving force of the reactions. High-energy electrons collide with gas molecules in their path, which generates radicals, ions, excited species, and photons [128]. These electron impact reactions can be represented as an Arrhenius equation in terms of gas and electron temperature. Therefore, various studies focus their efforts on predicting the properties of electrons (i.e., the electron energy distribution function, EEDF) [219].

3.2 Research Background

3.2.1 Research Gaps and Niche

Researchers have argued the need to study the kinetic model of tar degradation with NTP, especially the synergistic effect of different gases on the overall tar degradation rate [262]. Plasma reaction kinetic modelling is still an evolving subject and interpreting its method for tar cracking chemistry may be challenging. In this context, various studies have developed simpler lumped-species models that represent the changes in tar concentration between the input and output of gasification [208]. However, lumped kinetics are unable to represent the real phenomena behind plasma kinetic degradation.

Table 3-1 summarises the various modelling attempts at investigating tar cracking (or similar compounds). The PGM simplification of plasma chemistry is well aligned with the research direction of tar cracking kinetics. Whilst the interactions between tar and plasma species remain complex, simplifying these into a few hundred reactions within selected species (hypothesised to be the key reactions), would simplify the complex behaviour of plasma chemistry. This can allow interpretation

while preserving a level of accuracy consistent with modelling objectives. Such approach would be an appealing first step for modelling tar in NTP.

Table 3-1: Chapter 3 research novelty in comparison to other published work [93].

Study	Hydrocarbon	Other gases	Number of reactions	Plasma presented as
[226]	Heptane (C_7H_{16})	CO_2 O_2	157	As electron impact reactions
[231]	Propane (C_3H_6)	N_2 O_2 H_2O CO	21	As excited oxygen
[240]	Heptane	N_2	611	Heptane reforming only consists of radical reactions (Grimech)
[229]	Methane (CH_4)	-	2,174	The reaction kinetic consists of an electron impact reaction, excited hydrocarbon, radical and charged species.
[266]	Toluene ($C_6H_5CH_3$)	N_2 and O_2	266	Electron impact reaction, excited nitrogen, and oxygen.
[267]	Toluene	-	1,888	-
[268]	Benzene (C_6H_6) and phenol (C_6H_5OH)	-	>10,000	-
[269]	n-butylbenzene ($C_{10}H_{14}$) to naphthalene ($C_{10}H_8$)	-	4,330	-
This work	Heptane, phenol, toluene, styrene ($C_6H_5C_2H_3$), and naphthalene	CO_2, H_2, O_2, and Syngas	>1,900	As electron impact reactions (See Appendix A)

3.2.2 Chapter's Aim

This study aims to employ various bodies of knowledge on hydrocarbon reforming to produce a detailed chemical reaction kinetic to demonstrate a 0D NTP tar cracking reaction kinetic, utilising Global Plasma Model (GPM) framework. The goal of this chapter is to elucidate complex pathways, validate against experimental data, and contribute to the understanding of the NTP tar cracking at varying operating parameters.

As opposed to other similar simulation studies [270, 271], this study utilises a comprehensive reaction database complemented with electron impact reaction (Appendix A), where the model is further investigated under various operating conditions. The work begins by expanding the model of Wang et al. [226] for heptane reforming (Part I), which includes comprehensive electron impact reaction kinetics for various hydrocarbon chains. Subsequently, the reaction kinetics are expanded for tar cracking kinetics (phenol, toluene, and naphthalene, presenting tar class II, III, and IV, respectively) (in Part II). Model results are then compared and validated with experimental works [204, 208].

Finally, the reaction kinetic model is investigated in a syngas environment, mimicking real syngas and tar profiles from a waste gasification data [272]. The validated model is applied for tar cracking in waste gasification syngas (Part III). To verify this approach, Part IV evaluates the electron and system temperature along with the assumptions adopted in this work, comparing the results with other published work on tar cracking and plasma modelling. This aim aligns with the thesis's aim to investigate NTP's role in tar cracking and supporting the advancement of this research avenue. In contrast to others work, this work novelty lies in the comprehensive tar characterisation and

3.3 Methodology and Model Development

The aims of this chapter give rise to the following research questions:

1) How accurately does the PGM framework predict tar cracking and its resulting products?
2) What are the advantages and shortcomings of using detailed reaction kinetics for plasma modelling?
3) How do operational parameters (e.g., power, temperature, pressure, and residence time) affect tar conversion, syngas yield, tar output profile, and the overall reaction mechanism?

To answer these, reaction kinetics are modelled using ANSYS Chemkin-Pro to simulate a plasma reactor and compare this with experimental results (Part I and II). This comparison acts as a validation step. The validated model is later used to assess the impact of incoming tar in a syngas environment (Part III).

3.3.1 Modelling Method

Reaction kinetics are modelled as a zero-dimensional (0D) Plasma Perfectly Stirred Reactor (Plasma-PSR) model using ANSYS CHEMKIN-Pro [273]. The 0D Plasma PSR assumes a well-mixed reactor, ensuring high diffusivity and uniform distribution of plasma species across the reactor. The full details of reaction kinetics for Plasma-PSR can be found in the Chemkin Manual [274]. The main conservation equations are described as follows:

- Global mass balance equation:

$$\frac{\partial}{\partial t}(\rho V) = m_{in} - m_{out} = 0 \qquad \text{(Equation 3-1)}$$

where ρ and V are mass density and reactor volume, respectively. m_{in} and m_{out} are the inlet and outlet mass flow rates.

- Species conservation equation:

$$(\rho V)\frac{\partial Y_k}{\partial t} = m_{in}\left(Y_{k,in} - Y_k\right) + \omega_k V W_k \qquad \text{(Equation 3-2)}$$

where Y_k is the mass fraction of species k, ω_k and W_k are the molar rate of the chemical reaction and molecular weight for the species k, respectively (equation modified by Yue et al. [270]).

The plasma system model is described with electron impact reactions, influenced via the power deposition into the reactor. Electron-induced reactions are assumed to be independent of reactor conditions.

- Electron energy conservation equation:

$$\rho V\left[Y_e c_{ve}\frac{\partial T_e}{\partial t} - \frac{R}{W_e}T_e\frac{\partial Y_e}{\partial t}\right] = m_{in}Y_{e,in}c_{pe,in}\left(T_{e,in} - T_e\right) - Q_{loss}^{elas} - Q_{loss}^{inel} + Q_{source} \qquad \text{(Equation 3-3)}$$

where Q_{loss}^{elas}, and Q_{loss}^{inel} are the energy lost due to elastic and inelastic collisions, respectively. Q_{source} refers to the power deposition into the reactor, Y_e is the mass fraction of electron, c_{ve} and c_{pe} are electron constant specific heat capacity and electron constant pressure specific heat capacity, respectively. T_e indicates the electron temperature of the system, and R is the ideal gas constant.

- Power loss from elastic collision:

$$Q_{loss}^{elas} = \frac{3VR\rho_e}{W_e}\left(T_e - T_g\right)\sum_{k=1,k\neq e}^{K_g}\frac{W_e}{W_k}v_{ek} \qquad \text{(Equation 3-4)}$$

where, v_{ek} is momentum transfer collision frequency between electron and heavy species k.

- Power loss from inelastic collision:

$$Q_{loss}^{inel} = V\sum_{r=1}^{I_{er}}\Delta H_r q_r \qquad \text{(Equation 3-5)}$$

where ΔH_r is the net enthalpy change of the reaction determined by thermodynamic data. q_r is the net rate of progress of r reactions, described below.

- Gas reaction rate kinetics

$$k_{f,r,g} = A_{r,g}T_g{}^{\beta_{r,g}}\exp\left(-\frac{E_{r,g}}{R\,T_g}\right) \qquad \text{(Equation 3-6)}$$

- Electron reaction rate kinetics

$$k_{f,r,e} = A_{r,e}T_e{}^{\beta_{r,e}}\exp\left(-\frac{E_{r,e}}{R\,T_e}\right) \qquad \text{(Equation 3-7)}$$

where e and g are the physical properties of electrons and gas, respectively. $A_r$is a pre-exponential factor, $\beta_r$is dimensionless constant, and E_r is the activation energy.

- Chemical reaction progress rate

$$q_r = k_{f,r}\prod_{k=1}^{k=n}[X_k]^{v'_{kr}} - k_{b,r}\prod_{k=1}^{k=n}[X_k]^{v''_{kr}} \qquad \text{(Equation 3-8)}$$

where $k_{f,r}$ and $k_{b,r}$ are the forward and reverse rate constants for reaction r, and X_k is the molar concentration of species k. v'_{kr} and v''_{kr} is the stochiometric coefficient forward and reversed reaction respectively. For each gas species involved in the reaction, their thermodynamic and transport data are required by the model. The thermodynamic data are represented as polynomial coefficients, used to calculate the specific heat, enthalpy, and entropy of each reactant at a given temperature. Transport data refer to the molecular properties for the collision frequency of each species.

3.3.2 Reaction kinetics development

This study utilises two sets of reaction databases (Appendix A.1-A5). Firstly, heptane (Part I) reforming kinetics were obtained from Wang et al. [226] and supplemented with other sources [275, 276]. The model has 47 species and 183 reactions and was selected because of its comprehensive electron impact reactions for various hydrocarbon chains. Secondly, the tar cracking database (Part II and III) was collated from Metcalfe et al. [267], and supplemented with Wang et al. [226], Trushkin and Kochtov [266], and Curran et al. [269]. The model contains 343 gas species and >1960 reactions. Metcalfe et al. [267] was selected due to its comprehensive aromatic hydrocarbon reactions. Other works [271, 277] also used Metcalfe et al. [267] for plasma reaction modelling. Electron impact reactions act as the initiation rate described through EEDF, which is based on external studies. Meanwhile, the neutral-neutral reactions act as the rate limiting reactions dictated by the system's temperature. Figure 3-1 describes the strategy used to obtain the reaction kinetics for the plasma global model.

During the reaction kinetic development, several assumptions were made: (1) The reaction mechanism focuses on the electron and radical reactions, omitting the excited and ionised gases. This is because their interactions are still relatively unknown. Instead, these reactions are represented as simple gas radical generation such as (R192) $O+H_2 \leftrightarrow H+OH$ or (R1) $CO_2+H \leftrightarrow CO+OH$. (2) Larger hydrocarbon formation is outside the scope of the model; the database only accounts for a few reaction kinetics for larger hydrocarbon formation. (3) Plasma initial electron concentration is 1×10^{-8} mol/mol. The electron temperature is assumed to be 11,640 K [128, 270]. (4) No soot formation [226].

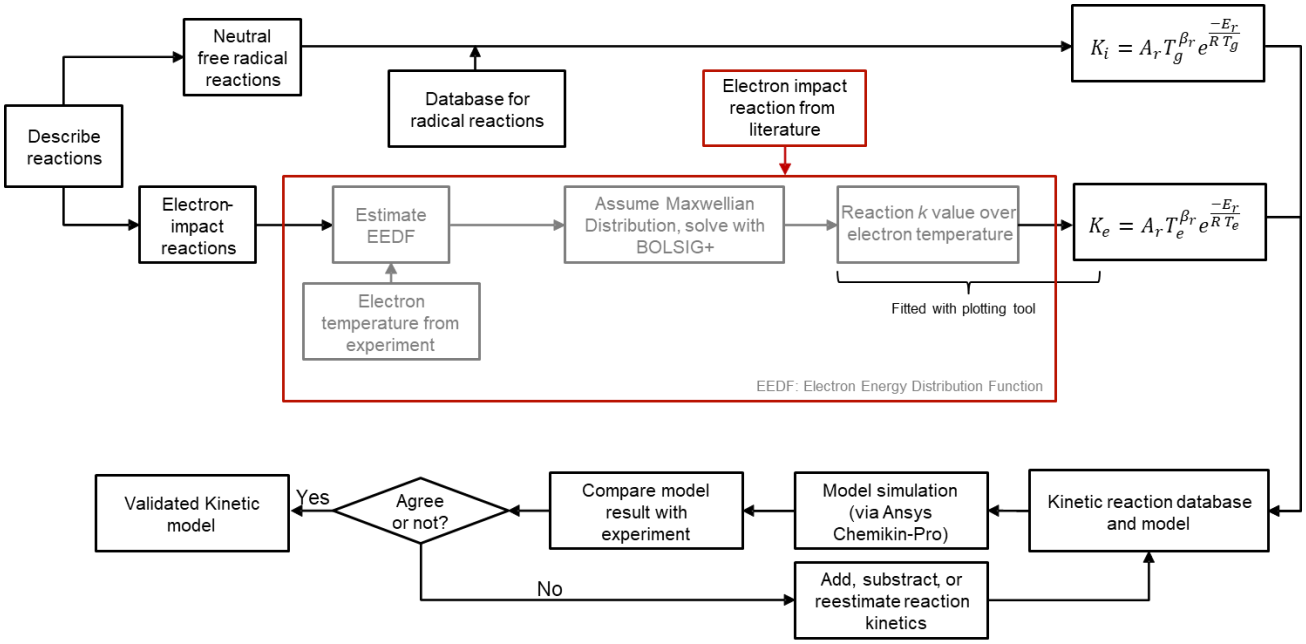

Figure 3-1: Strategy to obtain a global model for reaction kinetic modelling (modified from Zheng and Liu [128] and Chemkin [278]). For this study, EEDF kinetics were collected from other studies (see Appendix A).

3.3.3 Modelling parameters

The model operating parameters are outlined in Table 3-2. The operating conditions are used to simulate experimental data, acting as a validation step through predictive performance. The model and experimental results are then compared via the following success metrics:

1. Tar degradation (mol %), represents the NTP's ability to "crack" tar into simpler gases or smaller molecules. However, this metric does not account for the products or the carbon destination.

$$Tar\ degradation\ (X_{tar}, \%) = \frac{M_{tar\ in} - M_{tar\ out}}{M_{tar\ in}} \tag{3-9}$$

2. Yield (CO, CO_2, C_6H_6, etc. mol %), indicates the degree of tar cracking and the yield of desired gas products, categorised according to their function in syngas utilisation. Assuming tar is $C_xH_yO_z$, and the input is a mixture of only tar and CO_2,

$$CO\ Yield\ (y_{CO}, \%) = \frac{M_{CO}}{(x \times M_{C_xH_yO_z} \times X_{tar}) + (M_{CO_2} \times X_{CO_2})} \tag{3-10}$$

$$C_aH_b\ Yield\ \left(y_{C_aH_b}, \%\right) = \frac{a \times M_{C_aH_b}}{x \times M_{C_xH_yO_z} \times X_{tar}} \tag{3-11}$$

3. Output gas composition (mol/mol %), indicates the concentration of various gases and quantifies syngas purity [279].
4. The difference between results is quantified through Root Mean Square Error (RMSE).

$$RMSE = \sqrt{\frac{(Predicted\ data - experimental\ data)^2}{number\ of\ data\ points}} \quad (3\text{-}12)$$

It is important to note that the electron impact reactions adopted in this study may not be identical when compared to experimental data in Table 3-2, along with the adopted electron temperature that was based on the external study. The diversity in reactor designs, operating conditions, and data limitations hinder the creation of an identical model. This also applies to neutral-neutral reactions that are not always universally applicable [268]. Because of this complexity, this work focuses on comparing our model across studies, to examine its relevance, investigate its shortcomings and study the reaction mechanisms. Part IV of this work will discuss assumption and disparity between modelling studies and real conditions.

Table 3-2: Summary of operating conditions considered in this study.

Code	**H1**	**H2**	**H3**	**T1**	**T2**	**S1**	**S2**
Compound	Heptane	Heptane	Heptane	Tar	Tar	Tar	Tar
Part	I	I	I	II	II	III	IV
Context	Expanding work of Wang et al. on varying power [226]	Expanding work of Wang et al. on varying residence time [226]	Expanding work of Wang et al. model alone [226]	Comparing the tar model with Saleem et al. [208]	Comparing the tar model with Xu et al. [204]	Tar model at syngas environment based on Veksha et al. [272]	Sensitivity analysis on the model based
Gas temperature (K)	900	900	900	473-673	450	450	600-2300
Power (W)	30-36	36 W	25-(36)-50	10-40	20	10-(30)-100	10-100
Reactor volume (cm^3)	20	11.6-37.9	10-(20)-50	20	20	10-(20)-35	20
Residence time (sec)	10	5.8-18.9*	5-(10)-25	1.17	1.05	0.5-(1.17)-2	1.17
Reactor pressure (atm)	1.2	1.2	1-(1.2)-3	1.2	1.2	1-(1.2)-3	1.2
Gas Flowrate (cm^3/sec)	2	2	2	17	19	17	17
Gas temperature (K)	423	423	423	473-673	673	673	
Gas composition (mol/mol %)	13% C_7H_{16} 87% CO_2 1×10^{-6} % E	13% C_7H_{16} 87% CO_2 1×10^{-6} % E	1-(13)-92 % C_7H_{16} Varies CO_2 1×10^{-6} % E	12% $C_6H_5CH_3$ 88% H_2 1×10^{-6} % E	10% $C_{14}H_{10}$ 15% $C_6H_5CH_3$ 15% C_6H_5OH 30% H_2O 30% O_2 1×10^{-6} % E	6% $C_{14}H_{10}$ 9% $C_6H_5CH_3$ 4% $C_6H_5C_2H_3$ 1% C_6H_5OH 27% CO 32% H_2 14% CO_2 6% CH_4 1×10^{-6} % E	10% $C_{14}H_{10}$ 30% CO 30% H_2 15% CO_2 15% CH_4 1×10^{-6} % E

E: Electron concentration at the inlet. (), parentheses indicate the default value when other parameters are being investigated. * Adjusted value according to correction parameter.

3.4 Part I: Model Validation with Heptane

Figure 3-2 shows the comparison between the model and external experimental data for the reactor's yield and output gas composition. In an NTP reactor, supplying power to the electrode creates an electric field that boosts electron energy, accelerating the reaction as plasma power rises [95] (Eq. 3).

From Figure 3-2, A and C, the model prediction appears to visually match the external experimental data, validating the model at varying power. However, the opposite trend is predicted for H_2 gas yield. The experimental result shows a peak at 36 W and a decrease at 38 W, while the model predicts a consistent H_2 decrease with increasing power. This implies that the model achieves maximum H_2 yield at lower power, and H_2 starts to break down into H radicals as power increases further. However, this trend was not observable in the experiment due to the short half-life of H [280], meaning it may recombine into H_2 or H_2O and be detected as other species.

The model predicts an almost linear trend for CO yield and CO conversion (Figure 3-2, A), while the experimental result shows a peak at 38 W. This suggests that despite the model's capabilities, it may be unable to capture all phenomena occurring in the reaction system. Nonetheless, other models also show comparable outcomes. For instance, Sagese et al. [268] modelled benzene oxidation, predicting CO and C_2 yield peaks at lower temperatures than observed experimentally. Frassoldati et al. [281] similarly found an early peak in methane production from butane combustion in their model-experiment comparison.

Model-experiment disparities in various studies might stem from model assumptions. This study omits unsaturated and cyclic hydrocarbons, as well as soot, streamlining reactions and preventing by-product formation (Figure 3-5). While this simplifies the model, it hampers the examination of heptane conversion into complex hydrocarbons that could affect gas yield. Other experimental studies also find a similar trend where increasing power does improve hydrocarbon reforming and yield [282, 283].

Furthermore, this modelling work uses residence time as a parameter corrector. Parameter correction is a common practice in a modelling step to ensure result accuracy [284]. This is done by adjusting the parameter to meet the outcome, whether by trial and error or response calculation [285, 286]. A correction can also be made by introducing a constant [287].

For this model, parameter correction is required to normalise the ideal modelling condition to meet the experimental real-life condition. In the model, the Plasma PSR reactor ensures contact for every plasma species that is uniformly distributed throughout the reactor. The system also assumes no energy

loss [274]. In contrast, the reference experiment utilised a Gliding Arc Discharge (GAD). GAD produces a turbulent plasma arc that contains an excessive number of electrons and carries high energy, transforming adjacent gas into a reactive radical. The travelling arc influences temperature, creating distinct pockets of gas species and electron density. Species distribution may differ outside the arc. Another potential issue is that the adopted electron temperature in model may inaccurately reflect GAC's electron temperature [288-290]. The difference between the model and the experiment elucidates the need for parameter correction. Zheng and Liu [128] also adopted a similar method, where they define an "effective input power" for their modelling results. In their case, the model was unable to make accurate predictions at a higher power.

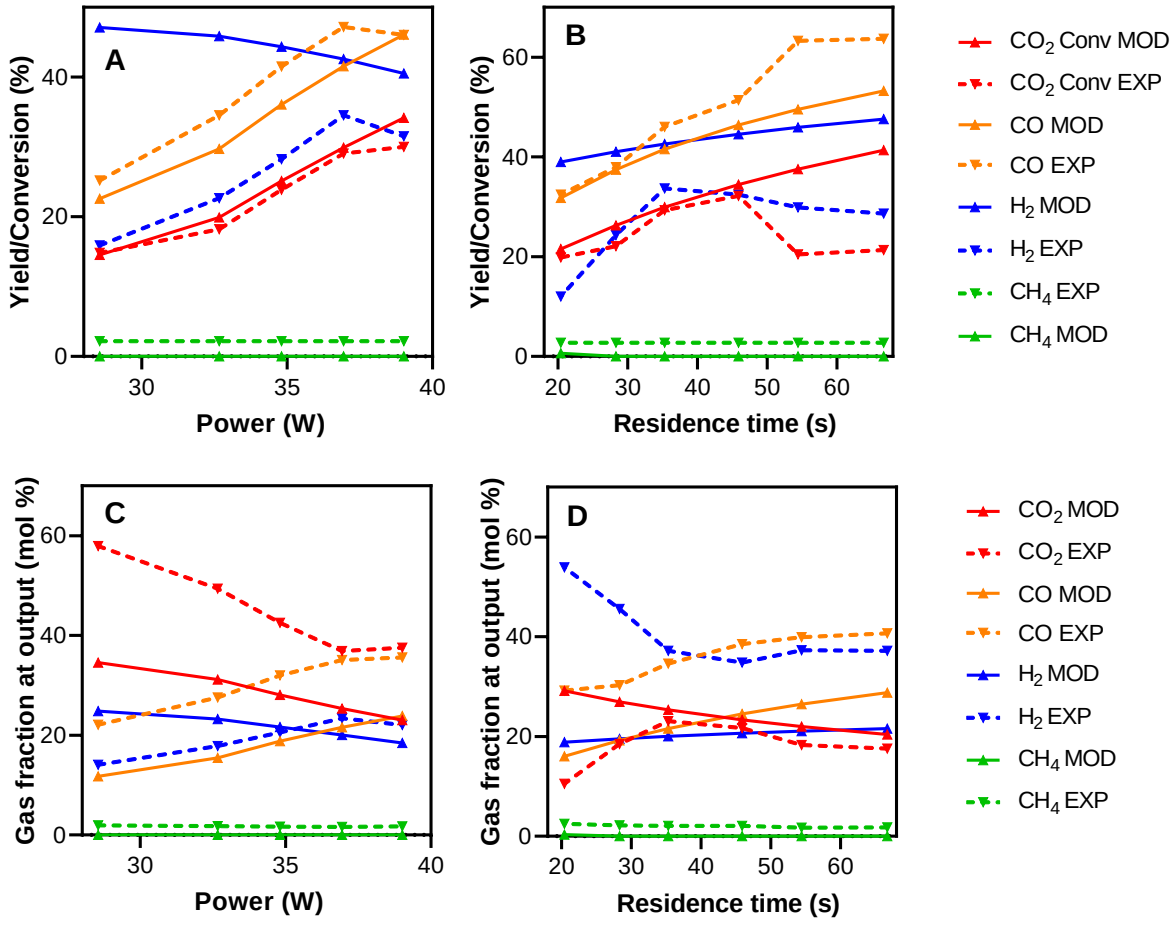

Figure 3-2: Comparison of experimental data and model predictions for yield-conversion (A and B) and output gas profile (C and D) for varying power (A and C; operating condition: Table 3-2, H1) and residence time (B and D; operating condition: Table 3-2, H2)

In this work, parameter correction is achieved by adjusting the residence time from 35.3 seconds in the experiment to 10 seconds in the model (71.7% reduction). The results show that the model has a

relatively linear response to changes in residence time, whilst the experimental result shows a peak of H_2 yield and CO_2 conversion at 35.3 and 45.9 seconds respectively (Figure 3-2, B). Similar to the power comparison, the model did not predict the peak of gas production and conversion. It is speculated that due to the model's perfectly stirred condition, an increase in residence time would not improve the reaction rate significantly (Figure 3-2, C and D). Meanwhile, the experimental condition would benefit greatly from increasing residence time as it increases the probability of hydrocarbon contact with plasma arc and other highly reactive species.

3.4.1 Standalone Model

Figure 3-3 and Figure 3-4 show the model effects of varying operating parameters.

At increasing power, the concentrations of acetylene (C_2H_2) and CO_2 at the output decrease while CO concentration increases. It is speculated that C_2H_2 is the critical pathway in the conversion of C_7H_{16} into CO (R36-R49). Increasing plasma power would favour C_2 and CO_2 conversion into CO. The increase in CO yield and CO_2 conversion with increasing power appears to slow down after 40 W. CO_2 is a major precursor for CO; however, CO_2 conversion into CO is a reversible reaction (R9-162). While this trend does not suggest that the reversible reaction is responsible for CO yield plateauing, a quenching method can be used to limit the reverse reaction. This can be done by adiabatic expansion or reactor cooling [291].

At increasing temperatures, an identical pattern emerges between power and temperature. For our model, most of the reaction kinetics for the higher hydrocarbons are dictated by neutral gas collision kinetics (Figure 3-5). The kinetics are described by the Arrhenius equation as a function of gas temperature (Equation 3-7), indicating the importance of temperature in determining the rate of reaction. Increasing power in the system does increase the temperature and energy of the electrons [292], which supports the neutral radical collision reactions. Saleem et al. [208] also studied the impact of temperature on hydrocarbon (toluene) cracking in a plasma environment. Interestingly, they found that increasing the reactor temperature (25- 400 °C) has a greater impact on tar conversion into smaller hydrocarbons than increasing plasma power (10 W to 40 W).

At increasing reactor pressure (compression), the process would favour the reversing of CO_2 conversion (reverse quenching process) [291]. This trend can be seen in Figure 3-4 (C), where CO_2 concentration increases while CO concentration decreases from 1 to 2 atm, suggesting that most of the carbon from heptane reforming was converted into CO_2. Hoang et al. [293] argue that increasing

reactor pressure supports hydrocarbon (ethanol) reforming into H_2, this is also shown in our model as Figure 3-4 (A) shows an increase in H_2 yield from 1 to 2 atm. Iwarere and Rohani [294] demonstrated that pressurised plasma can assist hydrocarbon reforming and improve methane yield, this is also shown in our model at 2 to 3 atm, where methane production is observed.

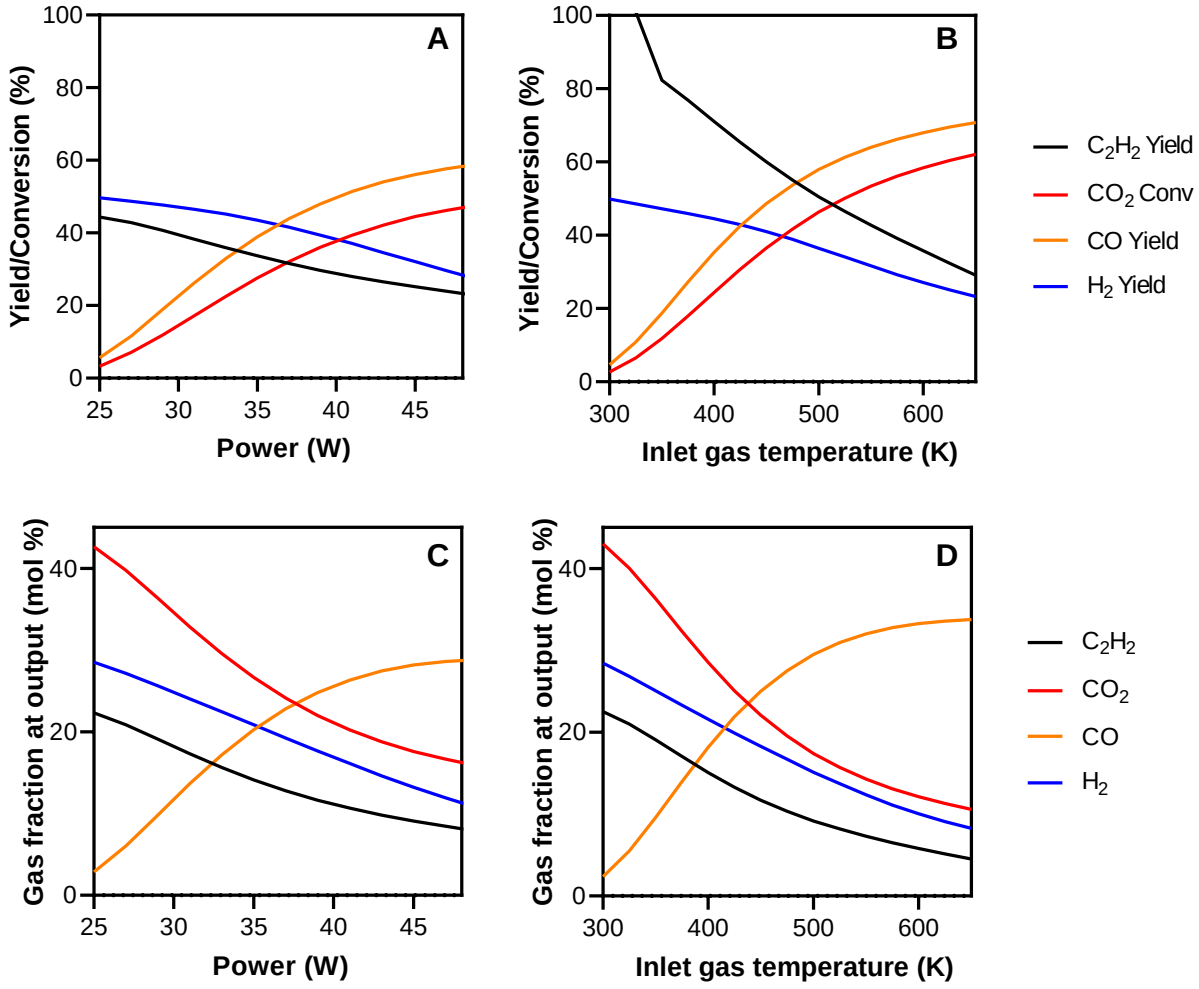

Figure 3-3: Model standalone result in terms of the gas yield (A and B) and output gas profile (C and D) at varying power (A and C) and inlet gas temperature (B and D (operating condition: Table 3-2, H3).

At increasing inlet C_7H_{16} concentration, the changing concentration significantly impacts the composition that alters the gas transport and reaction equilibrium. Wang et al. [192] evaluated naphthalene reforming with a plasma process, where they found that C_2H_2 formation is favoured at a high hydrocarbon concentration while CH_4 formation is at a low concentration. This is also demonstrated in our model (Figure 3-4, B and D) where there is a significant increase of H_2 and C_2H_2 yield when C_7H_{16} concentration increases from 0 to 0.25 mol/mol. However, the yield of all light gases (CH_4, H_2, C_2H_2) decreases as heptane concentration increases from 0.25-0.9 mol/mol. This suggests

that the incoming heptane is converted into other carbon products, potentially dispersed throughout C_3-C_4. The data implies that a high hydrocarbon concentration with a very low oxidant presence may result in an incomplete reforming process.

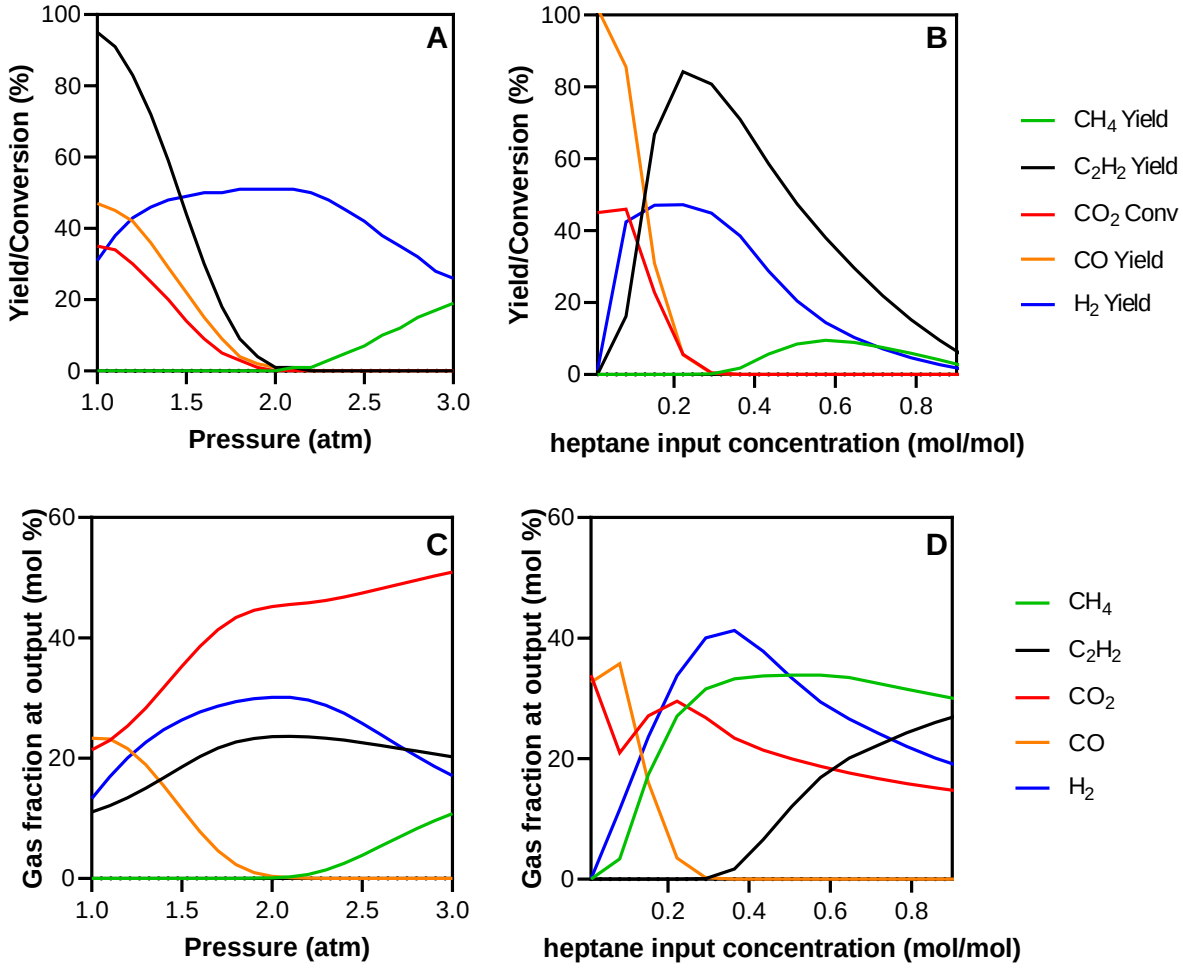

Figure 3-4: Model standalone result in terms of the gas yield (A and B) and output gas profile (C and D) at varying pressure (A and C) and heptane input concentration (B and D) (operating condition: Table 3-2, H3).

3.4.2 Reaction Mechanism

Figure 3-5 shows the reaction pathway. Despite the model's comprehensive inclusion of electron impact reactions with hydrocarbons [226], our model suggests that the electron impact reaction has a minimal role in hydrocarbon degradation. It is theorised that the electron temperature of 1.22 eV (~14,159 K) [295] is below the threshold energy for the n-heptane electron collision reaction (5.1 eV)

[226]. Instead, radicals generated via electron collisions in combination with the heat rise from the power applied are the contributing factors for hydrocarbon cracking [292].

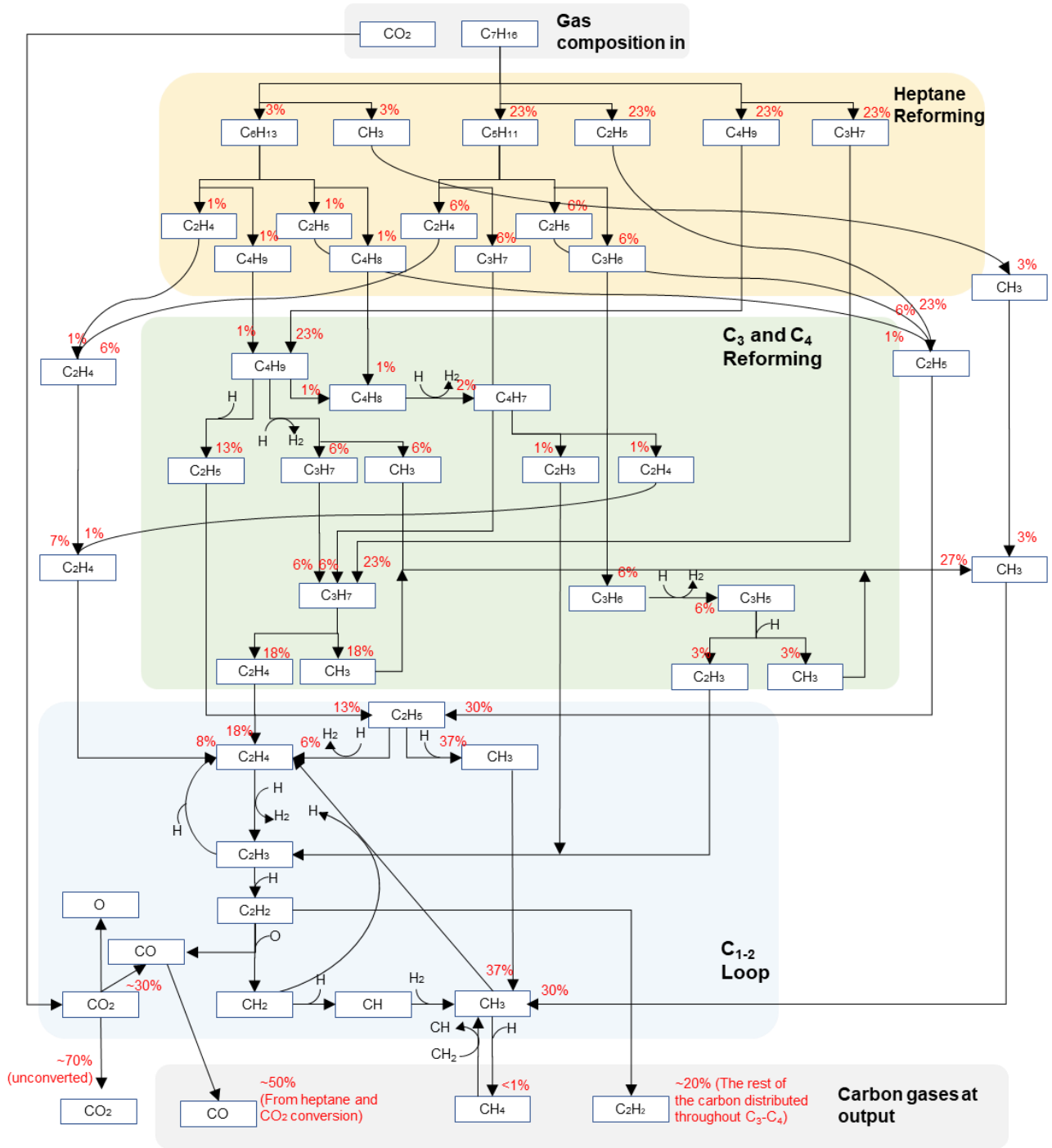

Figure 3-5: Reaction mechanism and pathway flux of n-heptane reforming at 36 W (Operating condition: Table 3-2 H1).

The model employed in this study simplifies the role of excited and ionised species in NTP, reducing them to their radical counterparts. Although there are modelling studies that assess the impact of these species with hydrocarbons [128, 229, 233, 242], these studies only assess small hydrocarbons (methane), resulting in a less complex interaction. Significant plasma research has been done on methane than higher hydrocarbon [219]. Most studies that study hydrocarbon and reactive plasma species are either obsolete or lumped kinetics [266, 296, 297], simplifying the reaction kinetics into only radical and/or electron impact reactions [298]. For example, Nagaraja et al. [240] and Benilov et al. [299] model plasma reforming of hydrocarbon fuels that only include the role of H O and OH radicals.

Figure 3-5 shows that heptane degradation is irreversible when it breaks down into C_5-C_3, where there is no indication that the carbon molecule recombines into a larger molecule. However, experimental studies indicate that hydrocarbon plasma reforming may produce a small portion of soot and might recombine into larger molecules [226, 300]. The reaction pathway becomes a loop-web network when the carbon molecules transform into C_1 and C_2. The mobile C_1 and C_2 species react with each other resulted in a loop reaction chain where C_1 atom recombined into C_2 molecule via reversible reaction networks. The reaction network is accomplished due to the extensive research on C_1 and C_2 reactions with radical species, with more recent directions to investigate the role of excited and ionised species [233, 301]. Moreover, throughout the model-experiment comparison, the collected experimental data shows the production of methane (< 5%) which is not presented in the model. However, a small portion of CH_3 is detected in the output. It is theorised that the remaining CH_4 breaks down into CH_3, as the reaction is reversible and further contributes to the abundance of H atom at the output (R32-35).

3.5 Part II: Tar Surrogates in NTP Reactor

3.5.1 Toluene

Toluene is considered to be the important precursor for tar, soot, and various PAH compounds, as well as being a reference fuel [302, 303]. Toluene relevancy has led to significant modelling work to predict toluene oxidation. This section models toluene cracking. The results are validated against the experimental work of Saleem et al. [208] on toluene cracking in a Dielectric Barrier Discharged (DBD) reactor with hydrogen plasma. Figure 3-6 shows model and external experimental data at varying power (10-40 W) and temperature (473-673 K) in terms of toluene conversion, lower hydrocarbon yield (LHC) and benzene yield. The experiment shows an agreement that can be observed, especially

at 673 K (Figure 3-6). It is important to highlight that although the model shows hig\agreement at high temperatures, the model diverge from experimental data at low temperature (473K).

At 473 K, the model predicts a significantly higher benzene yield compared to the external experimental data (Figure 3-6, A2). The external experimental data reported a low benzene yield (2-5%) and LHC (10-30%) despite the high toluene conversion rates (87-98%, Figure 3-6, A1). This finding suggests that the converted toluene is transformed into other products, possibly into larger PAHs. It is theorised that at 473 K, the experimental toluene transformed into larger PAHs compounds such as naphthalene or pyrene. The lower temperature promotes this transformation through unimolecular recombination [304]. In the given experimental setup, these PAH compounds typically condense and are not quantified for their yield. Relating this to the modelling work, the model does not comprehensively consider toluene conversion into larger PAHs. Instead, the excessive phenyl radicals in the model would be protonated by the rich hydrogen atom into benzene via R1917, resulting in the model over-predicting the benzene yield.

As the temperature increases, the experiment favours the production of benzene and LHC. At 673 K, the model can identically predict toluene conversion and LHC yield (RMSE = 1.51 and 72.35) along with the trend of lowering benzene yield at increasing power (RMSE = 547.77). This indicates that the model can precisely predict toluene conversion and gas products in a DBD reactor at high-temperature operating conditions (673 K, Figure 3-6 $C_{1\text{-}3}$). In comparison to other modelling work, Yue et al. [270] also demonstrate the capabilities of their modelling work to predict toluene degradation in a DBD plasma reactor, at varying power, inlet concentration, and gas flow rate. However, their study did not specify the model capabilities to predict the output products.

Figure 3-7 shows the reaction mechanism of toluene in hydrogen plasma based on the key reaction contribution ratio outlined in Figure 3-8. The model highlights the role of CH_3, CH_4, H_2 and H radicals, constantly donating and deprotonating the hydrocarbon. The incoming H_2 was transformed into H radical via R195 and R2140. The H-rich environment reforms the incoming toluene via two major pathways, (1) by replacing the methyl functional group to form benzene (C_6H_6, 55% of the incoming toluene, R1719) and (2) by stripping the most outer hydrogen atom of the toluene's methyl functional group to produce benzyl cation ($C_6H_5CH_2$, 54% of incoming toluene, R1694).

The abundance of the H atom encourages a collisional reaction of the toluene's methyl function, resulting in a substitution reaction to produce benzene. Benzene stability means that this pathway is unfavourable. Benzene resonance due to the lack of functional group encourages stability that disfavours cleavage/ring-opening reaction [305, 306]. Liang et al. [307] argue that benzene is more

stable than toluene in a plasma environment. According to the model, the benzene ring-opening reaction requires the formation of an aromatic functional group (such as phenol, phenolate (C_6H_5O), or toluene) to attack the aromatic double bond. This agrees with Liang et al. [308] and Li et al. [309]'s experimental data. However, as there are only H radicals, the few benzenes that reacted are converted into phenyl radicals, via R1916: $C_6H_6+H=C_6H_5+H_2$.

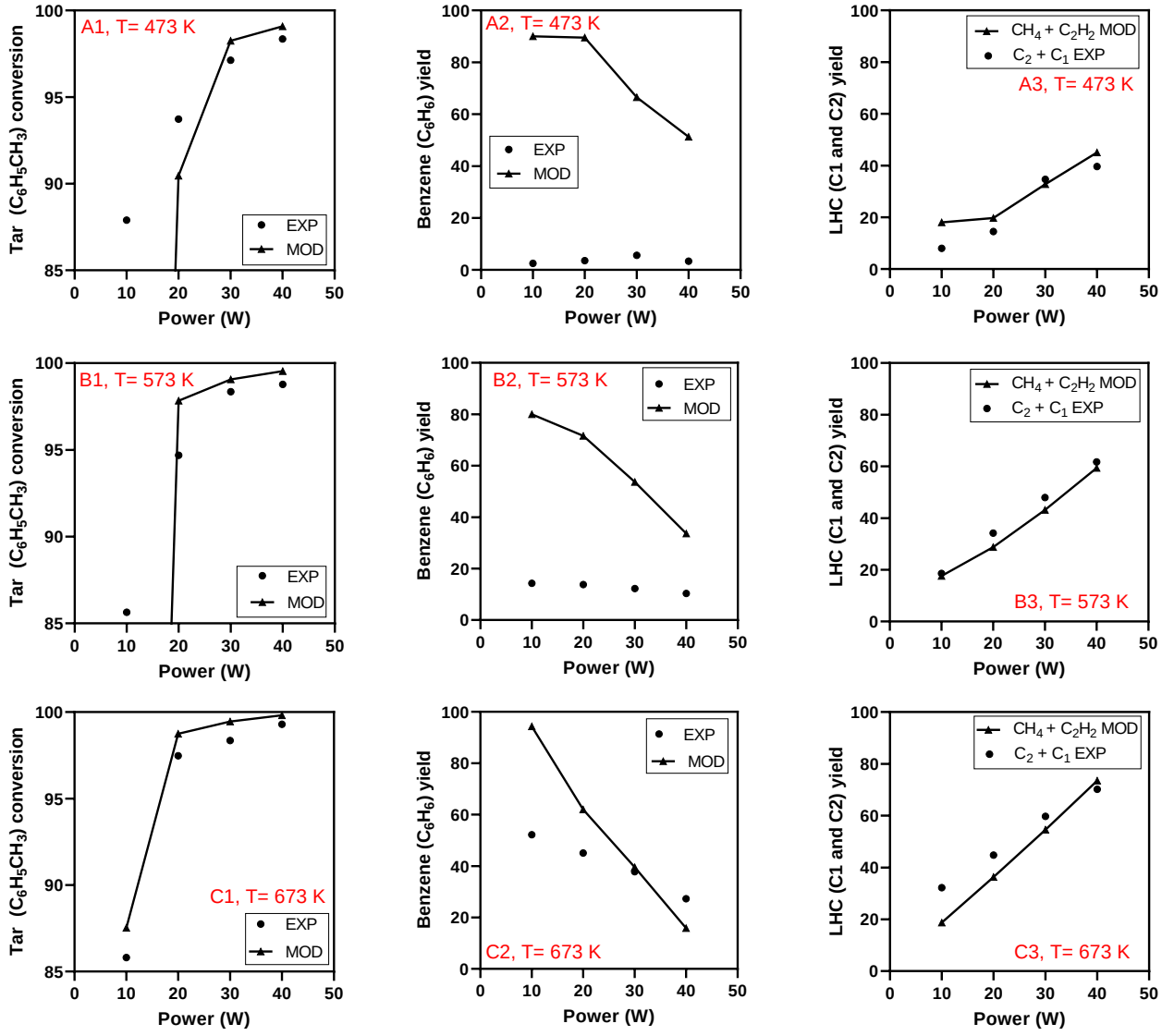

Figure 3-6: Comparison of experimental data (dots, collected from [208]) and model prediction (line) for toluene degradation (left), benzene yield (middle) and LHC yield (right) at varying power and temperature (operating condition: Table 3-2, T1) (RMSE: A1: 1934.19, B1: 1649.94, C1: 1.51, A2:5361.25, B2:2476.99, C2: 547.77, A3: 40.17, B3: 14.82, C3: 72.35)

In the second pathway, the produced benzyl cation still contains the benzene ring, the cation may recombine into larger compounds such as bi-benzyl ($C_{14}H_{14}$) or ethylbenzene ($C_6H_5C_2H_5$, R1746), but both of this pathway only account for a small fraction of the benzyl cation. Instead, the model suggests that the charged methyl attacks the double bond within the aromatic ring due to benzylic resonance [310], which produces cyclopentadiene anion (C_5H_5) and acetylene as a by-product via R1720: $C_6H_5CH_2=C_5H_5+C_2H_2$

Cyclopentadiene is a non-aromatic cyclic polyene with stability from orbital overlap and resonance, yet it lacks the optimal pi-bond overlap found in benzene for enhanced stability [311], making this compound the key intermediate compound. Yue et al. [270] also proposed a similar mechanism, the study theorised that the deprotonated OH group (phenolate) attacks the double bond. Experimentally, Liu et al. [283] speculate the presence of cyclopentane radicals in their tar cracking experiment, while Gao et al. [312] summarise various body of works that suggest cyclopentadiene presence in tar cracking mechanism.

Moreover, some of the alkene and alkyne radicals may recombine into a more stable compound, such as phenyl radical or benzene, (e.g., R725, 755, 2099), which is also proposed by Saleem et al. [200] and Fenglei et al. [313]. Benzene stability and recombination resulted in a high concentration at the output.

Comparing this with other hypothesised mechanisms, Fenglei et al. [313] suggest two similar pathways involving the formation of a benzyl cation and benzene. They also highlight the relevancy of cyclopentane as a ring-opening intermediate with C_3 radical recombination into aromatic rings. Vandenbroucke et al. [314] also suggest two similar pathways for toluene degradation. However, instead of benzene as the intermediate product, they theorised that the phenyl radical is the main product from the electron impact reaction between toluene and excited electrons, which later stabilise into benzene and phenol.

However, our model failed to highlight the direct ring-opening of toluene without the formation of intermediate species, as suggested by Fenglei et al. [313]. Nonetheless, more experimental data is required to confirm this mechanism. The stable conjugate structure (aromatic ring) in toluene prevents a direct ring opening [306]. Therefore, despite Fenglei et al.'s [313] theory on a direct ring opening, more evidence is needed to confirm the ability of plasma to perform a deep/direct aromatic ring oxidation [306].

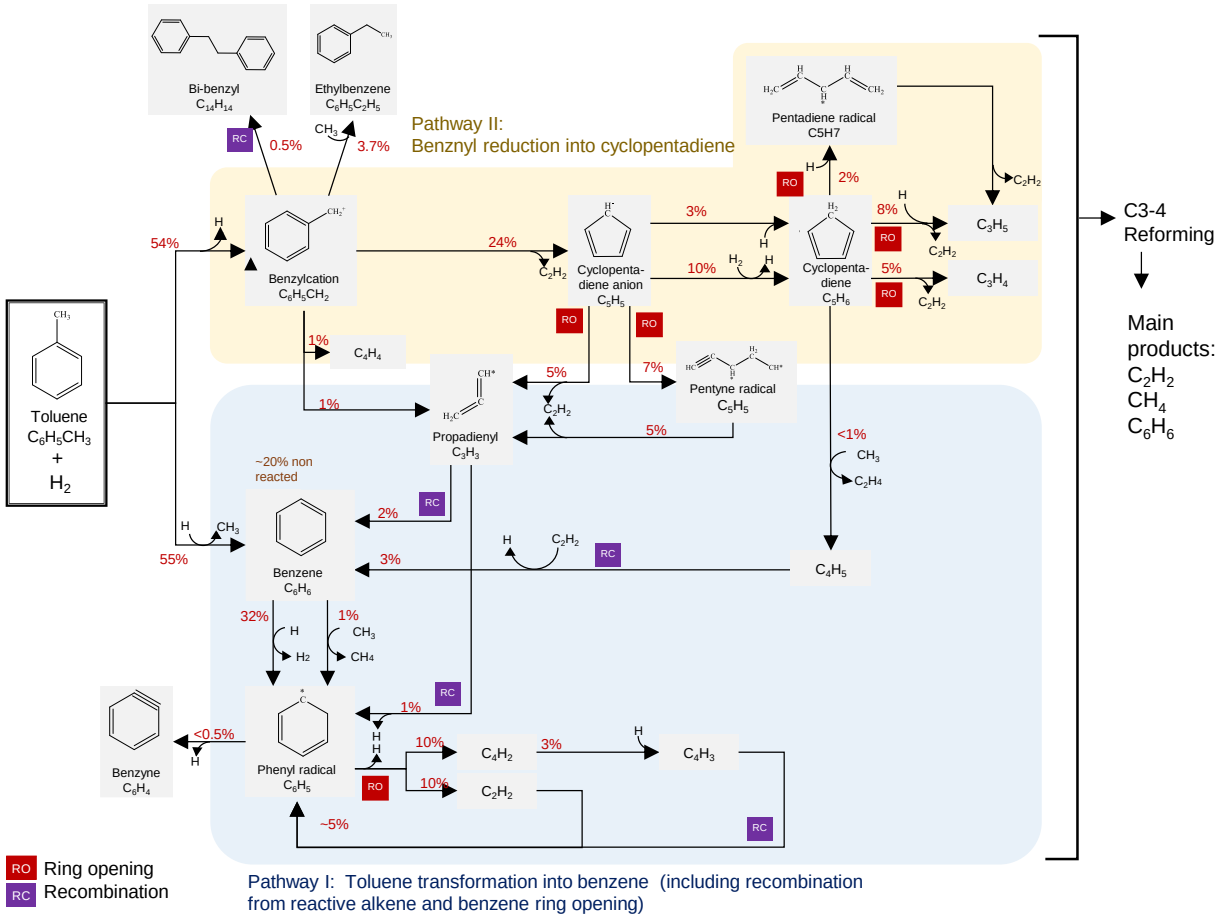

Figure 3-7: Hypothesised reaction mechanism pathway according to the modelling work, at 40 W and 673 K (operating condition: Table 3-2, T1)

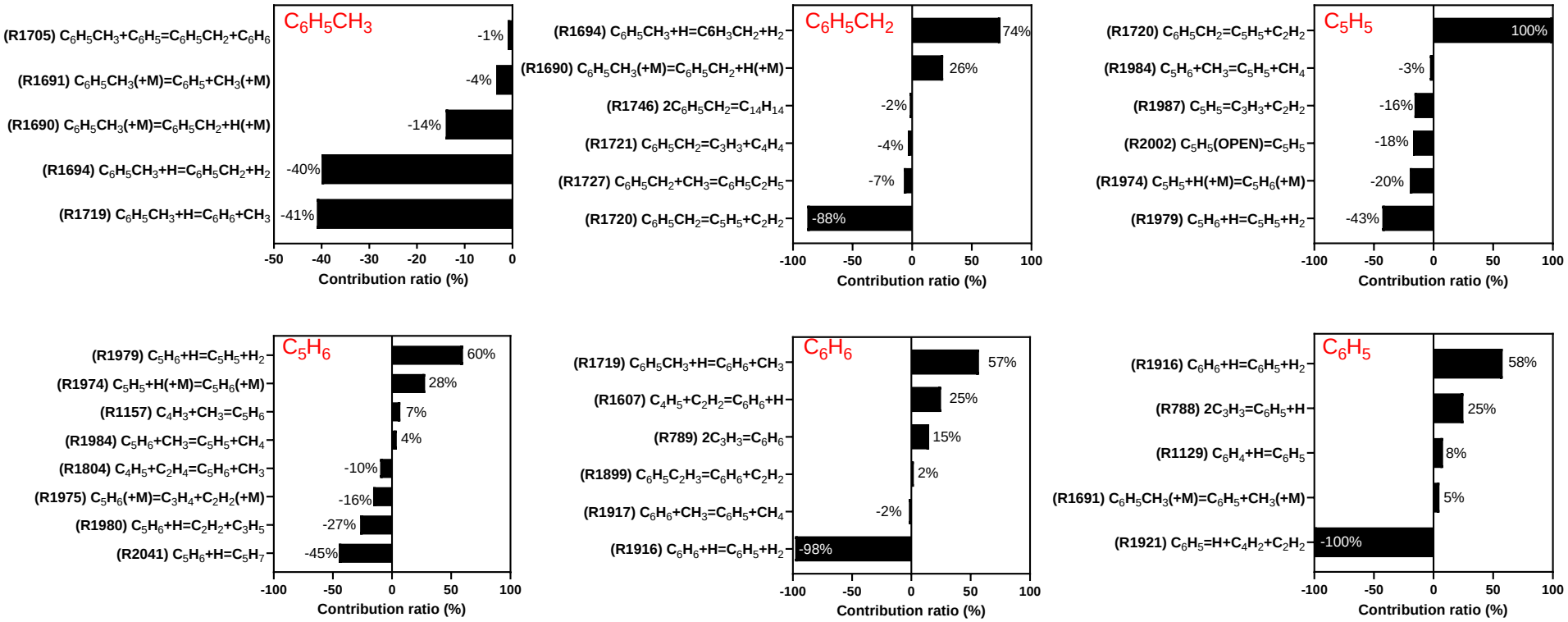

Figure 3-8: Consumption (negative) and production (positive) analysis of relevant tar species: Toluene ($C_6H_5CH_3$), benzyl cation ($C_6H_5CH_2$), cyclopentane (C_5H_6 and C_5H_5), benzene (C_6H_6), and phenyl radical (C_6H_5) in a hydrogen gas plasma environment, for 673 K and 40 W (operating condition: Table 3-2, T1).

3.5.2 Phenol, Toluene, and Naphthalene

This section reports on the model results from simulating three types of tar similar to the work of Xu et al. [204], who reform phenol, toluene, and naphthalene in a GAD reactor with steam (H_2O) and oxygen. While these gases are not present in syngas, this comparison provides a deep analysis of tar cracking in an oxygen-rich environment. The model prediction is validated against experimental data in Figure 3-9 at increasing temperatures.

Reaction kinetics for phenol and toluene are based on the work of Metcalfe et al. [267], whereas naphthalene cracking reaction is based on Curran et al. [269] (R2079 to R2138), which accounts for 3% of the overall tar cracking reactions. For toluene and phenol, the model predicts an increase in conversion rate over temperature, reaching 100% conversion. However, experimental data shows a maximum conversion of 94% and 87% at 873 K, respectively (Figure 3-9, A and B). Although increasing gas temperature should in theory improve hydrocarbon reactivity and yield, this is not reported in several experimental studies [204, 212]. This is because the 0D Plasma-PSR model guarantees the contact between every radical with incoming tar, enabling a full tar conversion, while this condition is not achievable in experimental GAD due to its physical limitation, such as ununiform species distribution and rapid residence time due to hot gas expansion.

Naphthalene is the only tar that is being under-predicted by the model, the smaller reaction kinetic database may influence this outcome (Figure 3-9, C). Naphthalene is considered a stable tar that is difficult to decompose [315]. Both model and experimental data show a maximum of ~73% of naphthalene conversion.

Increasing the temperature is expected to increase the yield of products such as CO, H_2, and C_2H_2, due to improved tar conversion and deep tar cracking by energetic radicals. However, this is not entirely reflected in experimental data, which show a relative plateau trend with a peak around 873 K (Figure 3-9, D-F). The experimental data reveal a decrease in tar conversion and gas yield from 873 K to 973 K. Xu et al. [204] attribute the decrease to gas density and conductivity changes at high temperatures, reducing effective discharge power. However, Saleem et al. [208] and Liu et al. [212] argue that higher temperature gas causes impurities from quartz and carbon deposition, hindering plasma's tar conversion ability. To address these limitations, fluid and reactor modelling can be used to investigate the behaviour of high-temperature gases in a plasma reactor and to account for impurities such as soot or carbon deposition.

Our model has a higher success in predicting tar degradation of Saleem et al. [208] at higher temperatures. This is possibly because Saleem et al.'s DBD reactor has a more uniform species distribution than a GAD [316] creating a scenario more akin to the 0D Plasma PSR model. This also elucidates the model's capabilities to predict experimental results at 600-800 K. At this temperature range, physical limitations are not prevalent, resulting in a high level of accuracy for the model. However, at extremely high temperatures (>900K), the system starts exhibiting complex behaviour that is not reflected in the 0D model. Plasma enters a transitional state between thermal and non-thermal plasma [317]. Furthermore, the physical limitations of high-temperature gas in an NTP reactor have not been fully investigated. This lack of understanding may lead to discrepancies between the model and experimental data, which can be problematic as certain syngas may reach temperatures up to 1,000 K when they exit the gasifier [318]. This challenge is also pointed out by Xu et al. [204] and Liu et al. [16], highlighting the need to investigate the synergetic effect between high temperature and NTP tar cracking.

Despite the model's limitations, the results agree with the experimental data. Nunnally et al. [319] also conducted similar simulation work but failed to provide experimental validation nor electron impact reactions consideration. In contrast, Shiels et al. [320] focused on the ionic reaction behaviour between ion molecules, including aromatic compounds, which is often overlooked in plasma reforming research.

Figure 3-11 and Figure 3-12 shows the key reaction contribution ratio of key reactions. The key reactions were established by the model via various conditions, namely the incoming gas species, operating conditions (plasma power, temperature, etc.), and reaction database. The key reactions are used to establish mechanism pathway of various tar degradation in plasma reactor shown in Figure 3-10.

For reaction mechanism, the incoming naphthalene transforms into naphthalene radical and anion (NAPH* and $NAPH^-$), achieved by deprotonating the H atom in its outer carbons (R2802 and R2804, Figure 3-11). The reactive ringside will undergo a ring-opening reaction to produce ethynlbenzaldehyde (C_9H_6O, R2809 and R2093) and naphtholate ($C_{10}H_7O$, R2088 and R2092). Naphtholate's reactive oxygen would attack the double bond inside the aromatic ring to produce CO while the tar converts into indenide (C_9H_7, Figure 3-11), an unstable compound that may convert into indene (C_9H_8). Both compounds are reactive and will eventually undergo a ring-opening reaction in their cyclopentane ring portion to produce ethynylbenzaldehyde (C9H6O, R2134, Figure 3-11). Ethynylbenzaldehyde would degrade via two main pathways, this happens when the C_2H_2 and CO

functional group leave the aromatic ring, leaving the unstable phenyl radical to undergo a ring-opening reaction into hexene (R2130) or remain cyclic (Benzyne, C_6H_4, R2135, Figure 3-12). Here, the compound transformed into a Class II tar. A small portion of naphthalene would also reform into larger PAHs with more than two rings (R2136). Xu et al. [204] and Mei et al. [321] suggested a similar pathway, where the incoming naphthalene would convert into idenide, indene, and naphthalene radical as its intermediate species upon elastic collision with reactive species. However, this study's model is missing the formation of methylnaphthalene ($C_{11}H_{10}$, Figure 3-12) as an intermediate species. Instead, the model shows the formation of naphtholate due to the rich oxygen environment.

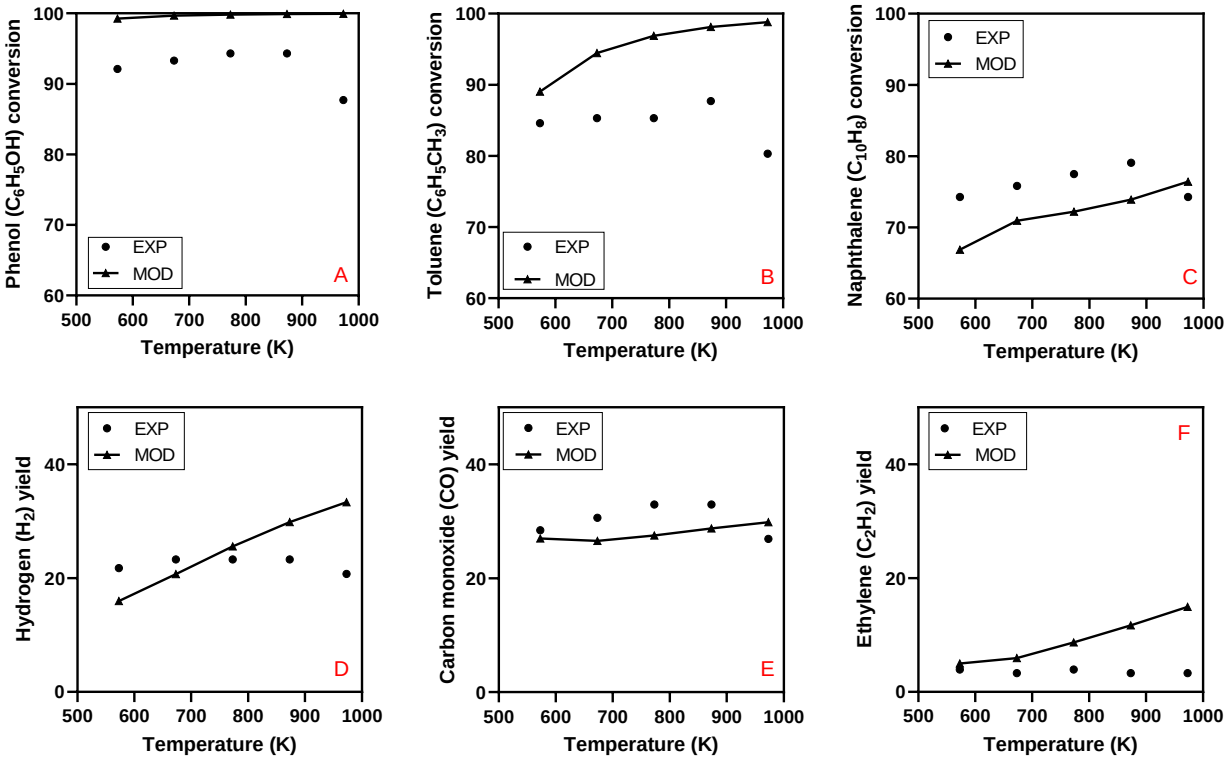

Figure 3-9: Comparison of experimental data (dots, from [204]) and model prediction (line) for tar degradation (A-C) and output gas yield (D-F) and varying temperature (operating condition: Table 3-2, T2 (RMSE=A: 60.84, B: 137.59, C: 27.57, D:49.49, E: 16.96, F: 47.57).

For toluene, ethylbenzene and its various forms of radicals become important pathways for toluene degradation. Ethylbenzene may transform into styrene ($C_6H_5C_2H_3$), where the ethene function would separate from the aromatic ring to produce phenyl radical and benzene (R1899 and R1905). Some of the benzyl cations recombine with reactive propyne (C_3H_3) to produce naphthalene (R2079). The active phenyl radical transforms into phenolate due to the abundance of oxygen, where the radical oxygen attacks the double bond inside the aromatic ring to produce cyclopentane. This is almost

identical to the previous mechanism (Section 3.5.1), but instead of methyl radical attacking the double bond inside the aromatic ring, it was the oxygen atom. Xu et al. [322] also proposed similar mechanisms, they argue that the system produced oxygenated aromatic compounds due to the rich oxygen plasma environment. Meanwhile, Xu et al. [207] hypothesised the transformation of toluene into styrene and phenol in the presence of an oxygen plasma environment.

For phenol, the OH radical function can directly break the double bond to form CO, opening the aromatic ring to produce cyclopentadiene (R1954). Phenol is also an intermediate species in the degradation of toluene via Toluene → Benzene → Phenol → Cyclopentadiene. The second pathway is Toluene → Styrene → Phenyl → Phenolate → Cyclopentadiene. Both toluene and naphthalene will reach class II tar, where the aromatic ring converts into cyclopentane. Naphthalene transformation works via Naphthalene → Naphtholate → Indenide → Ethylbenzaldehyde → Benzyne → Phenyl → Phenolate → Cyclopentadiene. Out of all tars, the reactivity goes by Phenol > Toluene > Naphthalene. Naphthalene is the least reactive due to its double aromatic ring. Naphthalene often being used to represent gravimetric tar and has been linked to soot precursor [323]. Phenol OH function makes it more reactive due to oxygen's lone pair that increases the aromatic electron density, resulting in higher reactivity than toluene or even benzene [324]. This makes phenol one of the intermediate species in the toluene and naphthalene cracking pathway, which agrees with Mei et al. [321] proposed reaction mechanism.

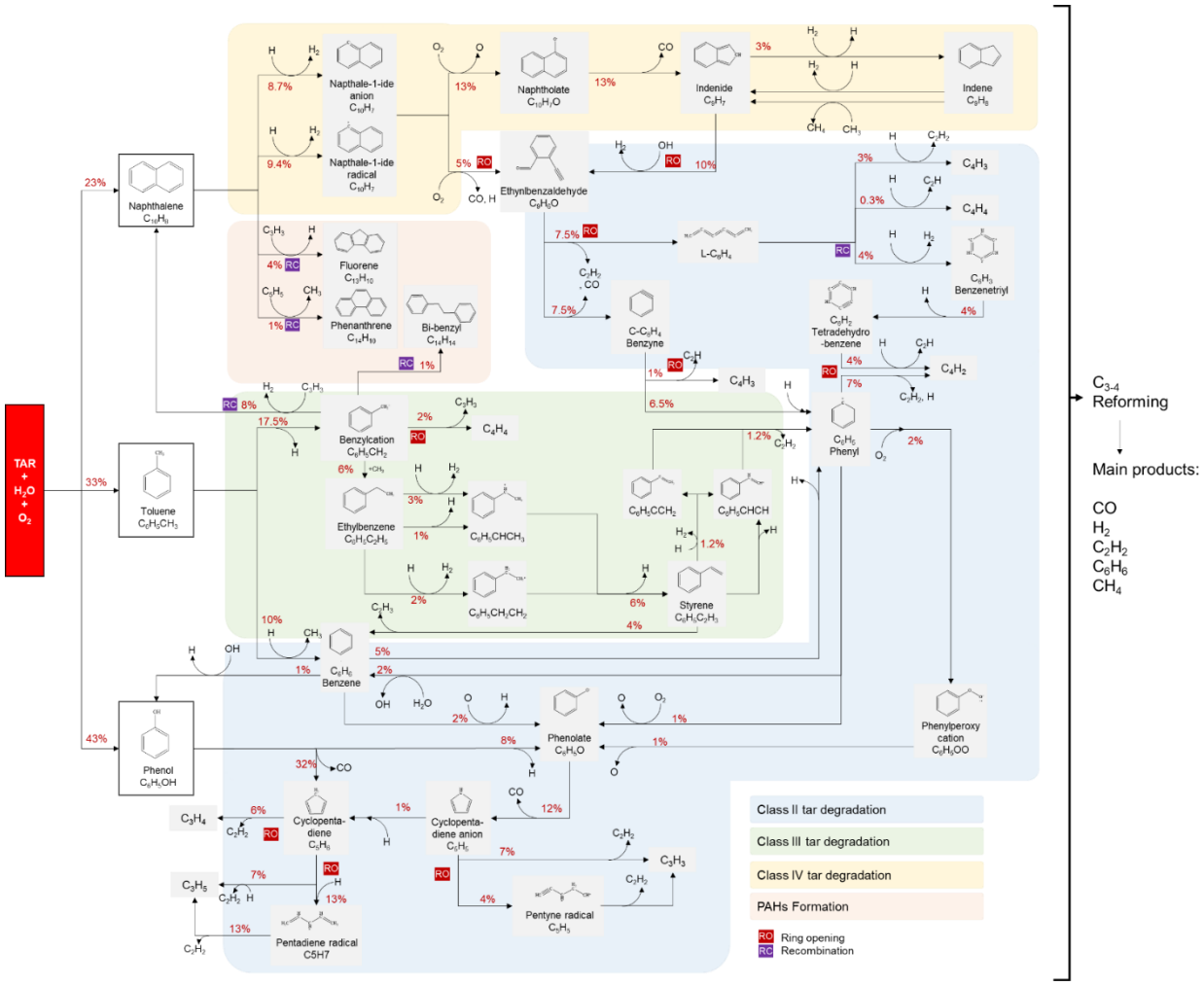

Figure 3-10: Hypothesised reaction mechanism pathway according to the modelling work at 673 K (operating condition: Table 3-2, T2).

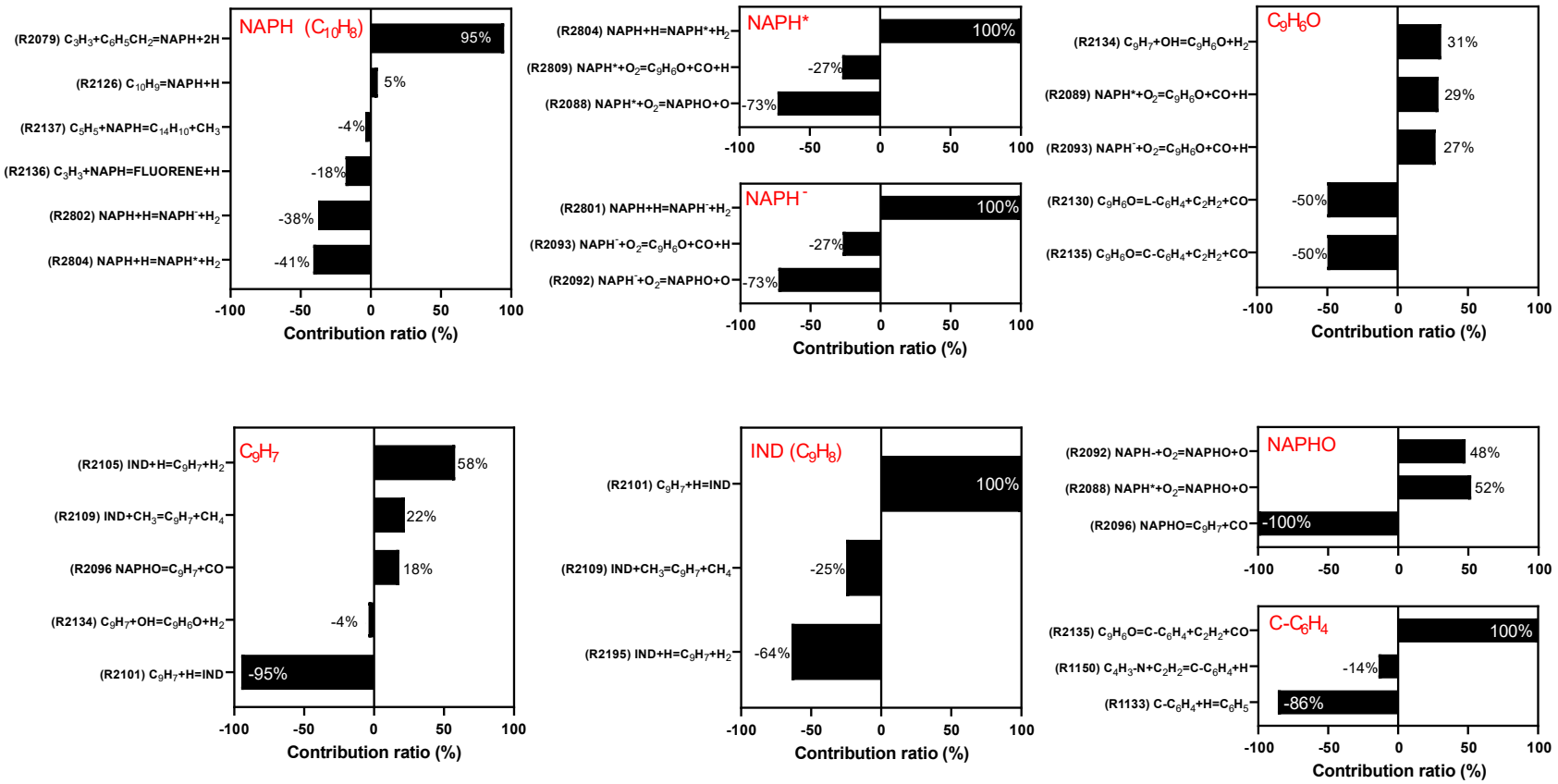

Figure 3-11: Consumption (negative) and production (positive) analysis of relevant tar species: Naphthalene ($C_{10}H_8$), Naphthalene radical, Naphthalene anion ($C_{10}H_8^-$), Ethynlbenzaldehyde (C_9H_6O), Indenide (C_9H_7), Indene (C_9H_8), Naphtholate ($C_{10}H_8O$), and benzyne (C_6H_4) in a oxygen and steam plasma for 673 K (operating condition: Table 3-2, T2).

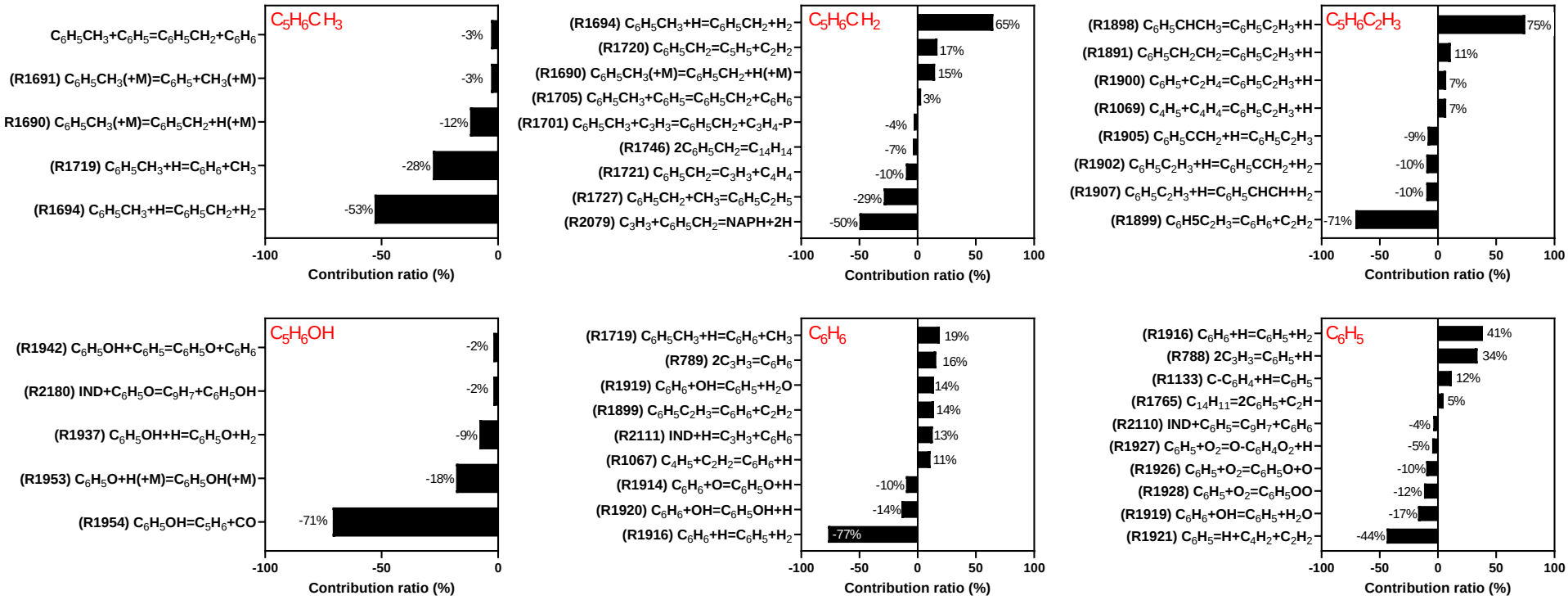

Figure 3-12: Consumption (negative) and production (positive) analysis of relevant tar species: Toluene ($C_6H_5CH_3$), benzylcation ($C_6H_5CH_2$), styrene ($C_6H_5C_2H_3$), phenol (C_6H_5OH), benzene (C_6H_6) and phenyl radical (C_6H_5) in an oxygen and steam plasma for 673 K (operating conditions: Table 3-2, T2).

3.6 Part III: Tar cracking in syngas environment

Although oxidative NTP tar cracking is preferred and has been investigated in various studies [204] [325], gasification restricts the oxygen content [41] producing an oxygen-poor syngas [326]. It is imperative to investigate the role of syngas gas species and tar cracking. Figure 3-13 shows the modelling result of the tar cracking in syngas at varying parameters. The tar and syngas composition was based on Veksha et al. [272], mimicking the real syngas and tar profile from waste gasification.

Increasing plasma power from 10 to 30 W would instantaneously improve toluene, styrene, and phenol conversion to almost 100%, but not naphthalene (Figure 3-13, A1). Naphthalene eventually reaches 100% conversion at 100 W, which is a relatively high operating condition. For the syngas conversion (Figure 3-13, B1), the model does not employ CO as an oxygen donor, possibly due to its strong chemical bond. In an NTP system, excited CO rarely produces O radicals. Capitelli et al. [327] suggest CO plasma dissociation often involves the collisions of two CO molecules to produce CO_2 and C. Because of this, the model predicts negative conversion (i.e., production) of CO, directly produced from CO_2 conversion and tar cracking.

The model predicts H_2 conversion and CH_4 production at low power, which reverses into H_2 production and CH_4 conversion above 30 W. It is speculated that at low power, the lack of tar conversion means that the yield and conversion for CH_4 and H_2 directly come from each two-gases equilibrium, where hydrogen dissociation is common due to its higher reactivity than methane, resulting in positive H_2 conversion and negative CH_4 conversion (Figure 3-13, B1). However, once the system sufficiently converts the incoming tar (~ 30 W). The tar starts releasing hydrogen atoms trapped as hydrocarbon, i.e., negative H_2 conversion. This is also characterised by a sudden dip in benzene concentration (Figure 3-13, D1). Methane conversion becomes more prominent as the system becomes more abundant with hydrogen gas (R32).

On the tar portion (Figure 3-13, A1), despite having almost 100% conversion of phenol, styrene, and toluene at low power (30 W), most of these tars were converted into benzene. As the power increases, benzene production is not favoured, and the produced benzene converts into smaller hydrocarbons due to the higher energy in the plasma reactor. Moreover, at low power, most naphthalene mostly converts into fluorene ($C_{13}H_{10}$, R2136). The reaction database does not account for fluorene conversion, which means that the fluorene decreases at increasing power resulting from naphthalene conversion favouring other pathways. The system favours fluorene production (R2136) at a low power possibly due to the C_3H_3 abundance that assists recombination reactions. This is also evidently shown as the benzene

concentration decreases at the same power range (40-60 W, Figure 3-13, D1). This finding highlights the importance of secondary and larger tar formations. Often, tar cracking studies focus on conversion and neglect the possibility of conversion into larger molecules or different classes of tar. Sun et al. [328] also model the formation of aromatic rings into larger PAHs. Capturing the trend of formation of larger PAHs in a shock tube reactor.

Whilst tar concentration eventually reaches a negligible concentration at a higher power, another challenge arises as most of the tar transformed into C_2H_2 instead of CO and H_2, making C_2H_2 a major product gas species (Figure 3-13, C1). Jamroz et al. [329] also found acetylene to be the major product of tar decomposition in a microwave plasma reactor. The presence of acetylene may pose an issue if the downstream processing requires high CO and H_2 purity. Acetylene abundance in the output is likely due to the deficiency in oxygen radicals that transform tar into phenol and phenolate which later convert it into CO and CH_4. Introducing oxygen or a catalyst into the plasma reactor may further assist in acetylene reforming into CO and H_2 [330].

Increasing residence time improves reaction conversion by increasing the probability of tar colliding with energetic species. Increasing residence time is a cost-effective method to ensure higher conversion and more gaseous tar being converted into smaller compounds [208]. In our model, increasing the residence time leads to an almost identical result as increasing plasma reactor power from 10 W to 50 W (Figure 3-13, A2-D2). Increasing residence time shows a positive improvement in tar degradation yet increasing it from 0.6 to 2 sec is found to be insufficient to fully degrade the incoming naphthalene. However, the model is a 0D kinetic model which means it neglects the interaction of incoming gas with the reactor surface and the fluid behaviour inside the reactor. The 0D model is limited to analysing the change of reactant and various species inside the reactor.

Increasing pressure reduces tar reactivity and conversion (Figure 3-13, A3) to a near zero (at >3 atm). The lack of tar conversion resulted in a consistent gas concentration at increasing pressure (Figure 3-13, C3). For the reacted class II and III tar at 1.0-2.0 atm (Figure 3-13, C3), the high pressure favours the conversion of the incoming hydrocarbon into methane instead of acetylene. This suggests that although increasing pressure decreases tar conversion, it increases methane selectivity. Increasing pressure may be used to produce syngas with purer content and eliminate C_2 impurities. For the syngas, Increasing reactor pressure would only increase the hydrogen conversion, which peaks at 1.75 atm (Figure 3-13, B3) since H_2 gas compression increases the reforming performance [331].

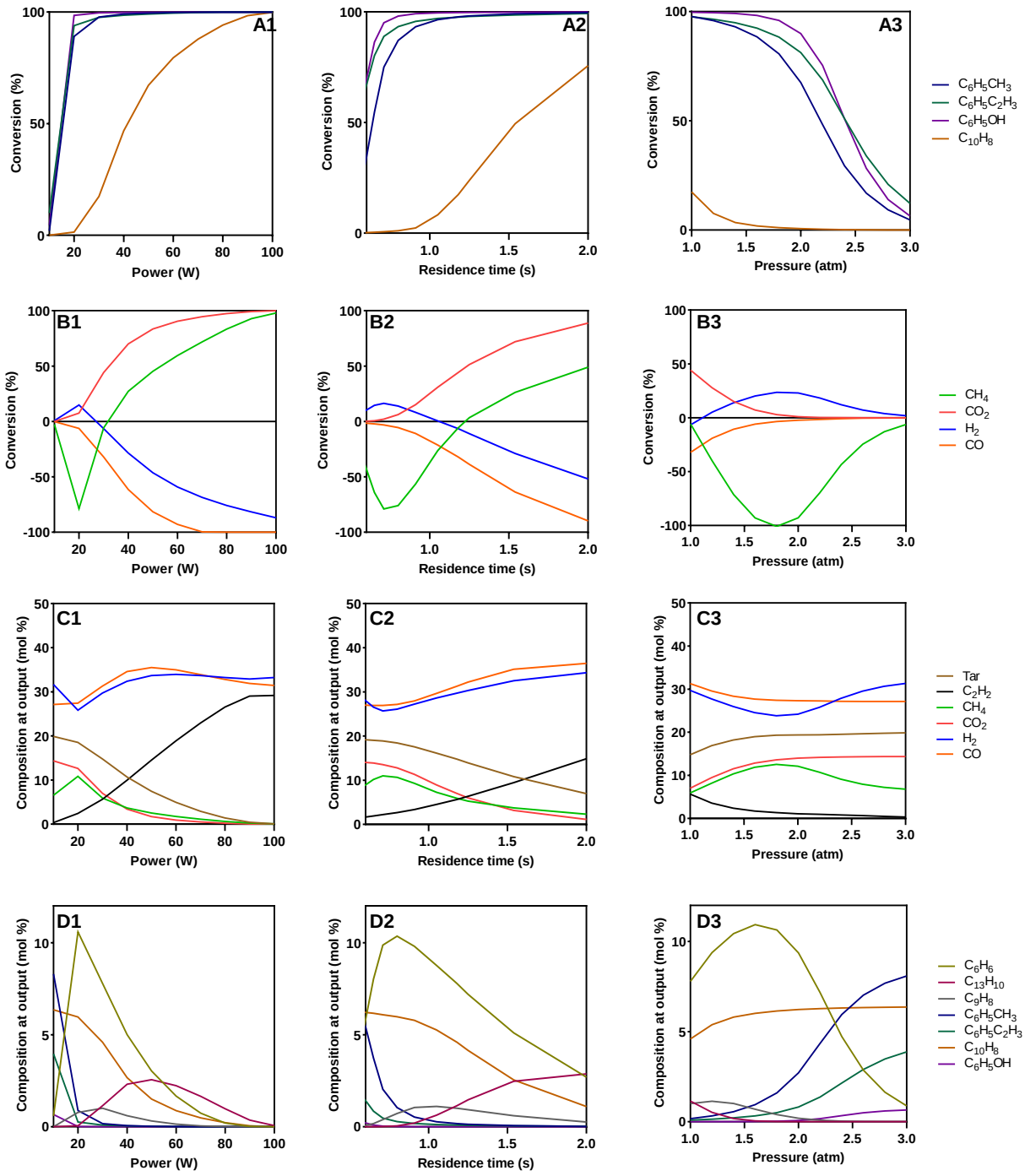

Figure 3-13: The conversion rate of incoming tar (A) and syngas (B) along with the output gas fraction at the output (C) and the detailed tar distribution (D), for varying power (1), reactor residence time (2), and reactor's pressure (3) (operating condition: Table 3-2, S1).

Above 2.5 atm, the lack of tar conversion is a result due to the model exclusion of reaction kinetic at this operating condition. Increasing pressure of aromatic compound endorsed the crystallisation process [332, 333], which is not included in this study reaction kinetic database. The exclusion of this

reaction kinetic is due to the utilised mode that primarily focus gas phase reforming kinetic. Experimentally, investigate study of high-pressure tar oxidation require a higher oxygen ratio, signifying the need of more oxidants is require for the lower PAH reactivity in a pressurised system [334, 335]. Furthermore, some studies highlight the benefits of pressure in retaining complex PAHs due to their low vapour pressure, i.e. their minimal tendency to stay as a vapour [336, 337]. Hence, increasing pressure in the system may contribute to tar condensation, resulting in tar bonding and increasing their particle size, which further reduce tar reactivity and plasma ability for tar cracking.

3.7 Part IV: Model verification

This part scrutinises the modelling approach and its assumptions. The model's power law kinetics are dictated by the system's temperature. Figure 3-14 compares tar cracking at increasing power, temperature, and temperature with low power (10 W). In comparison to NTP, the assistance of electron impact reactions and additional heating through power provide an abundance of radical generation for tar cracking. This is evidently demonstrated as the process benefits even from a low power addition (10 W), showing a reduction in temperature by ~500 K or 20 W in gas heating.

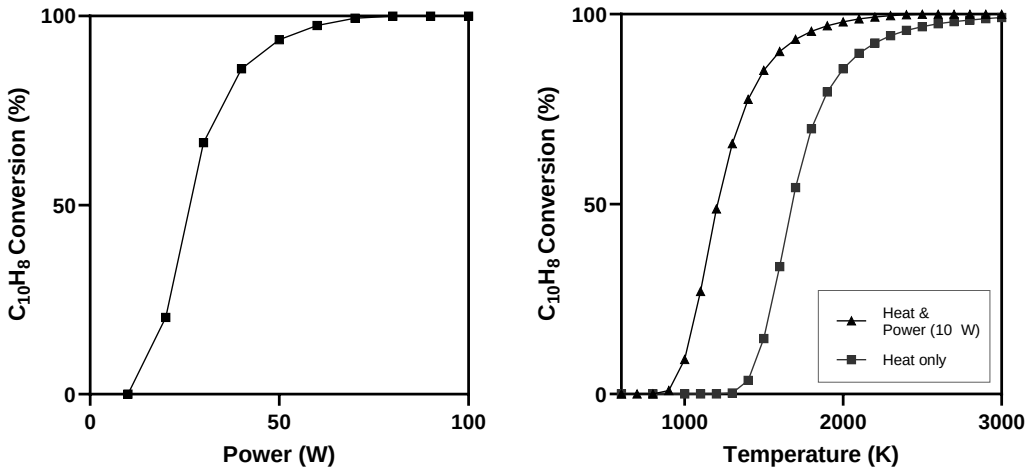

Figure 3-14: Tar (Naphthalene) cracking at increasing plasma power (left) and increasing temperature (right) (Table 3-2, S2)

Furthermore, NTP's main difference with thermal plasma is its difference in electron temperature. In this work, the electron temperature adopted is 10^4 K (around 1 eV), whereas other studies have employed electron temperature as high as 10^5 K (10 eV) [270]. Figure 3-15 shows the tar conversion over increasing electron temperature in the model. Increasing the electron temperature from 10^4 to 10^8 only improves tar degradation by 0.02%, while significant improvement is shown at a temperature

above 10^9 K. For comparison, thermal plasma is categorised when the electron temperature is equal to plasma temperature, at 10^6 to 10^8 K. Afterwards, it is considered a high-temperature plasma that is found in laser fusion [317]. From the reaction kinetics perspective, electron impact function as initiation reaction, producing radicals for hydrocarbon conversion [270, 338]. The role of electrons is restricted to generating radicals during the discharge stage, to produce radicals for tar cracking in the steady-state stage (afterglow) [266]. Increasing the electron temperature primarily supports the reforming of smaller gases during startup, which is assumed to be instantaneous by the 0D kinetic model in this study.

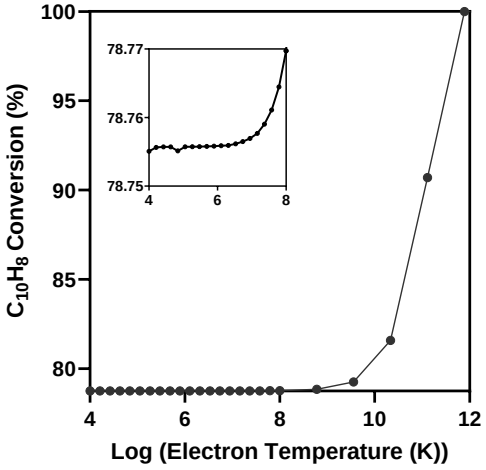

Figure 3-15: Tar (Naphthalene) degradation at increasing electron temperatures from 10^4 to 10^{12} K (Table 3-2, S2).

The data suggest that increasing the electron temperature within the NTP range has a minimal impact on tar cracking. This may be caused by radical collision dependency on reactor temperature instead of electron temperature. Additionally, the system may have achieved maximum radical generation from power heating, resulting in increasing electron temperature having negligible impact on radical generation and tar conversion. Moreover, the tar electron impact reaction has a minimal contribution compared to radical collision, which has also been previously demonstrated [270]. This suggests that increasing the electron temperature into the energy threshold above the hydrocarbon electron collisions would yield insignificant results since tar cracking reactions are dominated by radical collisions. Increasing power would result in a higher tar conversion that may have been influenced by other reactions independent to electron impact reactions, such as three body reactions or unimolecular decomposition. In these reactions, increasing power would increase the radical reactivity which supports a deeper tar cracking separate to electron temperature. Three body reactions can be used to represent electron collisions reactions that were demonstrated by [339-341]. Other plasma modelling

reactions also adopt three body reactions for plasma reforming which may originated from the oxidations database [226, 227]

Cha and Snoeckx [342] argued that thermochemistry governed by gas temperature has a more dominant effect on hydrocarbon reforming, which agrees with Hsu [338] and this work. This may be the explanation for some model omissions of electron impact reactions for hydrocarbon plasma reforming (e.g., [231, 240]). Furthermore, Yue et al. [270] and Wang et al. [226] adopted electron temperature between 1-1.22 eV (similar to this work), where they found negligible electron reactions impact despite deducing electron temperature from experimental data, implying is minimal contribution for tar cracking.

Therefore, increasing the model electron temperature within NTP exerts negligible impact on the tar cracking. This finding corroborates the adoption of lower electron temperature (1 eV) for well-mixed 0D reaction kinetic modelling of NTP tar cracking in this work which agrees with literatures.

Moreover, utilising power law kinetics in understanding plasma chemistry is a common strategy, along with the well-mixed 0D assumptions. Both methods are consensus assumptions demonstrated by other studies [226, 270, 298]. However, there has been discussion of their drawbacks, in terms of oversimplification and omission of complex plasma dynamics. For plasma modelling, despite the diverse modelling strategies reported, there is minimal evidence of the use of other methodology apart from reaction kinetics for the investigation of plasma chemistry. Although a more comprehensive set of reactive species can be adopted, this approach is rarely applied for tar-cracking chemistry. Further investigations are required to study the impact of diverse species on hydrocarbons. In addition, some studies have included transport phenomena and plasma dynamics simulation [224, 231], while this work assumed a 0-D well-mixed reactor. However, to focus on plasma dynamics, those studies often have to trade-off their accuracy by simplifying the reaction kinetic resulting in an oversimplification of the reaction kinetics database. In contrast, this work focus in modelling a comprehensive reaction kinetic, that can be applied in the future for a more complex reactor geometries, drawing the kinetic insight from this work's findings. Thus, the next step of this study is to utilise the key reaction pathway established in this study for fluid dynamic modelling in a plasma reactor, as this study well-mixed assumptions is only applied to small control volume. The well-mixed assumption necessitates parameter correction, enabling the modelling result to agree with non-perfect real-world experimental data, translating it from perfectly stirred reactor for practical application. This agreement demonstrates model accuracy despite its limitations from its assumptions, residence time was chosen as a parameter due to its suitability in reducing reaction rate to impose the imperfect conditions.

Table 3-3 reviews the parameter ranges where kinetic reaction rates are established, along with the experimental conditions against which the model is being validated. The main difference is the reactor design, where most oxidation reactions were established in a shock tube reactor experimental data use DBD and GAD. In addition, some parameters ranges may deviate in terms of temperature and tar concentration. However, the deviation is not within significant differences. A shock tube reactor is an imperative tool in characterising gas phase reaction kinetics, as it provides uniform distribution and homogenous reactions at varying parameters [343]. Applying these kinetics into other modelling work through validation is a commonly accepted method for simulation work. As the goal of this study is to understand the reaction mechanism, utilising reaction kinetics for investigating plasma chemistry further expands the consensus in the field and contributes to understanding plasma reaction chemistry. Future work may focus on reviewing hydrocarbon plasma reaction kinetics that maps the operating conditions and reactor configuration, establishing consensus amongst various modelling approach. (e.g. [268]). Furthermore, although the use of tar as compounds limits the model prediction for gravimetric tar and soot production, the diverse tar compound selected in this study provides an in-depth tar cracking reaction mechanism investigation that is unattainable with a lumped tar model.

Table 3-3:Comparison of parameter ranges between the reaction kinetic original development and the validation experimental data.

Type	Kinetic and validation experimental rage	Ref
Alkane electron collisions	The reaction kinetics were developed via EEDF estimation to estimate electron impact reactions based on heptane reforming in a GAD reactor with power ranging from 28 to 38 W and residence time of 20.4 to 66.7 s. The temperature was set to 423 K at atmospheric pressure.	[226]
Heptane oxidation	The reaction kinetics were established from shock tube flow reactors with a rapid compression machine. Pressure ranges from 1 – 42 atm with temperature of 550-1,700 K. The kinetics were affirmed with variance of ignition delay and species characterisation.	[344]
Hydrocarbon conversion	AramcoMech 1.3 was developed for various hydrocarbons and their derivatives, where the kinetics are validated against a shock tube, jet stirred, flow reactor and flame speed. The parameters range from 600-2,500 K and pressure of 1 to 10 atm. The kinetics were collected from [3]	[345]
Toluene oxidation	The reaction kinetics were developed in a flow reactor at temperatures ranging from 450 to 950 K for toluene up to 14% mol concentration, and residence time ranging from 0.3-2.5 s.	[267]
Naphthalene oxidation	Reaction kinetics were measured in a shock tube reactor over temperature ranging from 980-1,360 K, for pressure of 1-30 atm.	[269]
Toluene electron collision	The reaction kinetics were developed by investigating toluene conversion in a DBD reactor with volume of 23 cm^3, temperature ranging from 300-600 K, and toluene concentration ranging from 376-1,500 mg/m^3.	[266]

Toluene comparison	The experimental data were collected from a DBD reactor of toluene degradation at temperature of 300-673 K with power from 5-40 W for concentration from 2-82 g/m^3.	[208]
Tar mix comparison	The experimental data were collected from a GAD reactor of toluene, naphthalene and phenol blend degradation at temperature of 300-100 K, with power from 20-40 W for concentration from 2-26 mg/m^3.	[204]

3.8 Conclusion

This chapter demonstrates the use of a PGM framework to predict hydrocarbon tar degradation, validating it with external experimental data at varying power, residence time, and temperature. It is found that electron impact reactions mainly contribute to the reforming of lower hydrocarbons, while larger hydrocarbon reforming relies on radicals generated from electron collisions with incoming gases. The tar validation step elucidates the model's high accuracy for predicting tar conversion at a temperature range of 600-800 K. The model also has a higher success predicting results from the DBD reactor than the GAD reactor. It is theorised that the model exclusion of PAH formation contributes to this disparity at temperatures below 600 K. Meanwhile, thermal physical limitations such as runaway materials, gas expansion, and the plasma transitional state resulted in model disparity at temperatures above 800 K.

In a tar mixture, the reactivity increases from naphthalene to toluene to phenol, as the OH group in phenol makes it more reactive than toluene or benzene. Naphthalene and toluene reforming will eventually convert into class II (one aromatic ring tar), where the reactive function would attack the double bond inside the ring to produce cyclopentane. However, benzene formation is unfavourable due to its stability. Class II and III tar convert at low power (~30 W), but it is important to investigate the fate of these compounds. Often, conversion resulted in unfavourable benzene formation. This can be solved by increasing the plasma power or residence time, creating an environment that favours other pathways to support deep tar cracking. Conversion in a syngas environment results in a high acetylene yield due to the oxygen-poor environment. Oxygen can be introduced to generate the desirable CO and H_2 or pressurise the system to produce methane. This validated model reveals the current PGM capabilities, the high accuracy and comprehensive reaction database may be further used for process optimisation and fluid dynamic reactor simulation. The comprehensive reaction mechanism can be useful for investigating the tar conversion pathway, which can be applied for improving the gas of interest selectivity.

Chapter 4

Process Simulation of Non-Thermal Plasma Tar Cracking for Waste Gasification

The bulk of this chapter is currently under preparation for submission as the following manuscript: E. Sanjaya, G. Fimbres Weihs, and A. Abbas Process Simulation of Waste Gasification with Non-Thermal Plasma Tar Cracking Unit for Material and Energy Recovery.

4.1 Introduction

Gasification is a widely recognised technique that has gained prominence for its ability to convert various feedstocks, including waste materials, into syngas [41]. The production of syngas holds immense appeal due to its versatile applications. Energy recovery pathways can be achieved through boilers, gas turbines, or fuel cells [346]. Moreover, cleaned high-quality syngas can be synthesised into fuels and chemicals. For waste transformation, this essentially enables the pathway for chemical recycling [347].

Although gasification offers promising solutions encompassing fuel, chemicals, and power production, its practical implementation is marred by a range of technical challenges, especially in achieving a consistent production of high-quality syngas that meets the criteria. For instance, conventional air gasification produces syngas diluted with N_2, consequently reducing its heating value and potential energy recovery [348, 349]. To circumvent this, processes must adopt an O_2-based gasifying agent to generate syngas free from N_2 dilution. However, both air and oxygen gasification have proven to be insufficient to achieve a desirable H_2/CO ratio. For advanced value-adding processes, Fischer-Tropsch (FT) synthesis requires this ratio to be 1.6-2.05 depending on the catalyst [350], while methanol production requires 2.00 or more [351] [352], and syngas is considered suitable for hydrogen recovery when the H_2/CO ratio is above 3.00 [349]. To achieve this ratio, steam injection is crucial to generate more hydrogen content in syngas [353], which further complicates the overall process. Moreover, advanced syngas conversion demands a minimal CO_2 concentration in the syngas. Lastly, tar byproduct presents a significant impediment to the gasification process and has persisted as a

formidable obstacle since its initial industrial implementation [11]. High tar concentrations within syngas severely limit its potential applications, confining it primarily for boiler combustion.

Process simulation is a pivotal and cost-effective methodology to establish essential evidence in terms of predicting syngas yield under favourable conditions. This pragmatic tool is invaluable prior to commencing resource-intensive gasification experiments [64]. Process simulation stands as a cornerstone in facilitating gasification implementation, aiding in the prediction and optimisation of intricate processes. This approach has gained significant traction and has been a focal point of various studies, with process simulation evolving from simple models into complex gas phase kinetic reactions [65].

The methodologies employed in gasification process modelling vary depending on the study's objective. Each approach shows distinct technical advantages and drawbacks [65]. Whilst effective, it is important to establish boundary conditions for each study to maintain its accuracy. Modelling studies often fail to include a comprehensive selection of gas species and an internal understanding of reaction gasification reactions. This limitation is understandable given the intricate nature of gasification reactions. A review by Safarian et al. [65] summarises that gasification modelling often fails to address accurate tar models, comprehensive gas species, and/or cross-study validation.

Furthermore, recent research has demonstrated the potential of Non-Thermal Plasma (NTP) for effectively converting tar into syngas while retaining crucial syngas constituents. Although predominantly showcased on surrogate tar in laboratory-scale settings, this avenue of investigation has been gathering momentum, with more studies investigating its efficacy through reactor design and reaction kinetics [270]. Additionally, NTP exhibits the capability to convert unwanted CO_2 into CO via reforming reactions [354]. Despite its early research success, there is still a lack of studies that investigate NTP-gasification implementation. Plasma research for gasification is still dominated by thermal plasma, due to its research maturity [41]. This combined with the difficulty of predicting tar compounds and their behaviour in process simulation, has resulted in researchers often overlooking this avenue of research.

4.2 Research Background

4.2.1 Research Gaps and Niche

NTP Tar cracking has been demonstrated in bench scale, deemed as the attractive next step in a cost-effective tar removal. However, the feasibility of applying NTP techniques to remove tar in the context of MSW gasification remains unexplored. Furthermore, as the fundamental objective of NTP tar cracking is to produce high-quality syngas, it is logical to adopt a process that maximises the quality of syngas. Such pathway has not been authenticated as well. Hence, there is a gap between lab-scale results and potential implementation into advance waste gasification process.

Safarian et al. [65] concluded that the vast majority of modelling studies either neglect tar, assuming tar as inert, or simplify tar as one model compound (usually benzene or naphthalene). They argue that this oversimplification is due to tar complexity, resulting in a crucial errors between modelling and real-life scenarios (e.g [75]). The work presented in this chapter aims to further shrink this research gap by including three tar classes and their gas phase kinetic reaction.

Table 4-1: Chapter 4 novelty in comparison to other published studies.

Study	Compounds	Approach	Tar elimination	Syngas utilisation
[355]	CO, CO_2, CH_4, H_2, acidic gases	Yield correlation and enthalpy changes	Thermal plasma (Without tar consideration)	Turbine
[356]	CO, CO_2, CH_4, H_2, Tar (Ben)	Yield correlation and enthalpy changes	Catalyst (Fe_2O_3 and dolomite)	Methanol synthesis
[86]	CO, CO_2, CH_4, H_2, H_2O, N_2	Yield correlation and enthalpy changes	-	Energy recovery (combustion only)
[357]	N/A (Only consider the energy flow)	Energy balance	NTP (Without tar consideration)	Energy recovery
This work	CO, CO_2, CH_4, H_2, H_2O, N_2, C_2, C_3, C_4, C_5, Tar (Ben, Tol, Phen, Naph).	Yield correlation, Gas phase kinetic, Multilinear regression	NTP (reduced correlation)	Energy and material (methanol) recovery

Ben: Benzene, Tol: Toluene, Phen: Phenol, Naph: Naphthalene

Regarding NTP, Kwon and Im [357] demonstrated the energy analysis of a waste NTP gasification scenario. However, their inclusion of NTP reforming is not substantiated in terms of tar cracking ability nor advanced syngas reforming, rather, the study focused on the heat and energy balance across different EFW plants by assuming a constant power consumption to the NTP-gasification unit. In contrast, this chapter demonstrates the NTP efficacy in terms of tar cracking, syngas reforming, and

syngas profile, which is estimated via reduced correlations from Chapter 3. Furthermore, there are also minimal studies that evaluate tar cracking as a reduced correlation, with one study demonstrated by Wang et al. [358]. Providing a simplified yet accurate model for NTP tar cracking is crucial for this research field development.

Hence, this study's novelty lies in (1) comprehensive syngas and tar species modelling, (2) NTP tar cracking process simulation through reduced correlations, and (3) potential application of advanced syngas utilisation. Table 4-1 shows the comparison of other modelling studies and this chapter's novelty.

4.2.2 Chapter's Aim

This chapter aims to bridge the MSW gasification with NTP tar cracking, along with their potential application. To achieve this, process modelling methodology is adopted. The built gasification model is later equipped with an NTP tar cracking unit to eliminate the tar content in the produced syngas. The NTP tar cracking is modelled from the previously validated work (Chapter 3) via reduced correlation. The model is finally investigated for syngas recovery processes. This work aligns with the thesis's aim to investigate NTP efficacy for waste gasification through flowsheet (process) simulation in terms of tar cracking.

4.3 Methodology

To achieve the aims of this chapter, these research questions were developed:

1. How does the developed gasification model behave in comparison to experimental data and other modelling work? (Part I)
2. What is the optimisation model required to advance the process and bridge the research gaps? (Part II)
3. How to best incorporate the tar cracking reaction kinetics into the process modelling? what are the compromises and drawbacks of the given approach? (Part III)
4. How viable it is to use NTP tar cracking for cleaning syngas? (Part IV)

This chapter work is divided into four parts, investigating both the gasification and NTP tar cracking units. Figure 4-1 shows the methodology flowsheet for this Chapter.

Part I evaluates the waste gasification process modelling. The gasification process is formulated in Aspen Plus software, mimicking the four stages of gasification reactions, and later complemented with an NTP tar cracking unit. Figure 4-2 shows the formulated flowsheet along with the logic flowsheet to

develop the model through validation. This layout is a common flowsheet to simulate the gasification process in aspen, as demonstrated by [64, 77, 86, 359]. During the development of this model, these assumptions were adopted:

1. Ash is inert.
2. The process is in steady state with no pressure losses in the system. The reactor's internal mechanisms (e.g., pressure uniformity, fluidisation velocity, and temperature profile) are not considered as parameters in the model.
3. NH_3, H_2S, HCl, and heavy metals are not considered.
4. Gasification reactions are considered as: pyrolysis, decomposition, oxidation, and reduction [64, 65].
5. Tar compounds are C_6H_6, $C_6H_5CH_3$, C_6H_5OH, $C_{10}H_8$.
6. All gaseous components have ideal gas behaviour, syngas composed of: CO, H_2, CO_2, CH_4, C_2H_2, C_2H_6, C_3H_8, C_3H_3, C_4H_2, and C_5H_5.
7. The waste flow rate is 10 kg per hour, representing a pilot scale unit.

The waste feedstock and char were defined as their molecular structure using proximate and elemental analysis, described through PROXANAL and ULTANAL. These data are later used to estimate the feedstock enthalpy and density by defining them as non-conventional solids as HCOALGEN and DCOALIGT within the Aspen Plus software. The waste feedstock undergoes waste pyrolysis represented as yield correlation through RYIELD reactor, where the char portion decomposes in a RSTOIC. The syngas undergoes oxidation and reduction reactions represented through gas phase reaction kinetic modelled in RPLUG reactors. Pyrolysis correlations were adopted from Tungalang et al. [360] while the gas phase reaction kinetics were collected from various sources [64, 90, 361-366]. The crude syngas from Aspen Plus was simulated in Ansys Chemkin-Pro to represent the NTP tar cracking, where the result is converted into basis yield (kg/kg) and simulated in Aspen-plus using an RSTOIC reactor.

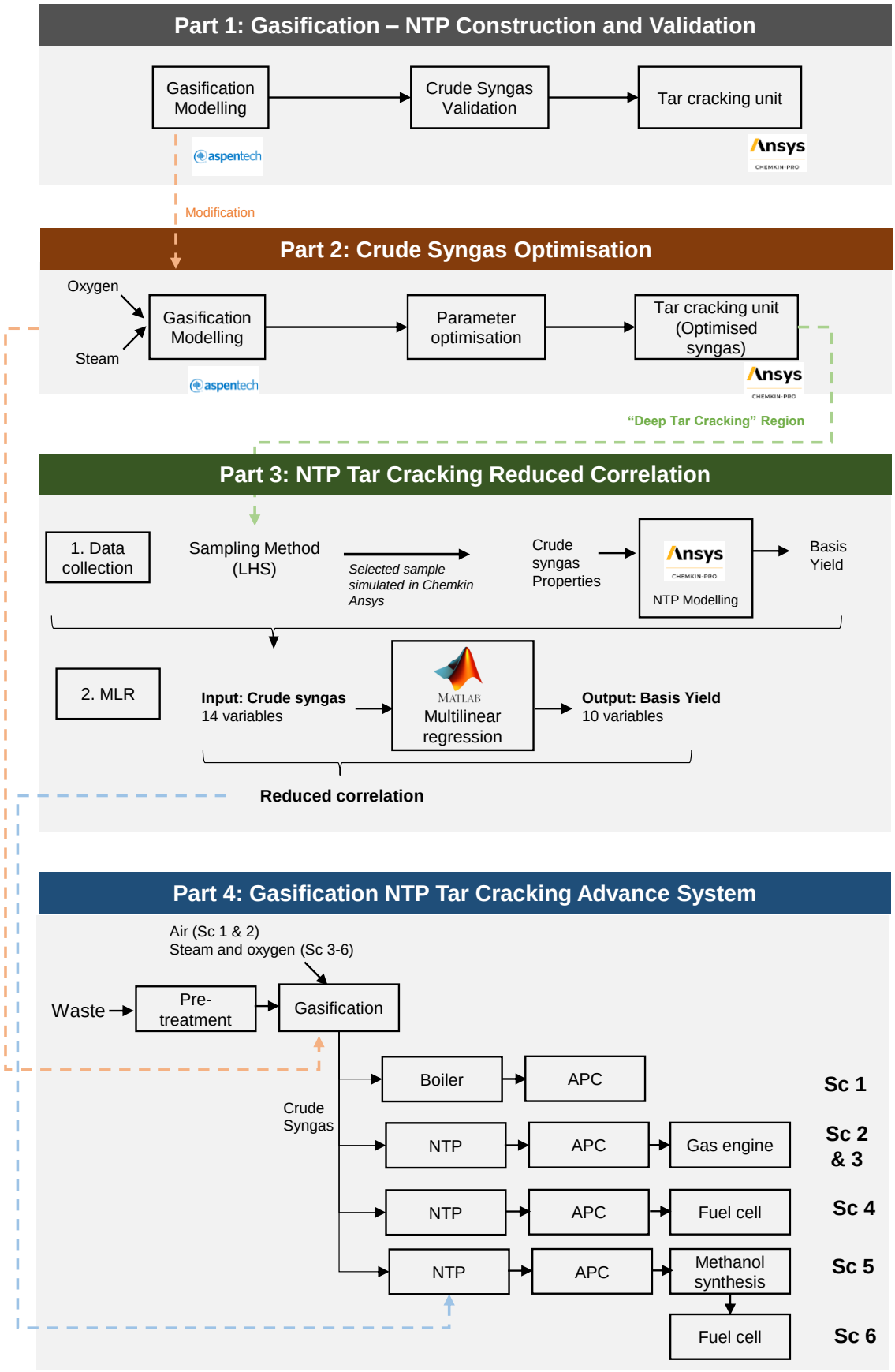

Figure 4-1: The methodology flowsheet for waste gasification-NTP tar cracking modelling.

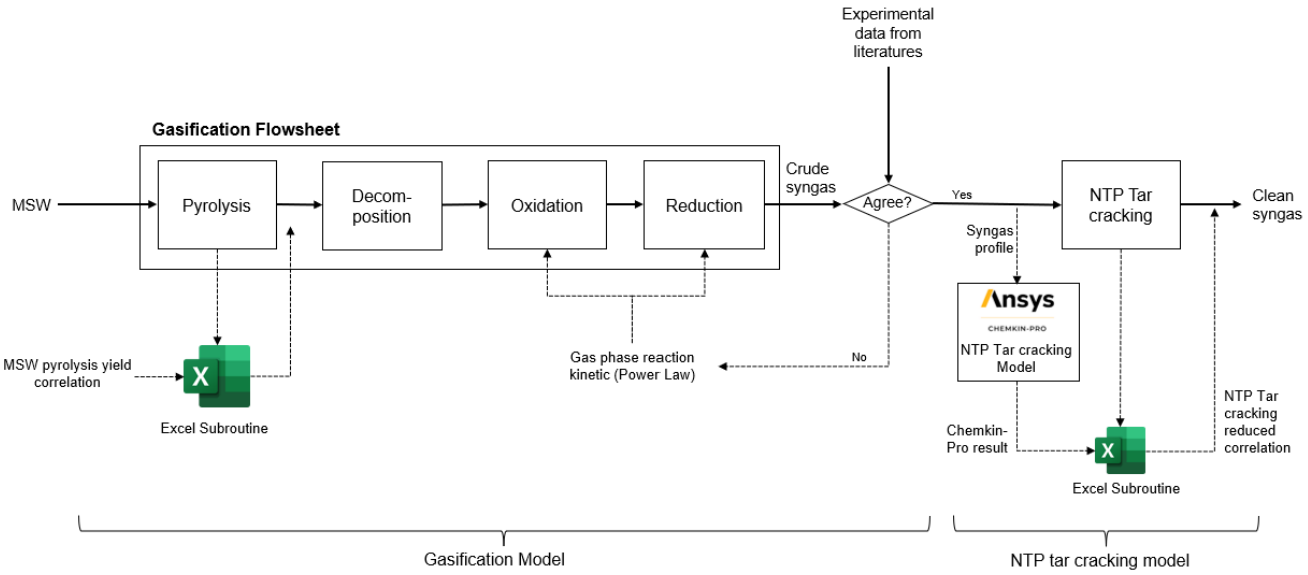

Figure 4-2: Flowsheet and logic in the development for the NTP tar cracking

Figure 4-3: Gasification process and reactor modelling

Process	Item (Figure 4-6)	Reactor type	Description	Modelling approach
Pyrolysis	R-1	RYIELD	Thermal decomposition of carbonaceous feedstock ranges between 500-700ºC	Yield correlation
Decomposition	R-3	RSTOIC	Char portions undergo decomposition reactions to produce elemental compounds. The conversion is assumed to be 100%	Stochiometric yield
Oxidation	R-5	RPLUG	Combustion of reactive gases to produces CO_2 and H_2O, the process generates a lot of heat that sustains the gasification reaction, temperature around 700-850ºC	Power law reaction kinetic
Reduction	R-6	RPLUG	As gasification operates below the stochiometric oxygen content, reduction reactions happen in the absence of oxygen, with predominantly endothermic reactions 800-1000ºC	Power law reaction kinetic
NTP tar cracking	R-8	RSTOIC	The tar and syngas portion further undergo reforming reactions, temperature and power are theorised to be the key parameters.	Yield correlation

Part II optimises the gasification process in terms of syngas quality through heating value (HV), Cold Gas Efficiency (CGE), and H_2/CO molar ratio, defined as:

$$Syngas\ HV(MJ/kg) = \sum(Compound\ heating\ value \times compound\ mass\ fraction) \qquad \text{Equation 4-1}$$

Where the heating value of CO, H_2, CH_4, C_2H_4, C_2H_6, and C_3H_8 are 10.1, 120.8, 50.0, 47.2, 47.5, and 46.3 MJ/kg respectively.

$$CGE = \frac{syngas\ heating\ value\ (MJ/kg)}{feedstock\ heating\ value\ (MJ/kg)}$$ Equation 4-2

$$Feedstock\ HV\ (MJ/kg) = 0.342\ x_C + 1.178\ x_H - 0.103\ x_O$$ Equation 4-3 [367]

This part identifies the favourable operating conditions for advanced syngas conversion. Furthermore, this part also establishes the boundary conditions and range for the reduced correlations of NTP tar reforming kinetic.

Part III explores the reduced correlations to represent the NTP tar cracking, aiming to predict the NTP product yield independent to the Ansys Chemkin-Pro software. This approach is adopted to achieve a streamlined waste gasification-NTP tar cracking model. Multilinear regression (MLR) was utilised to predict the basis yield of the NTP tar cracking.

	Input	Range						
X1	Temperature	750	1050	°C	→ MLR →	Y1	CO	kg/kg
X2	Flow rate	11.14	27.03	L/sec		Y2	CO_2	kg/kg
X3	CO	0.412	0.0781	mol/mol		Y3	H_2	kg/kg
X4	CO_2	0.065	0.3358	mol/mol		Y4	CH_4	kg/kg
X5	H_2	0.377	0.5607	mol/mol		Y5	C_2H_2 (C_2)	kg/kg
X6	CH_4	0.075	0.002	mol/mol		Y6	C_3H_3 (C_3)	kg/kg
X7	C_2H_4	0.017	0.0001	mol/mol		Y7	C_4H_8 (C_4)	kg/kg
X8	C_2H_6	0.013	0.0025	mol/mol		Y8	N_2	kg/kg
X9	C_7H_8	0.009	0.0046	mol/mol		Y9	H_2O	Kg/kg
X10	$C_{10}H_8$	0.001	0.0001	mol/mol		Y10	Tar	Kg/kg
X11	N_2	0.017	0.0089	mol/mol				
X12	C_6H_5OH	0.006	0.0031	mol/mol				
X13	C_6H_6	0.008	0.0042	mol/mol				
X14	Power	16	25	kW				

Figure 4-4: Input and output of the MLR reduced correlations.

Figure 4-4 shows the boundary conditions for the MLR established from Part II. 14 inputs (independent variables/predictors) and 11 outputs (dependent variables/target) were selected. Latin Hypercube Sampling (LHS) was used to randomise the input variables for 100 samples. These samples were later simulated in Ansys Chemkin Pro and the result was converted into basis yield (kg/kg). Further data treatment such as logarithmic and cross multiplication between variables were adopted to achieve the linear correlation. The input-output relationship is established based on the hypothesised reaction mechanism. Figure 4-5 shows the logic to select the input-output correlation. Matlab regress function was used to predict the MLR coefficients, where the predicted result and Ansys Chemki-pro result were compared and analysed through Root Mean Square Deviation (RMSD) (Equation 4-4).

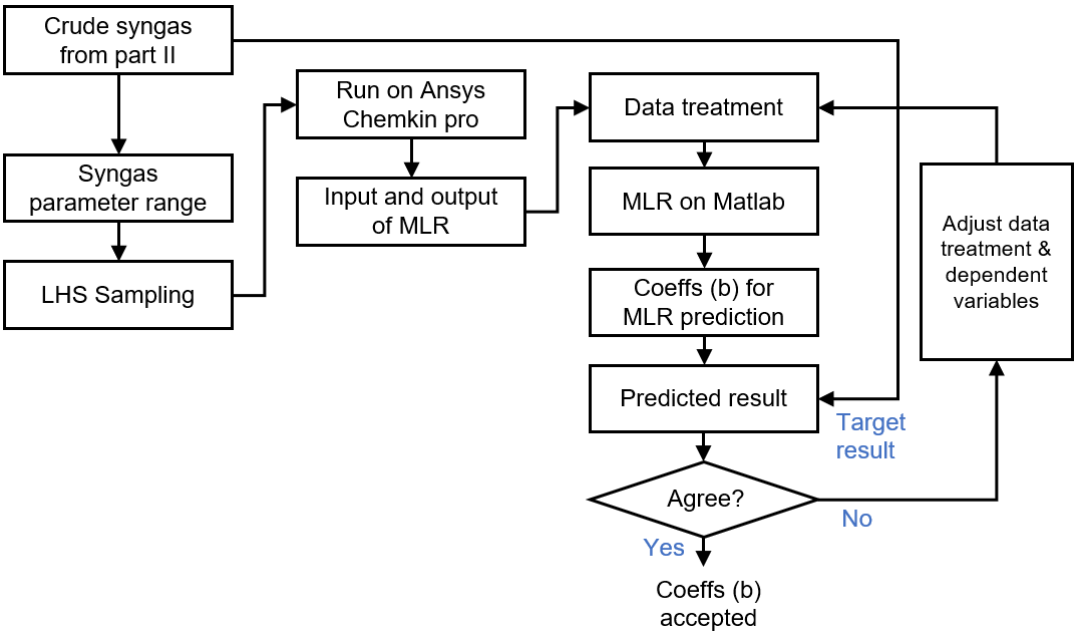

Figure 4-5: Flowsheet logic in selecting the dependent variables to predict the output.

$$RMSD = \sqrt{\frac{(Predictive\ value - Actual\ Value)^2}{Number\ of\ samples}} \qquad \text{Equation 4-4}$$

Part IV verify the validity of utilising NTP tar cracking for waste gasification, which was investigated through the products generated over energy required in the process. The scenarios are:

- Sc1: Air gasification, Boiler, and APC
- Sc2: Air gasification, NTP, APC, and gas turbine
- Sc3: O_2-Steam Gasification: Gasification, NTP, APC, and gas turbine
- Sc4: O_2-Steam Gasification, NTP, APC, and fuel cell
- Sc5: O_2-Steam Gasification, NTP, APC, and methanol synthesis
- Sc6: O_2-Steam Gasification, NTP, APC, methanol synthesis, and fuel cell.

Figure 4-6 shows the example of the gasification flowsheet utilised in this study, where the detail of the processes is explained in Table 4-2. For the energy generation, the model considered the heat from syngas' thermal energy, and it is heating value. The net power produced is later estimated from power generated deducted with the heat (Q) and power (W) used in the system, where the power generated is dependent on the energy recovery method. A similar heat and power combinations study has been evaluated by Kwon and Im [357]. Syngas thermal energy is defined as:

$$Syngas\ thermal\ energy\ \left({}^{kJ}/_{kg}\right) = m\ \left({}^{kg}/_{hr}\right) \times \Delta T\ (K) \times 0.399\ \left({}^{kJ}/_{kg.K}\right) \qquad \text{Equation 4-5}$$

Table 4-2: Unit process and design value for waste gasification with NTP Tar cracking.

Process	Block diagram	Design value	Ref
Pretreatment	B1	80-100 kWh per tonne of MSW for shredding and pelletising	[368]
Drying	B1	110-130 kWh per tonne of MSW	[368]
Gasification	R-1 to S-7	models assume a steady state process, meaning the only heating required is from air or oxygen.	[369]
Oxygen production	B2	51.3 kWh per tonne of oxygen production.	[370]
Gas preheating	HX-2	Air-specific heat is 1.005 kJ/kg K.	-
Steam production	HX-1	Water boiling conditions are assumed to be 2257 kJ/K while its water-specific heat is 4.184 kJ/kg K.	-
NTP tar cracking	R-8	18-20 kW established in this study.	-
APC	B3	3.06-5.22 kWh per tonne of MSW.	[357]
Gas boiler	B5	Recover 15-24% of syngas heating value.	[41]
Gas turbine	B5	Recover 26-35% of syngas heating value.	[41]
Fuel cells	B5	Recover 43.7% of syngas heating value.	[371]
Methanol synthesis	R-9	The syngas need to be heated from room temperature to 220-280 °C. The conversion is described as (RXN-24) $CO + 2H_2 \rightarrow CH_3OH, X = 35\%$	[356]

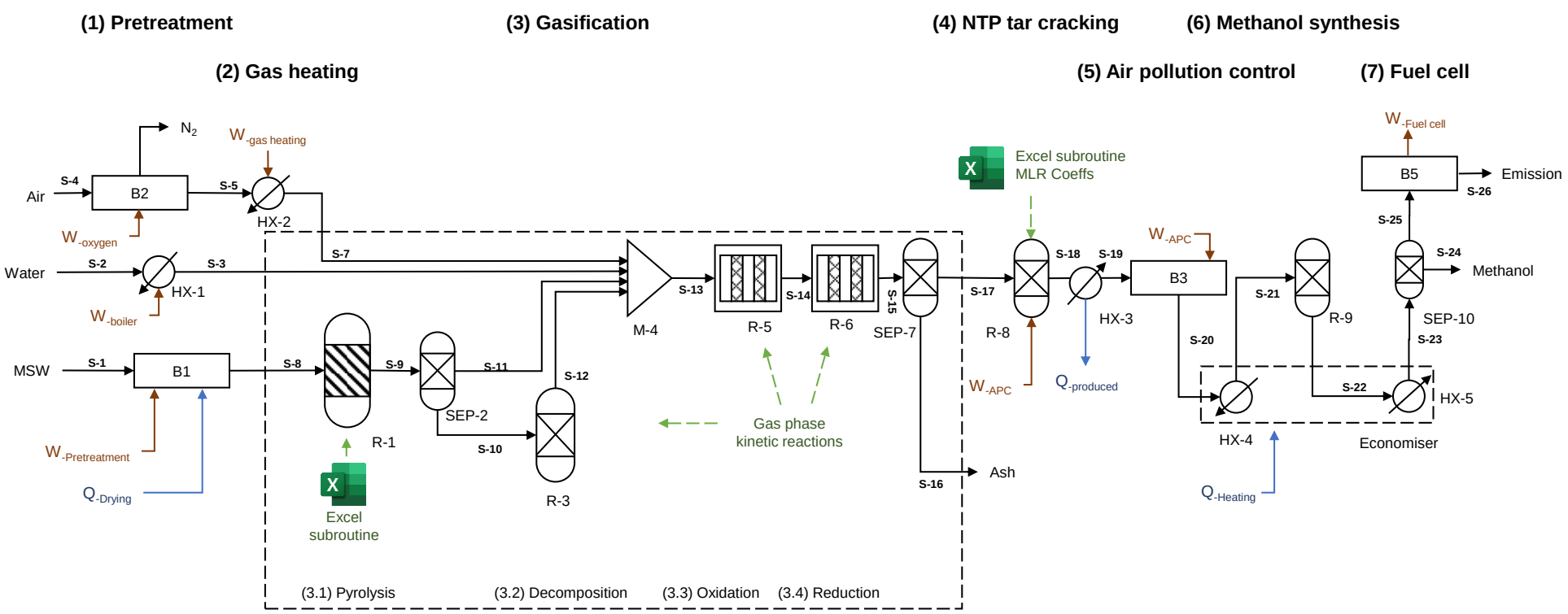

Figure 4-6: Schematic diagram of Scenario 6 for waste gasification NTP tar cracking with methanol synthesis and fuel cell energy recovery. Ful description of items is in Appendix B.1

4.4 Part I: Model construction and validation

4.4.1 Waste Gasification

During the gasification model construction, several parameters come into play that may influence the syngas result. Firstly, most gasification modelling studies describe waste as its molecular structure. Table 4-3 shows the comparison of different MSW molecular compositions used in gasification modelling. In this study, the proximate and ultimate analyses were based on MSW characterisation in the Australian suburbs of Brisbane [372]. It can be observed that Australian MSW is low in moisture due to the drying process to analyse the reconstituted sample and has a high HV.

Table 4-3: Comparison of various gasification feedstock elemental analysis

Ref	**[373]**	**[374]**	**[375]**	**[69]**	**[74]**	**[376]**	**[372]**
Based on	Pakistan's MSW	Tanzania's MSW	Sewage sludge	Unspecified RDF	Chinese MSW	Torrefied biomass	Australian MSW
Proximate analysis							
Moisture	51.87	59.79	8.7	1.9	-	4.5	-
VM	57	78.91	58.3	81.9	79.9	60	77.4
FC	12.19	10.54	-	-	14.6	34.5	15.1
Ash	30.81	10.55	41.7	16.2	5.7	1.0	7.6
Ultimate analysis (wt%)							
C	40.44	54.82	29.5	56.8	51.8	56.0	52.8
H	4.75	5.29	4.8	8.3	5.7	5.0	6.4
O	21.13	34.62	18.3	15.7	41.8	38.6	31.0
N	0.94	2.36	4.1	0.5	0.3	0.4	1.29
S	1.72	0.3	1.6	0.6	0.4	0.0	0.18
Cl	0.21	0.05	-	-	-	-	0.73
P	-	0.11	-	-	-		-
Ash	30.81	10.55	41.7	16.2	5.6	1.0	7.6
LHV	15.0	-	-	27.3	-	-	11.4
HHV	-	-	-	29.7	20.3	20.0	22.5

VM: Volatile matter, FC: Fixed carbon, HHV: higher heating value (MJ/kg), LLV: Lower heating value (MJ/kg), RDF: Refuse Derived Fuel, "-": Unreported

Table 4-4: Gasification modelling approaches in predicting pyrolysis yield (kg/kg of feedstock).

Study	**[64]**	**[90]**	**[360]**	**This work**
Pyrolysis estimation by	[377]	[378]	[379]	[90] and [360]
Feedstock	Various biomass	Wood chip	RDF	MSW
Prediction via	Linear correlation	Polynomial	The direct yield based on the experimental result	Adjusted to fit the study's objective
Gas compound				
CO	20	29.54	21.6	21.6
H_2	1	0.87	2.3	2.3
CH_4	3	1.21	5.4	5.4
CO_2	13	17.13	10.5	10.5
O_2	-	-	0.0	-
H_2O	-	24.05	5.0	5.0
N_2	-	-	0.9	0.9
Cl_2	-	-	0.2	Out of scope
S	-	-	1.6	Out of scope
C_2H_4	-	2.47	-	2.47
C_2H_6	-	2.05	1.8	2.05
C_3H_8	-	-	2.1	2.1
Tar compound				
C_6H_6	5.3 (total)	3.13	0.9	3.13
$C_6H_5CH_3$	-	4.06	-	4.06
C_6H_5OH	-	2.89	0.9	2.89
$C_{10}H_8$	-	0.41	-	0.41
$C_{16}H_{10}$	-	-	0.9	Out of scope
Other				
Char	12	24.22	11.6	36.8
Ash	-	-	29.3	Assumed to bed locked in char, released during decomposition
C	-	-	5.2	

The gasification reaction begins with pyrolysis. However, pyrolysis modelling itself is an evolving subject, with technical challenges such as waste inconsistency and reactor unpredictability. Revealing the true mechanisms of pyrolysis is a research field of its own [380]. There is currently a lack of consensus across research studies for pyrolysis modelling [381]. Since predicting pyrolysis reactions is out of this thesis' scope, the pyrolysis yield for this gasification modelling is derived from Tungalag et al. [360] and further complimented with Abdelouahed et al. [90] for the tar portion prediction. The mixed pyrolysis yield data is adopted due to Tungalag et al. consistent prediction for every tar

compound (0.9 wt/kg, Table 4-4), possibly resulting from tar complexity and characterisation error [65, 382]. Table 4-4 shows the pyrolysis yield used in this work.

Char is a solid product of pyrolysis [383], but in gasification, the high temperature converts char into reactive hot charcoal and leaves only elemental C and ash as solid by-products of gasification [65]. This study adopted 100% conversion by Puig Gamero (RXN-1, Table 4-5).

Table 4-5: Decomposition, oxidation, and reduction reactions

RXN	Name	Reaction	Kinetic	Ref
Decomposition				
1	Char cracking	$Char \rightarrow C + H_2 + N_2 + O_2 + Ash$	$X = 100\%$	[64]
Oxidation				
2	Methane partial oxidation	$CH_4 + 0.5\ O_2 \rightarrow CO + 2H_2$	$r = 1.58 \cdot 10^{10} \cdot e^{\frac{-2.02 \cdot 10^5}{RT}} [CH_4]^{0.7} [O_2]^{0.8}$	[361]
3	Elemental carbon partial oxidation	$\alpha C_{(s)} + 0.5\ O_2 \rightarrow 2(\alpha - 1)CO + (2 - \alpha)CO_2$	$r = 3.7 \cdot 10^{10} \cdot e^{\frac{-1.50 \cdot 10^5}{RT}} [O_2]$; $\alpha = \frac{1 + 2f}{1 + f}; f = 4.72 \cdot 10^{-3} \cdot e^{\frac{37{,}787}{RT}}$	[64]
4	Hydrogen oxidation	$H_2 + 0.5\ O_2 \rightarrow H_2O$	$r = 2.19 \cdot 10^{18} \cdot e^{\frac{-1.09 \cdot 10^5}{RT}} [O_2][H_2]$	[362]
5	Ethane oxidation	$C_2H_4 + 3\ O_2 \rightarrow 2CO_2 + 2H_2O$	$r = 1.58 \cdot 10^{14} \cdot e^{\frac{-1.66 \cdot 10^8}{RT}} [C_2H_4]^{0.7} [O_2]^{0.8}$	[363]
6	Ethane Partial oxidation	$C_2H_4 + 2\ O_2 \rightarrow 2CO + 2H_2O$	$r = 1.00 \cdot 10^{12} \cdot e^{\frac{-1.73 \cdot 10^5}{RT}} [C_2H_4]$	[364]
7	Propane decomposition	$C_3H_8 \rightarrow C_2H_4 + CH_4$	$r = 1.00 \cdot 10^{12} \cdot e^{\frac{-1.76 \cdot 10^5}{RT}} [C_3H_8]$	[364]
8	Propane oxidation	$C_3H_8 + 5O_2 \rightarrow 3CO_2 + 4H_2O$	$r = 1.00 \cdot 10^{12} \cdot e^{\frac{-1.73 \cdot 10^5}{RT}} [C_3H_8]$	[364]
9	Phenol partial oxidation	$C_6H_5OH + 4O_2 \rightarrow 6CO + 3H_2O$	$r = 6.55 \cdot 10^{2} \cdot e^{\frac{-8.02 \cdot 10^4}{RT}} [C_6H_5OH]^{0.5} [O_2]$	[361]
10	Naphthalene partial oxidation	$C_{10}H_8 + 5O_2 \rightarrow 10CO + 4H_2$	$r = 2.07 \cdot 10^{4} \cdot e^{\frac{8.02}{RT}} [C_{10}H_8][O_2]$	[365]
Reduction				
12	Methane steam reforming	$CH_4 + H_2O \rightarrow CO + 3H_2$	$r = 3.00 \cdot 10^{5} \cdot e^{\frac{-1.25 \cdot 10^5}{RT}} [CH_4][H_2O]$	[362]
13	Carbon steam reforming	$C + 1.2\ H_2O \rightarrow 0.8\ CO + 0.2CO_2 + 1.2H_2$	$r = 2.39 \cdot 10^{2} \cdot e^{\frac{-1.29 \cdot 10^5}{RT}} [C]$ (Simplified)	[361]
14	Carbon steam reforming	$C + H_2O \rightarrow CO + H_2$	$r = 6.33 \cdot 10^{1} \cdot e^{\frac{-1.41 \cdot 10^4}{RT}} [C]$ (Simplified)	[366]
15	Boudouard reaction	$C + CO_2 \rightarrow 2CO$	$r = 3.18 \cdot 10^{7} \cdot e^{\frac{-2.68 \cdot 10^5}{RT}} [C][CO]^{-1}$ (Simplified)	[361]
16	Methane reforming	$CH_4 \rightarrow C + 2H_2$	$r = 1.00 \cdot 10^{-1} \cdot e^{\frac{-2.63 \cdot 10^5}{RT}} [CH_4]$	[90]

RXN	Name	Reaction	Kinetic	Ref
17	Water gas shift reaction	$CO + H_2O \rightarrow CO_2 + H_2$	$r = 1.35 \cdot 10^5 \cdot e^{\frac{-1.02 \cdot 10^5}{RT}}[CO][H_2O]$	[90]
19	Naphthalene reforming	$C_{10}H_8 \rightarrow 6.5C + 0.5C_6H_6 + 1.5H_2 + 0.5CH_4$	$r = 1.70 \cdot 10^7 \cdot e^{\frac{-3.50 \cdot 10^5}{RT}}[C_{10}H_8]^{1.6}[H_2]^{-0.5}$	[64]
20	Phenol steam reforming	$C_6H_5OH + 3H_2O \rightarrow 4CO + 0.5C_2H_4 + CH_4 + H_2$	$r = 8.00 \cdot 10^{-3} \cdot e^{\frac{-4.99 \cdot 10^5}{RT}}[C_6H_5OH]$	[64]
21	Naphthalene stream forming	$C_{10}H_8 \rightarrow 9C + 0.167\ C_6H_6 + 3.5H_2$	$r = 3.40 \cdot 10^{14} \cdot e^{\frac{-3.50 \cdot 10^5}{RT}}[C_6H_5OH]$	[90]
22	Ethene steam reforming	$C_2H_4 + 2\ H_2O \rightarrow 2CO + 4H_2$	$r = 3.10 \cdot 10^2 \cdot e^{\frac{-1.50 \cdot 4}{RT}}[H_2O]^2[C_2H_4]$	[366]
23	Ethane steam reforming	$C_2H_6 + 2\ H_2O \rightarrow 2CO + 5H_2$	$r = 3.10 \cdot 10^2 \cdot e^{\frac{-1.50 \cdot 4}{RT}}[H_2O]^2[C_2H_4]$	[366]

The general kinetic reaction is $r = k \cdot e^{\frac{E_a}{RT}}$, where E_a is in J/mol.

The gas products are mixed with the gasifying agent (air) and undergo oxidation, where the gasifying agent is restricted to maintain a partial oxidation process. Afterwards, the gas undergoes gasification (reduction) reactions, where more gas and tar compounds break down into syngas. The gas phase kinetic reactions for oxidation and reduction are shown in Table 4-5 represented through power law kinetic.

Diverse gasification experimental data is collected for validation purposes (Table 4-6). However, upon investigation, it was found that the diversity in waste composition, reactor designs, and operating conditions employed by various researchers are bound to produce a unique and singular research result for the respective studies. Moreover, different studies may adopt different methods for estimating syngas composition [384], further contributing to the variability in experimental results. The lack of standardisation for syngas constitution exacerbates the wide range of variances observed across experimental studies, as evident in Table 4-6. Given the unique nature of each experimental condition, validating the model result solely based on syngas composition from one experimental data point may be futile. The syngas composition is destined to fluctuate even within the same experimental setup (shown in [375] and [384]).

For instance, the syngas profile from RDF-gasification in a fluidised bed by Arena et al. [69] exhibits a closer resemblance to the sewage sludge fluidised bed gasification by De Andres et al. [375], as opposed to another RDF-gasification by Del Alamo et al. [384]. It is theorised that De Alamo niche utilisation of a moving grate reactor promotes a more complete oxidation, resulting in lower levels of CO due to a longer residence time and enhanced oxidation process. However, the reactor theory lacks universal applicability, as evidenced by other fluidised bed gasification of various feedstock which do

not produce similar results [385, 386]. The existence of these discrepancies challenges the assumption that reactor conditions alone govern syngas composition, showcasing the complex intricacies of a multitude of factors that influence syngas composition. Elucidating all of these variables' influence on gasification reactions is beyond the scope of this thesis.

Thus, rather than validating the model with specific operating conditions to achieve an identical syngas composition (as demonstrated in modelling work [359, 373, 374]), an alternative validation approach is to focus on predicting trends generated across operating parameters to ensure the model's capability to represent waste gasification reaction across a changing operating condition. Figure 4-7 illustrates the validation between the modelled syngas and the experimental data of syngas at varying equivalence ratios (ER).

ER is considered to be the most crucial parameter influencing the syngas product profile [387]. Figure 4-7 demonstrates an agreement between the model and experimental data in terms of trendlines for most major gas species. To further assess the model's ability to predict the trends, Table 4-7 presents the gradients of linear correlations between the experimental results and the model employed in this study. Outliers across experimental studies are highlighted in red. Full gradient analysis is shown in Appendix B.2.

Table 4-6: Summary of syngas composition (vol %) across various waste (and biomass) gasification experiments and this modelling work

Study	Del Alamo et al. [384]	de Andrés et al. [375]	Arena et al. [69]	Naveed et al. [388]	Dudyński et al. [376]	de Diego et al. [386]	Puig-Gameo et al. [64]	Chang et al. [389]	Cai et al. [390]	Leung and Wang [385]	This work
Feedstock	UK's MSW turned into RDF	Sewage sludge	Unspecified RDF	UK MSW	Torrefied biomass	Biomass	Biomass	Biomass	Biomass + MSW	Tire Waste	MSW
Reactor	Moving grate gasifier	Fluidised bed gasifier	Fluidised bed gasifier	Downdraft gasifier	Downdraft gasifier	Fluidised bed gasifier	Fluidised bed	Downdraft gasifier	Tube reactor	Fluidised bed	General modelling
Operating condition	ENERGOS commercial scale MSW gasification	750-850 ºC, ER= 0.3, oxygen and steam	850ºC, ER=0.23-0.34	1000-1200ºC	750ºC	O_2 only, 1000 ºC	750-860ºC, ER: 0.17-0.35	200-1000ºC, ER=0.2-0.34	ER=0.1-0.4, 900ºC	ER=0.1-0.5, 500-800ºC	ER = 0.3, 950ºC
H_2	4.55	5.3-13.3 (9.5)	5.9-9.2 (7.7)	4.58	10.3	27.2	5-7.5 (6.5)	10.2-16.1 (13.3)	1.0-6.0 (3.5)	0.4-3.0 (1.5)	1.6
CO	0.97	6.3-9.6 (8.07)	7.9-9.1 (8.5)	14.89	29.0	21.7	14.0-22.0 (18.4)	8.4-12.1 (10.6)	21.0-42.0 (31.5)	18.0-36.0 (25.6)	29.4
CO_2	20.25	12.8-13.6 (13.3)	12.8-13.4 (12.8)	8.40	6.70	37.8	13-17.5 (15.7)	25.1-27.9 (26.4)	34.0-69.0 (51.5)		12.3
CH_4	7.12	2.6-3.3 (2.9)	6.6-8.3 (7.3)	1.54	2.40	9.20	3.5-5.7 (4.8)	2.2-4.2 (3.3)	4.0-13.8 (9.4)	2.5-6.3 (3.9)	2.2
N_2	65.97	58.3-67.7 (62.3)	-	67.34	48.3	0.00	49.0-54.0 (52.2)	42.5-51.2 (46.4)	-	-	48.9
O_2	0.50	-	-	1.20	0.00	0.00	-	-	-	-	0
C_2H_6	0.15	0.03-0.17 (0.076)	-	-	0.60	0.40	-	-	0.8-1.5 (1.1)	-	0.8
C_2H_2	0.27	-	-	-	-	-	-	-		-	-
C_2H_4	-	1.8-2.9 (2.1)	1.8-2.7 (2.1)	-	0.20	3.30	1.0-3.0 (2.2)	-	1.2-3.5 (2.5)	-	0.8
C_3H_8	0.20	-	-	-	0.10	0.30	-	-	-	-	0

The range shows the variance across the operating condition, with bracket value () indicating average.

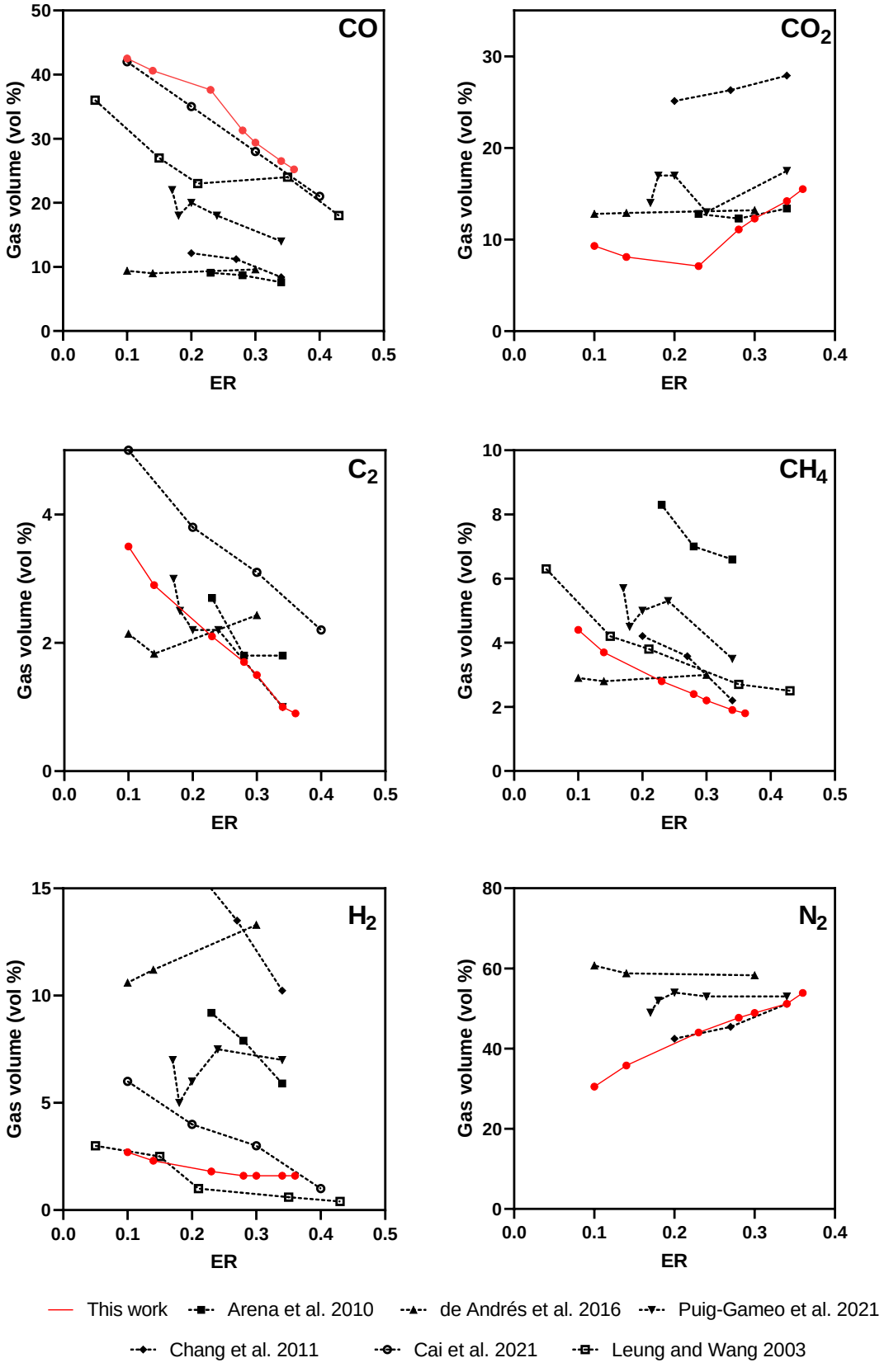

Figure 4-7: Modelling result and the experimental results across increasing ER.

Table 4-7: Linear gradient for the model and experimental literature result (See Appendix B.2).

Gas	This work	Arena et al. [69]	de Andres et al. [375]	Puig-Gamero et al. [64]	Chang et al. [389]	Cai et al. [390]	Leung and Wang [385]
CO	-68.8	-13.8	-1.78	-38.2	-26.8	-70	-39
CO_2	25.7	5.9	1.96	-	8.9	-	-
C_2	-9.7	-7.9	2.71*	-10.2	-	-9.1	-
CH_4	-9.5	-15.2	0.72*	-9.57	-14.5	-	-9.41
H_2	-4.1	-30.1	13.4*	6.53*	-40.1	-16	-7.61
N_2	85.5	-	-9.4*	12.8	62.5	-	-

*Indicates the outlier (positive or negative gradient trendline) against other literature work

The CO portion align with external experimental data collected from Cai et al. , where the reduction gradient agrees with Puig-Gamero et al. [64], Chang et al. [389], Leung and Wang [385] (Table 4-6). CO reduction over increasing ER is the result of a more complete combustion due to higher ER, converting it into CO_2. This is reflected in the CO_2 portion as it increases after ER=0.23 (RXN-17 to RXN-19, Table 4-5). The C_2 result also demonstrate an agreement when compared to the Arena et al. [69] and Puig-Gamero et al. [64] findings. C_2 analysis highlights the importance of establishing a diverse syngas analysis. Various studies omit C_2 analysis compounds, which may skew other syngas composition by normalising it into a limited light gas compounds [389] [391].

Among the studies, De Andres et al. [375] exhibit the most outliers in comparison to other studies including this work. The use of sewage sludge as a feedstock in their study leads to a higher H_2O-to-O_2 ratio in the lower ER (due to the higher sewage sludge flow rate), where the moisture excess in the system may reduce the internal gasification temperature [381]. The decrease in temperature may lead to an overall decrease in feedstock carbon conversion, as evidenced by their relatively linear CO and C_2 product trends, while others exhibit a strong negative gradient (Table 4-7). Moreover, the excess H_2O theory is further supported by the H_2 increase, while other studies, including this model, predicted a decrease in H_2 yield over increasing ER. The excess moisture promotes steam reforming reactions that produces more H_2 (RXN-12). This phenomenon reiterates the gasification process uniqueness for each experimental condition.

For the tar portion in syngas, the experimental result varies even greater than the syngas concentration among studies. Tar analysis may be challenging due to its (1) diverse chemical compounds, (2) varying concentrations amongst species, and (3) technical forensic difficulty (condensation, matrix effect, diverse sampling technique, etc.) [9, 392-394]. Furthermore, the reported experimental data suggest that tar in syngas does not exhibit a consistent pattern between various studies, whether it is the tar

concertation or the major tar species. For example, Chin et al. [395] reported a predominantly Class II Tar (Phenol). Meanwhile, Chianese et al. [396] show a high naphthalene concentration and negligible Class II and II tar. The large variance in literature experimental data created an obstacle for this model validation.

For the reaction kinetic, the limited understanding of tar generation mechanisms during gasification hinders an accurate tar production model. Most modelling studies rely on experimental data to assume the tar yield, rendering the model highly dependent on the input data [65]. Table 4-8 compares model results with reported experimental data. The comparison indicates that the model predicts Class II and III tar accurately when compared with Del Alamo et al. [384] and De Andres et al. [375] reported experimental data. However, the model underpredicts the naphthalene concentration. This discrepancy may arise from the mathematical correlation utilised in the model, which reported a low naphthalene tar yield [90, 378]. This finding agrees with other studies [394, 395, 397], which also reported a lower naphthalene concentration when compared to the other tar compounds.

Table 4-8: tar modelling result and experimental results (All values in g/Nm^3)

Tar compound	**[397]**	**[394]**	**[272]**	**[384]**	**[375]**	**This work**
Feedstock	Sewage sludge	Biomass	MSW	UK's MSW turned into RDF	Sewage sludge	MSW
Reactor	Downdraft gasifier	Fluidised bed gasifier	Downdraft gasifier	Moving grate	Fluidised bed gasifier	General modelling
Benzene	1.35	0.89	-	3.42	7.0-13.6 (8.8)	2.69-4.82 (3.50)
Class II (Phenol)	0.18	-	0.31	-	1.0-5.7 (3.2)	2.39-4.35 (3.22)
Class III (Toluene)	1.39	0.25	4.25	3.66	1.4-7.8 (4.6)	3.45-6.10 (4.47)
Class IV (Naphthalene)	0.09	0.28	4.01	4.50	2.0-3.9 (2.8)	0.02-0.01 (0.02)

The range shows the variance across the operating condition, with bracket value () indicating average.

Hence, while the model's naphthalene results may differ from experimental results, low naphthalene concentrations have been reported in other experimental studies. This indicates that the model captures the trend for predicting tar in syngas where one-ring hydrocarbon tar is more prevalent (Class II and III).

In summary, despite the uncontrollable challenges, such as syngas inconsistency and complexity in tar production and characterisation, the model effectively captures the general trends and tendencies of

waste gasification products. Thereby effectively simulating the reality of syngas and tar generation in a waste gasification process.

4.4.2 NTP tar cracking

The previous chapter established that the tar degradation mechanism is influenced by the syngas composition. Moreover, power was identified as the most influential factor in establishing whether the tar transformed into a secondary compound or fully degraded into smaller gases. Hence, this part modelled the crude syngas generated by the Aspen Plus model through the NTP tar cracking reaction kinetic database established in Chapter 3. The NTP tar cracking result is shown in Figure 4-8.

Analysis of Figure 4-8 reveals distinct operational regions. At lower power (<8 kW), tar conversion resulted in secondary tar compounds, notably C_9 and C_6, (Figure 4-8 A and B) This undesirable outcome suggests a need for higher power for effective tar cracking. In this zone, heightened methane production, attributed to toluene conversion into benzene, is evident in the increase of the CH_4 conversion trend (Figure 4-8 E).

Within the 8-15 kW range, high C_4, C_3, and C_2 basis yield signifies incomplete plasma tar cracking. Although breakdown into smaller compounds occurs, complete oxidation remains unachieved. This indicates incomplete tar cracking. Concurrently, H_2 and CO_2 increment has not achieved a steady line (Figure 4-8 D and E), suggesting that the NTP reactor has not achieved a complete tar cracking. Beyond 15 kW, Figure 4-8 A and B reported an almost undetectable presence of tar, while the CO_2 and CH_4 syngas portions were transformed into CO and H_2. water is identified to be a major by-product, possibly result of the phenol hydroxyl compound reacting with the excess H-radical (Figure 4-8 E), This zone is identified as a deep tar cracking zone.

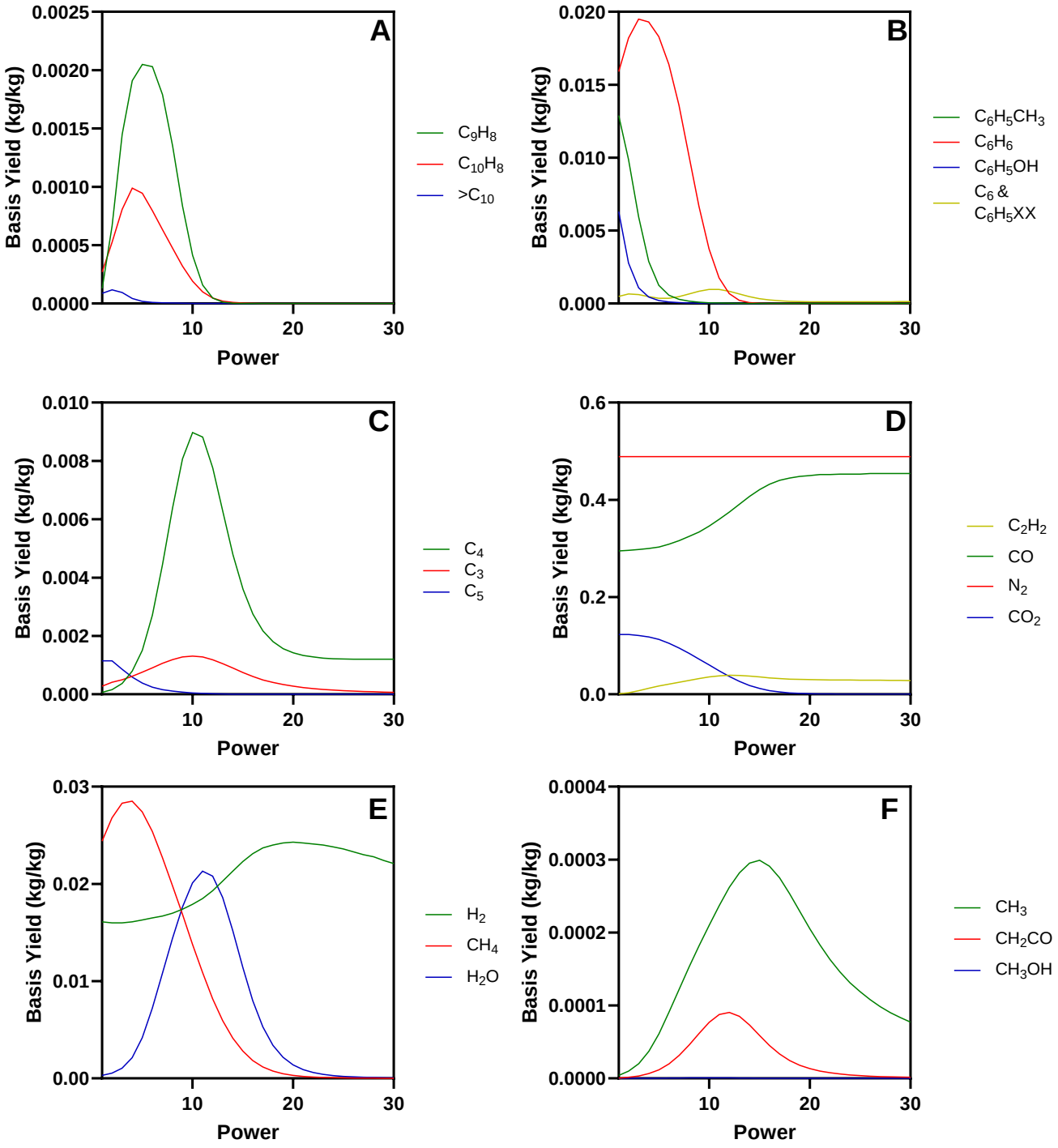

Figure 4-8: Ansys Chemkin-Pro basis yield (kg/kg) result of NTP tar cracking for (A) large tar, (B) single ring tar, (C) hydrocarbons, (D) Major gas products, (E) minor gas products, and (F) C1 compounds at increasing NTP reactor power from 1 to 30 kW. The regions are: Secondary tar generation (1-8 kW), incomplete tar cracking zone (8-15 kW) and deep tar cracking zone (>15 kW).

Table 4-9: Ansys Chemkin Pro result at 20 kW and the Aspen Plus adaptation.

ANSYS Chemkin Pro result at 20 kW reforming for 500 cm³ PSR		**RSOTIC basis yield in Aspen**	
Compound	**Basis Yield (kg/kg)**	**Compound**	**Basis Yield (kg/kg)**
CO	4.50×10^{-1}	CO	4.50×10^{-1}
CO_2	1.11×10^{-3}	CO_2	1.11×10^{-3}
H_2O	1.38×10^{-3}	H_2O	1.38×10^{-3}
H	4.21×10^{-4}		
H_2	2.43×10^{-2}	H_2	2.43×10^{-2}
N_2	4.89×10^{-1}	N_2	4.89×10^{-1}
CH_4	3.12×10^{-4}		
Hydrocarbons		**Hydrocarbons**	
CH_2O	2.51×10^{-7}		
CH_2CO	1.33×10^{-5}		
CH_3	2.05×10^{-4}		
C_1 Sum	2.18×10^{-4}	CH_4	5.31×10^{-4}
C_2H_5	7.78×10^{-8}		
C_2H_3	3.01×10^{-6}		
C_2H_6	1.25×10^{-7}		
C_2H_2	3.01×10^{-2}		
C_2H_4	1.41×10^{-5}		
C_2 Sum	3.01×10^{-2}	C_2H_2	3.01×10^{-2}
C_3H_4	6.13×10^{-6}		
C_3H_4	1.39×10^{-5}		
C_3H_3	2.56×10^{-4}		
C_3 Sum	2.76×10^{-4}	C_3H_3	2.76×10^{-4}
C_4H_5	1.78×10^{-7}		
C_4H_4	5.91×10^{-6}		
C_4H_2	1.41×10^{-3}		
C_4 Sum	1.42×10^{-3}	C_4H_2	1.42×10^{-3}
C_5H_5	3.97×10^{-7}	C_5H_5	3.97×10^{-7}
Tar (>C_6)		**Tar (>C_6)**	
C_6H_4	7.12×10^{-8}		
C_6H_2	1.24×10^{-4}		
$C_6H_4CH_3$	6.94×10^{-8}		
C_6H_6	5.63×10^{-8}	C_6H_6	1.24×10^{-4}
$C_6H_5CH_2$	5.42×10^{-8}		
$C_6H_5CH_3$	4.27×10^{-7}	$C_6H_5CH_3$	4.27×10^{-7}
C_6H_5OH	1.53×10^{-7}	C_6H_5OH	1.53×10^{-7}
$C_{10}H_8$	2.88×10^{-7}	$C_{10}H_8$	2.88×10^{-7}

NTP tar cracking objective should lie in the deep tar cracking zone, as this region provides a high tar conversion which contributes to a consistent gas yield. Consistent gas yield enables a more linear gas basis yield prediction and reliable outcome, reducing the complexity within the prediction model (Part III). The result of this basis yield is grouped and inputted in the gasification model. Table 4-2 shows the comparison of basis yield results from Ansys Chemkin Pro result and the value adopted into Aspen

Plus. The drawback of this approach is that the Aspen Plus model lacks the comprehensive product yield shown in Ansys Chemkin Pro modelling.

The utilisation of NTP tar cracking based on the Chemkin Ansys model for gasification relies on the premise that the NTP tar cracking model's properties remain relevant during scaling up and integrated into the waste gasification unit. Currently, there is an absence of studies that directly demonstrate the use of NTP tar cracking with waste gasification, resulting in limited insights into its potential upscaling [209, 398].

Table 4-10: Comparison of this modelling work vs. other experimental study

Study	**This work**	**[283]**	**[217]**	**[208]**	**[399]**	**[400]**	**[401]**
NTP Plasma	Plasma PSR (Ansys Chemkin)	AC GAD	AC GAD	DBD	Microwave torch	AC GAD	DBD
Surrogates tar	B, T, N, P	T	N	T	N	B	N
Tar content (g/Nm^3)	10.05	23.5	0.6-1.3%	33	4.2	0.12%	0.46
Flow rate (m^3/h)	94.03	0.23	0.48	0.0024	1.07	1.00	0.03
SEI (kWh/m^3)	0.19	0.30	1.00	0.98	0.93	0.17	0.02
Tar removal	98.8%	51.8%	79%	99%	99.0%	90.7%	83%

SEI: Specific Energy Input, B: Benzene, T: Toluene; N: Naphthalene, and P: Phenol

Although most researchers support the NTP's upscaling capability due to its straightforward design and cost-effectiveness [398, 402], the practicality of utilising NTP for gas cleaning in a high-capacity reforming remains uncharted [21]. Upscaling NTP requires elongating the tube reactor as increasing the discharge gap is not feasible, resulting in physical constraints [398]. Some examples of NTP upscaling are Xu et al. [403] investigation on a long DBD reactor (85 cm long) for tar cleaning (toluene), which is considered to be a pilot scale. Other NTP upscaling has been demonstrated in Volatile Organic Compounds (VOC) [404], organic wastewater treatment [405], and perfluoro pollutant abatement [406]. Furthermore, Rabinovich et al. [18] reported an upscaling of "warm" plasma through the gliding arc reactor to clean dirty pyrogas operating, but they also highlight that more parameter research is still required to upscaling the gliding arc reactor.

Hence, despite the favourable stance on NTP upscaling among experts, the upscaling of NTP tar cracking is still an evolving research direction [407]. In this study, the model operates under the assumption that upscaling is tenable. This means that the current scientific understanding of tar cracking (From Chapter 3) is reflected in NTP tar kinetic modelling and remains relevant to the scaled-up context.

From Figure 4-9, it is evident that tar conversion nearly reaches an imperceptible level (>99.99% Tar conversion), with the resultant hydrocarbon chain present at minimal concentration. Additionally, CO_2 and CH_4 reform into CO and H_2, along with water that can be removed via condensation. Although greater energy input augments tar conversion; high energy intake may diminish energy efficiency.

Table 4-10 comparative analysis reveals the model's performance with other NTP tar cracking studies. While this model's energy efficiency aligns relatively well with other studies, it should be noted that the model features lower tar concentrations. From the table, it is evident that the model shows agreement with experimental data, despite the inconsistency between different experimental data. It is important to note that the ideal conditions of the model may not translate into the real world, despite the similar tar removal rate. For instance, the model operates at a flowrate higher than experimental data, along with the limitation of tar species in comparison to real waste gasification plant [386].

In summary, the developed model produces result that align the external experimental data trends across studies, as shown in Table 4-7 and Table 4-10. The model produced the desired tar reduction and demonstrated the ability to simulate tar cracking reduction by transporting the data into ANSYS-Chemkin at the given crude syngas properties. Appendix B.3 shows the summary of the stream composition throughout the Aspen Plus model.

4.5 Part II: Gasification optimisation

This part delves into optimising syngas composition for advanced syngas recovery. Advanced syngas processing requires minimal N_2, CO_2, and tar concentrations, along with a heightened H_2/CO ratio. Pure oxygen injection, NTP tar cracking, and steam injection are adopted to facilitate these challenges. The result of Part II also provides the crude syngas range for NTP reduced correlation.

Air gasification often lacks the H_2/CO ratio required for advanced syngas processing, a concern also reflected in our model (Part I, H_2/CO =0.52). To address this, the model is simulated in pure oxygen and steam injection. Steam gasification is argued to produce the highest hydrogen yield out of any gasification modification [408].

Steam injection occurs before the reduction reactor. The addition of steam will further assist the reforming reactions that transform char into CO and CO_2 (RXN 13 and RXN 14 respectively). The excess of steam also converts CO into CO_2 and H_2 through a water gas shift reaction, which is argued to be the most important reaction in hydrogen production [409]. Although the production of H_2 is desirable in the system, the by-product of CO_2 may pose challenges, given certain syngas upgrading processes necessitate a low CO_2 concentration [279]. Steam also functions as an oxidant, converting methane and C_2 carbon (RXN 12 and RXN 22) into CO and H_2 [410].

Table 4-11 presents a comparison of the model's oxygen-steam gasification result with experimental data. Data limitation eliminates the ability to compare results at varying operating conditions. The model produces a result that has a numerical agreement with the external experimental data (Table 4-11); however, it is important to note that the excess steam flow rate may result in a bias where the gasification process produces excessive H_2 mole flow rates (50-65 mol%), skewing the result into predominantly H_2. Nevertheless, since H_2 is the gas of interest, it shows an agreement with experimental data.

Table 4-11: Comparison between external experimental data and the model for waste steam gasification

Study	**[411]**	**[412]**	**[413]**	**This Work**
Feedstock	Plastic waste	Wastewater sludge	MSW	MSW
Operating condition	800 ^oC with various catalysts at tube gasifier	900 ^oC at tube gasifier	Tube Gasifier	General Aspen Plus model at 950 ^oC
H_2	64.5	53.3	59.3	52.3
CH_4	3.0	8.7	3.5	3.9
CO	3.7	18.3	23.6	25.3
CO_2	6.5	19.1	8.7	14.0
C_2H_4	1.4	4.2	7.9	2.2

From modelling aspect, further research is still required to further understand waste-steam-gasification reaction kinetic. The current research gap is to understand the interaction between the H-radicals originated from steams and the diverse polymer feedstock (from MSW). Researcher hypothesised that the excess H radicals may result in an increased release of syngas during pyrolysis stage [414]. Other researchers demonstrate the distinct impact of steam on char porosity and potential syngas release [415] and its potential catalytic properties [416].This aspect has been investigated for biomass but not for plastic or waste stream [417].

Relating this to this work, the pyrolysis correlation accuracy may diminish, as it originates from air gasification data [360]. It is theorised that in steam gasification, the excess H-donor might influence polymer decomposition reactions and gas release during pyrolysis. In contrast, this work steam

reaction predominantly focus on gas-phase kinetic reforming [409]. Nevertheless, despite this knowledge gap, the comprehensive gas phase kinetic steam reforming still produces similar results with external experimental data shown in Table 4-11.

To investigate the parameter further, the model is being simulated at varying temperatures (750-1050 ^{o}C), steam flow rate (1-4 kg/h), and oxygen flow rate (1-4 kg/h). Figure 4-9 shows the surface response at varying gasification parameters. The syngas composition is shown in Figure 4-10, Appendix B.4, and B.5. High HV is desired when energy recovery via oxidation is the preferred utilisation of syngas [418]. Meanwhile, the H_2/CO ratio needs to achieve a specific concentration for syngas synthesis. Tar concentration is relevant for most syngas utilisation apart from direct combustion (boiler). Finally, CGE shows the overall gasification efficacy.

For HV, at zero oxidants, the HV is notably high (>12 MJ/kg). increasing steam flow rate elevates HV (maximum of 14.82 MJ/kg at 2 kg/h steam flow rate, Figure 4-9 A1). This was achieved due to the minimal oxidant presence that converts CO into CO_2, while the incoming H_2O transformed into a high heating value H_2 (141 MJ/kg). However, adding more steam is not always beneficial, as the H_2 production also converts the high heating value CO (~10 MJ/kg) into CO_2 (0 MJ/kg (RXN 17)). This is shown in Figure 4-10 (B1, O_2 = 0kg/h) where the CO mol concentration increases and peaks at 2 kg/h and decreases afterwards.

Increasing the oxygen flow rate would rapidly reduce the HV (Figure 4-9 A1, O_2= 0 to 4 kg/h) as it converts the high heating value hydrocarbons (~40 kJ/kg) and CO and CO_2. The high O_2 flow rate also disturbs H_2 production The high oxygen flow rate converts the H_2 back to H_2O via combustion. This can be observed in Figure 4-10 (A1) where there is a steady increase of H_2 concentration at increasing steam flow rate at O_2 = 0 kg/h. However, at a high oxygen flow rate (O_2 = 4kg/h) the H_2 concentration peaks at H_2O= 2 kg/h and diminish afterwards, as the H_2 concentration is combusted.

Although a low oxidants flow rate produces a high HV syngas, it is important to note that the low gas flow rate generates minimal gas yield. Moreover, this operating condition is considered a pyrolysis reaction that produces a high content of tar and other byproduct (char and oil) [419]. Other experimental studies also found a similar HV range of 8-15 MJ/kg [420] [421].

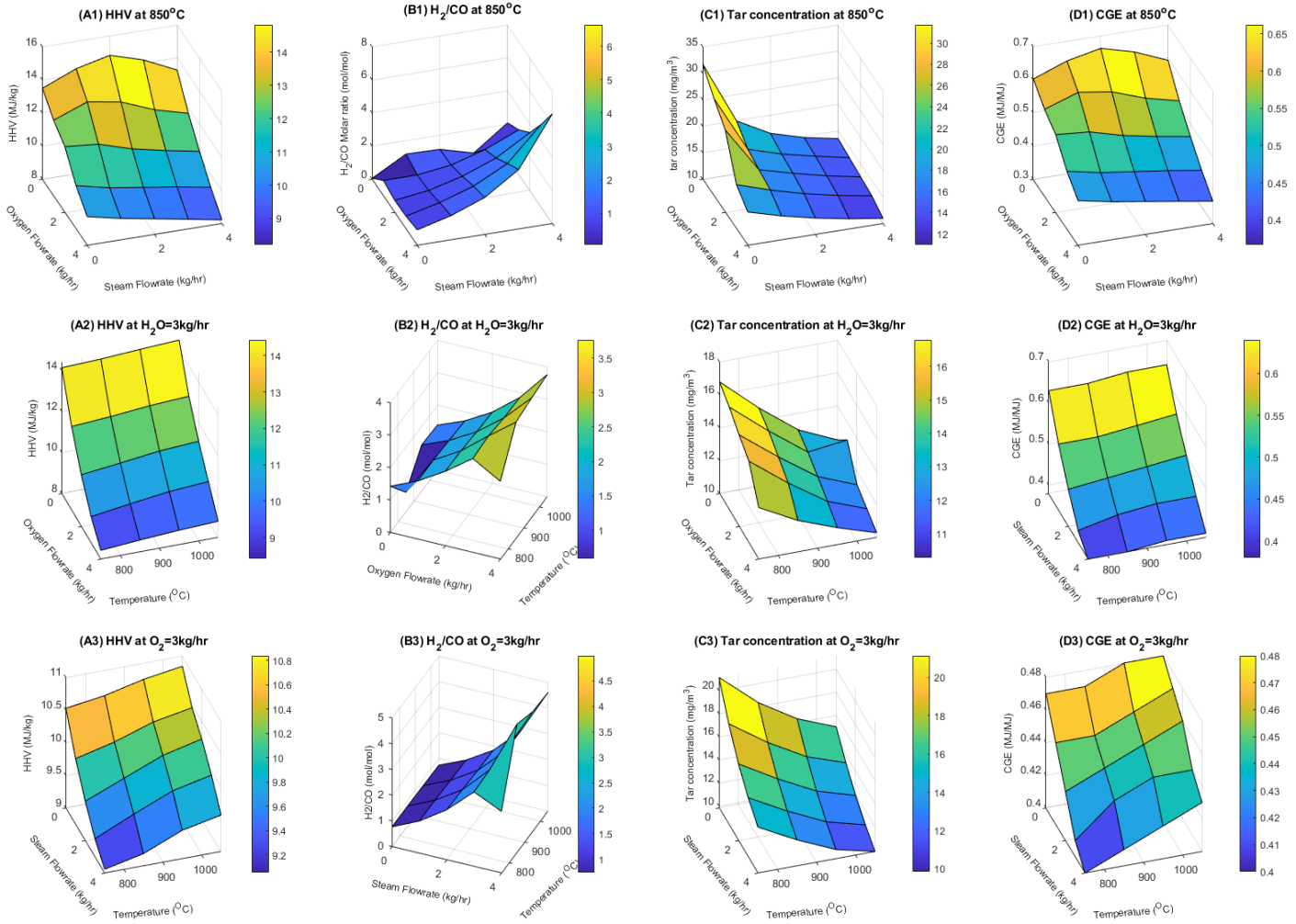

Figure 4-9: Crude Syngas properties of (A) HV, (B) H_2/CO Ratio, (C) Tar concentration and (D) CGE at varying temperature, oxygen, and steam flow rates, where (1) constant temperature (2) constant steam and (3) constant oxygen flow rate.

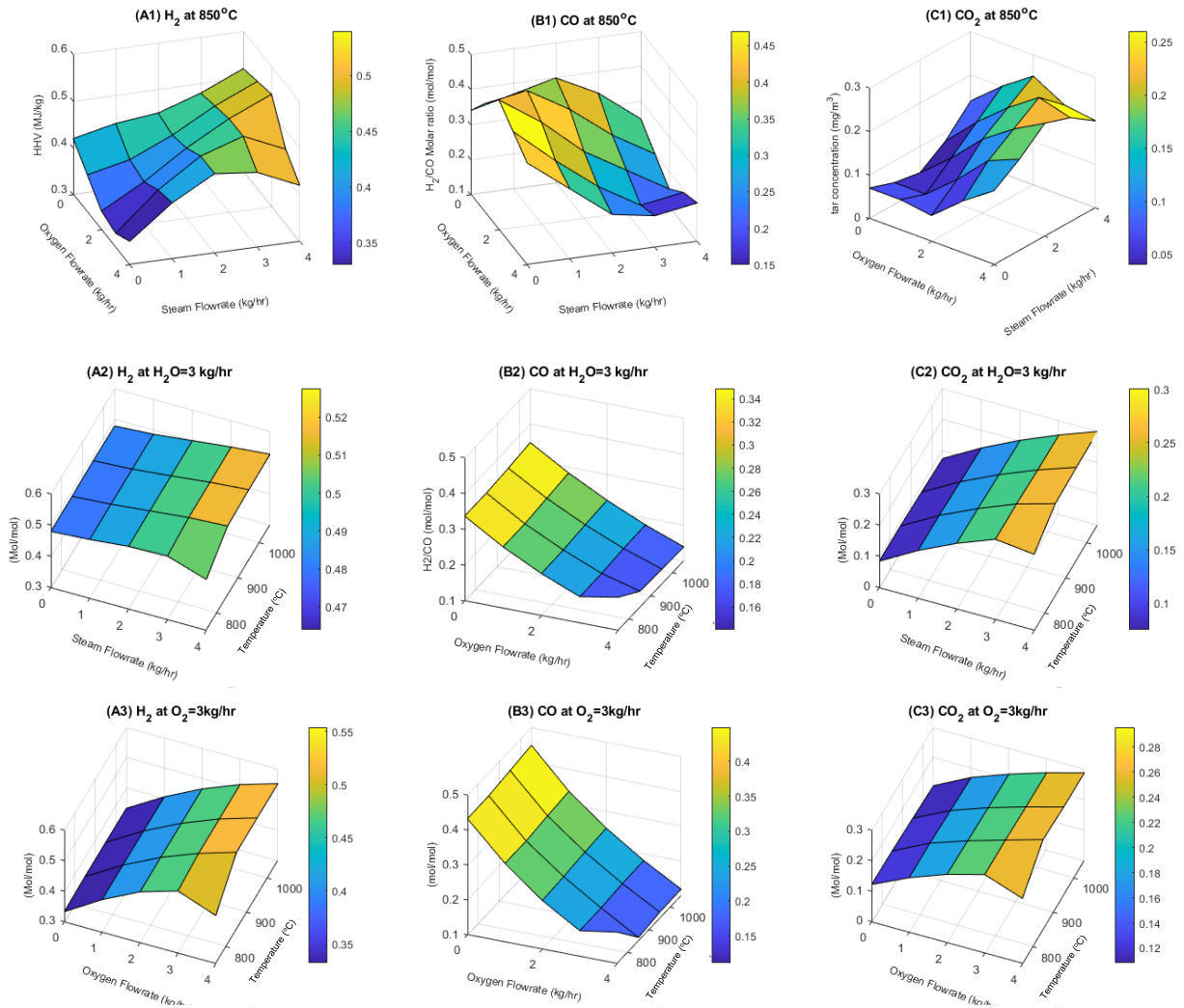

Figure 4-10: Syngas mol fraction of (A) H2, (B) CO, (C) CO_2, at varying temperature, oxygen, and steam flow rates, where (1) constant temperature (2) Constant Steam and (3) Constant Oxygen flow rate.

Increasing the temperature from 750 to 1050 ^{o}C shows a less pronounced effect on HV compared to the significant impact of raising steam or oxygen flow rates from 0 to 4 kg/h (Figure 4-10, A2 and A3). Temperature's influence was more evident when combined with increasing steam flow rate (Figure 4-9, A3), less so with oxygen flow rate (Figure 4-9, A2). This trend is likely due to oxygen's strong oxidising nature. Temperature exhibited a more substantial role in enhancing CGE (Figure 4-10, D3), as temperature increases endothermic reduction reactions. This result in a higher syngas production and overall efficiency [422]. Dalai et al. [423] also found no significant heating value increment at increasing gasification temperatures.

For H_2/CO, as the literature suggested, steam injection arose to be the most influential parameter in achieving high a H_2/CO ratio. Figure 4-9 B1 demonstrates this trend, where increasing steam injection from 0 to 4 kg/h elevates the H_2/CO ratio from 0.07 to 2.08 kg/h. Notably, at zero steam injection, increasing oxygen flow rates fails to enhance the H_2/CO ratio. However, under high steam flow rates (Figure 4-9, B1, H_2O = 4 kg/h), elevating the oxygen flow rate improves the ratio from 2.08 to 6.6 mol/mol. This is achieved because the introduced oxygen would react with the carbon monoxide, converting it into CO_2 via combustion and further increasing H_2/CO.

Increasing the temperature from 750 to 850 ^{o}C would increase the H_2/CO ratio, reaching a plateau thereafter (Figure 4-10 B2 and B3). This trend aligns with the decrease in H_2 molar concentration at lower temperatures (Figure 4-10 A2 and A3). The decrease may stem from lower temperatures enabling reaction completion at a lower oxidant flow rate, resulting in complete water gas shift reforming. Thus, high-temperature gasification is preferred to maintain reaction equilibria. Although steam injection is the primary method for enhancing the H_2/CO ratio, other approaches may include electrochemical reduction [424], chemical looping [425], and catalyst [426].

For tar concentrations, an outlier emerges with a high tar concentration at zero gasifying flow rate, reaching 31.73 mg/m^3 (Figure 4-9 C1). This outcome arises due to the system operating under pyrolysis conditions that produce complex by-products. Introducing oxidants (whether it is steam or oxygen) rapidly reduces the concentration. The model encompasses tar reforming via oxygen (RXN 9 and 10) and steam (RXN 20). Furthermore, increasing temperature significantly impacts tar concentration reduction, more distinct to other syngas parameters (HV and H_2/CO ratio). Low-temperature gasification (around 750 °C) is known to yield elevated levels of single-ring (polar) tar [427]. The model illustrates a decline in tar concentration from 16.79 mg/m^3 to 11.93 mg/m^3 with a temperature increase from 750 to 1050 °C (Figure 2 C2, O_2=0 kg/h). This is reflected as tar cracking reactions used in this work are more temperature-dependent than oxidants (e.g., RXN 19 and 21). Similarly, Cao et

al. [422] highlight the significance of maintaining high-temperature gasification to minimise tar generation.

Collectively, the data suggests that the steam and oxygen flow rate combination is the most influential parameter in producing sufficient H_2/CO and HV. They synergically control the syngas production and consequently the downstream processing. Restricting the oxidant's flow rate would improve HV but simultaneously produce higher tar concentration. Temperature adjustments from 750 to 1050 °C exert limited impact on HV and H_2/CO ratio; however, they significantly influence CGE and tar concentration reduction. Thus, maintaining higher temperatures is preferred to limit tar generation, enhance gas conversion, and uphold stable reaction equilibria relevant to the kinetic employed.

4.6 Part III: NTP tar cracking reduced order correlation

This part analyses the use of a reduced order correlation technique to develop a streamlined correlation of NTP tar cracking for process modelling. Sensitivity analysis was executed to establish the deep tar cracking zone. This is done as the full operating regime may not be representable in the linear regression. From the sensitivity analysis, it was established that >16 kW is sufficient to achieve full tar cracking (Appendix B.6 and B.7).

The MLR method is employed to establish a reduced order correlation representing NTP tar cracking. It is a widely used statistical approach to define linear relationships between multiple independent variables (predictors/input) and dependent variables (target/output). The resulting linear relationship is represented by coefficients, enabling predictions of output based on independent variables. MLR methods have demonstrated efficacy across various subjects, including medical [428], environmental [429], and circular economy studies [430].

The MLR correlations were individually deduced for each output with potential input (Table 4-12, Predictors coefficients). Full linear regression coefficients are provided in Appendix B.8. Figure 4-11 illustrates the actual and predicted MLR results, supported by MLR statistics in Table 4-12. The figure demonstrates a robust linear correlation, with R^2 values ranging from 66.9% to 94.7%, featuring significant p-values. For output gas yields with small concentrations (< 10^{-2} kg/kg basis yield), logarithmic predictions are used to prevent potential negative results and errors arising from MLR coefficient intercepts.

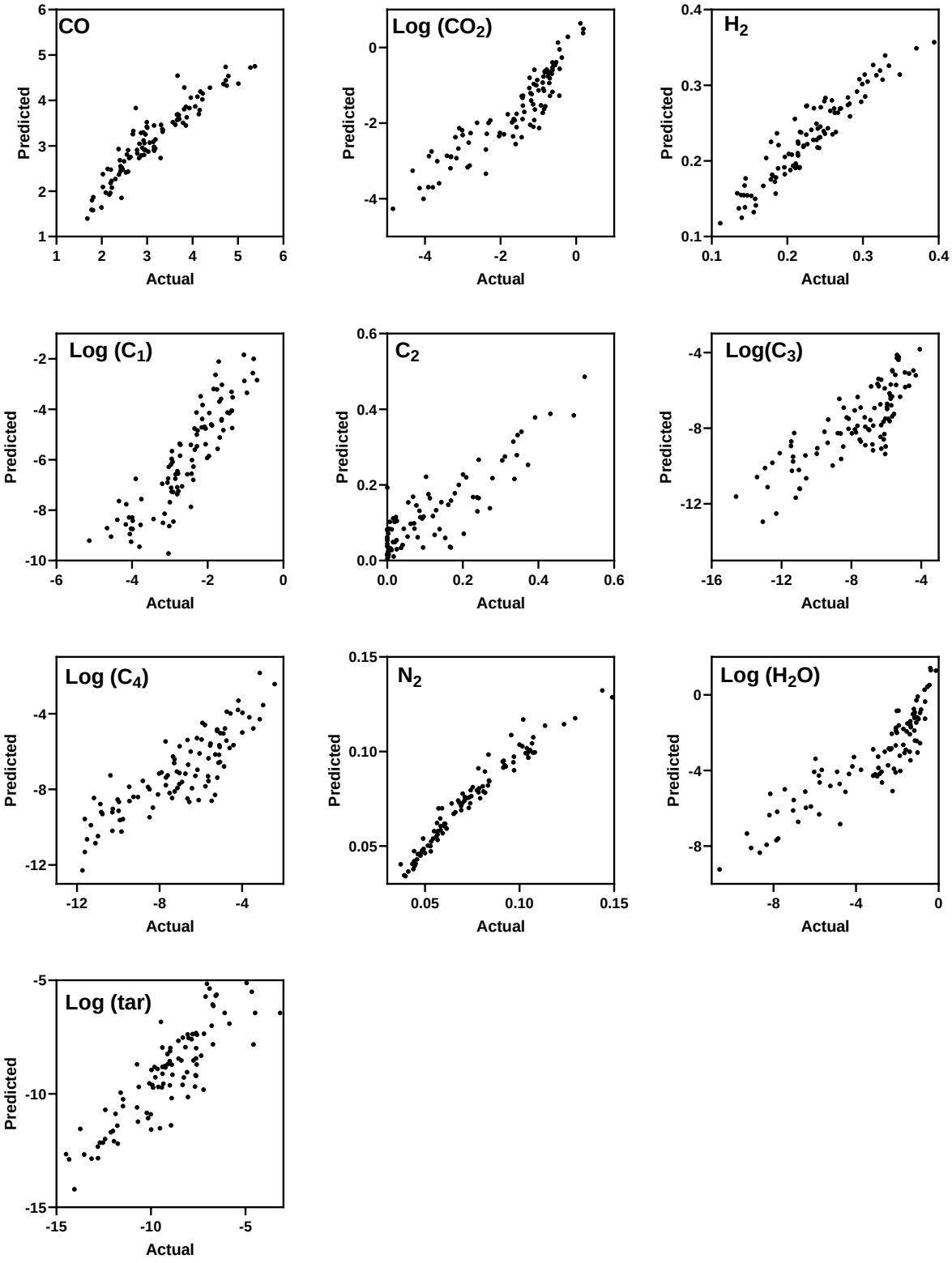

Figure 4-11: Comparison between actual and predicted MLR result for each gas compound, the R^2 is provided in Table 4-12.

Table 4-12: MLR statistical summary result.

Predicting	Predictor coefficients	R^2	F-stat	p-value	Error var	RMSD
CO	T, F, P, F^{-1}, P^{-1}, log (1), log (2), ones	87.6%	92.7	7.3×10^{-39}	0.10	0.30
Log (CO_2)	T, F, P, (2), F^{-1}, log (2), ones	82.7%	74.1	2.9×10^{-33}	1.35	0.49
H_2	F, P, (3), (5), (6), F^{-1}, P^{-1}, log (4), log (5), log (6), ones	89.4%	67.2	5.6×10^{-38}	4.55×10^{-04}	0.02
Log (C_1)	F, P, (3), (5), (6), P^{-1}, log (4), log (5), log (6), ones	80.2%	36.0	4.7×10^{-27}	1.17	6.38
C_2	T, F, P, (4×4), (4×6), (4×7), (4×8), (4×8), (4×10), (4×11), (5×5), (5×6), (5×8), (5×11), (6×6), (6×7), (6×10), (6×11), (7×5), (7×8), (7×7), (7×10), (7×11), (8×6), (8×8), (8×10), (8×11), (10×5), (10×10), (10×11), (11×11), ones	74.4%	6.7	1.1×10^{-10}	0.01	2.88
Log (C_3)		67.0%	4.4	1.47×10^{-07}	2.96	8.04
Log(C_4)		73.7%	6.2	2.23×10^{-10}	2.15	1.60
N_2	T, F, P, (10), log (10), ones	94.7%	333.0	3.52×10^{-58}	3.33×10^{-05}	7.54
Log (H_2O)	T, F, P, F^{-1}, P^{-1}, (2), (3), (3×3), (2×3), (3×2), ones	79.7%	34.9	1.41×10^{-26}	1.50	3.98
Log (tar)	T, F, P, (2×2), (2×9), (2×11), (2×12), (7×2), (7×7), (7×11), (8×7), (8×8), (8×11), (8×11), (10×7), (10×10), (10×11), (11×11), ones	73.9%	12.8	9.12×10^{-17}	1.82	6.73

Coefficients = T: Temperature, F: Flow rate, P: Power, 1: CO concentration, 2: CO_2 concentration, 3: H_2 concentration, 4: CH_4 concentration, 5: C_2H_4 concentration, 6: C_2H_6 concentration, 7: Toluene concentration, 8: Naphthalene concentration, 9: N_2 concentration, 10: Phenol concentration, 11: Benzene concentration, and Ones: Intercept

Regarding CO, the MLR correlation is predominantly influenced by CO_2 and the syngas physical condition. The high CO_2 concentration in the syngas will dissociate into CO and O radicals in a plasma reactor [224], significantly contributing to the CO yield. Similarly, for H_2, CO_2, H_2O, and C_1, the MLR is mainly dictated by inputs of the predecessor's compounds. This creates a streamlined correlation between inputs and outputs with a high R^2 ranging from 80.16% to 89.37%

However, for C_2 - C_4, the prediction becomes complicated due to their yields being influenced by (1) the recombination of smaller gases and (2) tar-cracking byproducts. Because of this, the quadratic method is adopted by multiplying tar concentrations and the small gases (C_1-C_2). The quadratic multiplication captures the synergistic impact between the two parameters governing the yield of these

compounds. The result shows a substantial linearity, albeit weaker than other correlations, as evidenced by predictions for log(C_3) with an R^2 value of 66.94%.

A similar method is adopted to predict the tar basis yield. Quadratic multiplication is done between tar input concentrations and CO_2. The inclusion of CO_2 is due to its role in donating the strong O radical that is imperative in the tar cracking process. The tar basis yield is also lumped into predicting tar instead of individual compounds due to tar's minuscule concentration ($<10^{-5}$ kg/kg).

Table 4-13: Ansys-Chemkin Pro result and predicted MLR result for scenarios A to C (Based on syngas in Table 3-2, Appendix B.9)

Compound	A actual	A predicted	B actual	B predicted	C actual	C predicted
CO	2.46	1.65	3.42	2.67	2.95	2.81
CO_2	1.96×10^{-4}	2.94×10^{-5}	9.81×10^{-3}	6.90×10^{-4}	3.55×10^{-4}	7.44×10^{-4}
H_2	0.18	0.15	0.26	0.22	0.20	0.20
C_1	9.65×10^{-4}	9.72×10^{-4}	8.72×10^{-3}	5.37×10^{-3}	1.06×10^{-3}	5.23×10^{-3}
C_2	0.35	0.19	0.29	0.21	0.22	0.21
C_3	4.43×10^{-3}	3.26×10^{-3}	4.77×10^{-3}	1.07×10^{-3}	3.44×10^{-3}	1.65×10^{-3}
C_4	1.94×10^{-2}	5.37×10^{-3}	1.07×10^{-2}	1.31×10^{-3}	7.91×10^{-3}	1.96×10^{-3}
N_2	6.40×10^{-2}	5.97×10^{-2}	7.40×10^{-2}	6.16×10^{-2}	6.19×10^{-2}	6.39×10^{-2}
H_2O	2.6×10^{-4}	1.21×10^{-3}	1.7×10^{-2}	3.01×10^{-3}	1.7×10^{-2}	7.38×10^{-3}
Tar	3.1×10^{-3}	6.54×10^{-4}	8.1×10^{-4}	1.88×10^{-4}	7.7×10^{-4}	1.91×10^{-4}

The robust R^2 values can be attributed to the utilisation of LHS, which ensures comprehensive parameter coverage, effective linear regression, and minimises potential co-linearity. However, it is important to note that while LHS enhances coverage, it may not fully capture the real statistical probability for syngas concentration yield. To analyse the MLR coefficients further, Table 4-13 presents data from the Chemkin-Ansys model from randomly selected syngas concentration from Part II (Syngas conditions shown in Appendix B.9). The predicted MLR result shows agreement with the Chemkin simulation result, affirming the ability of the MLR correlation to effectively represent NTP tar cracking and its potential applicability within the Aspen model.

Across the predicted result, the MLR shows a high accuracy ranging from 80.2% to 94.7% for smaller gases, while lower accuracy at 67.0% and 74.4% for C_2 to C_4. However, as this chapter focus on tar cracking and tar transformation into smaller gases in the deep tar cracking zone (established in Part I), the limited MLR accuracy for large hydrocarbons (C_2-C_4) would further result in a smaller error, which can be assumed to be negligible for this modelling work. Furthermore, it is essential to acknowledge that this validity is limited within the described gas concentration range. The grouping of tar compounds further implies that the reduced correlation ability to showcase actual compound products

is constrained, potentially leading to skewed results favouring specific species. Enhancing the model's scope can be achieved by incorporating additional compounds of interest, such as hypothesised radicals [431], and/or creating stages of degradation to “un-lump” the reaction kinetics [432].

In summary, the MLR correlation has predicts the NTP tar cracking with R^2 67.0% to 94,7%, simplifying the intricate reaction kinetics into linear correlations suitable for process simulation. The MLR exhibits satisfactory accuracy for light gases, but its performance is diminished for hydrocarbons and tars due to their more complex reaction mechanisms and minimal concentrations that distort the correlations. It is imperative to emphasise that the established correlation is only relevant for the given boundary condition.

4.7 Part IV: Waste Gasification and NTP tar cracking syngas recovery

This part converges the validated model (Part I), optimised operating condition (Part II), and reduced NTP tar cracking correlation (Part III) to explore the energy balance required to operate the process through multiple scenarios. The result for various energy recovery is shown in scenarios 1 to 4 (Figure 4-12 and Figure 4-13), meanwhile scenario 5 evaluates the material recovery, and scenario 6 for material-and-energy recovery (Figure 4-14 and Figure 4-15)

Waste gasification has been traditionally used for energy recover. Scenario 1 evaluates conventional air gasification with a boiler system for syngas combustion. As the syngas is immediately combusted, eliminating tar content is irrelevant. This approach yields a satisfactory amount of electricity at 0.77 kW/kg of waste. Chakraborty et al. [433] reported similar electrical production of 0.092–0.126 kW/kg of bulk waste, while Carotenuto et al. [434] reported higher energy generation of 2.54 kW/kg of dried sludge.If the process aims to employ a more advanced energy recovery with higher efficiency, the gas turbine may be adopted (Scenario 2). The system requires pre-APC cleaning and NTP tar cracking as gas turbines require tar lower than 5 mg/m^3 [12]. However, the high energy requirement for NTP tar cracking to clean syngas contaminated with N_2 results in the process requiring more energy than it can produce (0.024 kW per kg of waste, Figure 4-12). This finding elucidates that air gasification coupling with NTP tar cracking may be unsuitable for low-quality (N_2 diluted) syngas cleaning [435].

To improve the syngas quality, the system can substitute air gasification with O_2 and H_2O to increase its heating value and H_2/CO ratio [436] (Scenario 3). If this approach is adopted, the process can produce more energy than it consumes, producing a net energy of 0.2 kW/kg (Figure 4-12). However, this energy generation is significantly lower than conventional air gasification described in scenario 1. Figure 4-13 shows the evolution of energy produced by scenario 3 at increasing ER. A high ER flow

rate resulted in more complete oxidation and less CO, resulting in syngas with a lower heating value and subsequently lower energy recovery.

Scenario 4 evaluates the condition where the syngas produced has negligible impurities for fuel cell energy recovery. A fuel cell system requires minimal CO_2, N_2, and tar content, which is demonstrated by utilising the O_2-H_2O-gasification and NTP tar cracking system. Scenario 4 shows that this approach has the potential to generate energy as high as 0.69 kW per kg of waste, almost equal to conventional air gasification. A similar trend emerges as ER is increased, this is because fuel cells' energy recovery system also relies on the CO and H_2 content in syngas (Figure 4-13, 4A-4C). Although NTP appears to consume a substantial amount of power. The current power requirement of 1.80-2.00 kW/kg of waste is evidently lower than the thermal plasma requirement in the gasification process, where a study reported up to 45 kW/kg of waste [437]. Instead of energy recovery, NTP tar cracking production of tar-free syngas might enable its synthesis into methanol (Scenario 5). This pathway demonstrates the chemical recycling pathway of waste into other products [347]. Scenario 5 shows that the system produces 0.94 kg of methanol per kg of gasified waste. This is achieved when the steam flow rate of 2 kg/h at ER = 0.3 (Figure 4-15, 5C). In this scenario, increasing ER appears to be beneficial as it improves the H_2/CO ratio which is crucial in methanol synthesis. Other studies also found similar results, Zhang et al. [438] found that their model shows a yield of 0.39 kg of methanol per kg of gasified feedstock (woody biomass). Matveev et al. [439] show that 0.71 kg of kg of methanol per kg of gasified feedstock (rubber). As scenario 5 solely focuses on material synthesis, the external energy requirement in the gasification process follows an identical trend to the methanol yield (Figure 4-13, 5A-5C).

Scenario 6 evaluates the potential of capturing the uncreated syngas post-methanol synthesis for energy recovery via fuel cells. In this scenario, the low ER and H_2O flow rates are preferred (Figure 4-15 6A). This condition generates excess CO with a low H_2 yield (required in methanol synthesis), resulting in the process that retrieves most of syngas energy while having a low methanol yield. Because of this combination, the model shows that the gasification process can be self-sustaining requiring only 0.046 kW for the yield of 0.25 kg of methanol/kg of waste (Figure 4-15 6A ER=0.1). In contrast, Babarit et al. [440] estimate that it requires 11.2 kWh to produce 1 kg of methanol, via traditional natural gas synthesis.

However, as the ER and steam flow rate were increased, the rise in H_2/CO ratio led to more methanol production, subsequently lowering the post-syngas CO and H_2 concentration required for energy generation. Figure 4-15 (6C) shows that more external power is required when the process produces

more methanol, lowering the methanol productivity. Scenario 6 demonstrates that the co-production of methanol and power in series is not an ideal approach. Both processes demand the valuable species within syngas which creates competition. Both processes also favour different gasification conditions. A parallel process may be a better suitor, which is demonstrated in other studies that assess methanol and electricity co-production by using coal gasification [441, 442].

In summary, the high energy requirements of NTP tar cracking may lead to low energy production, as the energy generated from the syngas is primarily utilised internally for plasma power generation. This finding emphasises the need for NTP tar cracking advancement to focus on its efficiency, whether it is through reactor design, process retrofitting, or catalyst coupling [14], with the objective to minimise its energy expenditure while achieving deep tar cracking. Although energy recovery appears to be an unfavourable approach in this study, NTP tar cracking demonstrates its feasibility to produce tar-free syngas. Indicating that NTP tar cracking should be employed for advanced gasification process that demands "ultraclean" syngas for material synthesis. The data shows that the co-production of methanol and electricity is not ideal due to both processes competing for (1) favourable gasification operating conditions and (2) H_2 and CO in syngas. Nonetheless, it is important to note that the result of this study is constrained to the inputted data. Advanced processes such as air separation, methanol synthesis, and fuel cells are argued to be more complicated than the conventional air-boiler-waste-gasification process. Further analysis may be required, specifically in terms of a feasibility study in relation to process yield and capacity.

In the future, researchers should explore the possibility of improving NTP tar cracking efficiency to achieve deep tar cracking with lower energy intake, whether it is through novel reactor design, coupling with catalyst, or integration with other tar elimination strategies [14]. Process retrofitting studies such as renewable energy integration [14] and chemical looping [443] can be done to minimise external energy requirements. From the modelling point of view, future work may explore a multi-software interface program to bridge the process modelling with the NTP tar cracking reaction kinetic (e.g. CAPE-OPEN [444]).

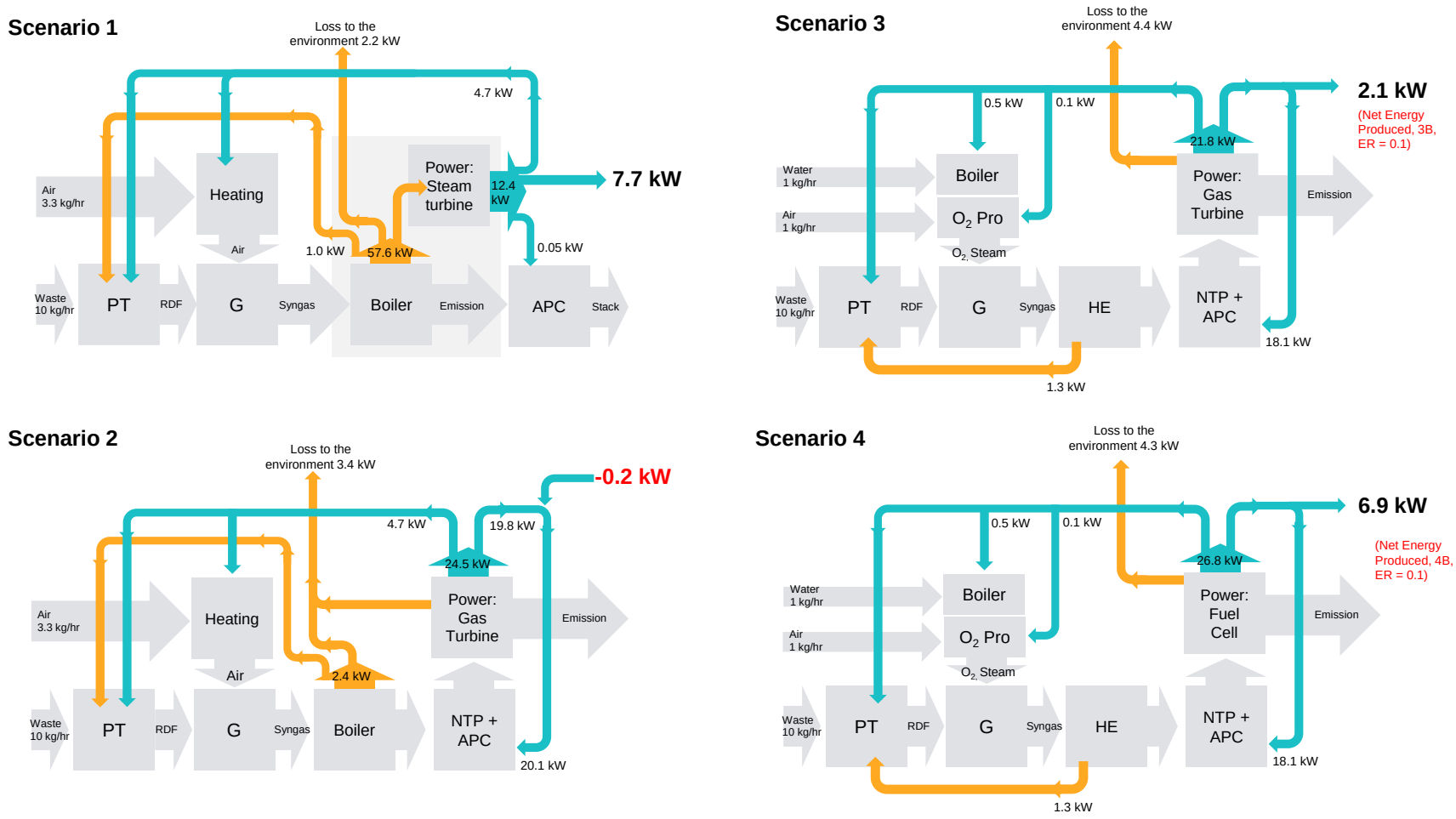

Not to scale, ➡ : Power, ➡ : Heat, ➡ : Material, PT: Pretreatment, G: Gasification, APC: Air Pollution Control, O_2 Pro: Oxygen Production, NTP: Non-thermal plasma tar cracking, HE: Heat recovery.

Figure 4-12: Flowchart for energy production scenarios one to four. Scenario 2 and 3 varying oxygen and steam injection is shown in Figure 4-13

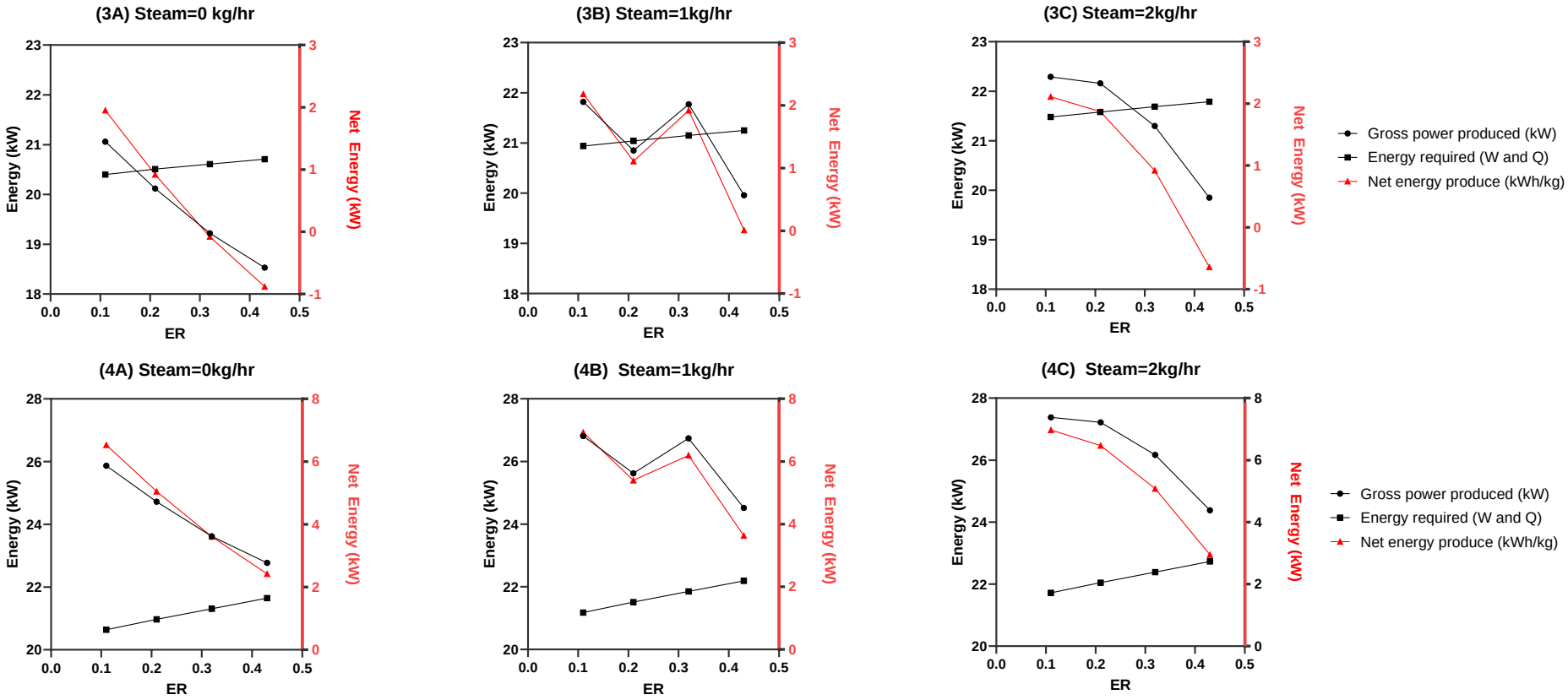

Figure 4-13: Energy produced from waste gasification at increasing ER for scenarios 3 and 4 for steam flow rate at 0 (A), 1 (B), and 2 (C) kg/h.

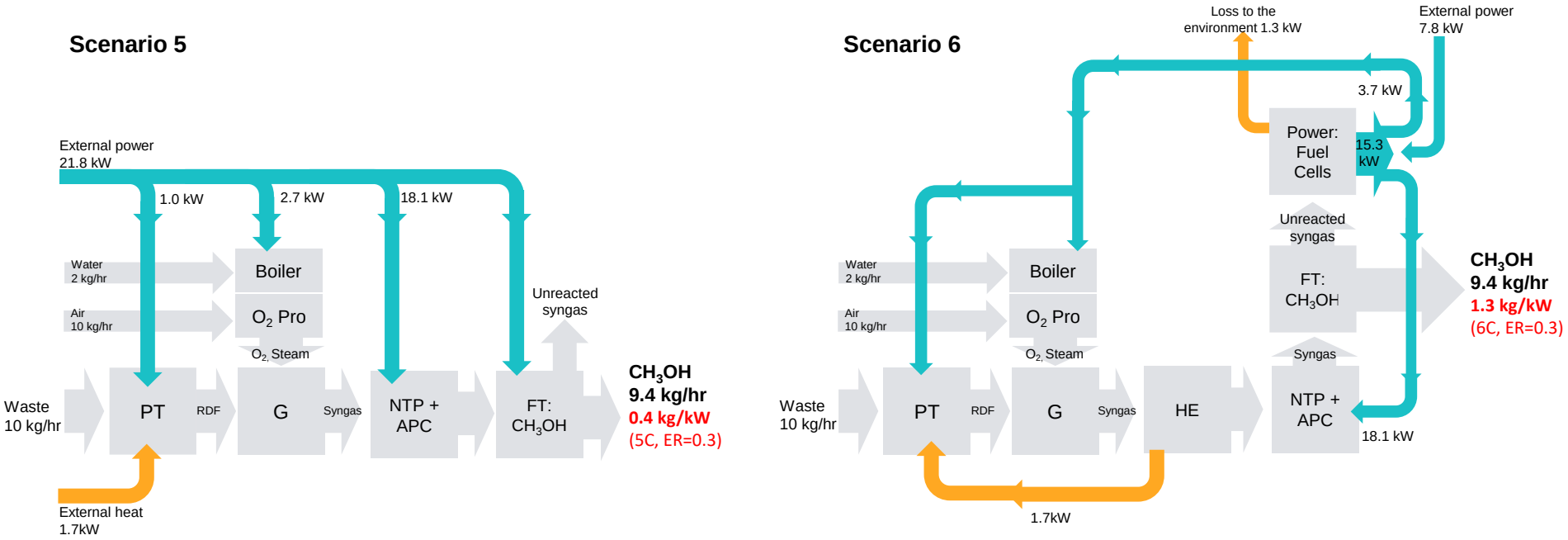

Not to scale, : Power, : Heat, : Material, PT: Pretreatment, G: Gasification, APC: Air Pollution Control, O_2 Pro: Oxygen Production, NTP: Non-thermal plasma tar cracking, FT: Fischer-Tropsch

Figure 4-14: Methanol production (scenario 5) and methanol-power production (scenario 6), where the methanol production (kg/h) and methanol efficiency (kg/kW) are shown in Figure 4-15.

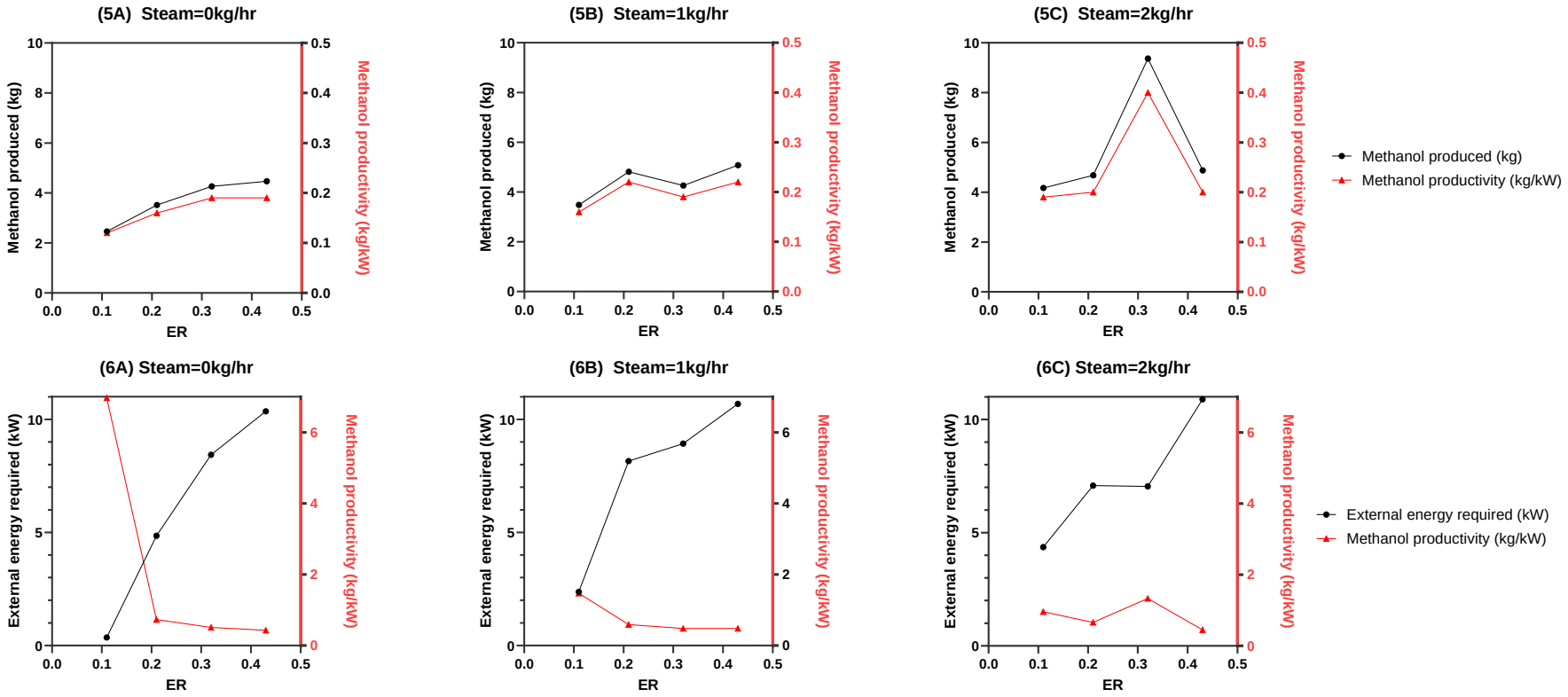

Figure 4-15: Methanol produced from waste gasification at increasing ER for scenarios 5 and 6 for steam flow rate at 0 (A), 1 (B), and 2 (C) kg/h.

4.8 Conclusion

This chapter conducted waste gasification modelling, validating the syngas composition against external experimental results collected from literature. The model predicts the syngas composition that shows agreement with the trends across varying ER was. However, traditional air gasification appears to be unsuitable for advanced syngas utilisation. Temperature, steam, and oxygen injections optimisations were executed. Elevated steam and oxygen flow rates enhance the H_2/CO ratio, while higher oxygen injection consistently lowers syngas heating value. Although temperature shows a minimal impact on the syngas quality, higher gasification temperature is favoured to maintain reaction consistency and lower tar production. Furthermore, The NTP tar cracking unit is represented using the MLR method, simplifying kinetic reactions into multilinear coefficients. The MLR coefficients were able to predict the reaction kinetic with negligible errors, with R^2 values ranging from 66.94% to 94.66%. Energy analysis of waste gasification NTP-tar cracking highlights the need to adopt advanced energy recovery (e.g., fuel cells), due to the high energy demand of NTP tar cracking. Consequently, the NTP tar cracking unit is better suited for product synthesis. Moreover, combined material and power production is not an ideal approach as both productions compete for the ideal operating conditions and valuable syngas species (CO and H_2).

Chapter 5
Analysis of Thermal Plasma Gasification Environmental Impact Studies

The bulk of this chapter have been published as the following manuscript: Sanjaya, E. and Abbas, A., 2023. Plasma gasification as an alternative energy-from-waste (EFW) technology for the circular economy: An environmental review. Resources, Conservation and Recycling, 189, p.106730.

5.1 Introduction

Energy-from-Waste (EFW) is a resource recovery option that lies between recycling and disposal (landfilling) in the waste hierarchy [28]. EFW has been predominantly absent in countries such as Australia due to constant regulatory hesitation and social backlash against EFW [30, 31]. Research effort continues to seek and identify EFW technologies alternative to incineration [33], but incineration remains the relevant EFW technology. Gasification, an alternative EFW technology, partially oxidises waste into synthetic gas (syngas) that can be combusted for energy, synthesized for fuel [34], or refined for hydrogen [35] and/or other chemicals [36]. The production of tar as a gasification by-product has however hampered the progress of this technology [264]. Tar condensation and agglomeration block piping and deactivate catalyst [9], restricting syngas application to only combustion. Tar in syngas confines the application of syngas to combustion, rather than advanced fuel and chemical production. [445, 446].

Tar removal can be done with plasma. Plasma is the fourth state of matter that consists of ionised gas that can induce tar reduction reactions, converting it into simpler gases [104], both thermal plasma and NTP. Thermal plasma gasification refers to the process of utilising thermal plasma to assist the gasification reactions while simultaneously reducing syngas' tar concentration [447]. Meanwhile, NTP utilisation has been demonstrated on a lab scale for surrogate tar compounds [16]. The low tar content in syngas from plasma gasification allows advanced syngas conversion that is unfeasible for conventional gasification [104]. As this technology has not been fully embraced as the preferred EFW,

a comprehensive understanding of technological & commercial readiness levels (TRL and CRL), environmental impact, and public perception need to be adequately understood before implementation and related policy development. As waste management option, it is imperative to explore the status and environmental impact of plasma gasification, in comparison to the more traditional waste management.

Moreover, LCA is an internationally well-known methodology for assessing the environmental impacts of products, processes, or services. LCA has become the preferred and standardised method to address waste management's footprint [250]. Although ISO14040/44 exists to govern the transparency and accountability of LCA studies, the principle still allows room for interpretation [251, 253] or perhaps misinterpretations. Laurent et al. [254] reported that malpractices exist across different LCA studies arising from not following the standard properly, such as omitting the system boundary, impact coverage, and sensitivity analysis [255]. Even within an appropriate framework, significant differences can still occur from identical data when processed by different models, eventually arriving at different conclusions [256]. Hence, transparency in LCA assumptions and scope is important to provide confidence in the result [251, 252]. This means reviewers have a crucial role in the assessment of whether certain LCA is suitable and follows ISO14040/44 [255]. Most researcher points out that LCA results are strongly influenced by geographical location, system boundary, scenarios, and functional unit [448]. Attempts to examine whether there is a straightforward pattern in waste management strategies often find complexity in the field, and variability in the LCA studies.

5.2 Research Background

5.2.1 Research Gaps and Niche

There is an absence of systematic analysis of environmental studies that assess advanced EFW to the more traditional incineration and landfilling. From the methodology perspective, LCA reviewers often do not systemically compare the LCA results. Benchmarking LCA's result for systematic analysis requires excessive data streamlining. Because of this, reviewers often resort to qualitative comparisons of different LCA results. Moreover, most LCA reviews focus mainly on comparing the different environmental impacts of recycling, landfilling, and incineration, with limited studies that consider the EFW technological diversity. Some reviewers emphasised the need to analyse advanced thermal

conversion in comparison to incineration, and its impact on the broader environment and waste management [250, 251, 449]. Table 5-1 shows this Chapter novelty.

Table 5-1: Chapter 5 novelty in comparison to other published work.

Ref	LCA analysed	Scope	Findings
Present work	25	Plasma & conventional gasification LCA	Quantitatively compare available LCA on plasma and conventional gasification. Plasma gasification has clear environmental benefits over landfilling and incineration; however, conventional gasification is only beneficial when compared to landfilling, not incineration. Plasma gasification may be a better suitor for CE, but clear incentives are necessary.
[450]	15	LCA studies on plastic waste management	Different LCA studies are tailored to each regional scenario, comparison should be done cautiously. While most studies find recycling to be favourable, a case study found recycling is not as favoured when transportation is considered
[451]	101	EFW environmental impact and uncertainty	While there is general agreement on incineration over landfilling, other EFW can affect different impact categories in contradicting ways. Selecting waste management should be case-specific (geographical location, social and economic aspects, etc.).
[452]	45	MSW management strategy	The article argues the need to target recyclable and organic management to minimise environmental impact. The review provides research gaps in waste management LCA.
[449]	27	Environmental impact of MSW management	Consensus agreement on favourable environmental impact for anaerobic digestion and landfill gas capture to produce electricity. Global warming impact is lower when incineration replaces landfilling but with uncertain health impact. Unclear conclusion on diversion of organic waste from anaerobic digestion to incineration
[448]	79	LCA of MSW management and strategy	Clear and defined scope is an important step in LCA. Sensitivity analysis is needed for a reliable result, yet it's only presented in 39% of LCA studied. A combination of recycling and resource recovery is the most appropriate strategy, however with high capital investment, this strategy is only suitable for high-income regions. For low-income areas, it is advised to promote waste reduction, or utilise cheap labour for decentralised recycling.

5.2.2 Chapter's Aim

This chapter aims to quantitively analyse each plasma and conventional gasification LCA to other waste management strategies, utilising a technique introduced by Villanueva and Wenzel [453] and later utilised for EFW by Istrate et al. [449]. This meta-analysis has not been utilised to assess gasification or thermal plasma gasification implementation. In comparison to the rest of the thesis, this chapter do not focus on the NTP as tar abatement strategy, rather, it focusses on is predecessor, that is the utilisation of thermal plasma for waste gasification. Nevertheless, this work aligns with the thesis as it concerns with plasma abatement method and its environmental implications. For NTP, its novelty resulted in the lack of LCA studies for this technology, which renders this chapter's ability to assess their LCA. NTP implementation with waste gasification LCA is presented in Chapter 6. Hence, in this chapter, plasma gasification refers to the thermal plasma aided waste gasification.

5.3 Meta-Analysis Methodology

In this chapter, meta-analysis comparisons were made to answer the following research question: Is the environmental performance of plasma gasification (PG) better than that of landfilling (LF) and other thermal conversion processes (incineration (INC), pyrolysis (PYRO) and gasification (GAS)). For comprehensiveness, the study also included the benchmarking of conventional gasification to landfilling and incineration.

The studies were obtained via the search engine Scopus Google Scholar. The keywords were "gasification", "life cycle", and "environment", with articles as late as November 2021. Because of the research question, the chapter is limited to LCA studies that compare different thermochemical processes. To minimise complexity in our exercise, this comparison omits the inclusion of the cascading process of gasification-pyrolysis, single scenario LCA, or LCA that evaluates feedstock variability. Moreover, due to the scarcity of plasma gasification LCA studies, the study also included a study that did not include energy recovery [454]. Table 5-2 summaries the LCA studies analysed in this chapter that is further elaborated in Table 5-4. The LCA work result is extracted and compared through meta-analysis methodology described in Figure 5-1.

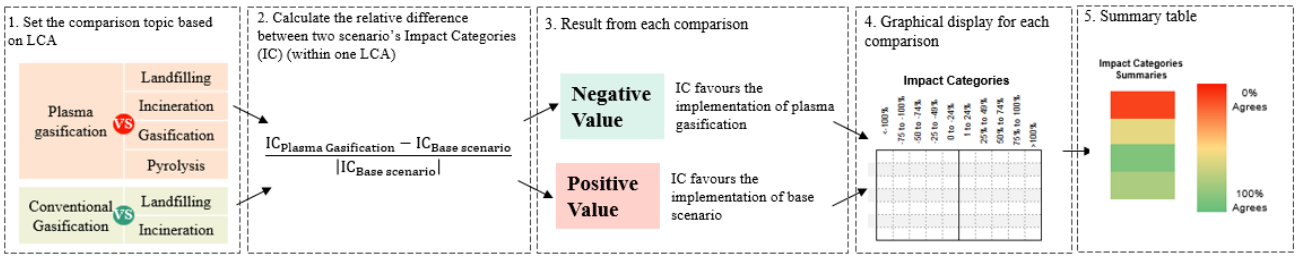

Figure 5-1: Methodology for environmental LCA comparative assessment of EFW technologies using relative differences of each impact category (modified from [449]).

Other reviewers have signalled the challenges in comparing results across LCA studies [252, 450]. The different system boundaries, assumptions and scenarios are bound to produce complexity in the benchmarking. To navigate the complexity, this study adopted a comparison method outlined by Istrate et al. [449]. Figure 5-1 shows the approach to estimating whether certain impact categories favour plasma gasification, which is later collected as a graphical display. Firstly, the result is extracted from each LCA. Secondly, the comparison between different scenarios is calculated through their relative difference, the result of the relative differences is later collected and mapped out as a graphical display. Finally, the trend, correlation, and causation were discussed. By doing this, the relative difference of plasma gasification to the base scenario can be drawn across different studies, without sacrificing the different scenario conditions across different LCA. The same approach is also used for conventional gasification technology. Table 5-3 outlines the impact categories assessed in this study. These impact categories were selected due to their relevancy and utilisation across LCA works.

As this chapter focuses on the impacts of different EFW technologies, it is understood that waste separation, transport, and supporting treatments have a significant impact on the result. However, singling out these variables can be challenging and requires a great deal of assumptions [252]. The adopted methodology is used to examine the trend across different scenarios without excessive data treatment.

Table 5-2: LCA studies included in this analysis study (Detailed descriptions in Appendix C).

Ref	Functional unit	Location	Model	Method	Comparison on				
					LF	GAS	PG	PYRO	INC
[455]	1 tonne of Refuse Derived Fuel (RDF) from landfill	Belgium	SimaPro	ReCiPe	X		X		
[456]	1 kg of MSW	United Kingdom	GaBi		X	X	X	X	X
[457]	1 kg industrial organic hazardous waste	Hungary	GaBI	CML		X	X	X	X
[454]	1 tonne of incineration fly ash		OpenLCA-Ecoinvent	ReCiPe	X		X		X
[458]	1 tonne of MSW	Global data	GaBI	CML			X		
[459]	1 tonne of MSW	Global data	GaBI	CML		X	X		X
[460]	1 tonne of MSW		GaBI	CML		X	X	X	X
[461]	1 tonne of MSW		GaBI	CML		X	X		
[462]	1 MJ of energy		SimaPro	Recipe			X		X
[463]	1 kg of waste and 1 MJ of gas produced	United Kingdom	Simapro	CML	X		X		X
[464]	1 tonne medical waste	China	OpenLCA-Ecoinvent;	CML			X	X	X
[465]	1 MJ of fuel	United State				X	X		
[466]	1 tonne of product gas	Singapore	GaBi	EDIP		X		X	
[467]	297,200 tonne per annum (tpa)	Italy	USES-LCA			X			X
[468]	1 tonne of solid waste	Europe	SimaPro	Impact 2002+		X			X
[469]	1 tonne of biomass	Japan	GEMIS			X			X
[470]	1 tonne of waste	Spain	SimaPro	Impact 2002+	X	X		X	X
[471]	1 tonne of MSW	USA	TRACI		X	X			X
[472]	1 tonne of MSW	South Europe			X	X			
[473]	1 MJ of energy	Spain	EcoInvent	ReCiPe		X			X
[474]	1 GWh of energy	Sweden	ORWARE		X	X			X
[475]	1 tonne of MSW	Indonesia			X	X			X
[476]	1000 tonnes of food waste	Singapore	GaBi	CML		X			X
[477]	1 tonne of MSW	China, France, Finland				X			X
[478]	1 MWh of energy		SimaPro	ReCiPe		X			
[479]	1 tonne of MSW	China	GaBi	EDIP		X			X
[480]	1 kg of mixed plastic and paper	Australia	SimaPro	CML	X	X			X

LF: Landfilling, GAS: Gasification, PG: Plasma Gasification, PYRO: Pyrolysis, INC: incineration

Table 5-3: Overview of LCA impact categories analysed in this chapter [481]

Impact Category	Abbreviation	Definition
Global Warming Potential	GWP	Multiple greenhouse gases and their impact on climate change, represented as relatives to CO_2. It can be reported as 20 years or 100 years (GWP20 and GWP100 respectively). GWP20 is used to evaluate strong greenhouse gases with shorter lifetime, such as methane.
Acidification Potential	AP	The impact of acidic gases such as nitrogen and sulphur oxides, on decreasing the pH value of rainwater and soil. It is represented as H^+ equivalent.
Abiotic Depletion Potential	AD	The consumption of non-living resources, the impact often separated as fossil fuels (AD-F, presented as MJ equivalent) and elemental (AD-F, presented as antimony equivalent). Other similar categories are Fossil Fuel Depletion (FFD) and Metal Depletion (MD)
Eutrophication potential	EP	Fertilising element (nitrogen and phosphorous) emission that will excessively enrich the ecosystem. It can be separated depending on its impact on freshwater and marine.
Photochemical ozone creation potential	POCP	Multiple gases that affect the creation of ozone in the lower atmospheric (smog) due to volatile organic compound reacting with sunlight. Various gases contribute to smog formation, it is represented as nitrogen oxides equivalent.
Ozone Depletion Potential	ODP	Air emissions of halon gases that destroy the protective ozone layer at the stratospheric layer, it is presented as chlorofluorocarbon (CFC-11) equivalent.
Human Health		Comprise of multiple categories such as human toxicity potential (HTP, from solid and air), Ionising radiation (IR), Respiratory inorganics, Climate Change on Human Health (CCHH) and Particulate Matter (PM) formation
Environmental impact		Other environmental impact such as ecotoxicity in freshwater (WE), marine (ME), and terrestrial (TE), land occupation in agriculture and urban (ALC, ULC), and primary energy demand (PED). Provide in Appendix C.1

Table 5-4: Case studies of different scenarios collected from various LCA studies (Appendix C.1).

Ref	Plasma Gasification/Conventional Gasification	Base scenario	Code
Plasma gasification vs Landfilling			
[456]	Sc6 Gasification + plasma cleaning	Sc1 Landfill	PGLF1
[454]	Sc1 Plasma vitrification	Sc4 Solidification and landfill	PGLF2
[460]	Co5 Plasma gasification	Co3 Landfill [456]	PGLF3
[463]	Sc5 Advance thermal two stage plasma gasification	Sc2 Separated organic into AD and other to recycling and landfill	PGLF4.1
	Sc5 Advance thermal two stage plasma gasification	Sc4 Separated organic into AD and other to landfill	PGLF4.2
Plasma gasification vs Incineration			
[455]	Sc1 Plasma gasification and landfilling of slag	Sc2 Incineration with landfilling bottom ash	PGINC1.1
	Sc1 Plasma gasification and landfilling of slag	Sc3 Incineration with bottom ash aggregate production	PGINC1.2
	Sc5 Plasma gasification with polymer cement production from slag	Sc2 Incineration with landfilling bottom ash	PGINC1.3
	Sc5 Plasma gasification with polymer cement production from slag	Sc3 Incineration with bottom ash aggregate production	PGINC1.4
[456]	Sc6 Gasification + plasma cleaning	Sc2 Incineration Sheffield	PGINC2.1
	Sc6 Gasification + plasma cleaning	Sc3 Incineration North Hykeham	PGINC2.2
[457]	Sc1 Plasma gasification and vitrification	Sc2 Incineration without APC	PGINC3.1
	Sc1 Plasma gasification and vitrification	Sc5 Incineration with APC	PGINC3.2
[454]	Sc1 Plasma vitrification	Sc3 Thermal treatment in rotary kiln	PGINC4
[459]	Sc3 Plasma gasification	Sc1 Incineration	PGINC5
[461]	Sc1 two stage plasma gasification	Sc2 Incineration	PGINC6
[462]	Sc1 Syngas-from-RDF combustion produced by plasma gasification	Sc2 Hard coal combustion	PGINC7.1
	Sc1 Syngas-from-RDF combustion produced by plasma gasification	Sc3 Mixture of RDF and hard coal	PGINC7.2
[463]	Sc5 Advance thermal two stage plasma gasification	Sc1 Separated organic into AD and other to recycling and incineration	PGINC8.1
	Sc5 Advance thermal two stage plasma gasification	Sc3 Separated organic into AD and other to incineration	PGINC8.2
[464]	Sc3 Plasma melting	Sc1 Rotary kiln incineration	PGINC9
Plasma Gasification vs Conventional Gasification			
[456]	Sc6 Gasification + plasma cleaning	Sc5 Gasification + syngas combustion	PGGAS1
[457]	Sc1 Plasma gasification and vitrification	Sc4 Gasification	PGGAS2
[459]	Sc3 Plasma gasification	Sc2 Gasification	PGGAS3
[465]	Sc2 Plasma gasification - Fischer Tropsch	Sc1 Conventional gasification - Fischer Tropsch	PGGAS4.1
	Sc2 Plasma gasification - Fischer Tropsch	Sc3 Conventional gasification - Alcohol synthesis	PGGAS4.2
Plasma Gasification vs Pyrolysis			
[456]	Sc6 Gasification + plasma cleaning	Sc4 Fast-pyrolysis + combustion	PGPYRO1
[457]	Sc1 Plasma gasification and vitrification	Sc3 Pyrolysis	PGPYRO2
[464]	Sc3 Plasma melting	Sc2 Pyrolysis-incineration	PGPYRO3
Gasification vs Landfill			
[456]	Sc5 Gasification + syngas combustion	Sc1 Landfill	GASLF1
[471]	Sc4 Gasification	Sc1 Landfill	GASLF2.1
	Sc4 Gasification	Sc2 Landfill gas capture	GASLF2.2
[472]	Sc3 fluidised bed gasification – Organic Rankine cycle	Sc5 Landfilling	GASLF3.1
	Sc2 fluidised bed gasification – Internal combustion engine	Sc5 Landfilling	GASLF3.2
[474]	Sc1 Gasification with catalytic combustion	Sc4 Landfilling with gas recovery	GASLF4.1

Ref	Plasma Gasification/Conventional Gasification	Base scenario	Code
	Sc2 Gasification with flame combustion	Sc4 Landfilling with gas recovery	GASLF4.2
[475]	Sc4 Gasification and AD	Sc1 Landfilling	GASLF5.1
	Sc6 Gasification	Sc1 Landfilling	GASLF5.2
	Sc4 Gasification and AD	Sc2 Landfilling with gas recovery	GASLF5.3
	Sc6 Gasification	Sc2 Landfilling with gas recovery	GASLF5.4
[480]	Sc3 Gasification Pyrolysis (mixed paper)	Sc1 Landfill (mixed paper)	GASLF6.1
	Sc6 Gasification Pyrolysis (mixed plastic)	Sc4 Landfill (mixed plastic)	GASLF6.2
[470]	Sc5 Mechanical recycling, gasification, and ash landfill	Sc1 Mechanical, biological recycling, and landfill	GASLF7.1
	Sc5 Mechanical recycling, gasification, and ash landfill	Sc2 Mechanical, biological recycling, and landfill gas capture	GASLF7.2
	Sc11 Gasification	Sc13 Landfill	GASLF7.3
	Sc11 Gasification	Sc14 Landfill gas capture	GASLF7.4
Gasification vs Incineration			
[456]	Sc6 Gasification + plasma cleaning	Sc2 Incineration Sheffield	GASINC1.1
	Sc6 Gasification + plasma cleaning	Sc3 Incineration North Hykeham	GASINC1.2
[457]	Sc4 Gasification	Sc2 Incineration without APC	GASINC2.1
	Sc4 Gasification	Sc5 Incineration with APC	GASINC2.2
[478]	Sc2 Gasification	Sc1 Incineration	GASINC3
[460]	Sc1 Low temperature gasification	Sc2 Incineration	GASINC4
[468]	Sc1 vertical shaft gasifier	Sc2 incineration	GASINC5
[469]	Sc2 Gasification	Sc1 Incineration	GASINC6.1
	Sc3 Gasification and Fischer-Tropsch	Sc1 Incineration	GASINC6.2
[470]	Sc5 Mechanical recycling, gasification, and ash landfill	Sc6 Mechanical recycling, incineration, and ash landfill	GASINC7.1
	Sc11 Gasification	Sc12 Incineration	GASINC7.2
[467]	Sc2 Wet fraction goes to AD, while mixed waste goes to gasification	Sc4 organic to AD wet fraction into Incineration	GASINC8
[471]	Sc4 Gasification	Sc3 Incineration	GASINC9
[473]	Sc2 Gasification	Sc1 Combustion	GASINC10
[474]	Sc1 Gasification with catalytic combustion	Sc3 Incineration	GASINC11.1
	Sc2 Gasification with flame combustion	Sc3 Incineration	GASINC11.2
[475]	Sc4 Gasification and AD	Sc5 Incineration	GASINC12.1
	Sc6 Gasification	Sc5 Incineration	GASINC12.2
	Sc4 Gasification and AD	Sc3 Incineration and AD	GASINC12.3
	Sc6 Gasification	Sc3 Incineration and AD	GASINC12.4
[476]	Sc4 AD – Gasification	Sc1 Incineration	GASINC13
[477]	Sc1 Gasification	Sc2 Mechanical-grate incineration	GASINC14.1
	Sc1 Gasification	Sc3 Fluidised bed incineration	GASINC14.2
[479]	Sc2 Gasification with steam turbine system	Sc1 Direction incineration	GASINC15.1
	Sc3 Gasification with gas turbine/ catalytic converter	Sc1 Direction incineration	GASINC15.2
	Sc4 Gasification with internal combustion engine	Sc1 Direction incineration	GASINC15.3
[480]	Sc3 Gasification Pyrolysis (mixed paper)	Sc2 Incineration (mixed paper)	GASINC16.1
	Sc6 Gasification Pyrolysis (mixed plastic)	Sc5 Incineration (mixed plastic)	GASINC16.2

5.4 Meta-Analysis Outcome

From the LCA's results, the relative difference is calculated and displayed in a graphical diagram ranging from -100% (the IC favours plasma/conventional gasification) to +100% (the IC favours base scenario). These graphical display shows the trend amongst the LCA work, enabling meta-analysis for selected impact categories.

Figure 5-2 shows the comparison between plasma gasification with landfilling, incineration, and conventional gasification. For comprehensiveness, Figure 5-3 shows the comparison between conventional gasification with landfilling and incineration. The details of each scenario are provided in Table 5-4 (full calculation is provided in Appendix C.2 and C.3).

The comparisons outcome is summarised in Table 5-5, showing the percentage of LCA works that found a positive impact on plasma and conventional gasification implementation.

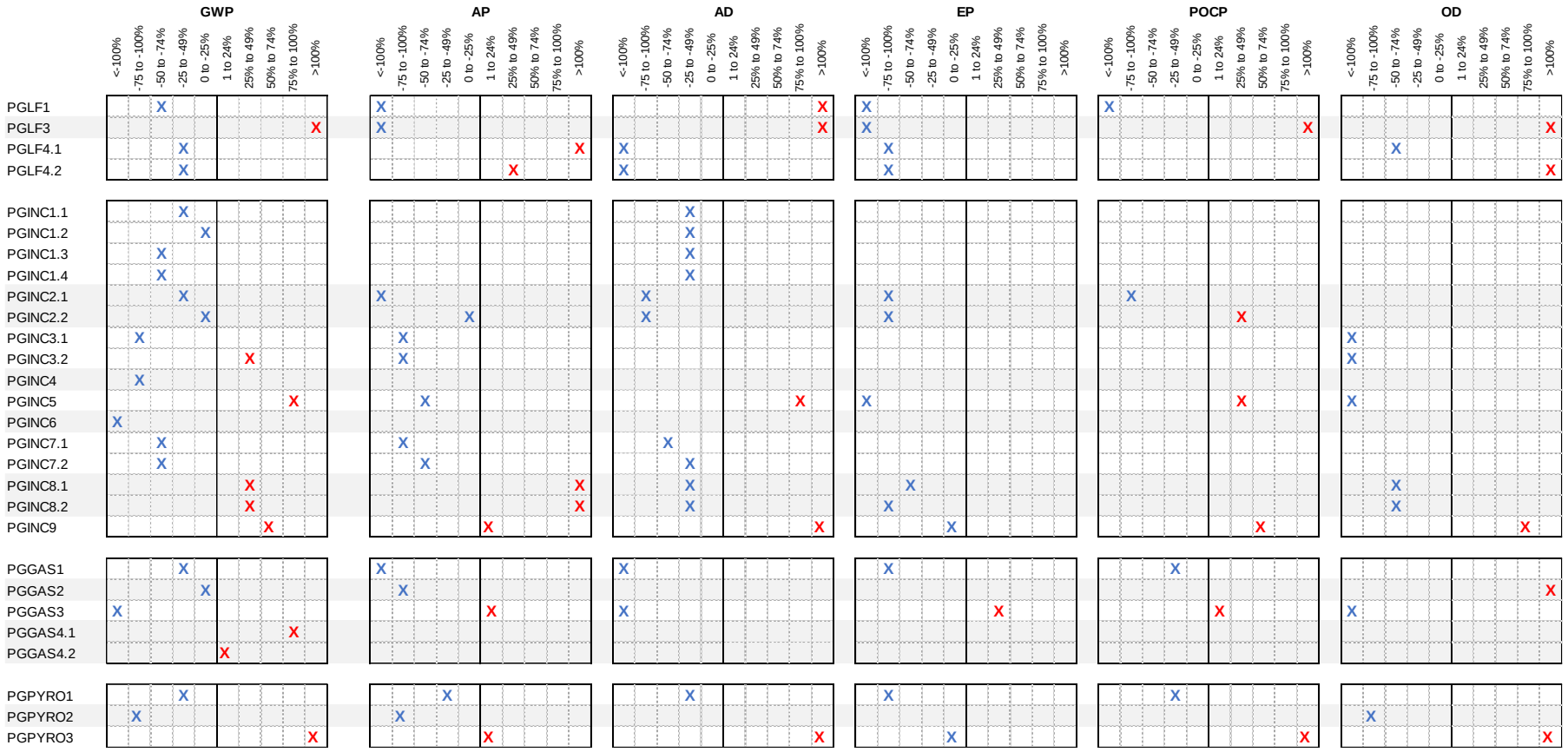

Figure 5-2: Various scenarios showing the relative differences of plasma gasification over landfilling, incineration, conventional gasification, and pyrolysis for selected impact categories (values are provided in Appendix C.3).

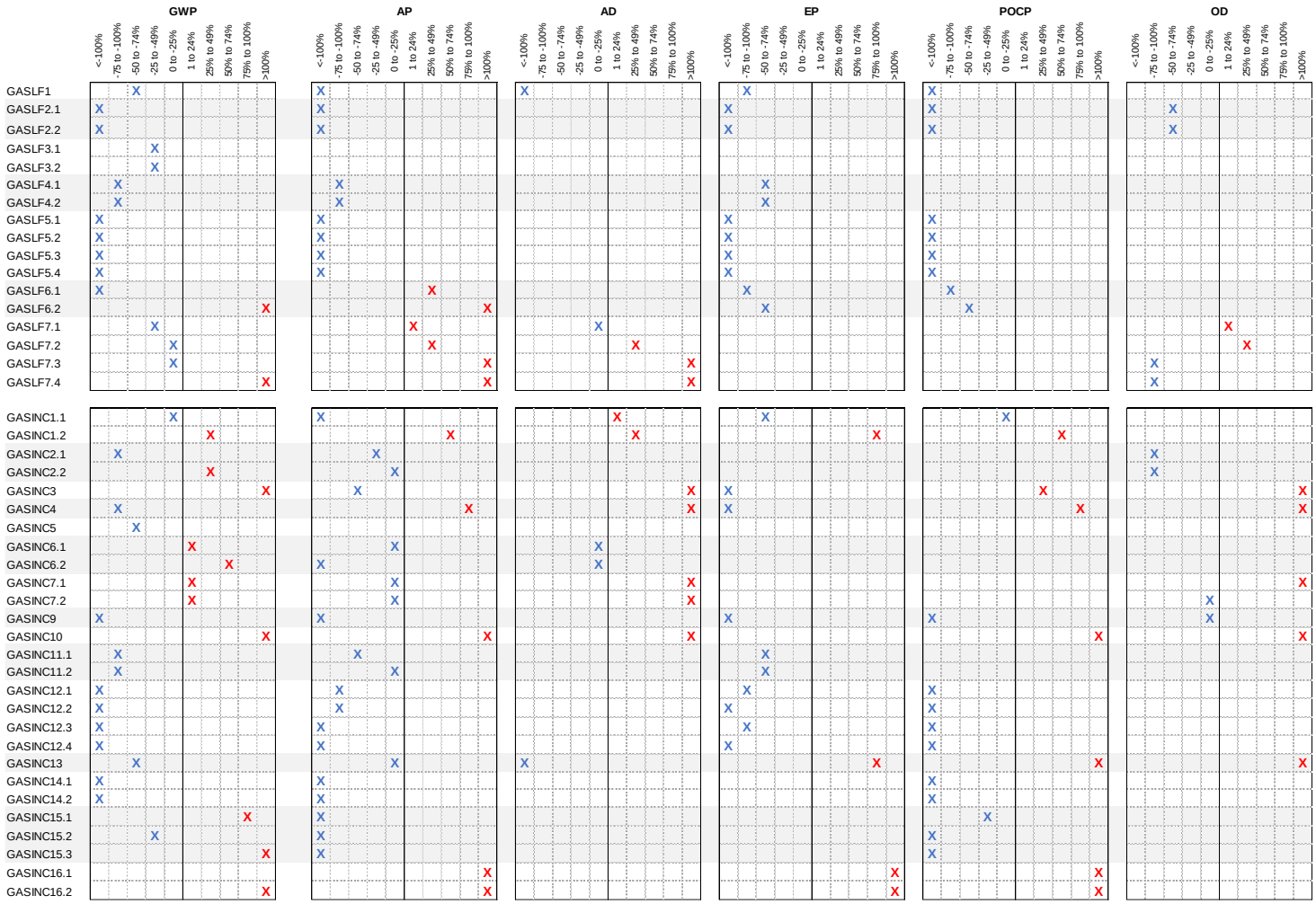

Figure 5-3: Various scenarios and the relative differences of plasma gasification over landfilling and incineration for selected impact categories (values are provided in Appendix C.4).

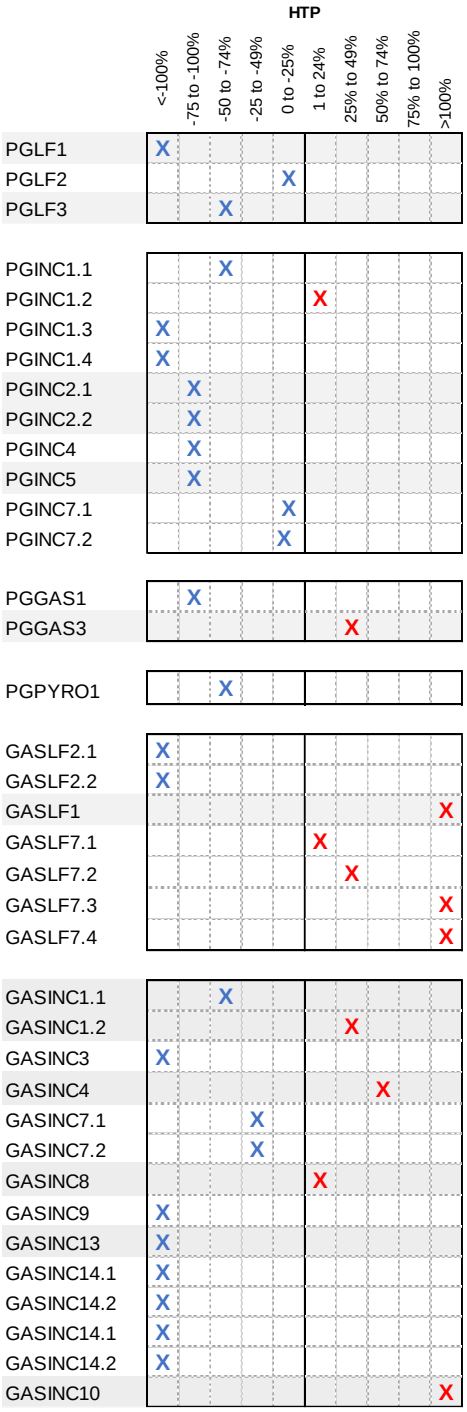

Figure 5-4: Various scenarios and the relative differences of plasma and conventional gasification over other waste management strategies for HTP.

Table 5-5: Percentage of analysed LCA that finds plasma gasification and conventional gasification implementation to be beneficial in terms of relative differences, along with the number of LCA (in bracket). If multiple comparisons are drawn from one LCA with contradicting outcome, the percentage is divided evenly.

Base case	**Comparison**	**GWP**		**AP**		**AD**		**EP**		**POCP**		**OD**		**HTP**	
Plasma gasification	Landfill	67%	(3)	67%	(3)	33%	(3)	100%	(3)	50%	(2)	25%	(2)	100%	(3)
	Incineration	61%	(9)	67%	(6)	67%	(6)	100%	(4)	17%	(3)	75%	(4)	95%	(5)
	Gasification	75%	(4)	67%	(3)	100%	(2)	50%	(2)	50%	(2)	50%	(2)	50%	(2)
	Pyrolysis	67%	(3)	67%	(3)	50%	(2)	100%	(2)	50%	(2)	50%	(2)	-	(1)
Gasification	Landfill	89%	(7)	67%	(6)	63%	(2)	100%	(5)	100%	(4)	75%	(2)	33%	(3)
	Incineration	56%	(15)	75%	(14)	29%	(7)	69%	(8)	45%	(10)	36%	(7)	61%	(8)

Disfavour base case — Favour base case

0% — 50% — 100%

5.5 Part I: Thermal Plasma Gasification

Regarding GWP, at least 61% of analysed LCAs found that plasma gasification has a lower impact than the other four scenarios. Landfilling is a significant methane producer. United States announced that their landfilling practice to be the third largest emission contributor, after fossil fuel and agriculture [482]. While this is true for waste's organic portion, plastic durability means it does not contribute to methane production [483]. However, when the temporal boundary is expanded, it becomes noticeable that plastic disposal impacts echo other sectors, such as prolonged air emission and supplementary fossil fuel consumption [484]. From the analysed LCAs, 67% of the LCA found that plasma gasification has a lower GWP than landfilling. However, The LCA result reported by Ramos et al. [460] contradicts other LCAs possibly because of the unclear adaptation methodology from Evangelisti et al. [456], which actually found plasma gasification to have lower GWP than landfilling. Landfilling type may also impact this result, methane from landfills is a potent GHG, and capturing this gas and converting it into carbon dioxide may reduce the overall GWP since it is a less potent GHG, other treatments such as pre-separation, wastewater treatment, and anaerobic digestion before landfilling may reduce the overall GWP from landfill [470]. Nonetheless, Evangelisti et al. [456]'s landfill scenario is equipped with gas capture, flaring, and energy production, the 50% emission outcome still leads to a more severe impact than plasma gasification. Similarly, Tagliaferri and Lettieri [463] find that despite the recycling and anaerobic digestion steps before landfilling, landfill GWP is still higher than plasma gasification.

However, both Tagliaferri and Lettieri [463] and Evangelisti et al. [456] reported an increase of GWP when the same plasma gasification is compared to incineration, even to the point where incineration GWP benefits outweigh plasma gasification (PGINC8.1 and PGINC8.2). The reduction is caused by parasitic load or energy consumption for plant operation, where their plasma gasification scenarios use diesel and natural gas-grid energy, respectively. Mannheim and Bodnár [457] and [459] also agree with Tagliaferri and Lettieri [463], however, the studies did not provide a clear explanation for this outcome. Furthermore, Zhao et al. [464] discovered that plasma melting technology is less beneficial than rotary kiln combustion when it comes to processing medical waste. The study claims that melting due to plasma's high energy requirement and low energy recovery affect the LCA result. Most LCAs that achieved positive GWP for plasma gasification use two stage plasma gasification, with GWP reduction ranging from 18% to 108% ([456, 461], Appendix C.2). The diversity in the incineration process means that every comparison is unique, and while generalised trend can be observed between different LCAs, the contributing factor may vary depending on the EFW scenarios.

Plasma gasification requires a steady supply of auxiliary fuel, while conventional gasification can be a self-sustaining process [107]. This means that plasma gasification's higher energy requirement will indirectly produce higher GWP. Despite this, 3 out of 4 LCAs reported that plasma gasification has less GWP than conventional gasification. Evangelisti et al. [456] demonstrate that plasma gasification's avoided burdens compensate the initial direct impact, lowering the overall GWP. The high compensation is supplied by high energy recovery (gas engine) and up-cycling bottom ash. In contrast, conventional gasification must rely on syngas combustion due to tar pollutant and bottom-ash landfilling, Ramos and Rouboa [459] and Mannheim and Bodnár [457] also establish a similar outcome. Suresh et al. [465] discover that plasma gasification energy requirement is too significant when the objective is jet fuel production. Two out of three LCAs found pyrolysis to be more detrimental than plasma gasification, this trend is possibly stemming from the limitations of pyrolysis. Traditionally, pyrolysis is used for oil and solid fuel production. However, when waste is used as the feedstock, pyrolysis may produces inconsistent process operations affecting products' quality [485]. Evangelisti et al. [456] and Mannheim and Bodnár [457] LCA only consider a pyrolysis-syngas-combustion scenario, followed by ash landfilling. The limited energy application reduces the avoided burden; thus, increasing the overall GWP. However, a consistent pyrolysis reaction can be expected from a homogenous feedstock, Zhao et al. [464] demonstrating that medical waste pyrolysis-incineration has less GWP than plasma melting technology. For most LCA, the energy source can significantly affect the overall GWP. To counter this, plasma gasification may achieve significant benefits with lowest environmental impacts if the energy source is renewable, as opposed to grid-mix, which is the case for most LCAs.

Regarding AP, there is a high degree of variability within analysed LCAs. Plasma gasification continuously oxidises waste while simultaneously producing acidic gases, directly contributing to AP [486]. However, when avoided burden is considered, plasma gasification's grid energy input and ash upcycling provide enough avoided emission to outweigh the initial impact, lowering the overall AP [456, 457]. Nonetheless, depending on the scenario, the avoided burdens may not be enough to counter the initial acidification impact. Tagliaferri and Lettieri [463] show that plasma gasification low energy production combined with high grid energy requirement produces a high overall AP due to uncompensated direct impact (PGLF4.1, PGLF4.2, PGINC8.1, & PGINC8.1). Other studies found the relative differences between plasma gasification to incineration are in the range of -23% (PGINC9) to 913% (PGINC2.1). Evangelisti et al. [456] believe that bottom ash recycling is the key to AP reduction. The study recorded an incineration plant that recycled its bottom ash and found a practically similar AP to plasma gasification (PGINC2.2). Meanwhile, López-Sabirón et al. [462] demonstrate the role

of sulphur composition in AP. In comparison to conventional gasification and pyrolysis, plasma gasification may be able to inhibit the formation of acidic gases. Plasma gasification extreme conditions break down feedstock without the need for excess oxidants, avoiding the formation of acidic gases [107]. This agrees with the finding where 67% of analysed LCAs found that plasma gasification has a lower AP as to pyrolysis and conventional gasification, with two disagreeing LCAs differing minimally at -1% (PGGAS3) and -7% (PGPYRO3).

Altogether, although plasma gasification's extreme operating conditions can inhibit the generation of acidic gases, there is a proper APC technique to reduce this impact, such as scrubber or reaction modification [487]. However, supplementary processes may drive more energy intake and depending on the energy source, more acidic gases can be emitted, such as if a plant utilises coal as an energy source [488]. As plasma generation often relies on grid energy, it is imperative to conduct an LCA to ensure that the avoided burden is enough to counteract the direct impact of the gasification reactions. AP variability emphasises the importance of a comprehensive system boundary and ash up-cycling. In this chapter, the use of renewable energy as input to plasma gasification is not reported.

Regarding AD, similar to AP and GWP, plasma gasification has higher energy consumption and would require more material consumption than landfilling (PGLF1 & PGLF2). Interestingly, Tagliaferri and Lettieri [463] demonstrate that plasma gasification has a lower AD impact than both incineration and landfilling, opposing the previous AP and GWP findings (PGLF 4.1 & PGLF4.2). Two possible explanations are (1) the auxiliary load from the organic separation and digestion process prior to landfilling and/or (2) the functional unit of 1 MJ influenced the LCA result to be energy-centric. The 1 MJ functional unit standardised the system boundary to meet this output, meaning that if a certain scenario is less resource intensive than others, the said scenario would operate at a higher consumption rate, thus more AD. Overall, most studies agree that plasma gasification has a lower AD impact than other thermochemical conversions, high energy recovery and bottom-ash upcycling may contribute to the avoided burdens. Ramos and Rouboa [459] and [464] contradict other studies stating that plasma gasification's higher AD impact is cause by diesel consumption and APC scrubber alkali injection, respectively.

Regarding EP, almost all comparisons made agree that plasma gasification has a lower impact on eutrophication than any other scenarios. Tagliaferri and Lettieri [463] claims that plasma extreme condition prevents the formation of ammonia, while [456] believes that ash vitrification locks the nutritional elements into the slag matrix.

Regarding POCP, most LCAs agree that plasma gasification can lead to more photochemical smog. Evangelisti et al. [456] landfilling scenario has a higher POCP resulting from the landfill gas flaring without adequate APC, contradicting Mannheim and Bodnár [457]. Furthermore, Evangelisti et al. [456] are the only LCA that finds their plasma gasification scenario to have a lower impact than other thermochemical conversions, arguing that ash vitrification is the key inhibitor. The argument is supported by the finding of lower POCP for incineration with ash upcycling (PGINC2.2). Whereas Zhao et al. [464] stated that plasma melting's fuel requirement is the direct contributor to the POCP.

Regarding OD, halogenated elements in the feedstock may be converted into a potent ozone depletion gas [459]. While this is possible, it is still unknown whether waste management is a significant contributor to OD [489]. In most circumstances, halogenated elements in waste (e.g. from PVC) would be converted into acidic gases (HCl) and ideally removed via APC [487]. However, plasma extreme conditions and waste heterogeneity may influence the formation and release of halogenated elements [490, 491]. From the analysed LCAs, it can be said that plasma gasification has a higher OD than landfilling, with Tagliaferri and Lettieri [463] being the only scenario to contradict this outcome. Moreover, plasma gasification can be a cleaner alternative to incineration in terms of OD (PGLF4.2). It is unclear if it has a lower OD to pyrolysis and conventional gasification.

In general, it is still inconclusive whether plasma gasification can contribute to more OD and POCP. More research is needed to confirm whether plasma interferes with the formation of certain gases, or it is primarily controlled by other variables, e.g., feedstock composition.

Regarding HTP, 95% of analysed LCAs agree that plasma gasification has a lower HTP than incineration or landfilling. The only scenario where incineration has lower HTP is when the said incineration recycles its bottom ash whilst plasma gasification landfills its slag (at 10% lower, PGINC1.2). Plasma gasification's vitrification process locks heavy metal into slag matrix [456], reducing the leaching potential and exposure via air. Moreover, the extreme heat also inhibits the formation of noxious compounds and persistent organic pollutants [107]. Landfill leachate is a widely known source of human toxicity, primarily through groundwater exposure [492, 493]. For incineration, while a strict APC is the norm [487], bottom & fly ash are susceptible to leaching. Ash requires further treatment before disposal or upcycling [494, 495], such as plasma vitrification [496, 497]. In terms of other thermal conversions, the two analysed LCAs produce contradicting result when comparing HTP in plasma and conventional gasification (PGGAS1 & PGGAS3). Likewise, a conclusion cannot be drawn for HTP in pyrolysis and plasma gasification due to the lack of LCA.

HTP, OD, and POCP comparison highlights the importance of LCA quantity. Often enough, studies with similar operating conditions and technology labelled as 'plasma gasification' resulted in contradicting outcomes, more LCAs would provide a higher degree of confidence while also allowing an opportunity to scrutinize each LCA's methodology.

5.6 Part II: Conventional Gasification

Regarding GWP, 89% of analysed LCAs agree that gasifying waste into syngas is more beneficial than the disposal strategy, with only two scenarios contradicting this. Demetrious and Crossin [480] discover an opposing trend when gasification is used for paper or plastic waste, concluding that is favourable to landfill separate mixed plastic waste than thermal treatment (GASLF6.2). Similar to plasma gasification, the benefits of gasification are reduced significantly when compared to incineration. [470] [470] outlined that landfill gas capture has lower GWP but it is unclear of its scenario's operating conditions (GASLF7.4). The assessment also found minimal benefits of gasification over landfilling (at 13% relative differences, PGLF7.2 and PGLF7.4) and drawbacks when compared to incineration (PGINC7.1 and PGINC7.2). The comparison became unclear when gasification was compared to incineration. Only 56% of the analysed LCAs find gasification to be more beneficial. The drawbacks may be caused by low energy recovery from the two two-stage gasification-combustion process. GWP comparison accentuates the importance of high energy recovery to improve avoided burden and compensate initial impact. This was emphasized by Evangelisti et al. [456] in the previous section and reconfirmed by Tang et al. [479] that gasification-gas turbine (PGINC15.2) has a lower GWP than gasification-steam turbine (PGINC15.1), making it more favourable when compared to incineration.

Regarding AP, 67% of analysed LCA find gasification to have a lower impact on AP. The meta-analysis outcome disparities may be caused by scenario complexity and system boundary, for example, Parascanu et al. [473] solely consider waste treatment while Fernández-Gonzalez et al. [470] evaluated a complex waste recycling and separation process prior to the treatment. Moreover, unlike GWP, 75% of analysed LCA agrees gasification has a lower AP than incineration, the few LCA that disagree may be influenced by feedstock impact (olive by-products, GASINC10) or inadequate APC. To reiterate, this impact can be minimised with appropriate APC, which was demonstrated by Evangelisti et al. [456] when comparing a gasification technology with two incinerations that employs different APC units (GASINC1.1 & GASINC1.2).

Regarding AD, gasification achieves lower AD than other scenarios when it has a high energy recovery (GASLF1 GASINC 6.1 & GASINC6.2), or when it is complemented with, separation, recycling, or anaerobic digestion (GASLF7.1 & GASINC13). Gasification-combustion process is a resource-intensive process, and without more advanced energy recovery (such as diesel engine or Fischer-Tropsch [469]). Without the mentioned modifications, it is unjustifiable to favour gasification over incineration, in terms of AD.

Regarding EP, all studies agree that gasification has a lower EP than landfilling, while 69% of the analysed LCA found that gasification has a lower EP than incineration. The LCAs that found incineration's EP to be lower than gasification achieve it by utilising catalytic reduction (GASINC1.2, GASINC16.1 & GASINC16.2), which reduces noxious pollutants into inert nitrogen gases [456, 480]. [476] [476]'s high EP may have resulted from process coupling with anaerobic digestion (GASINC13).

Regarding POCP and OD, most LCAs found that gasification has a lower impact when compared to landfilling, while the opposite for incineration. Photochemical smog is caused by volatile organic compounds and NOx (which are also acidic gases) [498]. Thus, APC can play an important role in reducing POCP. From Figure 5-4, a pattern emerges where the meta-analysis of the POCP comparison is similar to the AP comparison. Demetrious et al. [480] discovered that for separated waste, landfilling and incineration have lower OD impact while for mixed stream, gasification is favoured, an explanation for this phenomenon was not provided. In general, gasification adoption over incineration is not necessarily beneficial in terms of POCP and OD.

Regarding HTP, Coventry et al. [471] is the only LCA that finds gasification to have a lower HTP than landfilling (GASLF2.1 & GASLF2.2), stating that the avoided burden is the explanation. Although Evangelisti et al. [456] also consider avoided burdens, the LCA result contradicts Coventry et al. [471]'s findings. 61% of the analysed LCA agrees that conventional gasification has lower HTP than incineration, with the few studies that find otherwise credited the role of wastewater treatment (GASINC10) and an advanced APC (GASINC1.2 and GASINC4).

In relation to plasma gasification, there are more LCAs that assess gasification, providing more confidence in the trend. For GWP, Table 5-5 shows that significant LCAs favour gasification over landfilling while only 56% of LCAs favour gasification over incineration. For AP, the highest LCA agreement percentage occurred during gasification-incineration comparison (75% of analysed LCAs), although the high number of LCAs may be attributed to this meta-analysis trend. Surprisingly, only 33% and 61% of analysed LCAs find conventional gasification has HTP benefits over landfilling and

incineration, respectively, while it is almost unanimous that plasma gasification has a lower HTP in both scenarios. It is hypothesised that conventional gasification's ash-hazardous properties contribute to this trend. Conventional gasification ash is concentrated with heavy metals and other pollutants, and can easily leach into the environment [499], arguably easier as it is more concentrated with pollutants compared to untreated MSW in the landfill. Plasma gasification slag usually does not require further treatment and can be utilised/landfilled with minimal leaching [456]. This difference creates a stark contrast in the HTP of plasma and conventional gasification when compared to landfilling.

Overall, plasma gasification's lower environmental impact may be attributed to its cleaner syngas production and by-product (slag) utilisation. Clean syngas enable a more advanced energy recovery, meaning for the same energy production, less environmental impact will be produced. Meanwhile, reutilising by-products eliminates the environmental impact of virgin material production, contributing to the reduction of overall environmental impacts within the LCA study. Slag production, which is unique to plasma gasification, minimises leaching potentials that happen with untreated bottom ash from incineration and conventional gasification.

5.7 LCAs Takeaways

The variability across LCAs highlights the relevance of individual comparisons (Figure 5-2, Figure 5-3, Figure 5-4). From the technical standpoint, there is a diverse selection of technology and supplementary processes that fall under plasma and conventional gasification, making each LCA a unique scenario in its own right. A simple retrofitting such as APC chemical looping can reduce AP and GWP in plasma gasification by 80% and 90%, respectively [458].

From the feedstock standpoint, while in theory plasma gasification can process various types of waste, for a reliable process, incoming waste should be shredded and dried [32, 140]. Pre-treatment is an important step, as it supports further waste separation and ensures a steady plasma process, across every feedstock type [500]. [501] demonstrate that RDF plasma gasification has the lowest GWP when compared to biomass and unsorted waste, even when biogenic carbon is excluded. Khoo [466] also found a similar trend where RDF gasification has a lower GWP impact than MSW gasification. Interestingly, an LCA found that plastic waste gasification has more impact than landfilling [480], possibly because of the plastic non-biogenic carbon portion that minimally contributes to carbon emission. In general, there is an agreement for thermal treatment over landfilling for paper waste, while the same is unconfirmed for plastic and mixed waste [254].

Various articles have analysed EFW LCAs methodology and drawn advice for future researchers [250, 251, 255, 502, 503], while the Joint Research Centre (JRC) published a 'state-of-the-art' guideline for Waste Management LCA [504]. The lack of plasma gasification LCAs makes it unsuitable for a methodological review. However, some studies did not meet ISO14040/44 and do not specify a clear scope nor consider avoided emissions. Further work is needed to establish the role of methodologies and the inclusion of sensitivity analyses. Plasma gasification also relies on small-scale evidence, meaning LCA implementation may not provide the desired outcome [250]. For example, [456] compares plasma gasification at 100 kg per hour [57], to an incineration plant of 15,000 kg per hour [505]. From this review, future researchers may explore:

1. *A more complete LCA*, some LCA did not provide a full analysis and interpretation of every impact category [467, 506]. Inclusion of avoided burdens is favourable, along with 'hot spot' analysis [501], and biogenic carbon analysis [463]. Sensitivity analysis is also favourable [460, 502]. LCA should also consider obtaining data from industrial-scale operations, one that has a high TRL, and potentially assess its useful year in contrast to other waste management technology [451].
2. *LCA with co-assessment*, despite its excellence in assessing environmental impact, LCA can be complemented with other techniques such as Multi-Criteria Analysis (MCA) [507]. Extension methods such as Exegetic-LCA, Life Cycle Costing [508], or Social-LCA can supplement the environmental impact result [509].
3. *Process retrofitting and modification*, EFW co-processing should be embraced for a more advanced scenario. Co-process with digestion and recycling have been demonstrated in some LCA. Cascading process such as pyrolysis-gasification may improve conversion as the staged process allows a more complete breakdown [510-513]. Process augmentation is believed to be the next step in harmonising waste management and thermal treatment [514]. Future scenarios of LCA should be conducted before technology implementation, such as renewable energy [515, 516] or grid energy integrations [463].
4. *Opportunity as chemical recycling*, with some preliminary studies that demonstrate plasma process opportunity as a chemical recycling pathway [517], future researchers may explore its environmental impact and saving potential on plasma chemical recycling implementation. Such LCA have been demonstrated in lithium ion-battery (thermal plasma, [500]) and polylactic acid polymer (non-thermal plasma, not chemical recycling, but for manufacturing [518])

5.8 Conclusion

This chapter analysed 25 different LCA studies that compared thermal plasma gasification and conventional gasification to other waste management technologies, providing a meta-analysis comparison of existing LCA works. From the comparison, it is inconclusive whether conventional

gasification has a positive benefit when compared to incineration. However, from this study, it was found that a clear benefit exists in adopting plasma or conventional gasification over landfilling. Based on the GWP measure, the LCA analysis has shown that 61% of LCA studies favoured plasma gasification over incineration, and 67% of LCA studies favoured plasma gasification under the acidification impact category. Significantly, 100% of analysed LCAs found that plasma gasification has a lower impact than incineration eutrophication potential. These findings point to the potential of plasma gasification as an environmental technology suited for dealing with non-recyclable waste and residues. The key technological contributions to lowering environmental impact are identified as (1) adequate APC systems, (2) by-products upcycling, and (3) high energy recovery technology, and therefore are areas of focus for plasma gasification technology development. While technological advancement is necessary, there also is a need to incorporate the social and economic impact of plasma gasification when compared against other technologies.

Chapter 6

Environmental Impact of Waste Gasification with NTP Tar Cracking

The bulk of this chapter is currently under preparation for submission as the following manuscript: E. Sanjaya, G. Fimbres Weihs, and A. Abbas Environmental Impact of Potential NTP Tar Cracking Implementation for Waste Gasification.

6.1 Introduction

Waste management has become one of the most pressing challenges in modern history [1], casting a long shadow of environmental suffering [2]. Landfills release copious amounts of methane, a potent greenhouse gas into the atmosphere [3]. Incineration, though effective in reducing volume, raises concerns about emissions and pollutant dispersion [8]. The gravity of these environmental consequences necessitates a thorough examination of the environmental merits for each waste management method. Environmental study provides numerical validity to ensure the adoption of environmentally sound option [250].

However, the complexity of waste management presents a challenge to produce a cohesive environmental impact study. The diversity of approaches causes comparative assessment to be elusive. The intricate material flow calls for a tool capable of methodically assessing environmental impacts across diverse waste management scenarios. Life Cycle Assessment (LCA) is a systematic approach that has emerged to be preferred tool for this purpose. LCA provides a structured framework to comprehensively assess the environmental implications of products, processes, or activities. Guided by established ISO standards [251, 253], it facilitates a more objective comparison through a set of assumptions.

Among various waste management strategies, waste gasification has captured the attention of researchers and industry alike due to its promise of minimal environmental impacts and versatile products. Although gasification boasts numerous advantages, tar by-product generation remains a persistent issue. Tar hinders waste gasification implementation and advanced syngas recovery. In

recent years, researchers have demonstrated Non-Thermal Plasma (NTP) for tar cracking. NTP tar cracking has emerged as a valuable method as it distinguishes itself from other tar elimination strategies by directly destroying tar and enhancing syngas quality, while operating at a lower energy requirements [14]. As a novel technology, it is imperative to assess its environmental impact to authenticate its adoption as an environmentally sound solution.

6.2 Research Background

6.2.1 Research Gaps and Niche

Although LCA studies on gasification, incineration, and landfilling have been widely executed [8], the environmental impact of the potential NTP-based tar elimination process for waste gasification has not been explored. This research gap stems from the scarcity of studies done in this field. Previous chapters have highlighted the minimal study on understanding the technology's reactions and process implementation, resulting in the absence of environmental impact investigation. Table 6-1 shows the comparison of this LCA study with other works.

Table 6-1: Chapter 6 novelty in comparison to other published studies.

Study	Waste	Comparison	Main findings
[519]	Paper waste	Recycling, incineration, and bioethanol production	Production of bioethanol is shown to be the most favourable.
[468]	Solid waste	Incineration and gasification	Incineration (moving grate) has a slightly lower environmental impact
[480]	Paper and plastic packaging	Incineration, landfilling, and gasification-pyrolysis	Mixed paper may be treated in a thermal process while plastic is best for landfill
[456]	MSW	Incineration, landfilling, gasification, and plasma gasification	Thermal plasma gasification clean process shows the least environmental impact
This Work	MSW	Incineration, landfilling, gasification, plasma gasification, and gasification-NTP-tar cracking	NTP tar cracking lower energy intake has superiority over thermal plasma gasification.

6.2.2 Chapter's Aim

Hence, this chapter aims to investigate the environmental performance of NTP tar cracking implementation for waste gasification, producing ultraclean syngas suitable for advanced energy recovery (fuel cell) and material synthesis (methanol). The environmental performance is compared

against other more conventional scenarios, namely, landfilling, incineration, conventional gasification, and thermal plasma gasification. The Chapter's flow can be seen in Figure 6-1 where it follows the advised ISO LCA guidelines.

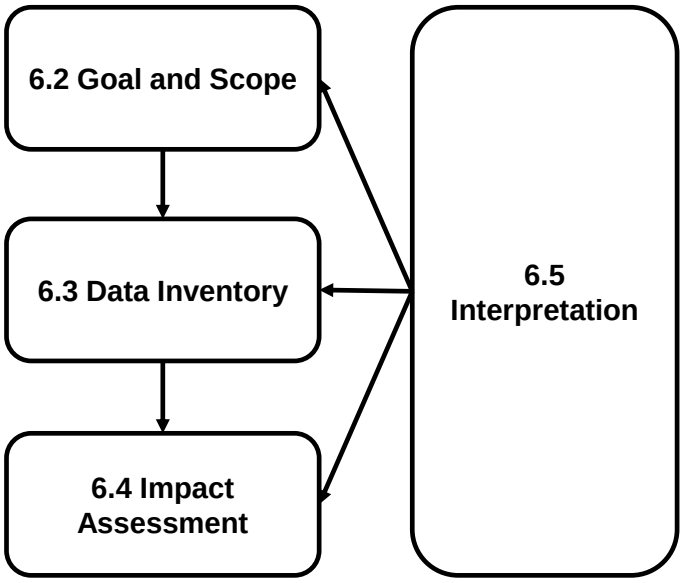

Figure 6-1: This chapter flows according to the ISO LCA Guidelines [253]

6.3 LCA Methodology and Data Inventory

In this LCA study, various waste management processes were defined as scenarios to investigate the environmental activity in relation to the functional unit defined through the study's objective. The functional unit utilised for this comparative LCA is one kilogram of MSW. Other studies that focused on energy generation adopted the 1 MJ [463]. Various software packages and data inventory databases exist to quantify the emissions. This study utilised the Ecoinvent version 3.6 with the Allocation at the Point of Substitution (APOS) system model [520]. Figure 6-2 shows the system boundary for this study. The main process for each scenario is described in the grey box while, acting as the foreground. The data inventory for the foreground mass balances is discussed in the next part. The product output for each scenario is considered by system expansions. The generation of valuable products was used to estimate the avoided potential environmental impact by substituting it on the market (i.e., avoided burden). For this study, the avoided burden is estimated to substitute the processes for:

1. Energy generated to substitute grid electricity for Australia according to the IEA World Energy Statistics and Balance [521].
2. Ferrous metal (FM) is assumed to substitute 1-to-1 to the process of low-alloyed steel production using an electric arc furnace.

3. Non-ferrous metal (NFM) is assumed to substitute 1-to-0.99 [522] in the process of aluminium production using a reverberatory furnace for casting[520].
4. Vitrified slag is assumed to substitute 1-to-1 to the process of crushed gravel aggregates (AGG) [520].
5. Methanol (MeOH) production substitutes 1-to-1 methanol synthesis from natural gas [523].

Meanwhile, the disposal of APC residue and bottom ash contributes to indirect environmental impact (i.e., indirect burden). For this study, APC residue indirect burden is represented as the landfilling of incineration residue, while bottom ash treatment is represented sanitary landfilling of incineration bottom ash for every scenario. The processes were provided in Ecoinvent version 3.6. Throughout the LCA, these assumptions were adopted:

1. The MSW composition does not affect the input-output of the boundary conditions.
2. Transportation, construction, capacity, and market fluctuation were not considered.
3. The emission impact on population density was unspecified.
4. Database on input, output, and emission were adjusted to fit the utilised database (Ecoinvent version 3.6, see Appendix D.1 and D.2).

For this study, Table 6-2 shows the life cycle impact category adopted for this study. The impact categories were selected based on data availability and relevancy to the objective. The method used in the simulation was ReCiPe Midpoint (H). ReCiPE is claimed to be improved from its predecessors (CML 2000), where it use a broad set of midpoint range and exclude the potential impact of future extraction [524].

Table 6-2: Impact categories adopted for this work.

Impact category	**Acronym**	**Units**
Global Warming potential	GWP	kg CO_2-Eq
Acidification potential	AP	kg SO_2-Eq
Eutrophication potential (Marine and freshwater)	EP	kg P-Eq and kg N-Eq
Photochemical ozone creation potential	POCP	kg NMVOC
Human Toxicity Potential	HTP	kg 1,4-DCB-Eq
Particulate Matter Formation Potential	PMFP	kg PM_{10}-Eq

GWP measures the extent to which a substance, when released into the atmosphere, contributes to global warming by trapping heat. GWP estimated the excessive fossil and biogenic origin GHG for 100 years [525]. AP represents the emissions of acidic gases that may return to earth, acidifying the soil and water via weather conditions. AP estimates the environmental harm caused by acidifying emissions, which may harm ecosystems, aquatic life, and vegetation. EP estimates the risk of nutrient-rich pollutants entering aquatic systems, causing excessive growth of algae and other aquatic plants, leading to oxygen depletion in the body of water, and eventually ecosystem. POCP measure the

scenario's emissions in gases that lead to the formation of ground-level ozone. Volatile organic compounds (VOCs) and nitrogen oxides (NOx) are the common responsible compounds. POCP is an important indicator in estimating air quality deterioration and human health. HTP assesses the potential harm to human health caused by emissions of toxic substances into the environment, which is estimated by the software through various emissions. Lastly, PMFP measures the scenario's impact on emissions to contribute to the formation and generation of particulate matter (PM), apart from PM directly, other compounds such as SO_2 and NO_x may react with air molecules to form small PM [526].

6.3.1 Life Cycle Data Inventory

For this study, the mass and energy balance for different base scenarios were mainly derived from Evangelisti et al. [456]. The data inventory is extracted and simulated within this Chapter's database to eliminate cross-study-assumption errors. As this chapter utilise Ecoinvent, taking the data directly from other database may provide different level of accuracy that distort the LCA result. Meanwhile, the background process data inventory is provided by the database (Ecoinvent version 3.6). This section will describe each scenario data's origin along with limitation analysis. Full data inventory is provided in Appendix D.1. and D.2.

6.3.1.1 Landfilling (LF)

The inventory database was collected from Evangelisti et al. [456], where they claim that the database was collected from the Gabi database [527]. The sanitary landfill meets the standard operating procedure including basic sealing and emission regulation. The landfill also captures 28% of the emission to be converted into energy while the rest is flared and emitted into the environment.

6.3.1.2 Incineration A (INC-A)

Incineration A's mass and energy balance were based on an existing plant in Sheffield UK. The plant utilises the moving grate combustor with a capacity of 28.3 tonnes per hour. Where the emission is treated with urea, limestone, and activated carbon to reduce pollution. The mass balance can be found in this report [528].

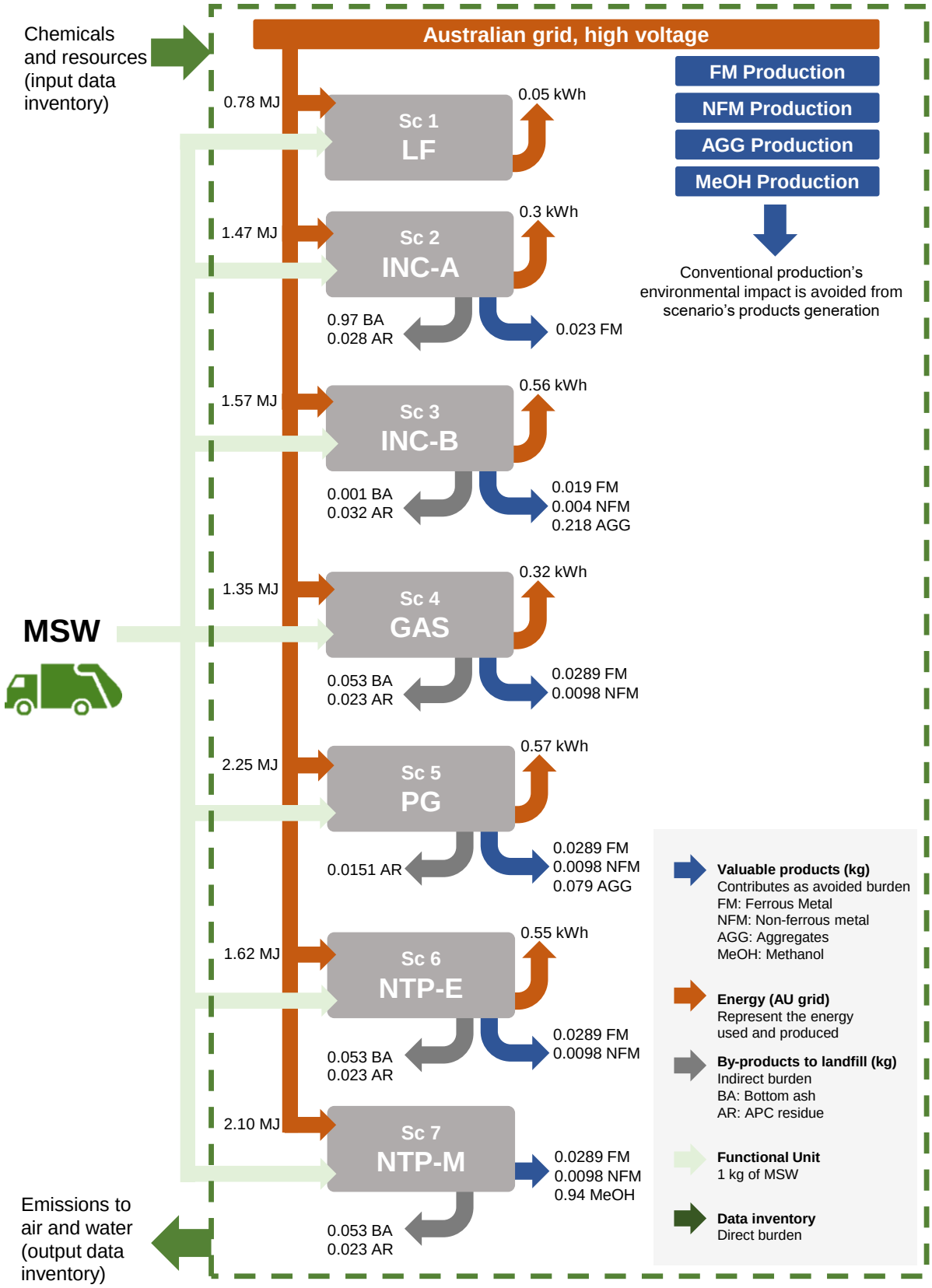

Figure 6-2: System boundary with mass and energy balance for each scenario (Data inventory in Appendix D.1 and D.2)

6.3.1.3 Incineration B (INC-B)

Incineration B was based on a more advanced incineration process that operates in Lincolnshire by FFC environment in North Hykeham UK. The process claims to utilise a reversed-acting grate a more advanced APC technique that injects ammonia to control the NOx production. Furthermore, the advanced combustion system also claims that it was able to harvest more energy from the combustion process and produce a higher net electrical efficiency of 23% [529].

6.3.1.4 Conventional gasification (GAS)

Conventional gasification converts waste into syngas using a moving grate gasifier. The syngas were directly combusted for energy in a steam-boiler system. The emission is cleaned via lime and activated carbon injection. Because of the conventional approach, the process substantially generates acidic gases, requiring more limestones in the APC practice to neutralise them. Bottom ash and APC are sent to the landfill while recycled scrap metal is recovered into the market contributing as avoided burden [530].

6.3.1.5 Thermal Plasma Gasification (PG)

Thermal gasification was based on Advanced Plasma Process (APP)'s plasma gasification process [57]. The pilot scale has been studied extensively both from experimental and modelling perspectives [144]. The process gasified waste in a fluidised bed. The produced syngas and ash were treated in a plasma reactor for tar cracking and ash vitrification. The process is claimed to generate a significant amount of energy from gas engines and the vitrified ash may be directly used as rock aggregates without further treatments. However, it is important to note that the mass balance for this process was based on Aspen simulation data that has been validated with experimental results of a pilot-scale reactor. Furthermore, the data inventory was collected from Evangelisti et al. [456] citing that personal communication was used for the mass and energy balance.

6.3.1.6 Gasification with NTP Tar cracking for Energy (NTP-E) and Methanol (NTP-M)

In these scenarios, the incoming waste is gasified into crude syngas, where it is treated and cleaned with NTP tar cracking and APC system to produce clean syngas. The clean syngas were later converted into energy in a fuel cell (NTP-E) or synthesised into methanol (NTP-M). The excess syngas is assumed to be combusted in a stack and released as emissions. full flowchart explanation and discussion are provided in Chapter 4.

Currently, there is a minimal industrial-scale implementation of NTP, limiting the data inventory available for environmental study. The data limitation is more pronounced for resource depletion and

detailed emissions. Because of this, NTP-LCA often rely on mass balance deduced from process simulation such as Anastasopoulou et al. [531]. For this study, the mass and energy balance, along with the emissions, were deduced from various sources, that is (1) the mass balance of another gasification scenarios (GAS and PG), (2) mass and energy balance from Chapter 4, and (3) mass balance and emission from other LCA study on fuel cells [532] and methanol production [523].

Regarding the data inventory, these assumptions were adopted. For energy resources, the PG operation reported utilisation of thermal plasma at 50-250 kW for 60 kg/h of RDF [145]. Meanwhile, Chapter 4 reported that NTP energy requirement was at 18 kWh for 10 kg/h of MSW. Translating this into these scenarios, and assuming that plasma generation is the most significant energy consumption, the primary energy requirements used in this study are 1.6 MJ and 2.1 MJ for NTP-E and NTP-M, respectively. The values were adjusted from PG's primary energy resource of 2.25 MJ reported by Evangelisti et al. [456]. The higher NTP-M scenario is due to the steam boiler.

For non-renewable element consumption, the inputs are assumed to equate to the conventional gasification scenario (GAS). This assumption is adopted due to negligible differences between GAS and NTP scenarios. Inherently, the NTP scenario's singular difference is the NTP tar cracking unit adoption, where the difference has been accounted for in the higher energy consumption. Furthermore, for NTP-E external input of fuel cell production is added to the inventory. This scenario utilises fuel cell production available within the Ecoinvent 3.6 database. The process provides data to produce 1 fuel cell for 125 kW production for 80,000 useful hours. The fuel cell unit is normalised against the energy generation. For NTP-M, the catalyst is assumed to be iron-based assumed to be useful for 3 years [533].

Similar to the non-renewable input, the emission output was assumed to equate to the GAS scenario. This adoption is made due to the lack of scientific understanding of NTP impacts in other pollutants, along with the similar implementation of APC requirements presented in the inputs, that is the high limestone and activated carbon flow rate. For the output, Evangelisti et al. [456] reported that PG produces 0.5 kWh per kg of MSW from 39% gas engine efficiency. Meanwhile, the fuel cell efficiency adopted in Chapter 4 was 43.7%. Thus, assuming a linear conversion, the NTP-E energy generation is 0.56 kWh per kg of MSW, which is slightly lower than the reported 0.69 kWh/kg in Chapter 4. For NTP-M, the methanol production is assumed to be 0.94 kg for 1 kg of MSW directly adopted from Chapter 4. This also reduces the CO_2 emissions by 35%.

The composite data inventory adopted for NTP scenarios is due to the nature of comparative LCA. To ensure valid comparison, the input and output levels of detail should be equal across scenarios. Directly

adopting a mass balance from Chapter 4 would create a distorted level of information as the study does not assess detailed emissions such as heavy metals and water emissions. Because of this, the Chapter 4 results were used as guidance and rationed with other gasification scenarios to produce a comprehensive, yet semi-accurate representation of waste gasification with NTP tar cracking. This approach enables homogeneous comparison across scenarios. Despite this limitation, this study still provides numerical evidence for the early-stage development of waste gasification with NTP tar cracking and the potential for chemical recycling [534]. The data details discrepancy also inhibits this work from utilising the comprehensive sanitary landfill and incineration scenarios provided by the Ecoinvent 3.6 database.

6.4 LCA Impact Assessment and Result

Figure 6-3 and Figure 6-4 shows the environmental impact of selected impact categories used in this LCA study. The numerical value can be found in Appendix D.3. The figures show LCA results direct environmental impact, accompanied by the potential emissions savings from product generations in negative value. The final environmental impact is shown in black showing the comparison of each waste management strategy for the six environmental impact categories.

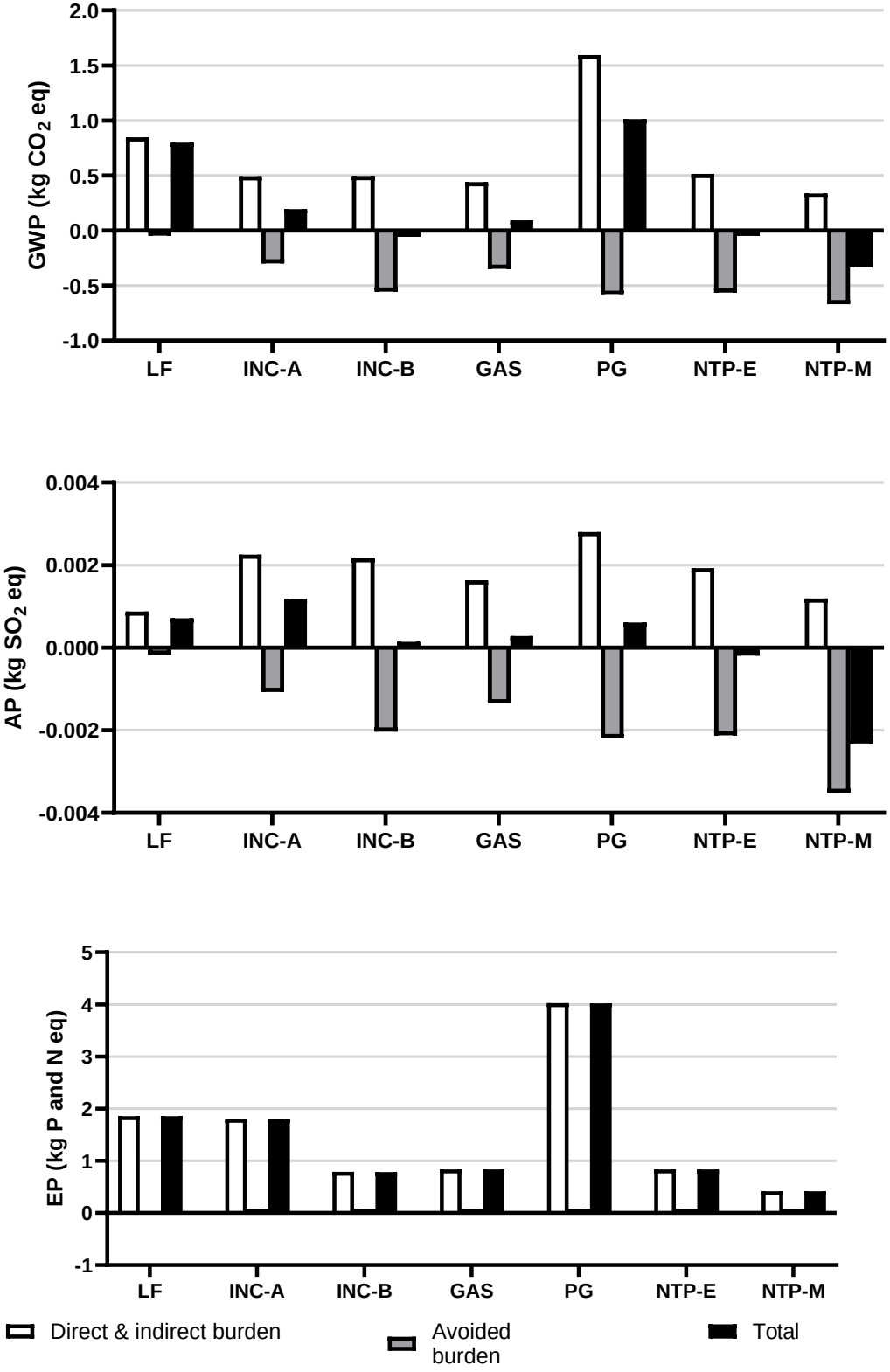

Figure 6-3: Environmental impact of the waste management scenarios for Global Warming Potential (GWP), Acidification Potential (AP), and Eutrophication Potential (EP)

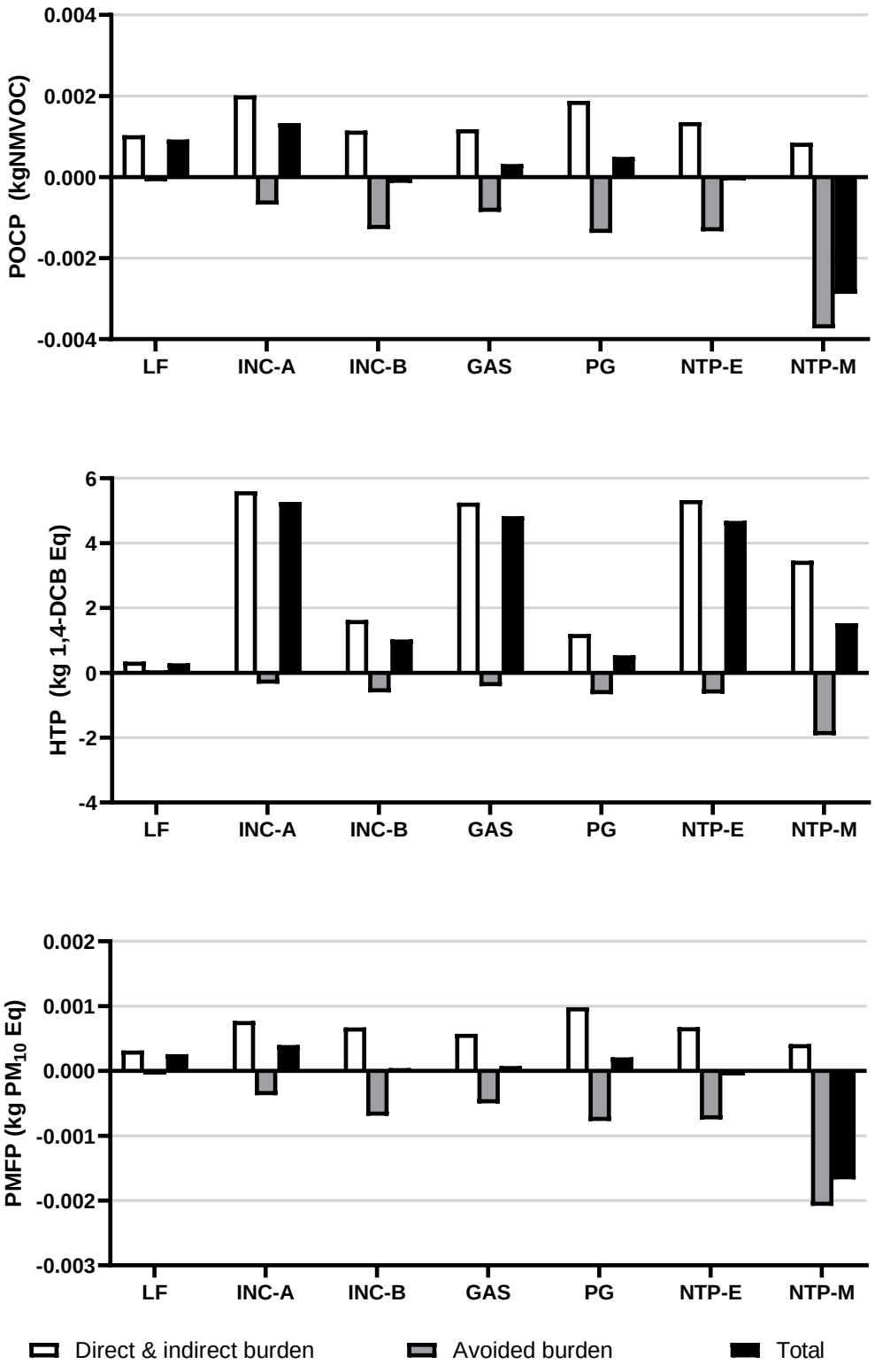

Figure 6-4: Environmental impact of the waste management scenarios for Photochemical ozon creation potential (POCP), Human Toxicity Potential (HTP), and Particulate Matter Formation Potential (PMFP)

6.5 LCA Interpretation and Discussion

For GWP, the LCA result shows that landfilling produces a high environmental impact (1.01 kg CO_2-Eq). This may be attributed to the landfill's substantial methane production. Methane is established to be 27-30 times more potent than CO_2 in GWP100, i.e, 100 years-time [535]. Furthermore, landfilling has the lowest avoided burden, primarily due to its limited capacity to generate valuable products for the market. In contrast, INC-A and INC-B exhibit significantly lower emissions (0.19 kg and -0.06 kg of CO_2-eq, respectively, Figure 6-3). INC-B's low environmental impact can be attributed to its robust energy recovery capabilities, producing nearly double the energy output of INC-A. The negative value indicates that the scenario emits less environmental impact compensated through avoided burden.

For energy generation, shown in Figure 6-5, The LCA demonstrates that both INC-B and NTP-E outperform the Australian grid in terms of GWP. The Australian power grid (AU grid) relies on coal combustion [536], resulting in a higher GWP when compared to INC-A and NTP-E. The database used in this study [520], reveals that AU grid data has almost three times GWP (0.94 kg CO_2-eq/kWh) than the UK grid (0.35 kg CO_2-eq/kWh) [536].

The combination of cleaner combustion practices and the production of scrap metal in INC-B contributes to a high avoided burden. Similarly, gasification (GAS) exhibits minimal overall GWP impact (0.09 kg of CO_2-eq). Figure 6-5 shows comparisons of direct GWP for different scenarios for 1 kWh power production. NTP-E and INC-B show almost similar GWP when compared to the Australian power grid. Meanwhile, the UK power grid has a lower environmental impact due to their usage of natural gas. PG has the highest GWP as the process consumed significant grid energy. INC-B and NTP-E shows the environmental benefits of EFW in terms of GWP [8].

Interestingly, the thermal plasma gasification (PG) LCA result shows the highest GWP impact out of the compared scenarios (1.59 kg of CO_2-eq, Figure 6-3). This burden persists despite the significant energy generation resulting in a high avoided burden from product generation (-0.58 kg of CO_2-eq, Figure 6-3). The high direct burden causes PG to produce the highest GWP out of every scenario (1.01 kg of CO_2-eq, Figure 6-3). This result does not agree with Evangelisti et al. [456]'s findings despite the identical data. This discrepancy is likely due to Evangelisti's plasma generation scenario independency from the grid power, instead, their study used unspecified fuel. This finding underscores the importance of avoiding fossil fuel-based energy for thermal plasma generation.

Furthermore, both NTP-E and NTP-M shows negative environmental impact. Suggesting that the direct environmental burden is compensated by the generation of valuable products. NTP-E's low

energy requirements enable emissions from the grid to be compensated by the high energy recovery via fuel cells. On the other hand, NTP-M demonstrates even greater emissions savings, as it transforms some of the waste's carbon into methanol instead of releasing it into the atmosphere. NTP-M exhibits a substantial avoided burden (0.67 kg of CO_2-eq, Figure 6-3). This is because conventional methanol production relies on natural gas synthesis that arguably produces significant emissions from mining and extraction [523]. NTP-M also has a lower GWP than NTP-E, this is because NTP-M convert some of the carbon emissions into methanol, locking it as product rather than emissions to the environment. GWP impact categories highlight the importance of energy flow into the process. The significant direct burden in PG and NTP processes signify the importance of renewable energy to support the process and reduces the direct environmental impact.

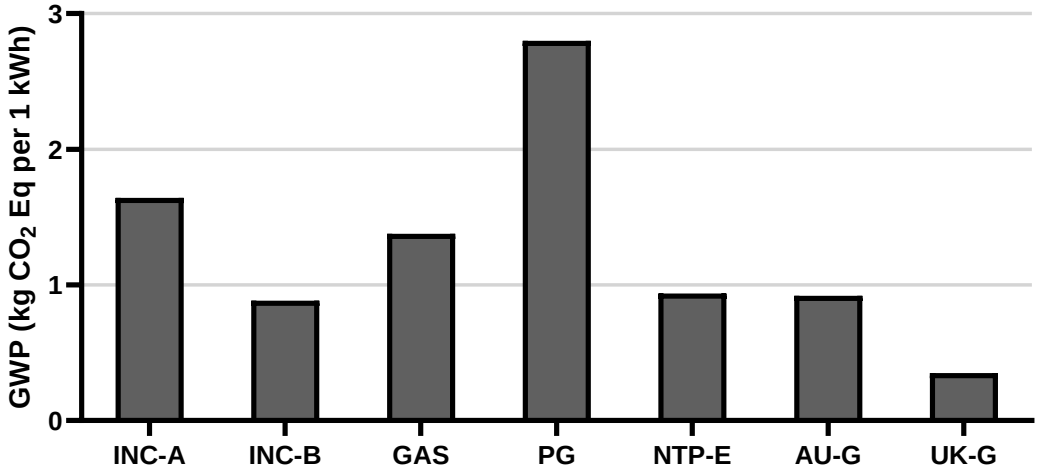

Figure 6-5: GWP comparison between the energy generation scenario in this study and AU and UK power grid (AU-G and UK-G)

For AP, landfilling exhibits a minimal impact, primarily because the decomposition of organic matter seldom generates potent acidic gases, releasing them gradually over an extended period. [537] In waste conversion, the AP is primarily influenced by the installed APC within each scenario. Notably, INC-A registers the highest environmental impact among the thermal processes. Although LF direct burden is not significantly higher than other scenarios, the low energy generation resulted in a less substantial avoided burden. In contrast, PG has the highest direct burden (0.0016 kg of SO_2 Eq, Figure 6-3); however, it is being compensated with its substantial energy production. AU grid relies heavily on coal combustion, which is a significant source of acidic gases [538]. Although APC measures are mandatory for coal combustion, environmental regulations may be less stringent compared to the EFW. This theory may explain the significant avoided burden provided found in this study. Similarly,

the production of methanol from natural gas requires substantial fossil fuel energy. Methanol from waste material (NTP-M) demonstrates a lower AP, resulting in a negative environmental burden of (-0.0023 kg of SO2 Eq, Figure 6-3). Processes may reduce their AP by installing a more advance acidic gas cleaning equipment.

For EP, it measures the excessive growth of algae and aquatic plants due to an increase in nutrient levels (such as nitrogen and phosphorus) in water bodies. Eutrophication can lead to oxygen depletion, harming aquatic life and ecosystems [481]. The LCA result reveals that the direct burden is the dominant contributor, with minimal environmental impact savings from the avoided burden (Figure 6-3). This outcome can be attributed to the limited inclusion of emissions to water in the inventory database. This underscores the critical importance of consistent data inventory practices across scenarios and database. In this LCA study, the database falls short in providing emissions to water, leading to a minimal avoided burden across all scenarios [520]. From the direct burden, it appears that GP shows the highest environmental impact whilst NTP-M shows the lowest. The high impact burden may be attributed to the less complex APC and unspecified wastewater treatment within the data inventory. It is important to note that this result contradicts other LCAs that has been done on thermal plasma gasification (Chapter 5). Further analysis in terms of data inventory and system boundary analysis may be required to establish a conclusive finding across studies.

For POCP, the impact primarily originates from halogenated methane by-products, a common ozone-depleting compound. POCP measuring the potential of a substance to form ground-level ozone through atmospheric reactions. It quantifies emissions of volatile organic compounds (VOCs) and nitrogen oxides (NOx) [481]. Thermal processes generally exhibit a higher impact than landfilling (0.0001 kg of NMVOC, Figure 6-4), with INC-B being an exception. This outlier arises due to the avoided burden from products generated, effectively offsetting the direct burden. NTP-M stands out with the lowest environmental impact, attributed to a high avoided burden [523]. POCP highlights the importance of products generation. For example, LF minimal commodity productions resulted in a high total POCP. This is also the case for INC-A, where the low energy recovery produces minimal avoided burden that is insufficient to compensate for the direct and indirect burden. Interestingly, INC-A and PG has a similar POCP, which may be cause by different factors. INC-A is due to high chemical requirement whilst PG is due to high energy requirement (See Appendix D.1). NTP-M methanol productions shows to produces a significant avoided savings that resulted in negative total burden (-0.0029 kg of NMVOC, Figure 6-4).

For HTP, the impact may originate from heavy metal leaching and emissions into water and air. This means that HTP considers various type of emissions with various factors. ot assesses the potential of a substance to cause harm to human health through exposure via inhalation, ingestion, or dermal contact. HTP considers factors such as the toxicity of emissions, exposure pathways, and the severity and duration of health effects [481]. In the case of sanitary landfilling (LF), the inert nature limits human exposure to the toxins, resulting in a low HTP. Among thermal processes, only INC-B and PG exhibit a low HTP (0.5 and 1.0 of 1,4-DCB kg-eq, Figure 6-4), while others register substantial impact (4.5 to 5.8 of 1,4-DCB kg-eq, Figure 6-4). INC-B's low environmental impact may be cause by its enhanced metal recovery capabilities, reclaiming toxic compounds into products [145]. Meanwhile, PG's slagging process immobilizes heavy metals into aggregate materials, resulting in minimal HTP. NTP's inability to produce slag due to lower temperature is evidently shown in this category. INC-A and GAS high HTP is due to the heavy metal emissions into the environment, which is the same case for NTP-E and NTP-M. Hence, more measures need to be implemented to ensure a lower HTP for NTP. NTP lack of slagging process does not bind the toxic ash into un-leachable matrix.

For PMFP, a similar trend with POCP is observed, with direct burden primarily attributed to SO_x and NO_x emissions. INC-B demonstrates a slightly lower direct burden than INC-A (0.00077 and 0.00067 kg of PM_{10}-eq, respectively), possibly due to the utilisation of ammonia injection to control NO_x production. Landfilling emerges with the lowest environmental impact (0.00026 kg of PM_{10}-eq, Figure 6-4), as it does not actively oxidise waste to generate smaller particles. Similar to other impact categories, NTP-M produces the largest avoided burden due to its high methanol production, producing overall negative environmental impact. NTP-M also has lower PMFP than NTP-E possibly due to lower carbon emissions. PG emerges as the highest PMFP direct burden but being compensated by the high energy generation in terms of avoided burden, which is not the case for INC-A.

In comparison to other studies, Śliwińska et al. [441] evaluated the co-production of power and methanol through coal gasification and reported a positive environmental impact upon implementation. However, the study also highlights that the novel methanol synthesis approach requires further evidence before implementation. Meanwhile, Stasiulaitiene et al. [539] compared plasma technology to conventional catalytic reduction methods. Their findings revealed that plasma technology exhibited better environmental performance for EP, AP, and HTP. However, the plasma process has a higher GWP, possibly attributable to its higher energy consumption, which is also observed in this study.

Overall, it is important to note the data limitation of this study. INC-B's mass balance was based on the design value that require validation with the operating plant [529]. Furthermore, more research is required to investigate impact NTP with other pollutants and its upscaling efficacy. The upscaling uncertainty extends to all scenarios. There is a wide capacity range across adopted data inventory, from 60 kg/h [145] to 28 tonnes per hour [528]. Additionally, inconsistencies in the chemical lists across data inventories between scenarios and databases are evident. The greater detail in the emissions list used to estimate avoided burdens may lead to an overestimation, producing a false favourable outcome.

Future LCA studies may integrate the emission inventory with a tertiary process, generating a more robust database. Furthermore, researchers should include the investigation of NTP reactors' impacts on other pollutants within syngas, more evidence is required on this front to enable a more in-depth environmental impact. Future work may also expand the system boundary to include waste separation, transport, and capacity impacts, accompanying the LCA study with in-depth sensitivity analysis. Moreover, future work should also explore the possibility of on-site energy generation as it may reduce the overall emissions. The research may include the changes as the grid evolves to cater more renewable energy.

6.6 Conclusion

This chapter has undertaken a comprehensive examination of waste management technology's environmental impact through a Life Cycle Assessment (LCA) method. The investigation has shed light on the complex interplay between waste resource recovery and its environmental impacts. The scenario investigated included landfilling (LF), Incineration (INC-A and INC-B), Gasification (GAS), thermal plasma gasification (PG), and gasification with NTP tar cracking for energy (NTP-E) and methanol (NTP-M) synthesis. The LCA quantified the direct burden through data inventory, which is offset by avoided burdens from the generation of valuable products. This methodology allows a more comprehensive analysis that included commodity production.

The LCA results highlight the importance of energy efficient processes. High energy recovery produces more avoided emissions, effectively reducing the total environmental impact. Similarly, the energy requirement had a significant influence on the direct environmental burden, particularly for Global Warming Potential (GWP) and Acidification Potential (AP). Grid power in this study (Australia) heavily relies on coal combustion, contributing to elevated CO_2 and acidic gas emissions. This was evidently shown for the PG scenario. PG shows that the high energy recovery did not compensate for the large direct emissions from plasma generation. This resulted in PG producing the

highest environmental impact in terms of GWP and AP. In contrast, NTP-E lower energy requirement translate into lower direct environmental impact, which is sufficiently compensated with avoided impact to produce negative GWP and AP. Interestingly, NTP-E process generates almost identical direct GWP in comparison to Australian grid. This highlights the importance of low energy processes and avoiding fossil fuel-based grid energy. On the other hand, although landfilling shows a considerable impact on GWP, AP, and Photochemical Ozone Creation Potential (POCP), it has a minimal Human Toxicity Potential (HTP) due to its inert nature. Moreover, the LCA highlight the paramount role of product generation, substituting the conventional process' environmental impact. This effect is particularly pronounced in NTP-M, where methanol production replaces conventionally produced methanol from natural gas, resulting in substantial avoided environmental impact.

Chapter 7

Conclusion and Perspectives

The perspectives of this chapter have been published as the following manuscript: Sanjaya, E. and Abbas, A., 2023. Plasma gasification as an alternative energy-from-waste (EFW) technology for the circular economy: An environmental review. Resources, Conservation and Recycling, 189, p.106730.

7.1 Thesis Main Conclusion

Tar in syngas is a persistent issue in gasification processes, it is critical to solve the tar problem for advancing gasification. Importantly, the improvements in gasification practicality extend beyond waste management. Its implementation may hold relevant for biomass conversion and gas synthesis. This highlights the substantial contribution of advancing plasma gasification technology. Despite thermal plasma's potential for cleaner synthesis, technical challenges like material fusing and high energy requirements persist, limiting its widespread adoption. Although organisations have explored thermal plasma gasification for energy from waste (EFW), many projects have been discontinued due to its high cost. Conversely, non-thermal plasma (NTP) tar cracking, demonstrated in bench-scale settings with DBD and GAD reactors, presents a promising avenue. However, further research is needed for its implementation, particularly in modelling investigations, which remain relatively underexplored due to the complexity of plasma modelling and its diverse applications.

Modelling of NTP tar cracking reaction kinetic aligns with external experimental data especially at 600-800 K. Model limitations in PAH formation may contribute to this disparity at temperatures lower than 600 K. Meanwhile, thermal physical limitations such as runaway materials, gas expansion, and the plasma transitional state may cause the disparity at temperatures above 800 K. Investigation into reaction mechanisms reveals a reactivity sequence from naphthalene to toluene to phenol, with the hydroxyl group in phenol enhancing its reactivity. Toluene and naphthalene undergo incomplete tar cracking at low power, resulting in benzene formation, necessitating higher plasma power. NTP tar cracking in syngas leads to an increased acetylene concentration.

The reaction kinetic is applied to a waste gasification process simulation through MLR reduced correlation, showing accuracy prediction ranging from 66.7% to 94.7%. Assessment across various

syngas recovery scenarios underscores the necessity for advanced energy recovery due to the high energy demand of NTP tar cracking. Material synthesis emerges as the preferred option, yielding high-quality tar-free syngas suitable for synthesis, with the potential to produce up to 0.94 kg of CH_3OH per kg of waste. However, the simultaneous production of materials and power faces challenges as both processes compete for ideal operating conditions and valuable syngas species.

For comprehensiveness, an in-depth examination of the current LCA studies on thermal plasma through meta-analysis comparison methodology. The meta-analysis shows a clear environmental benefit of thermal plasma gasification over incineration, while it is inconclusive for conventional gasification across 25 LCA works. The key technological contributions to lowering environmental impact are identified as adequate APC systems, by-product utilisation, and a high energy recovery technology.

The waste gasification with NTP tar cracking LCA shows superiority over other waste management strategies. It was revealed that this process is more beneficial than thermal plasma gasification. For thermal plasma gasification, the high energy recovery did not compensate for the large direct emissions from high energy requirements. NTP-gasification for methanol production shows the lowest environmental impact, as it substitutes the market with methanol produced from natural gas. The results show the significance of valuable product generation that contributes to the avoided burden by replacing the market with waste-originated commodities.

This thesis has presented the use of simulation techniques to further advance the NTP tar cracking research avenue and, consequently, its implementation in waste gasification. This thesis provides the "proof-of-concept" for the ideal NTP-tar cracking implementation through numerical validity along with its environmental impact.

7.2 Future Work

Firstly, further investigation is required to assess other species in NTP and their potential interactions with tar. Identifying these compounds should be followed by establishing their roles and reaction kinetics. From an experimental perspective, researchers should conduct in-depth analyses of secondary by-product yield, that is the liquid product produced in the solvent trap. Accurate estimations would provide a deeper understanding and may even lead to insights into potential secondary tar product generation. The lack of data from this angel resulting in the lack of validation.

Additionally, more evidence is needed for upscaling and studying NTP behaviour during upscaling, simply elongation NTP reactor is a challenging design approach. It may be worthwhile to explore novel reactor designs. Reactor design exploration may be integrated with other tar abatement strategy, such as catalyst and thermal decomposition. The solution for an effective tar cracking may not lies in one technology, but an integrated novel reactor.

Process simulation work may be expanded to encompass full plant simulation, including aspects such as oxygen purification and complex heat recovery methods. This comprehensive approach would allow for further feasibility assessments, techno-economic analysis, and capacity evaluations. Moreover, a more accurate model can be achieved by integrating multiple software simulations. In this case, each modelling software tailored for a specific process that predict each aspect independently.

Lastly, data inventory related to environmental impact should be standardised across various studies, including system boundaries for LCA. This standardisation may prevent biases caused by different techniques in environmental impacts estimation. The standard can be used for various waste management's LCA. In terms of future studies, researchers may explore the potential for co-production of recycling and material recovery. The optimal solution may not lie in a single technology but in a diverse collective approach to waste treatment. This may eliminate competition between recycling and other waste management strategies.

Overall, more investigation is still required to advance waste gasification. Despite this thesis' focus on the major tar issue, other limitation presence in waste gasification should be addressed as well. Challenges such as syngas synthesis, acidic gas generation, and other pollutants are still unresolved. Furthermore, this thesis has only focused on the tar degradation via surrogates' compound, future works may expand this by incorporating a more comprehensive tar database and its potential interactions. Addressing these issues may actualise the waste gasification.

7.3 Perspective on Circular Economy and Gasification

Circular Economy (CE) is a novel model that minimises waste by maximising the reuse and recycling of products and resources. It aims to break away from the traditional "take-make-dispose" linear model to create a more efficient and sustainable economic model [540]. Researchers and a growing consensus in the investment community believe that EFW, particularly incineration, is not the right candidate to be focused on when discussing the CE transition. The highlight should be placed on ma3terial recovery [25, 541, 542]. The destruction of material for energy purposes eliminates the potential of it being re-circulated. Nevertheless, EFW still has a clear sustainability role in mitigating GHG and eliminating

landfilling [543]. EFW can support CE by converting material that is destined to be landfilled into valuable energy[544], creating a thermodynamic approach for the 'closing-the-loop' strategy [545]. While feedstock competition with recycling may arise [156, 546], EFW technically supports recycling by recovering metal, destroying contaminants and toxins, and feeding the grid with a more sustainable energy source [38]. Due to entropy build-up, quality degradation is part of material recycling, meaning an infinite material cycle is impossible in traditional recycling approaches [25]. Recycling can be costly and labour-intensive [26], which also comes with social issues [547].

There is no singular silver bullet technology solution in CE, while recycling is suitable for many waste streams, EFW is necessary for hazardous, toxic, hygienic, and perishable waste. EFW can complement recycling in CE by consuming 'unsuitable to be recycled' waste [38, 544]. Different government organisations understand the role of EFW in a practical CE [548, 549], or as a transitional tool [37, 549, 550]. Nevertheless, the CE approach must be in place to avoid incineration overtaking the waste industry [37, 39, 551-553].

While robust, incineration energy products are limited to grid energy and focus on the high rate of consumption [554]. Gasification is arguably a better suitor for EFW in the CE because:

1. The diverse products can align with different CE strategies. Syngas can be combusted through a combined power cycle turbine for higher energy recovery [555] or routed into hydrocarbon conversion [543]. Bottom ash is converted into slag that can be easily repurposed for construction material without further treatment [556] (Figure 7-1).
2. The modular design can be easily retrofitted for future treatment, avoiding the lock-in investment that comes with incineration [557]. The pre and post-treatments provided more material separation [558]. The process can be translated into different sectors, such as co-processing with wastewater treatment [559] or anaerobic digestion [560]. This enables the opportunity for waste management parks targeting holistic treatment of process waste, and elimination of feedstock competition [561-564].
3. The smaller capacity provides an opportunity for decentralised waste treatment for smaller municipalities and local microgrids [565]. When waste separation is normalised, processing specific homogenous waste can provide a reliable reaction that enables a higher value-adding process [566, 567], this includes the possibility of chemical recycling [568, 569] and advanced biorefineries [570].
4. Some studies demonstrate that thermal plasma gasification has a lower generation of dioxins, NOx and flue gas than incineration, reducing the need for complicated APC [543, 565]. The smaller capacity may also reduce the cumulative exposure of air pollutants to the public.

7.4 Perspective on Gasification Implementation and EFW

The technical challenges in gasification transverse into economic feasibility challenges, making it a riskier investment when compared to incineration projects. High-quality syngas is required for commercialisation [558], this is achievable through consistent feedstock quality from waste separation. Thus, the lack of general support for new waste management solutions affects waste gasification implementation [570]. The public and investors are still sceptic about its feasibility and its environmental benefits [556]. Overall, extending plasma technology into EFW has been troublesome.

With air pollution representing a key backlash against EFW [571], installing a lengthy APC has become the norm for modern incineration [572]. With this push for a cleaner EFW plant, there is a concern that the pressing environmental targets and net zero policy could drive centralised mega incineration projects. A complex APC will consume more energy, reducing the net commodities to be sold to the grid. This makes EFW proponents design and install large capacity plants in pursuit of economies of scale [573].

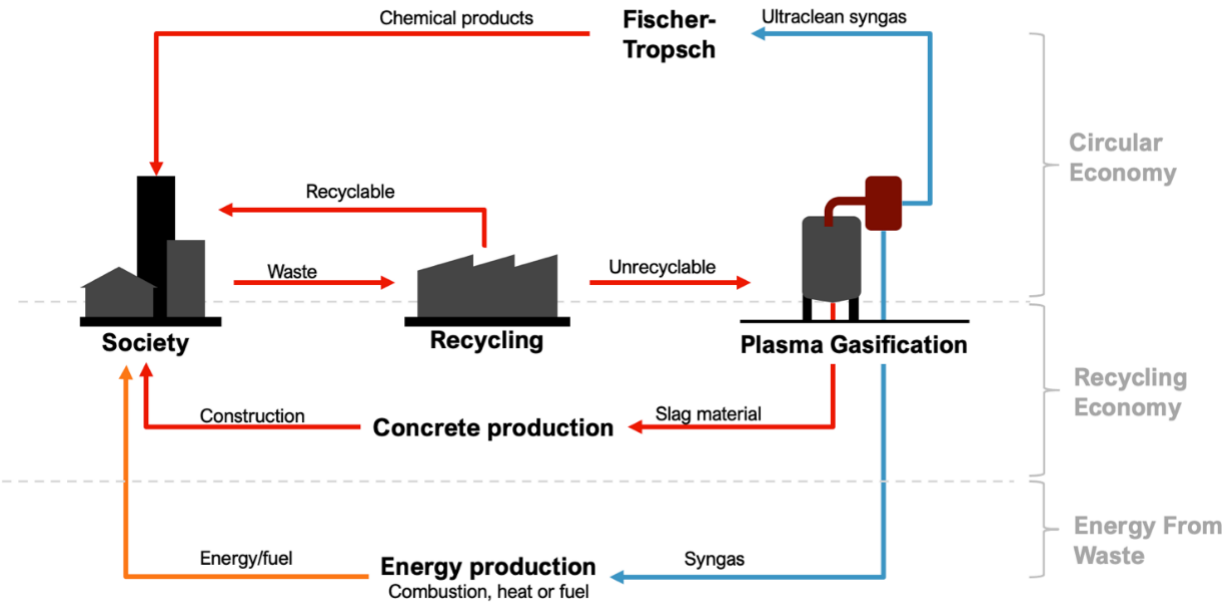

Figure 7-1: Potential of plasma (thermal and NTP) gasification in the circular economy

Since EFW is an umbrella term, air emissions policy and regulations often group incineration with other EFW technology, including plasma gasification, giving the perception that gasification has a slight variation to incineration [41]. Such grouping policy can restrict alternative EFW development since emerging technologies like waste gasification do not scale up as easily as moving grate incineration, reducing their ability to compensate for the complex APC system. Table 7-1 shows that

thermal plasma gasification can meet EFW and other technology regulations, apart from NOx and HCl limits which can be met by installing a catalytic converter and scrubber.

Separate regulations are required to support alternative EFW, giving them an alternative commercialisation pathway. Jurisdictions like the EU and the US implement less stringent regulations for smaller and/or older waste incineration and even produce a special regulation for alternative thermal EFW [574]. Table 7-2 shows the regulation on EFW emissions. This will also subsequently support the CE as the alternative EFW to open the market into fuel and chemical products.

Table 7-1: Emission comparison from different EFW (All unit is in mg/Nm^3, unless specified

Technology	Facility	Capacity (tpd)	APC	NOx	CO	SOx	PM	HCl	PCDD/Fs (mg/Nm^3)	Ref
Incineration	Milan, Italy	1232	Electrostatic precipitator, fabric filter, and SCR	41.4	5.5	0.44	0.09	1.9	0.005	[575]
Incineration BAT	Based on surveyed plants	-		2-7	10-50	5-40	-	2-7	0.01-0.06 ng/Nm^3	[487]
Gasification	Lahti, Finland	685	baghouse filter and SCR	161	2	7	2	1	0.002	[575]
	Unspecified, Japan	250	Baghouse filter, lime injection and SCR	20.9	6.2	3.3	1	3.7	0.006	[575, 576]
	Ebara TwinRec, Japan	420	Baghouse, lime injection, and SCR	29	-	<2.9	<1	<2	0.000051	[41, 577]
	Arena from Energos Norway	100	Baghouse filter, lime injection, activated carbon injection	42	-	19.8	0.24	3.61	0.0008	[41, 578]
Plasma gasification	Alter NRG Commercial plant, Utashinai, Japan	180	bag filter	206-244	-	5	<10	6-31	0.00059-0.00067	[156, 579, 580]
	Alter NRG pilot plant in Mihama-Mikata Japan	22	baghouse filter and activated carbon injection,	129-158	11.5-14.8	13	<16	86-93	-	[60, 580]
	Plasco Energy, Canada	110	Scrubber, precipitator, and absorber.	107	-	19	9.1	2.2	0.006	[41, 581]

Table 7-2: Concentration limits for various EFW technology (All unit is in mg/Nm^3, unless specified)

	EFW	Averaging Period	NOx	CO	SOx	PM	HCl	Comment	Document & Section
EU	Incineration	30 min	400	100	200	30	60	Two set of averaging periods (30 min and daily)	[582] Annex VI Part 3
		24 hours	150	50	40	10	2-7		[583]
	Cement kiln incineration	30 min	533-333	Flexible	33	20	6.67	Only need to meet 30 min averaging period, competent authority set the limit for CO and NOx	[582] Annex VI Part 4, Point 2
	Co-incineration (two stage pyrolysis or gasification)	30 min	No limit - 133	Unspecified	No limit - 133	33-20	Unspecified	Emission limit vary depending on the EFW capacity in terms of energy generation (MWth)	[582] Annex VI Part 4, Point 3
USA	New Incineration (≥ 250 tpd)	24 hours	240	98-244	67	15.6	32	New regulation for old and new EFW	[584] Table 1
	New Incineration (35-250 tpd)	24 hours	240-800	98-244	69	19	32	Different technology (fluidised bed rotary wall, etc) has different CO limit	[585] Table 1-4
NSW, Australia	New incineration	1 hour	250	80	100	20	50	Draft limit changed to meet with additional advice	[586] Table 1
	General activities (may include pyrolysis & gasification)	1 hour	64-357	89	Unspecified	36	71	Not tailored for waste management nor EFW	[587] Schedule 4 Group 6

for 100% compliance, converted into 273 K, 101.325 kPa (1 atm), 11% O2

References

[1] A. Zaman, Zero-Waste: A New Sustainability Paradigm for Addressing the Global Waste Problem, The Vision Zero Handbook: Theory, Technology and Management for a Zero Casualty Policy, Springer2022, pp. 1-24.

[2] P. Gautam, S. Kumar, Characterisation of hazardous waste landfill leachate and its reliance on landfill age and seasonal variation: a statistical approach, Journal of Environmental Chemical Engineering 9(4) (2021) 105496.

[3] T. Greicius, NASA Sensors to Help Detect Methane Emitted by Landfills, 2023. https://www.nasa.gov/feature/jpl/nasa-sensors-to-help-detect-methane-emitted-by-landfills.

[4] A.L.P. Silva, J.C. Prata, A.C. Duarte, D. Barcelò, T. Rocha-Santos, An urgent call to think globally and act locally on landfill disposable plastics under and after covid-19 pandemic: Pollution prevention and technological (Bio) remediation solutions, J Chemical Engineering Journal 426 (2021) 131201.

[5] H. Onoda, Smart approaches to waste management for post-COVID-19 smart cities in Japan, J IET Smart Cities 2(2) (2020) 89-94.

[6] European Parliament, Waste management in the EU: infographic with facts and figures, 2023. https://www.europarl.europa.eu/news/en/headlines/society/20180328STO00751/waste-management-in-the-eu-infographic-with-facts-and-figures.

[7] L. Makarichi, W. Jutidamrongphan, K.-a. Techato, The evolution of waste-to-energy incineration: A review, Renewable and Sustainable Energy Reviews 91 (2018) 812-821.

[8] E. Sanjaya, A. Abbas, Plasma gasification as an alternative energy-from-waste (EFW) technology for the circular economy: An environmental review, J Resources, Conservation Recycling 189 (2023) 106730.

[9] X. Zeng, Y. Ueki, R. Yoshiie, I. Naruse, F. Wang, Z. Han, G. Xu, Recent progress in tar removal by char and the applications: A comprehensive analysis, J Carbon Resources Conversion 3 (2020) 1-18.

[10] B.J. Mahler, P.C.V. Metre, J.L. Crane, A.W. Watts, M. Scoggins, E.S. Williams, Coal-tar-based pavement sealcoat and PAHs: implications for the environment, human health, and stormwater management, ACS Publications, 2012.

[11] T.A. Milne, R.J. Evans, N. Abatzaglou, Biomass gasifier"Tars": their nature, formation, and conversion, (1998).

[12] Y.G. Rueda, L. Helsen, The role of plasma in syngas tar cracking, J Biomass Conversion Biorefinery (2019) 1-15.

[13] Y.A. Gomez Rueda, Syngas Purification by Plasma Tar Cracking, (2021).

[14] F. Saleem, J. Harris, K. Zhang, A. Harvey, Non-thermal plasma as a promising route for the removal of tar from the product gas of biomass gasification–A critical review, J Chemical Engineering Journal 382 (2020) 122761.

[15] E. Gomez, D.A. Rani, C. Cheeseman, D. Deegan, M. Wise, A.J.J.o.h.m. Boccaccini, Thermal plasma technology for the treatment of wastes: a critical review, 161(2-3) (2009) 614-626.

[16] L. Liu, Z. Zhang, S. Das, S. Kawi, Reforming of tar from biomass gasification in a hybrid catalysis-plasma system: A review, J Applied Catalysis B: Environmental 250 (2019) 250-272.

[17] S.A. Nair, Corona plasma for tar removal, (2004).

[18] A. Rabinovich, G. Nirenberg, S. Kocagoz, M. Surace, C. Sales, A. Fridman, Scaling up of non-thermal gliding arc plasma systems for industrial applications, J Plasma Chemistry Plasma Processing 42(1) (2022) 35-50.

[19] R. Wang, Y. Yang, S. Chen, H. Jiang, P. Martin, Power calculation of pulse power-driven DBD plasma, J IEEE Transactions on Plasma Science 49(7) (2021) 2210-2216.

[20] M.Y. Arshad, M.A. Saeed, M.W. Tahir, H. Pawlak-Kruczek, A.S. Ahmad, L. Niedzwiecki, Advancing Sustainable Decomposition of Biomass Tar Model Compound: Machine Learning, Kinetic Modeling, and Experimental Investigation in a Non-Thermal Plasma Dielectric Barrier Discharge Reactor, J Energies 16(15) (2023) 5835.

[21] A.H. Khoja, M. Tahir, N.A.S. Amin, Recent developments in non-thermal catalytic DBD plasma reactor for dry reforming of methane, J Energy conversion management 183 (2019) 529-560.

[22] NSW Government, NSW Waste and Sustainable Materials Strategy 2041, 2021. https://www.dpie.nsw.gov.au/__data/assets/pdf_file/0006/385683/NSW-Waste-and-Sustainable-Materials-Strategy-2041.pdf. (Accessed 25 July 2022).

[23] S. Jones, Establishing political priority for regulatory interventions in waste management in Australia, J Australian Journal of Political Science 55(2) (2020) 211-227.

[24] NSW Government, Waste Less, Recycle More, 2016. https://www.epa.nsw.gov.au/-/media/epa/corporate-site/resources/waste/waste-less-recycle-more-2017-21-brochure-160538.pdf. (Accessed 25 July 2022).

[25] J. Korhonen, A. Honkasalo, J. Seppälä, Circular economy: the concept and its limitations, Ecological Economics 143 (2018) 37-46.

[26] L.J. Llorente-González, X. Vence, How labour-intensive is the circular economy? A policy-orientated structural analysis of the repair, reuse and recycling activities in the European Union, Resources Conservation and Recycling 162 (2020) 105033.

[27] R. Gray, What's the real price of getting rid of plastic packaging?, 2018. https://www.bbc.com/worklife/article/20180705-whats-the-real-price-of-getting-rid-of-plastic-packaging. (Accessed 25 July 2022).

[28] NSW EPA, NSW Energy from Waste Policy Statement, 2021. https://yoursay.epa.nsw.gov.au/energy-waste-policy-statement#:~:text=The%20NSW%20Energy%20from%20Waste%20Policy%20Statement%20sets%20out%20the,to%20industry%20and%20the%20community. (Accessed 25 July 2022).

[29] T. Karak, R. Bhagat, P. Bhattacharyya, Municipal solid waste generation, composition, and management: the world scenario, J Critical Reviews in Environmental Science and Technology 42(15) (2012) 1509-1630.

[30] R.J. Johnson, M.J. Scicchitano, Don’t call me NIMBY: Public attitudes toward solid waste facilities, J Environment and Behavior 44(3) (2012) 410-426.

[31] S. Shooshtarian, T. Maqsood, P. Wong, M. Khalfan, R. Yang, Review of energy recovery from construction and demolition waste in Australia, J. Constr. Eng. Manag. Innov 2 (2019) 112-130.

[32] S. Wood, M. Fanning, M. Venn, K. Whiting, Review of state-of-the-art Waste-to-Energy Technologies Stage Two- case Studies, 2013.

http://www.wtert.com.br/home2010/arquivo/noticias_eventos/WSP%20Waste%20to%20Energy%20Technical%20Report%20Stage%20Two.pdf. (Accessed 25 July 2022).

[33] H.D. Beyene, A.A. Werkneh, T.G. Ambaye, Current updates on waste to energy (WtE) technologies: a review, Renewable Energy Focus 24 (2018) 1-11.

[34] K.-W. Jun, H.-S. Roh, K.-S. Kim, J.-S. Ryu, K.-W. Lee, Catalytic investigation for Fischer–Tropsch synthesis from bio-mass derived syngas, J Applied Catalysis A: General 259(2) (2004) 221-226.

[35] Y. Byun, M. Cho, J.W. Chung, W. Namkung, H.D. Lee, S.D. Jang, Y.-S. Kim, J.-H. Lee, C.-R. Lee, S.-M.J.J.o.h.m. Hwang, Hydrogen recovery from the thermal plasma gasification of solid waste, Journal of Hazardous Materials 190(1-3) (2011) 317-323.

[36] Y. An, T. Lin, F. Yu, Y. Yang, L. Zhong, M. Wu, Y. Sun, Advances in direct production of value-added chemicals via syngas conversion, Science China Chemistry 60(7) (2017) 887-903.

[37] J. Malinauskaite, H. Jouhara, D. Czajczyńska, P. Stanchev, E. Katsou, P. Rostkowski, R.J. Thorne, J. Colón, S. Ponsá, F. Al-Mansour, Municipal solid waste management and waste-to-energy in the context of a circular economy and energy recycling in Europe, J Energy Conversion 141 (2017) 2013-2044.

[38] J. Van Caneghem, K. Van Acker, J. De Greef, G. Wauters, C. Vandecasteele, Waste-to-energy is compatible and complementary with recycling in the circular economy, J Clean Technologies nEnvironmental Policy 21(5) (2019) 925-939.

[39] EIA Bioenergy, Waste Incineration for the Future Scenario analysis and action plans, 2019 https://www.ieabioenergy.com/wp-content/uploads/2019/04/Waste-Energy-for-the-Future-IEA-version.pdf. (Accessed 25 July 2022).

[40] J. Whittaker, J. Kendall, Australian Paper to proceed with Victorian-first energy-from-waste project, 2019. https://www.abc.net.au/news/2019-02-07/victorian-first-energy-from-waste-project-gets-green-light/10791686. (Accessed 25 July 2022).

[41] U. Arena, Process and technological aspects of municipal solid waste gasification. A review, J Waste management 32(4) (2012) 625-639.

[42] W.A. Qazi, M.F. Abushammala, M.K. Younes, Waste-to-Energy Technologies: A literature review, J The Journal of Solid Waste Technology Management 44(4) (2018) 387-409.

[43] H.D. Beyene, A.A. Werkneh, T.G.J.R.E.F. Ambaye, Current updates on waste to energy (WtE) technologies: a review, 24 (2018) 1-11.

[44] A. Sanlisoy, M. Carpinlioglu, A review on plasma gasification for solid waste disposal, J International journal of hydrogen energy 42(2) (2017) 1361-1365.

[45] A.T. Sipra, N. Gao, H. Sarwar, Municipal solid waste (MSW) pyrolysis for bio-fuel production: A review of effects of MSW components and catalysts, J Fuel processing technology 175 (2018) 131-147.

[46] S. Ciuta, D. Tsiamis, M.J. Castaldi, Gasification of waste materials: technologies for generating energy, gas, and chemicals from municipal solid waste, biomass, nonrecycled plastics, sludges, and wet solid wastes, Academic Press2017.

[47] A. Kumar, S.R. Samadder, A review on technological options of waste to energy for effective management of municipal solid waste, J Waste Management 69 (2017) 407-422.

[48] Y. Yun, Gasification for Practical Applications, 2012.

[49] E.N. Kalogirou, Waste-to-Energy technologies and global applications, CRC Press2017.

[50] A. Buekens, Incineration technologies, Springer Science & Business Media2013.

[51] Y.-T. Chen, D.-S. Chang, Diffusion effect and learning effect: an examination on MSW recycling, J Journal of Cleaner Production 18(5) (2010) 496-503.

[52] L. Lombardi, E. Carnevale, A. Corti, A review of technologies and performances of thermal treatment systems for energy recovery from waste, J Waste management 37 (2015) 26-44.

[53] Y. Lin, X. Ma, X. Peng, Z. Yu, Hydrothermal carbonization of typical components of municipal solid waste for deriving hydrochars and their combustion behavior, J Bioresource Technology 243 (2017) 539-547.

[54] U.J.W.m. Arena, Process and technological aspects of municipal solid waste gasification. A review, 32(4) (2012) 625-639.

[55] G. Lopez, M. Artetxe, M. Amutio, J. Alvarez, J. Bilbao, M.J.R. Olazar, S.E. Reviews, Recent advances in the gasification of waste plastics. A critical overview, 82 (2018) 576-596.

[56] F. Fabry, C. Rehmet, V. Rohani, L.J.W. Fulcheri, B. Valorization, Waste gasification by thermal plasma: a review, 4(3) (2013) 421-439.

[57] R. Taylor, R. Ray, C. Chapman, Advanced thermal treatment of auto shredder residue and refuse derived fuel, J Fuel 106 (2013) 401-409.

[58] V. Popov, A. Bratsev, V. Kuznetsov, S. Shtengel, A. Ufimtsev, Plasma gasification of waste as a method of energy saving, Journal of Physics: Conference Series, IOP Publishing, 2011, p. 012015.

[59] D.M.Y. Maya, A.L.E. Sarmiento, C. de Sales, E. Oliveira, R. Andrade, Gasification of municipal solid waste for power generation in Brazil, a review of available technologies and their environmental benefits, J Journal of Chemistry Chemical Engineering 10 (2016) 249-255.

[60] D. Panepinto, V. Tedesco, E. Brizio, G. Genon, Environmental performances and energy efficiency for MSW gasification treatment, J Waste Biomass Valorization 6(1) (2015) 123-135.

[61] B. Vaish, B. Sharma, V. Srivastava, P. Singh, M.H. Ibrahim, R.P. Singh, Energy recovery potential and environmental impact of gasification for municipal solid waste, J Biofuels 10(1) (2019) 87-100.

[62] N. Agon, M. Hrabovský, O. Chumak, M. Hlína, V. Kopecký, A. Masláni, A. Bosmans, L. Helsen, S. Skoblja, G.J.W.m. Van Oost, Plasma gasification of refuse derived fuel in a single-stage system using different gasifying agents, 47 (2016) 246-255.

[63] S. Wood, M. Fanning, M. Venn, K. Whiting, Review of state-of-the-art Waste-to-Energy Technologies Stage Two- case Studies, in: WSP (Ed.) 2013.

[64] M. Puig-Gamero, D. Pio, L. Tarelho, P. Sánchez, L. Sanchez-Silva, Simulation of biomass gasification in bubbling fluidized bed reactor using aspen plus®, J Energy Conversion Management 235 (2021) 113981.

[65] S. Safarian, R. Unnþórsson, C. Richter, A review of biomass gasification modelling, J Renewable Sustainable Energy Reviews 110 (2019) 378-391.

[66] H.M.U. Ayub, M.A. Qyyum, K. Qadeer, M. Binns, A. Tawfik, M. Lee, Robustness enhancement of biomass steam gasification thermodynamic models for biohydrogen production: Introducing new correction factors, J Journal of Cleaner Production 321 (2021) 128954.

[67] J. Li, M. Suvarna, L. Pan, Y. Zhao, X. Wang, A hybrid data-driven and mechanistic modelling approach for hydrothermal gasification, J Applied Energy 304 (2021) 117674.

[68] G. Biancini, R. Moradi, L. Cioccolanti, B. Marchetti, M. Moglie, L. Del Zotto, A general model for air gasification of heterogenous municipal solid waste, J Energy Conversion Management 278 (2023) 116749.

[69] U. Arena, L. Zaccariello, M.L. Mastellone, Fluidized bed gasification of waste-derived fuels, J Waste Management 30(7) (2010) 1212-1219.

[70] F. Parrillo, F. Ardolino, G. Calì, D. Marotto, A. Pettinau, U. Arena, Fluidized bed gasification of eucalyptus chips: Axial profiles of syngas composition in a pilot scale reactor, J Energy 219 (2021) 119604.

[71] P. Rosha, H. Ibrahim, Hydrogen production via solid waste gasification with subsequent amine-based carbon dioxide removal using Aspen Plus, J International Journal of Hydrogen Energy 48(64) (2023) 24607-24618.

[72] F. Barontini, S. Frigo, R. Gabbrielli, P. Sica, Co-gasification of woody biomass with organic and waste matrices in a down-draft gasifier: An experimental and modeling approach, J Energy Conversion management 245 (2021) 114566.

[73] X. Wang, X. Wang, Y. Shao, B. Jin, Three-dimensional modelling of the multiphase hydrodynamics in a separated-gasification chemical looping combustion unit during full-loop operation, J Journal of Cleaner Production 275 (2020) 122782.

[74] S. Luo, Y. Zhou, C. Yi, Syngas production by catalytic steam gasification of municipal solid waste in fixed-bed reactor, J Energy Conversion Management 44(1) (2012) 391-395.

[75] D.K. Singh, J. Tirkey, Process modelling and thermodynamic performance optimization of biomass air gasification fuelled with waste poultry litter pellet by integrating Aspen plus with RSM, J Biomass Bioenergy 158 (2022) 106370.

[76] G. Diaz, N. Sharma, E. Leal-Quiros, A.J.I.J.o.H.E. Munoz-Hernandez, Enhanced hydrogen production using steam plasma processing of biomass: Experimental apparatus and procedure, 40(5) (2015) 2091-2098.

[77] H. Shafiq, S.U. Azam, A. Hussain, Steam gasification of municipal solid waste for hydrogen production using Aspen Plus® simulation, J Discover Chemical Engineering 1 (2021) 1-16.

[78] Y. Hu, K. Pang, L. Cai, Z. Liu, A multi-stage co-gasification system of biomass and municipal solid waste (MSW) for high quality syngas production, J Energy 221 (2021) 119639.

[79] P.R. Bhoi, R.L. Huhnke, A. Kumar, N. Indrawan, S. Thapa, Co-gasification of municipal solid waste and biomass in a commercial scale downdraft gasifier, J Energy 163 (2018) 513-518.

[80] M. Deraman, R.A. Rasid, M. Othman, L. Suli, Co-gasification of coal and empty fruit bunch in an entrained flow gasifier: A process simulation study, IOP Conference Series: Materials Science and Engineering, IOP Publishing, 2019, p. 012005.

[81] M.A. Adnan, M.M. Hossain, Gasification performance of various microalgae biomass–A thermodynamic study by considering tar formation using Aspen plus, J Energy conversion management 165 (2018) 783-793.

[82] G. Duman, M.A. Uddin, J. Yanik, Hydrogen production from algal biomass via steam gasification, J Bioresource technology 166 (2014) 24-30.

[83] M. Fernandez-Lopez, J. Pedroche, J.L. Valverde, L. Sanchez-Silva, Simulation of the gasification of animal wastes in a dual gasifier using Aspen Plus®, J Energy conversion management 140 (2017) 211-217.

[84] P. Kaushal, R. Tyagi, Advanced simulation of biomass gasification in a fluidized bed reactor using ASPEN PLUS, J Renewable energy 101 (2017) 629-636.

[85] S. Rapagnà, N. Jand, A. Kiennemann, P.U. Foscolo, Steam-gasification of biomass in a fluidised-bed of olivine particles, J Biomass bioenergy 19(3) (2000) 187-197.

[86] D.A. Ali, M.A. Gadalla, O.Y. Abdelaziz, C.P. Hulteberg, F.H. Ashour, Co-gasification of coal and biomass wastes in an entrained flow gasifier: Modelling, simulation and integration opportunities, J Journal of Natural Gas Science Engineering 37 (2017) 126-137.

[87] K. Xiangdong, W. Zhong, D. Wenli, Q. Feng, Three stage equilibrium model for coal gasification in entrained flow gasifiers based on aspen plus, J Chinese journal of chemical engineering 21(1) (2013) 79-84.

[88] J.H. Pauls, N. Mahinpey, E. Mostafavi, Simulation of air-steam gasification of woody biomass in a bubbling fluidized bed using Aspen Plus: A comprehensive model including pyrolysis, hydrodynamics and tar production, J Biomass bioenergy 95 (2016) 157-166.

[89] P. Lv, J. Chang, Z. Xiong, H. Huang, C. Wu, Y. Chen, J. Zhu, Biomass air− steam gasification in a fluidized bed to produce hydrogen-rich gas, J Energy fuels 17(3) (2003) 677-682.

[90] L. Abdelouahed, O. Authier, G. Mauviel, J.-P. Corriou, G. Verdier, A. Dufour, Detailed modeling of biomass gasification in dual fluidized bed reactors under Aspen Plus, J Energy fuels 26(6) (2012) 3840-3855.

[91] Ö.Ç. Mutlu, T. Zeng, Challenges and opportunities of modeling biomass gasification in Aspen Plus: A review, J Chemical Engineering Technology 43(9) (2020) 1674-1689.

[92] S. Srinivas, R.P. Field, H.J. Herzog, Modeling tar handling options in biomass gasification, J Energy Fuels 27(6) (2013) 2859-2873.

[93] H. Lateh, J. Taweekun, K. Maliwan, A. Ishak, The Removal of Mixed Tar in Biomass Fuel Gas through the Thermal and Catalytic Treatment Methods, IOP Conference Series: Materials Science and Engineering, IOP Publishing, 2020, p. 012141.

[94] M. Materazzi, P. Lettieri, L. Mazzei, R. Taylor, C. Chapman, Tar evolution in a two stage fluid bed–plasma gasification process for waste valorization, J Fuel processing technology 128 (2014) 146-157.

[95] V. Palma, M. Cortese, S. Renda, C. Ruocco, M. Martino, E. Meloni, A review about the recent advances in selected nonthermal plasma assisted solid–gas phase chemical processes, J Nanomaterials 10(8) (2020) 1596.

[96] European Union, Tar Measurement Standard, (2003).

[97] P.J. Woolcock, R.C.J.B. Brown, bioenergy, A review of cleaning technologies for biomass-derived syngas, 52 (2013) 54-84.

[98] M. Materazzi, R. Taylor, M. Cairns-Terry, Production of biohydrogen from gasification of waste fuels: Pilot plant results and deployment prospects, J Waste Management 94 (2019) 95-106.

[99] S. Anis, Z. Zainal, Tar reduction in biomass producer gas via mechanical, catalytic and thermal methods: A review, J Renewable sustainable energy reviews 15(5) (2011) 2355-2377.

[100] M. Nacken, L. Ma, K. Engelen, S. Heidenreich, G.V. Baron, Development of a tar reforming catalyst for integration in a ceramic filter element and use in hot gas cleaning, J Industrial engineering chemistry research 46(7) (2007) 1945-1951.

[101] M. Hu, M. Laghari, B. Cui, B. Xiao, B. Zhang, D. Guo, Catalytic cracking of biomass tar over char supported nickel catalyst, J Energy 145 (2018) 228-237.

[102] B. Ramadhani, T. Kivevele, J.H. Kihedu, Y.A. Jande, Biorefinery, Catalytic tar conversion and the prospective use of iron-based catalyst in the future development of biomass gasification: a review, J Biomass Conversion (2020) 1-24.

[103] M.W. Islam, A review of dolomite catalyst for biomass gasification tar removal, J Fuel 267 (2020) 117095.

[104] M. Oliveira, A. Ramos, T.M. Ismail, E. Monteiro, A. Rouboa, A Review on Plasma Gasification of Solid Residues: Recent Advances and Developments, J Energies 15(4) (2022) 1475.

[105] E. Gomez, D.A. Rani, C. Cheeseman, D. Deegan, Wise, A. Boccaccini, Thermal plasma technology for the treatment of wastes: a critical review, Journal of hazardous materials 161(2-3) (2009) 614-626.

[106] H.H. Kim, Nonthermal plasma processing for air-pollution control: a historical review, current issues, and future prospects, J Plasma Processes Polymers 1(2) (2004) 91-110.

[107] B. Ruj, S. Ghosh, Technological aspects for thermal plasma treatment of municipal solid waste—A review, J Fuel processing technology 126 (2014) 298-308.

[108] A.J.H.o.C.O. Gutsol, Warm discharges for fuel conversion, (2010) 323-353.

[109] V. Nehra, A. Kumar, H. Dwivedi, Atmospheric non-thermal plasma sources, J International Journal of Engineering 2(1) (2008) 53-68.

[110] A. Haji, M. Naebe, Cleaner dyeing of textiles using plasma treatment and natural dyes: A review, J Journal of Cleaner Production (2020) 121866.

[111] S. Samal, Thermal plasma technology: The prospective future in material processing, J Journal of cleaner production 142 (2017) 3131-3150.

[112] A.E. Ruark, Note on Events Distributed According to Chance, J Physical Review 65(9-10) (1944) 287-287.

[113] D.E. Kerr, Physics of Fully Ionized Gases, J Journal of the American Chemical Society 78(19) (1956) 5133-5134.

[114] N. Herlofson, Magneto-hydrodynamic waves in a compressible fluid conductor, J Nature 165(4208) (1950) 1020-1021.

[115] F. Haas, Quantum Plasmas, in: I.o. Physic (Ed.) 2017.

[116] M. Moynihan, Seven Ways to Model Plasma, 2018. https://www.thefusionpodcast.com/blog/2018/8/26/seven-ways-to-model-plasma.

[117] V. Bobrov, S. Trigger, I. Sokolov, Spectral energy distribution of the equilibrium radiation and its asymptotic behavior in ideal gaseous plasmas, J Physics of Plasmas 27(2) (2020) 022106.

[118] N. Yu, Y. Yang, R. Jourdain, M. Gourma, A. Bennett, F. Fang, Design and optimization of plasma jet nozzles based on computational fluid dynamics, J The international journal of advanced manufacturing technology 108(7) (2020) 2559-2568.

[119] M. Sheikholeslami, D.D. Ganji, External magnetic field effects on hydrothermal treatment of nanofluid: numerical and analytical studies, William Andrew2016.

[120] A. Lebouvier, S. Iwarere, D. Ramjugernath, L. Fulcheri, 3D magnetohydrodynamic modelling of a dc low-current plasma arc batch reactor at very high pressure in helium, J Journal of Physics D: Applied Physics 46(14) (2013) 145203.

[121] U. Shumlak, J. Loverich, Approximate Riemann solver for the two-fluid plasma model, J Journal of Computational Physics 187(2) (2003) 620-638.

[122] P. Huang, J. Hebeylein, E. Pfender, A two-fluid model of turbulence for a thermal plasma jet, J Plasma Chemistry Plasma Processing 15(1) (1995) 25-46.

[123] G. McKee, C. Petty, R. Waltz, C. Fenzi, R. Fonck, J. Kinsey, T. Luce, K. Burrell, D. Baker, E. Doyle, Non-dimensional scaling of turbulence characteristics and turbulent diffusivity, J Nuclear Fusion 41(9) (2001) 1235.

[124] T. Tatsuno, W. Dorland, A. Schekochihin, G. Plunk, M. Barnes, S. Cowley, G. Howes, Nonlinear phase mixing and phase-space cascade of entropy in gyrokinetic plasma turbulence, J Physical review letters 103(1) (2009) 015003.

[125] J.M. Dawson, Particle simulation of plasmas, J Reviews of modern physics 55(2) (1983) 403.

[126] M.W. Kunz, J.M. Stone, X.-N. Bai, Pegasus: a new hybrid-kinetic particle-in-cell code for astrophysical plasma dynamics, J Journal of Computational Physics 259 (2014) 154-174.

[127] G. Zhao, J. Mostaghimi, M. Boulos, The induction plasma chemical reactor: Part II. Kinetic model, J Plasma chemistry plasma processing 10(1) (1990) 151-166.

[128] H. Zheng, Q. Liu, Kinetic study of nonequilibrium plasma-assisted methane steam reforming, J Mathematical Problems in Engineering 2014 (2014).

[129] G. Manfredi, P.-A. Hervieux, J. Hurst, Fluid descriptions of quantum plasmas, J Reviews of Modern Plasma Physics 5(1) (2021) 1-38.

[130] C. Liu, K. Xu, Unified gas-kinetic wave-particle methods IV: Multi-species gas mixture and plasma transport, J Advances in Aerodynamics 3(1) (2021) 1-31.

[131] A. Gleizes, Perspectives on thermal plasma modelling, J Plasma Chemistry and Plasma Processing 35(3) (2015) 455-469.

[132] V. Shafranov, Electromagnetic waves in a plasma, J Reviews of plasma physics (1967) 1-157.

[133] F. Taccogna, S. Longo, M. Capitelli, Plasma-surface interaction model with secondary electron emission effects, J Physics of Plasmas 11(3) (2004) 1220-1228.

[134] S. Glenzer, W. Alley, K. Estabrook, J. De Groot, M. Haines, J. Hammer, J.-P. Jadaud, B. MacGowan, J. Moody, W. Rozmus, Thomson scattering from laser plasmas, J Physics of plasmas 6(5) (1999) 2117-2128.

[135] B. Ibrahimoglu, A. Cucen, M.Z. Yilmazoglu, Numerical modeling of a downdraft plasma gasification reactor, J International Journal of Hydrogen Energy 42(4) (2017) 2583-2591.

[136] M. Castela, B. Fiorina, A. Coussement, O. Gicquel, N. Darabiha, C.O. Laux, Modelling the impact of non-equilibrium discharges on reactive mixtures for simulations of plasma-assisted ignition in turbulent flows, J Combustion flame 166 (2016) 133-147.

[137] M. Materazzi, R. Taylor, P. Cozens, C. Manson-Whitton, Production of BioSNG from waste derived syngas: Pilot plant operation and preliminary assessment, J Waste Management 79 (2018) 752-762.

[138] M. Munir, I. Mardon, S. Al-Zuhair, A. Shawabkeh, N. Saqib, Plasma gasification of municipal solid waste for waste-to-value processing, J Renewable Sustainable Energy Reviews 116 (2019) 109461.

[139] J. Ren, J.-P. Cao, X.-Y. Zhao, F.-L. Yang, X.-Y. Wei, Recent advances in syngas production from biomass catalytic gasification: A critical review on reactors, catalysts, catalytic mechanisms and mathematical models, J Renewable Sustainable Energy Reviews 116 (2019) 109426.

[140] S. Ciuta, Gasification of waste materials : technologies for generating energy, gas, and chemicals from municipal solid waste, biomass, nonrecycled plastics, sludges, and wet solid wastes, Academic Press, London, 2018.

[141] Klean Industries, SPR Japan: World's Largest Waste-plastics-to-oil Recovery Plant (CHP Facility), 2015. http://www.kleanindustries.com/s/sapporo_plastics_pyrolysis_recycling_plant.asp.

[142] J. Favas, E. Monteiro, A.J.I.J.o.H.E. Rouboa, Hydrogen production using plasma gasification with steam injection, 42(16) (2017) 10997-11005.

[143] S. Morrin, P. Lettieri, C. Chapman, L. Mazzei, Two stage fluid bed-plasma gasification process for solid waste valorisation: Technical review and preliminary thermodynamic modelling of sulphur emissions, J Waste management 32(4) (2012) 676-684.

[144] S. Vecten, B. Herbert, M. Wilkinson, A. Shaw, N. Bimbo, R. Dawson, Integrated plasma gasification and SOFC system simulation using Aspen Plus, (2018).

[145] M. Materazzi, P. Lettieri, R. Taylor, C. Chapman, Performance analysis of RDF gasification in a two stage fluidized bed–plasma process, J Waste Management 47 (2016) 256-266.

[146] D. Lopez Varela, Artificial neural networks model for a plasma gasification reactor, University of Calgary, 2011.

[147] A. An'Shakov, V. Faleev, A. Danilenko, E. Urbakh, A. Urbakh, Investigation of plasma gasification of carbonaceous technogeneous wastes, J Thermophysics Aeromechanics 14(4) (2007) 607-616.

[148] R. Mourão, A.R. Marquesi, A.V. Gorbunov, G. Petraconi Filho, A.A. Halinouski, C. Otani, Thermochemical assessment of gasification process efficiency of biofuels industry waste with different plasma oxidants, J IEEE Transactions on Plasma Science 43(10) (2015) 3760-3767.

[149] A. Bratsev, I. Kumkova, V. Kuznetsov, V. Popov, A. Ufimtsev, Air plasma gasification of RDF as a prospective method for reduction of carbon dioxide emission, IOP Conference Series: Materials Science and Engineering, IOP Publishing, 2011, p. 012004.

[150] S. Achinas, E. Kapetanios, Efficiency evaluation of RDF plasma gasification process, J Energy Environment Research 3(1) (2013) 150.

[151] A. Perna, M. Minutillo, E.J.E. Jannelli, Hydrogen from intermittent renewable energy sources as gasification medium in integrated waste gasification combined cycle power plants: A performance comparison, 94 (2016) 457-465.

[152] A. Fourcault, F. Marias, U. Michon, Modelling of thermal removal of tars in a high temperature stage fed by a plasma torch, J Biomass bioenergy 34(9) (2010) 1363-1374.

[153] M. Materazzi, P. Lettieri, L. Mazzei, R. Taylor, C.J.F.p.t. Chapman, Tar evolution in a two stage fluid bed–plasma gasification process for waste valorization, 128 (2014) 146-157.

[154] M. Minutillo, A. Perna, D.J.E.C. Di Bona, Management, Modelling and performance analysis of an integrated plasma gasification combined cycle (IPGCC) power plant, 50(11) (2009) 2837-2842.

[155] N.K.C. Qing, N.A. Samiran, R. Abd Rashid, CFD Simulation analysis of Sub-Component in Municipal Solid Waste Gasification using Plasma Downdraft Technique, J CFD Letters 14(8) (2022) 63-70.

[156] K.P. Willis, S. Osada, K.L. Willerton, Plasma gasification: lessons learned at Eco-Valley WTE facility, 18th Annual North American Waste-to-Energy Conference, American Society of Mechanical Engineers, 2010, pp. 133-140.

[157] Westinghouse, Australian Waste to Energy Forum, Westinghouse Plasma Gasification: The Next Generation of Waste-to-Energy Solutions 2016. http://aien.com.au/wteforum/wp-content/uploads/2016/02/WillisK.pdf.

[158] E. Perchard, Air Products Shuts Down Tees Valley Development 2016. https://resource.co/article/air-products-shuts-down-tees-valley-development-10987.

[159] CHO Power, CENTRALE CHO MORCENX (in French), 2017. http://www.cho-power.com/nos-references/#centrale-morcenx/?lang=en.

[160] M. Materazzi, P. Lettieri, R. Taylor, C. Chapman, The fate of ashes and inorganics in a two-stage fluid particle system for waste valorization, J Procedia engineering 102 (2015) 936-944.

[161] M. Materazzi, R. Taylor, Plasma-assisted gasification for Waste-to-Fuels applications, J Industrial Engineering Chemistry Research 58(35) (2019) 15902-15913.

[162] S. Morrin, P. Lettieri, C. Chapman, R. Taylor, Fluid bed gasification–Plasma converter process generating energy from solid waste: Experimental assessment of sulphur species, J Waste management 34(1) (2014) 28-35.

[163] M. Materazzi, P. Lettieri, L. Mazzei, R. Taylor, C. Chapman, Thermodynamic modelling and evaluation of a two-stage thermal process for waste gasification, J Fuel 108 (2013) 356-369.

[164] J. Doherty, Waste-to-gas plant revived after administration, 2019. https://www.letsrecycle.com/news/latest-news/waste-to-gas-plant-revived-after-administration/.

[165] Advanced Plasma Power, Call for evidence, Response from Advanced Plasma Power Ltd, 2018. https://www.theccc.org.uk/wp-content/uploads/2018/12/Biomass-response-to-Call-for-Evidence-Advanced-Plasma-Power.pdf.

[166] ENERSOL Tech, PEGS® Gasification Systems, 2019. https://www.enersoltech.com/pegs.htm.

[167] Enersol Tech, Advanced Solution in Waste Management with Zero Defect and Zero Effect, 2019. https://ec.europa.eu/info/sites/default/files/21_radhakrishnan_srinivasan_.pdf.

[168] Q. Zhang, L. Dor, D. Fenigshtein, W. Yang, W. Blasiak, Gasification of municipal solid waste in the Plasma Gasification Melting process, J Applied Energy 90(1) (2012) 106-112.

[169] Q. Zhang, Y. Wu, L. Dor, W. Yang, W. Blasiak, A thermodynamic analysis of solid waste gasification in the Plasma Gasification Melting process, J Applied energy 112 (2013) 405-413.

[170] Q. Zhang, L. Dor, W. Yang, W. Blasiak, Eulerian model for municipal solid waste gasification in a fixed-bed plasma gasification melting reactor, J Energy fuels 25(9) (2011) 4129-4137.

[171] EURELCO, Development and optimization of a plasma gasification melting process, 2018. https://eurelco.org/2018/10/13/development-and-optimization-of-a-plasma-gasification-melting-process/.

[172] OMNI Conversion Technology, Omni200TM Gasification & Plasma Refining System (GPRSTM), 2021. https://omnict.com/wp-content/uploads/2021/04/OMNI-Process-Description-TMP-1202.pdf.

[173] Plasco Energy Group, Clean Economical Practical: Changing the Way Commnunities Deal with Waste, n.d. https://www.clubrunner.ca/Data/7040%5C1103%5CHTML%5C176256%5CPlasco_RotaryOttawaSouth_Presentation.pdf.

[174] OMNI Conversion Technology, OMNI CT Sells First OMNI200TM Hydrogen Unit, 2021. https://omnict.com/news-post/omni-ct-sells-first-omni200-hydrogen-unit/.

[175] Bellwether, The IMRG-Technology, 2017. https://bwrgas.wixsite.com/bellwether/imrg-technology.

[176] PEAT International, Plasma Thermal Desctruction and Recovery. http://www.peat.com/images/PEAT-International-Brochure.pdf.

[177] CISION PR Newswire, PEAT International Commissions Plasma Thermal Waste-to-Energy System in China, 2013. https://www.prnewswire.com/news-releases/peat-international-commissions-plasma-thermal-waste-to-energy-system-in-china-227230431.html.

[178] InEnTec, PEM Facilities, 2017. http://www.inentec.com/pem-facilities/.

[179] L. Rao, P. Carabin, G. Holcroft, Plasma Waste Gasification Decentralized Approach to Production of Energy From Waste, Pyrogenesis, 2010.

[180] Pyrogenesis, Plasma Toches, 2020. https://www.pyrogenesis.com/products-services/plasma-torches/.

[181] Clean the Air Energy Blog, SUCCESS FOR KOREAN PLASMA GASIFICATION FUEL CELL DEMO, 2012. http://energy.cleartheair.org.hk/?p=1218.

[182] GS Platech, S.M. Hwang, Present Status of Zero-Waste Technology Development and Examples of Public-Private Partnership, 2011. https://www.uncrd.or.jp/content/documents/Theme4-Hwang_GS%20Platech.pdf.

[183] M. Minutillo, A. Perna, D. Di Bona, Modelling and performance analysis of an integrated plasma gasification combined cycle (IPGCC) power plant, J Energy Conversion Management 50(11) (2009) 2837-2842.

[184] A. Mountouris, E. Voutsas, D.J.E.C. Tassios, Management, Solid waste plasma gasification: equilibrium model development and exergy analysis, 47(13-14) (2006) 1723-1737.

[185] G.S. Sturm, A.N. Muñoz, P. Aravind, G.D. Stefanidis, Microwave-driven plasma gasification for biomass waste treatment at miniature scale, J IEEE Transactions on Plasma Science 44(4) (2016) 670-678.

[186] N.D. Montiel-Bohórquez, A.F. Agudelo, J.F. Pérez, Modelling of an Integrated Plasma Gasification Combined Cycle power plant using Aspen Plus, J Journal of King Saud University-Engineering Sciences (2022).

[187] L. Liu, Z. Zhang, S. Das, S.J.A.C.B.E. Kawi, Reforming of tar from biomass gasification in a hybrid catalysis-plasma system: A review, 250 (2019) 250-272.

[188] K. Xiao, X. Li, J. Santoso, H. Wang, K. Zhang, J. Wu, D. Zhang, Synergistic effect of dielectric barrier discharge plasma and Mn catalyst on CO2 reforming of toluene, J Fuel 285 (2021) 119057.

[189] N. Indrawan, V. Plotnikov, S. Thapa, G.C. Diaz, A. Kumar, R.L. Huhnke, Preliminary evaluation of surface dielectric barrier discharge non-thermal plasma for reforming syngas derived from a downdraft gasifier, J Fuel 332 (2023) 126186.

[190] S. Wang, L. Zhao, W. Deng, Y. Ge, H. Wang, X. Li, Catalytic gasification of rice hull by dielectric barrier discharge non-thermal plasma over potassium catalyst, J International Journal of Hydrogen Energy 48(19) (2023) 6947-6958.

[191] M. Craven, Y. Wang, H. Yang, C. Wu, X. Tu, Integrated gasification and non-thermal plasma-catalysis system for cleaner syngas production from cellulose, J IOP SciNotes 1(2) (2020) 024001.

[192] Y. Wang, H. Yang, X. Tu, Plasma reforming of naphthalene as a tar model compound of biomass gasification, J Energy Conversion Management 187 (2019) 593-604.

[193] F. Saleem, A. Abbas, A. Rehman, A.H. Khoja, S.R. Naqvi, M.Y. Arshad, K. Zhang, A. Harvey, Decomposition of benzene as a biomass gasification tar in CH4 carrier gas using non-thermal plasma: Parametric and kinetic study, J Journal of the Energy Institute 102 (2022) 190-195.

[194] W.-J. Liang, L. Ma, H. Liu, J. Li, Toluene degradation by non-thermal plasma combined with a ferroelectric catalyst, J Chemosphere 92(10) (2013) 1390-1395.

[195] F. Saleem, A.H. Khoja, A. Khan, A. Rehman, S.R. Naqvi, U.Y. Qazi, K. Zhang, A. Harvey, Effect of non-thermal plasma dielectric barrier discharge reactor on the quality of biomass gasification product gas from the gasifier, J Journal of the Energy Institute 108 (2023) 101228.

[196] H. Zhang, R. Xu, J. Ananthanarasimhan, J. Zheng, J. Wan, K. Wang, B. Lan, J. Yan, X. Li, Destruction of biomass tar model compound in a rotating gliding arc plasma catalytic system: Contribution of typical transition metals in Ni-based bimetallic catalyst, J Fuel 323 (2022) 124385.

[197] D. Mei, S. Liu, J. Yanik, G. Lopez, M. Olazar, Z. Fang, X. Tu, Plasma-catalytic reforming of naphthalene and toluene as biomass tar over honeycomb catalysts in a gliding arc reactor, J ACS Sustainable Chemistry Engineering 10(27) (2022) 8958-8969.

[198] K. Sasujit, N. Homdoung, N. Tippayawong, Non-thermal plasma removal of naphthalene as tar model compound from biomass gasification, J Energy Reports 8 (2022) 97-103.

[199] U.H. Dahiru, F. Saleem, F.T. Al-sudani, K. Zhang, A.P. Harvey, Decomposition of benzene vapour using non-thermal plasmas: The effect of moisture content on eliminating solid residue, J Journal of Environmental Chemical Engineering 10(3) (2022) 107767.

[200] F. Saleem, A.H. Khoja, J. Umer, F. Ahmad, S.Z. Abbas, K. Zhang, A. Harvey, Removal of benzene as a tar model compound from a gas mixture using non-thermal plasma dielectric barrier discharge reactor, J Journal of the Energy Institute 96 (2021) 97-105.

[201] Y. Liu, J. Song, X. Diao, L. Liu, Y. Sun, Removal of tar derived from biomass gasification via synergy of non-thermal plasma and catalysis, J Science of The Total Environment 721 (2020) 137671.

[202] B. Xu, N. Wang, J. Xie, Y. Song, Y. Huang, W. Yang, X. Yin, C. Wu, Removal of toluene as a biomass tar surrogate by combining catalysis with nonthermal plasma: understanding the processing stability of plasma catalysis, J Catalysis Science Technology 10(20) (2020) 6953-6969.

[203] Z. Bo, S. Yang, J. Kong, J. Zhu, Y. Wang, H. Yang, X. Li, J. Yan, K. Cen, X. Tu, Solar-enhanced plasma-catalytic oxidation of toluene over a bifunctional graphene fin foam decorated with nanofin-like MnO2, J ACS catalysis 10(7) (2020) 4420-4432.

[204] R. Xu, F. Zhu, H. Zhang, P.M. Ruya, X. Kong, L. Li, X. Li, Simultaneous removal of toluene, naphthalene, and phenol as tar surrogates in a rotating gliding arc discharge reactor, J Energy Fuels 34(2) (2020) 2045-2054.

[205] B. Lee, D.-W. Kim, D.-W. Park, Decomposition of heptane by dielectric barrier discharge (DBD) plasma reactor having the segmented electrode: comparison of decomposition mechanisms to toluene, J Plasma Chemistry Plasma Processing 40 (2020) 61-77.

[206] I. Aminu, M.A. Nahil, P.T. Williams, Hydrogen from waste plastics by two-stage pyrolysis/low-temperature plasma catalytic processing, J Energy Fuels 34(9) (2020) 11679-11689.

[207] B. Xu, J. Xie, X. Yin, H. Liu, C. Sun, C. Wu, Mechanisms of toluene removal in relation to the main components of biosyngas in a catalytic nonthermal plasma process, J Energy Fuels 33(5) (2019) 4287-4301.

[208] F. Saleem, K. Zhang, A. Harvey, Temperature dependence of non-thermal plasma assisted hydrocracking of toluene to lower hydrocarbons in a dielectric barrier discharge reactor, J Chemical Engineering Journal 356 (2019) 1062-1069.

[209] F. Meng, X. Li, H. Liang, G. Wang, L. Lu, J. Liu, Non-thermal plasma degradation of tar in gasification syngas, J Chemical Engineering Processing-Process Intensification 145 (2019) 107656.

[210] M. Młotek, J. Woroszył, B. Ulejczyk, K. Krawczyk, Coupled plasma-catalytic system with rang 19pr catalyst for conversion of tar, J Scientific Reports 9(1) (2019) 13562.

[211] Y. Ma, J.D. Harding, X. Tu, Catalyst-free low temperature conversion of n-dodecane for co-generation of COx-free hydrogen and C2 hydrocarbons using a gliding arc plasma, J International Journal of Hydrogen Energy 44(48) (2019) 26158-26168.

[212] L. Liu, Q. Wang, J. Song, X. Yang, Y. Sun, Dry reforming of model biomass pyrolysis products to syngas by dielectric barrier discharge plasma, J International Journal of Hydrogen Energy 43(22) (2018) 10281-10293.

[213] R. Cimerman, D. Račková, K. Hensel, Tars removal by non-thermal plasma and plasma catalysis, J Journal of Physics D: Applied Physics 51(27) (2018) 274003.

[214] X. Kong, H. Zhang, X. Li, R. Xu, I. Mubeen, L. Li, J. Yan, Destruction of toluene, naphthalene and phenanthrene as model tar compounds in a modified rotating gliding arc discharge reactor, J Catalysts 9(1) (2018) 19.

[215] L. Liu, Q. Wang, J. Song, S. Ahmad, X. Yang, Y. Sun, Plasma-assisted catalytic reforming of toluene to hydrogen rich syngas, J Catalysis Science Technology 7(18) (2017) 4216-4231.

[216] S. Liu, D. Mei, M. Nahil, S. Gadkari, S. Gu, P. Williams, X. Tu, Hybrid plasma-catalytic steam reforming of toluene as a biomass tar model compound over Ni/Al2O3 catalysts, J Fuel Processing Technology 166 (2017) 269-275.

[217] Y.C. Yang, Y.N. Chun, Naphthalene destruction performance from tar model compound using a gliding arc plasma reformer, J Korean Journal of Chemical Engineering 28 (2011) 539-543.

[218] L. Yu, X. Li, X. Tu, Y. Wang, S. Lu, J. Yan, Decomposition of naphthalene by dc gliding arc gas discharge, J The Journal of Physical Chemistry A 114(1) (2010) 360-368.

[219] P.-A. Maitre, M.S. Bieniek, P.N. Kechagiopoulos, Plasma-enhanced catalysis for the upgrading of methane: A review of modelling and simulation methods, J Reaction Chemistry Engineering 5(5) (2020) 814-837.

[220] L. Alves, A. Bogaerts, V. Guerra, M. Turner, Foundations of modelling of nonequilibrium low-temperature plasmas, J Plasma Sources Science Technology 27(2) (2018) 023002.

[221] A. Hurlbatt, A.R. Gibson, S. Schröter, J. Bredin, A.P.S. Foote, P. Grondein, D. O'Connell, T. Gans, Concepts, capabilities, and limitations of global models: a review, J Plasma Processes Polymers 14(1-2) (2017) 1600138.

[222] N. Dyatko, I. Kochetov, A. Napartovich, A. Sukharev, EEDF: The software package for calculations of Electron Energy Distribution Function, (2015).

[223] Y. Wang, Y. Zhu, F. Tian, H. Dong, X. Fan, C. Du, L. Cui, H. Zheng, H. Teng, Lumped kinetic model for the hydrodeoxygenation of full-range middle-low temperature coal tar, J Reaction Kinetics, Mechanisms Catalysis 134(1) (2021) 179-198.

[224] H. Machrafi, S. Cavadias, J. Amouroux, CO2 valorization by means of dielectric barrier discharge, Journal of Physics: Conference Series, IOP Publishing, 2011, p. 012016.

[225] B. Wang, Y. Cheng, C. Wang, J. Zou, Steam reforming of methane in a gliding arc discharge reactor to produce hydrogen and its chemical kinetics study, J Chemical Engineering Science 253 (2022) 117560.

[226] B. Wang, S. Liu, Y. Peng, C. Wang, J. Zou, Heptane dry reforming and coupling with partial oxidation in gliding arc discharge plasma for H2 production, J Fuel Processing Technology 221 (2021) 106943.

[227] T. Nozaki, Nonthermal Plasma Conversion of Natural Gas to Oxygenates, Direct Natural Gas Conversion to Value-Added Chemicals, CRC Press2020, pp. 53-70.

[228] J. Pan, W. Meng, S. Li, J. Du, Numerical Investigations on Methane–Air Nanosecond Pulsed Dielectric Barrier Discharge Plasma-Assisted Combustion, J ACS omega 5(49) (2020) 31891-31901.

[229] S. Heijkers, M. Aghaei, A. Bogaerts, Plasma-based CH4 conversion into higher hydrocarbons and H2: modeling to reveal the reaction mechanisms of different plasma sources, J The Journal of Physical Chemistry C 124(13) (2020) 7016-7030.

[230] C. Xu, X. Tu, Plasma-assisted methane conversion in an atmospheric pressure dielectric barrier discharge reactor, J Journal of energy chemistry 22(3) (2013) 420-425.

[231] A.B. Oskooei, J. Koohsorkhi, M. Mehrpooya, Simulation of plasma-assisted catalytic reduction of NOx, CO, and HC from diesel engine exhaust with COMSOL, J Chemical Engineering Science 197 (2019) 135-149.

[232] C.R. McLarnon, B.M. Penetrante, Effect of reactor design on the plasma treatment of NOx, SAE INTERNATIONAL WARRENDALE PA, 1998.

[233] H. Zhang, W. Wang, X. Li, L. Han, M. Yan, Y. Zhong, X. Tu, Plasma activation of methane for hydrogen production in a N2 rotating gliding arc warm plasma: a chemical kinetics study, J Chemical Engineering Journal 345 (2018) 67-78.

[234] Z. Eckert, N. Tsolas, K. Togai, A. Chernukho, R.A. Yetter, I.V. Adamovich, Kinetics of plasma-assisted oxidation of highly diluted hydrocarbon mixtures excited by a repetitive nanosecond pulse discharge, J Journal of Physics D: Applied Physics 51(37) (2018) 374002.

[235] W.K. Metcalfe, S.M. Burke, S.S. Ahmed, H.J. Curran, A hierarchical and comparative kinetic modeling study of C1− C2 hydrocarbon and oxygenated fuels, J International Journal of Chemical Kinetics 45(10) (2013) 638-675.

[236] A. Konnov, Detailed reaction mechanism for small hydrocarbons combustion. Release 0.5, J http://homepages. vub. ac. be/~ akonnov/ (2000).

[237] S. Ponduri, M. Becker, S. Welzel, M. Van De Sanden, D. Loffhagen, R. Engeln, Fluid modelling of CO2 dissociation in a dielectric barrier discharge, J Journal of Applied Physics 119(9) (2016) 093301.

[238] J. Pan, L. Li, B. Chen, Y. Song, Y. Zhao, X. Xiu, Numerical simulation of evolution features of the atmospheric-pressure CF4 plasma generated by the pulsed dielectric barrier discharge, J The European Physical Journal D 70(6) (2016) 1-8.

[239] M. Maulois, M. Ribière, O. Eichwald, M. Yousfi, B. Azaïs, Chemical kinetics and relaxation of non-equilibrium air plasma generated by energetic photon and electron beams, J Physics of Plasmas 23(4) (2016) 043501.

[240] S. Nagaraja, W. Sun, V. Yang, Effect of non-equilibrium plasma on two-stage ignition of n-heptane, J Proceedings of the Combustion Institute 35(3) (2015) 3497-3504.

[241] J. Pan, Z. Tan, X. Wang, C. Sha, L. Nie, X. Chen, Effects of pulse parameters on the atmospheric-pressure dielectric barrier discharges driven by the high-voltage pulses in Ar and N2, J Plasma Sources Science Technology 23(6) (2014) 065019.

[242] R. Snoeckx, R. Aerts, X. Tu, A. Bogaerts, Plasma-based dry reforming: a computational study ranging from the nanoseconds to seconds time scale, J The Journal of Physical Chemistry C 117(10) (2013) 4957-4970.

[243] Q. Wang, B.-H. Yan, Y. Jin, Y. Cheng, Investigation of dry reforming of methane in a dielectric barrier discharge reactor, J Plasma Chemistry Plasma Processing 29(3) (2009) 217-228.

[244] H.J. Gallon, C. Whitehead, Dry reforming of methane using non-thermal plasma-catalysis, University of Manchester, 2011.

[245] F. Odeyemi, A. Rabinovich, A. Fridman, Gliding arc plasma-stimulated conversion of pyrogas into synthesis gas, J IEEE Transactions on Plasma Science 40(4) (2012) 1124-1130.

[246] W. Sun, M. Uddi, S.H. Won, T. Ombrello, C. Carter, Y. Ju, Kinetic effects of non-equilibrium plasma-assisted methane oxidation on diffusion flame extinction limits, J Combustion Flame 159(1) (2012) 221-229.

[247] T. Martens, A. Bogaerts, W. Brok, J. Dijk, The dominant role of impurities in the composition of high pressure noble gas plasmas, J Applied Physics Letters 92(4) (2008) 041504.

[248] C. De Bie, T. Martens, J. van Dijk, S. Paulussen, B. Verheyde, S. Corthals, A. Bogaerts, Dielectric barrier discharges used for the conversion of greenhouse gases: modeling the plasma chemistry by fluid simulations, J Plasma Sources Science mTechnology 20(2) (2011) 024008.

[249] A.A. Tropina, M. Uddi, Y. Ju, On the effect of nonequilibrium plasma on the minimum ignition energy—Part 1: Discharge model, J IEEE Transactions on Plasma Science 39(1) (2010) 615-623.

[250] B. Dastjerdi, V. Strezov, R. Kumar, J. He, M. Behnia, Comparative life cycle assessment of system solution scenarios for residual municipal solid waste management in NSW, Australia, J Science of The Total Environment 767 (2021) 144355.

[251] T.F. Astrup, D. Tonini, R. Turconi, A. Boldrin, Life cycle assessment of thermal waste-to-energy technologies: review and recommendations, J Waste management 37 (2015) 104-115.

[252] A. Bernstad, J. la Cour Jansen, Review of comparative LCAs of food waste management systems–current status and potential improvements, J Waste management 32(12) (2012) 2439-2455.

[253] ISO, ISO 14040/44 international standard, J Environmental Management-Life Cycle Assessment-Principles Framework. International Organisation for Standardization (2006).

[254] A. Laurent, I. Bakas, J. Clavreul, A. Bernstad, M. Niero, E. Gentil, M.Z. Hauschild, T.H. Christensen, Review of LCA studies of solid waste management systems–Part I: Lessons learned and perspectives, J Waste Management Research 34(3) (2014) 573-588.

[255] A. Laurent, J. Clavreul, A. Bernstad, I. Bakas, M. Niero, E. Gentil, T.H. Christensen, M.Z. Hauschild, Review of LCA studies of solid waste management systems–Part II: Methodological guidance for a better practice, J Waste management 34(3) (2014) 589-606.

[256] J. Winkler, B. Bilitewski, Comparative evaluation of life cycle assessment models for solid waste management, J Waste management 27(8) (2007) 1021-1031.

[257] S. Lotfi, W. Ma, K. Austin, A. Kumar, A wet packed-bed scrubber for removing tar from biomass producer gas, J Fuel processing technology 193 (2019) 197-203.

[258] A.K.S. Parihar, T. Hammer, G. Sridhar, Development and testing of tube type wet ESP for the removal of particulate matter and tar from producer gas, J Renewable energy 74 (2015) 875-883.

[259] R. Zwart, A. Van der Drift, A. Bos, H. Visser, M. Cieplik, H. Könemann, Oil‐based gas washing—Flexible tar removal for high‐efficient production of clean heat and power as well as

sustainable fuels and chemicals, J Environmental Progress Sustainable Energy: An Official Publication of the American Institute of Chemical Engineers 28(3) (2009) 324-335.

[260] B. Pathak, D. Kapatel, P. Bhoi, A. Sharma, D. Vyas, Design and development of sand bed filter for upgrading producer gas to IC engine quality fuel, J International Energy Journal 8(1) (2007).

[261] A. Surjosatyo, M.B. Anggriawan, A.A. Hermawan, H. Dafiqurrohman, Comparison between secondary thermal cracking methods and venturi scrubber filtering in order to reduce tar in biomass gasification, J Energy Procedia 158 (2019) 749-754.

[262] J. Ashok, N. Dewangan, S. Das, P. Hongmanorom, M.H. Wai, K. Tomishige, S. Kawi, Recent progress in the development of catalysts for steam reforming of biomass tar model reaction, J Fuel Processing Technology 199 (2020) 106252.

[263] F.N. Cayan, M. Zhi, S.R. Pakalapati, I. Celik, N. Wu, R. Gemmen, Effects of coal syngas impurities on anodes of solid oxide fuel cells, J Journal of Power Sources 185(2) (2008) 595-602.

[264] J. Han, H.J.R. Kim, s.e. reviews, The reduction and control technology of tar during biomass gasification/pyrolysis: an overview, Renewable and sustainable energy reviews 12(2) (2008) 397-416.

[265] A.P. Harvey, I.A. Mohammed, U. Dahiru, K. Zhang, Opportunities for process intensification using non-thermal plasmas, J Current Opinion in Chemical Engineering 41 (2023) 100930.

[266] A. Trushkin, I. Kochetov, Simulation of toluene decomposition in a pulse-periodic discharge operating in a mixture of molecular nitrogen and oxygen, J Plasma physics reports 38 (2012) 407-431.

[267] W. Metcalfe, S. Dooley, F. Dryer, Comprehensive detailed chemical kinetic modeling study of toluene oxidation, J Energy Fuels 25(11) (2011) 4915-4936.

[268] C. Saggese, A. Frassoldati, A. Cuoci, T. Faravelli, E. Ranzi, A wide range kinetic modeling study of pyrolysis and oxidation of benzene, J Combustion flame 160(7) (2013) 1168-1190.

[269] H.J. Curran, W.J. Pitz, H. Nakamura, C.J. Tobin, D. Darcy, M. Mehl, C.K. Westbrook, W.K. Metcalfe, An experimental and modeling study of shock tube and rapid compression machine ignition of n-butylbenzene/air mixtures, J Combustion Flame (2013).

[270] W. Yue, W. Lei, Y. Dong, C. Shi, Q. Lu, X. Cui, X. Wang, Y. Chen, J. Zhang, Toluene degradation in air/H2O DBD plasma: A reaction mechanism investigation based on detailed kinetic modeling and emission spectrum analysis, J Journal of Hazardous Materials 448 (2023) 130894.

[271] W. Wang, Q. Li, Q. Wang, J. Zhang, J. Liu, Tar steam reforming during biomass gasification: kinetic model and reaction pathway, J Clean Technologies Environmental Policy (2022) 1-12.

[272] A. Veksha, A. Giannis, G. Yuan, J. Tng, W.P. Chan, V.W.-C. Chang, G. Lisak, T.-T. Lim, Distribution and modeling of tar compounds produced during downdraft gasification of municipal solid waste, J Renewable energy 136 (2019) 1294-1303.

[273] R.J. Kee, F.M. RUpley, E. Meeks, J.A. Miller, CHEMKIN-III: A FORTRAN chemical kinetics package for the analysis of gas-phase chemical and plasma kinetics, 1996. https://www.osti.gov/biblio/481621.

[274] ANSYS, ANSYS Chemkin-Pro Input Manual, in: A. Inc (Ed.) Ansys Inc, 2021.

[275] Sichuan University, Combustion Dynamics Center of Sichuan University Sichuan Aerospace Power Technology Co., Ltd., n.d. https://cds.scu.edu.cn/.

[276] M. Mehl, W.J. Pitz, C.K. Westbrook, H.J. Curran, Kinetic modeling of gasoline surrogate components and mixtures under engine conditions, J International Journal of Chemical Kinetics 33(1) (2011) 193-200.

[277] K. Norinaga, Y. Sakurai, R. Sato, J.-i. Hayashi, Numerical simulation of thermal conversion of aromatic hydrocarbons in the presence of hydrogen and steam using a detailed chemical kinetic model, J Chemical engineering journal 178 (2011) 282-290.

[278] ANSYS, Introduction to Ansys Chemkin Pro, Lesson 8: Plasma Reactors, 2021.

[279] NTEL, Syngas Optimized for Intended Products, 2002. https://netl.doe.gov/research/coal/energy-systems/gasification/gasifipedia/syngas-optimization.

[280] K. Priya Arjunan, A. Morss Clyne, Hydroxyl radical and hydrogen peroxide are primarily responsible for dielectric barrier discharge plasma - induced angiogenesis, J Plasma Processes Polymers 8(12) (2011) 1154-1164.

[281] A. Frassoldati, A. Cuoci, T. Faravelli, U. Niemann, E. Ranzi, R. Seiser, K. Seshadri, An experimental and kinetic modeling study of n-propanol and iso-propanol combustion, J Combustion Flame 157(1) (2010) 2-16.

[282] F. Saleem, K. Zhang, A. Harvey, Role of CO2 in the conversion of toluene as a tar surrogate in a nonthermal plasma dielectric barrier discharge reactor, J Energy Fuels 32(4) (2018) 5164-5170.

[283] S. Liu, D. Mei, L. Wang, X. Tu, Steam reforming of toluene as biomass tar model compound in a gliding arc discharge reactor, J Chemical Engineering Journal 307 (2017) 793-802.

[284] R. Hizmeri, M. Izzeldin, M. Tsionas, A simple model correction for modelling and forecasting (un) reliable realized volatility, J Available at SSRN 3639116 (2021).

[285] M. Prieß, S. Koziel, T. Slawig, Surrogate-based optimization of climate model parameters using response correction, J Journal of Computational Science 2(4) (2011) 335-344.

[286] G.W. Sileshi, A critical review of forest biomass estimation models, common mistakes and corrective measures, J Forest Ecology Management 329 (2014) 237-254.

[287] S. Wauters, G. Marin, Kinetic modeling of coke formation during steam cracking, J Industrial engineering chemistry research 41(10) (2002) 2379-2391.

[288] L. Lie, W. Bin, Y. Chi, W. Chengkang, Characteristics of gliding arc discharge plasma, J Plasma Science Technology 8(6) (2006) 653.

[289] J. Gao, C. Kong, J. Zhu, A. Ehn, T. Hurtig, Y. Tang, S. Chen, M. Aldén, Z. Li, Visualization of instantaneous structure and dynamics of large-scale turbulent flames stabilized by a gliding arc discharge, J Proceedings of the Combustion Institute 37(4) (2019) 5629-5636.

[290] N. Aleksandrov, S. Kindysheva, I. Kochetov, Kinetics of low-temperature plasmas for plasma-assisted combustion and aerodynamics, J Plasma Sources Science Technology 23(1) (2014) 015017.

[291] A. Bogaerts, G. Centi, Plasma technology for CO2 conversion: a personal perspective on prospects and gaps, J Frontiers in Energy Research 8 (2020) 111.

[292] H. Conrads, M. Schmidt, Plasma generation and plasma sources, J Plasma Sources Science Technology 9(4) (2000) 441.

[293] T.Q. Hoang, X. Zhu, L.L. Lobban, R.G. Mallinson, Effects of gap and elevated pressure on ethanol reforming in a non-thermal plasma reactor, J Journal of Physics D: Applied Physics 44(27) (2011) 274003.

[294] S. Iwarere, V. Rohani, D. Ramjugernath, F. Fabry, L. Fulcheri, Hydrocarbons synthesis from syngas by very high pressure plasma, J Chemical Engineering Journal 241 (2014) 1-8.

[295] Swarthmore College, Information and notes for use with PrismSpect modeling and data display, n.d.

https://astro.swarthmore.edu/~cohen/projects/prismspect/notes.html#:~:text=X%2Dray%20astronomers%20and%20high,to%2011.6%20million%20degrees%20Kelvin.

[296] G. Gerasimov, Kinetic mechanisms of electron-beam induced polycyclic aromatic hydrocarbons transformation in flue gases, J Plasma Chemistry Plasma Processing 35 (2015) 895-911.

[297] I. Kosarev, N. Aleksandrov, S. Kindysheva, l.S. Starikovskaia, A.Y. Starikovskii, Kinetics of ignition of saturated hydrocarbons by nonequilibrium plasma: C2H6-to C5H12-containing mixtures, J Combustion flame 156(1) (2009) 221-233.

[298] F. Marias, R. Demarthon, A. Bloas, J. Robert-Arnouil, Modeling of tar thermal cracking in a plasma reactor, J Fuel Processing Technology 149 (2016) 139-152.

[299] M. Benilov, G. Naidis, Modeling of hydrogen-rich gas production by plasma reforming of hydrocarbon fuels, J International Journal of Hydrogen Energy 31(6) (2006) 769-774.

[300] B. Yan, Y. Cheng, T. Li, Y. Cheng, Detailed kinetic modeling of acetylene decomposition/soot formation during quenching of coal pyrolysis in thermal plasma, J Energy 121 (2017) 10-20.

[301] A.C. DeFilippo, J.-Y. Chen, Modeling plasma-assisted methane–air ignition using pre-calculated electron impact reaction rates, J Combustion Flame 172 (2016) 38-48.

[302] E. Ranzi, A. Frassoldati, R. Grana, A. Cuoci, T. Faravelli, A. Kelley, C.K. Law, Hierarchical and comparative kinetic modeling of laminar flame speeds of hydrocarbon and oxygenated fuels, J Progress in Energy Combustion Science 38(4) (2012) 468-501.

[303] M. Pelucchi, C. Cavallotti, T. Faravelli, S. Klippenstein, H-Abstraction reactions by OH, HO 2, O, O 2 and benzyl radical addition to O 2 and their implications for kinetic modelling of toluene oxidation, J Physical Chemistry Chemical Physics 20(16) (2018) 10607-10627.

[304] C. Wang, Y. Wang, H. Herath, Polycyclic aromatic hydrocarbons (PAHs) in biochar–Their formation, occurrence and analysis: A review, J Organic Geochemistry 114 (2017) 1-11.

[305] M.R. Crimmin, Benzene rings broken for chemical synthesis, Nature Publishing Group UK London, 2021.

[306] H. Wang, L. Chen, L. Xiao, K. Li, Y. Sun, F. Dong, Engineering the surface delocalized electrons facilitates the ring-opening for deep toluene oxidation, J Journal of Catalysis 413 (2022) 417-424.

[307] Y. Liang, Y. Xue, D. Fang, T. Tan, Z. Jiang, W. Shangguan, J. Yang, Y. Pan, Reaction mechanism of toluene decomposition in non-thermal plasma: How does it compare with benzene?, J Fundamental Research (2022).

[308] Y. Liang, J. Li, Y. Xue, T. Tan, Z. Jiang, Y. He, W. Shangguan, J. Yang, Y. Pan, Benzene decomposition by non-thermal plasma: A detailed mechanism study by synchrotron radiation photoionization mass spectrometry and theoretical calculations, J Journal of Hazardous Materials 420 (2021) 126584.

[309] Y. Li, H. Yuan, X. Zhou, J. Liang, Y. Liu, D. Chang, D. Yang, Degradation of Benzene Using Dielectric Barrier Discharge Plasma Combined with Transition Metal Oxide Catalyst in Air, J Catalysts 12(2) (2022) 203.

[310] University of Calgary, https://www.chem.ucalgary.ca/courses/350/Carey5th/Ch11/ch11-9.html, n.d. https://www.chem.ucalgary.ca/courses/350/Carey5th/Ch11/ch11-9.html.

[311] LibreText, 15.6: Other Cyclic Polyenes: Huckel 's Rule, n.d. https://chem.libretexts.org/Bookshelves/Organic_Chemistry/Map%3A_Organic_Chemistry_(Vollhardt_and_Schore)/15%3A_Benzene_and_Aromaticity%3A_Electrophilic_Aromatic_Substitution/15.06%3A_Other__Cyclic__Polyenes%3A__Huckel_'s_Rule.

[312] N. Gao, M.H. Milandile, C. Quan, L. Rundong, Critical assessment of plasma tar reforming during biomass gasification: A review on advancement in plasma technology, J Journal of Hazardous Materials 421 (2022) 126764.

[313] H. Fenglei, L. Mengyu, Z. Huangrong, L. Ting, L. Dandan, Z. Shuo, G. Wenwen, L. Fang, Product analysis and mechanism of toluene degradation by low temperature plasma with single dielectric barrier discharge, J Journal of Saudi Chemical Society 24(9) (2020) 673-682.

[314] A.M. Vandenbroucke, R. Morent, N.D. Geyter, C. Leys, Decomposition of toluene with plasma-catalysis: A review, J Journal of Advanced Oxidation Technologies 15(2) (2012) 232-241.

[315] L. Devi, K.J. Ptasinski, F.J. Janssen, Decomposition of naphthalene as a biomass tar over pretreated olivine: effect of gas composition, kinetic approach, and reaction scheme, J Industrial engineering chemistry research 44(24) (2005) 9096-9104.

[316] H. Ghomi, N.N. Safa, S. Ghasemi, Investigation on a DBD plasma reactor, J IEEE Transactions on plasma science 39(11) (2011) 2104-2105.

[317] A. Gutsol, Warm discharges for fuel conversion, J Handbook of Combustion: Online (2010) 323-353.

[318] K. Kwiatkowski, J. Krzysztoforski, K. Bajer, M. Dudyński, Bioenergy from feathers gasification–Efficiency and performance analysis, J Biomass bioenergy 59 (2013) 402-411.

[319] T. Nunnally, A. Tsangaris, A. Rabinovich, G. Nirenberg, I. Chernets, A. Fridman, Gliding arc plasma oxidative steam reforming of a simulated syngas containing naphthalene and toluene, J International journal of hydrogen energy 39(23) (2014) 11976-11989.

[320] O.J. Shiels, J.A. Turner, P. Kelly, S.J. Blanksby, G. da Silva, A.J. Trevitt, Modelling reaction kinetics of distonic radical ions: a systematic investigation of phenyl-type radical addition to unsaturated hydrocarbons, J Faraday Discussions 238 (2022) 475-490.

[321] D. Mei, Y. Wang, S. Liu, M. Alliati, H. Yang, X. Tu, Plasma reforming of biomass gasification tars using mixed naphthalene and toluene as model compounds, J Energy Conversion Management 195 (2019) 409-419.

[322] W. Xu, B. Chen, X. Jiang, F. Xu, X. Chen, L. Chen, J. Wu, M. Fu, D. Ye, Effect of calcium addition in plasma catalysis for toluene removal by Ni/ZSM-5: Acidity/basicity, catalytic activity and reaction mechanism, J Journal of hazardous materials 387 (2020) 122004.

[323] T. Namioka, Y.-i. Son, M. Sato, K. Yoshikawa, Practical method of gravimetric tar analysis that takes into account a thermal cracking reaction scheme, J Energy fuels 23(12) (2009) 6156-6162.

[324] R. Koch, R. Knispel, M. Elend, M. Siese, C. Zetzsch, Consecutive reactions of aromatic-OH adducts with NO, NO 2 and O 2: benzene, naphthalene, toluene, m-and p-xylene, hexamethylbenzene, phenol, m-cresol and aniline, J Atmospheric Chemistry Physics 7(8) (2007) 2057-2071.

[325] D.H. Lee, K.-T. Kim, M.S. Cha, Y.-H. Song, Effect of excess oxygen in plasma reforming of diesel fuel, J International journal of hydrogen energy 35(10) (2010) 4668-4675.

[326] N.D. Couto, V.B. Silva, E. Monteiro, A. Rouboa, Assessment of municipal solid wastes gasification in a semi-industrial gasifier using syngas quality indices, J Energy 93 (2015) 864-873.

[327] M. Capitelli, G. Colonna, G. D'Ammando, V. Laporta, A. Laricchiuta, Nonequilibrium dissociation mechanisms in low temperature nitrogen and carbon monoxide plasmas, J Chemical Physics 438 (2014) 31-36.

[328] W. Sun, A. Hamadi, S. Abid, N. Chaumeix, A. Comandini, Detailed experimental and kinetic modeling study of toluene/C2 pyrolysis in a single-pulse shock tube, J Combustion Flame 226 (2021) 129-142.

[329] P. Jamróz, W. Kordylewski, M. Wnukowski, Microwave plasma application in decomposition and steam reforming of model tar compounds, J Fuel Processing Technology 169 (2018) 1-14.

[330] O. Guaitella, F. Thevenet, E. Puzenat, C. Guillard, A. Rousseau, C2H2 oxidation by plasma/TiO2 combination: Influence of the porosity, and photocatalytic mechanisms under plasma exposure, J Applied Catalysis B: Environmental 80(3-4) (2008) 296-305.

[331] R.K. Prasad, A.K. Agarwal, Development and comparative experimental investigations of laser plasma and spark plasma ignited hydrogen enriched compressed natural gas fueled engine, J Energy 216 (2021) 119282.

[332] F.P. Fabbiani, D.R. Allan, S. Parsons, C.R. Pulham, Exploration of the high-pressure behaviour of polycyclic aromatic hydrocarbons: naphthalene, phenanthrene and pyrene, J Acta Crystallographica Section B: Structural Science 62(5) (2006) 826-842.

[333] L. Ciabini, M. Santoro, F.A. Gorelli, R. Bini, V. Schettino, S. Raugei, Triggering dynamics of the high-pressure benzene amorphization, J Nature materials 6(1) (2007) 39-43.

[334] Y. Zhang, K.P. Somers, M. Mehl, W.J. Pitz, R.F. Cracknell, H.J. Curran, Probing the antagonistic effect of toluene as a component in surrogate fuel models at low temperatures and high pressures. A case study of toluene/dimethyl ether mixtures, J Proceedings of the Combustion Institute 36(1) (2017) 413-421.

[335] R. Sivaramakrishnan, R. Tranter, K. Brezinsky, High-pressure, high-temperature oxidation of toluene, J Combustion flame 139(4) (2004) 340-350.

[336] H.I. Abdel-Shafy, M.S. Mansour, A review on polycyclic aromatic hydrocarbons: source, environmental impact, effect on human health and remediation, J Egyptian journal of petroleum 25(1) (2016) 107-123.

[337] S. Lundstedt, P. Haglund, L. Öberg, Simultaneous extraction and fractionation of polycyclic aromatic hydrocarbons and their oxygenated derivatives in soil using selective pressurized liquid extraction, J Analytical Chemistry 78(9) (2006) 2993-3000.

[338] W.L. Hsu, Gas‐phase kinetics during microwave plasma‐assisted diamond deposition: Is the hydrocarbon product distribution dictated by neutral‐neutral interactions?, J Journal of applied physics 72(7) (1992) 3102-3109.

[339] Y.S. Sayasov, Three-body electron recombination in plasma, J Bull. Soc. Fribourgeoise Sci. Naturelles 65(1) (1976) 76-87.

[340] N.L. Aleksandrov, Three-body electron attachment to a molecule, J Soviet Physics Uspekhi 31(2) (1988) 101.

[341] T. Owano, C. Kruger, R. Beddini, Electron-ion three-body recombination coefficient of argon, J AIAA journal 31(1) (1993) 75-82.

[342] M.S. Cha, R. Snoeckx, Plasma technology–Preparing for the electrified future, J Frontiers in Mechanical Engineering 8 (2022) 903379.

[343] K. Bhaskaran, P. Roth, The shock tube as wave reactor for kinetic studies and material systems, Progress in energy combustion science 28(2) (2002) 151-192.

[344] H.J. Curran, P. Gaffuri, W.J. Pitz, C.K. Westbrook, A comprehensive modeling study of n-heptane oxidation, J Combustion flame 114(1-2) (1998) 149-177.

[345] University of Galway, AramcoMech 1.3, n.g. https://www.universityofgalway.ie/combustionchemistrycentre/mechanismdownloads/aramcomech13/#. (Accessed 10 October 2023.

[346] J. Hanna, W.Y. Lee, Y. Shi, A.F. Ghoniem, Fundamentals of electro-and thermochemistry in the anode of solid-oxide fuel cells with hydrocarbon and syngas fuels, J Progress in energy combustion science 40 (2014) 74-111.

[347] O. Dogu, M. Pelucchi, R. Van de Vijver, P.H. Van Steenberge, D.R. D'hooge, A. Cuoci, M. Mehl, A. Frassoldati, T. Faravelli, K.M. Van Geem, The chemistry of chemical recycling of solid plastic waste via pyrolysis and gasification: State-of-the-art, challenges, and future directions, J Progress in Energy

Combustion Science 84 (2021) 100901.

[348] J.P. Ciferno, J.J. Marano, Benchmarking biomass gasification technologies for fuels, chemicals and hydrogen production, J US Department of Energy. National Energy Technology Laboratory (2002).

[349] P.F. Schubert, C.A. Bayens, L. Weick, M.O. Haid, Expanding markets for GTL fuels and specialty products, J Studies in Surface Science Catalysis 136 (2001) 459-464.

[350] M. Ostadi, E. Rytter, M. Hillestad, Boosting carbon efficiency of the biomass to liquid process with hydrogen from power: The effect of H2/CO ratio to the Fischer-Tropsch reactors on the production and power consumption, J Biomass Bioenergy 127 (2019) 105282.

[351] H.J. Chae, J.-H. Kim, S.C. Lee, H.-S. Kim, S.B. Jo, J.-H. Ryu, T.Y. Kim, C.H. Lee, S.J. Kim, S.-H. Kang, Catalytic technologies for CO hydrogenation for the production of light hydrocarbons and middle distillates, J Catalysts 10(1) (2020) 99.

[352] C. Du, P. Lu, N. Tsubaki, Efficient and new production methods of chemicals and liquid fuels by carbon monoxide hydrogenation, J ACS omega 5(1) (2019) 49-56.

[353] D.H. Tay, R.T. Ng, D.K. Ng, Modular optimization approach for process synthesis and integration of an integrated biorefinery, Computer Aided Chemical Engineering, Elsevier2012, pp. 1045-1049.

[354] S. Xu, H. Chen, C. Hardacre, X. Fan, Non-thermal plasma catalysis for CO2 conversion and catalyst design for the process, J Journal of Physics D: Applied Physics 54(23) (2021) 233001.

[355] L. Mazzoni, I. Janajreh, Plasma gasification of municipal solid waste with variable content of plastic solid waste for enhanced energy recovery, J International Journal of Hydrogen Energy 42(30) (2017) 19446-19457.

[356] M. Puig-Gamero, J. Argudo-Santamaria, J. Valverde, P. Sánchez, L. Sanchez-Silva, Three integrated process simulation using aspen plus®: Pine gasification, syngas cleaning and methanol synthesis, J Energy conversion management 177 (2018) 416-427.

[357] S. Kwon, S.-k. Im, Feasibility of non-thermal plasma gasification for a waste-to-energy power plant, J Energy Conversion Management 251 (2022) 114978.

[358] Y. Wang, Z. Liao, S. Mathieu, F. Bin, X. Tu, Prediction and evaluation of plasma arc reforming of naphthalene using a hybrid machine learning model, J Journal of Hazardous Materials 404 (2021) 123965.

[359] N. Ramzan, A. Ashraf, S. Naveed, A. Malik, Simulation of hybrid biomass gasification using Aspen plus: A comparative performance analysis for food, municipal solid and poultry waste, J Biomass bioenergy 35(9) (2011) 3962-3969.

[360] A. Tungalag, B. Lee, M. Yadav, O. Akande, Yield prediction of MSW gasification including minor species through ASPEN plus simulation, J Energy 198 (2020) 117296.

[361] W.M. Champion, C.D. Cooper, K.R. Mackie, P. Cairney, Development of a chemical kinetic model for a biosolids fluidized-bed gasifier and the effects of operating parameters on syngas quality, J Journal of the Air

Waste Management Association 64(2) (2014) 160-174.

[362] A.M. Gonzalez, E.E.S. Lora, J.C.E. Palacio, Syngas production from oil sludge gasification and its potential use in power generation systems: An energy and exergy analysis, J Energy 169 (2019) 1175-1190.

[363] G. Groppi, E. Tronconi, P. Forzatti, M. Berg, Mathematical modelling of catalytic combustors fuelled by gasified biomasses, J Catalysis Today 59(1-2) (2000) 151-162.

[364] D.P. Ross, H.-m. Yan, D.-k. Zhang, Modelling of a laboratory-scale bubbling fluidised-bed gasifier with feeds of both char and propane, J Fuel 83(14-15) (2004) 1979-1990.

[365] A. Ahmed, A. Salmiaton, T. Choong, W.W. Azlina, Review of kinetic and equilibrium concepts for biomass tar modeling by using Aspen Plus, J Renewable Sustainable Energy Reviews 52 (2015) 1623-1644.

[366] N. Couto, V. Silva, E. Monteiro, A. Rouboa, Exergy analysis of Portuguese municipal solid waste treatment via steam gasification, J Energy conversion management 134 (2017) 235-246.

[367] S. Klebingat, T. Kempka, M. Schulten, R. Azzam, T.M. Fernández-Steeger, Optimization of synthesis gas heating values and tar by-product yield in underground coal gasification, J Fuel 229 (2018) 248-261.

[368] P. Breeze, Energy from waste, Academic Press2017.

[369] G. Perkins, V. Sahajwalla, Steady-state model for estimating gas production from underground coal gasification, J Energy Fuels 22(6) (2008) 3902-3914.

[370] T. Banaszkiewicz, M. Chorowski, Energy consumption of air-separation adsorption methods, J Entropy 20(4) (2018) 232.

[371] A. Habibollahzade, M.A. Rosen, Syngas-fueled solid oxide fuel cell functionality improvement through appropriate feedstock selection and multi-criteria optimization using Air/O2-enriched-air gasification agents, J Applied Energy 286 (2021) 116497.

[372] D. Roberts, Characterisation of chemical composition and energy content of green waste and municipal solid waste from Greater Brisbane, Australia, J Waste management 41 (2015) 12-19.

[373] M. Mehdi, S.A.A. Taqvi, A.A. Shaikh, S. Khan, S.R. Naqvi, M. Shahbaz, D. Juchelková, Aspen plus simulation model of municipal solid waste gasification of metropolitan city for syngas production, J Fuel processing technology 344 (2023) 128128.

[374] R.E. Moshi, Y.A.C. Jande, T.T. Kivevele, W. Kim, Simulation and performance analysis of municipal solid waste gasification in a novel hybrid fixed bed gasifier using Aspen plus, J Energy Sources, Part A: Recovery, Utilization, Environmental Effects (2020) 1-13.

[375] J.M. de Andrés, E. Roche, A. Narros, M.E. Rodríguez, Characterisation of tar from sewage sludge gasification. Influence of gasifying conditions: Temperature, throughput, steam and use of primary catalysts, J Fuel processing technology 180 (2016) 116-126.

[376] M. Dudyński, J.C. van Dyk, K. Kwiatkowski, M. Sosnowska, Biomass gasification: Influence of torrefaction on syngas production and tar formation, J Fuel processing technology 131 (2015) 203-212.

[377] D. Neves, H. Thunman, A. Matos, L. Tarelho, A. Gómez-Barea, Characterization and prediction of biomass pyrolysis products, J Progress in energy combustion Science 37(5) (2011) 611-630.

[378] A. Dufour, E. Masson, P. Girods, Y. Rogaume, A. Zoulalian, Evolution of aromatic tar composition in relation to methane and ethylene from biomass pyrolysis-gasification, J Energy Fuels 25(9) (2011) 4182-4189.

[379] I. Janajreh, M. Al Shrah, Numerical and experimental investigation of downdraft gasification of wood chips, J Energy Conversion Management 65 (2013) 783-792.

[380] S. Hameed, A. Sharma, V. Pareek, H. Wu, Y. Yu, A review on biomass pyrolysis models: Kinetic, network and mechanistic models, J Biomass bioenergy 123 (2019) 104-122.

[381] Z. Kaczor, Z. Buliński, S. Werle, Modelling approaches to waste biomass pyrolysis: a review, J Renewable Energy 159 (2020) 427-443.

[382] J. Hernández, R. Ballesteros, G. Aranda, Characterisation of tars from biomass gasification: Effect of the operating conditions, J Energy 50 (2013) 333-342.

[383] D. Chen, L. Yin, H. Wang, P. He, Pyrolysis technologies for municipal solid waste: a review, J Waste management 34(12) (2014) 2466-2486.

[384] G. Del Alamo, A. Hart, A. Grimshaw, P. Lundstrøm, Characterization of syngas produced from MSW gasification at commercial-scale ENERGOS Plants, J Waste management 32(10) (2012) 1835-1842.

[385] D. Leung, C. Wang, Fluidized-bed gasification of waste tire powders, J Fuel Processing Technology 84(1-3) (2003) 175-196.

[386] L. De Diego, F. García-Labiano, P. Gayán, A. Abad, T. Mendiara, J. Adánez, M. Nacken, S. Heidenreich, Tar abatement for clean syngas production during biomass gasification in a dual fluidized bed, J Fuel processing technology 152 (2016) 116-123.

[387] S. Salaudeen, P. Arku, A. Dutta, Gasification of plastic solid waste and competitive technologies, Plastics to energy, Elsevier2019, pp. 269-293.

[388] S. Naveed, N. Ramzan, A. Malik, M. Akram, A comparative study of gasification of food waste (FW), poultry waste (PW), municipal solid waste (MSW) and used tires (UT), J The Nucleus 46(3) (2009) 77-81.

[389] A.C. Chang, H.-F. Chang, F.-J. Lin, K.-H. Lin, C.-H. Chen, Biomass gasification for hydrogen production, J International Journal of Hydrogen Energy 36(21) (2011) 14252-14260.

[390] J. Cai, R. Zeng, W. Zheng, S. Wang, J. Han, K. Li, M. Luo, X. Tang, Synergistic effects of co-gasification of municipal solid waste and biomass in fixed-bed gasifier, J Process Safety Environmental Protection 148 (2021) 1-12.

[391] M. Bassyouni, S.W. ul Hasan, M. Abdel-Aziz, S.-S. Abdel-hamid, S. Naveed, A. Hussain, F.N. Ani, Date palm waste gasification in downdraft gasifier and simulation using ASPEN HYSYS, J Energy conversión management 88 (2014) 693-699.

[392] S. Varjani, Efficient removal of tar employing dolomite catalyst in gasification: Challenges and opportunities, J Science of The Total Environment 836 (2022) 155721.

[393] T. Fujiyoshi, T. Ikami, T. Sato, K. Kikukawa, M. Kobayashi, H. Ito, A. Yamamoto, Evaluation of the matrix effect on gas chromatography–mass spectrometry with carrier gas containing ethylene glycol as an analyte protectant, J Journal of Chromatography A 1434 (2016) 136-141.

[394] S. Osipovs, Comparison of efficiency of two methods for tar sampling in the syngas, J Fuel 103 (2013) 387-392.

[395] B.L.F. Chin, A. Gorin, H.B. Chua, F. Twaiq, Experimental investigation on tar produced from palm shells derived syngas using zeolite HZSM-5 catalyst, J Journal of the Energy Institute 89(4) (2016) 713-724.

[396] S. Chianese, S. Fail, M. Binder, R. Rauch, H. Hofbauer, A. Molino, A. Blasi, D. Musmarra, Experimental investigations of hydrogen production from CO catalytic conversion of tar rich syngas by biomass gasification, J Catalysis Today 277 (2016) 182-191.

[397] T. Phuphuakrat, N. Nipattummakul, T. Namioka, S. Kerdsuwan, K. Yoshikawa, Characterization of tar content in the syngas produced in a downdraft type fixed bed gasification system from dried sewage sludge, J Fuel 89(9) (2010) 2278-2284.

[398] E. Delikonstantis, F. Cameli, M. Scapinello, V. Rosa, K.M. Van Geem, G.D. Stefanidis, Low-carbon footprint chemical manufacturing using plasma technology, J Current Opinion in Chemical Engineering 38 (2022) 100857.

[399] R.M. Eliott, M.F. Nogueira, A.S. Silva Sobrinho, B.A. Couto, H.S. Maciel, P.T. Lacava, Tar reforming under a microwave plasma torch, J Energy fuels 27(2) (2013) 1174-1181.

[400] Y.N. Chun, S.C. Kim, K. Yoshikawa, Removal characteristics of tar benzene using the externally oscillated plasma reformer, J Chemical Engineering Processing: Process Intensification 57 (2012) 65-74.

[401] Z. Wu, J. Wang, J. Han, S. Yao, S. Xu, P. Martin, Naphthalene decomposition by dielectric barrier discharges at atmospheric pressure, J IEEE Transactions on Plasma Science 45(1) (2016) 154-161.

[402] A. George, B. Shen, M. Craven, Y. Wang, D. Kang, C. Wu, X. Tu, A Review of Non-Thermal Plasma Technology: A novel solution for CO2 conversion and utilization, J Renewable Sustainable Energy Reviews 135 (2021) 109702.

[403] M. Xu, Y. Fukuyama, K. Nakai, Z. Liu, Y. Sumiya, A. Okino, Characteristics of Double-Layer, Large-Flow Dielectric Barrier Discharge Plasma Source for Toluene Decomposition, J Plasma 6(2) (2023) 212-224.

[404] P. Liang, W. Jiang, L. Zhang, J. Wu, J. Zhang, D. Yang, Experimental studies of removing typical VOCs by dielectric barrier discharge reactor of different sizes, J Process Safety Environmental Protection 94 (2015) 380-384.

[405] D. Gerrity, B.D. Stanford, R.A. Trenholm, S.A. Snyder, An evaluation of a pilot-scale nonthermal plasma advanced oxidation process for trace organic compound degradation, J Water Research 44(2) (2010) 493-504.

[406] S.-H. Han, H.-W. Park, T.-H. Kim, D.-W. Park, Large scale treatment of perfluorocompounds using a thermal plasma scrubber, J 청정기술 17(3) (2011) 250-258.

[407] C.A. Aggelopoulos, Recent advances of cold plasma technology for water and soil remediation: A critical review, J Chemical Engineering Journal 428 (2022) 131657.

[408] P. Parthasarathy, K.S. Narayanan, Hydrogen production from steam gasification of biomass: influence of process parameters on hydrogen yield–a review, J Renewable energy 66 (2014) 570-579.

[409] M.A. Babatabar, M. Saidi, Hydrogen production via integrated configuration of steam gasification process of biomass and water‐gas shift reaction: Process simulation and optimization, J International Journal of Energy Research 45(13) (2021) 19378-19394.

[410] F. Gallucci, R. Liberatore, L. Sapegno, E. Volponi, P. Venturini, F. Rispoli, E. Paris, M. Carnevale, A. Colantoni, Influence of oxidant agent on syngas composition: Gasification of hazelnut shells through an updraft reactor, J Energies 13(1) (2019) 102.

[411] C. Wu, P.T. Williams, Hydrogen production by steam gasification of polypropylene with various nickel catalysts, J Applied Catalysis B: Environmental 87(3-4) (2009) 152-161.

[412] N. Nipattummakul, I. Ahmed, S. Kerdsuwan, A.K. Gupta, High temperature steam gasification of wastewater sludge, Applied Energy Volume 87, Issue 12, (2010).

[413] U. Lee, J. Chung, H.A. Ingley, High-temperature steam gasification of municipal solid waste, rubber, plastic and wood, J Energy Fuels 28(7) (2014) 4573-4587.

[414] K. Burra, A. Gupta, Synergistic effects in steam gasification of combined biomass and plastic waste mixtures, J Applied energy 211 (2018) 230-236.

[415] H. Tian, Q. Hu, J. Wang, L. Liu, Y. Yang, A.V. Bridgwater, Steam gasification of Miscanthus derived char: the reaction kinetics and reactivity with correlation to the material composition and microstructure, J Energy conversion and management 219 (2020) 113026.

[416] M. Shahbaz, A. Inayat, D.O. Patrick, M. Ammar, The influence of catalysts in biomass steam gasification and catalytic potential of coal bottom ash in biomass steam gasification: a review, J Renewable Sustainable Energy Reviews 73 (2017) 468-476.

[417] S.S. Siwal, Q. Zhang, C. Sun, S. Thakur, V.K. Gupta, V.K. Thakur, Energy production from steam gasification processes and parameters that contemplate in biomass gasifier–A review, J Bioresource technology 297 (2020) 122481.

[418] D. Panepinto, V. Tedesco, E. Brizio, G. Genon, Environmental performances and energy efficiency for MSW gasification treatment, J Waste Biomass Valorization 6 (2015) 123-135.

[419] A. Antelava, N. Jablonska, A. Constantinou, G. Manos, S.A. Salaudeen, A. Dutta, S.M. Al-Salem, Energy potential of plastic waste valorization: A short comparative assessment of pyrolysis versus gasification, J Energy Fuels 35(5) (2021) 3558-3571.

[420] C. Borgianni, P. De Filippis, F. Pochetti, M. Paolucci, Gasification process of wastes containing PVC, J Fuel 81(14) (2002) 1827-1833.

[421] P.G. Rutberg, V.A. Kuznetsov, E.O. Serba, S.D. Popov, A.V. Surov, G.V. Nakonechny, A.V. Nikonov, Novel three-phase steam–air plasma torch for gasification of high-caloric waste, J Applied energy 108 (2013) 505-514.

[422] Y. Cao, Q. Wang, J. Du, J. Chen, Oxygen-enriched air gasification of biomass materials for high-quality syngas production, J Energy conversion management 199 (2019) 111628.

[423] A.K. Dalai, N. Batta, I. Eswaramoorthi, G.J. Schoenau, Gasification of refuse derived fuel in a fixed bed reactor for syngas production, J Waste Management 29(1) (2009) 252-258.

[424] B. Kumar, J.P. Brian, V. Atla, S. Kumari, K.A. Bertram, R.T. White, J.M. Spurgeon, Controlling the product syngas H2: CO ratio through pulsed-bias electrochemical reduction of CO2 on copper, J Acs Catalysis 6(7) (2016) 4739-4745.

[425] Q. Liu, C. Hu, B. Peng, C. Liu, Z. Li, K. Wu, H. Zhang, R. Xiao, High H2/CO ratio syngas production from chemical looping co-gasification of biomass and polyethylene with CaO/Fe2O3 oxygen carrier, J Energy Conversion Management 199 (2019) 111951.

[426] N.D. Subramanian, J. Gao, X. Mo, J.G. Goodwin Jr, W. Torres, J.J. Spivey, La and/or V oxide promoted Rh/SiO2 catalysts: Effect of temperature, H2/CO ratio, space velocity, and pressure on ethanol selectivity from syngas, J Journal of catalysis 272(2) (2010) 204-209.

[427] R. Zwart, S. Van der Heijden, R. Emmen, J.D. Bentzen, J. Ahrenfeldt, P. Stoholm, J. Krogh, Tar removal from low-temperature gasifiers, (2010).

[428] S. Kalantary, A. Jahani, R. Jahani, MLR and Ann approaches for prediction of synthetic/natural nanofibers diameter in the environmental and medical applications, J Scientific reports 10(1) (2020) 8117.

[429] D. Xie, X. Li, T. Zhou, Y. Feng, Estimating the contribution of environmental variables to water quality in the postrestoration littoral zones of Taihu Lake using the APCS-MLR model, J Science of The Total Environment 857 (2023) 159678.

[430] F.E. Yatim, I. Boumanchar, B. Srhir, Y. Chhiti, C. Jama, F.E.M.h. Alaoui, Waste-to-energy as a tool of circular economy: Prediction of higher heating value of biomass by artificial neural network (ANN) and multivariate linear regression (MLR), J Waste Management 153 (2022) 293-303.

[431] Z. Chen, X. Yu, X. Huang, S. Zhang, Prediction of reaction rate constants of hydroxyl radical with organic compounds, J Journal of the Chilean Chemical Society 59(1) (2014) 2252-2259.

[432] X. Zhang, K.K. Yalamanchi, S.M. Sarathy, A functional-group-based approach to modeling real-fuel combustion chemistry–I: Prediction of stoichiometric parameters for lumped pyrolysis reactions, J Combustion Flame 227 (2021) 497-509.

[433] M. Chakraborty, C. Sharma, J. Pandey, P.K. Gupta, Assessment of energy generation potentials of MSW in Delhi under different technological options, J Energy Conversion Management 75 (2013) 249-255.

[434] A. Carotenuto, S. Di Fraia, N. Massarotti, S. Sobek, M.R. Uddin, L. Vanoli, S. Werle, Sewage Sludge Gasification Process Optimization for Combined Heat and Power Generation, J Energies 16(12) (2023) 4742.

[435] I.B. Lee, I.S. Woo, M.C. Lee, Effects of nitrogen dilution on the NOx and CO emission of H2/CO/CH4 syngases in a partially-premixed gas turbine model combustor, J International journal of hydrogen energy 41(35) (2016) 15841-15851.

[436] Z. McCaffrey, P. Thy, M. Long, M. Oliveira, L. Wang, L. Torres, T. Aktas, B.-S. Chiou, W. Orts, B.M. Jenkins, Air and steam gasification of almond biomass, J Frontiers in energy research 7 (2019) 84.

[437] G. Galeno, M. Minutillo, A. Perna, From waste to electricity through integrated plasma gasification/fuel cell (IPGFC) system, J international journal of hydrogen energy 36(2) (2011) 1692-1701.

[438] Y. Zhang, J. Xiao, L. Shen, Simulation of methanol production from biomass gasification in interconnected fluidized beds, J Industrial engineering chemistry research 48(11) (2009) 5351-5359.

[439] A. Matveev, A. Dubinin, S. Shcheklein, Steam gasification of waste tires for the purpose of methanol production, J International Multidisciplinary Scientific GeoConference: SGEM 18(4.2) (2018) 175-182.

[440] A. Babarit, E. Body, J.-C. Gilloteaux, J.-F. Hétet, Energy and economic performance of the FARWIND energy system for sustainable fuel production from the far-offshore wind energy resource, 2019 Fourteenth International Conference on Ecological Vehicles and Renewable Energies (EVER), IEEE, 2019, pp. 1-10.

[441] A. Śliwińska, D. Burchart-Korol, A. Smoliński, Environmental life cycle assessment of methanol and electricity co-production system based on coal gasification technology, J Science of the Total Environment 574 (2017) 1571-1579.

[442] G.-j. Liu, Z. Li, M.-h. Wang, W.-d. Ni, Energy savings by co-production: A methanol/electricity case study, J Applied Energy 87(9) (2010) 2854-2859.

[443] N.M. Nguyen, F. Alobaid, P. Dieringer, B. Epple, Biomass-based chemical looping gasification: Overview and recent developments, J Applied Sciences 11(15) (2021) 7069.

[444] J. van Baten, M. Pons, CAPE - OPEN: Interoperability in Industrial Flowsheet Simulation Software, J Chemie Ingenieur Technik 86(7) (2014) 1052-1064.

[445] P.J. Woolcock, R.C. Brown, A review of cleaning technologies for biomass-derived syngas, Biomass and Bioenergy 52 (2013) 54-84.

[446] Y.G. Rueda, L.J. Helsen, The role of plasma in syngas tar cracking, Biomass Conversion Biorefinery (2019) 1-15.

[447] F. Fabry, C. Rehmet, V. Rohani, L. Fulcheri, Waste gasification by thermal plasma: a review, J Waste Biomass Valorization 4(3) (2013) 421-439.

[448] A. Iqbal, X. Liu, G.-H. Chen, Municipal solid waste: Review of best practices in application of life cycle assessment and sustainable management techniques, J Science of The Total Environment 729 (2020) 138622.

[449] I.-R. Istrate, D. Iribarren, J.-L. Gálvez-Martos, J. Dufour, Review of life-cycle environmental consequences of waste-to-energy solutions on the municipal solid waste management system, Resources, conservation & recycling 157 (2020) 104778.

[450] H. Alhazmi, F.H. Almansour, Z. Aldhafeeri, Plastic Waste Management: A Review of Existing Life Cycle Assessment Studies, J Sustainability 13(10) (2021) 5340.

[451] B. Dastjerdi, V. Strezov, M.A. Rajaeifar, R. Kumar, M. Behnia, A systematic review on life cycle assessment of different waste to energy valorization technologies, J Journal of Cleaner Production 290 (2021) 125747.

[452] J. Zhang, Q. Qin, G. Li, C.-H. Tseng, Sustainable municipal waste management strategies through life cycle assessment method: A review, Journal of Environmental Management 287 (2021) 112238.

[453] A. Villanueva, H. Wenzel, Paper waste–recycling, incineration or landfilling? A review of existing life cycle assessments, J Waste management 27(8) (2007) S29-S46.

[454] S.-L. Pei, T.-L. Chen, S.-Y. Pan, Y.-L. Yang, Z.-H. Sun, Y.-J. Li, Addressing environmental sustainability of plasma vitrification technology for stabilization of municipal solid waste incineration fly ash, J Journal of Hazardous Materials 398 (2020) 122959.

[455] M. Danthurebandara, S. Van Passel, I. Vanderreydt, K. Van Acker, Environmental and economic performance of plasma gasification in Enhanced Landfill Mining, J Waste Management 45 (2015) 458-467.

[456] S. Evangelisti, C. Tagliaferri, R. Clift, P. Lettieri, R. Taylor, C. Chapman, Life cycle assessment of conventional and two-stage advanced energy-from-waste technologies for municipal solid waste treatment, J Journal of Cleaner Production 100 (2015) 212-223.

[457] V. Mannheim, I. Bodnár, Life Cycle Assessment for Thermic Treatments of Organic Industrial Waste, Enviro-management, 2012.

[458] H. Qi, P. Cui, Z. Liu, Z. Xu, D. Yao, Y. Wang, Z. Zhu, S. Yang, Conceptual design and comprehensive analysis for novel municipal sludge gasification-based hydrogen production via plasma gasifier, J Energy Conversion Management 245 (2021) 114635.

[459] A. Ramos, A. Rouboa, Renewable energy from solid waste: Life cycle analysis and social welfare, J Environmental impact assessment review 85 (2020) 106469.

[460] A. Ramos, C.A. Teixeira, A. Rouboa, Assessment study of an advanced gasification strategy at low temperature for syngas generation, J International Journal of Hydrogen Energy 43(21) (2018) 10155-10166.

[461] A. Ramos, C.A. Teixeira, A. Rouboa, Environmental assessment of municipal solid waste by two-stage plasma gasification, J Energies 12(1) (2019) 137.

[462] A.M. López-Sabirón, K. Fleiger, S. Schäfer, J. Antoñanzas, A. Irazustabarrena, A. Aranda-Usón, G.A. Ferreira, Refuse derived fuel (RDF) plasma torch gasification as a feasible route to produce low environmental impact syngas for the cement industry, J Waste Management Research 33(8) (2015) 715-722.

[463] C. Tagliaferri, P. Lettieri, Methane from waste: Thermal and biological technologies compared under a life cycle assessment perspective, Substitute Natural Gas from Waste, Elsevier2019, pp. 275-315.

[464] H.-L. Zhao, L. Wang, F. Liu, H.-Q. Liu, N. Zhang, Y.-W. Zhu, Energy, environment and economy assessment of medical waste disposal technologies in China, J Science of The Total Environment 796 (2021) 148964.

[465] P. Suresh, R. Malina, M.D. Staples, S. Lizin, H. Olcay, D. Blazy, M.N. Pearlson, S.R. Barrett, Life cycle greenhouse gas emissions and costs of production of diesel and jet fuel from municipal solid waste, J Environmental science technology 52(21) (2018) 12055-12065.

[466] H.H. Khoo, Life cycle impact assessment of various waste conversion technologies, J Waste management 29(6) (2009) 1892-1900.

[467] M. Schiavon, M. Ragazzi, E. Rada, G. Merler, Proposal for the correct management of the life cycle assessment results from integrated municipal solid waste treatment, J WIT Trans. Ecol. Environ 180 (2014) 163-173.

[468] U. Arena, F. Ardolino, F. Di Gregorio, A life cycle analysis of two combustion and gasification-based waste-to-energy units, J Proceedings Venice (2014).

[469] J. Portugal-Pereira, L. Lee, Economic and environmental benefits of waste-to-energy technologies for debris recovery in disaster-hit Northeast Japan, J Journal of Cleaner Production 112 (2016) 4419-4429.

[470] J.-M. Fernández-Gonzalez, A.L. Grindlay, F. Serrano-Bernardo, M.I. Rodríguez-Rojas, M. Zamorano, Economic and environmental review of Waste-to-Energy systems for municipal solid waste management in medium and small municipalities, J Waste Management 67 (2017) 360-374.

[471] Z.A. Coventry, R. Tize, A.T. Karunanithi, Comparative life cycle assessment of solid waste management strategies, J Clean Technologies Environmental Policy 18(5) (2016) 1515-1524.

[472] C. Aracil, P. Haro, D. Fuentes-Cano, A. Gómez-Barea, Implementation of waste-to-energy options in landfill-dominated countries: Economic evaluation and GHG impact, J Waste Management 76 (2018) 443-456.

[473] M. Parascanu, P. Sánchez, G. Soreanu, J. Valverde, L. Sanchez-Silva, Environmental assessment of olive pomace valorization through two different thermochemical processes for energy production, J Journal of Cleaner Production 186 (2018) 771-781.

[474] G. Assefa, O. Eriksson, B. Frostell, Technology assessment of thermal treatment technologies using ORWARE, J Energy conversion management 46(5) (2005) 797-819.

[475] M. Gunamantha, Life cycle assessment of municipal solid waste treatment to energy options: Case study of KARTAMANTUL region, Yogyakarta, J Renewable energy 41 (2012) 277-284.

[476] H. Tong, Y. Shen, J. Zhang, C.-H. Wang, T.S. Ge, Y.W. Tong, A comparative life cycle assessment on four waste-to-energy scenarios for food waste generated in eateries, J Applied Energy 225 (2018) 1143-1157.

[477] J. Dong, Y. Tang, A. Nzihou, Y. Chi, E. Weiss-Hortala, M. Ni, Z. Zhou, Comparison of waste-to-energy technologies of gasification and incineration using life cycle assessment: Case studies in Finland, France and China, J Journal of Cleaner Production 203 (2018) 287-300.

[478] A. Ramos, J. Berzosa, F. Clarens, M. Marin, A. Rouboa, Environmental and socio-economic assessment of cork waste gasification: Life cycle and cost analysis, J Journal of Cleaner Production 249 (2020) 119316.

[479] Y. Tang, J. Dong, G. Li, Y. Zheng, Y. Chi, A. Nzihou, E. Weiss-Hortala, C. Ye, Environmental and exergetic life cycle assessment of incineration-and gasification-based waste to energy systems in China, J Energy Conversion 205 (2020) 118002.

[480] A. Demetrious, E.t. Crossin, Life cycle assessment of paper and plastic packaging waste in landfill, incineration, and gasification-pyrolysis, Journal of Material Cycles and Waste Management 21(4) (2019) 850-860.

[481] Eco Chain, Impact Categories (LCA) – Overview, 2020. https://ecochain.com/knowledge/impact-categories-lca/. (Accessed 25 July 2022).

[482] S. Nanda, F. Berruti, Municipal solid waste management and landfilling technologies: a review, J Environmental Chemistry Letters 19(2) (2021) 1433-1456.

[483] R. Harrabin, Should we burn or bury waste plastic?, 2018. https://www.bbc.com/news/science-environment-43120041. (Accessed 25 July 2022).

[484] D. Lazarevic, E. Aoustin, N. Buclet, N. Brandt, Plastic waste management in the context of a European recycling society: Comparing results and uncertainties in a life cycle perspective, J Resources, Conservation & Recycling 55(2) (2010) 246-259.

[485] D. Chen, L. Yin, H. Wang, P. He, Reprint of: pyrolysis technologies for municipal solid waste: a review, J Waste management 37 (2015) 116-136.

[486] I. Dincer, M.A. Rosen, Thermal energy storage systems and applications, John Wiley & Sons2021.

[487] F. Neuwahl, G. Cusano, J.G. Benavides, S. Holbrook, S. Roudier, Best Available Techniques (BAT) Reference Document for Waste Incineration, J EUR 29971 (2019) 2020-01.

[488] L. Ji, S. Lu, J. Yang, C. Du, Z. Chen, A. Buekens, J. Yan, Municipal solid waste incineration in China and the issue of acidification: A review, J Waste Management Research 34(4) (2016) 280-297.

[489] E. Hodson, D. Martin, R. Prinn, The municipal solid waste landfill as a source of ozone-depleting substances in the United States and United Kingdom, J Atmospheric Chemistry Physics 10(4) (2010) 1899-1910.

[490] M. Materazzi, P. Lettieri, L. Mazzei, R. Taylor, C. Chapman, Fate and behavior of inorganic constituents of RDF in a two stage fluid bed-plasma gasification plant, J Fuel 150 (2015) 473-485.

[491] M. Laaksonen, Simulation and Optimization of an Air Pollution Control System Dealing with Flue Gases from Combustion of Syngas Produced through a Municipal Solid Waste Plasma Gasification and Melting Process, 2012.

[492] D. Baderna, F. Caloni, E. Benfenati, Investigating landfill leachate toxicity in vitro: A review of cell models and endpoints, J Environment international 122 (2019) 21-30.

[493] E.R. Rogers, R.S. Zalesny Jr, C.-H. Lin, A systematic approach for prioritizing landfill pollutants based on toxicity: Applications and opportunities, J Journal of Environmental Management 284 (2021) 112031.

[494] X.-G. Li, Y. Lv, B.-G. Ma, Q.-B. Chen, X.-B. Yin, S.-W. Jian, Utilization of municipal solid waste incineration bottom ash in blended cement, J Journal of Cleaner Production 32 (2012) 96-100.

[495] D. Blasenbauer, F. Huber, J. Lederer, M.J. Quina, D. Blanc-Biscarat, A. Bogush, E. Bontempi, J. Blondeau, J.M. Chimenos, H. Dahlbo, Legal situation and current practice of waste incineration bottom ash utilisation in Europe, J Waste Management 102 (2020) 868-883.

[496] M. Čarnogurská, M. Lázár, M. Puškár, M. Lengyelová, J. Václav, Ľ. Širillová, Measurement and evaluation of properties of MSW fly ash treated by plasma, J Measurement 62 (2015) 155-161.

[497] T. Cheng, J. Chu, C. Tzeng, Y. Chen, Treatment and recycling of incinerated ash using thermal plasma technology, J Waste Management 22(5) (2002) 485-490.

[498] US EPA, Photochemical smog - What it means for us, 2004. https://www.epa.sa.gov.au/files/8238_info_photosmog.pdf. (Accessed 25 July 2022).

[499] L. Sivula, A. Oikari, J. Rintala, Toxicity of waste gasification bottom ash leachate, J Waste management 32(6) (2012) 1171-1178.

[500] M.A. Rajaeifar, M. Raugei, B. Steubing, A. Hartwell, P.A. Anderson, O. Heidrich, Life cycle assessment of lithium‐ion battery recycling using pyrometallurgical technologies, J Journal of Industrial Ecology 25(6) (2021) 1560-1571.

[501] S. Evangelisti, C. Tagliaferri, R. Clift, P. Lettieri, R. Taylor, C. Chapman, Integrated gasification and plasma cleaning for waste treatment: A life cycle perspective, J Waste Management 43 (2015) 485-496.

[502] F. Mayer, R. Bhandari, S. Gäth, Critical review on life cycle assessment of conventional and innovative waste-to-energy technologies, J Science of the Total Environment 672 (2019) 708-721.

[503] J. Cleary, Life cycle assessments of municipal solid waste management systems: A comparative analysis of selected peer-reviewed literature, J Environment international 35(8) (2009) 1256-1266.

[504] S. Manfredi, R. Pant, D.W. Pennington, A. Versmann, Supporting environmentally sound decisions for waste management with LCT and LCA, J The International Journal of Life Cycle Assessment 16(9) (2011) 937-939.

[505] A. Kane, FCC'S LINCOLN INCINERATOR OFFICIALLY OPENS, 2014. https://resource.co/article/fcc%E2%80%99s-lincoln-incinerator-officially-opens-6992. (Accessed 25 July 2022).

[506] J.-L. Shie, C.-Y. Chang, C.-S. Chen, D.-G. Shaw, Y.-H. Chen, W.-H. Kuan, H.-K. Ma, Energy life cycle assessment of rice straw bio-energy derived from potential gasification technologies, J Bioresource technology 102(12) (2011) 6735-6741.

[507] M. Herva, E. Roca, Ranking municipal solid waste treatment alternatives based on ecological footprint and multi-criteria analysis, J Ecological Indicators 25 (2013) 77-84.

[508] F. De Menna, J. Dietershagen, M. Loubiere, M. Vittuari, Life cycle costing of food waste: A review of methodological approaches, J Waste Management 73 (2018) 1-13.

[509] Z. Zhou, Y. Tang, Y. Chi, M. Ni, A. Buekens, Waste-to-energy: A review of life cycle assessment and its extension methods, J Waste Management Research 36(1) (2018) 3-16.

[510] R.J. Saft, Life cycle assessment of a pyrolysis/gasification plant for hazardous paint waste, J The International Journal of Life Cycle Assessment 12(4) (2007) 230-238.

[511] A.U. Zaman, Life cycle assessment of pyrolysis–gasification as an emerging municipal solid waste treatment technology, J International Journal of Environmental Science Technology 10(5) (2013) 1029-1038.

[512] A.U. Zaman, Comparative study of municipal solid waste treatment technologies using life cycle assessment method, J International Journal of Environmental Science Technology 7(2) (2010) 225-234.

[513] A. Demetrious, K. Verghese, P. Stasinopoulos, E. Crossin, Comparison of alternative methods for managing the residual of material recovery facilities using life cycle assessment, J Resources, Conservation Recycling 136 (2018) 33-45.

[514] B. Sharma, Y. Goswami, S. Sharma, S. Shekhar, Inherent roadmap of conversion of plastic waste into energy and its life cycle assessment: a frontrunner compendium, J Renewable Sustainable Energy Reviews 146 (2021) 111070.

[515] K. Zeng, D. Gauthier, J. Soria, G. Mazza, G. Flamant, Solar pyrolysis of carbonaceous feedstocks: A review, J Solar Energy 156 (2017) 73-92.

[516] J. Zeaiter, F. Azizi, M. Lameh, D. Milani, H.Y. Ismail, A. Abbas, Waste tire pyrolysis using thermal solar energy: An integrated approach, J Renewable Energy 123 (2018) 44-51.

[517] M. Solis, S. Silveira, Technologies for chemical recycling of household plastics–A technical review and TRL assessment, J Waste Management 105 (2020) 128-138.

[518] E. Benetto, C. Jury, E. Igos, J. Carton, P. Hild, C. Vergne, J. Di Martino, Using atmospheric plasma to design multilayer film from polylactic acid and thermoplastic starch: A screening Life Cycle Assessment, J Journal of Cleaner Production 87 (2015) 953-960.

[519] L. Wang, R. Templer, R.J. Murphy, A Life Cycle Assessment (LCA) comparison of three management options for waste papers: Bioethanol production, recycling and incineration with energy recovery, J Bioresource Technology 120 (2012) 89-98.

[520] Ecoinvent, System Models, n.d. https://ecoinvent.org/the-ecoinvent-database/system-models/#:~:text=of%20cut%2Doff.-,Allocation%20at%20the%20Point%20of%20Substitution,as%20the%20APOS%20system%20model.\.

[521] International Energy Agency, World Energy Balances, (2016).

[522] C. Koffler, J. Florin, Tackling the downcycling issue—A revised approach to value-corrected substitution in life cycle assessment of aluminum (VCS 2.0), J Sustainability 5(11) (2013) 4546-4560.

[523] N. Jungbluth, M. Chudacoff, A. Dauriat, F. Dinkel, G. Doka, M. Faist Emmenegger, E. Gnansounou, N. Kljun, K. Schleiss, M. Spielmann, Life cycle inventories of bioenergy, J Final report ecoinvent data v2. 0 17 (2007).

[524] National Institute for Public Health and the Environment, LCIA: the ReCiPe mode, 2018. https://www.rivm.nl/en/life-cycle-assessment-lca/recipe.

[525] A. Kendall, Time-adjusted global warming potentials for LCA and carbon footprints, J The International Journal of Life Cycle Assessment 17 (2012) 1042-1049.

[526] J.B. Guinée, Handbook on life cycle assessment: operational guide to the ISO standards, Springer Science & Business Media2002.

[527] Sphera, Search Life Cycle Assessment Datasets (fka GaBi), (n.d).

[528] Sheffield Energy Recovery Facility, ANNUAL PERFORMANCE REPORT 2012, (2012).

[529] Lincolnshire, Energy from Waste, n.d. https://lincolnshire.fccenvironment.co.uk/.

[530] Knowsley Council, Knowsley Industrial Park, (2012).

[531] A. Anastasopoulou, S. Butala, J. Lang, V. Hessel, Q. Wang, Life cycle assessment of the nitrogen fixation process assisted by plasma technology and incorporating renewable energy, J Industrial Engineering Chemistry Research 55(29) (2016) 8141-8153.

[532] H. Althaus, M. Chudacoff, R. Hischier, N. Jungbluth, M. Osses, A. Primas, Life cycle inventories of chemicals, J Ecoinvent report 2 (2007).

[533] D.H. Chun, J.C. Park, S.Y. Hong, J.T. Lim, C.S. Kim, H.-T. Lee, J.-I. Yang, S. Hong, H. Jung, Highly selective iron-based Fischer–Tropsch catalysts activated by CO2-containing syngas, J Journal of catalysis 317 (2014) 135-143.

[534] C. Moretti, B. Corona, V. Rühlin, T. Götz, M. Junginger, T. Brunner, I. Obernberger, L. Shen, Combining biomass gasification and solid oxid fuel cell for heat and power generation: An early-stage life cycle assessment, J Energies 13(11) (2020) 2773.

[535] US EPA, Understanding Global Warming Potentials, 2023. https://www.epa.gov/ghgemissions/understanding-global-warming-potentials.

[536] International Energy Agency, Key world energy statistics, International Energy Agency Paris2007.

[537] C. Ramprasad, H.C. Teja, V. Gowtham, V. Vikas, Quantification of landfill gas emissions and energy production potential in Tirupati Municipal solid waste disposal site by LandGEM mathematical model, J MethodsX 9 (2022) 101869.

[538] X. Cui, R.M. Bustin, L. Chikatamarla, Adsorption - induced coal swelling and stress: Implications for methane production and acid gas sequestration into coal seams, J Journal of Geophysical Research: Solid Earth 112(B10) (2007).

[539] I. Stasiulaitiene, D. Martuzevicius, V. Abromaitis, M. Tichonovas, J. Baltrusaitis, R. Brandenburg, A. Pawelec, A. Schwock, Comparative life cycle assessment of plasma-based and traditional exhaust gas treatment technologies, J Journal of Cleaner Production 112 (2016) 1804-1812.

[540] Ellen MacArthur Foundation, What is Circular Economy, 2022. https://ellenmacarthurfoundation.org/topics/circular-economy-introduction/overview.

[541] P. Ghisellini, C. Cialani, S. Ulgiati, A review on circular economy: the expected transition to a balanced interplay of environmental and economic systems, J Journal of Cleaner production 114 (2016) 11-32.

[542] M.A. Reuter, A. van Schaik, J. Gutzmer, N. Bartie, A. Abadías-Llamas, Challenges of the Circular Economy: A Material, Metallurgical, and Product Design Perspective, J Annual Review of Materials Research 49 (2019).

[543] N. AlQattan, M. Acheampong, F.M. Jaward, F.C. Ertem, N. Vijayakumar, T. Bello, Reviewing the potential of Waste-to-Energy (WTE) technologies for Sustainable Development Goal (SDG) numbers seven and eleven, J Renewable Energy Focus 27 (2018) 97-110.

[544] E. Rada, M. Ragazzi, V. Torretta, G. Castagna, L. Adami, L. Cioca, Circular economy and waste to energy, AIP Conference Proceedings, AIP Publishing, 2018, p. 030050.

[545] T. Tomić, D.R. Schneider, The role of energy from waste in circular economy and closing the loop concept–Energy analysis approach, J Renewable Sustainable Energy Reviews 98 (2018) 268-287.

[546] A. Luthra, Waste-to-Energy and Recycling, J Economic Political Weekly 52(13) (2017) 51.

[547] N. Ferronato, V. Torretta, Waste mismanagement in developing countries: A review of global issues, J International journal of environmental research public health 16(6) (2019) 1060.

[548] Government of Japan, The 4th Fundamental Plan for Establishing a Sound Material-Cycle Society, 2018. https://www.env.go.jp/en/recycle/smcs/index.html. (Accessed 25 July 2022).

[549] W. McDowall, Y. Geng, B. Huang, E. Barteková, R. Bleischwitz, S. Türkeli, R. Kemp, T. Doménech, Circular economy policies in China and Europe, J Journal of Industrial Ecology 21(3) (2017) 651-661.

[550] European Commission, Implementation of the Circular Economy Action Plan, 2019. http://ec.europa.eu/environment/circular-economy/index_en.htm. (Accessed 25 July 2022).

[551] E.C. Rada, L.-I. Cioca, G. Ionescu, Energy recovery from Municipal Solid Waste in EU: proposals to assess the management performance under a circular economy perspective, MATEC Web of Conferences, EDP Sciences, 2017, p. 05006.

[552] S.-Y. Pan, M.A. Du, I.-T. Huang, I.-H. Liu, E. Chang, P.-C. Chiang, Strategies on implementation of waste-to-energy (WTE) supply chain for circular economy system: a review, J Journal of Cleaner Production 108 (2015) 409-421.

[553] Z. Zhongming, L. Linong, Z. Wangqiang, L. Wei, Waste to Energy in the Age of the Circular Economy: Best Practice Handbook, 2020.

[554] S. Achinas, An overview of the technological applicability of plasma gasification process, J Contemporary Environmental Issues and Challenges in Era of Climate Change (2020) 261-275.

[555] B. Welt, Plasma gasification can enable circular economy sustainability for packaging, 2019. https://www.packworld.com/issues/sustainability/blog/13377446/plasma-gasification-can-enable-circular-economy-sustainability-for-packaging. (Accessed 25 July 2022).

[556] M. Pourali, Application of plasma gasification technology in waste to energy challenges and opportunities, 2009 IEEE PES/IAS Conference on Sustainable Alternative Energy (SAE), IEEE, 2009, pp. 1-6.

[557] H. Corvellec, M.J.Z. Campos, P. Zapata, Infrastructures, lock-in, and sustainable urban development: the case of waste incineration in the Göteborg Metropolitan Area, J Journal of cleaner production 50 (2013) 32-39.

[558] M. Klavins, V. Bisters, J. Burlakovs, Small scale gasification application and perspectives in circular economy, J Scientific Journal of Riga Technical University. Environmental Climate Technologies 22(1) (2018) 42-54.

[559] N.P. Lumley, D.F. Ramey, A.L. Prieto, R.J. Braun, T.Y. Cath, J.M. Porter, Techno-economic analysis of wastewater sludge gasification: A decentralized urban perspective, J Bioresource technology 161 (2014) 385-394.

[560] M. Pecchi, M. Baratieri, Coupling anaerobic digestion with gasification, pyrolysis or hydrothermal carbonization: A review, J Renewable Sustainable Energy Reviews 105 (2019) 462-475.

[561] Q. Zhu, E.A. Lowe, Y.a. Wei, D. Barnes, Industrial symbiosis in China: a case study of the Guitang Group, Journal of Industrial Ecology 11(1) (2007) 31-42.

[562] N.B. Jacobsen, Industrial symbiosis in Kalundborg, Denmark: a quantitative assessment of economic and environmental aspects, J Journal of industrial ecology 10(1-2) (2006) 239-255.

[563] D. Gibbs, P. Deutz, Implementing industrial ecology? Planning for eco-industrial parks in the USA, J Geoforum 36(4) (2005) 452-464.

[564] B.H. Roberts, The application of industrial ecology principles and planning guidelines for the development of eco-industrial parks: an Australian case study, J Journal of Cleaner Production 12(8-10) (2004) 997-1010.

[565] S. Consonni, F. Viganò, Waste gasification vs. conventional Waste-To-Energy: A comparative evaluation of two commercial technologies, J Waste management 32(4) (2012) 653-666.

[566] B. Bahor, M. Van Brunt, WTE: Sustainable Waste and Materials Management, J Recovery of Materials Energy from Urban Wastes: A Volume in the Encyclopedia of Sustainability Science Technology, Second Edition (2019) 439-454.

[567] M.L. Mastellone, Technical description and performance evaluation of different packaging plastic waste management's systems in a circular economy perspective, J Science of the total environment 718 (2020) 137233.

[568] O. Dogu, M. Pelucchi, R. Van de Vijver, P.H. Van Steenberge, D.R. D'hooge, A. Cuoci, M. Mehl, A. Frassoldati, T. Faravelli, K.M. Van Geem, The chemistry of chemical recycling of solid plastic waste via pyrolysis and gasification: State-of-the-art, challenges, and future directions, J Progress in Energy Combustion Science 84 (2021) 100901.

[569] D. Fytili, A. Zabaniotou, Circular economy synergistic opportunities of decentralized thermochemical systems for bioenergy and biochar production fueled with agro-industrial wastes with environmental sustainability and social acceptance: a review, J Current Sustainable/Renewable Energy Reports 5(2) (2018) 150-155.

[570] M.U. Khan, B. Ahring, T. Garcia-Perez, M. Garcia-Perez, Valorization of municipal solid waste in biorefineries for the creation of a circular economy: role of emerging technologies, Current Developments in Biotechnology and Bioengineering, Elsevier2020, pp. 323-347.

[571] Z. Wan, J. Chen, B. Craig, Lessons learned from Huizhou, China's unsuccessful waste-to-energy incinerator project: Assessment and policy recommendations, J Utilities Policy 33 (2015) 63-68.

[572] Stantec Consulting, A Technical Review of Municipal Solid Waste Thermal Treatment Practices, 2011. http://www.mercuryconvention.org/Portals/11/documents/meetings/EG1/waste_to_energy_part_3.pdf. (Accessed 25 July 2022).

[573] L. Yassin, P. Lettieri, S. Simons, A. Germana, Energy recovery from thermal processing of waste: a review, Proceedings of the Institution of Civil Engineers-Engineering Sustainability, Thomas Telford Ltd, 2005, pp. 97-103.

[574] US EPA, Advance Notice of Proposed Rulemaking on Pyrolysis and Gasification Units, 2021. https://www.epa.gov/stationary-sources-air-pollution/advance-notice-proposed-rulemaking-pyrolysis-and-gasification. (Accessed 25 July 2022).

[575] J. Dong, Y. Tang, A. Nzihou, Y. Chi, E. Weiss-Hortala, M. Ni, Life cycle assessment of pyrolysis, gasification and incineration waste-to-energy technologies: Theoretical analysis and case study of commercial plants, J Science of the Total Environment 626 (2018) 744-753.

[576] N. Tanigaki, K. Manako, M. Osada, Co-gasification of municipal solid waste and material recovery in a large-scale gasification and melting system, J Waste Management 32(4) (2012) 667-675.

[577] K. Yoshikawa, Gasification and Liquefaction Alternatives to Incineration in Japan, J Renewable Energy Systems (2013) 728-743.

[578] ENERGOS, ENERGOS Gasification Technology: . https://www.energos.com/technology-solutions/. (Accessed 25 July 2022).

[579] Alter NRG, Alter NRG: A leading Provider of Clean Energy Solutions, 2010. http://energy.cleartheair.org.hk/wp-content/uploads/2013/05/NAWTEC_2010_Presentation_FINAL.pdf. (Accessed 25 July 2022).

[580] Juniper Consultancy Ltd., Independent Waste technology report, 2008. http://energy.cleartheair.org.hk/wp-content/uploads/2013/09/Westinghouse_Plasma_Gasification.pdf. (Accessed 25 July 2022).

[581] Plasco Technologies, Plasco Conversion Technologies, 2020. https://globalsyngas.org/wp-content/conference-presentations/2020/2020-w2-d1-a3-GSTCpresentation.pdf. (Accessed 25 July 2022).

[582] European Union Directive, Directive 2010/75/EU of the European Parliament and of the Council, 2010. https://eur-lex.europa.eu/legal-content/EN/TXT/?uri=celex%3A32010L0075. (Accessed 25 July 2022).

[583] European Union Directive, Commosion implementing Decision (EU) 2019/2010 of 12 November 2019 establishing the best available techniques (BAT) conclusions, under Directive 2010/75/EU of the European Parliament and of the Council, for waste incineration, 312 (2019) 55-92.

[584] US EPA, Large Municipal Waste Combustors (LMWC): New Source Performance Standards (NSPS) and Emissions Guidelines, 2007. https://www.epa.gov/stationary-sources-air-pollution/large-municipal-waste-combustors-lmwc-new-source-performance. (Accessed 25 July 2022).

[585] US EPA, Small Municipal Waste Combustors (SMWC): New Source Performance Standards (NSPS) and Emission Guidelines (EG), 2003. https://www.epa.gov/stationary-sources-air-pollution/small-municipal-waste-combustors-smwc-new-source-performance. (Accessed 25 July 2022).

[586] NSW Government, Energy from Waste With additional advice as at November 2020, 2020. https://www.chiefscientist.nsw.gov.au/__data/assets/pdf_file/0019/357400/FINAL-Report_EFW-with-additional-advice.pdf. (Accessed 25 July 2022).

[587] NSW EPA, Protection of the Environment Operations (Clean Air) Regulation 2010, 2010. https://legislation.nsw.gov.au/view/pdf/asmade/sl-2010-428. (Accessed 25 July 2022).

Appendix A: NTP Tar Cracking Reaction Mechanism

Appendix A.1 Heptane Reforming Reactions

References based on Appendix A.6

Reactions	**Code**	$A_{r,g}$	$\beta_{r,g}$	$E_{r,g}$	**Ref**
$CO_2 + H \rightarrow CO + OH$	R1	2.51×10^{15}	0	$2.69\times10^{+04}$	[a]
$C + O_2 \rightarrow CO + O$	R2	5.80×10^{13}	0	576	[a]
$C + OH \rightarrow CO + H$	R3	5.00×10^{13}	0	0	[a]
$CH + H \rightarrow C + H_2$	R4	1.10×10^{14}	0	0	[a]
$CH + H_2 \rightarrow CH_2 + H$	R5	1.11×10^{8}	1.79	1670	[a]
$CH_2 + CH \rightarrow C_2H_2 + H$	R6	4.00×10^{13}	0	0	[a]
$CH_2 + CH_2 \rightarrow C_2H_2 + H_2$	R7	3.20×10^{13}	0	0	[a]
$CH_2 + H_2 \rightarrow H + CH_3$	R8	5.00×10^{5}	2	7230	[a]
$CO + O_2 \rightarrow CO_2 + O$	R9	1.12×10^{12}	0	47700	[a]
$CO + OH \rightarrow CO_2 + H$	R10	5.76×10^{12}	-0.664	331.83	[a]
$CO + OH \rightarrow CO_2 + H$	R11	7.04×10^{4}	2.053	-355.67	[a]
$H + H + CO_2 \rightarrow H_2 + CO_2$	R12	5.50×10^{20}	-2	0	[a]
$H + H + H_2 \rightarrow H_2 + H_2$	R13	9.00×10^{0}	-0.6	0	[a]
$H + H + H_2O \rightarrow H_2 + H_2O$	R14	5.62×10^{19}	-1.25	0	[a]
$O + H_2 \rightarrow H + OH$	R15	4.59×10^{4}	2.7	6260	[a]
$OH + OH \rightarrow O + H_2O$	R16	3.97×10^{1}	1.4	-2110	[a]
$CH_2* + H \rightarrow CH + H_2$	R17	3.00×10^{13}	0	0	[a]
$CH_2* + O \rightarrow CO + H_2$	R18	1.50×10^{13}	0	0	[a]
$CH_2* + H_2 \rightarrow CH_3 + H$	R19	7.00×10^{13}	0	0	[a]
$CH_2* + O_2 \rightleftharpoons H + OH + CO$	R20	2.80×10^{13}	0	0	[a]
$CH_2* + O_2 \rightleftharpoons CO + H_2O$	R21	1.20×10^{13}	0	0	[a]
$CH_2* + H_2O \rightleftharpoons CH_2 + H_2O$	R22	3.00×10^{13}	0	0	[a]
$CH_2* + CO \rightleftharpoons CH_2 + CO$	R23	9.00×10^{12}	0	0	[a]
$CH_2* + CO_2 \rightleftharpoons CH_2 + CO_2$	R24	7.00×10^{12}	0	0	[a]
$CH_3 + CH_2* \rightleftharpoons C_2H_4 + H$	R25	1.20×10^{13}	0	-570	[a]
$C_2H_6 + CH_2* \rightleftharpoons C_2H_5 + CH_3$	R26	4.00×10^{13}	0	-550	[a]
$C_2H_4 + CH_2* \rightleftharpoons C_3H_5 + H$	R27	5.00×10^{13}	0	0	[a]
$C_2H_4 + CH_3 \rightleftharpoons C_2H_3 + CH_4$	R28	2.27×10^{5}	2	9200	[a]
$CH_4 + CH_2* \rightleftharpoons CH_3 + CH_3$	R29	1.60×10^{13}	0	-570	[a]

Reactions	Code	$A_{r,g}$	$\beta_{r,g}$	$E_{r,g}$	Ref
$CH_3 + CH_2 \rightleftharpoons C_2H_4 + H$	R30	4.00×10^{13}	0	0	[a]
$CH_3 + CH_3 \rightleftharpoons H + C_2H_5$	R31	4.99×10^{12}	0.1	10600	[a]
$CH_4 + H \rightleftharpoons CH_3 + H_2$	R32	6.60×10^{8}	1.62	10840	[a]
$CH_4 + O \rightleftharpoons CH_3 + OH$	R33	1.02×10^{9}	1.5	8600	[a]
$CH_4 + CH \rightleftharpoons C_2H_4 + H$	R34	6.00×10^{13}	0	0	[a]
$CH_4 + CH_2 \rightleftharpoons CH_3 + CH_3$	R35	2.46×10^{6}	2	8270	[a]
$C_2H_2 + O \rightarrow CH_2 + CO$	R36	4.08×10^{5}* (4.08×10^{4})	2	2000	[a]
$C_2H_2 + OH \rightarrow CH_3 + CO$	R37	4.83×10^{-1} * (4.83×10^{-4})	0* (4)	-2000	[a]
$C_2H_2 + CH_3 \rightleftharpoons C_3H_4 + H$	R38	2.56×10^{9}	1.1	13644	[a]
$C_2H_2 + CH_3 \rightleftharpoons C_3H_5$	R39	4.99×10^{22}	-4.39	18850	[a]
$C_2H_2 + OH \rightleftharpoons C_2H + H_2O$	R40	3.37×10^{7}	2	14000	[b]
$C_2H_2 + OH \rightleftharpoons HCCOH + H$	R41	5.04×10^{5}	2.3	13500	[b]
$C_2H_2 + OH \rightleftharpoons CH_2CO + H$	R42	2.18×10^{-4}	4.5	-1000	[b]
$C_2H_2 + OH \rightleftharpoons CH_2CO + H$	R43	2.00×10^{11}	0	0	[b]
$C_2H_2 + OH \rightleftharpoons CH_3 + CO$	R44	4.83×10^{-4}	4	-2000	[b]
$HCCOH + H \rightleftharpoons CH_2CO + H$	R45	1.00×10^{13}	0	0	[b]
$C_2H_2 + O \rightleftharpoons CH_2 + CO$	R46	6.12×10^{6}	2	1900	[b]
$C_2H_2 + O \rightleftharpoons HCCO + H$	R47	1.43×10^{7}	2	1900	[b]
$C_2H_2 + O \rightleftharpoons C_2H + OH$	R48	3.16×10^{15}	-0.6	15000	[b]
$C_2H_2 + CH_3 \rightleftharpoons C_2H + CH_4$	R49	1.81×10^{11}	0	17289	[b]
$C_2H_2 + O_2 \rightleftharpoons HCCO + OH$	R50	4.00×10^{7}	1.5	30100	[b]
$C_2H_2 + M \rightleftharpoons C_2H + H + M$	R51	4.20×10^{16}	0	107000	[b]
$C_2H_2 + H + M \rightleftharpoons C_2H_3 + M$	R52	3.11×10^{11}	0.58	2589	[b]
$C_2H + H_2 \rightleftharpoons C_2H_2 + H$	R53	4.09×10^{5}	2.39	864.3	[b]
$C_2H + O \rightleftharpoons CH + CO$	R54	5.00×10^{13}	0	0	[b]
$C_2H + OH \rightleftharpoons HCCO + H$	R55	2.00×10^{13}	0	0	[b]
$C_2H + O_2 \rightleftharpoons CO + CO + H$	R56	9.04×10^{12}	0	-457	[b]
$HCCO + O \rightleftharpoons H + CO + CO$	R57	8.00×10^{13}	0	0	[b]
$HCCO + O \rightleftharpoons CH + CO_2$	R58	2.95×10^{13}	0	1113	[b]
$HCCO + O_2 \rightleftharpoons HCO + CO + O$	R59	2.50×10^{8}	1	0	[b]
$HCCO + O_2 \rightleftharpoons CO_2 + HCO$	R60	2.40×10^{11}	0	-854	[b]
$HCCO + CH \rightleftharpoons C_2H_2 + CO$	R61	5.00×10^{13}	0	0	[b]
$HCCO + HCCO \rightleftharpoons C_2H_2 + CO + CO$	R62	1.00×10^{13}	0	0	[b]
$CH_2CO + O \rightleftharpoons CO_2 + CH_2$	R63	1.00×10^{12} (W_1) * $8E^{12}$ (W_2) * ($1.75E^{12}$)	0	1350	[b]
$CH_2CO + H \rightleftharpoons CH_3 + CO$	R64	7.00×10^{12}	0	3011	[b]
$CH_2CO + H \rightleftharpoons HCCO + H_2$	R65	2.00×10^{14}	0	8000	[b]
$CH_2CO + O \rightleftharpoons HCCO + OH$	R66	1.00×10^{13}	0	8000	[b]
$CH_2CO + OH \rightleftharpoons HCCO + H_2O$	R67	1.00×10^{13}	0	2000	[b]

Reactions	Code	$A_{r,g}$	$\beta_{r,g}$	$E_{r,g}$	Ref
$CH_2CO + M \rightleftharpoons CH_2 + CO + M$	R68	3.00×10^{14}	0	70980	[b]
$C_2H_3 + H \rightleftharpoons C_2H_2 + H_2$	R69	9.00×10^{13}	0	0	[a]
$C_2H_3 + O \rightleftharpoons CH_3 + CO$	R70	4.80×10^{13}	0	0	[a]
$C_2H_3 + CH_3 \rightleftharpoons C_2H_2 + CH_4$	R71	3.92×10^{11}	0	0	[a]
$C_2H_3 + CH_3 \rightleftharpoons C_3H_5 + H$	R72	1.50×10^{24}	-2.83	18618	[a]
$C_2H_3 + C_2H_3 \rightleftharpoons C_2H_2 + C_2H_4$	R73	9.60×10^{11}	0	0	[a]
$C_2H_4 + H \rightleftharpoons C_2H_3 + H_2$	R74	5.07×10^{5}	1.9	12950	[a]
$C_2H_4 + O \rightleftharpoons C_2H_3 + OH$	R75	1.51×10^{7}	1.9	3740	[a]
$C_2H_4 + CH \rightleftharpoons C_3H_4 + H$	R76	3.00×10^{13}	0	0	[a]
$C_2H_4 + CH_2 \rightleftharpoons C_3H_5 + H$	R77	2.00×10^{13}	0	6000	[a]
$C_2H_4 + CH_3 \rightleftharpoons C_3H_7$	R78	3.30×10^{11}	0	7700	[a]
$C_2H_4 + C_2H_3 \rightleftharpoons C_4H_7$	R79	7.93×10^{38}	-8.47	14220	[a]
$C_2H_5 + H \rightleftharpoons C_2H_4 + H_2$	R80	2.00×10^{12}	0	0	[a]
$C_2H_5 + C_2H_3 \rightleftharpoons C_3H_5 + CH_3$	R81	3.90×10^{32}	-5.22	19747	[a]
$C_2H_6 + H \rightleftharpoons C_2H_5 + H_2$	R82	1.15×10^{8}	1.9	7530	[a]
$C_2H_6 + O \rightleftharpoons C_2H_5 + OH$	R83	8.98×10^{7}	1.92	5690	[a]
$C_2H_6 + CH_3 \rightleftharpoons C_2H_5 + CH_4$	R84	6.14×10^{6}	1.74	10450	[a]
$C_3H_4 + O \rightleftharpoons C_2H_4 + CO$	R85	2.00×10^{7}	1.8	1000	[a]
$C_3H_4 + H \rightleftharpoons C_3H_5$	R86	4.91×10^{60}	-14.37	31644	[a]
$C_3H_5 + H \rightleftharpoons C_3H_4 + H_2$	R87	1.80×10^{13}	0	0	[a]
$C_3H_5 + CH_3 \rightleftharpoons C_3H_4 + CH_4$	R88	3.00×10^{12}	-0.32	-131	[a]
$C_3H_6 + H \rightleftharpoons C_2H_4 + CH_3$	R89	8.00×10^{21}	-2.39	11180	[a]
$C_3H_6 + H \rightleftharpoons C_3H_5 + H_2$	R90	1.73×10^{5}	2.5	2490	[a]
$C_3H_6 + O \rightleftharpoons C_3H_5 + OH$	R91	1.80×10^{11}	0.7	5880	[a]
$C_3H_6 + CH_3 \rightleftharpoons C_3H_5 + CH_4$	R92	2.20×10^{2}	3.5	5675	[a]
$C_3H_7 + H \rightleftharpoons C_2H_5 + CH_3$	R93	3.70×10^{24}	-2.92	12505	[a]
$C_3H_7 + H \rightleftharpoons C_3H_6 + H_2$	R94	1.80×10^{12}	0	0	[a]
$C_3H_7 + CH_3 \rightleftharpoons CH_4 + C_3H_6$	R95	1.10×10^{13}	0	0	[a]
$C_3H_8 + H \rightleftharpoons H_2 + C_3H_7$	R96	1.30×10^{6}	2.4	4471	[a]
$C_3H_8 + O \rightleftharpoons C_3H_7 + OH$	R97	1.90×10^{5}	2.68	3716	[a]
$C_3H_8 + CH_3 \rightleftharpoons CH_4 + C_3H_7$	R98	1.51	3.46	5480	[a]
$C_4H_6 + H \rightleftharpoons C_2H_4 + C_2H_3$	R99	1.00×10^{13}	0	4700	[a]
$C_4H_6 + H \rightleftharpoons C_3H_4 + CH_3$	R100	2.60×10^{5}	2.5	1000	[a]
$C_4H_7 \rightleftharpoons C_4H_6 + H$	R101	2.48×10^{53}	-12.3	52000	[a]
$C_4H_7 + H \rightleftharpoons CH_3 + C_3H_5$	R102	2.00×10^{21}	-2	11000	[a]
$C_4H_7 + H \rightleftharpoons C_4H_6 + H_2$	R103	1.80×10^{12}	0	0	[a]
$C_4H_7 + CH_3 \rightleftharpoons C_4H_6 + CH_4$	R104	1.10×10^{13}	0	0	[a]
$C_4H_8 + H \rightleftharpoons C_2H_4 + C_2H_5$	R105	1.60×10^{22}	-2.39	11180	[a]
$C_4H_8 + H \rightleftharpoons C_3H_6 + CH_3$	R106	3.20×10^{22}	-2.39	11180	[a]
$C_4H_8 + O \rightleftharpoons C_4H_7 + OH$	R107	1.50×10^{13}	0	5760	[a]

Reactions	Code	$A_{r,g}$	$\beta_{r,g}$	$E_{r,g}$	Ref
$C_4H_8 + O \rightleftharpoons C_4H_7 + OH$	R108	2.60×10^{13}	0	4470	[a]
$C_4H_8 + H \rightleftharpoons C_4H_7 + H_2$	R109	3.40×10^{5}	2.5	2490	[a]
$C_4H_8 + CH_3 \rightleftharpoons C_4H_7 + CH_4$	R110	4.4	3.5	5675	[a]
$C_4H_9 + H \rightleftharpoons C_2H_5 + C_2H_5$	R111	3.70×10^{24}	-2.92	12505	[a]
$C_4H_9 + H \rightleftharpoons C_4H_8 + H_2$	R112	1.80×10^{12}	0	0	[a]
$C_4H_9 + CH_3 \rightleftharpoons C_4H_8 + CH_4$	R113	1.10×10^{13}	0	0	[a]
$C_4H_9 + H \rightleftharpoons C_3H_7 + CH_3$	R114	1.90×10^{35}	-5.83	22470	[a]
$C_4H_9 + O \rightleftharpoons C_4H_8 + OH$	R115	1.80×10^{14}	0	0	[a]
$C_4H_{10} + H \rightleftharpoons C_4H_9 + H_2$	R116	2.40×10^{6}	2.4	4471	[a]
$C_4H_{10} + O \rightleftharpoons C_4H_9 + OH$	R117	4.90×10^{6}	2.4	5500	[a]
$C_4H_{10} + CH_3 \rightleftharpoons C_4H_9 + CH_4$	R118	3	3.46	5480	[a]
$C_7H_{16} \rightleftharpoons CH_3 + C_6H_{13}$	R119	3.50×10^{19}	-0.86	8.71×10+04	[a]
$C_7H_{16} \rightleftharpoons C_2H_5 + C_5H_{11}$	R120	8.30×10^{22}	-1.6	8.83×10+04	[a]
$C_7H_{16} \rightleftharpoons C_3H_7 + C_4H_9$	R121	8.30×10^{22}	-1.6	8.83×10+04	[a]
$C_7H_{16} + H \rightleftharpoons C_7H_{15} + H_2$	R122	5.61×10^{5}	2	7.70×10+03	[a]
$C_7H_{16} + CH_3 \rightleftharpoons C_7H_{15} + CH_4$	R123	1.32×10^{12}	0	1.16×10+04	[a]
$C_7H_{16} + C_2H_5 \rightleftharpoons C_7H_{15} + C_2H_6$	R124	1.00×10^{11}	0	1.34×10+04	[a]
$C_7H_{16} + C_2H_3 \rightleftharpoons C_7H_{15} + C_2H_4$	R125	1.00×10^{12}	0	1.80×10+04	[a]
$C_7H_{16} + O \rightleftharpoons C_7H_{15} + OH$	R126	1.00×10^{14}	0	7.86×10+03	[a]
$C_7H_{16} + OH \rightleftharpoons C_7H_{15} + H_2O$	R127	8.58×10^{6}	1.1	1.81×10+03	[a]
$C_7H_{15} \rightleftharpoons C_2H_4 + C_5H_{11}$	R128	2.00×10^{13}	0	2.86×10+04	[a]
$C_7H_{15} \rightleftharpoons C_3H_6 + C_4H_9$	R129	2.00×10^{13}	0	2.86×10+04	[a]
$C_7H_{15} \rightleftharpoons C_3H_7 + C_4H_8$	R130	2.00×10^{13}	0	2.86×10+04	[a]
$C_7H_{15} \rightleftharpoons CH_3 + C_6H_{12}$	R131	8.00×10^{12}	0	3.30×10+04	[a]
$CH_3 + C_6H_{12} \rightleftharpoons C_7H_{15}$	R132	2.00×10^{11}	0	7.22×10+03	[a]
$C_7H_{15} \rightleftharpoons C_2H_5 + C_5H_{10}$	R133	4.00×10^{13}	0	2.86×10+04	[a]
$C_6H_{13} \rightleftharpoons C_2H_4 + C_4H_9$	R134	2.00×10^{13}	0	2.86×10+04	[a]
$C_5H_{11} \rightleftharpoons C_2H_4 + C_3H_7$	R135	2.00×10^{13}	0	2.86×10+04	[a]
$C_6H_{12} \rightleftharpoons C_3H_7 + C_3H_5$	R136	2.50×10^{16}	0	7.10×10+04	[a]
$C_6H_{12} + H \rightleftharpoons C_6H_{11} + H_2$	R137	2.64×10^{4}	2.5	-2.56×10+03	[a]
$C_6H_{12} + CH_3 \rightleftharpoons C_6H_{11} + CH_4$	R138	5.76×10^{4}	3.5	2.18×10+03	[a]
$C_6H_{12} + O \rightleftharpoons C_6H_{11} + OH$	R139	4.80×10^{10}	0.7	1.00×10+03	[a]
$C_6H_{12} \rightleftharpoons C_3H_6 + C_3H_6$	R140	1.60×10^{13}	0	5.64×10+04	[a]
$C_5H_{10} \rightleftharpoons C_2H_5 + C_3H_5$	R141	2.50×10^{16}	0	7.10×10+04	[a]
$C_5H_{10} + H \rightleftharpoons C_5H_9 + H_2$	R142	2.64×10^{4}	2.5	-2.56×10+03	[a]
$C_5H_{10} + CH_3 \rightleftharpoons C_5H_9 + CH_4$	R143	5.76×10^{5}	3.5	2.18×10+03	[a]
$C_5H_{10} + O \rightleftharpoons C_5H_9 + OH$	R144	4.80×10^{10}	0.7	1.00×10+03	[a]
$C_5H_{10} \rightleftharpoons C_2H_4 + C_3H_6$	R145	2.40×10^{13}	0	5.64×10+04	[a]
$C_6H_{13} \rightleftharpoons CH_3 + C_5H_{10}$	R146	8.00×10^{12}	0	3.30×10+04	[a]

Reactions	Code	$A_{r,g}$	$\beta_{r,g}$	$E_{r,g}$	Ref
$CH_3 + C_5H_{10} \rightleftharpoons C_6H_{13}$	R147	2.00×10^{11}	0	7.22×10+03	[a]
$C_6H_{13} \rightleftharpoons C_2H_5 + C_4H_8$	R148	2.00×10^{13}	0	2.86×10+04	[a]
$C_5H_{11} \rightleftharpoons C_2H_5 + C_3H_6$	R149	2.00×10^{13}	0	2.86×10+04	[a]
$C_6H_{11} \rightleftharpoons C_2H_5 + C_4H_6$	R150	2.51×10^{13}	0	3.00×10+04	[a]
$C_5H_9 \rightleftharpoons CH_3 + C_4H_6$	R151	2.51×10^{13}	0	3.00×10+04	[a]

*r×10-estimated value, with original value is in bracket (), for the kinetic of $k_{f,r,e} = A_{r,g}T_g^{\beta_{r,g}}\exp\left(-\frac{E_{r,g}}{R.T_g}\right)$

Appendix A.2 Methane Reforming Reactions

References based on Appendix A.6

Reactions	Code	$A_{r,g}$	$\beta_{r,g}$	$E_{r,g}$	Ref
$CH_4 + OH \rightleftharpoons CH_3 + H_2O$	R152	4.13×10^{i3}	0	6456	[c]
$CH_4 + O_2 \rightleftharpoons CH_3 + HO_2$	R153	1.04×10^{i3}	0	56938	[c]
$CH_4 + M \rightleftharpoons CH_3 + H + M$	R154	3.00×10^{16}	0	85800	[c]
H_2 / 2.00 / H_2O / 6.00 / CO / 1.50 / CO_2 / 2.00 / CH_4 / 2.00 /					
$CH_3 + OH \rightleftharpoons CH_2 + H_2O$	R155	7.00×10^{12}	0	0	[c]
$CH_3 + O_2 \rightleftharpoons CH_2O + OH$	R156	6.38×10^{11}	0	13500	[c]
$CH_2O + HO_2 \rightleftharpoons HCO + H_2O_2$	R157	6.42×10^{12}	0	18008	[c]
$CH_2O + O_2 \rightleftharpoons HCO + HO_2$	R158	7.07×10^{16}	0	46720	[c]
$CH_2 + O_2 \rightleftharpoons HCO + OH$	R159	8.06×10^{12}	0	1500	[c]
$HCO + O_2 \rightleftharpoons CO + HO_2$	R160	3.70×10^{13}	0	3110	[c]
$HCO + M \rightleftharpoons H + CO + M$	R161	1.05×10^{14}* (9.72×10^{11})	0	13000	[c]
H_2 / 2.00 / H_2O / 6.00 / CO / 1.50 / CO_2 / 2.00 / CH_4 / 2.00 /					
$CO + OH \rightleftharpoons H + CO_2$	R162	9.72×10^{5}	0	2631	[c]
$H_2 + OH \rightleftharpoons H + H_2O$	R163	4.38×10^{13}	0	6990	[c]
$H_2 + O_2 \rightleftharpoons HO_2 + H$	R164	1.76×10^{14}	0	57816	[c]
$H_2 + O \rightleftharpoons H + OH$	R165	6.83×10^{13}	0	10384	[c]
$H_2 + M \rightleftharpoons H + H + M$	R166	3.33×10^{14}	0	102072	[c]
H_2 / 2.50 / H_2O / 12.00 / CO / 1.90 / CO_2 / 3.80 / CH_4 / 2.00 /					
$HO_2 + H \rightleftharpoons OH + OH$	R167	7.08×10^{13}	0	1500	[c]
$H + O_2 (+M) \rightleftharpoons HO_2 (+M)$	R168	1.14×10^{14}	0	0	[c]
LOW / 2.28×10^{-15} 0 0 /					
H_2 / 1.30 / CO / 1.90 / CO_2 / 3.80 / H_2O / 10.00 / CH_4 / 2.00 /					
$O_2 + H \rightleftharpoons O + OH$	R169	1.04×10^{14}	0	15600	[c]

$H + H + M \rightleftharpoons H_2 + M$	R170	1.78×10^{18}	-1	0	[c]
$O + H + M \rightleftharpoons OH + M$	R171	9.43×10^{18}	-1	0	[d]
H_2 / 2.5 / H_2O / 12.0 / CO / 1.5 / CO_2 / 2.0 / CH_4 / 2.0 / $CO_2 + M \rightleftharpoons CO + O + M$	R172	6.89×10^{9}	0	11625	[d]

*r×10-estimated value, with original value is in bracket (), for the kinetic of $k_{f,r,e} = A_{r,g}T_g^{\beta_{r,g}}\exp\left(-\frac{E_{r,g}}{R.T_g}\right)$

Appendix A.3 Heptane Electron Impact Reactions

References based on Appendix A.6

Reactions	**Code**	$A_{r,e}$	$\beta_{r,e}$	$E_{r,e}$	**Ref**
$C_2H_2 + E \rightarrow CH + CH + E$	R173	2.35×10^{-7}	0.594	13.4	[a]
$C_2H_4 + E \rightarrow CH + CH_3 + E$	R174	6.00×10^{-7}	0.738	10.4	[a]
$C_2H_4 + E \rightarrow CH_2 + CH_2 + E$	R175	6.54×10^{-7}	0.694	10.8	[a]
$C_2H_4 + E \rightarrow CH_4 + C + E$	R176	6.15×10^{-7}	0.689	9.94	[a]
$C_7H_{16} + E \rightarrow C_3H_6 + C_4H_8 + 2H + E$	R177	9.41×10^{-9}	0	21.6	[a]
$C_7H_{16} + E \rightarrow C_3H_6 + C_4H_9 + H + E$	R178	1.74×10^{-9}	0.1422	27.1	[a]
$C_7H_{16} + E \rightarrow C_3H_7 + C_4H_8 + H + E$	R179	1.51×10^{-9}	0.1485	19.5	[a]
$C_7H_{16} + E \rightarrow C_3H_7 + C_4H_9 + E$	R180	2.28×10^{-9}	0.2309	10.4	[a]
$C_7H_{16} + E \rightarrow C_5H_{10} + C_2H_4 + 2H + E$	R181	6.17×10^{-10}	0.16	27.9	[a]
$C_7H_{16} + E \rightarrow C_5H_{10} + C_2H_5 + H + E$	R182	2.22×10^{-9}	0.1211	27.1	[a]
$C_7H_{16} + E \rightarrow C_5H_{11} + C_2H_4 + H + E$	R183	9.12×10^{-9}	0	33.9	[a]
$C_7H_{16} + E \rightarrow C_5H_{11} + C_2H_5 + E$	R184	2.23×10^{-9}	0.2039	10.6	[a]
$C_7H_{16} + E \rightarrow C_6H_{13} + CH_3 + E$	R185	2.08×10^{-9}	0.2044	10.9	[a]
$C_7H_{16} + E \rightarrow C_7H_{15} + H + E$	R186	3.24×10^{-9}	0.1647	12.1	[a]
$CH_4 + E \rightarrow CH_2 + H_2 + E$	R187	6.08×10^{-8}	0.16	11.8	[a]
$CH_4 + E \rightarrow CH_3 + H + E$	R188	4.15×10^{-7}	0.181	11.6	[a]
$CO_2 + E \rightarrow CO + O + E$	R189	2.90×10^{-9}	0.3015	12.1	[a]
$H_2 + E \rightarrow H + H + E$	R190	9.53×10^{-8}	0.241	12.1	[a]

Electron impact reaction is assumed to be dependent to electron temperature, and with excitation loss equivalent to the E_r value, for the kinetic of $k_{f,r,e} = A_{r,e}T_e^{\beta_{r,e}}\exp\left(-\frac{E_{r,e}}{R.T_e}\right)$

Appendix A.4 Tar reforming kinetic reactions

Toluene, benzene, phenol, and naphthalene reforming kinetic, references based on Appendix A.6

Reactions	**Code**	$A_{r,g}$	$\beta_{r,g}$	$E_{r,g}$	**Ref**
$H+O_2 \rightleftharpoons O+OH$	R191	3.55×10^{15}	-0.4	16599	[e]
$O+H_2 \rightleftharpoons H+OH$	R192	5.08×10^{4}	2.7	6290	[e]
$H_2+OH \rightleftharpoons H_2O+H$	R193	2.16×10^{8}	1.5	3430	[e]
$O+H_2O \rightleftharpoons OH+OH$	R194	2.97×10^{6}	2	13400	[e]
$H_2+M \rightleftharpoons H+H+M$	R195	4.58×10^{19}	-1.4	104380	[e]
$H_2+AR \rightleftharpoons H+H+AR$	R196	5.84×10^{18}	-1.1	104380	[e]
$H_2+HE \rightleftharpoons H+H+HE$	R197	5.84×10^{18}	-1.1	104380	[e]
$O+O+M \rightleftharpoons O_2+M$	R198	6.16×10^{15}	-0.5	0	[e]
$O+O+AR \rightleftharpoons O_2+AR$	R199	1.89×10^{13}	0	-1788	[e]
$O+O+HE \rightleftharpoons O_2+HE$	R200	1.89×10^{13}	0	-1788	[e]
$O+H+M \rightleftharpoons OH+M$	R201	4.71×10^{18}	-1	0	[e]
$H+OH+M \rightleftharpoons H_2O+M$	R202	3.80×10^{22}	-2	0	[e]
$H+O_2(+M) \rightleftharpoons HO_2(+M)$	R203	1.48×10^{12}	0.6	0	[e]
$HO_2+H \rightleftharpoons H_2+O_2$	R204	1.66×10^{13}	0	823	[e]
$HO_2+H \rightleftharpoons OH+OH$	R205	7.08×10^{13}	0	295	[e]
$HO_2+O \rightleftharpoons O_2+OH$	R206	3.25×10^{13}	0	0	[e]
$HO_2+OH \rightleftharpoons H_2O+O_2$	R207	2.89×10^{13}	0	-497	[e]
$HO_2+HO_2 \rightleftharpoons H_2O_2+O_2$	R208	4.20×10^{14}	0	11982	[e]
$HO_2+HO_2 \rightleftharpoons H_2O_2+O_2$	R209	1.30×10^{11}	0	-1629.3	[e]
$H_2O_2(+M) \rightleftharpoons OH+OH(+M)$	R210	2.95×10^{14}	0	48430	[e]
$H_2O_2+H \rightleftharpoons H_2O+OH$	R211	2.41×10^{13}	0	0.00×10+00	[e]
$H_2O_2+H \rightleftharpoons HO_2+H_2$	R212	4.82×10^{13}	0	7950	[e]
$H_2O_2+O \rightleftharpoons OH+HO_2$	R213	9.55×10^{6}	2	3970	[e]
$H_2O_2+OH \rightleftharpoons HO_2+H_2O$	R214	1.00×10^{12}	0	0	[e]
$H_2O_2+OH \rightleftharpoons HO_2+H_2O$	R215	5.80×10^{14}	0	9557	[e]
$CO+O(+M) \rightleftharpoons CO_2(+M)$	R216	1.80×10^{10}	0	2384	[e]
$CO+O_2 \rightleftharpoons CO_2+O$	R217	2.53×10^{12}	0	47700	[e]
$CO+HO_2 \rightleftharpoons CO_2+OH$	R218	3.01×10^{13}	0	23000	[e]
$CO+OH \rightleftharpoons CO_2+H$	R219	2.23×10^{5}	1.9	-1158.7	[e]
$HCO+M \rightleftharpoons H+CO+M$	R220	4.75×10^{11}	0.7	14874	[e]
$HCO+O_2 \rightleftharpoons CO+HO_2$	R221	7.58×10^{12}	0	410	[e]
$HCO+H \rightleftharpoons CO+H_2$	R222	7.23×10^{13}	0	0	[e]
$HCO+O \rightleftharpoons CO+OH$	R223		0	0	[e]
$HCO+OH \rightleftharpoons CO+H_2O$	R224	3.02×10^{13}	0	0	[e]
$HCO+O \rightleftharpoons CO_2+H$	R225	3.02×10^{13}	0	0	[e]

Reactions	Code	$A_{r,g}$	$\beta_{r,g}$	$E_{r,g}$	Ref
HCO+HO₂⇌CO₂+OH+H	R226	3.00×10¹³	0	0	[e]
HCO+CH₃⇌CO+CH₄	R227	3.00×10¹³	0	0	[e]
HCO+HCO⇌H₂+CO+CO	R228	2.65×10¹³	0	0	[e]
HCO+HCO⇌CH₂O+CO	R229	3.00×10¹²	0	0	[e]
HCO+O₂⇌O₂CHO	R230	3.00×10¹³	0	-1100	[e]
CH₂O+O₂CHO⇌HCO+HO₂CHO	R231	1.20×10¹¹	0	11660	[e]
HO₂CHO⇌OCHO+OH	R232	1.99×10¹²	0	40150	[e]
H+CO₂+M⇌OCHO+M	R233	5.01×10¹⁴	0	29000	[e]
CH₂O+M⇌HCO+H+M	R234	7.50×10¹³	-6.3	99900	[e]
CH₂O+M⇌CO+H₂+M	R235	3.30×10³⁹	-8	97510	[e]
CH₂O+H⇌HCO+H₂	R236	3.10×10⁴⁵	1.9	2748.6	[e]
CH₂O+O⇌HCO+OH	R237	5.74×10⁷	0	3080	[e]
CH₂O+OH⇌HCO+H₂O	R238	1.81×10¹³	1.2	-447	[e]
CH₂O+O₂⇌HCO+HO₂	R239	3.43×10⁹	3	52000	[e]
CH₂O+HO₂⇌HCO+H₂O₂	R240	1.23×10⁶	2.5	10210	[e]
CH₂O+CH₃⇌HCO+CH₄	R241	4.11×10⁴	5.4	998	[e]
CH₂O+HO₂⇌OCH₂O₂H	R242	3.64×10⁻⁶	0	11900	[e]
OCH₂O₂H⇌HOCH₂O₂	R243	1.50×10¹¹	0	8600	[e]
HOCH₂O+HO2⇌HOCH₂O₂H+O2	R244	3.00×10¹¹	0	-3275	[e]
HOCH₂O+OH⇌HOCH₂O₂H	R245	3.50×10¹⁰	0	0	[e]
CH₃+O⇌CH₂O+H	R246	8.43×10¹³	0	0	[e]
CH₃+O₂⇌CH₃O+O	R247	1.99×10¹⁸	-1.6	29230	[e]
CH₃+O₂⇌CH₂O+OH	R248	3.51×10⁻¹	3.5	7380	[e]
CH₃+HO₂⇌CH₃O+OH	R249	2.41×10¹⁰	0.8	-2325	[e]
CH₃+CH₃(+M)⇌C₂H₆(+M)	R250	2.28×10¹⁵	-0.7	174.9	[e]
CH₃+H(+M)⇌CH₄(+M)	R251	1.27×10¹⁶	-0.6	383	[e]
CH₄+H⇌CH₃+H₂	R252	5.47×10⁷	2	11210	[e]
CH₄+O⇌CH₃+OH	R253	3.15×10¹²	0.5	10290	[e]
CH₄+OH⇌CH₃+H₂O	R254	5.72×10⁶	2	2639	[e]
CH₃+HO₂⇌CH₄+O₂	R255	3.16×10¹²	0	0	[e]
CH₄+HO₂⇌CH₃+H₂O₂	R256	1.81×10¹¹	0	18580	[e]
CH₃+CH₃OH⇌CH₄+CH₃O	R257	1.44×10¹	3.1	6935	[e]
CH₃O+CH₃⇌CH₂O+CH₄	R258	1.20×10¹³	0	0	[e]
CH₃O+H⇌CH₂O+H₂	R259	2.00×10¹³	0	0	[e]
CH₃+O₂(+M)⇌CH₃O₂(+M)	R260	1.01×10⁸	1.6	0	[e]
CH₃O₂+CH₂O⇌CH₃O₂H+HCO	R261	1.99×10¹²	0	11660	[e]
CH₄+CH₃O₂⇌CH₃+CH₃O₂H	R262	1.81×10¹¹	0	18480	[e]
CH₃OH+CH₃O₂⇌CH₂OH+CH₃O₂H	R263	1.81×10¹²	0	13710	[e]
CH₃O₂+CH₃⇌CH₃O+CH₃O	R264	5.08×10¹²	0	-1411	[e]
CH₃O₂+HO₂⇌CH₃O₂H+O₂	R265	2.47×10¹¹	0	-1570	[e]

Reactions	Code	$A_{r,g}$	$\beta_{r,g}$	$E_{r,g}$	Ref
$CH_3O_2+CH_3O_2 \rightleftharpoons CH_2O+CH_3OH+O_2$	R266	3.11×10^{14}	-1.6	-1051	[e]
$CH_3O_2+CH_3O_2 \rightleftharpoons O_2+CH_3O+CH_3O$	R267	1.40×10^{16}	-1.6	1860	[e]
$CH_3O_2+H \rightleftharpoons CH_3O+OH$	R268	9.60×10^{13}	0	0	[e]
$CH_3O_2+O \rightleftharpoons CH_3O+O_2$	R269	3.60×10^{13}	0	0	[e]
$CH_3O_2+OH \rightleftharpoons CH_3OH+O_2$	R270	6.00×10^{13}	0	0	[e]
$CH_3O_2H \rightleftharpoons CH_3O+OH$	R271	6.31×10^{14}	0	42300	[e]
$CH_2OH+M \rightleftharpoons CH_2O+H+M$	R272	1.00×10^{14}	0	25100	[e]
$CH_2OH+H \rightleftharpoons CH_2O+H_2$	R273	6.00×10^{12}	0	0	[e]
$CH_2OH+H \rightleftharpoons CH_3+OH$	R274	9.64×10^{13}	0	0	[e]
$CH_2OH+O \rightleftharpoons CH_2O+OH$	R275	4.20×10^{13}	0	0	[e]
$CH_2OH+OH \rightleftharpoons CH_2O+H_2O$	R276	2.40×10^{13}	0	0	[e]
$CH_2OH+O_2 \rightleftharpoons CH_2O+HO_2$	R277	2.41×10^{14}	0	5017	[e]
$CH_2OH+O_2 \rightleftharpoons CH_2O+HO_2$	R278	1.51×10^{15}	-1	0	[e]
$CH_2OH+HO_2 \rightleftharpoons CH_2O+H_2O_2$	R279	1.20×10^{13}	0	0	[e]
$CH_2OH+HCO \rightleftharpoons CH_3OH+CO$	R280	1.00×10^{13}	0	0	[e]
$CH_2OH+HCO \rightleftharpoons CH_2O+CH_2O$	R281	1.50×10^{13}	0	0	[e]
$2CH_2OH \rightleftharpoons CH_3OH+CH_2O$	R282	3.00×10^{12}	0	0	[e]
$CH_2OH+CH_3O \rightleftharpoons CH_3OH+CH_2O$	R283	2.40×10^{13}	0	0	[e]
$CH_2OH+HO_2 \rightleftharpoons HOCH_2O+OH$	R284	1.00×10^{13}	0	0	[e]
$CH_3O+M \rightleftharpoons CH_2O+H+M$	R285	8.30×10^{17}	-1.2	15500	[e]
$CH_3O+H \rightleftharpoons CH_3+OH$	R286	3.20×10^{13}	0	0	[e]
$CH_3O+O \rightleftharpoons CH_2O+OH$	R287	6.00×10^{12}	0	0	[e]
$CH_3O+OH \rightleftharpoons CH_2O+H_2O$	R288	1.80×10^{13}	0	0	[e]
$CH_3O+O_2 \rightleftharpoons CH_2O+HO_2$	R289	9.03×10^{13}	0	11980	[e]
$CH_3O+O_2 \rightleftharpoons CH_2O+HO_2$	R290	2.20×10^{10}	0	1748	[e]
$CH_3O+HO_2 \rightleftharpoons CH_2O+H_2O_2$	R291	3.00×10^{11}	0	0	[e]
$CH_3O+CO \rightleftharpoons CH_3+CO_2$	R292	1.60×10^{13}	0	11800	[e]
$CH_3O+HCO \rightleftharpoons CH_3OH+CO$	R293	9.00×10^{13}	0	0	[e]
$2CH_3O \rightleftharpoons CH_3OH+CH_2O$	R294	6.00×10^{13}	0	0	[e]
$OH+CH_3(+M) \rightleftharpoons CH_3OH(+M)$	R295	2.79×10^{18}	-1.4	1330	[e]
$H+CH_2OH(+M) \rightleftharpoons CH_3OH(+M)$	R296	1.06×10^{12}	0.5	86	[e]
$H+CH_3O(+M) \rightleftharpoons CH_3OH(+M)$	R297	2.43×10^{12}	0.5	50	[e]
$CH_3OH+H \rightleftharpoons CH_2OH+H_2$	R298	3.20×10^{13}	0	6095	[e]
$CH_3OH+H \rightleftharpoons CH_3O+H_2$	R299	8.00×10^{12}	0	6095	[e]
$CH_3OH+O \rightleftharpoons CH_2OH+OH$	R300	3.88×10^{5}	2.5	3080	[e]
$CH_3OH+OH \rightleftharpoons CH_3O+H_2O$	R301	1.00×10^{6}	2.1	496.7	[e]
$CH_3OH+OH \rightleftharpoons CH_2OH+H_2O$	R302	7.10×10^{6}	1.8	-596	[e]
$CH_3OH+O_2 \rightleftharpoons CH_2OH+HO_2$	R303	2.05×10^{13}	0	44900	[e]
$CH_3OH+HCO \rightleftharpoons CH_2OH+CH_2O$	R304	9.64×10^{3}	2.9	13110	[e]
$CH_3OH+HO_2 \rightleftharpoons CH_2OH+H_2O_2$	R305	3.98×10^{13}	0	19400	[e]

Reactions	Code	$A_{r,g}$	$\beta_{r,g}$	$E_{r,g}$	Ref
$CH_3OH+CH_3 \rightleftharpoons CH_2OH+CH_4$	R306	3.19×10^{1}	3.2	7172	[e]
$CH_3O+CH_3OH \rightleftharpoons CH_3OH+CH_2OH$	R307	3.00×10^{11}	0	4060	[e]
$CH_3+CH_3 \rightleftharpoons H+C_2H_5$	R308	4.99×10^{12}	0.1	10600	[e]
$CH_4+CH_2 \rightleftharpoons CH_3+CH_3$	R309	2.46×10^{6}	2	8270	[e]
$CH_4+CH_2(S) \rightleftharpoons CH_3+CH_3$	R310	1.60×10^{13}	0	-570	[e]
$CH_3+OH \rightleftharpoons CH_2+H_2O$	R311	5.60×10^{7}	1.6	5420	[e]
$CH_3+OH \rightleftharpoons CH_2(S)+H_2O$	R312	2.50×10^{13}	0	0	[e]
$CH_3+CH_2 \rightleftharpoons C_2H_4+H$	R313	4.00×10^{13}	0	0	[e]
$CH_3+CH_2(S) \rightleftharpoons C_2H_4+H$	R314	1.20×10^{13}	0	-570	[e]
$CH_3O+H \rightleftharpoons CH_2(S)+H_2O$	R315	1.60×10^{13}	0	0	[e]
$CH_2(S)+H_2O(+M) \rightleftharpoons CH_3OH(+M)$	R316	4.82×10^{17}	-1.2	1145	[e]
$CH_2+H(+M) \rightleftharpoons CH_3(+M)$	R317	2.50×10^{16}	-0.8	0	[e]
$CH_2+O \rightleftharpoons HCO+H$	R318	8.00×10^{13}	0	0	[e]
$CH_2+OH \rightleftharpoons CH_2O+H$	R319	2.00×10^{13}	0	0	[e]
$CH_2+H_2 \rightleftharpoons H+CH_3$	R320	5.00×10^{5}	2	7230	[e]
$CH_2+O_2 \rightleftharpoons HCO+OH$	R321	1.32×10^{13}	0	1500	[e]
$CH_2+HO_2 \rightleftharpoons CH_2O+OH$	R322	2.00×10^{13}	0	0	[e]
$CH_2+CO(+M) \rightleftharpoons CH_2CO(+M)$	R323	8.10×10^{11}	0.5	4510	[e]
$CH_2+CH_2 \rightleftharpoons C_2H_2+H_2$	R324	3.20×10^{13}	0	0	[e]
$CH_2(S)+M \rightleftharpoons CH_2+M$	R325	9.00×10^{12}	0	600	[e]
$CH_2(S)+H_2O \rightleftharpoons CH_2+H_2O$	R326	3.00×10^{13}	0	0	[e]
$CH_2(S)+CO \rightleftharpoons CH_2+CO$	R327	9.00×10^{12}	0	0	[e]
$CH_2(S)+CO_2 \rightleftharpoons CH_2+CO_2$	R328	7.00×10^{12}	0	0	[e]
$CH_2(S)+AR \rightleftharpoons CH_2+AR$	R329	9.00×10^{12}	0	600	[e]
$CH_2(S)+O \rightleftharpoons CO+H_2$	R330	1.50×10^{13}	0	0	[e]
$CH_2(S)+O \rightleftharpoons HCO+H$	R331	1.50×10^{13}	0	0	[e]
$CH_2(S)+OH \rightleftharpoons CH_2O+H$	R332	3.00×10^{13}	0	0	[e]
$CH_2(S)+H_2 \rightleftharpoons CH_3+H$	R333	7.00×10^{13}	0	0	[e]
$CH_2(S)+O_2 \rightleftharpoons H+OH+CO$	R334	2.80×10^{13}	0	0	[e]
$CH_2(S)+O_2 \rightleftharpoons CO+H_2O$	R335	1.20×10^{13}	0	0	[e]
$CH_2(S)+CO_2 \rightleftharpoons CH_2O+CO$	R336	1.40×10^{13}	0	0	[e]
$CH_2(S)+H \rightleftharpoons CH+H_2$	R337	3.00×10^{13}	0	0	[e]
$CH_2+H \rightleftharpoons CH+H_2$	R338	1.00×10^{18}	-1.6	0	[e]
$CH_2+OH \rightleftharpoons CH+H_2O$	R339	1.13×10^{7}	2	3000	[e]
$CH+O_2 \rightleftharpoons HCO+O$	R340	3.30×10^{13}	0	0	[e]
$CH+H \rightleftharpoons C+H_2$	R341	5.00×10^{13}	0	0	[e]
$CH+O \rightleftharpoons CO+H$	R342	5.70×10^{13}	0	0	[e]
$CH+OH \rightleftharpoons HCO+H$	R343	3.00×10^{13}	0	0	[e]
$CH_2+H \rightleftharpoons CH+H_2$	R344	2.70×10^{11}	0.7	25700	[e]

Reactions	Code	$A_{r,g}$	$\beta_{r,g}$	$E_{r,g}$	Ref
$CH+H_2O \rightleftharpoons H+CH_2O$	R345	1.71×10^{13}	0	-755	[e]
$CH+CO_2 \rightleftharpoons HCO+CO$	R346	1.70×10^{12}	0	685	[e]
$HOCH_2O \rightleftharpoons HCOOH+H$	R347	1.00×10^{14}	0	14900	[e]
$CH_2O+OH \rightleftharpoons HOCH_2O$	R348	4.50×10^{15}	-1.1	0	[e]
$HCOOH+M \rightleftharpoons CO+H_2O+M$	R349	2.30×10^{13}	0	50000	[e]
$HCOOH+M \rightleftharpoons CO_2+H_2+M$	R350	1.50×10^{16}	0	57000	[e]
$HCOOH \rightleftharpoons HCO+OH$	R351	4.59×10^{18}	-0.5	108300	[e]
$HCOOH+OH \rightleftharpoons H_2O+CO_2+H$	R352	2.62×10^{6}	2.1	916	[e]
$HCOOH+OH \rightleftharpoons H_2O+CO+OH$	R353	1.85×10^{7}	1.5	-962	[e]
$HCOOH+H \rightleftharpoons H_2+CO_2+H$	R354	4.24×10^{6}	2.1	4868	[e]
$HCOOH+H \rightleftharpoons H_2+CO+OH$	R355	6.03×10^{13}	-0.3	2988	[e]
$HCOOH+CH_3 \rightleftharpoons CH_4+CO+OH$	R356	3.90×10^{-7}	5.8	2200	[e]
$HCOOH+HO_2 \rightleftharpoons H_2O_2+CO+OH$	R357	1.00×10^{12}	0	11920	[e]
$HCOOH+O \rightleftharpoons CO+OH+OH$	R358	1.77×10^{18}	-1.9	2975	[e]
$C_2H_5+H(+M) \rightleftharpoons C_2H_6(+M)$	R359	5.21×10^{17}	-1	1580	[e]
$C_2H_6+H \rightleftharpoons C_2H_5+H_2$	R360	1.15×10^{8}	1.9	7530	[e]
$C_2H_6+O \rightleftharpoons C_2H_5+OH$	R361	3.55×10^{6}	2.4	5830	[e]
$C_2H_6+OH \rightleftharpoons C_2H_5+H_2O$	R362	1.48×10^{7}	1.9	950	[e]
$C_2H_6+O_2 \rightleftharpoons C_2H_5+HO_2$	R363	6.03×10^{13}	0	51870	[e]
$C_2H_6+CH_3 \rightleftharpoons C_2H_5+CH_4$	R364	1.51×10^{-7}	6	6047	[e]
$C_2H_6+HO_2 \rightleftharpoons C_2H_5+H_2O_2$	R365	3.46×10^{31}	3.6	16920	[e]
$C_2H_6+CH_3O_2 \rightleftharpoons C_2H_5+CH_3O_2H$	R366	1.94×10^{21}	3.6	17100	[e]
$C_2H_6+CH_3O \rightleftharpoons C_2H_5+CH_3OH$	R367	2.41×10^{11}	0	7090	[e]
$C_2H_6+CH \rightleftharpoons C_2H_5+CH_2$	R368	1.10×10^{14}	0	-260	[e]
$CH_2(S)+C_2H_6 \rightleftharpoons CH_3+C_2H_5$	R369	1.20×10^{14}	0	0	[e]
$H+C_2H_4(+M) \rightleftharpoons C_2H_5(+M)$	R370	8.10×10^{11}	0.5	1820	[e]
$H_2+CH_3O_2 \rightleftharpoons H+CH_3O_2H$	R371	1.50×10^{14}	0	26030	[e]
$H_2+C_2H_5O_2 \rightleftharpoons H+C_2H_5O_2H$	R372	1.50×10^{14}	0	26030	[e]
$C_2H_4+C_2H_4 \rightleftharpoons C_2H_5+C_2H_3$	R373	4.82×10^{14}	0	71530	[e]
$CH_3+C_2H_5 \rightleftharpoons CH_4+C_2H_4$	R374	1.18×10^{4}	2.5	-2921	[e]
$C_2H_5+H \rightleftharpoons C_2H_4+H_2$	R375	2.00×10^{12}	0	0	[e]
$C_2H_5+O \rightleftharpoons CH_3CHO+H$	R376	1.10×10^{14}	0	0	[e]
$C_2H_5+HO_2 \rightleftharpoons C_2H_5O+OH$	R377	1.10×10^{13}	0	0	[e]
$CH_3O_2+C_2H_5 \rightleftharpoons CH_3O+C_2H_5O$	R378	8.00×10^{12}	0	-1000	[e]
$C_2H_5O+O_2 \rightleftharpoons CH_3CHO+HO_2$	R379	4.28×10^{10}	0	1097	[e]
$CH_3+CH_2O \rightleftharpoons C_2H_5O$	R380	3.00×10^{11}	0	6336	[e]
$CH_3CHO+H \rightleftharpoons C_2H_5O$	R381	8.00×10^{12}	0	6400	[e]
$C_2H_5+O_2 \rightleftharpoons C_2H_5O_2$	R382	2.88×10^{56}	-13.8	14620	[e]
$C_2H_5O_2+CH_2O \rightleftharpoons C_2H_5O_2H+HCO$	R383	1.99×10^{12}	0	11660	[e]
$CH_4+C_2H_5O_2 \rightleftharpoons CH_3+C_2H_5O_2H$	R384	1.81×10^{11}	0	18480	[e]

Reactions	Code	$A_{r,g}$	$\beta_{r,g}$	$E_{r,g}$	Ref
$CH_3OH+C_2H_5O_2 \rightleftharpoons CH_2OH+C_2H_5O_2H$	R385	1.81×10^{12}	0	13710	[e]
$C_2H_5O_2+HO_2 \rightleftharpoons C_2H_5O_2H+O_2$	R386	1.75×10^{10}	0	-3275	[e]
$C_2H_6+C_2H_5O_2 \rightleftharpoons C_2H_5+C_2H_5O_2H$	R387	8.60×10^{0}	3.8	17200	[e]
$C_2H_5O_2H \rightleftharpoons C_2H_5O+OH$	R388	6.31×10^{14}	0	42300	[e]
$C_2H_5+O_2 \rightleftharpoons C_2H_4O_2H$	R389	1.81×10^{45}	-11.5	14600	[e]
$C_2H_5+O_2 \rightleftharpoons C_2H_4+HO_2$	R390	7.56×10^{14}	-1	4749	[e]
$C_2H_5+O_2 \rightleftharpoons C_2H_4+HO_2$	R391	4.00×10^{-1}	3.9	13620	[e]
$C_2H_5+O_2 \rightleftharpoons C_2H_4O_1\text{-}2+OH$	R392	1.63×10^{11}	-0.3	6150	[e]
$C_2H_5+O_2 \rightleftharpoons CH_3CHO+OH$	R393	8.26×10^{2}	2.4	5285	[e]
$C_2H_4O_2H \rightleftharpoons C_2H_5O_2$	R394	1.20×10^{36}	-8.1	27020	[e]
$C_2H_5O_2 \rightleftharpoons CH_3CHO+OH$	R395	2.52×10^{41}	-10.2	43710	[e]
$C_2H_5O_2 \rightleftharpoons C_2H_4+HO_2$	R396	1.82×10^{38}	-8.4	37890	[e]
$C_2H_5O_2 \rightleftharpoons C_2H_4O_1\text{-}2 + OH$	R397	4.00×10^{43}	-10.5	45580	[e]
$C_2H_4O_2H \rightleftharpoons C_2H_4O_1\text{-}2 + OH$	R398	8.85×10^{30}	-6.1	20660	[e]
$C_2H_4O_2H \rightleftharpoons C_2H_4 + HO_2$	R399	3.98×10^{34}	-7.2	23250	[e]
$C_2H_4O_2H \rightleftharpoons CH_3CHO + OH$	R400	1.19×10^{34}	-9	29210	[e]
$C_2H_4O_1\text{-}2 \rightleftharpoons CH_3 + HCO$	R401	3.63×10^{13}	0	57200	[e]
$C_2H_4O_1\text{-}2 \rightleftharpoons CH_3CHO$	R402	7.41×10^{12}	0	53800	[e]
$C_2H_4O_1\text{-}2 + OH \rightleftharpoons C_2H_3O_1\text{-}2 + H_2O$	R403	1.78×10^{13}	0	3610	[e]
$C_2H_4O_1\text{-}2 + H \rightleftharpoons C_2H_3O_1\text{-}2 + H_2$	R404	8.00×10^{13}	0	9680	[e]
$C_2H_4O_1\text{-}2 + HO_2 \rightleftharpoons C_2H_3O_1\text{-}2 + H_2O_2$	R405	1.13×10^{13}	0	30430	[e]
$C_2H_4O_1\text{-}2 + CH_3O_2 \rightleftharpoons C_2H_3O_1\text{-}2 + CH_3O_2H$	R406	1.13×10^{13}	0	30430	[e]
$C_2H_4O_1\text{-}2 + C_2H_5O_2 \rightleftharpoons C_2H_4O_1\text{-}2C_2H_5O_2H$	R407	1.13×10^{13}	0	30430	[e]
$C_2H_4O_1\text{-}2 + CH_3 \rightleftharpoons C_2H_3O_1\text{-}2 + CH_4$	R408	1.07×10^{12}	0	11830	[e]
$C_2H_4O_1\text{-}2 + CH_3O \rightleftharpoons C_2H_3O_1\text{-}2 + CH_3OH$	R409	1.20×10^{11}	0	6750	[e]
$C_2H_3O_1\text{-}2 \rightleftharpoons CH_3CO$	R410	8.50×10^{14}	0	14000	[e]
$C_2H_3O_1\text{-}2 \rightleftharpoons CH_2CHO$	R411	1.00×10^{14}	0	14000	[e]
$CH_3+HCO \rightleftharpoons CH_3CHO$	R412	1.75×10^{13}	0	0	[e]
$CH_3CHO+H \rightleftharpoons CH_3CO+H_2$	R413	1.11×10^{13}	0	3110	[e]
$CH_3CHO+O \rightleftharpoons CH_3CO+OH$	R414	5.94×10^{12}	0	1868	[e]
$CH_3CHO+OH \rightleftharpoons CH_3CO+H_2O$	R415	2.00×10^{6}	1.8	1300	[e]
$CH_3CHO+O_2 \rightleftharpoons CH_3CO+HO_2$	R416	3.01×10^{13}	0	39150	[e]
$CH_3CHO+CH_3 \rightleftharpoons CH_3CO+CH_4$	R417	1.76×10^{3}	2.8	4950	[e]
$CH_3CHO+HO_2 \rightleftharpoons CH_3CO+H_2O_2$	R418	3.01×10^{12}	0	11920	[e]
$CH_3O_2+CH_3CHO \rightleftharpoons CH_3O_2H+CH_3CO$	R419	3.01×10^{12}	0	11920	[e]
$CH_3CHO+CH_3CO_3 \rightleftharpoons CH_3CO+CH_3CO_3H$	R420	3.01×10^{12}	0	11920	[e]
$CH_3CHO+OH \rightleftharpoons CH_3+HCOOH$	R421	3.00×10^{15}	-1.1	0	[e]
$CH_3CHO+OH \rightleftharpoons CH_2CHO+H_2O$	R422	1.72×10^{5}	2.4	815	[e]
$CH_3CO(+M) \rightleftharpoons CH_3+CO(+M)$	R423	3.00×10^{12}	0	16720	[e]

Reactions	Code	$A_{r,g}$	$\beta_{r,g}$	$E_{r,g}$	Ref
$CH_3CO+H \rightleftharpoons CH_2CO+H_2$	R424	2.00×10^{13}	0	0	[e]
$CH_3CO+O \rightleftharpoons CH_2CO+OH$	R425	2.00×10^{13}	0	0	[e]
$CH_3CO+CH_3 \rightleftharpoons CH_2CO+CH_4$	R426	5.00×10^{13}	0	0	[e]
$CH_3CO+O_2 \rightleftharpoons CH_3CO_3$	R427	1.20×10^{11}	0	-1100	[e]
$CH_3CO_3+HO_2 \rightleftharpoons CH_3CO_3H+O_2$	R428	1.75×10^{10}	0	-3275	[e]
$H_2O_2+CH_3CO_3 \rightleftharpoons HO_2+CH_3CO_3H$	R429	2.41×10^{12}	0	9936	[e]
$CH_4+CH_3CO_3 \rightleftharpoons CH_3+CH_3CO_3H$	R430	1.81×10^{11}	0	18480	[e]
$CH_2O+CH_3CO_3 \rightleftharpoons HCO+CH_3CO_3H$	R431	1.99×10^{12}	0	11660	[e]
$C_2H_6+CH_3CO_3 \rightleftharpoons C_2H_5+CH_3CO_3H$	R432	1.70×10^{13}	0	20460	[e]
$CH_3CO_3H \rightleftharpoons CH_3CO_2+OH$	R433	5.01×10^{14}	0	40150	[e]
$CH_3CO_2+M \rightleftharpoons CH_3+CO_2+M$	R434	4.40×10^{15}	0	10500	[e]
$CH_2CO+H \rightleftharpoons CH_2CHO$	R435	5.00×10^{13}	0	12300	[e]
$CH_2CHO+O_2 \rightleftharpoons CH_2O+CO+OH$	R436	2.00×10^{13}	0	4200	[e]
$CH_2CO+H \rightleftharpoons CH_3+CO$	R437	1.10×10^{13}	0	3400	[e]
$CH_2CO+H \rightleftharpoons HCCO+H_2$	R438	2.00×10^{14}	0	8000	[e]
$CH_2CO+O \rightleftharpoons CH_2+CO_2$	R439	1.75×10^{12}	0	1350	[e]
$CH_2CO+O \rightleftharpoons HCCO+OH$	R440	1.00×10^{13}	0	8000	[e]
$CH_2CO+OH \rightleftharpoons HCCO+H_2O$	R441	1.00×10^{13}	0	2000	[e]
$CH_2CO+OH \rightleftharpoons CH_2OH+CO$	R442	2.00×10^{12}	0	-1010	[e]
$CH_2(S)+CH_2CO \rightleftharpoons C_2H_4+CO$	R443	1.60×10^{14}	0	0	[e]
$HCCO+OH \rightleftharpoons H_2+CO+CO$	R444	1.00×10^{14}	0	0	[e]
$H+HCCO \rightleftharpoons CH_2(S)+CO$	R445	1.10×10^{13}	0	0	[e]
$HCCO+O \rightleftharpoons H+CO+CO$	R446	8.00×10^{13}	0	0	[e]
$HCCO+O_2 \rightleftharpoons OH+CO+CO$	R447	4.20×10^{10}	0	850	[e]
$HCCO+M \rightleftharpoons CH+CO+M$	R448	6.50×10^{15}	0	58820	[e]
$CH+CH_2O \rightleftharpoons H+CH_2CO$	R449	9.46×10^{13}	0	-515	[e]
$CH+HCCO \rightleftharpoons CO+C_2H_2$	R450	5.00×10^{13}	0	0	[e]
$C_2H_3+H(+M) \rightleftharpoons C_2H_4(+M)$	R451	1.36×10^{14}	0.2	660	[e]
$C_2H_4(+M) \rightleftharpoons C_2H_2+H_2(+M)$	R452	8.00×10^{12}	0.4	88770	[e]
$C_2H_4+H \rightleftharpoons C_2H_3+H_2$	R453	5.07×10^{7}	1.9	12950	[e]
$C_2H_4+O \rightleftharpoons CH_3+HCO$	R454	8.56×10^{6}	1.9	183	[e]
$C_2H_4+O \rightleftharpoons CH_2CHO+H$	R455	4.99×10^{6}	1.9	183	[e]
$C_2H_4+OH \rightleftharpoons C_2H_3+H_2O$	R456	1.80×10^{6}	2	2500	[e]
$C_2H_4+CH_3 \rightleftharpoons C_2H_3+CH_4$	R457	6.62×10^{0}	3.7	9500	[e]
$C_2H_4+O_2 \rightleftharpoons C_2H_3+HO_2$	R458	4.00×10^{13}	0	58200	[e]
$C_2H_4+CH_3O \rightleftharpoons C_2H_3+CH_3OH$	R459	1.20×10^{11}	0	6750	[e]
$C_2H_4+CH_3O_2 \rightleftharpoons C_2H_3+CH_3O_2H$	R460	2.23×10^{12}	0	17190	[e]
$C_2H_4+C_2H_5O_2 \rightleftharpoons C_2H_3+C_2H_5O_2H$	R461	2.23×10^{12}	0	17190	[e]
$C_2H_4+CH_3CO_3 \rightleftharpoons C_2H_3+CH_3CO_3H$	R462	1.13×10^{13}	0	30430	[e]
$C_2H_4+CH_3O_2 \rightleftharpoons C_2H_4O1\text{-}2+CH_3O$	R463	2.82×10^{12}	0	17110	[e]

Reactions	Code	$A_{r,g}$	$\beta_{r,g}$	$E_{r,g}$	Ref
$C_2H_4+C_2H_5O_2 \rightleftharpoons C_2H_4O1\text{-}2+C_2H_5O$	R464	2.82×10^{12}	0	17110	[e]
$C_2H_4+HO_2 \rightleftharpoons C_2H_4O1\text{-}2+OH$	R465	2.23×10^{12}	0	17190	[e]
$CH+CH_4 \rightleftharpoons C_2H_4+H$	R466	6.00×10^{13}	0	0	[e]
$C_2H_2+H(+M) \rightleftharpoons C_2H_3(+M)$	R467	5.60×10^{12}	0	2400	[e]
$C_2H_3+O_2 \rightleftharpoons HCO+CH_2O$	R468	4.58×10^{16}	-1.4	1015	[e]
$C_2H_3+O_2 \rightleftharpoons HO_2+C_2H_2$	R469	1.34×10^{6}	1.6	-384	[e]
$C_2H_3+O_2 \rightleftharpoons O+CH_2CHO$	R470	1.00×10^{11}	0.3	11	[e]
$CH_3+C_2H_3 \rightleftharpoons CH_4+C_2H_2$	R471	3.92×10^{11}	0	0	[e]
$C_2H_3+H \rightleftharpoons C_2H_2+H_2$	R472	3.00×10^{13}	0	0	[e]
$C_2H_3+OH \rightleftharpoons C_2H_2+H_2O$	R473	5.00×10^{12}	0	0	[e]
$C_2H+H(+M) \rightleftharpoons C_2H_2(+M)$	R474	1.00×10^{17}	0	0	[e]
$C_2H_2+O_2 \rightleftharpoons HCCO+OH$	R475	2.00×10^{8}	1.5	30100	[e]
$O+C_2H_2 \rightleftharpoons C_2H+OH$	R476	4.60×10^{19}	-1.4	28950	[e]
$C_2H_2+O \rightleftharpoons CH_2+CO$	R477	6.94×10^{6}	2	1900	[e]
$C_2H_2+O \rightleftharpoons HCCO+H$	R478	1.35×10^{7}	2	1900	[e]
$C_2H_2+OH \rightleftharpoons C_2H+H_2O$	R479	3.37×10^{7}	2	14000	[e]
$C_2H_2+OH \rightleftharpoons CH_2CO+H$	R480	3.24×10^{13}	0	12000	[e]
$C_2H_2+OH \rightleftharpoons CH_3+CO$	R481	4.83×10^{-4}	4	-2000	[e]
$OH+C_2H_2 \rightleftharpoons H+HCCOH$	R482	5.04×10^{5}	2.3	13500	[e]
$H+HCCOH \rightleftharpoons H+CH_2CO$	R483	1.00×10^{13}	0	0	[e]
$C_2H_5OH(+M) \rightleftharpoons CH_2OH+CH_3(+M)$	R484	5.71×10^{23}	-1.7	94400	[e]
$C_2H_5OH(+M) \rightleftharpoons C_2H_5+OH(+M)$	R485	2.40×10^{23}	-1.6	99540	[e]
$C_2H_5OH(+M) \rightleftharpoons C_2H_4+H_2O(+M)$	R486	2.79×10^{13}	0.1	66140	[e]
$C_2H_5OH(+M) \rightleftharpoons CH_3CHO+H_2(+M)$	R487	7.24×10^{11}	0.1	91010	[e]
$C_2H_5OH+O_2 \rightleftharpoons P(C_2H_4OH)+HO_2$	R488	2.00×10^{13}	0	52800	[e]
$C_2H_5OH+O_2 \rightleftharpoons S(C_2H_4OH)+HO_2$	R489	1.50×10^{13}	0	50150	[e]
$C_2H_5OH+OH \rightleftharpoons P(C_2H_4OH)+H_2O$	R490	1.74×10^{11}	0.3	600	[e]
$C_2H_5OH+OH \rightleftharpoons S(C_2H_4OH)+H_2O$	R491	4.64×10^{11}	0.1	0	[e]
$C_2H_5OH+OH \rightleftharpoons C_2H_5O+H_2O$	R492	7.46×10^{11}	0.3	1634	[e]
$C_2H_5OH+H \rightleftharpoons P(C_2H_4OH)+H_2$	R493	1.23×10^{7}	1.8	5098	[e]
$C_2H_5OH+H \rightleftharpoons S(C_2H_4OH)+H_2$	R494	2.58×10^{7}	1.6	2827	[e]
$C_2H_5OH+H \rightleftharpoons C_2H_5O+H_2$	R495	1.50×10^{7}	1.6	3038	[e]
$C_2H_5OH+HO_2 \rightleftharpoons P(C_2H_4OH)+H_2O_2$	R496	1.23×10^{4}	2.5	15750	[e]
$C_2H_5OH+HO_2 \rightleftharpoons S(C_2H_4OH)+H_2O_2$	R497	8.20×10^{3}	2.5	10750	[e]
$C_2H_5OH+HO_2 \rightleftharpoons C_2H_5O+H_2O_2$	R498	2.50×10^{12}	0	24000	[e]
$C_2H_5OH+CH_3O_2 \rightleftharpoons P(C_2H_4OH)+CH_3O_2H$	R499	1.23×10^{4}	2.5	15750	[e]
$C_2H_5OH+CH_3O_2 \rightleftharpoons S(C_2H_4OH)+CH_3O_2H$	R500	8.20×10^{3}	2.5	10750	[e]
$C_2H_5OH+CH_3O_2 \rightleftharpoons C_2H_5O+CH_3O_2H$	R501	2.50×10^{12}	0	24000	[e]
$C_2H_5OH+O \rightleftharpoons P(C_2H_4OH)+OH$	R502	9.41×10^{7}	1.7	5459	[e]
$C_2H_5OH+O \rightleftharpoons S(C_2H_4OH)+OH$	R503	1.88×10^{7}	1.9	1824	[e]

Reactions	Code	$A_{r,g}$	$\beta_{r,g}$	$E_{r,g}$	Ref
$C_2H_5OH+O \rightleftharpoons C_2H_5O+OH$	R504	1.58×10^{7}	2	4448	[e]
$C_2H_5OH+CH_3 \rightleftharpoons P(C_2H_4OH)+CH_4$	R505	1.33×10^{2}	3.2	9362	[e]
$C_2H_5OH+CH_3 \rightleftharpoons S(C_2H_4OH)+CH_4$	R506	4.44×10^{2}	2.9	7690	[e]
$C_2H_5OH+CH_3 \rightleftharpoons C_2H_5O+CH_4$	R507	1.34×10^{2}	2.9	7452	[e]
$C_2H_5OH+C_2H_5 \rightleftharpoons P(C_2H_4OH)+C_2H_6$	R508	5.00×10^{10}	0	13400	[e]
$C_2H_5OH+C_2H_5 \rightleftharpoons S(C_2H_4OH)+C_2H_6$	R509	5.00×10^{10}	0	10400	[e]
$C_2H_4+OH \rightleftharpoons P(C_2H_4OH)$	R510	4.17×10^{20}	-2.8	1240	[e]
$S(C_2H_4OH)+M \rightleftharpoons CH_3CHO+H+M$	R511	1.00×10^{14}	0	25000	[e]
$O_2C_2H_4OH \rightleftharpoons P(C_2H_4OH)+O_2$	R512	3.90×10^{16}	-1	30000	[e]
$O_2C_2H_4OH \rightleftharpoons OH+CH_2O+CH_2O$	R513	3.12×10^{9}	0	18900	[e]
$S(C_2H_4OH)+O_2 \rightleftharpoons CH_3CHO+HO_2$	R514	3.81×10^{6}	2	1641	[e]
$CH_3COCH_3(+M) \rightleftharpoons CH_3CO+CH_3(+M)$	R515	7.11×10^{21}	-1.6	84680	[e]
$CH_3COCH_3+OH \rightleftharpoons CH_3COCH_2+H_2O$	R516	1.25×10^{5}	2.5	445	[e]
$CH_3COCH_3+H \rightleftharpoons CH_3COCH_2+H_2$	R517	9.80×10^{5}	2.4	5160	[e]
$CH_3COCH_3+O \rightleftharpoons CH_3COCH_2+OH$	R518	5.13×10^{11}	0.2	4890	[e]
$CH_3COCH_3+CH_3 \rightleftharpoons CH_3COCH_2+CH_4$	R519	3.96×10^{11}	0	9784	[e]
$CH_3COCH_3+CH_3O \rightleftharpoons CH_3COCH_2+CH_3OH$	R520	4.34×10^{11}	0	6460	[e]
$CH_3COCH_3+O_2 \rightleftharpoons CH_3COCH_2+HO_2$	R521	6.03×10^{13}	0	48500	[e]
$CH_3COCH_3 + HO_2 \rightleftharpoons CH_3COCH_2 + H_2O_2$	R522	1.70×10^{13}	0	20460	[e]
$CH_3COCH_3 + CH_3O_2 \rightleftharpoons CH_3COCH_2 + CH_3O_2H$	R523	1.70×10^{13}	0	20460	[e]
$CH_3COCH_2 \rightleftharpoons CH_2CO + CH_3$	R524	1.00×10^{14}	0	31000	[e]
$CH_3COCH_2 + O_2 \rightleftharpoons CH_3COCH_2O_2$	R525	1.20×10^{11}	0	-1100	[e]
$CH_3COCH_3 + CH_3COCH_2O_2 \rightleftharpoons CH_3COCH_2 + CH_3COCH_2O_2H$	R526	1.00×10^{11}	0	5000	[e]
$CH_2O + CH_3COCH_2O_2 \rightleftharpoons HCO + CH_3COCH_2O_2H$	R527	1.29×10^{11}	0	9000	[e]
$HO_2 + CH_3COCH_2O_2 \rightleftharpoons CH_3COCH_2O_2H + O_2$	R528	1.00×10^{12}	0	0	[e]
$CH_3COCH_2O_2H \rightleftharpoons CH_3COCH_2O + OH$	R529	1.00×10^{16}	0	43000	[e]
$CH_3CO + CH_2O \rightleftharpoons CH_3COCH_2O$	R530	1.00×10^{11}	0	11900	[e]
$C_2H_3 + HCO \rightleftharpoons C_2H_3CHO$	R531	1.81×10^{13}	0	0	[e]
$C_2H_3CHO + H \rightleftharpoons C_2H_3CO + H_2$	R532	1.34×10^{13}	0	3300	[e]
$C_2H_3CHO + O \rightleftharpoons C_2H_3CO + OH$	R533	5.94×10^{12}	0	1868	[e]
$C_2H_3CHO + H \rightleftharpoons C_2H_4 + HCO$	R534	2.00×10^{13}	0	3500	[e]
$C_2H_3CHO + O \rightleftharpoons CH_2CO + HCO + H$	R535	5.00×10^{7}	1.8	76	[e]
$C_2H_3CHO + OH \rightleftharpoons C_2H_3CO + H_2O$	R536	9.24×10^{6}	1.5	-962	[e]
$C_2H_3CHO + O_2 \rightleftharpoons C_2H_3CO + HO_2$	R537	1.00×10^{13}	0	40700	[e]
$C_2H_3CHO + HO_2 \rightleftharpoons C_2H_3CO + H_2O_2$	R538	3.01×10^{12}	0	11920	[e]
$C_2H_3CHO + CH_3 \rightleftharpoons C_2H_3CO + CH_4$	R539	2.61×10^{6}	1.8	5911	[e]
$C_2H_3CHO + C_2H_3 \rightleftharpoons C_2H_3CO + C_2H_4$	R540	1.74×10^{12}	0	8440	[e]
$C_2H_3CHO + CH_3O \rightleftharpoons C_2H_3CO + CH_3OH$	R541	1.00×10^{12}	0	3300	[e]
$C_2H_3CHO + CH_3O_2 \rightleftharpoons C_2H_3CO + CH_3O_2H$	R542	3.01×10^{12}	0	11920	[e]

Reactions	Code	$A_{r,g}$	$\beta_{r,g}$	$E_{r,g}$	Ref
$C_2H_3 + CO \rightleftharpoons C_2H_3CO$	R543	1.51×10^{11}	0	4810	[e]
$C_2H_3CO + O_2 \rightleftharpoons CH_2CHO + CO_2$	R544	5.40×10^{20}	-2.7	7000	[e]
$C_2H_3CO + O \rightleftharpoons C_2H_3 + CO_2$	R545	1.00×10^{14}	0	0	[e]
$C_2H_5 + HCO \rightleftharpoons C_2H_5CHO$	R546	1.81×10^{13}	0	0	[e]
$C_2H_5CHO + H \rightleftharpoons C_2H_5CO + H_2$	R547	4.00×10^{13}	0	4200	[e]
$C_2H_5CHO + O \rightleftharpoons C_2H_5CO + OH$	R548	5.00×10^{12}	0	1790	[e]
$C_2H_5CHO + OH \rightleftharpoons C_2H_5CO + H_2O$	R549	2.69×10^{10}	0.8	-340	[e]
$C_2H_5CHO + CH_3 \rightleftharpoons C_2H_5CO + CH_4$	R550	2.61×10^{6}	1.8	5911	[e]
$C_2H_5CHO + HO_2 \rightleftharpoons C_2H_5CO + H_2O_2$	R551	2.80×10^{12}	0	13600	[e]
$C_2H_5CHO + CH_3O \rightleftharpoons C_2H_5CO + CH_3OH$	R552	1.00×10^{12}	0	3300	[e]
$C_2H_5CHO + CH_3O_2 \rightleftharpoons C_2H_5CO + CH_3O_2H$	R553	3.01×10^{12}	0	11920	[e]
$C_2H_5CHO + C_2H_5 \rightleftharpoons C_2H_5CO + C_2H_6$	R554	1.00×10^{12}	0	8000	[e]
$C_2H_5CHO + C_2H_5O \rightleftharpoons C_2H_5CO + C_2H_5OH$	R555	6.03×10^{11}	0	3300	[e]
$C_2H_5CHO + C_2H_5O_2 \rightleftharpoons C_2H_5CO + C_2H_5O_2H$	R556	3.01×10^{12}	0	11920	[e]
$C_2H_5CHO + O_2 \rightleftharpoons C_2H_5CO + HO_2$	R557	1.00×10^{13}	0	40700	[e]
$C_2H_5CHO + CH_3CO_3 \rightleftharpoons C_2H_5CO + CH_3CO_3H$	R558	3.01×10^{12}	0	11920	[e]
$C_2H_5CHO + C_2H_3 \rightleftharpoons C_2H_5CO + C_2H_4$	R559	1.70×10^{12}	0	8440	[e]
$C_2H_5 + CO \rightleftharpoons C_2H_5CO$	R560	1.51×10^{11}	0	4810	[e]
$CH_3OCH_3(+M) \rightleftharpoons CH_3 + CH_3O(+M)$	R561	4.85×10^{21}	-1.6	83130	[e]
$CH_3OCH_3 + OH \rightleftharpoons CH_3OCH_2 + H_2O$	R562	9.35×10^{5}	2.3	-781	[e]
$CH_3OCH_3 + H \rightleftharpoons CH_3OCH_2 + H_2$	R563	3.61×10^{4}	2.9	2996	[e]
$CH_3OCH_3 + O \rightleftharpoons CH_3OCH_2 + OH$	R564	7.75×10^{8}	1.4	2250	[e]
$CH_3OCH_3 + HO_2 \rightleftharpoons CH_3OCH_2 + H_2O_2$	R565	1.34×10^{13}	0	17690	[e]
$CH_3OCH_3 + CH_3O_2 \rightleftharpoons CH_3OCH_2 + CH_3O_2H$	R566	1.34×10^{13}	0	17690	[e]
$CH_3OCH_3 + CH_3 \rightleftharpoons CH_3OCH_2 + CH_4$	R567	1.44×10^{-6}	5.7	5699	[e]
$CH_3OCH_3 + O_2 \rightleftharpoons CH_3OCH_2 + HO_2$	R568	4.10×10^{13}	0	44910	[e]
$CH_3OCH_3 + CH_3O \rightleftharpoons CH_3OCH_2 + CH_3OH$	R569	6.02×10^{11}	0	4074	[e]
$CH_3OCH_3 + CH_3OCH_2O_2 \rightleftharpoons CH_3OCH_2 + CH_3OCH_2O_2H$	R570	5.00×10^{12}	0	17690	[e]
$CH_3OCH_3 + O_2CHO \rightleftharpoons CH_3OCH_2 + HO_2CHO$	R571	4.42×10^{4}	2.6	13910	[e]
$CH_3OCH_3 + OCHO \rightleftharpoons CH_3OCH_2 + HCOOH$	R572	1.00×10^{13}	0	17690	[e]
$CH_3OCH_2 \rightleftharpoons CH_2O + CH_3$	R573	1.60×10^{13}	0	25500	[e]
$CH_3OCH_2 + CH_3O \rightleftharpoons CH_3OCH_3 + CH_2O$	R574	2.41×10^{13}	0	0	[e]
$CH_3OCH_2 + CH_2O \rightleftharpoons CH_3OCH_3 + HCO$	R575	5.49×10^{3}	2.8	5862	[e]
$CH_3OCH_2 + CH_3CHO \rightleftharpoons CH_3OCH_3 + CH_3CO$	R576	1.26×10^{12}	0	8499	[e]
$CH_3OCH_2 + O_2 \rightleftharpoons CH_3OCH_2O_2$	R577	2.00×10^{12}	0	0	[e]
$CH_3OCH_2O_2 + CH_2O \rightleftharpoons CH_3OCH_2O_2H + HCO$	R578	1.00×10^{12}	0	11660	[e]
$CH_3OCH_2O_2 + CH_3CHO \rightleftharpoons CH_3OCH_2O_2H + CH_3CO$	R579	2.80×10^{12}	0	13600	[e]
$CH_3OCH_2O_2 + CH_3OCH_2O_2 \rightleftharpoons O_2 + CH_3OCH_2O + CH_3OCH_2O$	R580	2.21×10^{23}	-4.5	0	[e]

Reactions	Code	$A_{r,g}$	$\beta_{r,g}$	$E_{r,g}$	Ref
$CH_3OCH_2O + OH \rightleftharpoons CH_3OCH_2O_2H$	R581	2.00×10^{13}	0	0	[e]
$CH_3O + CH_2O \rightleftharpoons CH_3OCH_2O$	R582	1.00×10^{11}	0	11900	[e]
$CH_3OCH_2O + O_2 \rightleftharpoons CH_3OCHO + HO_2$	R583	5.00×10^{10}	0	500	[e]
$CH_3OCHO + H \rightleftharpoons CH_3OCH_2O$	R584	1.00×10^{13}	0	7838	[e]
$CH_3OCH_2O_2 \rightleftharpoons CH_2OCH_2O_2H$	R585	6.00×10^{10}	0	21580	[e]
$CH_2OCH_2O_2H \rightleftharpoons OH + CH_2O + CH_2O$	R586	1.50×10^{13}	0	20760	[e]
$CH_2OCH_2O_2H + O_2 \rightleftharpoons O_2CH_2OCH_2O_2H$	R587	7.00×10^{11}	0	0	[e]
$O_2CH_2OCH_2O_2H \rightleftharpoons HO_2CH_2OCHO + OH$	R588	4.00×10^{10}	0	18580	[e]
$HO_2CH_2OCHO \rightleftharpoons OCH_2OCHO + OH$	R589	2.00×10^{16}	0	40500	[e]
$CH_2O + OCHO \rightleftharpoons OCH_2OCHO$	R590	1.25×10^{11}	0	11900	[e]
$OCH_2OCHO \rightleftharpoons HOCH_2OCO$	R591	1.00×10^{11}	0	14000	[e]
$HOCH_2O + CO \rightleftharpoons HOCH_2OCO$	R592	1.50×10^{11}	0	4800	[e]
$CH_2OH + CO_2 \rightleftharpoons HOCH_2OCO$	R593	1.50×10^{11}	0	35720	[e]
$CH_2OCHO + H \rightleftharpoons CH_3OCHO$	R594	1.00×10^{14}	0	0	[e]
$CH_3OCO + H \rightleftharpoons CH_3OCHO$	R595	1.00×10^{14}	0	0	[e]
$CH_3OCHO(+M) \rightleftharpoons CH_3OH + CO(+M)$	R596	1.00×10^{14}	0	62500	[e]
$CH_3O + HCO \rightleftharpoons CH_3OCHO$	R597	3.00×10^{13}	0	0	[e]
$CH_3 + OCHO \rightleftharpoons CH_3OCHO$	R598	1.00×10^{13}	0	0	[e]
$CH_3OCHO + O_2 \rightleftharpoons CH_3OCO + HO_2$	R599	1.00×10^{13}	0	49700	[e]
$CH_3OCHO + O_2 \rightleftharpoons CH_2OCHO + HO_2$	R600	2.05×10^{13}	0	52000	[e]
$CH_3OCHO + OH \rightleftharpoons CH_3OCO + H_2O$	R601	1.58×10^{7}	1.8	934	[e]
$CH_3OCHO + OH \rightleftharpoons CH_2OCHO + H_2O$	R602	5.27×10^{9}	1	1586	[e]
$CH_3OCHO + HO_2 \rightleftharpoons CH_3OCO + H_2O_2$	R603	4.82×10^{3}	2.6	13910	[e]
$CH_3OCHO + HO_2 \rightleftharpoons CH_2OCHO + H_2O_2$	R604	2.38×10^{4}	2.5	16490	[e]
$CH_3OCHO + O \rightleftharpoons CH_3OCO + OH$	R605	2.76×10^{5}	2.5	2830	[e]
$CH_3OCHO + O \rightleftharpoons CH_2OCHO + OH$	R606	9.80×10^{5}	2.4	4750	[e]
$CH_3OCHO + H \rightleftharpoons CH_3OCO + H_2$	R607	6.50×10^{5}	2.4	4471	[e]
$CH_3OCHO + H \rightleftharpoons CH_2OCHO + H_2$	R608	6.65×10^{5}	2.5	6756	[e]
$CH_3OCHO + CH_3 \rightleftharpoons CH_3OCO + CH_4$	R609	7.55×10^{-1}	3.5	5481	[e]
$CH_3OCHO + CH_3 \rightleftharpoons CH_2OCHO + CH_4$	R610	4.52×10^{-1}	3.6	7154	[e]
$CH_3OCHO + CH_3O \rightleftharpoons CH_3OCO + CH_3OH$	R611	5.48×10^{11}	0	5000	[e]
$CH_3OCHO + CH_3O \rightleftharpoons CH_2OCHO + CH_3OH$	R612	2.17×10^{11}	0	6458	[e]
$CH_3OCHO + CH_3O_2 \rightleftharpoons CH_3OCO + CH_3O_2H$	R613	4.82×10^{3}	2.6	13910	[e]
$CH_3OCHO + CH_3O_2 \rightleftharpoons CH_2OCHO + CH_3O_2H$	R614	2.38×10^{4}	2.5	16490	[e]
$CH_3OCHO + HCO \rightleftharpoons CH_3OCO + CH_2O$	R615	5.40×10^{6}	1.9	17010	[e]
$CH_3OCHO + HCO \rightleftharpoons CH_2OCHO + CH_2O$	R616	1.02×10^{5}	2.5	18430	[e]
$CH_3OCO \rightleftharpoons CH_2OCHO$	R617	1.63×10^{12}	-0.2	40670	[e]
$CH_3 + CO_2 \rightleftharpoons CH_3OCO$	R618	4.76×10^{7}	1.5	34700	[e]

Reactions	Code	$A_{r,g}$	$\beta_{r,g}$	$E_{r,g}$	Ref
$CH_3O + CO \rightleftharpoons CH_3OCO$	R619	1.55×10^{6}	2	5730	[e]
$CH_2O + HCO \rightleftharpoons CH_2OCHO$	R620	1.50×10^{11}	0	11900	[e]
$C_3H_8(+M) \rightleftharpoons CH_3 + C_2H_5(+M)$	R621	1.29×10^{37}	-5.8	97380	[e]
$NC_3H_7 + H \rightleftharpoons C_3H_8$	R622	1.00×10^{14}	0	0	[e]
$IC_3H_7 + H \rightleftharpoons C_3H_8$	R623	1.00×10^{14}	0	0	[e]
$C_3H_8 + O_2 \rightleftharpoons IC_3H_7 + HO_2$	R624	2.00×10^{13}	0	49640	[e]
$C_3H_8 + O_2 \rightleftharpoons NC_3H_7 + HO_2$	R625	6.00×10^{13}	0	52290	[e]
$H + C_3H_8 \rightleftharpoons H_2 + IC_3H_7$	R626	1.30×10^{6}	2.4	4471	[e]
$H + C_3H_8 \rightleftharpoons H_2 + NC_3H_7$	R627	1.33×10^{6}	2.5	6756	[e]
$C_3H_8 + O \rightleftharpoons IC_3H_7 + OH$	R628	5.49×10^{5}	2.5	3140	[e]
$C_3H_8 + O \rightleftharpoons NC_3H_7 + OH$	R629	3.71×10^{6}	2.4	5505	[e]
$C_3H_8 + OH \rightleftharpoons NC_3H_7 + H_2O$	R630	1.05×10^{10}	1	1586	[e]
$C_3H_8 + OH \rightleftharpoons IC_3H_7 + H_2O$	R631	4.67×10^{7}	1.6	-35	[e]
$C_3H_8 + HO_2 \rightleftharpoons IC_3H_7 + H_2O_2$	R632	5.88×10^{4}	2.5	14860	[e]
$C_3H_8 + HO_2 \rightleftharpoons NC_3H_7 + H_2O_2$	R633	8.10×10^{4}	2.5	16690	[e]
$CH_3 + C_3H_8 \rightleftharpoons CH_4 + IC_3H_7$	R634	6.40×10^{4}	2.2	7520	[e]
$CH_3 + C_3H_8 \rightleftharpoons CH_4 + NC_3H_7$	R635	9.04×10^{-1}	3.6	7154	[e]
$IC_3H_7 + C_3H_8 \rightleftharpoons NC_3H_7 + C_3H_8$	R636	3.00×10^{10}	0	12900	[e]
$C_2H_3 + C_3H_8 \rightleftharpoons C_2H_4 + IC_3H_7$	R637	1.00×10^{11}	0	10400	[e]
$C_2H_3 + C_3H_8 \rightleftharpoons C_2H_4 + NC_3H_7$	R638	1.00×10^{11}	0	10400	[e]
$C_2H_5 + C_3H_8 \rightleftharpoons C_2H_6 + IC_3H_7$	R639	1.00×10^{11}	0	10400	[e]
$C_2H_5 + C_3H_8 \rightleftharpoons C_2H_6 + NC_3H_7$	R640	1.00×10^{11}	0	10400	[e]
$C_3H_8 + C_3H_5\text{-}A \rightleftharpoons NC_3H_7 + C_3H_6$	R641	7.94×10^{11}	0	20500	[e]
$C_3H_8 + C_3H_5\text{-}A \rightleftharpoons IC_3H_7 + C_3H_6$	R642	7.94×10^{11}	0	16200	[e]
$C_3H_8 + CH_3O \rightleftharpoons NC_3H_7 + CH_3OH$	R643	3.00×10^{11}	0	7000	[e]
$C_3H_8 + CH_3O \rightleftharpoons IC_3H_7 + CH_3OH$	R644	3.00×10^{11}	0	7000	[e]
$CH_3O_2 + C_3H_8 \rightleftharpoons CH_3O_2H + NC_3H_7$	R645	8.10×10^{4}	2.5	16690	[e]
$CH_3O_2 + C_3H_8 \rightleftharpoons CH_3O_2H + IC_3H_7$	R646	5.88×10^{4}	2.5	14860	[e]
$C_2H_5O_2 + C_3H_8 \rightleftharpoons C_2H_5O_2H + NC_3H_7$	R647	8.10×10^{4}	2.5	16690	[e]
$C_2H_5O_2 + C_3H_8 \rightleftharpoons C_2H_5O_2H + IC_3H_7$	R648	5.88×10^{4}	2.5	14860	[e]
$NC_3H_7O_2 + C_3H_8 \rightleftharpoons NC_3H_7O_2H + NC_3H_7$	R649	1.70×10^{13}	0	20460	[e]
$NC_3H_7O_2 + C_3H_8 \rightleftharpoons NC_3H_7O_2H + IC_3H_7$	R650	2.00×10^{12}	0	17000	[e]
$IC_3H_7O_2 + C_3H_8 \rightleftharpoons IC_3H_7O_2H + NC_3H_7$	R651	1.70×10^{13}	0	20460	[e]
$IC_3H_7O_2 + C_3H_8 \rightleftharpoons IC_3H_7O_2H + IC_3H_7$	R652	2.00×10^{12}	0	17000	[e]
$C_3H_8 + CH_3CO_3 \rightleftharpoons IC_3H_7 + CH_3CO_3H$	R653	2.00×10^{12}	0	17000	[e]
$C_3H_8 + CH_3CO_3 \rightleftharpoons NC_3H_7 + CH_3CO_3H$	R654	1.70×10^{13}	0	20460	[e]
$C_3H_8 + O_2CHO \rightleftharpoons NC_3H_7 + HO_2CHO$	R655	5.52×10^{4}	2.5	16480	[e]
$C_3H_8 + O_2CHO \rightleftharpoons IC_3H_7 + HO_2CHO$	R656	1.48×10^{4}	2.6	13910	[e]

Reactions	Code	$A_{r,g}$	$\beta_{r,g}$	$E_{r,g}$	Ref
$H + C_3H_6 \rightleftharpoons IC_3H_7$	R657	2.64×10^{13}	0	2160	[e]
$IC_3H_7 + H \rightleftharpoons C_2H_5 + CH_3$	R658	2.00×10^{13}	0	0	[e]
$IC_3H_7 + O_2 \rightleftharpoons C_3H_6 + HO_2$	R659	4.50×10^{-19}	0	5020	[e]
$IC_3H_7 + OH \rightleftharpoons C_3H_6 + H_2O$	R660	2.41×10^{13}	0	0	[e]
$IC_3H_7 + O \rightleftharpoons CH_3COCH_3 + H$	R661	4.82×10^{13}	0	0	[e]
$IC_3H_7 + O \rightleftharpoons CH_3CHO + CH_3$	R662	4.82×10^{13}	0	0	[e]
$NC_3H_7 \rightleftharpoons CH_3 + C_2H_4$	R663	9.97×10^{40}	-8.6	41430	[e]
$NC_3H_7 \rightleftharpoons H + C_3H_6$	R664	8.78×10^{39}	-8.1	46580	[e]
$NC_3H_7 + O_2 \rightleftharpoons C_3H_6 + HO_2$	R665	3.00×10^{-19}	0	3000	[e]
$C_2H_5CHO + NC_3H_7 \rightleftharpoons C_2H_5CO + C_3H_8$	R666	1.70×10^{12}	0	8440	[e]
$C_2H_5CHO + IC_3H_7 \rightleftharpoons C_2H_5CO + C_3H_8$	R667	1.70×10^{12}	0	8440	[e]
$C_2H_5CHO + C_3H_5\text{-}A \rightleftharpoons C_2H_5CO + C_3H_6$	R668	1.70×10^{12}	0	8440	[e]
$C_3H_5\text{-}A + H\ (+M) \rightleftharpoons C_3H_6\ (+M)$	R669	2.00×10^{14}	0	0	[e]
$C_2H_3 + CH_3\ (+M) \rightleftharpoons C_3H_6\ (+M)$	R670	2.50×10^{13}	0	0	[e]
$C_3H_6 \rightleftharpoons C_3H_5\text{-}S + H$	R671	7.71×10^{69}	-16.1	140000	[e]
$C_3H_6 \rightleftharpoons C_3H_5\text{-}T + H$	R672	5.62×10^{71}	-16.6	139300	[e]
$C_3H_6 + O \rightleftharpoons C_2H_5 + HCO$	R673	1.58×10^{7}	1.8	-1216	[e]
$C_3H_6 + O \rightleftharpoons CH_2CO + CH_3 + H$	R674	2.50×10^{7}	1.8	76	[e]
$C_3H_6 + O \rightleftharpoons CH_3CHCO + H + H$	R675	2.50×10^{7}	1.8	76	[e]
$C_3H_6 + O \rightleftharpoons C_3H_5\text{-}A + OH$	R676	5.24×10^{11}	0.7	5884	[e]
$C_3H_6 + O \rightleftharpoons C_3H_5\text{-}S + OH$	R677	1.20×10^{11}	0.7	8959	[e]
$C_3H_6 + O \rightleftharpoons C_3H_5\text{-}T + OH$	R678	6.03×10^{10}	0.7	7632	[e]
$C_3H_6 + OH \rightleftharpoons C_3H_5\text{-}A + H_2O$	R679	3.12×10^{6}	2	-298	[e]
$C_3H_6 + OH \rightleftharpoons C_3H_5\text{-}S + H_2O$	R680	2.11×10^{6}	2	2778	[e]
$C_3H_6 + OH \rightleftharpoons C_3H_5\text{-}T + H_2O$	R681	1.11×10^{6}	2	1451	[e]
$C_3H_6 + HO_2 \rightleftharpoons C_3H_5\text{-}A + H_2O_2$	R682	2.70×10^{4}	2.5	12340	[e]
$C_3H_6 + HO_2 \rightleftharpoons C_3H_5\text{-}S + H_2O_2$	R683	1.80×10^{4}	2.5	27620	[e]
$C_3H_6 + HO_2 \rightleftharpoons C_3H_5\text{-}T + H_2O_2$	R684	9.00×10^{3}	2.5	23590	[e]
$C_3H_6 + H \rightleftharpoons C_2H_4 + CH_3$	R685	3.30×10^{24}	-3	15610	[e]
$C_3H_6 + H \rightleftharpoons C_3H_5\text{-}A + H_2$	R686	1.73×10^{5}	2.5	2490	[e]
$C_3H_6 + H \rightleftharpoons C_3H_5\text{-}T + H_2$	R687	4.00×10^{5}	2.5	9790	[e]
$C_3H_6 + H \rightleftharpoons C_3H_5\text{-}S + H_2$	R688	8.04×10^{5}	2.5	12283	[e]
$C_3H_6 + O_2 \rightleftharpoons C_3H_5\text{-}A + HO_2$	R689	4.00×10^{12}	0	39900	[e]
$C_3H_6 + O_2 \rightleftharpoons C_3H_5\text{-}S + HO_2$	R690	2.00×10^{12}	0	62900	[e]
$C_3H_6 + O_2 \rightleftharpoons C_3H_5\text{-}T + HO_2$	R691	1.40×10^{12}	0	60700	[e]
$C_3H_6 + CH_3 \rightleftharpoons C_3H_5\text{-}A + CH_4$	R692	2.21×10	3.5	5675	[e]
$C_3H_6 + CH_3 \rightleftharpoons C_3H_5\text{-}S + CH_4$	R693	1.35×10	3.5	12850	[e]
$C_3H_6 + CH_3 \rightleftharpoons C_3H_5\text{-}T + CH_4$	R694	8.40×10^{-1}	3.5	11660	[e]

Reactions	Code	$A_{r,g}$	$\beta_{r,g}$	$E_{r,g}$	Ref
$C_3H_6 + C_2H_5 \rightleftharpoons C_3H_5\text{-}A + C_2H_6$	R695	1.00×10^{11}	0	9800	[e]
$C_3H_6 + CH_3CO_3 \rightleftharpoons C_3H_5\text{-}A + CH_3CO_3H$	R696	3.24×10^{11}	0	14900	[e]
$C_3H_6 + CH_3O_2 \rightleftharpoons C_3H_5\text{-}A + CH_3O_2H$	R697	3.24×10^{11}	0	14900	[e]
$C_3H_6 + HO_2 \rightleftharpoons C_3H_6O_{1\text{-}2} + OH$	R698	1.29×10^{12}	0	14900	[e]
$C_3H_6 + C_2H_5O_2 \rightleftharpoons C_3H_5\text{-}A + C_2H_5O_2H$	R699	3.24×10^{11}	0	14900	[e]
$C_3H_6 + NC_3H_7O_2 \rightleftharpoons C_3H_5\text{-}A + NC_3H_7O_2H$	R700	3.24×10^{11}	0	14900	[e]
$C_3H_6 + IC_3H_7O_2 \rightleftharpoons C_3H_5\text{-}A + IC_3H_7O_2H$	R701	3.24×10^{11}	0	14900	[e]
$C_3H_6 + OH \rightleftharpoons C_3H_6OH$	R702	9.93×10^{11}	0	-960	[e]
$C_3H_6OH + O_2 \rightleftharpoons HOCH_3CHO$	R703	1.20×10^{11}	0	-1100	[e]
$HOCH_3O_2 \rightleftharpoons CH_3CHO + CH_2O + OH$	R704	1.25×10^{10}	0	18900	[e]
$C_3H_5\text{-}A + H \rightleftharpoons C_3H_4\text{-}A + H_2$	R705	1.80×10^{13}	0	0	[e]
$C_3H_5\text{-}A + O \rightleftharpoons C_2H_3CHO + H$	R706	6.00×10^{13}	0	0	[e]
$C_3H_5\text{-}A + OH \rightleftharpoons C_2H_3CHO + H + H$	R707	1.60×10^{20}	-1.6	26330	[e]
$C_3H_5\text{-}A + OH \rightleftharpoons C_3H_4\text{-}A + H_2O$	R708	6.00×10^{12}	0	0	[e]
$C_3H_5\text{-}A + O_2 \rightleftharpoons C_3H_4\text{-}A + HO_2$	R709	2.18×10^{21}	-2.9	30755	[e]
$C_3H_5\text{-}A + O_2 \rightleftharpoons CH_3CO + CH_2O$	R710	7.14×10^{15}	-1.2	21046	[e]
$C_3H_5\text{-}A + O_2 \rightleftharpoons C_2H_3CHO + OH$	R711	2.47×10^{13}	-0.5	23017	[e]
$C_3H_5\text{-}A + HCO \rightleftharpoons C_3H_6 + CO$	R712	6.00×10^{13}	0	0	[e]
$C_3H_5\text{-}A + CH_3(+M) \rightleftharpoons C_4H_{8\text{-}1}(+M)$	R713	1.00×10^{14}	-0.3	-262.3	[e]
$C_3H_5\text{-}A + CH_3 \rightleftharpoons C_3H_4\text{-}A + CH_4$	R714	3.00×10^{12}	-0.3	-131	[e]
$C_3H_5\text{-}A \rightleftharpoons C_3H_5\text{-}T$	R715	4.86×10^{53}	-12.8	75883	[e]
$C_3H_5\text{-}A \rightleftharpoons C_3H_5\text{-}S$	R716	9.70×10^{48}	-11.7	73700	[e]
$C_2H_2 + CH_3 \rightleftharpoons C_3H_5\text{-}A$	R717	1.04×10^{51}	-11.9	36476	[e]
$C_3H_5\text{-}A + CH_3O_2 \rightleftharpoons C_3H_5O + CH_3O$	R718	7.00×10^{12}	0	-1000	[e]
$C_3H_5\text{-}A + C_2H_5 \rightleftharpoons C_2H_6 + C_3H_4\text{-}A$	R719	4.00×10^{11}	0	0	[e]
$C_3H_5\text{-}A + C_2H_5 \rightleftharpoons C_2H_4 + C_3H_6$	R720	4.00×10^{11}	0	0	[e]
$C_3H_5\text{-}A + C_2H_3 \rightleftharpoons C_2H_4 + C_3H_4\text{-}A$	R721	1.00×10^{12}	0	0	[e]
$C_3H_5\text{-}A + C_3H_5\text{-}A \rightleftharpoons C_3H_4\text{-}A + C_3H_6$	R722	8.43×10^{10}	0	-262	[e]
$C_3H_5\text{-}A + C_2H_2 \rightleftharpoons C_8H_6$	R723	1.00×10^{12}	0	6883.4	[e]
$C_3H_5\text{-}A + C_2H_3 \rightleftharpoons C_5H_6 + H + H$	R724	1.60×10^{35}	-14	61137.7	[e]
$C_3H_5\text{-}A + C_3H_3 \rightleftharpoons C_6H_6 + H + H$	R725	5.60×10^{20}	-2.5	1696.9	[e]
$C_3H_5\text{-}A + HO_2 \rightleftharpoons C_3H_5O + OH$	R726	7.00×10^{12}	0	-1000	[e]
$C_2H_2 + CH_3 \rightleftharpoons C_3H_5\text{-}S$	R727	2.40×10^{38}	-8.2	17100	[e]
$C_3H_5\text{-}S + H \rightleftharpoons C_3H_4\text{-}P + H_2$	R728	3.34×10^{12}	0	0	[e]
$C_3H_5\text{-}S + O \rightleftharpoons C_2H_4 + HCO$	R729	6.00×10^{13}	0	0	[e]
$C_3H_5\text{-}S + OH \rightleftharpoons C_2H_4 + HCO + H$	R730	5.00×10^{12}	0	0	[e]
$C_3H_5\text{-}S + O_2 \rightleftharpoons CH_3CHO + HCO$	R731	1.00×10^{11}	0	0	[e]
$C_3H_5\text{-}S + HO_2 \rightleftharpoons C_2H_4 + HCO + OH$	R732	2.00×10^{13}	0	0	[e]

Reactions	Code	$A_{r,g}$	$\beta_{r,g}$	$E_{r,g}$	Ref
C_3H_5-S + HCO ⇌ C_3H_6 + CO	R733	9.00×10^{13}	0	0	[e]
C_3H_5-S + CH_3 ⇌ C_3H_4-P + CH_4	R734	1.00×10^{11}	0	0	[e]
C_2H_2 + CH_3 ⇌ C_3H_5-T	R735	7.31×10^{25}	-5.1	21150	[e]
C_3H_5-T ⇌ C_3H_5-S	R736	5.10×10^{52}	-13.4	57200	[e]
C_3H_5-T + H ⇌ C_3H_4-P + H_2	R737	3.34×10^{12}	0	0	[e]
C_3H_5-T + O ⇌ CH_3 + CH_2CO	R738	6.00×10^{13}	0	0	[e]
C_3H_5-T + OH ⇌ CH_3 + CH_2CO + H	R739	5.00×10^{12}	0	0	[e]
C_3H_5-T + O_2 ⇌ CH_3CO + CH_2O	R740	1.00×10^{11}	0	0	[e]
C_3H_5-T + HO_2 ⇌ CH_3 + CH_2CO + OH	R741	2.00×10^{13}	0	0	[e]
C_3H_5-T + HCO ⇌ C_3H_6 + CO	R742	9.00×10^{13}	0	0	[e]
C_3H_5-T + CH_3 ⇌ C_3H_4-P + CH_4	R743	1.00×10^{11}	0	0	[e]
C_2H_2 + CH_3 ⇌ C_3H_4-A + H	R744	9.20×10^{10}	0.5	23950	[e]
C_3H_4-A + H ⇌ C_3H_3 + H_2	R745	1.30×10^{6}	2	5500	[e]
C_3H_4-A + H ⇌ C_3H_5-S	R746	2.60×10^{31}	-6.2	18700	[e]
C_3H_4-A + H ⇌ C_3H_5-T	R747	6.98×10^{44}	-9.7	14032	[e]
C_3H_4-A + H ⇌ C_3H_5-A	R748	7.34×10^{54}	-12.1	26187	[e]
C_3H_4-A + O ⇌ C_2H_4 + CO	R749	2.00×10^{7}	1.8	1000	[e]
C_3H_4-A + OH ⇌ C_3H_3 + H_2O	R750	5.30×10^{6}	2	2000	[e]
C_3H_4-A + CH_3 ⇌ C_3H_3 + CH_4	R751	1.30×10^{12}	0	7700	[e]
C_3H_4-A + C_2H ⇌ C_2H_2 + C_3H_3	R752	1.00×10^{13}	0	0	[e]
C_3H_4-A + C_3H_4-A ⇌ C_3H_5-A + C_3H_3	R753	5.00×10^{14}	0	64746.7	[e]
C_3H_4-A + C_3H_5-A ⇌ C_3H_3 + C_3H_6	R754	2.00×10^{11}	0	7700	[e]
C_3H_4-A + C_3H_3 ⇌ C_6H_6 + H	R755	1.40×10^{12}	0	9990.4	[e]
C_3H_4-P ⇌ CC_3H_4	R756	3.92×10^{40}	-8.7	68706	[e]
C_3H_4-P ⇌ C_3H_4-A	R757	3.12×10^{58}	-13.1	92680	[e]
C_3H_4-P + H ⇌ C_3H_4-A + H	R758	1.93×10^{18}	-1	11523	[e]
C_3H_4-P + H ⇌ C_3H_5-T	R759	9.62×10^{47}	-10.6	15910	[e]
C_3H_4-P + H ⇌ C_3H_5-S	R760	1.00×10^{34}	-6.9	8900	[e]
C_3H_4-P + H ⇌ C_3H_5-A	R761	9.02×10^{59}	-13.9	33953	[e]
C_3H_4-P + H ⇌ C_3H_3 + H_2	R762	1.30×10^{6}	2	5500	[e]
C_3H_4-P + C_3H_3 ⇌ C_3H_4-A + C_3H_3	R763	6.14×10^{6}	1.7	10450	[e]
C_3H_4-P + O ⇌ HCCO + CH_3	R764	7.30×10^{12}	0	2250	[e]
C_3H_4-P + O ⇌ C_2H_4 + CO	R765	1.00×10^{13}	0	2250	[e]
C_3H_4-P + OH ⇌ C_3H_3 + H_2O	R766	1.00×10^{6}	2	100	[e]
C_3H_4-P + C_2H ⇌ C_2H_2 + C_3H_3	R767	1.00×10^{13}	0	0	[e]
C_3H_4-P + CH_3 ⇌ C_3H_3 + CH_4	R768	1.80×10^{12}	0	7700	[e]
C_2H_2 + CH_3 ⇌ C_3H_4-P + H	R769	2.51×10^{11}	0.6	15453	[e]
C_3H_4-P + C_2H_3 ⇌ C_3H_3 + C_2H_4	R770	1.00×10^{12}	0	7700	[e]

Reactions	Code	$A_{r,g}$	$\beta_{r,g}$	$E_{r,g}$	Ref
C_3H_4-P + C_3H_5-A ⇌ C_3H_3 + C_3H_6	R771	1.00×10^{12}	0	7700	[e]
CC_3H_4 ⇌ C_3H_4-A	R772	4.33×10^{41}	-8.9	50475	[e]
C_3H_3 + H ⇌ C_3H_4-P	R773	1.50×10^{13}	0	0	[e]
C_3H_3 + H ⇌ C_3H_4-A	R774	2.50×10^{12}	0	0	[e]
C_3H_3 + H ⇌ C_3H_2 + H_2	R775	5.00×10^{13}	0	1000	[e]
C_3H_3 + O ⇌ CH_2O + C_2H	R776	2.00×10^{13}	0	0	[e]
C_3H_3 + OH ⇌ C_3H_2 + H_2O	R777	2.00×10^{13}	0	0	[e]
C_3H_3 + O_2 ⇌ CH_2CO + HCO	R778	3.00×10^{10}	0	2868	[e]
C_3H_3 + HO_2 ⇌ OH + CO + C_2H_3	R779	8.00×10^{11}	0	0	[e]
C_3H_3 + HO_2 ⇌ C_3H_4-A + O_2	R780	3.00×10^{11}	0	0	[e]
C_3H_3 + HO_2 ⇌ C_3H_4-P + O_2	R781	2.50×10^{12}	0	0	[e]
C_3H_3 + HCO ⇌ C_3H_4-A + CO	R782	2.50×10^{13}	0	0	[e]
C_3H_3 + HCO ⇌ C_3H_4-P + CO	R783	2.50×10^{13}	0	0	[e]
C_3H_3 + HCCO ⇌ C_4H_4 + CO	R784	2.50×10^{13}	0	0	[e]
C_3H_3 + CH ⇌ C_4H_3-I + H	R785	5.00×10^{13}	0	0	[e]
C_3H_3 + CH_2 ⇌ C_4H_4 + H	R786	5.00×10^{13}	0	0	[e]
C_3H_3 + CH_3(+M) ⇌ C_4H_{612}(+M)	R787	1.50×10^{12}	0	0	[e]
C_3H_3 + C_3H_3 ⇌ C_6H_5 + H	R788	5.00×10^{12}	0	0	[e]
C_3H_3 + C_3H_3 ⇌ C_6H_6	R789	2.00×10^{12}	0	0	[e]
C_3H_3 + C_4H_6 ⇌ $C_6H_5CH_3$ + H	R790	6.53×10^{5}	1.3	-4611	[e]
C_2H_5 + C_2H ⇌ C_3H_3 + CH_3	R791	1.81×10^{13}	0	0	[e]
C_3H_2 + H ⇌ C_3H_3	R792	1.00×10^{13}	0	0	[e]
C_3H_2 + O ⇌ C_2H_2 + CO	R793	6.80×10^{13}	0	0	[e]
C_3H_2 + OH ⇌ HCO + C_2H_2	R794	6.80×10^{13}	0	0	[e]
C_3H_2 + O_2 ⇌ HCCO + H + CO	R795	2.00×10^{12}	0	1000	[e]
C_3H_2 + CH ⇌ C_4H_2 + H	R796	5.00×10^{13}	0	0	[e]
C_3H_2 + CH_2 ⇌ C_4H_3-N + H	R797	5.00×10^{13}	0	0	[e]
C_3H_2 + CH_3 ⇌ C_4H_4 + H	R798	5.00×10^{12}	0	0	[e]
C_3H_2 + HCCO ⇌ C_4H_3-N + CO	R799	1.00×10^{13}	0	0	[e]
C_3H_2 + C_3H_3 ⇌ C_6H_5	R800	7.00×10^{12}	0	0	[e]
C_3H_2 + O_2 ⇌ HCO + HCCO	R801	5.00×10^{13}	0	0	[e]
CH_3CHCO + OH ⇌ C_2H_5 + CO_2	R802	1.73×10^{12}	0	-1010	[e]
CH_3CHCO + OH ⇌ SC_2H_4OH + CO	R803	2.00×10^{12}	0	-1010	[e]
CH_3CHCO + H ⇌ C_2H_5 + CO	R804	4.40×10^{12}	0	1459	[e]
CH_3CHCO + O ⇌ CH_3CHO + CO	R805	3.20×10^{12}	0	-437	[e]
NC_3H_7 + HO_2 ⇌ NC_3H_7O + OH	R806	7.00×10^{12}	0	-1000	[e]
IC_3H_7 + HO_2 ⇌ IC_3H_7O + OH	R807	7.00×10^{12}	0	-1000	[e]
CH_3O_2 + NC_3H_7 ⇌ CH_3O + NC_3H_7O	R808	7.00×10^{12}	0	-1000	[e]
CH_3O_2 + IC_3H_7 ⇌ CH_3O + IC_3H_7O	R809	7.00×10^{12}	0	-1000	[e]

Reactions	Code	$A_{r,g}$	$\beta_{r,g}$	$E_{r,g}$	Ref
$NC_3H_7 + O_2 \rightleftharpoons NC_3H_7O_2$	R810	4.52×10^{12}	0	0	[e]
$IC_3H_7 + O_2 \rightleftharpoons IC_3H_7O_2$	R811	7.54×10^{12}	0	0	[e]
$NC_3H_7O_2 + CH_2O \rightleftharpoons NC_3H_7O_2H + HCO$	R812	5.60×10^{12}	0	13600	[e]
$NC_3H_7O_2 + CH_3CHO \rightleftharpoons NC_3H_7O_2H + CH_3CO$	R813	2.80×10^{12}	0	13600	[e]
$IC_3H_7O_2 + CH_2O \rightleftharpoons IC_3H_7O_2H + HCO$	R814	5.60×10^{12}	0	13600	[e]
$IC_3H_7O_2 + CH_3CHO \rightleftharpoons IC_3H_7O_2H + CH_3CO$	R815	2.80×10^{12}	0	13600	[e]
$NC_3H_7O_2 + HO_2 \rightleftharpoons NC_3H_7O_2H + O_2$	R816	1.75×10^{10}	0	-3275	[e]
$IC_3H_7O_2 + HO_2 \rightleftharpoons IC_3H_7O_2H + O_2$	R817	1.75×10^{10}	0	-3275	[e]
$C_2H_4 + NC_3H_7O_2 \rightleftharpoons C_2H_3 + NC_3H_7O_2H$	R818	1.13×10^{13}	0	30430	[e]
$C_2H_4 + IC_3H_7O_2 \rightleftharpoons C_2H_3 + IC_3H_7O_2H$	R819	1.13×10^{13}	0	30430	[e]
$CH_3OH + NC_3H_7O_2 \rightleftharpoons CH_2OH + NC_3H_7O_2H$	R820	6.30×10^{12}	0	19360	[e]
$CH_3OH + IC_3H_7O_2 \rightleftharpoons CH_2OH + IC_3H_7O_2H$	R821	6.30×10^{12}	0	19360	[e]
$C_2H_3CHO + NC_3H_7O_2 \rightleftharpoons C_2H_3CO + NC_3H_7O_2H$	R822	2.80×10^{12}	0	13600	[e]
$C_2H_3CHO + IC_3H_7O_2 \rightleftharpoons C_2H_3CO + IC_3H_7O_2H$	R823	2.80×10^{12}	0	13600	[e]
$CH_4 + NC_3H_7O_2 \rightleftharpoons CH_3 + NC_3H_7O_2H$	R824	1.12×10^{13}	0	24640	[e]
$CH_4 + IC_3H_7O_2 \rightleftharpoons CH_3 + IC_3H_7O_2H$	R825	1.12×10^{13}	0	24640	[e]
$NC_3H_7O_2 + CH_3O_2 \rightleftharpoons NC_3H_7O + CH_3O + O_2$	R826	1.40×10^{16}	-1.6	1860	[e]
$IC_3H_7O_2 + CH_3O_2 \rightleftharpoons IC_3H_7O + CH_3O + O_2$	R827	1.40×10^{16}	-1.6	1860	[e]
$H_2 + NC_3H_7O_2 \rightleftharpoons H + NC_3H_7O_2H$	R828	3.01×10^{13}	0	26030	[e]
$H_2 + IC_3H_7O_2 \rightleftharpoons H + IC_3H_7O_2H$	R829	3.01×10^{13}	0	26030	[e]
$IC_3H_7O_2 + C_2H_6 \rightleftharpoons IC_3H_7O_2H + C_2H_5$	R830	1.70×10^{13}	0	20460	[e]
$NC_3H_7O_2 + C_2H_6 \rightleftharpoons NC_3H_7O_2H + C_2H_5$	R831	1.70×10^{13}	0	20460	[e]
$IC_3H_7O_2 + C_2H_5CHO \rightleftharpoons IC_3H_7O_2H + C_2H_5CO$	R832	2.00×10^{11}	0	9500	[e]
$NC_3H_7O_2 + C_2H_5CHO \rightleftharpoons NC_3H_7O_2H + C_2H_5CO$	R833	2.00×10^{11}	0	9500	[e]
$IC_3H_7O_2 + CH_3CO_3 \rightleftharpoons IC_3H_7O + CH_3CO_2 + O_2$	R834	1.40×10^{16}	-1.6	1860	[e]
$NC_3H_7O_2 + CH_3CO_3 \rightleftharpoons NC_3H_7O + CH_3CO_2 + O_2$	R835	1.40×10^{16}	-1.6	1860	[e]
$IC_3H_7O_2 + C_2H_5O_2 \rightleftharpoons IC_3H_7O + C_2H_5O + O_2$	R836	1.40×10^{16}	-1.6	1860	[e]
$NC_3H_7O_2 + C_2H_5O_2 \rightleftharpoons NC_3H_7O + C_2H_5O + O_2$	R837	1.40×10^{16}	-1.6	1860	[e]
$IC_3H_7O_2 + IC_3H_7O_2 \rightleftharpoons O_2 + IC_3H_7O + IC_3H_7O$	R838	1.40×10^{16}	-1.6	1860	[e]
$NC_3H_7O_2 + NC_3H_7O_2 \rightleftharpoons O_2 + NC_3H_7O + NC_3H_7O$	R839	1.40×10^{16}	-1.6	1860	[e]
$IC_3H_7O_2 + NC_3H_7O_2 \rightleftharpoons IC_3H_7O + NC_3H_7O + O_2$	R840	1.40×10^{16}	-1.6	1860	[e]
$IC_3H_7O_2 + CH_3 \rightleftharpoons IC_3H_7O + CH_3O$	R841	7.00×10^{12}	0	-1000	[e]
$IC_3H_7O_2 + C_2H_5 \rightleftharpoons IC_3H_7O + C_2H_5O$	R842	7.00×10^{12}	0	-1000	[e]
$IC_3H_7O_2 + IC_3H_7 \rightleftharpoons IC_3H_7O + IC_3H_7O$	R843	7.00×10^{12}	0	-1000	[e]
$IC_3H_7O_2 + NC_3H_7 \rightleftharpoons IC_3H_7O + NC_3H_7O$	R844	7.00×10^{12}	0	-1000	[e]
$IC_3H_7O_2 + C_3H_5\text{-}A \rightleftharpoons IC_3H_7O + C_3H_5O$	R845	7.00×10^{12}	0	-1000	[e]
$NC_3H_7O_2 + CH_3 \rightleftharpoons NC_3H_7O + CH_3O$	R846	7.00×10^{12}	0	-1000	[e]
$NC_3H_7O_2 + C_2H_5 \rightleftharpoons NC_3H_7O + C_2H_5O$	R847	7.00×10^{12}	0	-1000	[e]

Reactions	Code	$A_{r,g}$	$\beta_{r,g}$	$E_{r,g}$	Ref
$NC_3H_7O_2 + IC_3H_7 \rightleftharpoons NC_3H_7O + IC_3H_7O$	R848	7.00×10^{12}	0	-1000	[e]
$NC_3H_7O_2 + NC_3H_7 \rightleftharpoons NC_3H_7O + NC_3H_7O$	R849	7.00×10^{12}	0	-1000	[e]
$NC_3H_7O_2 + C_3H_5\text{-}A \rightleftharpoons NC_3H_7O + C_3H_5O$	R850	7.00×10^{12}	0	-1000	[e]
$NC_3H_7O_2H \rightleftharpoons NC_3H_7O + OH$	R851	1.50×10^{16}	0	42500	[e]
$IC_3H_7O_2H \rightleftharpoons IC_3H_7O + OH$	R852	9.45×10^{15}	0	42600	[e]
$C_2H_5 + CH_2O \rightleftharpoons NC_3H_7O$	R853	1.00×10^{11}	0	3496	[e]
$C_2H_5CHO + H \rightleftharpoons NC_3H_7O$	R854	4.00×10^{12}	0	6260	[e]
$CH_3 + CH_3CHO \rightleftharpoons IC_3H_7O$	R855	1.00×10^{11}	0	9256	[e]
$CH_3COCH_3 + H \rightleftharpoons IC_3H_7O$	R856	2.00×10^{12}	0	7270	[e]
$IC_3H_7O + O_2 \rightleftharpoons CH_3COCH_3 + HO_2$	R857	9.09×10^{9}	0	390	[e]
$NC_3H_7O_2 \rightleftharpoons C_3H_6OOH_{1\text{-}2}$	R858	6.00×10^{11}	0	26850	[e]
$NC_3H_7O_2 \rightleftharpoons C_3H_6OOH_{1\text{-}3}$	R859	1.12×10^{11}	0	24400	[e]
$IC_3H_7O_2 \rightleftharpoons C_3H_6OOH_{2\text{-}1}$	R860	1.80×10^{12}	0	29400	[e]
$IC_3H_7O_2 \rightleftharpoons C_3H_6OOH_{2\text{-}2}$	R861	1.23×10^{35}	-7	48880	[e]
$C_3H_6OOH_{1\text{-}2} \rightleftharpoons C_3H_6O_{1\text{-}2} + OH$	R862	6.00×10^{11}	0	22000	[e]
$C_3H_6OOH_{1\text{-}3} \rightleftharpoons C_3H_6O_{1\text{-}3} + OH$	R863	7.50×10^{10}	0	15250	[e]
$C_3H_6OOH_{2\text{-}1} \rightleftharpoons C_3H_6O_{1\text{-}2} + OH$	R864	6.00×10^{11}	0	22000	[e]
$C_3H_6 + HO_2 \rightleftharpoons C_3H_6OOH_{1\text{-}2}$	R865	1.00×10^{11}	0	11000	[e]
$C_3H_6 + HO_2 \rightleftharpoons C_3H_6OOH_{2\text{-}1}$	R866	1.00×10^{11}	0	11750	[e]
$C_3H_6OOH_{1\text{-}3} \rightleftharpoons OH + CH_2O + C_2H_4$	R867	3.04×10^{15}	-0.8	27400	[e]
$C_3H_6OOH_{2\text{-}1} \rightleftharpoons C_2H_3OOH + CH_3$	R868	6.54×10^{27}	-5.1	38320	[e]
$C_3H_6OOH_{1\text{-}2} \rightleftharpoons C_2H_4 + CH_2O + OH$	R869	1.31×10^{33}	-7	48120	[e]
$C_3H_6OOH_{2\text{-}2} \rightleftharpoons CH_3COCH_3 + OH$	R870	9.00×10^{14}	0	1500	[e]
$C_3H_6OOH_{1\text{-}2} + O_2 \rightleftharpoons C_3H_6OOH_{1\text{-}2}O_2$	R871	5.00×10^{12}	0	0	[e]
$C_3H_6OOH_{1\text{-}3} + O_2 \rightleftharpoons C_3H_6OOH_{1\text{-}3}O_2$	R872	4.52×10^{12}	0	0	[e]
$C_3H_6OOH_{2\text{-}1} + O_2 \rightleftharpoons C_3H_6OOH_{2\text{-}1}O_2$	R873	4.52×10^{12}	0	0	[e]
$C_3H_6OOH_{1\text{-}2}O_2 \rightleftharpoons C_3KET_{12} + OH$	R874	6.00×10^{11}	0	26400	[e]
$C_3H_6OOH_{1\text{-}3}O_2 \rightleftharpoons C_3KET_{13} + OH$	R875	7.50×10^{10}	0	21400	[e]
$C_3H_6OOH_{2\text{-}1}O_2 \rightleftharpoons C_3KET_{21} + OH$	R876	3.00×10^{11}	0	23850	[e]
$C_3H_6OOH_{2\text{-}1}O_2 \rightleftharpoons C_3H_{51\text{-}2,3}OOH$	R877	1.12×10^{11}	0	24400	[e]
$C_3H_6OOH_{1\text{-}2}O_2 \rightleftharpoons C_3H_{51\text{-}2,3}OOH$	R878	9.00×10^{11}	0	29400	[e]
$C_3H_{51\text{-}2,3}OOH \rightleftharpoons AC_3H_5OOH + HO_2$	R879	2.56×10^{13}	-0.5	17770	[e]
$C_3H_6OOH_{1\text{-}3}O_2 \rightleftharpoons C_3H_{52\text{-}1,3}OOH$	R880	6.00×10^{11}	0	26850	[e]
$C_3H_{52\text{-}1,3}OOH \rightleftharpoons AC_3H_5OOH + HO_2$	R881	1.15×10^{14}	-0.6	17250	[e]
$C_3KET_{12} \rightleftharpoons CH_3CHO + HCO + OH$	R882	9.45×10^{15}	0	43000	[e]
$C_3KET_{13} \rightleftharpoons CH_2O + CH_2CHO + OH$	R883	1.00×10^{16}	0	43000	[e]
$C_3KET_{21} \rightleftharpoons CH_2O + CH_3CO + OH$	R884	1.00×10^{16}	0	43000	[e]
$C_3H_5O + OH \rightleftharpoons AC_3H_5OOH$	R885	2.00×10^{13}	0	0	[e]

Reactions	Code	$A_{r,g}$	$\beta_{r,g}$	$E_{r,g}$	Ref
$C_3H_5O \rightleftharpoons C_2H_3CHO + H$	R886	1.00×10^{14}	0	29100	[e]
$C_2H_3 + CH_2O \rightleftharpoons C_3H_5O$	R887	1.50×10^{11}	0	10600	[e]
$C_3H_5O + O_2 \rightleftharpoons C_2H_3CHO + HO_2$	R888	1.00×10^{12}	0	6000	[e]
$C_2H_3OOH \rightleftharpoons CH_2CHO + OH$	R889	8.40×10^{14}	0	43000	[e]
$C_3H_6O_{1-2} \rightleftharpoons C_2H_4 + CH_2O$	R890	6.00×10^{14}	0	60000	[e]
$C_3H_6O_{1-2} + OH \rightleftharpoons CH_2O + C_2H_3 + H_2O$	R891	5.00×10^{12}	0	0	[e]
$C_3H_6O_{1-2} + H \rightleftharpoons CH_2O + C_2H_3 + H_2$	R892	2.63×10^{7}	2	5000	[e]
$C_3H_6O_{1-2} + O \rightleftharpoons CH_2O + C_2H_3 + OH$	R893	8.43×10^{13}	0	5200	[e]
$C_3H_6O_{1-2} + HO_2 \rightleftharpoons CH_2O + C_2H_3 + H_2O_2$	R894	1.00×10^{13}	0	15000	[e]
$C_3H_6O_{1-2} + CH_3O_2 \rightleftharpoons CH_2O + C_2H_3 + CH_3O_2H$	R895	1.00×10^{13}	0	19000	[e]
$C_3H_6O_{1-2} + CH_3 \rightleftharpoons CH_2O + C_2H_3 + CH_4$	R896	2.00×10^{11}	0	10000	[e]
$C_3H_6O_{1-3} \rightleftharpoons C_2H_4 + CH_2O$	R897	6.00×10^{14}	0	60000	[e]
$C_3H_6O_{1-3} + OH \rightleftharpoons CH_2O + C_2H_3 + H_2O$	R898	5.00×10^{12}	0	0	[e]
$C_3H_6O_{1-3} + O \rightleftharpoons CH_2O + C_2H_3 + OH$	R899	8.43×10^{13}	0	5200	[e]
$C_3H_6O_{1-3} + H \rightleftharpoons CH_2O + C_2H_3 + H_2$	R900	2.63×10^{7}	2	5000	[e]
$C_3H_6O_{1-3} + CH_3O_2 \rightleftharpoons CH_2O + C_2H_3 + CH_3O_2H$	R901	1.00×10^{13}	0	19000	[e]
$C_3H_6O_{1-3} + HO_2 \rightleftharpoons CH_2O + C_2H_3 + H_2O_2$	R902	1.00×10^{13}	0	15000	[e]
$C_3H_6O_{1-3} + CH_3 \rightleftharpoons CH_2O + C_2H_3 + CH_4$	R903	2.00×10^{11}	0	10000	[e]
$IC_3H_7O_2 \rightleftharpoons C_3H_6 + HO_2$	R904	1.01×10^{43}	-9.4	41490	[e]
$NC_3H_7O_2 \rightleftharpoons C_3H_6 + HO_2$	R905	5.04×10^{38}	-8.1	40490	[e]
$C_4H_{10}(+M) \rightleftharpoons C_2H_5 + C_2H_5(+M)$	R906	2.72×10^{15}	0	75610	[e]
$C_4H_{10}(+M) \rightleftharpoons NC_3H_7 + CH_3(+M)$	R907	4.28×10^{14}	0	69900	[e]
$PC_4H_9 + H \rightleftharpoons C_4H_{10}$	R908	3.61×10^{13}	0	0	[e]
$SC_4H_9 + H \rightleftharpoons C_4H_{10}$	R909	3.61×10^{13}	0	0	[e]
$C_4H_{10} + O_2 \rightleftharpoons PC_4H_9 + HO_2$	R910	6.00×10^{13}	0	52340	[e]
$C_4H_{10} + O_2 \rightleftharpoons SC_4H_9 + HO_2$	R911	4.00×10^{13}	0	49800	[e]
$C_4H_{10} + C_3H_5\text{-}A \rightleftharpoons PC_4H_9 + C_3H_6$	R912	7.94×10^{11}	0	20500	[e]
$C_4H_{10} + C_3H_5\text{-}A \rightleftharpoons SC_4H_9 + C_3H_6$	R913	3.16×10^{11}	0	16400	[e]
$C_4H_{10} + C_2H_5 \rightleftharpoons PC_4H_9 + C_2H_6$	R914	1.58×10^{11}	0	12300	[e]
$C_4H_{10} + C_2H_5 \rightleftharpoons SC_4H_9 + C_2H_6$	R915	1.00×10^{11}	0	10400	[e]
$C_4H_{10} + C_2H_3 \rightleftharpoons PC_4H_9 + C_2H_4$	R916	1.00×10^{12}	0	18000	[e]
$C_4H_{10} + C_2H_3 \rightleftharpoons SC_4H_9 + C_2H_4$	R917	8.00×10^{11}	0	16800	[e]
$C_4H_{10} + CH_3 \rightleftharpoons PC_4H_9 + CH_4$	R918	9.04×10^{-1}	3.6	7154	[e]
$C_4H_{10} + CH_3 \rightleftharpoons SC_4H_9 + CH_4$	R919	3.02×10^{0}	3.5	5481	[e]
$C_4H_{10} + H \rightleftharpoons PC_4H_9 + H_2$	R920	1.88×10^{5}	2.8	6280	[e]
$C_4H_{10} + H \rightleftharpoons SC_4H_9 + H_2$	R921	2.60×10^{6}	2.4	4471	[e]
$C_4H_{10} + OH \rightleftharpoons PC_4H_9 + H_2O$	R922	1.05×10^{10}	1	1586	[e]
$C_4H_{10} + OH \rightleftharpoons SC_4H_9 + H_2O$	R923	9.34×10^{7}	1.6	-35	[e]

Reactions	Code	$A_{r,g}$	$\beta_{r,g}$	$E_{r,g}$	Ref
$C_4H_{10} + O \rightleftharpoons PC_4H_9 + OH$	R924	1.13×10^{14}	0	7850	[e]
$C_4H_{10} + O \rightleftharpoons SC_4H_9 + OH$	R925	5.62×10^{13}	0	5200	[e]
$C_4H_{10} + HO_2 \rightleftharpoons PC_4H_9 + H_2O_2$	R926	8.10×10^{4}	2.5	16690	[e]
$C_4H_{10} + HO_2 \rightleftharpoons SC_4H_9 + H_2O_2$	R927	1.18×10^{5}	2.5	14860	[e]
$C_4H_{10} + CH_3O \rightleftharpoons PC_4H_9 + CH_3OH$	R928	3.00×10^{11}	0	7000	[e]
$C_4H_{10} + CH_3O \rightleftharpoons SC_4H_9 + CH_3OH$	R929	6.00×10^{11}	0	7000	[e]
$C_4H_{10} + C_2H_5O \rightleftharpoons PC_4H_9 + C_2H_5OH$	R930	3.00×10^{11}	0	7000	[e]
$C_4H_{10} + C_2H_5O \rightleftharpoons SC_4H_9 + C_2H_5OH$	R931	6.00×10^{11}	0	7000	[e]
$C_4H_{10} + PC_4H_9 \rightleftharpoons SC_4H_9 + C_4H_{10}$	R932	1.00×10^{11}	0	10400	[e]
$C_4H_{10} + CH_3CO_3 \rightleftharpoons PC_4H_9 + CH_3CO_3H$	R933	1.70×10^{13}	0	20460	[e]
$C_4H_{10} + CH_3CO_3 \rightleftharpoons SC_4H_9 + CH_3CO_3H$	R934	1.12×10^{13}	0	17700	[e]
$C_4H_{10} + O_2CHO \rightleftharpoons PC_4H_9 + HO_2CHO$	R935	1.68×10^{13}	0	20440	[e]
$C_4H_{10} + O_2CHO \rightleftharpoons SC_4H_9 + HO_2CHO$	R936	1.12×10^{13}	0	17690	[e]
$CH_3O_2 + C_4H_{10} \rightleftharpoons CH_3O_2H + PC_4H_9$	R937	8.10×10^{4}	2.5	16690	[e]
$CH_3O_2 + C_4H_{10} \rightleftharpoons CH_3O_2H + SC_4H_9$	R938	1.18×10^{5}	2.5	14860	[e]
$C_2H_5O_2 + C_4H_{10} \rightleftharpoons C_2H_5O_2H + PC_4H_9$	R939	1.70×10^{13}	0	20460	[e]
$C_2H_5O_2 + C_4H_{10} \rightleftharpoons C_2H_5O_2H + SC_4H_9$	R940	1.12×10^{13}	0	17700	[e]
$NC_3H_7O_2 + C_4H_{10} \rightleftharpoons NC_3H_7O_2H + PC_4H_9$	R941	1.70×10^{13}	0	20460	[e]
$NC_3H_7O_2 + C_4H_{10} \rightleftharpoons NC_3H_7O_2H + SC_4H_9$	R942	1.12×10^{13}	0	17700	[e]
$IC_3H_7O_2 + C_4H_{10} \rightleftharpoons IC_3H_7O_2H + PC_4H_9$	R943	1.70×10^{13}	0	20460	[e]
$IC_3H_7O_2 + C_4H_{10} \rightleftharpoons IC_3H_7O_2H + SC_4H_9$	R944	1.12×10^{13}	0	17700	[e]
$PC_4H_9O_2 + C_3H_8 \rightleftharpoons PC_4H_9O_2H + NC_3H_7$	R945	1.70×10^{13}	0	20460	[e]
$PC_4H_9O_2 + C_3H_8 \rightleftharpoons PC_4H_9O_2H + IC_3H_7$	R946	2.00×10^{12}	0	17000	[e]
$PC_4H_9O_2 + C_4H_{10} \rightleftharpoons PC_4H_9O_2H + PC_4H_9$	R947	1.70×10^{13}	0	20460	[e]
$PC_4H_9O_2 + C_4H_{10} \rightleftharpoons PC_4H_9O_2H + SC_4H_9$	R948	1.12×10^{13}	0	17700	[e]
$SC_4H_9O_2 + C_3H_8 \rightleftharpoons SC_4H_9O_2H + NC_3H_7$	R949	1.70×10^{13}	0	20460	[e]
$SC_4H_9O_2 + C_3H_8 \rightleftharpoons SC_4H_9O_2H + IC_3H_7$	R950	2.00×10^{12}	0	17000	[e]
$SC_4H_9O_2 + C_4H_{10} \rightleftharpoons SC_4H_9O_2H + PC_4H_9$	R951	1.70×10^{13}	0	20460	[e]
$SC_4H_9O_2 + C_4H_{10} \rightleftharpoons SC_4H_9O_2H + SC_4H_9$	R952	1.12×10^{13}	0	17700	[e]
$C_2H_5 + C_2H_4 \rightleftharpoons PC_4H_9$	R953	1.32×10^{4}	2.5	6130	[e]
$C_3H_6 + CH_3 \rightleftharpoons SC_4H_9$	R954	1.76×10^{4}	2.5	6130	[e]
$C_4H_{81}\text{-} + H \rightleftharpoons PC_4H_9$	R955	2.50×10^{11}	0.5	2620	[e]
$C_4H_{82}\text{-} + H \rightleftharpoons SC_4H_9$	R956	2.50×10^{11}	0.5	2620	[e]
$C_4H_{81}\text{-} + H \rightleftharpoons SC_4H_9$	R957	4.24×10^{11}	0.5	1230	[e]
$PC_4H_9 + O_2 \rightleftharpoons C_4H_{81}\text{-} + HO_2$	R958	2.00×10^{-18}	0	5000	[e]
$SC_4H_9 + O_2 \rightleftharpoons C_4H_{81}\text{-} + HO_2$	R959	2.00×10^{-18}	0	5000	[e]
$SC_4H_9 + O_2 \rightleftharpoons C_4H_{82}\text{-} + HO_2$	R960	2.00×10^{-18}	0	5000	[e]
$C_2H_3 + C_2H_5 \rightleftharpoons C_4H_{81}$	R961	9.00×10^{12}	0	0	[e]

Reactions	Code	$A_{r,g}$	$\beta_{r,g}$	$E_{r,g}$	Ref
$H + C_4H_{7\text{-}3} \rightleftharpoons C_4H_{81}$	R962	5.00×10^{13}	0	0	[e]
$C_4H_{8\text{-}1} + O_2 \rightleftharpoons C_4H_{7\text{-}3} + HO_2$	R963	2.00×10^{13}	0	37190	[e]
$C_4H_{8\text{-}1} + H \rightleftharpoons C_4H_{7\text{-}1} + H_2$	R964	7.81×10^{5}	2.5	12290	[e]
$C_4H_{8\text{-}1} + H \rightleftharpoons C_4H_{7\text{-}2} + H_2$	R965	3.90×10^{5}	2.5	5821	[e]
$C_4H_{8\text{-}1} + H \rightleftharpoons C_4H_{7\text{-}3} + H_2$	R966	3.38×10^{5}	2.4	207	[e]
$C_4H_{8\text{-}1} + H \rightleftharpoons C_4H_{7\text{-}14} + H_2$	R967	6.65×10^{5}	2.5	6756	[e]
$C_4H_{8\text{-}1} + OH \rightleftharpoons C_4H_{7\text{-}1} + H_2O$	R968	2.14×10^{6}	2	2778	[e]
$C_4H_{8\text{-}1} + OH \rightleftharpoons C_4H_{7\text{-}2} + H_2O$	R969	2.22×10^{6}	2	1451	[e]
$C_4H_{8\text{-}1} + OH \rightleftharpoons C_4H_{7\text{-}3} + H_2O$	R970	2.76×10^{4}	2.6	-1919	[e]
$C_4H_{8\text{-}1} + OH \rightleftharpoons C_4H_{7\text{-}4} + H_2O$	R971	5.27×10^{9}	1	1586	[e]
$C_4H_{8\text{-}1} + CH_3 \rightleftharpoons C_4H_{7\text{-}3} + CH_4$	R972	3.69×10^{0}	3.3	4002	[e]
$C_4H_{8\text{-}1} + CH_3 \rightleftharpoons C_4H_{7\text{-}4} + CH_4$	R973	4.52×10^{-1}	3.6	7154	[e]
$C_4H_{8\text{-}1} + HO_2 \rightleftharpoons C_4H_{7\text{-}3} + H_2O_2$	R974	4.82×10^{3}	2.5	10530	[e]
$C_4H_{8\text{-}1} + HO_2 \rightleftharpoons C_4H_{7\text{-}4} + H_2O_2$	R975	2.38×10^{3}	2.5	16490	[e]
$C_4H_{8\text{-}1} + CH_3O_2 \rightleftharpoons C_4H_{7\text{-}3} + CH_3O_2H$	R976	4.82×10^{3}	2.5	10530	[e]
$C_4H_{8\text{-}1} + CH_3O_2 \rightleftharpoons C_4H_{7\text{-}4} + CH_3O_2H$	R977	2.38×10^{3}	2.5	16490	[e]
$C_4H_{8\text{-}1} + CH_3O \rightleftharpoons C_4H_{7\text{-}3} + CH_3OH$	R978	4.00×10^{1}	2.9	8609	[e]
$C_4H_{8\text{-}1} + CH_3O \rightleftharpoons C_4H_{7\text{-}4} + CH_3OH$	R979	2.17×10^{11}	0	6458	[e]
$C_4H_{8\text{-}1} + CH_3CO_3 \rightleftharpoons C_4H_{7\text{-}3} + CH_3CO_3H$	R980	1.00×10^{11}	0	8000	[e]
$C_4H_{8\text{-}1} + C_3H_5\text{-A} \rightleftharpoons C_4H_{7\text{-}3} + C_3H_6$	R981	7.90×10^{10}	0	12400	[e]
$C_4H_{7\text{-}13} + C_4H_{7\text{-}13} \rightleftharpoons C_4H_{8\text{-}1} + C_4H_6$	R982	1.60×10^{12}	0	0	[e]
$C_4H_{8\text{-}1} + C_2H_5O_2 \rightleftharpoons C_4H_{7\text{-}3} + C_2H_5O_2H$	R983	1.40×10^{12}	0	14900	[e]
$C_4H_{8\text{-}1} + NC_3H_7O_2 \rightleftharpoons C_4H_{7\text{-}3} + NC_3H_7O_2H$	R984	1.40×10^{12}	0	14900	[e]
$C_4H_{8\text{-}1} + IC_3H_7O_2 \rightleftharpoons C_4H_{7\text{-}3} + IC_3H_7O_2H$	R985	1.40×10^{12}	0	14900	[e]
$C_4H_{8\text{-}1} + PC_4H_9O_2 \rightleftharpoons C_4H_{7\text{-}3} + PC_4H_9O_2H$	R986	1.40×10^{12}	0	14900	[e]
$C_4H_{8\text{-}1} + SC_4H_9O_2 \rightleftharpoons C_4H_{7\text{-}3} + SC_4H_9O_2H$	R987	1.40×10^{12}	0	14900	[e]
$C_4H_{8\text{-}1} + CH_3O_2 \rightleftharpoons C_4H_8O_{1\text{-}2} + CH_3O$	R988	1.00×10^{12}	0	14340	[e]
$H + C_4H_{7\text{-}3} \rightleftharpoons C_4H_{8\text{-}2}$	R989	5.00×10^{13}	0	0	[e]
$C_4H_{8\text{-}2} + O_2 \rightleftharpoons C_4H_{7\text{-}3} + HO_2$	R990	4.00×10^{13}	0	39390	[e]
$C_4H_{8\text{-}2} + H \rightleftharpoons C_4H_{7\text{-}3} + H_2$	R991	3.46×10^{5}	2.5	2492	[e]
$C_4H_{8\text{-}2} + OH \rightleftharpoons C_4H_{7\text{-}3} + H_2O$	R992	6.24×10^{6}	2	-298	[e]
$C_4H_{8\text{-}2} + CH_3 \rightleftharpoons C_4H_{7\text{-}3} + CH_4$	R993	4.42×10^{0}	3.5	5675	[e]
$C_4H_{8\text{-}2} + HO_2 \rightleftharpoons C_4H_{7\text{-}3} + H_2O_2$	R994	1.93×10^{4}	2.6	13910	[e]
$C_4H_{8\text{-}2} + CH_3O_2 \rightleftharpoons C_4H_{7\text{-}3} + CH_3O_2H$	R995	1.93×10^{4}	2.6	13910	[e]
$C_4H_{8\text{-}2} + CH_3O \rightleftharpoons C_4H_{7\text{-}3} + CH_3OH$	R996	1.80×10^{1}	3	11990	[e]
$C_4H_{8\text{-}2} + C_2H_5O_2 \rightleftharpoons C_4H_{7\text{-}3} + C_2H_5O_2H$	R997	3.20×10^{12}	0	14900	[e]
$C_4H_{8\text{-}2} + NC_3H_7O_2 \rightleftharpoons C_4H_{7\text{-}3} + NC_3H_7O_2H$	R998	3.20×10^{12}	0	14900	[e]
$C_4H_{8\text{-}2} + IC_3H_7O_2 \rightleftharpoons C_4H_{7\text{-}3} + IC_3H_7O_2H$	R999	3.20×10^{12}	0	14900	[e]

Reactions	Code	$A_{r,g}$	$\beta_{r,g}$	$E_{r,g}$	Ref
$C_4H_{8-2} + PC_4H_9O_2 \rightleftharpoons C_4H_{71-3} + PC_4H_9O_2H$	R1000	3.20×10^{12}	0	14900	[e]
$C_4H_{8-2} + SC_4H_9O_2 \rightleftharpoons C_4H_{71-3} + SC_4H_9O_2H$	R1001	3.20×10^{12}	0	14900	[e]
$C_4H_{8-1} + HO_2 \rightleftharpoons C_4H_8O_{1-2} + OH$	R1002	1.00×10^{12}	0	14340	[e]
$C_4H_{8-2} + HO_2 \rightleftharpoons C_4H_8O_{2-3} + OH$	R1003	5.62×10^{11}	0	12310	[e]
$C_4H_{8-2} + CH_3O_2 \rightleftharpoons C_4H_8O_{2-3} + CH_3O$	R1004	5.62×10^{11}	0	12310	[e]
$C_4H_{8-1} + OH \rightleftharpoons C_4H_8OH_{-1}$	R1005	4.75×10^{12}	0	-782	[e]
$C_4H_{8-2} + OH \rightleftharpoons C_4H_8OH_{-2}$	R1006	4.75×10^{12}	0	-782	[e]
$C_4H_8OH_{-1} + O_2 \rightleftharpoons C_4H_8OH_{-1}O_2$	R1007	2.00×10^{12}	0	0	[e]
$C_4H_8OH_{-2} + O_2 \rightleftharpoons C_4H_8OH_{-2}O_2$	R1008	2.00×10^{12}	0	0	[e]
$C_4H_8OH_{-1}O_2 \rightleftharpoons C_2H_5CHO + CH_2O + OH$	R1009	1.00×10^{16}	0	25000	[e]
$C_4H_8OH_{-2}O_2 \rightleftharpoons OH + CH_3CHO + CH_3CHO$	R1010	1.00×10^{16}	0	25000	[e]
$C_2H_2 + C_2H_5 \rightleftharpoons C_4H_{71-1}$	R1011	2.00×10^{11}	0	7800	[e]
$C_3H_{4-}A + CH_3 \rightleftharpoons C_4H_{71-2}$	R1012	2.00×10^{11}	0	7800	[e]
$C_2H_4 + C_2H_3 \rightleftharpoons C_4H_{71-4}$	R1013	2.00×10^{11}	0	7800	[e]
$C_3H_{4-}P + CH_3 \rightleftharpoons C_4H_{72-2}$	R1014	1.00×10^{11}	0	7800	[e]
$C_4H_6 + H \rightleftharpoons C_4H_{71-3}$	R1015	4.00×10^{13}	0	1300	[e]
$C_4H_{71-3} + C_2H_5 \rightleftharpoons C_4H_{8-1} + C_2H_4$	R1016	2.59×10^{12}	0	-131	[e]
$C_4H_{71-3} + CH_3O \rightleftharpoons C_4H_{8-1} + CH_2O$	R1017	2.41×10^{13}	0	0	[e]
$C_4H_{71-3} + O \rightleftharpoons C_2H_3CHO + CH_3$	R1018	6.03×10^{13}	0	0	[e]
$C_4H_{71-3} + HO_2 \rightleftharpoons C_4H_7O + OH$	R1019	9.64×10^{12}	0	0	[e]
$C_4H_{71-3} + CH_3O_2 \rightleftharpoons C_4H_7O + CH_3O$	R1020	9.64×10^{12}	0	0	[e]
$C_3H_{5-}A + C_4H_{71-3} \rightleftharpoons C_3H_6 + C_4H_6$	R1021	6.31×10^{12}	0	0	[e]
$C_4H_{71-3} + O_2 \rightleftharpoons C_4H_6 + HO_2$	R1022	1.00×10^{9}	0	0	[e]
$H + C_4H_{71-3} \rightleftharpoons C_4H_6 + H_2$	R1023	3.16×10^{13}	0	0	[e]
$C_2H_5 + C_4H_{71-3} \rightleftharpoons C_4H_6 + C_2H_6$	R1024	3.98×10^{12}	0	0	[e]
$C_2H_3 + C_4H_{71-3} \rightleftharpoons C_2H_4 + C_4H_6$	R1025	3.98×10^{12}	0	0	[e]
$C_4H_{71-3} + C_2H_5O_2 \rightleftharpoons C_4H_7O + C_2H_5O$	R1026	3.80×10^{12}	0	-1200	[e]
$IC_3H_7O_2 + C_4H_{71-3} \rightleftharpoons IC_3H_7O + C_4H_7O$	R1027	3.80×10^{12}	0	-1200	[e]
$NC_3H_7O_2 + C_4H_{71-3} \rightleftharpoons NC_3H_7O + C_4H_7O$	R1028	3.80×10^{12}	0	-1200	[e]
$C_4H_7O \rightleftharpoons CH_3CHO + C_2H_3$	R1029	7.94×10^{14}	0	19000	[e]
$C_4H_7O \rightleftharpoons C_2H_3CHO + CH_3$	R1030	7.94×10^{14}	0	19000	[e]
$C_4H_6 \rightleftharpoons C_4H_{5-}I + H$	R1031	5.70×10^{36}	-6.3	112353	[e]
$C_4H_6 \rightleftharpoons C_4H_{5-}N + H$	R1032	5.30×10^{44}	-8.6	123608	[e]
$C_4H_6 \rightleftharpoons C_4H_4 + H_2$	R1033	2.50×10^{15}	0	94700	[e]
$C_4H_6 + H \rightleftharpoons C_4H_{5-}N + H_2$	R1034	1.33×10^{6}	2.5	12240	[e]
$C_4H_6 + H \rightleftharpoons C_4H_{5-}I + H_2$	R1035	6.65×10^{5}	2.5	9240	[e]
$C_4H_6 + H \rightleftharpoons C_2H_4 + C_2H_3$	R1036	5.45×10^{30}	-4.5	21877	[e]
$C_4H_6 + H \rightleftharpoons C_3H_{4-}P + CH_3$	R1037	2.00×10^{12}	0	7000	[e]

Reactions	Code	$A_{r,g}$	$\beta_{r,g}$	$E_{r,g}$	Ref
$C_4H_6 + H \rightleftharpoons C_3H_4\text{-}A + CH_3$	R1038	2.00×10^{12}	0	7000	[e]
$C_4H_6 + O \rightleftharpoons C_4H_5\text{-}N + OH$	R1039	7.50×10^{6}	1.9	3740	[e]
$C_4H_6 + O \rightleftharpoons C_4H_5\text{-}I + OH$	R1040	7.50×10^{6}	1.9	3740	[e]
$C_4H_6 + O \rightleftharpoons CH_3CHCHCO + H$	R1041	1.50×10^{8}	1.4	-860	[e]
$C_4H_6 + O \rightleftharpoons CH_2CHCHCHO + H$	R1042	4.50×10^{8}	1.4	-860	[e]
$C_4H_6 + OH \rightleftharpoons C_4H_5\text{-}N + H_2O$	R1043	6.20×10^{6}	2	3430	[e]
$C_4H_6 + OH \rightleftharpoons C_4H_5\text{-}I + H_2O$	R1044	3.10×10^{6}	2	430	[e]
$C_4H_6 + HO_2 \rightleftharpoons C_4H_6O_{25} + OH$	R1045	1.20×10^{12}	0	14000	[e]
$C_4H_6 + HO_2 \rightleftharpoons C_2H_3CHOCH_2 + OH$	R1046	4.80×10^{12}	0	14000	[e]
$C_4H_6 + CH_3 \rightleftharpoons C_4H_5\text{-}N + CH_4$	R1047	2.00×10^{14}	0	22800	[e]
$C_4H_6 + CH_3 \rightleftharpoons C_4H_5\text{-}I + CH_4$	R1048	1.00×10^{14}	0	19800	[e]
$C_4H_6 + C_2H_3 \rightleftharpoons C_4H_5\text{-}N + C_2H_4$	R1049	5.00×10^{13}	0	22800	[e]
$C_4H_6 + C_2H_3 \rightleftharpoons C_4H_5\text{-}I + C_2H_4$	R1050	2.50×10^{13}	0	19800	[e]
$C_4H_6 + C_3H_3 \rightleftharpoons C_4H_5\text{-}N + C_3H_4\text{-}A$	R1051	1.00×10^{13}	0	22500	[e]
$C_4H_6 + C_3H_3 \rightleftharpoons C_4H_5\text{-}I + C_3H_4\text{-}A$	R1052	5.00×10^{12}	0	19500	[e]
$C_4H_6 + C_3H_5\text{-}A \rightleftharpoons C_4H_5\text{-}N + C_3H_6$	R1053	1.00×10^{13}	0	22500	[e]
$C_4H_6 + C_3H_5\text{-}A \rightleftharpoons C_4H_5\text{-}I + C_3H_6$	R1054	5.00×10^{12}	0	19500	[e]
$C_4H_6 + C_2H_3 \rightleftharpoons C_6H_6 + H_2 + H$	R1055	5.62×10^{11}	0	3240	[e]
$C_4H_{71\text{-}4} \rightleftharpoons C_4H_6 + H$	R1056	1.85×10^{48}	-10.5	51770	[e]
$C_4H_5\text{-}N \rightleftharpoons C_4H_5\text{-}I$	R1057	1.50×10^{67}	-16.9	59100	[e]
$C_4H_5\text{-}N + H \rightleftharpoons C_4H_5\text{-}I + H$	R1058	3.10×10^{26}	-3.4	17423	[e]
$C_4H_5\text{-}N + H \rightleftharpoons C_4H_4 + H_2$	R1059	1.50×10^{13}	0	0	[e]
$C_4H_5\text{-}N + OH \rightleftharpoons C_4H_4 + H_2O$	R1060	2.00×10^{12}	0	0	[e]
$C_4H_5\text{-}N + HCO \rightleftharpoons C_4H_6 + CO$	R1061	5.00×10^{12}	0	0	[e]
$C_4H_5\text{-}N + HO_2 \rightleftharpoons C_2H_3 + CH_2CO + OH$	R1062	6.60×10^{12}	0	0	[e]
$C_4H_5\text{-}N + H_2O_2 \rightleftharpoons C_4H_6 + HO_2$	R1063	1.21×10^{10}	0	-596	[e]
$C_4H_5\text{-}N + HO_2 \rightleftharpoons C_4H_6 + O_2$	R1064	6.00×10^{11}	0	0	[e]
$C_4H_5\text{-}N + O_2 \rightleftharpoons CH_2CHCHCHO + O$	R1065	3.00×10^{11}	0.3	11	[e]
$C_4H_5\text{-}N + O_2 \rightleftharpoons HCO + C_2H_3CHO$	R1066	9.20×10^{16}	-1.4	1010	[e]
$C_4H_5\text{-}N + C_2H_2 \rightleftharpoons C_6H_6 + H$	R1067	1.60×10^{16}	-1.3	5400	[e]
$C_4H_5\text{-}N + C_2H_3 \rightleftharpoons C_6H_6 + H_2$	R1068	1.84×10^{-13}	7.1	-3611	[e]
$C_4H_5\text{-}N + C_4H_4 \rightleftharpoons C_6H_5C_2H_3 + H$	R1069	3.16×10^{11}	0	600	[e]
$C_4H_5\text{-}I + H \rightleftharpoons C_4H_4 + H_2$	R1070	3.00×10^{13}	0	0	[e]
$C_4H_5\text{-}I + H \rightleftharpoons C_3H_3 + CH_3$	R1071	2.00×10^{13}	0	2000	[e]
$C_4H_5\text{-}I + OH \rightleftharpoons C_4H_4 + H_2O$	R1072	4.00×10^{12}	0	0	[e]
$C_4H_5\text{-}I + HCO \rightleftharpoons C_4H_6 + CO$	R1073	5.00×10^{12}	0	0	[e]
$C_4H_5\text{-}I + HO_2 \rightleftharpoons C_4H_6 + O_2$	R1074	6.00×10^{11}	0	0	[e]
$C_4H_5\text{-}I + HO_2 \rightleftharpoons C_2H_3 + CH_2CO + OH$	R1075	6.60×10^{12}	0	0	[e]

Reactions	Code	$A_{r,g}$	$\beta_{r,g}$	$E_{r,g}$	Ref
$C_4H_5\text{-}I + H_2O_2 \rightleftharpoons C_4H_6 + HO_2$	R1076	1.21×10^{10}	0	-596	[e]
$C_4H_5\text{-}I + O_2 \rightleftharpoons CH_2CO + CH_2CHO$	R1077	2.16×10^{10}	0	2500	[e]
$C_4H_5\text{-}I + C_4H_4 \rightleftharpoons C_6H_5C_2H_3 + H$	R1078	5.00×10^{14}	0	25000	[e]
$C_4H_5\text{-}_2 \rightleftharpoons C_4H_5\text{-}I$	R1079	1.50×10^{67}	-16.9	59100	[e]
$C_4H_5\text{-}_2 + H \rightleftharpoons C_4H_5\text{-}I + H$	R1080	3.10×10^{26}	-3.4	17423	[e]
$C_4H_5\text{-}_2 + HO_2 \rightleftharpoons OH + C_2H_2 + CH_3CO$	R1081	8.00×10^{11}	0	0	[e]
$C_4H_5\text{-}_2 + O_2 \rightleftharpoons CH_3CO + CH_2CO$	R1082	2.16×10^{10}	0	2500	[e]
$C_4H_5\text{-}_2 + C_2H_2 \rightleftharpoons C_6H_6 + H$	R1083	5.00×10^{14}	0	25000	[e]
$C_4H_5\text{-}_2 + C_2H_4 \rightleftharpoons C_5H_6 + CH_3$	R1084	5.00×10^{14}	0	25000	[e]
$C_4H_5\text{-}_2 + C_4H_4 \rightleftharpoons C_6H_5C_2H_3 + H$	R1085	5.00×10^{14}	0	25000	[e]
$C_4H_6\text{-}_2 \rightleftharpoons C_4H_5\text{-}I + H$	R1086	4.20×10^{15}	0	92600	[e]
$C_4H_6\text{-}_2 + H \rightleftharpoons C_4H_6 + H$	R1087	2.00×10^{13}	0	4000	[e]
$C_4H_6\text{-}_2 + H \rightleftharpoons C_4H_5\text{-}I + H_2$	R1088	1.70×10^{5}	2.5	2490	[e]
$C_4H_6\text{-}_2 + H \rightleftharpoons C_3H_4\text{-}A + CH_3$	R1089	2.00×10^{13}	0	2000	[e]
$C_4H_6\text{-}_2 + H \rightleftharpoons C_3H_4\text{-}P + CH_3$	R1090	2.00×10^{13}	0	2000	[e]
$C_4H_6\text{-}_2 + CH_3 \rightleftharpoons C_4H_5\text{-}I + CH_4$	R1091	7.00×10^{13}	0	18500	[e]
$C_4H_6\text{-}_2 + O \rightleftharpoons CH_2CO + C_2H_4$	R1092	1.20×10^{8}	1.6	327	[e]
$C_4H_6\text{-}_2 + O \rightleftharpoons C_4H_5\text{-}I + OH$	R1093	1.80×10^{11}	0.7	5880	[e]
$C_4H_6\text{-}_2 + OH \rightleftharpoons C_4H_5\text{-}I + H_2O$	R1094	3.10×10^{6}	2	-298	[e]
$C_4H_6\text{-}_2 \rightleftharpoons C_4H_6$	R1095	3.00×10^{13}	0	65000	[e]
$C_4H_6\text{-}_2 \rightleftharpoons C_4H_6$	R1096	3.00×10^{13}	0	65000	[e]
$C_4H_6\text{-}_2 \rightleftharpoons C_4H_6\text{-}_2$	R1097	3.00×10^{13}	0	67000	[e]
$C_4H_6\text{-}_2 + H \rightleftharpoons C_4H_6\text{-}_2 + H$	R1098	2.00×10^{13}	0	4000	[e]
$C_4H_6\text{-}_2 + H \rightleftharpoons C_4H_5\text{-}_2 + H_2$	R1099	3.40×10^{5}	2.5	2490	[e]
$C_4H_6\text{-}_2 + H \rightleftharpoons CH_3 + C_3H_4\text{-}P$	R1100	2.60×10^{5}	2.5	1000	[e]
$C_4H_6\text{-}_2 \rightleftharpoons H + C_4H_5\text{-}_2$	R1101	5.00×10^{15}	0	87300	[e]
$C_4H_6\text{-}_2 + CH_3 \rightleftharpoons C_4H_5\text{-}_2 + CH_4$	R1102	1.40×10^{14}	0	18500	[e]
$C_2H_3CHOCH_2 \rightleftharpoons C_4H_6O_{23}$	R1103	2.00×10^{14}	0	50600	[e]
$C_4H_6O_{23} \rightleftharpoons CH_3CHCHCHO$	R1104	1.95×10^{13}	0	49400	[e]
$C_4H_6O_{23} \rightleftharpoons C_2H_4 + CH_2CO$	R1105	5.75×10^{15}	0	69300	[e]
$C_4H_6O_{23} \rightleftharpoons C_2H_2 + C_2H_4O_{1\text{-}2}$	R1106	1.00×10^{16}	0	75800	[e]
$C_4H_6O_{25} \rightleftharpoons C_4H_4O + H_2$	R1107	5.30×10^{12}	0	48500	[e]
$C_4H_4O \rightleftharpoons CO + C_3H_4\text{-}P$	R1108	1.78×10^{15}	0	77500	[e]
$C_4H_4O \rightleftharpoons C_2H_2 + CH_2CO$	R1109	5.01×10^{14}	0	77500	[e]
$CH_3CHCHCHO \rightleftharpoons C_3H_6 + CO$	R1110	3.90×10^{14}	0	69000	[e]
$CH_3CHCHCHO + H \rightleftharpoons CH_2CHCHCHO + H_2$	R1111	1.70×10^{5}	2.5	2490	[e]
$CH_3CHCHCHO + H \rightleftharpoons CH_3CHCHCO + H_2$	R1112	1.00×10^{5}	2.5	2490	[e]
$CH_3CHCHCHO + H \rightleftharpoons CH_3 + C_2H_3CHO$	R1113	4.00×10^{21}	-2.4	11180	[e]

Reactions	Code	$A_{r,g}$	$\beta_{r,g}$	$E_{r,g}$	Ref
$CH_3CHCHCHO + H \rightleftharpoons C_3H_6 + HCO$	R1114	4.00×10^{21}	-2.4	11180	[e]
$CH_3CHCHCHO + CH_3 \rightleftharpoons CH_2CHCHCHO + CH_4$	R1115	2.10×10^{0}	3.5	5675	[e]
$CH_3CHCHCHO + CH_3 \rightleftharpoons CH_3CHCHCO + CH_4$	R1116	1.10×10^{0}	3.5	5675	[e]
$CH_3CHCHCHO + C_2H_3 \rightleftharpoons CH_2CHCHCHO + C_2H_4$	R1117	2.21×10^{0}	3.5	4682	[e]
$CH_3CHCHCHO + C_2H_3 \rightleftharpoons CH_3CHCHCO + C_2H_4$	R1118	1.11×10^{0}	3.5	4682	[e]
$CH_3CHCHCO \rightleftharpoons C_3H_5\text{-}S + CO$	R1119	1.00×10^{14}	0	30000	[e]
$CH_3CHCHCO + H \rightleftharpoons CH_3CHCHCHO$	R1120	1.00×10^{14}	0	0	[e]
$CH_2CHCHCHO \rightleftharpoons C_3H_5\text{-}A + CO$	R1121	1.00×10^{14}	0	25000	[e]
$CH_2CHCHCHO + H \rightleftharpoons CH_3CHCHCHO$	R1122	1.00×10^{14}	0	0	[e]
$C_6H_2 + H \rightleftharpoons C_6H_3$	R1123	1.10×10^{30}	-4.9	10800	[e]
$C_6H_3 + H \rightleftharpoons C_4H_2 + C_2H_2$	R1124	2.80×10^{23}	-2.5	10780	[e]
$C_6H_3 + H \rightleftharpoons L\text{-}C_6H_4$	R1125	3.40×10^{43}	-9	12120	[e]
$C_6H_3 + H \rightleftharpoons C_6H_2 + H_2$	R1126	3.00×10^{13}	0	0	[e]
$C_6H_3 + OH \rightleftharpoons C_6H_2 + H_2O$	R1127	4.00×10^{12}	0	0	[e]
$C_6H_3 + O_2 \rightarrow CO + C_3H_2 + HCCO$	R1128	5.00×10^{11}	0	0	[e]
$L\text{-}C_6H_4 + H \rightleftharpoons C_6H_5$	R1129	1.70×10^{78}	-19.7	31400	[e]
$L\text{-}C_6H_4 + H \rightleftharpoons C\text{-}C_6H_4 + H$	R1130	1.40×10^{54}	-11.7	34500	[e]
$L\text{-}C_6H_4 + H \rightleftharpoons C_6H_3 + H_2$	R1131	1.33×10^{6}	2.5	9240	[e]
$L\text{-}C_6H_4 + OH \rightleftharpoons C_6H_3 + H_2O$	R1132	3.10×10^{6}	2	430	[e]
$C\text{-}C_6H_4 + H \rightleftharpoons C_6H_5$	R1133	2.40×10^{60}	-13.7	29500	[e]
$C_4H_4 + H \rightleftharpoons C_4H_5\text{-}N$	R1134	1.30×10^{51}	-11.9	16500	[e]
$C_4H_4 + H \rightleftharpoons C_4H_5\text{-}I$	R1135	4.90×10^{51}	-11.9	17700	[e]
$C_4H_4 + H \rightleftharpoons C_4H_3\text{-}N + H_2$	R1136	6.65×10^{5}	2.5	12240	[e]
$C_4H_4 + H \rightleftharpoons C_4H_3\text{-}I + H_2$	R1137	3.33×10^{5}	2.5	9240	[e]
$C_4H_4 + OH \rightleftharpoons C_4H_3\text{-}N + H_2O$	R1138	3.10×10^{7}	2	3430	[e]
$C_4H_4 + OH \rightleftharpoons C_4H_3\text{-}I + H_2O$	R1139	1.55×10^{7}	2	430	[e]
$C_4H_4 + O \rightleftharpoons C_3H_3 + HCO$	R1140	6.00×10^{8}	1.4	-860	[e]
$C_4H_4 + C_2H \rightleftharpoons L\text{-}C_6H_4 + H$	R1141	1.20×10^{13}	0	0	[e]
$C_4H_3\text{-}N \rightleftharpoons C_4H_3\text{-}I$	R1142	4.10×10^{43}	-9.5	53000	[e]
$C_4H_3\text{-}N + H \rightleftharpoons C_4H_3\text{-}I + H$	R1143	2.50×10^{20}	-1.7	10800	[e]
$C_4H_3\text{-}N + H \rightleftharpoons C_2H_2 + H_2CC$	R1144	6.30×10^{25}	-3.3	10014	[e]
$C_4H_3\text{-}N + H \rightleftharpoons C_4H_4$	R1145	2.00×10^{47}	-10.3	13070	[e]
$C_4H_3\text{-}N + H \rightleftharpoons C_4H_2 + H_2$	R1146	3.00×10^{13}	0	0	[e]
$C_4H_3\text{-}N + OH \rightleftharpoons C_4H_2 + H_2O$	R1147	2.00×10^{12}	0	0	[e]
$C_4H_3\text{-}N + C_2H_2 \rightleftharpoons L\text{-}C_6H_4 + H$	R1148	2.50×10^{14}	-0.6	10600	[e]
$C_4H_3\text{-}N + C_2H_2 \rightleftharpoons C_6H_5$	R1149	9.60×10^{70}	-17.8	31300	[e]
$C_4H_3\text{-}N + C_2H_2 \rightleftharpoons C\text{-}C_6H_4 + H$	R1150	6.90×10^{46}	-10	30100	[e]
$C_4H_3\text{-}I + H \rightleftharpoons C_2H_2 + H_2CC$	R1151	2.80×10^{23}	-2.5	10780	[e]
$C_4H_3\text{-}I + H \rightleftharpoons C_4H_4$	R1152	3.40×10^{43}	-9	12120	[e]

Reactions	Code	$A_{r,g}$	$\beta_{r,g}$	$E_{r,g}$	Ref
$C_4H_3\text{-}I + H \rightleftharpoons C_4H_2 + H_2$	R1153	6.00×10^{13}	0	0	[e]
$C_4H_3\text{-}I + OH \rightleftharpoons C_4H_2 + H_2O$	R1154	4.00×10^{12}	0	0	[e]
$C_4H_3\text{-}I + O_2 \rightleftharpoons HCCO + CH_2CO$	R1155	7.86×10^{16}	-1.8	0	[e]
$C_4H_3\text{-}I + CH_2 \rightleftharpoons C_3H_4\text{-}A + C_2H$	R1156	2.00×10^{13}	0	0	[e]
$C_4H_3\text{-}I + CH_3 \rightleftharpoons C_5H_6$	R1157	1.00×10^{12}	0	0	[e]
$C_4H_2 + H \rightleftharpoons C_4H_3\text{-}N$	R1158	1.10×10^{42}	-8.7	15300	[e]
$C_4H_2 + H \rightleftharpoons C_4H_3\text{-}I$	R1159	1.10×10^{30}	-4.9	10800	[e]
$C_4H_2 + O \rightleftharpoons C_3H_2 + CO$	R1160	2.70×10^{13}	0	1720	[e]
$C_4H_2 + OH \rightleftharpoons H_2C_4O + H$	R1161	6.60×10^{12}	0	-410	[e]
$C_4H_2 + C_2H \rightleftharpoons C_6H_2 + H$	R1162	9.60×10^{13}	0	0	[e]
$C_4H_2 + C_2H \rightleftharpoons C_6H_3$	R1163	4.50×10^{37}	-7.7	7100	[e]
$H_2C_4O + H \rightleftharpoons C_2H_2 + HCCO$	R1164	5.00×10^{13}	0	3000	[e]
$H_2C_4O + OH \rightleftharpoons CH_2CO + HCCO$	R1165	1.00×10^{7}	2	2000	[e]
$H_2CC + H \rightleftharpoons C_2H_2 + H$	R1166	1.00×10^{14}	0	0	[e]
$H_2CC + OH \rightleftharpoons CH_2CO + H$	R1167	2.00×10^{13}	0	0	[e]
$H_2CC + O_2 \rightleftharpoons HCO + HCO$	R1168	1.00×10^{13}	0	0	[e]
$H_2CC + C_2H_2(+M) \rightleftharpoons C_4H_4(+M)$	R1169	3.50×10^{5}	2.1	-2400	[e]
$H_2CC + C_2H_4 \rightleftharpoons C_4H_6$	R1170	1.00×10^{12}	0	0	[e]
$C_4H_8O_{1\text{-}2} + OH \rightleftharpoons CH_2O + C_3H_5\text{-}A + H_2O$	R1171	5.00×10^{12}	0	0	[e]
$C_4H_8O_{1\text{-}2} + H \rightleftharpoons CH_2O + C_3H_5\text{-}A + H_2$	R1172	5.00×10^{12}	0	0	[e]
$C_4H_8O_{1\text{-}2} + O \rightleftharpoons CH_2O + C_3H_5\text{-}A + OH$	R1173	5.00×10^{12}	0	0	[e]
$C_4H_8O_{1\text{-}2} + HO_2 \rightleftharpoons CH_2O + C_3H_5\text{-}A + H_2O_2$	R1174	1.00×10^{13}	0	15000	[e]
$C_4H_8O_{1\text{-}2} + CH_3O_2 \rightleftharpoons CH_2O + C_3H_5\text{-}A + CH_3O_2H$	R1175	1.00×10^{13}	0	19000	[e]
$C_4H_8O_{1\text{-}2} + CH_3 \rightleftharpoons CH_2O + C_3H_5\text{-}A + CH_4$	R1176	2.00×10^{11}	0	10000	[e]
$C_4H_8O_{1\text{-}3} + OH \rightleftharpoons CH_2O + C_3H_5\text{-}A + H_2O$	R1177	5.00×10^{12}	0	0	[e]
$C_4H_8O_{1\text{-}3} + H \rightleftharpoons CH_2O + C_3H_5\text{-}A + H_2$	R1178	5.00×10^{12}	0	0	[e]
$C_4H_8O_{1\text{-}3} + O \rightleftharpoons CH_2O + C_3H_5\text{-}A + OH$	R1179	5.00×10^{12}	0	0	[e]
$C_4H_8O_{1\text{-}3} + HO_2 \rightleftharpoons CH_2O + C_3H_5\text{-}A + H_2O_2$	R1180	1.00×10^{13}	0	15000	[e]
$C_4H_8O_{1\text{-}3} + CH_3O_2 \rightleftharpoons CH_2O + C_3H_5\text{-}A + CH_3O_2H$	R1181	1.00×10^{13}	0	19000	[e]
$C_4H_8O_{1\text{-}3} + CH_3 \rightleftharpoons CH_2O + C_3H_5\text{-}A + CH_4$	R1182	2.00×10^{11}	0	10000	[e]
$C_4H_8O_{1\text{-}4} + OH \rightleftharpoons CH_2O + C_3H_5\text{-}A + H_2O$	R1183	5.00×10^{12}	0	0	[e]
$C_4H_8O_{1\text{-}4} + H \rightleftharpoons CH_2O + C_3H_5\text{-}A + H_2$	R1184	5.00×10^{12}	0	0	[e]
$C_4H_8O_{1\text{-}4} + O \rightleftharpoons CH_2O + C_3H_5\text{-}A + OH$	R1185	5.00×10^{12}	0	0	[e]
$C_4H_8O_{1\text{-}4} + HO_2 \rightleftharpoons CH_2O + C_3H_5\text{-}A + H_2O_2$	R1186	1.00×10^{13}	0	15000	[e]
$C_4H_8O_{1\text{-}4} + CH_3O_2 \rightleftharpoons CH_2O + C_3H_5\text{-}A + CH_3O_2H$	R1187	1.00×10^{13}	0	19000	[e]
$C_4H_8O_{1\text{-}4} + CH_3 \rightleftharpoons CH_2O + C_3H_5\text{-}A + CH_4$	R1188	2.00×10^{11}	0	10000	[e]
$C_4H_8O_{2\text{-}3} + OH \rightleftharpoons CH_2O + C_3H_5\text{-}A + H_2O$	R1189	5.00×10^{12}	0	0	[e]
$C_4H_8O_{2\text{-}3} + H \rightleftharpoons CH_2O + C_3H_5\text{-}A + H_2$	R1190	5.00×10^{12}	0	0	[e]

Reactions	Code	$A_{r,g}$	$\beta_{r,g}$	$E_{r,g}$	Ref
$C_4H_8O_{2-3} + O \rightleftharpoons CH_2O + C_3H_5\text{-}A + OH$	R1191	5.00×10^{12}	0	0	[e]
$C_4H_8O_{2-3} + HO_2 \rightleftharpoons CH_2O + C_3H_5\text{-}A + H_2O_2$	R1192	1.00×10^{13}	0	15000	[e]
$C_4H_8O_{2-3} + CH_3O_2 \rightleftharpoons CH_2O + C_3H_5\text{-}A + CH_3O_2H$	R1193	1.00×10^{13}	0	19000	[e]
$C_4H_8O_{2-3} + CH_3 \rightleftharpoons CH_2O + C_3H_5\text{-}A + CH_4$	R1194	2.00×10^{11}	0	10000	[e]
$PC_4H_9 + O_2 \rightleftharpoons PC_4H_9O_2$	R1195	4.52×10^{12}	0	0	[e]
$SC_4H_9 + O_2 \rightleftharpoons SC_4H_9O_2$	R1196	7.54×10^{12}	0	0	[e]
$SC_4H_9O_2 + CH_2O \rightleftharpoons SC_4H_9O_2H + HCO$	R1197	5.60×10^{12}	0	13600	[e]
$SC_4H_9O_2 + CH_3CHO \rightleftharpoons SC_4H_9O_2H + CH_3CO$	R1198	2.80×10^{12}	0	13600	[e]
$SC_4H_9O_2 + HO_2 \rightleftharpoons SC_4H_9O_2H + O_2$	R1199	1.75×10^{10}	0	-3275	[e]
$IC_3H_7O_2 + PC_4H_9 \rightleftharpoons IC_3H_7O + PC_4H_9O$	R1200	7.00×10^{12}	0	-1000	[e]
$IC_3H_7O_2 + SC_4H_9 \rightleftharpoons IC_3H_7O + SC_4H_9O$	R1201	7.00×10^{12}	0	-1000	[e]
$NC_3H_7O_2 + PC_4H_9 \rightleftharpoons NC_3H_7O + PC_4H_9O$	R1202	7.00×10^{12}	0	-1000	[e]
$NC_3H_7O_2 + SC_4H_9 \rightleftharpoons NC_3H_7O + SC_4H_9O$	R1203	7.00×10^{12}	0	-1000	[e]
$SC_4H_9O_2 + SC_4H_9O_2 \rightleftharpoons O_2 + SC_4H_9O + SC_4H_9O$	R1204	1.40×10^{16}	-1.6	1860	[e]
$SC_4H_9O_2 + NC_3H_7O_2 \rightleftharpoons SC_4H_9O + NC_3H_7O + O_2$	R1205	1.40×10^{16}	-1.6	1860	[e]
$SC_4H_9O_2 + IC_3H_7O_2 \rightleftharpoons SC_4H_9O + IC_3H_7O + O_2$	R1206	1.40×10^{16}	-1.6	1860	[e]
$SC_4H_9O_2 + C_2H_5O_2 \rightleftharpoons SC_4H_9O + C_2H_5O + O_2$	R1207	1.40×10^{16}	-1.6	1860	[e]
$SC_4H_9O_2 + CH_3O_2 \rightleftharpoons SC_4H_9O + CH_3O + O_2$	R1208	1.40×10^{16}	-1.6	1860	[e]
$SC_4H_9O_2 + CH_3CO_3 \rightleftharpoons SC_4H_9O + CH_3CO_2 + O_2$	R1209	1.40×10^{16}	-1.6	1860	[e]
$PC_4H_9O_2 + HO_2 \rightleftharpoons PC_4H_9O + OH + O_2$	R1210	1.40×10^{-14}	-1.6	1860	[e]
$SC_4H_9O_2 + HO_2 \rightleftharpoons SC_4H_9O + OH + O_2$	R1211	1.40×10^{-14}	-1.6	1860	[e]
$H_2 + PC_4H_9O_2 \rightleftharpoons H + PC_4H_9O_2H$	R1212	3.01×10^{13}	0	26030	[e]
$H_2 + SC_4H_9O_2 \rightleftharpoons H + SC_4H_9O_2H$	R1213	3.01×10^{13}	0	26030	[e]
$C_2H_6 + PC_4H_9O_2 \rightleftharpoons C_2H_5 + PC_4H_9O_2H$	R1214	1.70×10^{13}	0	20460	[e]
$C_2H_6 + SC_4H_9O_2 \rightleftharpoons C_2H_5 + SC_4H_9O_2H$	R1215	1.70×10^{13}	0	20460	[e]
$PC_4H_9O_2 + C_2H_5CHO \rightleftharpoons PC_4H_9O_2H + C_2H_5CO$	R1216	2.00×10^{11}	0	9500	[e]
$SC_4H_9O_2 + C_2H_5CHO \rightleftharpoons SC_4H_9O_2H + C_2H_5CO$	R1217	2.00×10^{11}	0	9500	[e]
$SC_4H_9O_2 + CH_3 \rightleftharpoons SC_4H_9O + CH_3O$	R1218	7.00×10^{12}	0	-1000	[e]
$SC_4H_9O_2 + C_2H_5 \rightleftharpoons SC_4H_9O + C_2H_5O$	R1219	7.00×10^{12}	0	-1000	[e]
$SC_4H_9O_2 + IC_3H_7 \rightleftharpoons SC_4H_9O + IC_3H_7O$	R1220	7.00×10^{12}	0	-1000	[e]
$SC_4H_9O_2 + NC_3H_7 \rightleftharpoons SC_4H_9O + NC_3H_7O$	R1221	7.00×10^{12}	0	-1000	[e]
$SC_4H_9O_2 + PC_4H_9 \rightleftharpoons SC_4H_9O + PC_4H_9O$	R1222	7.00×10^{12}	0	-1000	[e]
$SC_4H_9O_2 + SC_4H_9 \rightleftharpoons SC_4H_9O + SC_4H_9O$	R1223	7.00×10^{12}	0	-1000	[e]
$SC_4H_9O_2 + C_3H_5\text{-}A \rightleftharpoons SC_4H_9O + C_3H_5O$	R1224	7.00×10^{12}	0	-1000	[e]
$PC_4H_9O_2 + CH_2O \rightleftharpoons PC_4H_9O_2H + HCO$	R1225	5.60×10^{12}	0	13600	[e]
$PC_4H_9O_2 + CH_3CHO \rightleftharpoons PC_4H_9O_2H + CH_3CO$	R1226	2.80×10^{12}	0	13600	[e]
$PC_4H_9O_2 + HO_2 \rightleftharpoons PC_4H_9O_2H + O_2$	R1227	1.75×10^{10}	0	-3275	[e]
$C_3H_6 + PC_4H_9O_2 \rightleftharpoons C_3H_5\text{-}A + PC_4H_9O_2H$	R1228	3.24×10^{11}	0	14900	[e]

Reactions	Code	$A_{r,g}$	$\beta_{r,g}$	$E_{r,g}$	Ref
$C_3H_6 + SC_4H_9O_2 \rightleftharpoons C_3H_5\text{-}A + SC_4H_9O_2H$	R1229	3.24×10^{11}	0	14900	[e]
$C_2H_4 + PC_4H_9O_2 \rightleftharpoons C_2H_3 + PC_4H_9O_2H$	R1230	1.13×10^{13}	0	30430	[e]
$C_2H_4 + SC_4H_9O_2 \rightleftharpoons C_2H_3 + SC_4H_9O_2H$	R1231	1.13×10^{13}	0	30430	[e]
$CH_3OH + PC_4H_9O_2 \rightleftharpoons CH_2OH + PC_4H_9O_2H$	R1232	6.30×10^{12}	0	19360	[e]
$CH_3OH + SC_4H_9O_2 \rightleftharpoons CH_2OH + SC_4H_9O_2H$	R1233	6.30×10^{12}	0	19360	[e]
$C_2H_3CHO + PC_4H_9O_2 \rightleftharpoons C_2H_3CO + PC_4H_9O_2H$	R1234	2.80×10^{12}	0	13600	[e]
$C_2H_3CHO + SC_4H_9O_2 \rightleftharpoons C_2H_3CO + SC_4H_9O_2H$	R1235	2.80×10^{12}	0	13600	[e]
$CH_4 + PC_4H_9O_2 \rightleftharpoons CH_3 + PC_4H_9O_2H$	R1236	1.12×10^{13}	0	24640	[e]
$CH_4 + SC_4H_9O_2 \rightleftharpoons CH_3 + SC_4H_9O_2H$	R1237	1.12×10^{13}	0	24640	[e]
$C_4H_{71}\text{-}_3 + PC_4H_9O_2 \rightleftharpoons C_4H_7O + PC_4H_9O$	R1238	7.00×10^{12}	0	-1000	[e]
$C_4H_{71}\text{-}_3 + SC_4H_9O_2 \rightleftharpoons C_4H_7O + SC_4H_9O$	R1239	7.00×10^{12}	0	-1000	[e]
$H_2O_2 + PC_4H_9O_2 \rightleftharpoons HO_2 + PC_4H_9O_2H$	R1240	2.40×10^{12}	0	10000	[e]
$H_2O_2 + SC_4H_9O_2 \rightleftharpoons HO_2 + SC_4H_9O_2H$	R1241	2.40×10^{12}	0	10000	[e]
$PC_4H_9O_2 + PC_4H_9O_2 \rightleftharpoons O_2 + PC_4H_9O + PC_4H_9O$	R1242	1.40×10^{16}	-1.6	1860	[e]
$PC_4H_9O_2 + SC_4H_9O_2 \rightleftharpoons PC_4H_9O + SC_4H_9O + O_2$	R1243	1.40×10^{16}	-1.6	1860	[e]
$PC_4H_9O_2 + NC_3H_7O_2 \rightleftharpoons PC_4H_9O + NC_3H_7O + O_2$	R1244	1.40×10^{16}	-1.6	1860	[e]
$PC_4H_9O_2 + IC_3H_7O_2 \rightleftharpoons PC_4H_9O + IC_3H_7O + O_2$	R1245	1.40×10^{16}	-1.6	1860	[e]
$PC_4H_9O_2 + C_2H_5O_2 \rightleftharpoons PC_4H_9O + C_2H_5O + O_2$	R1246	1.40×10^{16}	-1.6	1860	[e]
$PC_4H_9O_2 + CH_3O_2 \rightleftharpoons PC_4H_9O + CH_3O + O_2$	R1247	1.40×10^{16}	-1.6	1860	[e]
$PC_4H_9O_2 + CH_3CO_3 \rightleftharpoons PC_4H_9O + CH_3CO_2 + O_2$	R1248	1.40×10^{16}	-1.6	1860	[e]
$PC_4H_9O_2 + CH_3 \rightleftharpoons PC_4H_9O + CH_3O$	R1249	7.00×10^{12}	0	-1000	[e]
$PC_4H_9O_2 + C_2H_5 \rightleftharpoons PC_4H_9O + C_2H_5O$	R1250	7.00×10^{12}	0	-1000	[e]
$PC_4H_9O_2 + IC_3H_7 \rightleftharpoons PC_4H_9O + IC_3H_7O$	R1251	7.00×10^{12}	0	-1000	[e]
$PC_4H_9O_2 + NC_3H_7 \rightleftharpoons PC_4H_9O + NC_3H_7O$	R1252	7.00×10^{12}	0	-1000	[e]
$PC_4H_9O_2 + PC_4H_9 \rightleftharpoons PC_4H_9O + PC_4H_9O$	R1253	7.00×10^{12}	0	-1000	[e]
$PC_4H_9O_2 + SC_4H_9 \rightleftharpoons PC_4H_9O + SC_4H_9O$	R1254	7.00×10^{12}	0	-1000	[e]
$PC_4H_9O_2 + C_3H_5\text{-}A \rightleftharpoons PC_4H_9O + C_3H_5O$	R1255	7.00×10^{12}	0	-1000	[e]
$PC_4H_9 + HO_2 \rightleftharpoons PC_4H_9O + OH$	R1256	7.00×10^{12}	0	-1000	[e]
$SC_4H_9 + HO_2 \rightleftharpoons SC_4H_9O + OH$	R1257	7.00×10^{12}	0	-1000	[e]
$CH_3O_2 + PC_4H_9 \rightleftharpoons CH_3O + PC_4H_9O$	R1258	7.00×10^{12}	0	-1000	[e]
$CH_3O_2 + SC_4H_9 \rightleftharpoons CH_3O + SC_4H_9O$	R1259	7.00×10^{12}	0	-1000	[e]
$PC_4H_9O_2H \rightleftharpoons PC_4H_9O + OH$	R1260	1.50×10^{16}	0	42500	[e]
$SC_4H_9O_2H \rightleftharpoons SC_4H_9O + OH$	R1261	9.45×10^{15}	0	41600	[e]
$NC_3H_7 + CH_2O \rightleftharpoons PC_4H_9O$	R1262	5.00×10^{10}	0	3457	[e]
$CH_3 + C_2H_5CHO \rightleftharpoons SC_4H_9O$	R1263	5.00×10^{10}	0	9043	[e]
$C_2H_5 + CH_3CHO \rightleftharpoons SC_4H_9O$	R1264	3.33×10^{10}	0	6397	[e]
$PC_4H_9O_2 \rightleftharpoons C_4H_8OOH_1\text{-}_2$	R1265	2.00×10^{11}	0	26850	[e]
$PC_4H_9O_2 \rightleftharpoons C_4H_8OOH_1\text{-}_3$	R1266	2.50×10^{10}	0	20850	[e]

Reactions	Code	$A_{r,g}$	$\beta_{r,g}$	$E_{r,g}$	Ref
$PC_4H_9O_2 \rightleftharpoons C_4H_8OOH_{1\text{-}4}$	R1267	4.69×10^{9}	0	22350	[e]
$SC_4H_9O_2 \rightleftharpoons C_4H_8OOH_{2\text{-}1}$	R1268	3.00×10^{11}	0	29400	[e]
$SC_4H_9O_2 \rightleftharpoons C_4H_8OOH_{2\text{-}3}$	R1269	2.00×10^{11}	0	26850	[e]
$SC_4H_9O_2 \rightleftharpoons C_4H_8OOH_{2\text{-}4}$	R1270	3.75×10^{10}	0	24400	[e]
$PC_4H_9O_2 \rightleftharpoons C_4H_{8\text{-}1} + HO_2$	R1271	5.04×10^{38}	-8.1	40490	[e]
$SC_4H_9O_2 \rightleftharpoons C_4H_{8\text{-}1} + HO_2$	R1272	5.07×10^{42}	-9.4	41490	[e]
$SC_4H_9O_2 \rightleftharpoons C_4H_{8\text{-}2} + HO_2$	R1273	5.04×10^{38}	-8.1	40490	[e]
$C_4H_{8\text{-}1} + HO_2 \rightleftharpoons C_4H_8OOH_{1\text{-}2}$	R1274	1.00×10^{11}	0	11000	[e]
$C_4H_{8\text{-}1} + HO_2 \rightleftharpoons C_4H_8OOH_{2\text{-}1}$	R1275	1.00×10^{11}	0	11750	[e]
$C_4H_{8\text{-}2} + HO_2 \rightleftharpoons C_4H_8OOH_{2\text{-}3}$	R1276	1.00×10^{11}	0	11750	[e]
$C_4H_8OOH_{1\text{-}2} \rightleftharpoons C_4H_8O_{1\text{-}2} + OH$	R1277	6.00×10^{11}	0	22000	[e]
$C_4H_8OOH_{1\text{-}3} \rightleftharpoons C_4H_8O_{1\text{-}3} + OH$	R1278	7.50×10^{10}	0	15250	[e]
$C_4H_8OOH_{1\text{-}4} \rightleftharpoons C_4H_8O_{1\text{-}4} + OH$	R1279	9.38×10^{9}	0	6000	[e]
$C_4H_8OOH_{2\text{-}1} \rightleftharpoons C_4H_8O_{1\text{-}2} + OH$	R1280	6.00×10^{11}	0	22000	[e]
$C_4H_8OOH_{2\text{-}3} \rightleftharpoons C_4H_8O_{2\text{-}3} + OH$	R1281	6.00×10^{11}	0	22000	[e]
$C_4H_8OOH_{2\text{-}4} \rightleftharpoons C_4H_8O_{1\text{-}3} + OH$	R1282	7.50×10^{10}	0	15250	[e]
$C_4H_8OOH_{1\text{-}1} \rightleftharpoons NC_3H_7CHO + OH$	R1283	9.00×10^{14}	0	1500	[e]
$C_4H_8OOH_{2\text{-}2} \rightleftharpoons C_2H_5COCH_3 + OH$	R1284	9.00×10^{14}	0	1500	[e]
$C_4H_8OOH_{1\text{-}3} \rightleftharpoons OH + CH_2O + C_3H_6$	R1285	6.64×10^{13}	-0.2	29900	[e]
$C_4H_8OOH_{2\text{-}4} \rightleftharpoons OH + CH_3CHO + C_2H_4$	R1286	1.94×10^{18}	-1.6	26790	[e]
$C_4H_8OOH_{1\text{-}2} + O_2 \rightleftharpoons C_4H_8OOH_{1\text{-}2}O_2$	R1287	7.54×10^{12}	0	0	[e]
$C_4H_8OOH_{1\text{-}3} + O_2 \rightleftharpoons C_4H_8OOH_{1\text{-}3}O_2$	R1288	7.54×10^{12}	0	0	[e]
$C_4H_8OOH_{1\text{-}4} + O_2 \rightleftharpoons C_4H_8OOH_{1\text{-}4}O_2$	R1289	4.52×10^{12}	0	0	[e]
$C_4H_8OOH_{2\text{-}1} + O_2 \rightleftharpoons C_4H_8OOH_{2\text{-}1}O_2$	R1290	4.52×10^{12}	0	0	[e]
$C_4H_8OOH_{2\text{-}3} + O_2 \rightleftharpoons C_4H_8OOH_{2\text{-}3}O_2$	R1291	7.54×10^{12}	0	0	[e]
$C_4H_8OOH_{2\text{-}4} + O_2 \rightleftharpoons C_4H_8OOH_{2\text{-}4}O_2$	R1292	4.52×10^{12}	0	0	[e]
$C_4H_8OOH_{1\text{-}2}O_2 \rightleftharpoons NC_4KET_{12} + OH$	R1293	2.00×10^{11}	0	26400	[e]
$C_4H_8OOH_{1\text{-}3}O_2 \rightleftharpoons NC_4KET_{13} + OH$	R1294	2.50×10^{10}	0	21400	[e]
$C_4H_8OOH_{1\text{-}4}O_2 \rightleftharpoons NC_4KET_{14} + OH$	R1295	3.12×10^{9}	0	19350	[e]
$C_4H_8OOH_{2\text{-}1}O_2 \rightleftharpoons NC_4KET_{21} + OH$	R1296	1.00×10^{11}	0	23850	[e]
$C_4H_8OOH_{2\text{-}3}O_2 \rightleftharpoons NC_4KET_{23} + OH$	R1297	1.00×10^{11}	0	23850	[e]
$C_4H_8OOH_{2\text{-}4}O_2 \rightleftharpoons NC_4KET_{24} + OH$	R1298	1.25×10^{10}	0	17850	[e]
$NC_4KET_{12} \rightleftharpoons C_2H_5CHO + HCO + OH$	R1299	1.05×10^{16}	0	41600	[e]
$NC_4KET_{13} \rightleftharpoons CH_3CHO + CH_2CHO + OH$	R1300	1.05×10^{16}	0	41600	[e]
$NC_4KET_{14} \rightleftharpoons CH_2CH_2CHO + CH_2O + OH$	R1301	1.50×10^{16}	0	42000	[e]
$NC_4KET_{21} \rightleftharpoons CH_2O + C_2H_5CO + OH$	R1302	1.50×10^{16}	0	42000	[e]
$NC_4KET_{23} \rightleftharpoons CH_3CHO + CH_3CO + OH$	R1303	1.05×10^{16}	0	41600	[e]
$NC_4KET_{24} \rightleftharpoons CH_2O + CH_3COCH_2 + OH$	R1304	1.50×10^{16}	0	42000	[e]

Reactions	Code	$A_{r,g}$	$\beta_{r,g}$	$E_{r,g}$	Ref
$C_2H_5COCH_3 + OH \rightleftharpoons CH_2CH_2COCH_3 + H_2O$	R1305	7.55×10^{9}	1	1586	[e]
$C_2H_5COCH_3 + OH \rightleftharpoons CH_3CHCOCH_3 + H_2O$	R1306	8.45×10^{11}	0	-228	[e]
$C_2H_5COCH_3 + OH \rightleftharpoons C_2H_5COCH_2 + H_2O$	R1307	5.10×10^{11}	0	1192	[e]
$C_2H_5COCH_3 + HO_2 \rightleftharpoons CH_2CH_2COCH_3 + H_2O_2$	R1308	2.38×10^{4}	2.5	16490	[e]
$C_2H_5COCH_3 + HO_2 \rightleftharpoons CH_3CHCOCH_3 + H_2O_2$	R1309	2.00×10^{11}	0	8698	[e]
$C_2H_5COCH_3 + HO_2 \rightleftharpoons C_2H_5COCH_2 + H_2O_2$	R1310	2.38×10^{4}	2.5	14690	[e]
$C_2H_5COCH_3 + O \rightleftharpoons CH_2CH_2COCH_3 + OH$	R1311	2.25×10^{13}	0	7700	[e]
$C_2H_5COCH_3 + O \rightleftharpoons CH_3CHCOCH_3 + OH$	R1312	3.07×10^{13}	0	3400	[e]
$C_2H_5COCH_3 + O \rightleftharpoons C_2H_5COCH_2 + OH$	R1313	5.00×10^{12}	0	5962	[e]
$C_2H_5COCH_3 + H \rightleftharpoons CH_2CH_2COCH_3 + H_2$	R1314	9.16×10^{6}	2	7700	[e]
$C_2H_5COCH_3 + H \rightleftharpoons CH_3CHCOCH_3 + H_2$	R1315	4.46×10^{6}	2	3200	[e]
$C_2H_5COCH_3 + H \rightleftharpoons C_2H_5COCH_2 + H_2$	R1316	9.30×10^{12}	0	6357	[e]
$C_2H_5COCH_3 + O_2 \rightleftharpoons CH_2CH_2COCH_3 + HO_2$	R1317	2.05×10^{13}	0	51310	[e]
$C_2H_5COCH_3 + O_2 \rightleftharpoons CH_3CHCOCH_3 + HO_2$	R1318	1.55×10^{13}	0	41970	[e]
$C_2H_5COCH_3 + O_2 \rightleftharpoons C_2H_5COCH_2 + HO_2$	R1319	2.05×10^{13}	0	49150	[e]
$C_2H_5COCH_3 + CH_3 \rightleftharpoons CH_2CH_2COCH_3 + CH_4$	R1320	3.19×10^{1}	3.2	7172	[e]
$C_2H_5COCH_3 + CH_3 \rightleftharpoons CH_3CHCOCH_3 + CH_4$	R1321	1.74×10^{0}	3.5	3680	[e]
$C_2H_5COCH_3 + CH_3 \rightleftharpoons C_2H_5COCH_2 + CH_4$	R1322	1.62×10^{11}	0	9630	[e]
$C_2H_5COCH_3 + CH_3O \rightleftharpoons CH_2CH_2COCH_3 + CH_3OH$	R1323	2.17×10^{11}	0	6460	[e]
$C_2H_5COCH_3 + CH_3O \rightleftharpoons CH_3CHCOCH_3 + CH_3OH$	R1324	1.45×10^{11}	0	2771	[e]
$C_2H_5COCH_3 + CH_3O \rightleftharpoons C_2H_5COCH_2 + CH_3OH$	R1325	2.17×10^{11}	0	4660	[e]
$C_2H_5COCH_3 + CH_3O_2 \rightleftharpoons CH_2CH_2COCH_3 + CH_3O_2H$	R1326	3.01×10^{12}	0	19380	[e]
$C_2H_5COCH_3 + CH_3O_2 \rightleftharpoons CH_3CHCOCH_3 + CH_3O_2H$	R1327	2.00×10^{12}	0	15250	[e]
$C_2H_5COCH_3 + CH_3O_2 \rightleftharpoons C_2H_5COCH_2 + CH_3O_2H$	R1328	3.01×10^{12}	0	17580	[e]
$C_2H_5COCH_3 + C_2H_3 \rightleftharpoons CH_2CH_2COCH_3 + C_2H_4$	R1329	5.00×10^{11}	0	10400	[e]
$C_2H_5COCH_3 + C_2H_3 \rightleftharpoons CH_3CHCOCH_3 + C_2H_4$	R1330	3.00×10^{11}	0	3400	[e]
$C_2H_5COCH_3 + C_2H_3 \rightleftharpoons C_2H_5COCH_2 + C_2H_4$	R1331	6.15×10^{10}	0	4278	[e]
$C_2H_5COCH_3 + C_2H_5 \rightleftharpoons CH_2CH_2COCH_3 + C_2H_6$	R1332	5.00×10^{10}	0	13400	[e]
$C_2H_5COCH_3 + C_2H_5 \rightleftharpoons CH_3CHCOCH_3 + C_2H_6$	R1333	3.00×10^{10}	0	8600	[e]
$C_2H_5COCH_3 + C_2H_5 \rightleftharpoons C_2H_5COCH_2 + C_2H_6$	R1334	5.00×10^{10}	0	11600	[e]
$CH_3CHCOCH_3 + O_2 \rightleftharpoons CH_3CHOOCOCH_3$	R1335	1.00×10^{11}	0	0	[e]
$CH_3CHOOCOCH_3 \rightleftharpoons CH_2CHOOHCOCH_3$	R1336	8.90×10^{12}	0	29700	[e]
$C_2H_3COCH_3 + HO_2 \rightleftharpoons CH_2CHOOHCOCH_3$	R1337	7.00×10^{10}	0	7800	[e]
$CH_2CH_2CHO \rightleftharpoons C_2H_4 + HCO$	R1338	3.13×10^{13}	-0.5	24590	[e]
$CH_2CH_2COCH_3 \rightleftharpoons C_2H_4 + CH_3CO$	R1339	1.00×10^{14}	0	18000	[e]
$C_2H_5COCH_2 \rightleftharpoons CH_2CO + C_2H_5$	R1340	1.00×10^{14}	0	35000	[e]
$C_2H_3COCH_3 + H \rightleftharpoons CH_3CHCOCH_3$	R1341	5.00×10^{12}	0	1200	[e]
$CH_3CHCO + CH_3 \rightleftharpoons CH_3CHCOCH_3$	R1342	1.23×10^{11}	0	7800	[e]

Reactions	Code	$A_{r,g}$	$\beta_{r,g}$	$E_{r,g}$	Ref
$NC_3H_7CHO + O_2 \rightleftharpoons NC_3H_7CO + HO_2$	R1343	1.20×10^{5}	2.5	37560	[e]
$NC_3H_7CHO + OH \rightleftharpoons NC_3H_7CO + H_2O$	R1344	2.00×10^{6}	1.8	-1300	[e]
$NC_3H_7CHO + H \rightleftharpoons NC_3H_7CO + H_2$	R1345	4.14×10^{9}	1.1	2320	[e]
$NC_3H_7CHO + O \rightleftharpoons NC_3H_7CO + OH$	R1346	5.94×10^{12}	0	1868	[e]
$NC_3H_7CHO + HO_2 \rightleftharpoons NC_3H_7CO + H_2O_2$	R1347	4.09×10^{4}	2.5	10200	[e]
$NC_3H_7CHO + CH_3 \rightleftharpoons NC_3H_7CO + CH_4$	R1348	2.89×10^{-3}	4.6	3210	[e]
$NC_3H_7CHO + CH_3O \rightleftharpoons NC_3H_7CO + CH_3OH$	R1349	1.00×10^{12}	0	3300	[e]
$NC_3H_7CHO + CH_3O_2 \rightleftharpoons NC_3H_7CO + CH_3O_2H$	R1350	4.09×10^{4}	2.5	10200	[e]
$NC_3H_7CHO + OH \rightleftharpoons C_3H_6CHO_1 + H_2O$	R1351	5.28×10^{9}	1	1586	[e]
$NC_3H_7CHO + OH \rightleftharpoons C_3H_6CHO_2 + H_2O$	R1352	4.68×10^{7}	1.6	-35	[e]
$NC_3H_7CHO + OH \rightleftharpoons C_3H_6CHO_3 + H_2O$	R1353	5.52×10^{2}	3.1	-1176	[e]
$NC_3H_7CHO + HO_2 \rightleftharpoons C_3H_6CHO_1 + H_2O_2$	R1354	2.38×10^{4}	2.5	16490	[e]
$NC_3H_7CHO + HO_2 \rightleftharpoons C_3H_6CHO_2 + H_2O_2$	R1355	9.64×10^{3}	2.6	13910	[e]
$NC_3H_7CHO + HO_2 \rightleftharpoons C_3H_6CHO_3 + H_2O_2$	R1356	3.44×10^{12}	0.1	17880	[e]
$NC_3H_7CHO + CH_3O_2 \rightleftharpoons C_3H_6CHO_1 + CH_3O_2H$	R1357	2.38×10^{4}	2.5	16490	[e]
$NC_3H_7CHO + CH_3O_2 \rightleftharpoons C_3H_6CHO_2 + CH_3O_2H$	R1358	9.64×10^{3}	2.6	13910	[e]
$NC_3H_7CHO + CH_3O_2 \rightleftharpoons C_3H_6CHO_3 + CH_3O_2H$	R1359	3.44×10^{12}	0.1	17880	[e]
$NC_3H_7CO \rightleftharpoons NC_3H_7 + CO$	R1360	1.00×10^{11}	0	9600	[e]
$C_3H_6CHO_1 \rightleftharpoons C_2H_4 + CH_2CHO$	R1361	7.40×10^{11}	0	21970	[e]
$C_2H_5CHCO + H \rightleftharpoons C_3H_6CHO_3$	R1362	5.00×10^{12}	0	1200	[e]
$C_2H_3CHO + CH_3 \rightleftharpoons C_3H_6CHO_3$	R1363	1.23×10^{11}	0	7800	[e]
$SC_3H_5CHO + H \rightleftharpoons C_3H_6CHO_2$	R1364	5.00×10^{12}	0	2900	[e]
$C_3H_6 + HCO \rightleftharpoons C_3H_6CHO_2$	R1365	1.00×10^{11}	0	6000	[e]
$C_2H_5CHCO + OH \rightleftharpoons NC_3H_7 + CO_2$	R1366	3.73×10^{12}	0	-1010	[e]
$C_2H_5CHCO + H \rightleftharpoons NC_3H_7 + CO$	R1367	4.40×10^{12}	0	1459	[e]
$C_2H_5CHCO + O \rightleftharpoons C_3H_6 + CO_2$	R1368	3.20×10^{12}	0	-437	[e]
$SC_3H_5CHO + OH \rightleftharpoons SC_3H_5CO + H_2O$	R1369	2.69×10^{10}	0.8	-340	[e]
$SC_3H_5CO \rightleftharpoons C_3H_5\text{-}S + CO$	R1370	8.60×10^{15}	0	23000	[e]
$SC_3H_5CHO + HO_2 \rightleftharpoons SC_3H_5CO + H_2O_2$	R1371	1.00×10^{12}	0	11920	[e]
$SC_3H_5CHO + CH_3 \rightleftharpoons SC_3H_5CO + CH_4$	R1372	3.98×10^{12}	0	8700	[e]
$SC_3H_5CHO + O \rightleftharpoons SC_3H_5CO + OH$	R1373	7.18×10^{12}	0	1389	[e]
$SC_3H_5CHO + O_2 \rightleftharpoons SC_3H_5CO + HO_2$	R1374	4.00×10^{13}	0	37600	[e]
$SC_3H_5CHO + H \rightleftharpoons SC_3H_5CO + H_2$	R1375	2.60×10^{12}	0	2600	[e]
$C_2H_3COCH_3 + OH \rightleftharpoons CH_3CHO + CH_3CO$	R1376	1.00×10^{11}	0	0	[e]
$C_2H_3COCH_3 + OH \rightleftharpoons CH_2CO + C_2H_3 + H_2O$	R1377	5.10×10^{11}	0	1192	[e]
$C_2H_3COCH_3 + HO_2 \rightleftharpoons CH_2CHO + CH_3CO + OH$	R1378	6.03×10^{9}	0	7949	[e]
$C_2H_3COCH_3 + HO_2 \rightleftharpoons CH_2CO + C_2H_3 + H_2O_2$	R1379	8.50×10^{12}	0	20460	[e]
$C_2H_3COCH_3 + CH_3O_2 \rightleftharpoons CH_2CHO + CH_3CO + CH_3O$	R1380	3.97×10^{11}	0	17050	[e]

Reactions	Code	$A_{r,g}$	$\beta_{r,g}$	$E_{r,g}$	Ref
$C_2H_3COCH_3 + CH_3O_2 \rightleftharpoons CH_2CO + C_2H_3 + CH_3O_2H$	R1381	3.01×10^{12}	0	17580	[e]
$IC_4H_{10}(+M) \rightleftharpoons CH_3 + IC_3H_7(+M)$	R1382	4.83×10^{16}	0	79900	[e]
$IC_4H_{10} \rightleftharpoons TC_4H_9 + H$	R1383	2.51×10^{98}	-23.8	145300	[e]
$IC_4H_{10} \rightleftharpoons IC_4H_9 + H$	R1384	9.85×10^{95}	-23.1	147600	[e]
$IC_4H_{10} + H \rightleftharpoons TC_4H_9 + H_2$	R1385	1.81×10^{6}	2.5	6756	[e]
$IC_4H_{10} + H \rightleftharpoons IC_4H_9 + H_2$	R1386	6.02×10^{5}	2.4	2583	[e]
$IC_4H_{10} + CH_3 \rightleftharpoons TC_4H_9 + CH_4$	R1387	1.36×10^{0}	3.6	7154	[e]
$IC_4H_{10} + CH_3 \rightleftharpoons IC_4H_9 + CH_4$	R1388	9.04×10^{-1}	3.5	4598	[e]
$IC_4H_{10} + OH \rightleftharpoons TC_4H_9 + H_2O$	R1389	5.73×10^{10}	0.5	63	[e]
$IC_4H_{10} + OH \rightleftharpoons IC_4H_9 + H_2O$	R1390	2.29×10^{8}	1.5	776	[e]
$IC_4H_{10} + C_2H_5 \rightleftharpoons IC_4H_9 + C_2H_6$	R1391	1.51×10^{12}	0	10400	[e]
$IC_4H_{10} + C_2H_5 \rightleftharpoons TC_4H_9 + C_2H_6$	R1392	1.00×10^{11}	0	7900	[e]
$IC_4H_{10} + HO_2 \rightleftharpoons IC_4H_9 + H_2O_2$	R1393	1.22×10^{5}	2.5	16690	[e]
$IC_4H_{10} + HO_2 \rightleftharpoons TC_4H_9 + H_2O_2$	R1394	1.50×10^{4}	2.5	12260	[e]
$IC_4H_{10} + O \rightleftharpoons TC_4H_9 + OH$	R1395	1.97×10^{5}	2.4	1150	[e]
$IC_4H_{10} + O \rightleftharpoons IC_4H_9 + OH$	R1396	4.05×10^{7}	2	5136	[e]
$IC_4H_{10} + CH_3O \rightleftharpoons IC_4H_9 + CH_3OH$	R1397	4.80×10^{11}	0	7000	[e]
$IC_4H_{10} + CH_3O \rightleftharpoons TC_4H_9 + CH_3OH$	R1398	1.90×10^{10}	0	2800	[e]
$IC_4H_{10} + O_2 \rightleftharpoons IC_4H_9 + HO_2$	R1399	1.80×10^{14}	0	46000	[e]
$IC_4H_{10} + O_2 \rightleftharpoons TC_4H_9 + HO_2$	R1400	2.04×10^{13}	0	41350	[e]
$IC_4H_{10} + CH_3O_2 \rightleftharpoons IC_4H_9 + CH_3O_2H$	R1401	1.22×10^{5}	2.5	16690	[e]
$IC_4H_{10} + C_2H_5O_2 \rightleftharpoons IC_4H_9 + C_2H_5O_2H$	R1402	2.55×10^{13}	0	20460	[e]
$IC_4H_{10} + CH_3CO_3 \rightleftharpoons IC_4H_9 + CH_3CO_3H$	R1403	2.55×10^{13}	0	20460	[e]
$IC_4H_{10} + NC_3H_7O_2 \rightleftharpoons IC_4H_9 + NC_3H_7O_2H$	R1404	2.55×10^{13}	0	20460	[e]
$IC_4H_{10} + IC_3H_7O_2 \rightleftharpoons IC_4H_9 + IC_3H_7O_2H$	R1405	2.55×10^{13}	0	20460	[e]
$IC_4H_{10} + IC_4H_9O_2 \rightleftharpoons IC_4H_9 + IC_4H_9O_2H$	R1406	2.55×10^{13}	0	20460	[e]
$IC_4H_{10} + TC_4H_9O_2 \rightleftharpoons IC_4H_9 + TC_4H_9O_2H$	R1407	2.55×10^{13}	0	20460	[e]
$IC_4H_{10} + O_2CHO \rightleftharpoons IC_4H_9 + HO_2CHO$	R1408	2.52×10^{13}	0	20440	[e]
$IC_4H_{10} + O_2CHO \rightleftharpoons TC_4H_9 + HO_2CHO$	R1409	2.80×10^{12}	0	16010	[e]
$IC_4H_{10} + SC_4H_9O_2 \rightleftharpoons IC_4H_9 + SC_4H_9O_2H$	R1410	2.25×10^{13}	0	20460	[e]
$IC_4H_{10} + SC_4H_9O_2 \rightleftharpoons TC_4H_9 + SC_4H_9O_2H$	R1411	2.80×10^{12}	0	16000	[e]
$IC_4H_{10} + PC_4H_9O_2 \rightleftharpoons IC_4H_9 + PC_4H_9O_2H$	R1412	2.25×10^{13}	0	20460	[e]
$IC_4H_{10} + PC_4H_9O_2 \rightleftharpoons TC_4H_9 + PC_4H_9O_2H$	R1413	2.80×10^{12}	0	16000	[e]
$IC_4H_{10} + CH_3O_2 \rightleftharpoons TC_4H_9 + CH_3O_2H$	R1414	1.50×10^{4}	2.5	12260	[e]
$IC_4H_{10} + C_2H_5O_2 \rightleftharpoons TC_4H_9 + C_2H_5O_2H$	R1415	2.80×10^{12}	0	16000	[e]
$IC_4H_{10} + CH_3CO_3 \rightleftharpoons TC_4H_9 + CH_3CO_3H$	R1416	2.80×10^{12}	0	16000	[e]
$IC_4H_{10} + NC_3H_7O_2 \rightleftharpoons TC_4H_9 + NC_3H_7O_2H$	R1417	2.80×10^{12}	0	16000	[e]
$IC_4H_{10} + IC_3H_7O_2 \rightleftharpoons TC_4H_9 + IC_3H_7O_2H$	R1418	2.80×10^{12}	0	16000	[e]

Reactions	Code	$A_{r,g}$	$\beta_{r,g}$	$E_{r,g}$	Ref
$IC_4H_{10} + IC_4H_9O_2 \rightleftharpoons TC_4H_9 + IC_4H_9O_2H$	R1419	2.80×10^{12}	0	16000	[e]
$IC_4H_{10} + TC_4H_9O_2 \rightleftharpoons TC_4H_9 + TC_4H_9O_2H$	R1420	2.80×10^{12}	0	16000	[e]
$IC_4H_{10} + IC_4H_9 \rightleftharpoons TC_4H_9 + IC_4H_{10}$	R1421	2.50×10^{10}	0	7900	[e]
$IC_4H_9 + HO_2 \rightleftharpoons IC_4H_9O + OH$	R1422	7.00×10^{12}	0	-1000	[e]
$TC_4H_9 + HO_2 \rightleftharpoons TC_4H_9O + OH$	R1423	7.00×10^{12}	0	-1000	[e]
$CH_3O_2 + IC_4H_9 \rightleftharpoons CH_3O + IC_4H_9O$	R1424	7.00×10^{12}	0	-1000	[e]
$CH_3O_2 + TC_4H_9 \rightleftharpoons CH_3O + TC_4H_9O$	R1425	7.00×10^{12}	0	-1000	[e]
$IC_4H_9 \rightleftharpoons IC_4H_8 + H$	R1426	4.98×10^{32}	-6.2	40070	[e]
$IC_4H_9 \rightleftharpoons C_3H_6 + CH_3$	R1427	1.64×10^{37}	-7.4	38670	[e]
$TC_4H_9 \rightleftharpoons H + IC_4H_8$	R1428	4.65×10^{46}	-9.8	55080	[e]
$TC_4H_9 + O_2 \rightleftharpoons IC_4H_8 + HO_2$	R1429	2.00×10^{-18}	0	5000	[e]
$IC_4H_9 + O_2 \rightleftharpoons IC_4H_8 + HO_2$	R1430	2.00×10^{-18}	0	5000	[e]
$NC_3H_7O_2 + IC_4H_9 \rightleftharpoons NC_3H_7O + IC_4H_9O$	R1431	7.00×10^{12}	0	-1000	[e]
$NC_3H_7O_2 + TC_4H_9 \rightleftharpoons NC_3H_7O + TC_4H_9O$	R1432	7.00×10^{12}	0	-1000	[e]
$NC_3H_7O_2 + IC_4H_7 \rightleftharpoons NC_3H_7O + IC_4H_7O$	R1433	7.00×10^{12}	0	-1000	[e]
$SC_4H_9O_2 + IC_4H_9 \rightleftharpoons SC_4H_9O + IC_4H_9O$	R1434	7.00×10^{12}	0	-1000	[e]
$SC_4H_9O_2 + TC_4H_9 \rightleftharpoons SC_4H_9O + TC_4H_9O$	R1435	7.00×10^{12}	0	-1000	[e]
$PC_4H_9O_2 + IC_4H_9 \rightleftharpoons PC_4H_9O + IC_4H_9O$	R1436	7.00×10^{12}	0	-1000	[e]
$PC_4H_9O_2 + TC_4H_9 \rightleftharpoons PC_4H_9O + TC_4H_9O$	R1437	7.00×10^{12}	0	-1000	[e]
$PC_4H_9O_2 + IC_4H_7 \rightleftharpoons PC_4H_9O + IC_4H_7O$	R1438	7.00×10^{12}	0	-1000	[e]
$SC_4H_9O_2 + IC_4H_7 \rightleftharpoons SC_4H_9O + IC_4H_7O$	R1439	7.00×10^{12}	0	-1000	[e]
$IC_4H_9 + O_2 \rightleftharpoons IC_4H_9O_2$	R1440	2.26×10^{12}	0	0	[e]
$TC_4H_9 + O_2 \rightleftharpoons TC_4H_9O_2$	R1441	1.41×10^{13}	0	0	[e]
$IC_4H_9O_2 + C_4H_{10} \rightleftharpoons IC_4H_9O_2H + SC_4H_9$	R1442	1.12×10^{13}	0	17700	[e]
$TC_4H_9O_2 + C_4H_{10} \rightleftharpoons TC_4H_9O_2H + SC_4H_9$	R1443	1.12×10^{13}	0	17700	[e]
$IC_4H_9O_2 + C_4H_{10} \rightleftharpoons IC_4H_9O_2H + PC_4H_9$	R1444	1.70×10^{13}	0	20460	[e]
$TC_4H_9O_2 + C_4H_{10} \rightleftharpoons TC_4H_9O_2H + PC_4H_9$	R1445	1.70×10^{13}	0	20460	[e]
$IC_3H_7O_2 + IC_4H_9 \rightleftharpoons IC_3H_7O + IC_4H_9O$	R1446	7.00×10^{12}	0	-1000	[e]
$IC_3H_7O_2 + TC_4H_9 \rightleftharpoons IC_3H_7O + TC_4H_9O$	R1447	7.00×10^{12}	0	-1000	[e]
$IC_3H_7O_2 + IC_4H_7 \rightleftharpoons IC_3H_7O + IC_4H_7O$	R1448	7.00×10^{12}	0	-1000	[e]
$IC_4H_9O_2 + C_3H_6 \rightleftharpoons IC_4H_9O_2H + C_3H_5\text{-}A$	R1449	3.24×10^{11}	0	14900	[e]
$TC_4H_9O_2 + C_3H_6 \rightleftharpoons TC_4H_9O_2H + C_3H_5\text{-}A$	R1450	3.24×10^{11}	0	14900	[e]
$IC_4H_9O_2 + IC_4H_8 \rightleftharpoons IC_4H_9O_2H + IC_4H_7$	R1451	1.40×10^{12}	0	14900	[e]
$TC_4H_9O_2 + IC_4H_8 \rightleftharpoons TC_4H_9O_2H + IC_4H_7$	R1452	1.40×10^{12}	0	14900	[e]
$PC_4H_9O_2 + IC_4H_8 \rightleftharpoons PC_4H_9O_2H + IC_4H_7$	R1453	1.40×10^{12}	0	14900	[e]
$SC_4H_9O_2 + IC_4H_8 \rightleftharpoons SC_4H_9O_2H + IC_4H_7$	R1454	1.40×10^{12}	0	14900	[e]
$IC_3H_7O_2 + IC_4H_8 \rightleftharpoons IC_3H_7O_2H + IC_4H_7$	R1455	1.40×10^{12}	0	14900	[e]
$NC_3H_7O_2 + IC_4H_8 \rightleftharpoons NC_3H_7O_2H + IC_4H_7$	R1456	1.40×10^{12}	0	14900	[e]

Reactions	Code	$A_{r,g}$	$\beta_{r,g}$	$E_{r,g}$	Ref
$IC_4H_9O_2 + C_4H_{8-1} \rightleftharpoons IC_4H_9O_2H + C_4H_{71-3}$	R1457	1.40×10^{12}	0	14900	[e]
$TC_4H_9O_2 + C_4H_{8-1} \rightleftharpoons TC_4H_9O_2H + C_4H_{71-3}$	R1458	1.40×10^{12}	0	14900	[e]
$IC_4H_9O_2 + C_4H_{8-2} \rightleftharpoons IC_4H_9O_2H + C_4H_{71-3}$	R1459	1.40×10^{12}	0	14900	[e]
$TC_4H_9O_2 + C_4H_{8-2} \rightleftharpoons TC_4H_9O_2H + C_4H_{71-3}$	R1460	1.40×10^{12}	0	14900	[e]
$CC_4H_8O + OH \rightleftharpoons CH_2O + C_3H_5\text{-}A + H_2O$	R1461	5.00×10^{12}	0	0	[e]
$CC_4H_8O + H \rightleftharpoons CH_2O + C_3H_5\text{-}A + H_2$	R1462	3.51×10^{7}	2	5000	[e]
$CC_4H_8O + O \rightleftharpoons CH_2O + C_3H_5\text{-}A + OH$	R1463	1.12×10^{14}	0	5200	[e]
$CC_4H_8O + HO_2 \rightleftharpoons CH_2O + C_3H_5\text{-}A + H_2O_2$	R1464	1.00×10^{13}	0	15000	[e]
$CC_4H_8O + CH_3O_2 \rightleftharpoons CH_2O + C_3H_5\text{-}A + CH_3O_2H$	R1465	1.00×10^{13}	0	19000	[e]
$CC_4H_8O + CH_3 \rightleftharpoons CH_2O + C_3H_5\text{-}A + CH_4$	R1466	2.00×10^{11}	0	10000	[e]
$C_2H_4 + TC_4H_9O_2 \rightleftharpoons C_2H_3 + TC_4H_9O_2H$	R1467	7.00×10^{11}	0	17110	[e]
$TC_4H_9O_2 + CH_4 \rightleftharpoons TC_4H_9O_2H + CH_3$	R1468	1.13×10^{13}	0	20460	[e]
$H_2 + TC_4H_9O_2 \rightleftharpoons H + TC_4H_9O_2H$	R1469	3.01×10^{13}	0	26030	[e]
$TC_4H_9O_2 + C_2H_6 \rightleftharpoons TC_4H_9O_2H + C_2H_5$	R1470	1.70×10^{13}	0	20460	[e]
$TC_4H_9O_2 + C_3H_8 \rightleftharpoons TC_4H_9O_2H + IC_3H_7$	R1471	2.00×10^{12}	0	17000	[e]
$TC_4H_9O_2 + C_3H_8 \rightleftharpoons TC_4H_9O_2H + NC_3H_7$	R1472	1.70×10^{13}	0	20460	[e]
$TC_4H_9O_2 + CH_3OH \rightleftharpoons TC_4H_9O_2H + CH_2OH$	R1473	6.30×10^{12}	0	19360	[e]
$TC_4H_9O_2 + C_2H_5OH \rightleftharpoons TC_4H_9O_2H + PC_2H_4OH$	R1474	6.30×10^{12}	0	19360	[e]
$TC_4H_9O_2 + C_2H_5OH \rightleftharpoons TC_4H_9O_2H + SC_2H_4OH$	R1475	4.20×10^{12}	0	15000	[e]
$IC_4H_9O_2 + CH_3CHO \rightleftharpoons IC_4H_9O_2H + CH_3CO$	R1476	2.80×10^{12}	0	13600	[e]
$TC_4H_9O_2 + CH_3CHO \rightleftharpoons TC_4H_9O_2H + CH_3CO$	R1477	2.80×10^{12}	0	13600	[e]
$IC_4H_9O_2 + C_2H_3CHO \rightleftharpoons IC_4H_9O_2H + C_2H_3CO$	R1478	2.80×10^{12}	0	13600	[e]
$TC_4H_9O_2 + C_2H_3CHO \rightleftharpoons TC_4H_9O_2H + C_2H_3CO$	R1479	2.80×10^{12}	0	13600	[e]
$IC_4H_9O_2 + C_2H_5CHO \rightleftharpoons IC_4H_9O_2H + C_2H_5CO$	R1480	2.80×10^{12}	0	13600	[e]
$TC_4H_9O_2 + C_2H_5CHO \rightleftharpoons TC_4H_9O_2H + C_2H_5CO$	R1481	2.80×10^{12}	0	13600	[e]
$IC_4H_9O_2 + HO_2 \rightleftharpoons IC_4H_9O_2H + O_2$	R1482	1.75×10^{10}	0	-3275	[e]
$TC_4H_9O_2 + HO_2 \rightleftharpoons TC_4H_9O_2H + O_2$	R1483	1.75×10^{10}	0	-3275	[e]
$IC_4H_9O_2 + H_2O_2 \rightleftharpoons IC_4H_9O_2H + HO_2$	R1484	2.40×10^{12}	0	10000	[e]
$TC_4H_9O_2 + H_2O_2 \rightleftharpoons TC_4H_9O_2H + HO_2$	R1485	2.40×10^{12}	0	10000	[e]
$IC_4H_9O_2 + CH_2O \rightleftharpoons IC_4H_9O_2H + HCO$	R1486	1.30×10^{11}	0	9000	[e]
$TC_4H_9O_2 + CH_2O \rightleftharpoons TC_4H_9O_2H + HCO$	R1487	1.30×10^{11}	0	9000	[e]
$IC_4H_9O_2 + CH_3O_2 \rightleftharpoons IC_4H_9O + CH_3O + O_2$	R1488	1.40×10^{16}	-1.6	1860	[e]
$TC_4H_9O_2 + CH_3O_2 \rightleftharpoons TC_4H_9O + CH_3O + O_2$	R1489	1.40×10^{16}	-1.6	1860	[e]
$IC_4H_9O_2 + C_2H_5O_2 \rightleftharpoons IC_4H_9O + C_2H_5O + O_2$	R1490	1.40×10^{16}	-1.6	1860	[e]
$TC_4H_9O_2 + C_2H_5O_2 \rightleftharpoons TC_4H_9O + C_2H_5O + O_2$	R1491	1.40×10^{16}	-1.6	1860	[e]
$IC_4H_9O_2 + CH_3CO_3 \rightleftharpoons IC_4H_9O + CH_3CO_2 + O_2$	R1492	1.40×10^{16}	-1.6	1860	[e]
$TC_4H_9O_2 + CH_3CO_3 \rightleftharpoons TC_4H_9O + CH_3CO_2 + O_2$	R1493	1.40×10^{16}	-1.6	1860	[e]
$IC_4H_9O_2 + IC_4H_9O_2 \rightleftharpoons O_2 + IC_4H_9O + IC_4H_9O$	R1494	1.40×10^{16}	-1.6	1860	[e]

Reactions	Code	$A_{r,g}$	$\beta_{r,g}$	$E_{r,g}$	Ref
$IC_4H_9O_2 + TC_4H_9O_2 \rightleftharpoons IC_4H_9O + TC_4H_9O + O_2$	R1495	1.40×10^{16}	-1.6	1860	[e]
$TC_4H_9O_2 + TC_4H_9O_2 \rightleftharpoons O_2 + TC_4H_9O + TC_4H_9O$	R1496	1.40×10^{16}	-1.6	1860	[e]
$IC_4H_9O_2 + PC_4H_9O_2 \rightleftharpoons IC_4H_9O + PC_4H_9O + O_2$	R1497	1.40×10^{16}	-1.6	1860	[e]
$TC_4H_9O_2 + PC_4H_9O_2 \rightleftharpoons TC_4H_9O + PC_4H_9O + O_2$	R1498	1.40×10^{16}	-1.6	1860	[e]
$IC_4H_9O_2 + SC_4H_9O_2 \rightleftharpoons IC_4H_9O + SC_4H_9O + O_2$	R1499	1.40×10^{16}	-1.6	1860	[e]
$TC_4H_9O_2 + SC_4H_9O_2 \rightleftharpoons TC_4H_9O + SC_4H_9O + O_2$	R1500	1.40×10^{16}	-1.6	1860	[e]
$IC_4H_9O_2 + NC_3H_7O_2 \rightleftharpoons IC_4H_9O + NC_3H_7O + O_2$	R1501	1.40×10^{16}	-1.6	1860	[e]
$TC_4H_9O_2 + NC_3H_7O_2 \rightleftharpoons TC_4H_9O + NC_3H_7O + O_2$	R1502	1.40×10^{16}	-1.6	1860	[e]
$IC_4H_9O_2 + IC_3H_7O_2 \rightleftharpoons IC_4H_9O + IC_3H_7O + O_2$	R1503	1.40×10^{16}	-1.6	1860	[e]
$TC_4H_9O_2 + IC_3H_7O_2 \rightleftharpoons TC_4H_9O + IC_3H_7O + O_2$	R1504	1.40×10^{16}	-1.6	1860	[e]
$IC_4H_9O_2 + HO_2 \rightleftharpoons IC_4H_9O + OH + O_2$	R1505	1.40×10^{16}	-1.6	1860	[e]
$TC_4H_9O_2 + HO_2 \rightleftharpoons TC_4H_9O + OH + O_2$	R1506	1.40×10^{16}	-1.6	1860	[e]
$IC_4H_9O_2 + CH_3 \rightleftharpoons IC_4H_9O + CH_3O$	R1507	7.00×10^{12}	0	-1000	[e]
$IC_4H_9O_2 + C_2H_5 \rightleftharpoons IC_4H_9O + C_2H_5O$	R1508	7.00×10^{12}	0	-1000	[e]
$IC_4H_9O_2 + IC_3H_7 \rightleftharpoons IC_4H_9O + IC_3H_7O$	R1509	7.00×10^{12}	0	-1000	[e]
$IC_4H_9O_2 + NC_3H_7 \rightleftharpoons IC_4H_9O + NC_3H_7O$	R1510	7.00×10^{12}	0	-1000	[e]
$IC_4H_9O_2 + PC_4H_9 \rightleftharpoons IC_4H_9O + PC_4H_9O$	R1511	7.00×10^{12}	0	-1000	[e]
$IC_4H_9O_2 + SC_4H_9 \rightleftharpoons IC_4H_9O + SC_4H_9O$	R1512	7.00×10^{12}	0	-1000	[e]
$IC_4H_9O_2 + IC_4H_9 \rightleftharpoons IC_4H_9O + IC_4H_9O$	R1513	7.00×10^{12}	0	-1000	[e]
$IC_4H_9O_2 + TC_4H_9 \rightleftharpoons IC_4H_9O + TC_4H_9O$	R1514	7.00×10^{12}	0	-1000	[e]
$IC_4H_9O_2 + C_3H_5\text{-}A \rightleftharpoons IC_4H_9O + C_3H_5O$	R1515	7.00×10^{12}	0	-1000	[e]
$IC_4H_9O_2 + C_4H_{71}\text{-}_3 \rightleftharpoons IC_4H_9O + C_4H_7O$	R1516	7.00×10^{12}	0	-1000	[e]
$IC_4H_9O_2 + IC_4H_7 \rightleftharpoons IC_4H_9O + IC_4H_7O$	R1517	7.00×10^{12}	0	-1000	[e]
$TC_4H_9O_2 + CH_3 \rightleftharpoons TC_4H_9O + CH_3O$	R1518	7.00×10^{12}	0	-1000	[e]
$TC_4H_9O_2 + C_2H_5 \rightleftharpoons TC_4H_9O + C_2H_5O$	R1519	7.00×10^{12}	0	-1000	[e]
$TC_4H_9O_2 + IC_3H_7 \rightleftharpoons TC_4H_9O + IC_3H_7O$	R1520	7.00×10^{12}	0	-1000	[e]
$TC_4H_9O_2 + NC_3H_7 \rightleftharpoons TC_4H_9O + NC_3H_7O$	R1521	7.00×10^{12}	0	-1000	[e]
$TC_4H_9O_2 + PC_4H_9 \rightleftharpoons TC_4H_9O + PC_4H_9O$	R1522	7.00×10^{12}	0	-1000	[e]
$TC_4H_9O_2 + SC_4H_9 \rightleftharpoons TC_4H_9O + SC_4H_9O$	R1523	7.00×10^{12}	0	-1000	[e]
$TC_4H_9O_2 + IC_4H_9 \rightleftharpoons TC_4H_9O + IC_4H_9O$	R1524	7.00×10^{12}	0	-1000	[e]
$TC_4H_9O_2 + TC_4H_9 \rightleftharpoons TC_4H_9O + TC_4H_9O$	R1525	7.00×10^{12}	0	-1000	[e]
$TC_4H_9O_2 + C_3H_5\text{-}A \rightleftharpoons TC_4H_9O + C_3H_5O$	R1526	7.00×10^{12}	0	-1000	[e]
$TC_4H_9O_2 + C_4H_{71}\text{-}_3 \rightleftharpoons TC_4H_9O + C_4H_7O$	R1527	7.00×10^{12}	0	-1000	[e]
$TC_4H_9O_2 + IC_4H_7 \rightleftharpoons TC_4H_9O + IC_4H_7O$	R1528	7.00×10^{12}	0	-1000	[e]
$IC_4H_9O_2 + C_2H_4 \rightleftharpoons IC_4H_9O_2H + C_2H_3$	R1529	2.00×10^{11}	0	6000	[e]
$IC_4H_9O_2 + CH_4 \rightleftharpoons IC_4H_9O_2H + CH_3$	R1530	1.13×10^{13}	0	20460	[e]
$H_2 + IC_4H_9O_2 \rightleftharpoons H + IC_4H_9O_2H$	R1531	3.01×10^{13}	0	26030	[e]
$IC_4H_9O_2 + C_2H_6 \rightleftharpoons IC_4H_9O_2H + C_2H_5$	R1532	1.70×10^{13}	0	20460	[e]

Reactions	Code	$A_{r,g}$	$\beta_{r,g}$	$E_{r,g}$	Ref
$IC_4H_9O_2 + C_3H_8 \rightleftharpoons IC_4H_9O_2H + IC_3H_7$	R1533	2.00×10^{12}	0	17000	[e]
$IC_4H_9O_2 + C_3H_8 \rightleftharpoons IC_4H_9O_2H + NC_3H_7$	R1534	1.70×10^{13}	0	20460	[e]
$IC_4H_9O_2 + CH_3OH \rightleftharpoons IC_4H_9O_2H + CH_2OH$	R1535	6.30×10^{12}	0	19360	[e]
$IC_4H_9O_2 + C_2H_5OH \rightleftharpoons IC_4H_9O_2H + PC_2H_4OH$	R1536	6.30×10^{12}	0	19360	[e]
$IC_4H_9O_2 + C_2H_5OH \rightleftharpoons IC_4H_9O_2H + SC_2H_4OH$	R1537	4.20×10^{12}	0	15000	[e]
$IC_4H_9O_2H \rightleftharpoons IC_4H_9O + OH$	R1538	1.50×10^{16}	0	42500	[e]
$TC_4H_9O_2H \rightleftharpoons TC_4H_9O + OH$	R1539	5.95×10^{15}	0	42540	[e]
$IC_4H_9O + HO_2 \rightleftharpoons IC_3H_7CHO + H_2O_2$	R1540	1.00×10^{12}	0	0	[e]
$IC_4H_9O + OH \rightleftharpoons IC_3H_7CHO + H_2O$	R1541	1.81×10^{13}	0	0	[e]
$IC_4H_9O + CH_3 \rightleftharpoons IC_3H_7CHO + CH_4$	R1542	2.40×10^{13}	0	0	[e]
$IC_4H_9O + O \rightleftharpoons IC_3H_7CHO + OH$	R1543	6.00×10^{12}	0	0	[e]
$IC_4H_9O + H \rightleftharpoons IC_3H_7CHO + H_2$	R1544	1.99×10^{13}	0	0	[e]
$IC_4H_9O \rightleftharpoons IC_3H_7CHO + H$	R1545	4.00×10^{14}	0	21500	[e]
$IC_4H_9O \rightleftharpoons CH_2O + IC_3H_7$	R1546	2.00×10^{14}	0	17500	[e]
$CH_3COCH_3 + CH_3 \rightleftharpoons TC_4H_9O$	R1547	1.50×10^{11}	0	11900	[e]
$IC_4H_9O + O_2 \rightleftharpoons IC_3H_7CHO + HO_2$	R1548	1.93×10^{11}	0	1660	[e]
$TC_4H_9O + O_2 \rightleftharpoons IC_4H_8O + HO_2$	R1549	8.10×10^{11}	0	4700	[e]
$IC_4H_8O \rightleftharpoons IC_3H_7CHO$	R1550	4.18×10^{13}	0	52720	[e]
$IC_4H_8O + OH \rightleftharpoons IC_3H_6CHO + H_2O$	R1551	1.25×10^{12}	0	0	[e]
$IC_4H_8O + H \rightleftharpoons IC_3H_6CHO + H_2$	R1552	1.25×10^{12}	0	0	[e]
$IC_4H_8O + HO_2 \rightleftharpoons IC_3H_6CHO + H_2O_2$	R1553	2.50×10^{12}	0	15000	[e]
$IC_4H_8O + CH_3O_2 \rightleftharpoons IC_3H_6CHO + CH_3O_2H$	R1554	2.50×10^{12}	0	19000	[e]
$IC_4H_8O + CH_3 \rightleftharpoons IC_3H_6CHO + CH_4$	R1555	5.00×10^{10}	0	10000	[e]
$IC_4H_8O + O \rightleftharpoons IC_3H_6CHO + OH$	R1556	1.25×10^{12}	0	0	[e]
$TC_3H_6CHO + H \rightleftharpoons IC_3H_7CHO$	R1557	2.00×10^{14}	0	0	[e]
$IC_3H_7 + HCO \rightleftharpoons IC_3H_7CHO$	R1558	1.81×10^{13}	0	0	[e]
$IC_3H_7CHO + HO_2 \rightleftharpoons IC_3H_7CO + H_2O_2$	R1559	3.00×10^{12}	0	11920	[e]
$IC_3H_7CHO + HO_2 \rightleftharpoons TC_3H_6CHO + H_2O_2$	R1560	8.00×10^{10}	0	11920	[e]
$IC_3H_7CHO + CH_3 \rightleftharpoons IC_3H_7CO + CH_4$	R1561	3.98×10^{12}	0	8700	[e]
$IC_3H_7CHO + O \rightleftharpoons IC_3H_7CO + OH$	R1562	7.18×10^{12}	0	1389	[e]
$IC_3H_7CHO + O_2 \rightleftharpoons IC_3H_7CO + HO_2$	R1563	4.00×10^{13}	0	37600	[e]
$IC_3H_7CHO + OH \rightleftharpoons IC_3H_7CO + H_2O$	R1564	2.69×10^{10}	0.8	-340	[e]
$IC_3H_7CHO + OH \rightleftharpoons TC_3H_6CHO + H_2O$	R1565	1.68×10^{12}	0	-781	[e]
$IC_3H_7CHO + H \rightleftharpoons IC_3H_7CO + H_2$	R1566	2.60×10^{12}	0	2600	[e]
$IC_3H_7CHO + OH \rightleftharpoons IC_3H_6CHO + H_2O$	R1567	3.12×10^{6}	2	-298	[e]
$IC_3H_7CHO + HO_2 \rightleftharpoons IC_3H_6CHO + H_2O_2$	R1568	2.74×10^{4}	2.5	15500	[e]
$IC_3H_7CHO + CH_3O_2 \rightleftharpoons IC_3H_6CHO + CH_3O_2H$	R1569	4.76×10^{4}	2.5	16490	[e]
$IC_3H_7 + CO \rightleftharpoons IC_3H_7CO$	R1570	1.50×10^{11}	0	4810	[e]

Reactions	Code	$A_{r,g}$	$\beta_{r,g}$	$E_{r,g}$	Ref
$C_3H_6 + HCO \rightleftharpoons IC_3H_6CHO$	R1571	1.00×10^{11}	0	7800	[e]
$C_2H_3CHO + CH_3 \rightleftharpoons IC_3H_6CHO$	R1572	1.00×10^{11}	0	7800	[e]
$IC_4H_8 + OH \rightleftharpoons IC_4H_8OH$	R1573	9.93×10^{11}	0	-960	[e]
$IC_4H_8OH + O_2 \rightleftharpoons IO_2C_4H_8OH$	R1574	1.20×10^{11}	0	-1100	[e]
$IO_2C_4H_8OH \rightleftharpoons CH_3COCH_3 + CH_2O + OH$	R1575	1.25×10^{10}	0	18900	[e]
$IC_4H_9O_2 \rightleftharpoons IC_4H_8O_2H\text{-}I$	R1576	7.50×10^{10}	0	24400	[e]
$TC_4H_9O_2 \rightleftharpoons TC_4H_8O_2H\text{-}I$	R1577	9.00×10^{11}	0	29400	[e]
$IC_4H_9O_2 \rightleftharpoons IC_4H_8O_2H\text{-}T$	R1578	1.00×10^{11}	0	24100	[e]
$IC_4H_9O_2 \rightleftharpoons IC_4H_8 + HO_2$	R1579	4.53×10^{35}	-7.2	39490	[e]
$TC_4H_9O_2 \rightleftharpoons IC_4H_8 + HO_2$	R1580	1.52×10^{43}	-9.4	41490	[e]
$IC_4H_8O_2H\text{-}I + O_2 \rightleftharpoons IC_4H_8OOH\text{-}IO_2$	R1581	2.26×10^{12}	0	0	[e]
$TC_4H_8O_2H\text{-}I + O_2 \rightleftharpoons TC_4H_8OOH\text{-}IO_2$	R1582	2.26×10^{12}	0	0	[e]
$IC_4H_8O_2H\text{-}T + O_2 \rightleftharpoons IC_4H_8OOH\text{-}TO_2$	R1583	1.41×10^{13}	0	0	[e]
$IC_4H_8OOH\text{-}IO_2 \rightleftharpoons IC_4KETII + OH$	R1584	2.50×10^{10}	0	21400	[e]
$IC_4H_8OOH\text{-}TO_2 \rightleftharpoons IC_4KETIT + OH$	R1585	2.00×10^{11}	0	26400	[e]
$IC_4KETII \rightleftharpoons CH_2O + C_2H_5CO + OH$	R1586	1.50×10^{16}	0	42000	[e]
$IC_4KETIT \rightleftharpoons CH_3COCH_3 + HCO + OH$	R1587	9.50×10^{15}	0	42540	[e]
$IC_4H_8 + HO_2 \rightleftharpoons TC_4H_8O_2H\text{-}I$	R1588	3.97×10^{11}	0	12620	[e]
$IC_4H_8 + HO_2 \rightleftharpoons IC_4H_8O_2H\text{-}T$	R1589	3.97×10^{11}	0	12620	[e]
$IC_4H_8O_2H\text{-}I \rightleftharpoons CC_4H_8O + OH$	R1590	7.50×10^{10}	0	15250	[e]
$IC_4H_8O_2H\text{-}T \rightleftharpoons IC_4H_8O + OH$	R1591	6.00×10^{11}	0	22000	[e]
$TC_4H_8O_2H\text{-}I \rightleftharpoons IC_4H_8O + OH$	R1592	6.00×10^{11}	0	22000	[e]
$IC_4H_8O_2H\text{-}I \rightleftharpoons OH + CH_2O + C_3H_6$	R1593	8.45×10^{15}	-0.7	29170	[e]
$IC_4H_8 \rightleftharpoons C_3H_5\text{-}T + CH_3$	R1594	1.92×10^{66}	-14.2	128100	[e]
$IC_4H_8 \rightleftharpoons IC_4H_7 + H$	R1595	3.07×10^{55}	-11.5	114300	[e]
$IC_4H_8 + H \rightleftharpoons C_3H_6 + CH_3$	R1596	5.68×10^{33}	-5.7	20000	[e]
$IC_4H_8 + H \rightleftharpoons IC_4H_7 + H_2$	R1597	3.40×10^{5}	2.5	2492	[e]
$IC_4H_8 + O \rightleftharpoons CH_2CO + CH_3 + CH_3$	R1598	3.33×10^{7}	1.8	76	[e]
$IC_4H_8 + O \rightleftharpoons IC_3H_6CO + H + H$	R1599	1.66×10^{7}	1.8	76	[e]
$IC_4H_8 + O \rightleftharpoons IC_4H_7 + OH$	R1600	1.21×10^{11}	0.7	7633	[e]
$IC_4H_8 + CH_3 \rightleftharpoons IC_4H_7 + CH_4$	R1601	4.42×10^{0}	3.5	5675	[e]
$IC_4H_8 + HO_2 \rightleftharpoons IC_4H_7 + H_2O_2$	R1602	1.93×10^{4}	2.6	13910	[e]
$IC_4H_8 + O_2CHO \rightleftharpoons IC_4H_7 + HO_2CHO$	R1603	1.93×10^{4}	2.6	13910	[e]
$IC_4H_8 + O_2 \rightleftharpoons IC_4H_7 + HO_2$	R1604	6.00×10^{12}	0	39900	[e]
$IC_4H_8 + C_3H_5\text{-}A \rightleftharpoons IC_4H_7 + C_3H_6$	R1605	7.94×10^{11}	0	20500	[e]
$IC_4H_8 + C_3H_5\text{-}S \rightleftharpoons IC_4H_7 + C_3H_6$	R1606	7.94×10^{11}	0	20500	[e]
$IC_4H_8 + C_3H_5\text{-}T \rightleftharpoons IC_4H_7 + C_3H_6$	R1607	7.94×10^{11}	0	20500	[e]
$IC_4H_8 + OH \rightleftharpoons IC_4H_7 + H_2O$	R1608	5.20×10^{6}	2	-298	[e]

Reactions	Code	$A_{r,g}$	$\beta_{r,g}$	$E_{r,g}$	Ref
$IC_4H_8 + O \rightleftharpoons IC_3H_7 + HCO$	R1609	1.58×10^{7}	1.8	-1216	[e]
$IC_4H_8 + CH_3O_2 \rightleftharpoons IC_4H_7 + CH_3O_2H$	R1610	1.93×10^{4}	2.6	13910	[e]
$IC_4H_8 + HO_2 \rightleftharpoons IC_4H_8O + OH$	R1611	1.29×10^{12}	0	13340	[e]
$IC_4H_7 + O_2 \rightleftharpoons IC_3H_5CHO + OH$	R1612	2.47×10^{13}	-0.5	23020	[e]
$IC_4H_7 + O_2 \rightleftharpoons CH_3COCH_2 + CH_2O$	R1613	7.14×10^{15}	-1.2	21050	[e]
$IC_4H_7 + O_2 \rightleftharpoons C_3H_4\text{-}A + CH_2O + OH$	R1614	7.29×10^{29}	-5.7	21450	[e]
$IC_4H_7 + O \rightleftharpoons IC_3H_5CHO + H$	R1615	6.03×10^{13}	0	0	[e]
$IC_4H_7 \rightleftharpoons C_3H_4\text{-}A + CH_3$	R1616	1.23×10^{47}	-9.7	74260	[e]
$CH_3O_2 + IC_4H_7 \rightleftharpoons CH_3O + IC_4H_7O$	R1617	7.00×10^{12}	0	-1000	[e]
$IC_4H_7 + HO_2 \rightleftharpoons IC_4H_7O + OH$	R1618	7.00×10^{12}	0	-1000	[e]
$C_3H_5\text{-}T + CH_2O \rightleftharpoons IC_4H_7O$	R1619	1.00×10^{11}	0	12600	[e]
$IC_4H_7O \rightleftharpoons IC_4H_6OH$	R1620	1.39×10^{11}	0	15600	[e]
$IC_4H_7O \rightleftharpoons IC_3H_5CHO + H$	R1621	5.00×10^{13}	0	29100	[e]
$IC_4H_6OH + H_2 \rightleftharpoons IC_4H_7OH + H$	R1622	2.16×10^{4}	2.4	18990	[e]
$IC_4H_7OH + O_2 \rightleftharpoons IC_4H_6OH + HO_2$	R1623	6.00×10^{13}	0	39900	[e]
$IC_4H_6OH + CH_2O \rightleftharpoons IC_4H_7OH + HCO$	R1624	6.30×10^{8}	1.9	18190	[e]
$IC_4H_6OH + IC_4H_8 \rightleftharpoons IC_4H_7OH + IC_4H_7$	R1625	4.70×10^{2}	3.3	19840	[e]
$IC_4H_6OH + H \rightleftharpoons IC_4H_7OH$	R1626	1.00×10^{14}	0	0	[e]
$IC_4H_6OH + H_2O_2 \rightleftharpoons IC_4H_7OH + HO_2$	R1627	7.83×10^{5}	2	13580	[e]
$C_3H_4\text{-}A + CH_2OH \rightleftharpoons IC_4H_6OH$	R1628	1.00×10^{11}	0	9200	[e]
$IC_4H_7O + O_2 \rightleftharpoons IC_3H_5CHO + HO_2$	R1629	3.00×10^{10}	0	1649	[e]
$IC_4H_7O + HO_2 \rightleftharpoons IC_3H_5CHO + H_2O_2$	R1630	3.00×10^{11}	0	0	[e]
$IC_4H_7O + CH_3 \rightleftharpoons IC_3H_5CHO + CH_4$	R1631	2.40×10^{13}	0	0	[e]
$IC_4H_7O + O \rightleftharpoons IC_3H_5CHO + OH$	R1632	6.00×10^{12}	0	0	[e]
$IC_4H_7O + OH \rightleftharpoons IC_3H_5CHO + H_2O$	R1633	1.81×10^{13}	0	0	[e]
$IC_4H_7O + H \rightleftharpoons IC_3H_5CHO + H_2$	R1634	1.99×10^{13}	0	0	[e]
$IC_3H_5CHO + OH \rightleftharpoons IC_3H_5CO + H_2O$	R1635	2.69×10^{10}	0.8	-340	[e]
$IC_3H_5CHO + HO_2 \rightleftharpoons IC_3H_5CO + H_2O_2$	R1636	1.00×10^{12}	0	11920	[e]
$IC_3H_5CHO + CH_3 \rightleftharpoons IC_3H_5CO + CH_4$	R1637	3.98×10^{12}	0	8700	[e]
$IC_3H_5CHO + O \rightleftharpoons IC_3H_5CO + OH$	R1638	7.18×10^{12}	0	1389	[e]
$IC_3H_5CHO + O_2 \rightleftharpoons IC_3H_5CO + HO_2$	R1639	2.00×10^{13}	0	40700	[e]
$IC_3H_5CHO + H \rightleftharpoons IC_3H_5CO + H_2$	R1640	2.60×10^{12}	0	2600	[e]
$C_3H_5\text{-}T + CO \rightleftharpoons IC_3H_5CO$	R1641	1.51×10^{11}	0	4809	[e]
$TC_3H_6CHO + HO_2 \rightleftharpoons TC_3H_6OCHO + OH$	R1642	9.64×10^{12}	0	0	[e]
$TC_3H_6OCHO \rightleftharpoons CH_3COCH_3 + HCO$	R1643	3.98×10^{13}	0	9700	[e]
$IC_3H_5CHO + H \rightleftharpoons TC_3H_6CHO$	R1644	1.30×10^{13}	0	1200	[e]
$IC_3H_6CO + H \rightleftharpoons TC_3H_6CHO$	R1645	1.30×10^{13}	0	4800	[e]
$TC_3H_6CHO + H_2 \rightleftharpoons IC_3H_7CHO + H$	R1646	2.16×10^{5}	2.4	18990	[e]

Reactions	Code	$A_{r,g}$	$\beta_{r,g}$	$E_{r,g}$	Ref
$IC_4H_7O + OH \rightleftharpoons IC_4H_7OOH$	R1647	1.00×10^{11}	0	0	[e]
$IC_4H_7O + H \rightleftharpoons IC_4H_7OH$	R1648	4.00×10^{13}	0	0	[e]
$IC_4H_7OH + H \rightleftharpoons IC_4H_8OH$	R1649	1.00×10^{13}	0	1200	[e]
$IC_4H_7O + H_2 \rightleftharpoons IC_4H_7OH + H$	R1650	9.05×10^{6}	2	17830	[e]
$IC_4H_7 + OH \rightleftharpoons IC_4H_7OH$	R1651	3.00×10^{13}	0	0	[e]
$IC_4H_7OH + HCO \rightleftharpoons IC_4H_7O + CH_2O$	R1652	3.02×10^{11}	0	18160	[e]
$TC_3H_6CHO + CH_2O \rightleftharpoons IC_3H_7CHO + HCO$	R1653	2.52×10^{8}	1.9	18190	[e]
$TC_3H_6CHO + IC_4H_8 \rightleftharpoons IC_3H_7CHO + IC_4H_7$	R1654	4.70×10^{2}	3.3	19840	[e]
$IC_3H_6CO + OH \rightleftharpoons IC_3H_7 + CO_2$	R1655	1.73×10^{12}	0	-1010	[e]
$TC_3H_6CHO + OH \rightleftharpoons TC_3H_6OHCHO$	R1656	5.00×10^{13}	0	0	[e]
$TC_3H_6OH + HCO \rightleftharpoons TC_3H_6OHCHO$	R1657	1.81×10^{13}	0	0	[e]
$CH_3COCH_3 + H \rightleftharpoons TC_3H_6OH$	R1658	1.00×10^{12}	0	0	[e]
$IC_3H_5OH + H \rightleftharpoons TC_3H_6OH$	R1659	1.30×10^{13}	0	1560	[e]
$C_3H_5\text{-}T + OH \rightleftharpoons IC_3H_5OH$	R1660	5.00×10^{13}	0	0	[e]
$TC_3H_6CHO + O_2 \rightleftharpoons TC_3H_6O_2CHO$	R1661	1.99×10^{17}	-2.1	0	[e]
$TC_3H_6O_2CHO \rightleftharpoons IC_3H_5O_2HCHO$	R1662	6.00×10^{11}	0	29880	[e]
$TC_3H_6O_2CHO \rightleftharpoons TC_3H_6O_2HCO$	R1663	1.00×10^{11}	0	25750	[e]
$IC_3H_5CHO + HO_2 \rightleftharpoons IC_3H_5O_2HCHO$	R1664	2.23×10^{11}	0	10600	[e]
$TC_3H_6O_2HCO \rightleftharpoons CH_3COCH_3 + CO + OH$	R1665	4.24×10^{18}	-1.4	4800	[e]
$TC_3H_6OH + O_2 \rightleftharpoons CH_3COCH_3 + HO_2$	R1666	2.23×10^{13}	0	0	[e]
$IC_3H_6CO + OH \rightleftharpoons TC_3H_6OH + CO$	R1667	2.00×10^{12}	0	-1010	[e]
$TC_3H_6CHO + O_2 \rightleftharpoons IC_3H_5CHO + HO_2$	R1668	2.72×10^{-19}	0	7240	[e]
$TC_3H_6CHO + O_2 \rightleftharpoons CH_3COCH_3 + CO + OH$	R1669	3.62×10^{-20}	0	0	[e]
$TC_3H_6CHO + HO_2 \rightleftharpoons IC_3H_7CHO + O_2$	R1670	3.68×10^{12}	0	1310	[e]
$TC_3H_6CHO + CH_3 \rightleftharpoons IC_3H_5CHO + CH_4$	R1671	3.01×10^{12}	-0.3	-131	[e]
$TC_4H_8CHO \rightleftharpoons IC_3H_5CHO + CH_3$	R1672	1.00×10^{13}	0	26290	[e]
$TC_4H_8CHO \rightleftharpoons IC_4H_8 + HCO$	R1673	8.52×10^{12}	0	20090	[e]
$TC_4H_8CHO + O_2 \rightleftharpoons O_2C_4H_8CHO$	R1674	2.00×10^{12}	0	0	[e]
$O_2C_4H_8CHO \rightleftharpoons O_2HC_4H_8CO$	R1675	2.16×10^{11}	0	15360	[e]
$IC_4H_8O_2H\text{-}T + CO \rightleftharpoons O_2HC_4H_8CO$	R1676	1.50×10^{11}	0	4809	[e]
$IC_4H_7O + IC_4H_8 \rightleftharpoons IC_4H_7OH + IC_4H_7$	R1677	2.70×10^{11}	0	4000	[e]
$IC_4H_6OH + HO_2 \rightleftharpoons CH_2CCH_2OH + CH_2O + OH$	R1678	1.45×10^{13}	0	0	[e]
$IC_4H_8 + CH_2CCH_2OH \rightleftharpoons IC_4H_7 + C_3H_5OH$	R1679	7.94×10^{11}	0	20500	[e]
$CH_2CCH_2OH + H_2O_2 \rightleftharpoons C_3H_5OH + HO_2$	R1680	3.01×10^{9}	0	2583	[e]
$C_3H_5OH + OH \rightleftharpoons CH_2CCH_2OH + H_2O$	R1681	5.06×10^{12}	0	5960	[e]
$C_3H_5OH + H \rightleftharpoons CH_2CCH_2OH + H_2$	R1682	3.90×10^{5}	2.5	5821	[e]
$C_3H_5OH + O_2 \rightleftharpoons CH_2CCH_2OH + HO_2$	R1683	4.00×10^{13}	0	60690	[e]
$C_3H_5OH + CH_3 \rightleftharpoons CH_2CCH_2OH + CH_4$	R1684	2.40×10^{11}	0	8030	[e]

Reactions	Code	$A_{r,g}$	$\beta_{r,g}$	$E_{r,g}$	Ref
$CH_2CCH_2OH + CH_3 \rightleftharpoons IC_4H_7OH$	R1685	3.00×10^{13}	0	0	[e]
$CH_2CCH_2OH + H \rightleftharpoons C_3H_5OH$	R1686	1.00×10^{14}	0	0	[e]
$CH_2CCH_2OH + O_2 \rightleftharpoons CH_2OH + CO + CH_2O$	R1687	4.34×10^{12}	0	0	[e]
$CH_2CCH_2OH \rightleftharpoons C_2H_2 + CH_2OH$	R1688	2.16×10^{40}	-8.3	45110	[e]
$C_3H_4\text{-A} + OH \rightleftharpoons CH_2CCH_2OH$	R1689	8.50×10^{12}	0	2000	[e]
$C_6H_5CH_3(+M) \rightleftharpoons C_6H_5CH_2 + H(+M)$	R1690	2.78×10^{15}	0.2	91168	[e]
$C_6H_5CH_3(+M) \rightleftharpoons C_6H_5 + CH_3(+M)$	R1691	1.95×10^{27}	-3.2	107447	[e]
$C_6H_5CH_3 + O_2 \rightleftharpoons C_6H_5CH_2 + HO_2$	R1692	2.18×10^{7}	2.5	46045	[e]
$C_6H_5CH_3 + HO_2 \rightleftharpoons C_6H_5CH_2 + H_2O_2$	R1693	3.97×10^{11}	0	14069.4	[e]
$C_6H_5CH_3 + H \rightleftharpoons C_6H_5CH_2 + H_2$	R1694	6.47×10^{0}	4	3384	[e]
$C_6H_5CH_3 + OH \rightleftharpoons C_6H_5CH_2 + H_2O$	R1695	1.77×10^{5}	2.4	-602	[e]
$C_6H_5CH_3 + O \rightleftharpoons C_6H_5CH_2 + OH$	R1696	6.30×10^{11}	0	0	[e]
$C_6H_5CH_3 + CH_3 \rightleftharpoons C_6H_5CH_2 + CH_4$	R1697	2.94×10^{11}	0	9245	[e]
$C_6H_5CH_3 + HCO \rightleftharpoons C_6H_5CH_2 + CH_2O$	R1698	3.77×10^{13}	0	23787.4	[e]
$C_6H_5CH_3 + C_2H_3 \rightleftharpoons C_6H_5CH_2 + C_2H_4$	R1699	4.00×10^{12}	0	8000	[e]
$C_6H_5CH_3 + C_3H_5\text{-A} \rightleftharpoons C_6H_5CH_2 + C_3H_6$	R1700	1.60×10^{12}	0	15100	[e]
$C_6H_5CH_3 + C_3H_3 \rightleftharpoons C_6H_5CH_2 + C_3H_4\text{-P}$	R1701	1.60×10^{12}	0	15100	[e]
$C_6H_5CH_3 + C_4H_5\text{-I} \rightleftharpoons C_6H_5CH_2 + C_4H_6$	R1702	1.60×10^{12}	0	15100	[e]
$C_6H_5CH_3 + C_4H_5\text{-N} \rightleftharpoons C_6H_5CH_2 + C_4H_6$	R1703	1.60×10^{12}	0	15100	[e]
$C_6H_5CH_3 + C_5H_5 \rightleftharpoons C_6H_5CH_2 + C_5H_6$	R1704	1.60×10^{12}	0	11100	[e]
$C_6H_5CH_3 + C_6H_5 \rightleftharpoons C_6H_5CH_2 + C_6H_6$	R1705	7.90×10^{13}	0	12000	[e]
$C_6H_5CH_3 + C_6H_5O \rightleftharpoons C_6H_5CH_2 + C_6H_5OH$	R1706	5.43×10^{12}	0	20923	[e]
$C_6H_5CH_3 + C_6H_4CH_3 \rightleftharpoons C_6H_5CH_2 + C_6H_5CH_3$	R1707	7.90×10^{13}	0	12000	[e]
$C_6H_5CH_3 + OC_6H_4CH_3 \rightleftharpoons C_6H_5CH_2 + HO_3C_6H_4CH_3$	R1708	1.60×10^{11}	0	15100	[e]
$C_6H_5CH_3 + C_6H_5CH_2OO \rightleftharpoons C_6H_5CH_2 + BZCOOH$	R1709	4.00×10^{11}	0	14000	[e]
$C_6H_5CH_3 + C_6H_5CH_2O \rightleftharpoons C_6H_5CH_2 + C_6H_5CH_2OH$	R1710	1.60×10^{11}	0	11100	[e]
$C_6H_5CH_3 + HO_3C_6H_4CH_2 \rightleftharpoons C_6H_5CH_2 + HO_3C_6H_4CH_3$	R1711	1.60×10^{11}	0	15100	[e]
$C_6H_5CH_3 + H \rightleftharpoons C_6H_4CH_3 + H_2$	R1712	5.00×10^{8}	1	16800	[e]
$C_6H_5CH_3 + O \rightleftharpoons C_6H_4CH_3 + OH$	R1713	1.66×10^{13}	0	14700	[e]
$C_6H_5CH_3 + OH \rightleftharpoons C_6H_4CH_3 + H_2O$	R1714	1.33×10^{8}	1.4	1450	[e]
$C_6H_5CH_3 + HO_2 \rightleftharpoons C_6H_4CH_3 + H_2O_2$	R1715	3.33×10^{11}	0	28900	[e]
$C_6H_5CH_3 + CH_3 \rightleftharpoons C_6H_4CH_3 + CH_4$	R1716	1.60×10^{12}	0	15000	[e]
$C_6H_5CH_3 + O \rightleftharpoons OC_6H_4CH_3 + H$	R1717	1.70×10^{13}	0	3600	[e]
$C_6H_5CH_3 + OH \rightleftharpoons HO_3C_6H_4CH_3 + H$	R1718	1.10×10^{2}	3.2	5590	[e]
$C_6H_5CH_3 + H \rightleftharpoons C_6H_6 + CH_3$	R1719	9.49×10^{5}	2	944	[e]
$C_6H_5CH_2 \rightleftharpoons C_5H_5 + C_2H_2$	R1720	6.00×10^{13}	0	70000	[e]
$C_6H_5CH_2 \rightleftharpoons C_3H_3 + C_4H_4$	R1721	2.00×10^{14}	0	83600	[e]
$C_6H_5CH_2 + O \rightleftharpoons C_6H_5CHO + H$	R1722	2.11×10^{14}	0	0	[e]

Reactions	Code	$A_{r,g}$	$\beta_{r,g}$	$E_{r,g}$	Ref
$C_6H_5CH_2 + O \rightleftharpoons C_6H_5 + CH_2O$	R1723	1.19×10^{14}	0	0	[e]
$C_6H_5CH_2 + OH \rightleftharpoons C_6H_5CH_2OH$	R1724	2.00×10^{13}	0	0	[e]
$C_6H_5CH_2 + HO_2 \rightleftharpoons BZCOOH$	R1725	6.75×10^{44}	-17.5	-45232	[e]
$C_6H_5CH_2 + HO_2 \rightleftharpoons C_6H_5CH_2O + OH$	R1726	1.00×10^{13}	0	0	[e]
$C_6H_5CH_2 + CH_3 \rightleftharpoons C_6H_5C_2H_5$	R1727	1.19×10^{13}	0	221	[e]
$C_6H_4CH_3 + O_2 \rightleftharpoons OC_6H_4CH_3 + O$	R1728	2.60×10^{13}	0	6100	[e]
$C_6H_4CH_3 + O_2 \rightleftharpoons O\text{-}C_6H_4O_2 + CH_3$	R1729	3.00×10^{13}	0	9000	[e]
$C_6H_4CH_3 + H \rightleftharpoons C_6H_5CH_3$	R1730	1.00×10^{14}	0	0	[e]
$C_6H_4CH_3 + H \rightleftharpoons C_6H_5CH_2 + H$	R1731	1.00×10^{13}	0	0	[e]
$C_6H_4CH_3 + O \rightleftharpoons OC_6H_4CH_3$	R1732	1.00×10^{14}	0	0	[e]
$C_6H_4CH_3 + OH \rightleftharpoons HOC_6H_4CH_3$	R1733	1.00×10^{13}	0	0	[e]
$C_6H_4CH_3 + HO_2 \rightleftharpoons OC_6H_4CH_3 + OH$	R1734	5.00×10^{12}	0	0	[e]
$C_6H_5CH_2OO(+M) \rightleftharpoons C_6H_5CH_2 + O_2(+M)$	R1735	4.17×10^{36}	-7.1	32235	[e]
$C_6H_5CH_2OO + H \rightleftharpoons BZCOOH$	R1736	1.00×10^{14}	0	0	[e]
$C_6H_5CH_2OO + HO_2 \rightleftharpoons BZCOOH + O_2$	R1737	2.00×10^{11}	0	0	[e]
$C_6H_5CH_2OO + C_6H_5CH_2OO \rightleftharpoons C_6H_5CH_2OH + C_6H_5CHO + O_2$	R1738	1.40×10^{10}	0	-720	[e]
$C_6H_5CH_2OO + C_6H_5CH_2OO \rightleftharpoons C_6H_5CH_2O + C_6H_5CH_2O + O_2$	R1739	6.30×10^{10}	0	-720	[e]
$C_6H_5CH_2O + OH \rightleftharpoons BZCOOH$	R1740	2.00×10^{13}	0	0	[e]
$C_6H_5CH_2O \rightleftharpoons C_6H_5CHO + H$	R1741	1.99×10^{13}	0	18728	[e]
$C_6H_5CH_2O \rightleftharpoons C_6H_5 + CH_2O$	R1742	8.55×10^{13}	0	26017	[e]
$C_6H_5CH_2O + O_2 \rightleftharpoons C_6H_5CHO + HO_2$	R1743	6.00×10^{10}	0	1600	[e]
$OC_6H_4CH_3 \rightleftharpoons C_6H_6 + CO + H$	R1744	7.60×10^{11}	0	43800	[e]
$OC_6H_4CH_3 + H \rightleftharpoons HOC_6H_4CH_3$	R1745	1.00×10^{14}	0	0	[e]
$C_6H_5CH_2 + C_6H_5CH_2 \rightleftharpoons C_{14}H_{14}$	R1746	5.00×10^{12}	0	454	[e]
$C_{14}H_{14} \rightleftharpoons C_{14}H_{13} + H$	R1747	1.00×10^{16}	0	83660	[e]
$C_{14}H_{14} + H \rightleftharpoons C_{14}H_{13} + H_2$	R1748	3.16×10^{12}	0	0	[e]
$C_{14}H_{14} + O_2 \rightleftharpoons C_{14}H_{13} + HO_2$	R1749	2.80×10^{12}	0	35000	[e]
$C_{14}H_{14} + O \rightleftharpoons C_{14}H_{13} + OH$	R1750	8.40×10^{11}	0	-2000	[e]
$C_{14}H_{14} + OH \rightleftharpoons C_{14}H_{13} + H_2O$	R1751	7.00×10^{9}	1	-1100	[e]
$C_{14}H_{14} + HO_2 \rightleftharpoons C_{14}H_{13} + H_2O_2$	R1752	5.40×10^{11}	0	12000	[e]
$C_{14}H_{14} + CH_3 \rightleftharpoons C_{14}H_{13} + CH_4$	R1753	2.20×10^{12}	0	9100	[e]
$C_{14}H_{14} + C_3H_5\text{-}A \rightleftharpoons C_{14}H_{13} + C_3H_6$	R1754	2.20×10^{12}	0	9100	[e]
$C_{14}H_{14} + C_6H_5CH_2 \rightleftharpoons C_{14}H_{13} + C_6H_5CH_3$	R1755	2.20×10^{11}	0	9100	[e]
$C_{14}H_{14} + C_6H_5 \rightleftharpoons C_{14}H_{13} + C_6H_6$	R1756	1.06×10^{14}	0	9949	[e]
$C_{14}H_{14} + C_6H_5O \rightleftharpoons C_{14}H_{13} + C_6H_5OH$	R1757	5.43×10^{12}	0	20923	[e]
$C_{14}H_{13} \rightleftharpoons C_{14}H_{12} + H$	R1758	7.90×10^{15}	0	51864	[e]
$C_{14}H_{13} + O_2 \rightleftharpoons C_6H_5CHO + C_6H_5CH_2O$	R1759	3.94×10^{50}	-11.5	42250	[e]

Reactions	Code	$A_{r,g}$	$\beta_{r,g}$	$E_{r,g}$	Ref
$C_{14}H_{13} + HO_2 \rightleftharpoons C_6H_5CH_2 + C_6H_5CHO + OH$	R1760	1.92×10^{13}	0	0	[e]
$C_{14}H_{12} + O_2 \rightleftharpoons HO_2 + C_{14}H_{11}$	R1761	4.00×10^{13}	0	58200	[e]
$C_{14}H_{12} + H \rightleftharpoons C_{14}H_{11} + H_2$	R1762	8.42×10^{-3}	4.6	2583	[e]
$C_{14}H_{12} + OH \rightleftharpoons C_{14}H_{11} + H_2O$	R1763	2.02×10^{13}	0	5955	[e]
$C_{14}H_{12} + O \rightleftharpoons C_6H_5CO + C_6H_5CH_2$	R1764	7.95×10^{3}	1.7	657.4	[e]
$C_{14}H_{11} \rightarrow C_6H_5 + C_2H + C_6H_5$	R1765	1.07×10^{25}	-2.2	88474.6	[e]
$C_{14}H_{11} + O_2 \rightleftharpoons C_6H_5CO + C_6H_5CHO$	R1766	1.70×10^{29}	-5.3	6500	[e]
$C_{14}H_{12} + O \rightleftharpoons C_{14}H_{11} + OH$	R1767	4.20×10^{11}	0	-1940	[e]
$C_{14}H_{12} + HO_2 \rightleftharpoons C_{14}H_{11} + H_2O_2$	R1768	2.70×10^{11}	0	11640	[e]
$C_{14}H_{12} + CH_3 \rightleftharpoons C_{14}H_{11} + CH_4$	R1769	1.10×10^{12}	0	8827	[e]
$C_{14}H_{12} + C_3H_5\text{-}A \rightleftharpoons C_{14}H_{11} + C_3H_6$	R1770	1.10×10^{12}	0	8827	[e]
$C_{14}H_{12} + C_6H_5O \rightleftharpoons C_{14}H_{11} + C_6H_5OH$	R1771	5.43×10^{12}	0	20923	[e]
$C_{14}H_{12} + C_6H_5CH_2 \rightleftharpoons C_{14}H_{11} + C_6H_5CH_3$	R1772	1.10×10^{11}	0	8827	[e]
$C_{14}H_{13} + O_2 \rightleftharpoons C_{14}H_{13}OO$	R1773	8.00×10^{12}	0	0	[e]
$C_{14}H_{13} + HO_2 \rightleftharpoons C_{14}H_{13}O + OH$	R1774	7.00×10^{12}	0	-1000	[e]
$C_6H_5CH_2 + C_6H_5CHO \rightleftharpoons C_{14}H_{13}O$	R1775	1.00×10^{11}	0	12900	[e]
$C_{14}H_{13}OOH + C_6H_5CH_2 \rightleftharpoons C_{14}H_{13}OO + C_6H_5CH_3$	R1776	1.44×10^{10}	0	17700	[e]
$C_{14}H_{13}OO + HO_2 \rightleftharpoons C_{14}H_{13}OOH + O_2$	R1777	1.75×10^{10}	0	-3275	[e]
$C_{14}H_{13}OO + H_2O_2 \rightleftharpoons C_{14}H_{13}OOH + HO_2$	R1778	2.40×10^{12}	0	10000	[e]
$C_{14}H_{13}O + OH \rightleftharpoons C_{14}H_{13}OOH$	R1779	2.00×10^{13}	0	0	[e]
$C_{14}H_{13}OO \rightleftharpoons C_{14}H_{12}OOH$	R1780	2.59×10^{12}	0	21374	[e]
$C_{14}H_{12} + HO_2 \rightleftharpoons C_{14}H_{12}OOH$	R1781	1.00×10^{11}	0	10530	[e]
$C_{14}H_{12}OOH + O_2 \rightleftharpoons C_{14}H_{12}O_2H^{-1}O_2$	R1782	8.00×10^{12}	0	0	[e]
$C_{14}H_{12}O_2H^{-1}O_2 \rightleftharpoons C_{14}H_{11}O^{-1}O_2H + OH$	R1783	1.30×10^{12}	0	18374	[e]
$C_{14}H_{11}O^{-1}O_2H \rightleftharpoons C_6H_5CO + C_6H_5CO + OH$	R1784	1.00×10^{16}	0	43000	[e]
$C_6H_5CHO \rightleftharpoons C_6H_5CO + H$	R1785	4.00×10^{15}	0	83700	[e]
$C_6H_5CHO + O_2 \rightleftharpoons C_6H_5CO + HO_2$	R1786	7.00×10^{11}	0	39500	[e]
$C_6H_5CHO + H \rightleftharpoons C_6H_6 + HCO$	R1787	5.80×10^{13}	0	8100	[e]
$C_6H_5CHO + H \rightleftharpoons C_6H_5CO + H_2$	R1788	4.00×10^{13}	0	3200	[e]
$C_6H_5CHO + O \rightleftharpoons C_6H_5CO + OH$	R1789	6.00×10^{12}	0	1800	[e]
$C_6H_5CHO + OH \rightleftharpoons C_6H_5CO + H_2O$	R1790	7.80×10^{12}	0	0	[e]
$C_6H_5CHO + HO_2 \rightleftharpoons C_6H_5CO + H_2O_2$	R1791	3.00×10^{12}	0	11000	[e]
$C_6H_5CHO + CH_3 \rightleftharpoons C_6H_5CO + CH_4$	R1792	2.00×10^{-6}	5.6	1500	[e]
$C_6H_5CHO + C_2H_5 \rightleftharpoons C_6H_5CO + C_2H_6$	R1793	1.30×10^{12}	0	7500	[e]
$C_6H_5CHO + C_3H_5\text{-}A \rightleftharpoons C_6H_5CO + C_3H_6$	R1794	1.30×10^{12}	0	11500	[e]
$C_6H_5CHO + C_4H_5\text{-}I \rightleftharpoons C_6H_5CO + C_4H_6$	R1795	1.30×10^{12}	0	11500	[e]
$C_6H_5CHO + C_4H_5\text{-}N \rightleftharpoons C_6H_5CO + C_4H_6$	R1796	1.30×10^{12}	0	7500	[e]
$C_6H_5CHO + C_5H_5 \rightleftharpoons C_6H_5CO + C_5H_6$	R1797	1.30×10^{11}	0	11500	[e]
$C_6H_5CHO + C_6H_5 \rightleftharpoons C_6H_5CO + C_6H_6$	R1798	1.30×10^{11}	0	11500	[e]

Reactions	Code	$A_{r,g}$	$\beta_{r,g}$	$E_{r,g}$	Ref
$C_6H_5CHO + C_6H_5CH_2 \rightleftharpoons C_6H_5CO + C_6H_5CH_3$	R1799	1.30×10^{11}	0	11500	[e]
$C_6H_5CHO + C_6H_5O \rightleftharpoons C_6H_5CO + C_6H_5OH$	R1800	1.30×10^{11}	0	11500	[e]
$C_6H_5CHO + OC_6H_4CH_3 \rightleftharpoons C_6H_5CO + HO_3C_6H_4CH_3$	R1801	1.30×10^{11}	0	11500	[e]
$C_6H_5CHO + HO_3C_6H_4CH_2 \rightleftharpoons C_6H_5CO + HO_3C_6H_4CH_3$	R1802	1.30×10^{11}	0	11500	[e]
$C_6H_5CO \rightleftharpoons C_6H_5 + CO$	R1803	4.00×10^{14}	0	29500	[e]
$HO_3C_6H_4CH_3 + O_2 \rightleftharpoons OC_6H_4CH_3 + HO_2$	R1804	1.00×10^{13}	0	38900	[e]
$HO_3C_6H_4CH_3 + O_2 \rightleftharpoons HO_3C_6H_4CH_2 + HO_2$	R1805	2.10×10^{12}	0	39700	[e]
$HO_3C_6H_4CH_3 + H \rightleftharpoons C_6H_5OH + CH_3$	R1806	5.80×10^{13}	0	8100	[e]
$HO_3C_6H_4CH_3 + H \rightleftharpoons OC_6H_4CH_3 + H_2$	R1807	1.20×10^{14}	0	12400	[e]
$HO_3C_6H_4CH_3 + O \rightleftharpoons OC_6H_4CH_3 + OH$	R1808	1.30×10^{13}	0	2900	[e]
$HO_3C_6H_4CH_3 + OH \rightleftharpoons OC_6H_4CH_3 + H_2O$	R1809	1.40×10^{8}	1.4	-960	[e]
$HO_3C_6H_4CH_3 + HO_2 \rightleftharpoons OC_6H_4CH_3 + H_2O_2$	R1810	1.00×10^{12}	0	10000	[e]
$HO_3C_6H_4CH_3 + CH_3 \rightleftharpoons OC_6H_4CH_3 + CH_4$	R1811	1.80×10^{11}	0	7700	[e]
$HO_3C_6H_4CH_3 + C_6H_5 \rightleftharpoons OC_6H_4CH_3 + C_6H_6$	R1812	4.90×10^{12}	0	4400	[e]
$HO_3C_6H_4CH_3 + C_5H_5 \rightleftharpoons OC_6H_4CH_3 + C_5H_6$	R1813	4.90×10^{11}	0	9400	[e]
$HO_3C_6H_4CH_3 + C_3H_5\text{-A} \rightleftharpoons OC_6H_4CH_3 + C_3H_6$	R1814	4.90×10^{11}	0	9400	[e]
$HO_3C_6H_4CH_3 + C_4H_5\text{-I} \rightleftharpoons OC_6H_4CH_3 + C_4H_6$	R1815	4.90×10^{11}	0	9400	[e]
$HO_3C_6H_4CH_3 + C_4H_5\text{-N} \rightleftharpoons OC_6H_4CH_3 + C_4H_6$	R1816	4.90×10^{11}	0	9400	[e]
$HO_3C_6H_4CH_3 + C_6H_5O \rightleftharpoons OC_6H_4CH_3 + C_6H_5OH$	R1817	4.90×10^{11}	0	9400	[e]
$HO_3C_6H_4CH_3 + H \rightleftharpoons HO_3C_6H_4CH_2 + H_2$	R1818	1.20×10^{14}	0	8400	[e]
$HO_3C_6H_4CH_3 + O \rightleftharpoons HO_3C_6H_4CH_2 + OH$	R1819	6.30×10^{11}	0	0	[e]
$HO_3C_6H_4CH_3 + OH \rightleftharpoons HO_3C_6H_4CH_2 + H_2O$	R1820	5.20×10^{9}	1	870	[e]
$HO_3C_6H_4CH_3 + HO_2 \rightleftharpoons HO_3C_6H_4CH_2 + H_2O_2$	R1821	4.00×10^{11}	0	14000	[e]
$HO_3C_6H_4CH_3 + CH_3 \rightleftharpoons HO_3C_6H_4CH_2 + CH_4$	R1822	1.60×10^{12}	0	11100	[e]
$HO_3C_6H_4CH_3 + C_3H_5\text{-A} \rightleftharpoons HO_3C_6H_4CH_2 + C_3H_6$	R1823	1.60×10^{12}	0	15100	[e]
$HO_3C_6H_4CH_3 + C_3H_3 \rightleftharpoons HO_3C_6H_4CH_2 + C_3H_4\text{-P}$	R1824	1.60×10^{12}	0	15100	[e]
$HO_3C_6H_4CH_3 + C_4H_5\text{-I} \rightleftharpoons HO_3C_6H_4CH_2 + C_4H_6$	R1825	1.60×10^{12}	0	15100	[e]
$HO_3C_6H_4CH_3 + C_4H_5\text{-N} \rightleftharpoons HO_3C_6H_4CH_2 + C_4H_6$	R1826	1.60×10^{12}	0	11100	[e]
$HO_3C_6H_4CH_3 + C_5H_5 \rightleftharpoons HO_3C_6H_4CH_2 + C_5H_6$	R1827	1.60×10^{11}	0	15100	[e]
$HO_3C_6H_4CH_3 + C_6H_5 \rightleftharpoons HO_3C_6H_4CH_2 + C_6H_6$	R1828	7.90×10^{13}	0	12000	[e]
$HO_3C_6H_4CH_3 + C_6H_5O \rightleftharpoons HO_3C_6H_4CH_2 + C_6H_5OH$	R1829	1.60×10^{11}	0	15100	[e]
$HO_3C_6H_4CH_3 + C_6H_4CH_3 \rightleftharpoons OC_6H_4CH_3 + C_6H_5CH_3$	R1830	7.90×10^{13}	0	12000	[e]
$HO_3C_6H_4CH_3 + OC_6H_4CH_3 \rightleftharpoons HO_3C_6H_4CH_2 + HO_3C_6H_4CH_3$	R1831	1.60×10^{11}	0	15100	[e]
$HO_3C_6H_4CH_3 + C_6H_5CH_2OO \rightleftharpoons HO_3C_6H_4CH_2 +$ BZCOOH	R1832	4.00×10^{11}	0	14000	[e]
$HO_3C_6H_4CH_3 + C_6H_5CH_2O \rightleftharpoons HO_3C_6H_4CH_2 + C_6H_5CH_2OH$	R1833	1.60×10^{11}	0	11100	[e]
$HO_3C_6H_4CH_2 + O_2 \rightleftharpoons HO_3C_6H_4CH_2OO$	R1834	4.60×10^{11}	0	-380	[e]

Reactions	Code	$A_{r,g}$	$\beta_{r,g}$	$E_{r,g}$	Ref
$HO_3C_6H_4CH_2 + O_2 \rightleftharpoons HO_3C_6H_4CH_2O + O$	R1835	6.30×10^{12}	0	40000	[e]
$HO_3C_6H_4CH_2 + H \rightleftharpoons HO_3C_6H_4CH_3$	R1836	1.00×10^{14}	0	0	[e]
$HO_3C_6H_4CH_2 + HO_2 \rightleftharpoons HO_3C_6H_4CH_2OOH$	R1837	5.00×10^{12}	0	0	[e]
$HO_3C_6H_4CH_2 + CH_3 \rightleftharpoons C_6H_5OH + C_2H_4$	R1838	5.00×10^{12}	0	0	[e]
$HO_3C_6H_4CH_2OO \rightleftharpoons HO_3C_6H_4CHO + OH$	R1839	3.40×10^{9}	1	37500	[e]
$HO_3C_6H_4CH_2O \rightleftharpoons HO_3C_6H_4CHO + H$	R1840	2.00×10^{13}	0	27500	[e]
$HO_3C_6H_4CH_2O + O_2 \rightleftharpoons HO_3C_6H_4CHO + HO_2$	R1841	6.00×10^{10}	0	1600	[e]
$HO_3C_6H_4CHO + H \rightleftharpoons HO_3C_6H_4CO + H_2$	R1842	4.00×10^{13}	0	3200	[e]
$HO_3C_6H_4CHO + O \rightleftharpoons HO_3C_6H_4CO + OH$	R1843	6.00×10^{12}	0	1800	[e]
$HO_3C_6H_4CHO + OH \rightleftharpoons HO_3C_6H_4CO + H_2O$	R1844	7.80×10^{12}	0	0	[e]
$HO_3C_6H_4CHO + HO_2 \rightleftharpoons HO_3C_6H_4CO + H_2O_2$	R1845	3.00×10^{12}	0	11000	[e]
$HO_3C_6H_4CHO + CH_3 \rightleftharpoons HO_3C_6H_4CO + CH_4$	R1846	2.00×10^{-6}	5.6	1500	[e]
$HO_3C_6H_4CO \rightleftharpoons C_6H_5O + CO$	R1847	4.00×10^{14}	0	29500	[e]
$HO_3C_6H_4CH_2O + OH \rightleftharpoons HO_3C_6H_4CH_2OOH$	R1848	2.00×10^{13}	0	0	[e]
$C_6H_5CH_2OH + O_2 \rightleftharpoons C_6H_5CHOH + HO_2$	R1849	1.40×10^{12}	0	34000	[e]
$C_6H_5CH_2OH + O_2 \rightleftharpoons C_6H_5CH_2O + HO_2$	R1850	2.00×10^{14}	0	41400	[e]
$C_6H_5CH_2OH + H \rightleftharpoons C_6H_6 + CH_2OH$	R1851	5.80×10^{13}	0	8100	[e]
$C_6H_5CH_2OH + H \rightleftharpoons C_6H_5CHOH + H_2$	R1852	8.00×10^{13}	0	6400	[e]
$C_6H_5CH_2OH + O \rightleftharpoons C_6H_5CHOH + OH$	R1853	4.20×10^{11}	0	-2000	[e]
$C_6H_5CH_2OH + OH \rightleftharpoons C_6H_5CHOH + H_2O$	R1854	3.90×10^{9}	1	-1100	[e]
$C_6H_5CH_2OH + HO_2 \rightleftharpoons C_6H_5CHOH + H_2O_2$	R1855	2.70×10^{11}	0	12000	[e]
$C_6H_5CH_2OH + CH_3 \rightleftharpoons C_6H_5CHOH + CH_4$	R1856	1.10×10^{12}	0	9100	[e]
$C_6H_5CH_2OH + C_3H_3 \rightleftharpoons C_6H_5CHOH + C_3H_4\text{-P}$	R1857	1.10×10^{12}	0	13100	[e]
$C_6H_5CH_2OH + C_3H_5\text{-A} \rightleftharpoons C_6H_5CHOH + C_3H_6$	R1858	1.10×10^{12}	0	13100	[e]
$C_6H_5CH_2OH + C_4H_5\text{-I} \rightleftharpoons C_6H_5CHOH + C_4H_6$	R1859	1.10×10^{12}	0	13100	[e]
$C_6H_5CH_2OH + C_4H_5\text{-N} \rightleftharpoons C_6H_5CHOH + C_4H_6$	R1860	1.10×10^{12}	0	13100	[e]
$C_6H_5CH_2OH + C_5H_5 \rightleftharpoons C_6H_5CHOH + C_5H_6$	R1861	1.10×10^{12}	0	9100	[e]
$C_6H_5CH_2OH + C_6H_5 \rightleftharpoons C_6H_5CHOH + C_6H_6$	R1862	5.20×10^{13}	0	10000	[e]
$C_6H_5CH_2OH + C_6H_5O \rightleftharpoons C_6H_5CHOH + C_6H_5OH$	R1863	1.10×10^{11}	0	13100	[e]
$C_6H_5CH_2OH + C_6H_5CH_2 \rightleftharpoons C_6H_5CHOH + C_6H_5CH_3$	R1864	1.10×10^{11}	0	13100	[e]
$C_6H_5CH_2OH + C_6H_4CH_3 \rightleftharpoons C_6H_5CHOH + C_6H_5CH_3$	R1865	5.20×10^{13}	0	10000	[e]
$C_6H_5CH_2OH + OC_6H_4CH_3 \rightleftharpoons C_6H_5CHOH + HO_3C_6H_4CH_3$	R1866	1.10×10^{11}	0	13100	[e]
$C_6H_5CH_2OH + HO_3C_6H_4CH_2 \rightleftharpoons C_6H_5CHOH + HO_3C_6H_4CH_3$	R1867	1.10×10^{11}	0	13100	[e]
$C_6H_5CH_2OH + C_6H_5CH_2O \rightleftharpoons C_6H_5CHOH + C_6H_5CH_2OH$	R1868	1.10×10^{11}	0	9100	[e]
$C_6H_5CHOH \rightleftharpoons C_6H_5CHO + H$	R1869	2.00×10^{14}	0	23300	[e]
$C_6H_5C_2H_5 + H \rightleftharpoons C_6H_6 + C_2H_5$	R1870	1.20×10^{13}	0	5100	[e]

Reactions	Code	$A_{r,g}$	$\beta_{r,g}$	$E_{r,g}$	Ref
$C_6H_5C_2H_5 + H \rightleftharpoons C_6H_5CHCH_3 + H_2$	R1871	3.97×10^{2}	3.4	3120	[e]
$C_6H_5C_2H_5 + OH \rightleftharpoons C_6H_5CHCH_3 + H_2O$	R1872	5.17×10^{9}	1	870	[e]
$C_6H_5C_2H_5 + O_2 \rightleftharpoons C_6H_5CHCH_3 + HO_2$	R1873	1.81×10^{12}	0	39740	[e]
$C_6H_5C_2H_5 + O_2 \rightleftharpoons C_6H_5CH_2CH_2 + HO_2$	R1874	1.20×10^{13}	0	49000	[e]
$C_6H_5C_2H_5 + O \rightleftharpoons C_6H_5CHCH_3 + OH$	R1875	3.90×10^{9}	1	-1100	[e]
$C_6H_5C_2H_5 + HO_2 \rightleftharpoons C_6H_5CHCH_3 + H_2O_2$	R1876	2.70×10^{11}	0	12000	[e]
$C_6H_5C_2H_5 + CH_3 \rightleftharpoons C_6H_5CHCH_3 + CH_4$	R1877	1.10×10^{12}	0	9100	[e]
$C_6H_5C_2H_5 + C_3H_5\text{-}A \rightleftharpoons C_6H_5CHCH_3 + C_3H_6$	R1878	1.10×10^{12}	0	13100	[e]
$C_6H_5C_2H_5 + C_4H_5\text{-}I \rightleftharpoons C_6H_5CHCH_3 + C_4H_6$	R1879	1.10×10^{12}	0	13100	[e]
$C_6H_5C_2H_5 + C_4H_5\text{-}N \rightleftharpoons C_6H_5CHCH_3 + C_4H_6$	R1880	1.10×10^{12}	0	13100	[e]
$C_6H_5C_2H_5 + C_5H_5 \rightleftharpoons C_6H_5CHCH_3 + C_5H_6$	R1881	1.10×10^{12}	0	9100	[e]
$C_6H_5C_2H_5 + C_6H_5O \rightleftharpoons C_6H_5CHCH_3 + C_6H_5OH$	R1882	1.10×10^{12}	0	13100	[e]
$C_6H_5C_2H_5 + C_6H_5CH_2 \rightleftharpoons C_6H_5CHCH_3 + C_6H_5CH_3$	R1883	1.10×10^{12}	0	13100	[e]
$C_6H_5C_2H_5 + OC_6H_4CH_3 \rightleftharpoons C_6H_5CHCH_3 + HO_3C_6H_4CH_3$	R1884	1.10×10^{11}	0	13100	[e]
$C_6H_5C_2H_5 + HO_3C_6H_4CH_2 \rightleftharpoons C_6H_5CHCH_3 + HO_3C_6H_4CH_3$	R1885	1.10×10^{11}	0	13100	[e]
$C_6H_5C_2H_5 + H \rightleftharpoons C_6H_5CH_2CH_2 + H_2$	R1886	2.80×10^{7}	2	7700	[e]
$C_6H_5C_2H_5 + O \rightleftharpoons C_6H_5CH_2CH_2 + OH$	R1887	5.10×10^{13}	0	7800	[e]
$C_6H_5C_2H_5 + OH \rightleftharpoons C_6H_5CH_2CH_2 + H_2O$	R1888	2.70×10^{6}	2	400	[e]
$C_6H_5C_2H_5 + HO_2 \rightleftharpoons C_6H_5CH_2CH_2 + H_2O_2$	R1889	6.00×10^{11}	0	17000	[e]
$C_6H_5C_2H_5 + CH_3 \rightleftharpoons C_6H_5CH_2CH_2 + CH_4$	R1890	3.00×10^{-1}	4	8200	[e]
$C_6H_5CH_2CH_2 \rightleftharpoons C_6H_5C_2H_3 + H$	R1891	1.60×10^{13}	0	43500	[e]
$C_6H_5CH_2CH_2 \rightleftharpoons C_2H_4 + C_6H_5$	R1892	7.10×10^{14}	0	43500	[e]
$C_6H_5CHCH_3 + O_2 \rightleftharpoons C_6H_5C_2H_3 + HO_2$	R1893	7.00×10^{11}	0	15000	[e]
$C_6H_5CH_2CH_2 + O_2 \rightleftharpoons C_6H_5C_2H_3 + HO_2$	R1894	1.50×10^{12}	0	5000	[e]
$C_6H_5CHCH_3 + HO_2 \rightleftharpoons C_6H_5CHO + CH_3 + OH$	R1895	5.00×10^{12}	0	0	[e]
$C_6H_5CH_2CH_2 + HO_2 \rightleftharpoons C_6H_5CH_2 + CH_2O + OH$	R1896	5.00×10^{12}	0	0	[e]
$C_6H_5C_2H_5 \rightleftharpoons C_6H_5CHCH_3 + H$	R1897	2.51×10^{15}	0	81262	[e]
$C_6H_5CHCH_3 \rightleftharpoons C_6H_5C_2H_3 + H$	R1898	3.16×10^{13}	0	50669	[e]
$C_6H_5C_2H_3 \rightleftharpoons C_6H_6 + C_2H_2$	R1899	1.58×10^{11}	0	58440	[e]
$C_6H_5 + C_2H_4 \rightleftharpoons C_6H_5C_2H_3 + H$	R1900	2.51×10^{12}	0	6200	[e]
$C_6H_5C_2H_3 + O \rightleftharpoons C_6H_5 + CH_2CHO$	R1901	3.50×10^{13}	0	2832	[e]
$C_6H_5C_2H_3 + H \rightleftharpoons C_6H_5CCH_2 + H_2$	R1902	3.23×10^{7}	2.1	15842	[e]
$C_6H_5C_2H_3 + OH \rightleftharpoons C_6H_5CCH_2 + H_2O$	R1903	2.11×10^{13}	0	4571	[e]
$C_6H_5CCH_2 + O_2 \rightleftharpoons C_6H_5O + CH_2CO$	R1904	1.88×10^{12}	0	7469	[e]
$C_6H_5CCH_2 + H \rightleftharpoons C_6H_5C_2H_3$	R1905	1.11×10^{16}	-0.8	690	[e]
$C_6H_5 + C_2H_2 \rightleftharpoons C_6H_5CCH_2$	R1906	1.10×10^{41}	-8.6	18152	[e]
$C_6H_5C_2H_3 + H \rightleftharpoons C_6H_5CHCH + H_2$	R1907	5.07×10^{7}	1.9	12951	[e]
$C_6H_5C_2H_3 + OH \rightleftharpoons C_6H_5CHCH + H_2O$	R1908	2.02×10^{13}	0	5955	[e]

Reactions	Code	$A_{r,g}$	$\beta_{r,g}$	$E_{r,g}$	Ref
$C_6H_5C_2H_3 + O \rightleftharpoons C_6H_5CHCH + OH$	R1909	7.55×10^{6}	1.9	3736	[e]
$C_6H_5 + C_2H_2 \rightleftharpoons C_6H_5CHCH$	R1910	6.70×10^{34}	-7	10987	[e]
$C_6H_5C_2H_3 + O_2 \rightleftharpoons C_6H_5CCH_2 + HO_2$	R1911	2.00×10^{13}	0	57900	[e]
$C_6H_5 + H(+M) \rightleftharpoons C_6H_6(+M)$	R1912	1.00×10^{14}	0	0	[e]
$C_6H_6 + O_2 \rightleftharpoons C_6H_5 + HO_2$	R1913	6.30×10^{13}	0	60000	[e]
$C_6H_6 + O \rightleftharpoons C_6H_5O + H$	R1914	2.20×10^{13}	0	4530	[e]
$C_6H_6 + O \rightleftharpoons C_6H_5 + OH$	R1915	2.00×10^{13}	0	14700	[e]
$C_6H_6 + H \rightleftharpoons C_6H_5 + H_2$	R1916	2.50×10^{14}	0	16000	[e]
$C_6H_6 + CH_3 \rightleftharpoons C_6H_5 + CH_4$	R1917	7.32×10^{12}	0	18920	[e]
$C_6H_6 + HO_2 \rightleftharpoons C_6H_5 + H_2O_2$	R1918	5.50×10^{12}	0	28900	[e]
$C_6H_6 + OH \rightleftharpoons C_6H_5 + H_2O$	R1919	1.20×10^{9}	4.1	-301	[e]
$C_6H_6 + OH \rightleftharpoons C_6H_5OH + H$	R1920	1.32×10^{2}	3.2	5590	[e]
$C_6H_5 \rightleftharpoons H + C_4H_2 + C_2H_2$	R1921	4.30×10^{12}	0.6	77294	[e]
$C_6H_5 + CH_2O \rightleftharpoons C_6H_6 + HCO$	R1922	8.55×10^{4}	2.2	38	[e]
$C_6H_5 + CH_2O \rightleftharpoons C_6H_5CHO + H$	R1923	2.91×10^{4}	2.1	-411	[e]
$C_6H_5 + HCO \rightleftharpoons C_6H_6 + CO$	R1924	8.55×10^{4}	2.2	38	[e]
$C_6H_5 + HO_2 \rightleftharpoons C_6H_5O + OH$	R1925	5.00×10^{12}	0	0	[e]
$C_6H_5 + O_2 \rightleftharpoons C_6H_5O + O$	R1926	2.60×10^{13}	0	6120	[e]
$C_6H_5 + O_2 \rightleftharpoons O\text{-}C_6H_4O_2 + H$	R1927	3.00×10^{13}	0	8980	[e]
$C_6H_5 + O_2 \rightleftharpoons C_6H_5OO$	R1928	1.86×10^{13}	-0.2	-711	[e]
$C_6H_5OO \rightleftharpoons C_6H_5O + O$	R1929	1.27×10^{15}	-0.2	38536	[e]
$C_6H_5OO + C_6H_5CH_3 \rightleftharpoons C_6H_5OOH + C_6H_5CH_2$	R1930	4.00×10^{11}	0	14000	[e]
$C_6H_5O + OH \rightleftharpoons C_6H_5OOH$	R1931	2.00×10^{13}	0	0	[e]
$C_6H_5OO + C_6H_5OH \rightleftharpoons C_6H_5OOH + C_6H_5O$	R1932	1.33×10^{11}	0	14000	[e]
$C_6H_5 + C_2H_5 \rightleftharpoons C_6H_5C_2H_5$	R1933	5.00×10^{12}	0	0	[e]
$C_6H_5 + C_2H_3 \rightleftharpoons C_6H_5C_2H_3$	R1934	5.00×10^{12}	0	0	[e]
$C_6H_5OH + O_2 \rightleftharpoons C_6H_5O + HO_2$	R1935	1.00×10^{13}	0	38800	[e]
$C_6H_5OH + O \rightleftharpoons OC_6H_4OH + H$	R1936	1.60×10^{13}	0	3400	[e]
$C_6H_5OH + H \rightleftharpoons C_6H_5O + H_2$	R1937	1.20×10^{14}	0	12400	[e]
$C_6H_5OH + O \rightleftharpoons C_6H_5O + OH$	R1938	1.30×10^{13}	0	2900	[e]
$C_6H_5OH + OH \rightleftharpoons C_6H_5O + H_2O$	R1939	1.40×10^{8}	1.4	-960	[e]
$C_6H_5OH + HO_2 \rightleftharpoons C_6H_5O + H_2O_2$	R1940	1.00×10^{12}	0	10000	[e]
$C_6H_5OH + CH_3 \rightleftharpoons C_6H_5O + CH_4$	R1941	1.80×10^{11}	0	7700	[e]
$C_6H_5OH + C_6H_5 \rightleftharpoons C_6H_5O + C_6H_6$	R1942	4.90×10^{12}	0	4400	[e]
$C_6H_5OH + C_3H_5\text{-}A \rightleftharpoons C_6H_5O + C_3H_6$	R1943	4.90×10^{11}	0	9400	[e]
$C_6H_5OH + C_4H_5\text{-}I \rightleftharpoons C_6H_5O + C_4H_6$	R1944	4.90×10^{11}	0	9400	[e]
$C_6H_5OH + H \rightleftharpoons C_6H_4OH + H_2$	R1945	1.70×10^{14}	0	16000	[e]
$C_6H_5OH + O \rightleftharpoons C_6H_4OH + OH$	R1946	2.00×10^{13}	0	14700	[e]

Reactions	Code	$A_{r,g}$	$\beta_{r,g}$	$E_{r,g}$	Ref
$C_6H_5OH + OH \rightleftharpoons C_6H_4OH + H_2O$	R1947	1.40×10^{13}	0	4600	[e]
$C_6H_5OH + HO_2 \rightleftharpoons C_6H_4OH + H_2O_2$	R1948	4.00×10^{11}	0	28900	[e]
$C_6H_5OH + CH_3 \rightleftharpoons C_6H_4OH + CH_4$	R1949	2.00×10^{12}	0	15000	[e]
$C_6H_4OH + O_2 \rightleftharpoons OC_6H_4OH + O$	R1950	2.10×10^{13}	0	6100	[e]
$C_6H_4OH + H \rightleftharpoons C_6H_5OH$	R1951	1.00×10^{14}	0	0	[e]
$OC_6H_4OH \rightleftharpoons C_5H_4OH + CO$	R1952	7.40×10^{11}	0	43800	[e]
$C_6H_5O + H(+M) \rightleftharpoons C_6H_5OH(+M)$	R1953	2.00×10^{14}	0	0	[e]
$C_6H_5OH \rightleftharpoons C_5H_6 + CO$	R1954	4.31×10^{15}	-0.6	74115	[e]
$C_6H_5O \rightleftharpoons CO + C_5H_5$	R1955	2.00×10^{11}	0	43900	[e]
$C_6H_5O + H \rightleftharpoons CO + C_5H_6$	R1956	1.00×10^{13}	0	0	[e]
$C_6H_5O + O \rightleftharpoons C_5H_5 + CO_2$	R1957	1.00×10^{13}	0	0	[e]
$C_6H_5O + O \rightleftharpoons OC_6H_4OH$	R1958	2.60×10^{10}	0.5	800	[e]
$C_6H_5O + HO_2 \rightleftharpoons O\text{-}OC_6H_5OJ + OH$	R1959	2.00×10^{12}	0	0	[e]
$P\text{-}C_6H_4O_2 + H \rightleftharpoons P\text{-}OC_6H_5OJ$	R1960	4.00×10^{12}	0	9740	[e]
$O\text{-}C_6H_4O_2 + H \rightleftharpoons O\text{-}OC_6H_5OJ$	R1961	4.00×10^{12}	0	6960	[e]
$C_6H_5O + O \rightleftharpoons P\text{-}C_6H_4O_2 + H$	R1962	4.25×10^{13}	0	0	[e]
$C_6H_5O + O \rightleftharpoons O\text{-}C_6H_4O_2 + H$	R1963	8.50×10^{13}	0	0	[e]
$O\text{-}C_6H_4O_2 \rightleftharpoons C_5H_4O + CO$	R1964	1.00×10^{12}	0	40000	[e]
$P\text{-}C_6H_4O_2 \rightleftharpoons C_5H_4O + CO$	R1965	3.70×10^{11}	0	59000	[e]
$P\text{-}C_6H_4O_2 + H \rightleftharpoons C_5H_5O + CO$	R1966	2.50×10^{13}	0	4700	[e]
$P\text{-}C_6H_4O_2 + H \rightleftharpoons P\text{-}C_6H_3O_2 + H_2$	R1967	2.00×10^{12}	0	8100	[e]
$P\text{-}C_6H_4O_2 + O \rightleftharpoons P\text{-}C_6H_3O_2 + OH$	R1968	1.40×10^{13}	0	14700	[e]
$P\text{-}C_6H_4O_2 + OH \rightleftharpoons P\text{-}C_6H_3O_2 + H_2O$	R1969	1.00×10^{6}	2	4000	[e]
$P\text{-}C_6H_3O_2 + H \rightleftharpoons P\text{-}C_6H_4O_2$	R1970	1.00×10^{14}	0	0	[e]
$P\text{-}C_6H_3O_2 + H \rightleftharpoons 2C_2H_2 + 2CO$	R1971	1.00×10^{14}	0	0	[e]
$P\text{-}C_6H_3O_2 + O \rightleftharpoons C_2H_2 + HCCO + 2CO$	R1972	1.00×10^{14}	0	0	[e]
$P\text{-}C_6H_4O_2 + O \rightleftharpoons 2CO + C_2H_2 + CH_2CO$	R1973	3.00×10^{13}	0	5000	[e]
$C_5H_5 + H(+M) \rightleftharpoons C_5H_6(+M)$	R1974	2.60×10^{14}	0	0	[e]
$C_5H_6(+M) \rightleftharpoons C_3H_4\text{-}A + C_2H_2(+M)$	R1975	3.80×10^{17}	0	104000	[e]
$C_5H_6 + O_2 \rightleftharpoons C_5H_5 + HO_2$	R1976	4.00×10^{13}	0	37150	[e]
$C_5H_6 + HO_2 \rightleftharpoons C_5H_5 + H_2O_2$	R1977	1.10×10^{4}	2.6	12900	[e]
$C_5H_6 + OH \rightleftharpoons C_5H_5 + H_2O$	R1978	3.08×10^{6}	2	0	[e]
$C_5H_6 + H \rightleftharpoons C_5H_5 + H_2$	R1979	7.20×10^{13}	0	3500	[e]
$C_5H_6 + H \rightleftharpoons C_2H_2 + C_3H_5\text{-}A$	R1980	7.74×10^{36}	-6.2	32890	[e]
$C_5H_6 + O \rightleftharpoons C_5H_5 + OH$	R1981	4.80×10^{4}	2.7	1100	[e]
$C_5H_6 + C_2H_3 \rightleftharpoons C_5H_5 + C_2H_4$	R1982	1.20×10^{-1}	4	0	[e]
$C_5H_6 + C_6H_5O \rightleftharpoons C_5H_5 + C_6H_5OH$	R1983	3.16×10^{11}	0	8000	[e]
$C_5H_6 + CH_3 \rightleftharpoons C_5H_5 + CH_4$	R1984	1.80×10^{-1}	4	0	[e]

Reactions	Code	$A_{r,g}$	$\beta_{r,g}$	$E_{r,g}$	Ref
$C_5H_6 + C_6H_5 \rightleftharpoons C_5H_5 + C_6H_6$	R1985	1.00×10^{-1}	4	0	[e]
$C_5H_6 + C_5H_5 \rightleftharpoons C_6H_6 + C_4H_5\text{-}N$	R1986	5.00×10^{9}	0	0	[e]
$C_5H_5 \rightleftharpoons C_3H_3 + C_2H_2$	R1987	1.98×10^{68}	-15	124900	[e]
$C_5H_5 + O \rightleftharpoons C_4H_5\text{-}N + CO$	R1988	3.20×10^{13}	-0.2	440	[e]
$C_5H_5 + O \rightleftharpoons C_5H_4O + H$	R1989	5.80×10^{13}	0	20	[e]
$C_5H_5 + OH \rightleftharpoons C_5H_5OH$	R1990	6.50×10^{14}	-0.8	-2730	[e]
$C_5H_5 + OH \rightleftharpoons C_5H_5OH$	R1991	1.10×10^{43}	-8.8	18730	[e]
$C_5H_5 + OH \rightleftharpoons C_5H_5OH$	R1992	1.10×10^{59}	-13.1	33450	[e]
$C_5H_5 + OH \rightleftharpoons C_5H_4OH + H$	R1993	3.50×10^{57}	-12.2	48350	[e]
$C_5H_5 + OH \rightleftharpoons C_4H_6 + CO$	R1994	4.00×10^{14}	0	4500	[e]
$C_5H_5 + HO_2 \rightleftharpoons C_5H_5O + OH$	R1995	6.30×10^{29}	-4.7	11650	[e]
$C_5H_5 + O_2 \rightleftharpoons VK + HCO$	R1996	6.00×10^{18}	-2.5	10970	[e]
$VK + H \rightleftharpoons C_3H_5\text{-}A + CO$	R1997	6.60×10^{13}	0	2740	[e]
$VK + H \rightleftharpoons C_3H_5\text{-}A + CO$	R1998	5.90×10^{6}	2	1300	[e]
$VK + O \rightleftharpoons CH_2CHO + HCCO$	R1999	3.00×10^{8}	1.4	-860	[e]
$VK + OH \rightleftharpoons C_3H_5\text{-}A + CO_2$	R2000	3.00×10^{12}	0	0	[e]
$C_3H_3 + C_2H_2 \rightleftharpoons C\#CC^*CCJ$	R2001	4.11×10^{72}	-18.2	45400	[e]
$C\#CC^*CCJ \rightleftharpoons C_5H_5$	R2002	8.00×10^{13}	0	34058.3	[e]
$C\#CC^*CCJ + H \rightleftharpoons C_5H_6$	R2003	1.00×10^{14}	0	0	[e]
$C\#CC^*CCJ + H \rightleftharpoons C_5H_6\text{-}L$	R2004	1.00×10^{10}	0	0	[e]
$C_5H_6\text{-}L + O \rightleftharpoons C\#CC^*CCJ + OH$	R2005	1.00×10^{10}	0	0	[e]
$C_5H_6\text{-}L + OH \rightleftharpoons C\#CC^*CCJ + H_2O$	R2006	1.00×10^{10}	0	0	[e]
$C_5H_5OH + H \rightleftharpoons C_5H_4OH + H_2$	R2007	3.20×10^{12}	0	0	[e]
$C_5H_5OH + H \rightleftharpoons C_5H_5O + H_2$	R2008	4.00×10^{13}	0	6094	[e]
$C_5H_5OH + OH \rightleftharpoons C_5H_4OH + H_2O$	R2009	5.50×10^{12}	0	1731	[e]
$C_5H_5OH + OH \rightleftharpoons C_5H_5O + H_2O$	R2010	1.00×10^{13}	0	1697	[e]
$C_5H_5OH + O \rightleftharpoons C_5H_4OH + OH$	R2011	4.70×10^{11}	0	0	[e]
$C_5H_5OH + O \rightleftharpoons C_5H_5O + OH$	R2012	1.00×10^{13}	0	4683	[e]
$C_5H_5OH + HO_2 \rightleftharpoons C_5H_4OH + H_2O_2$	R2013	3.60×10^{3}	2.5	10531	[e]
$C_5H_5OH + HO_2 \rightleftharpoons C_5H_5O + H_2O_2$	R2014	1.00×10^{13}	0	15800	[e]
$C_5H_5O \rightleftharpoons C_5H_4O + H$	R2015	2.90×10^{32}	-6.5	21220	[e]
$C_5H_5O \rightleftharpoons C_4H_5\text{-}N + CO$	R2016	1.10×10^{79}	-19.6	66250	[e]
$C_5H_5O \rightleftharpoons CJ^*CC^*CC^*O$	R2017	2.00×10^{13}	0	14338	[e]
$CJ^*CC^*CC^*O \rightleftharpoons C^*CC^*CCJ^*O$	R2018	4.30×10^{11}	-1.1	4118	[e]
$C_4H_5\text{-}N + CO \rightleftharpoons C^*CC^*CCJ^*O$	R2019	1.51×10^{11}	0	4810	[e]
$CJCCCCO \rightleftharpoons C_2H_2 + CJCC^*O$	R2020	3.00×10^{13}	0	43710	[e]
$CJ^*CC^*O \rightleftharpoons C_2H_3CO$	R2021	1.40×10^{9}	1	32100	[e]
$C_2H_2 + HCO \rightleftharpoons CJ^*CC^*O$	R2022	7.77×10^{6}	1.4	7755	[e]
$C_5H_4OH + H \rightleftharpoons C_5H_5OH$	R2023	1.00×10^{14}	0	0	[e]

Reactions	Code	$A_{r,g}$	$\beta_{r,g}$	$E_{r,g}$	Ref
$C_5H_4OH + H \rightleftharpoons C_5H_4O + H_2$	R2024	2.10×10^{13}	0	54000	[e]
$C_5H_4OH + O_2 \rightleftharpoons C_5H_4O + HO_2$	R2025	3.00×10^{13}	0	5000	[e]
$C_5H_4O \rightleftharpoons CO + C_2H_2 + C_2H_2$	R2026	5.70×10^{32}	-6.8	68500	[e]
$C_5H_4O \rightleftharpoons CO + C_2H_2 + C_2H_2$	R2027	6.20×10^{41}	-7.9	98700	[e]
$C_5H_4O + H \rightleftharpoons C_4H_5\text{-}N + CO$	R2028	2.10×10^{61}	-13.3	40810	[e]
$C_5H_4O + O \rightleftharpoons C_4H_4 + CO_2$	R2029	1.00×10^{13}	0	2000	[e]
$C_5H_4O + H \rightleftharpoons C_5H_3O + H_2$	R2030	2.00×10^{12}	0	8100	[e]
$C_5H_4O + O \rightleftharpoons C_5H_3O + OH$	R2031	1.40×10^{13}	0	1470	[e]
$C_5H_4O + OH \rightleftharpoons C_5H_3O + H_2O$	R2032	1.10×10^{8}	1.4	1450	[e]
$C_5H_3O + H \rightleftharpoons C_5H_4O$	R2033	1.00×10^{14}	0	0	[e]
$C_5H_3O + O_2 \rightarrow CO_2 + C_2H_2 + HCCO$	R2034	9.70×10^{58}	-13.5	38180	[e]
$C_5H_3O \rightarrow C_2H_2 + CO + C_2H$	R2035	2.00×10^{13}	0	51000	[e]
$C_5H_7 \rightleftharpoons C^*CCJC^*C$	R2036	3.20×10^{15}	0	39500	[e]
$C_5H_7 + H \rightleftharpoons C_5H_6 + H_2$	R2037	3.60×10^{12}	0	0	[e]
$C_5H_7 + O \rightleftharpoons C_5H_6 + OH$	R2038	1.00×10^{13}	0	0	[e]
$C_5H_7 + OH \rightleftharpoons C_5H_6 + H_2O$	R2039	2.40×10^{13}	0	0	[e]
$C_5H_7 + O_2 \rightleftharpoons OC_5H_7O$	R2040	8.90×10^{24}	-3.8	20000	[e]
$C_5H_6 + H \rightleftharpoons C_5H_7$	R2041	2.40×10^{73}	-17.9	31500	[e]
$C_5H_6 + H \rightleftharpoons C^*CCJC^*C$	R2042	1.10×10^{14}	-0.2	3100	[e]
$C_5H_6 + O \rightleftharpoons C_5H_5O + H$	R2043	8.90×10^{12}	-0.1	590	[e]
$C_5H_6 + O \rightleftharpoons C_5H_5O + H$	R2044	5.60×10^{12}	-0.1	200	[e]
$C_5H_6 + OH \rightleftharpoons C^*CCJC^*COH$	R2045	1.10×10^{13}	-0.1	870	[e]
$C_5H_6 + HO_2 \rightleftharpoons C_5H_7 + O_2$	R2046	1.30×10^{15}	-1.1	9530	[e]
$C_5H_6 + HCO \rightleftharpoons C_5H_5 + CH_2O$	R2047	1.08×10^{8}	1.9	16000	[e]
$C_5H_6 + C_2H_3 \rightleftharpoons C_6H_6 + CH_3$	R2048	2.10×10^{67}	-16.1	42460	[e]
$C_5H_6 + C_4H_5\text{-}I \rightleftharpoons C_5H_5 + C_4H_6$	R2049	6.00×10^{12}	0	0	[e]
$C^*CCJC^*C \rightleftharpoons C^*CC^*CCJ$	R2050	5.40×10^{11}	-0.7	60	[e]
$C^*CC^*CCJ + H \rightleftharpoons C^*CC^*CC$	R2051	2.30×10^{20}	-1.6	3020	[e]
$C^*CC^*CC + H \rightleftharpoons C_4H_6 + CH_3$	R2052	5.20×10^{71}	-16.4	51000	[e]
$C^*CC^*CC + H \rightleftharpoons C^*CC^*CCJ + H_2$	R2053	7.00×10^{6}	2	5000	[e]
$C^*CC^*CC + OH \rightleftharpoons C^*CC^*CCJ + H_2O$	R2054	7.00×10^{6}	2	0	[e]
$C^*CCJC^*C + O_2 \rightleftharpoons C_2H_3CHO + CH_2CHO$	R2055	1.20×10^{36}	-7.2	33600	[e]
$C^*CC^*CCJ + H \rightleftharpoons C_4H_5\text{-}N + CH_3$	R2056	2.90×10^{26}	-2.2	36770	[e]
$C^*CCJC^*C + O \rightleftharpoons C_2H_3CHO + C_2H_3$	R2057	2.00×10^{14}	0	0	[e]
$C^*CC^*CCJ + OH \rightleftharpoons C^*CC^*CCOH$	R2058	1.50×10^{13}	0	0	[e]
$C^*CC^*CCJ + O_2 \rightleftharpoons C^*CCJC^*O + CH_2O$	R2059	8.20×10^{10}	0.2	9140	[e]
$C^*CC^*CCOH + H \rightleftharpoons C_4H_6 + CH_2OH$	R2060	2.50×10^{34}	-6.1	16250	[e]
$OC_5H_7O + O_2 \rightleftharpoons OC_4H_6O + HOCO$	R2061	6.30×10^{5}	-7.2	33600	[e]
$C^*CCJC^*COH + O_2 \rightleftharpoons HOC^*CC^*O + CH_2CHO$	R2062	1.20×10^{36}	-7.2	33600	[e]

Reactions	Code	$A_{r,g}$	$\beta_{r,g}$	$E_{r,g}$	Ref
HOC*CC*O + OH ⇌ HOC*CCJ*O + H_2O	R2063	2.69×10^{10}	0.8	-340	[e]
HOC*CC*O+HO_2⇌HOC*CCJ*O+$H2O_2$	R2064	1.00×10^{12}	0	11920	[e]
HOC*CC*O+CH_3⇌HOC*CCJ*O+CH_4	R2065	3.98×10^{12}	0	8700	[e]
HOC*CC*O+O⇌HOC*CCJ*O+OH	R2066	7.18×10^{12}	0	1389	[e]
HOC*CC*O+O_2⇌HOC*CCJ*O+HO_2	R2067	2.00×10^{13}	0	40700	[e]
HOC*CC*O+H⇌HOC*CCJ*O+H_2	R2068	2.60×10^{12}	0	2600	[e]
C_2H_2OH + CO ⇌ HOC*CCJ*O	R2069	1.51×10^{11}	0	4810	[e]
C_2H_2 + OH ⇌ C_2H_2OH	R2070	9.93×10^{11}	0	-960	[e]
OC_4H_6O + H ⇌ OC_4H_5O + H_2	R2071	2.30×10^{10}	1.1	3279	[e]
OC_4H_6O + OH ⇌ OC_4H_5O + H_2O	R2072	3.50×10^{9}	1.2	-447	[e]
OC_4H_5O + O_2 ⇌ $O_2CCHOOJ$ + C_2H_4	R2073	1.60×10^{45}	-9.9	20670	[e]
$O_2CCHOOJ$ ⇌ HOCO + CO_2	R2074	3.00×10^{13}	0	4000	[e]
C*CCJC*O⇌⇌ C_3H_5-A + CO	R2075	6.10×10^{5}	0.9	-1120	[e]
C*CCJC*O + O_2 ⇌ C_2H_3CHO + HOCO	R2076	1.20×10^{36}	-7.2	33600	[e]
HOCO ⇌ CO + OH	R2077	1.19×10^{14}	0.1	36460	[e]
HOCO ⇌ CO_2 + H	R2078	8.22×10^{11}	0.4	35340	[e]
C_3H_3 + $C_6H_5CH_2$ ⇌ NAPH + 2H	R2079	6.03×10^{11}	0	0	[f]
NAPH ⇌ $NAPH^-$ + H	R2080	8.60×10^{60}	-12.5	148076	[f]
NAPH + H ⇌ $NAPH^-$ + H_2	R2081	2.65×10^{8}	1.9	17096.1	[f]
NAPH + OH ⇌ $NAPH^-$ + H_2O	R2082	9.63×10^{2}	3	4373.8	[f]
NAPH ⇌ NAPH* + H	R2083	8.60×10^{60}	-12.5	148076	[f]
NAPH + H ⇌ NAPH* + H_2	R2084	2.65×10^{8}	1.9	17096.1	[f]
NAPH + OH ⇌ NAPH* + H_2O	R2085	9.63×10^{2}	3	4373.8	[f]
NAPH + C_2H_3 ⇌ $NAPH^-$ + C_2H_4	R2086	4.08×10^{-1}	4	8803	[f]
NAPH + C_2H_3 ⇌ NAPH* + C_2H_4	R2087	4.08×10^{-1}	4	8803	[f]
NAPH* + O_2 ⇌ NAPHO + O	R2088	8.57×10^{20}	-2.3	7189.3	[f]
NAPH* + O_2 → C_9H_6O + CO + H	R2089	3.00×10^{13}	0	8981.8	[f]
NAPH* + O ⇌ NAPHO	R2090	1.00×10^{14}	0	0	[f]
NAPH* + OH ⇌ NAPHO + H	R2091	3.00×10^{13}	0	0	[f]
$NAPH^-$ + O_2 ⇌ NAPHO + O	R2092	8.57×10^{20}	-2.3	7189.3	[f]
$NAPH^-$ + O_2 → C_9H_6O + CO + H	R2093	3.00×10^{13}	0	8981.8	[f]
$NAPH^-$ + O ⇌ NAPHO	R2094	1.00×10^{14}	0	0	[f]
$NAPH^-$ + OH ⇌ NAPHO + H	R2095	3.00×10^{13}	0	0	[f]
NAPHO ⇌ C_9H_7 + CO	R2096	2.90×10^{10}	0	36424.5	[f]
NAPHO + O → C_9H_6O + CO + H	R2097	1.68×10^{14}	0	0	[f]
NAPHO + O_2 → C_9H_6O + CO + OH	R2098	6.51×10^{7}	1.3	17667.3	[f]
C_2H_2 + C_4H_5-N ⇌ C_6H_6 + H	R2099	1.65×10^{16}	-1	9481	[f]
C_2H_2 + C_4H_5-N ⇌ FULVENE + H	R2100	1.23×10^{20}	-2	16200	[f]
C_9H_7 + H ⇌ IND	R2101	1.00×10^{14}	0	0	[f]

Reactions	Code	$A_{r,g}$	$\beta_{r,g}$	$E_{r,g}$	Ref
IND + O_2 ⇌ C_9H_7 + HO_2	R2102	4.00×10^{13}	0	37150	[f]
IND + HO_2 ⇌ C_9H_7 + H_2O_2	R2103	1.10×10^{4}	2.6	12900	[f]
IND + OH ⇌ C_9H_7 + H_2O	R2104	3.08×10^{6}	2	0	[f]
IND + H ⇌ C_9H_7 + H_2	R2105	1.70×10^{5}	2.5	2484	[f]
IND + O ⇌ C_9H_7 + OH	R2106	4.80×10^{4}	2.7	1100	[f]
IND + C_2H_3 ⇌ C_9H_7 + C_2H_4	R2107	1.20×10^{-1}	4	0	[f]
IND + C_6H_5O ⇌ C_9H_7 + C_6H_5OH	R2108	3.16×10^{11}	0	8000	[f]
IND + CH_3 ⇌ C_9H_7 + CH_4	R2109	1.80×10^{-1}	4	0	[f]
IND + C_6H_5 ⇌ C_9H_7 + C_6H_6	R2110	1.00×10^{-1}	4	0	[f]
IND + H ⇌ C_3H_3 + C_6H_6	R2111	2.00×10^{13}	0	0	[f]
$C_{10}H_{10}$ + O_2 ⇌ $C_{10}H_9$ + HO_2	R2112	4.00×10^{13}	0	37150	[f]
$C_{10}H_{10}$ + HO_2 ⇌ $C_{10}H_9$ + H_2O_2	R2113	1.10×10^{4}	2.6	12900	[f]
$C_{10}H_{10}$ + OH ⇌ $C_{10}H_9$ + H_2O	R2114	3.08×10^{6}	2	0	[f]
$C_{10}H_{10}$ + C_5H_5 ⇌ C_5H_6 + $C_{10}H_9$	R2115	1.10×10^{11}	0	5505	[f]
$C_{10}H_{10}$ + C_4H_5-N ⇌ $C_{10}H_9$ + C_4H_6	R2116	1.00×10^{-1}	4	0	[f]
$C_{10}H_{10}$ + H ⇌ $C_{10}H_9$ + H_2	R2117	1.70×10^{5}	2.5	2484	[f]
$C_{10}H_{10}$ + O ⇌ $C_{10}H_9$ + OH	R2118	4.80×10^{4}	2.7	1100	[f]
$C_{10}H_9$ + HO_2 → C_6H_5CHO + C_3H_3 + OH	R2119	5.00×10^{12}	0	0	[f]
$C_{10}H_{10}$ + C_2H_3 ⇌ $C_{10}H_9$ + C_2H_4	R2120	1.20×10^{-1}	4	0	[f]
$C_{10}H_{10}$ + C_6H_5O ⇌ $C_{10}H_9$ + C_6H_5OH	R2121	3.16×10^{11}	0	8000	[f]
$C_{10}H_{10}$ + CH_3 ⇌ $C_{10}H_9$ + CH_4	R2122	1.80×10^{-1}	4	0	[f]
$C_{10}H_{10}$ + C_6H_5 ⇌ $C_{10}H_9$ + C_6H_6	R2123	1.00×10^{-1}	4	0	[f]
C_5H_5 + C_5H_5 → $C_{10}H_9$ + H	R2124	5.24×10^{14}	-0.9	3650	[f]
C_5H_5 + C_5H_5 ⇌ $C_{10}H_{10}$	R2125	8.00×10^{12}	0	3000	[f]
$C_{10}H_9$ ⇌ NAPH + H	R2126	3.00×10^{13}	0	39000	[f]
$C_{10}H_9$ + H ⇌ $C_{10}H_{10}$	R2127	2.00×10^{14}	0	0	[f]
$C_{10}H_{10}$ + H ⇌ C_4H_5-N + C_6H_6	R2128	2.00×10^{13}	0	0	[f]
$C_{10}H_{10}$ + OH ⇌ $CH_2CHCHCHO$ + C_6H_6	R2129	1.00×10^{14}	0	0	[f]
C_9H_6O → L-C_6H_4 + C_2H_2 + CO	R2130	3.37×10^{44}	-8	108675.9	[f]
C_9H_7 + O ⇌ C_9H_6O + H	R2131	2.80×10^{13}	0	0	[f]
C_9H_7 + O_2 ⇌ C_9H_6O + OH	R2132	1.74×10^{7}	1.3	17667.3	[f]
C_9H_7 + HO_2 → C_9H_6O + H + OH	R2133	1.24×10^{13}	0	0	[f]
C_9H_7 + OH → C_9H_6O + H_2	R2134	4.08×10^{12}	0	0	[f]
C_9H_6O → C-C_6H_4 + C_2H_2 + CO	R2135	3.37×10^{44}	-8	108675.9	[f]
C_3H_3 + NAPH → FLUORENE + H	R2136	3.00×10^{12}	0	23000	[f]
C_5H_5 + NAPH → $C_{14}H_{10}$ + CH_3	R2137	3.00×10^{12}	0	23000	[f]
C_6H_5 + NAPH → $C_{16}H_{10}$ + H + H_2	R2138	3.00×10^{12}	0	10000	[f]

for the kinetic of $k_{f,r,e} = A_{r,g}T_g^{\beta_{r,g}}\exp\left(-\frac{E_{r,g}}{R.T_g}\right)$

Appendix A.5 Tar electron reactions

Summary of electron impact reactions used for tar kinetic reforming, reference on Appendix A.6.

Reactions	Code	$A_{r,e}$	$\beta_{r,e}$	$E_{r,e}$	Ref
$CO_2 + E \rightarrow CO + O + E$	R2139	2.90×10^{-9}	0.3	12.1	[c]
$H_2 + E \rightarrow H + H + E$	R2140	9.53×10^{-8}	0.2	12.1	[c]
$CH_4 + E \rightarrow CH_2 + H_2 + E$	R2141	6.08×10^{-8}	0.2	11.8	[c]
$CH_4 + E \rightarrow CH_3 + H + E$	R2142	4.15×10^{-7}	0.2	11.6	[c]
$C_2H_2 + E \rightarrow CH + CH + E$	R2143	2.35×10^{-7}	0.6	13.4	[c]
$C_2H_4 + E \rightarrow CH_4 + C + E$	R2144	6.15×10^{-7}	0.7	9.9	[c]
$C_2H_4 + E \rightarrow CH_2 + CH_2 + E$	R2145	6.54×10^{-7}	0.7	10.8	[c]
$C_2H_4 + E \rightarrow CH + CH_3 + E$	R2146	6.00×10^{-7}	0.7	10.4	[c]
$C_6H_5CH_3 + E \rightleftharpoons C_6H_5CH_2 + H + E$	R2147	1.00×10^{-9}	0	12.1	[g]
$C_6H_5CH_3 + E \rightleftharpoons C_6H_5 + CH_3 + E$	R2148	1.00×10^{-9}	0	12.1	[g]
$C_3H_3 + C_6H_5CH_2 + E \rightarrow NAPH + 2H + E$	R2149	1.00×10^{-9}	0	12.1	Estimated in this work
$IND + E \rightarrow C_9H_7 + H + E$	R2150	1.00×10^{-9}	0	12.1	Estimated in this work

Electron impact reaction is assumed to be dependent to electron temperature, and with excitation loss equivalent to the E_r value, for the kinetic of $k_{f,r,e} = A_{r,e}T_e^{\beta_{r,e}}\exp\left(-\frac{E_{r,e}}{R.T_e}\right)$

Appendix A.6 Reaction References

[a] Wang, Baowei, et al. "Heptane dry reforming and coupling with partial oxidation in gliding arc discharge plasma for H2 production." Fuel Processing Technology 221 (2021): 106943.

[b] Curran, H. J., P. Gaffuri, W. J. Pitz, and C. K. Westbrook, "A Comprehensive Modeling Study of n-Heptane Oxidation" Combustion and Flame 114:149-177 (1998): https://combustion.llnl.gov/mechanisms/alkanes/n-heptan×10-detailed-mechanism-version-3

[c] J. Xue, S. Xi, F. Wang, An extensive study on skeletal mechanism reduction for the oxidation of C0–C4 fuels, Combustion and Flame 214 (2020) 184–198.: Methane combustion https://cds.scu.edu.cn/ckl/database/mech -

[d] Yin Rou, Xue Jie, Wang Jingbo, Li Xiangyuan. Construction of n-decane simplification mechanism and its application in numerical simulation of engine combustion [J]. Propulsion Technology: 1-7, [2021-08-02].https://doi.org/10.13675/j.cnki.tjjs.190789m n decane combustion: http://cds.scu.edu.cn/ckl/database/mech#

[e] Metcalfe, W. K., S. Dooley, and F. L. Dryer. "Comprehensive detailed chemical kinetic modeling study of toluene oxidation." Energy & Fuels 25.11 (2011): 4915-4936.

[f] H. Nakamura, D. Darcy, M. Mehl, C.J. Tobin, W.K. Metcalfe, W.J. Pitz, C.K. Westbrook, H.J. Curran, Combustion and Flame 161 (2014) 49-64. http://dx.doi.org/10.1016/j.combustflame.2013.08.002: https://combustion.llnl.gov/mechanisms/aromatic-and-pah-formation/toluen×10-ethyl-propyl-butyl-benzene

[g] Trushkin, A. N., and I. V. Kochetov. "Simulation of toluene decomposition in a puls×10-periodic discharge operating in a mixture of molecular nitrogen and oxygen." Plasma physics reports 38 (2012): 407-431.

Appendix B: Process Simulation Information

Appendix B.1 Items and description of waste gasification flowsheet

Unit	Description
B1	Pretreatment block (shredding, pelletising, and drying)
B2	Oxygen production block
B3	Air pollution control block
B4	Energy recovery (fuel cell) block
R-1	Pyrolysis reactor
SEP-2	Separate char from syngas
R-3	Decomposition reactor
M-4	Mixing syngas with gasifying agent
R-5	Oxidation reactor
R-6	Reduction reactor
SEP-7	Separate syngas from ash
R-8	NTP tar cracking reactor
R-9	Methanol synthesis yield reactor
SEP-10	Separate methanol and syngas
HX-1	Boiler
HX-2	Gas heater
HX-3	Syngas cooler
HX-4	Syngas heater
HX-5	Product Cooler

Stream	Description
S-1	MSW
S-2	Water
S-3	Steam
S-4	Air
S-5	Air/O_2
S-7	Heated Air/O_2
S-8	RDF
S-9	Syngas/Char
S-10	Char
S-11	Syngas
S-12	Syngas/Ash
S-13	Mixed gas
S-14	Oxidation product
S-15	Reduction product
S-16	Ash
S-17	Crude syngas
S-18	Clean Syngas
S-19	Cooled clean syngas
S-20	Cleaned syngas
S-21	Heated syngas
S-22	Syngas/methanol
S-23	Syngas/methanol
S-24	Methanol
S-25	Syngas
S-26	Emission

Appendix B.2 Crude Syngas Analysis

Modelling result and experimental result syngas trend over varying ER and the linear correlation

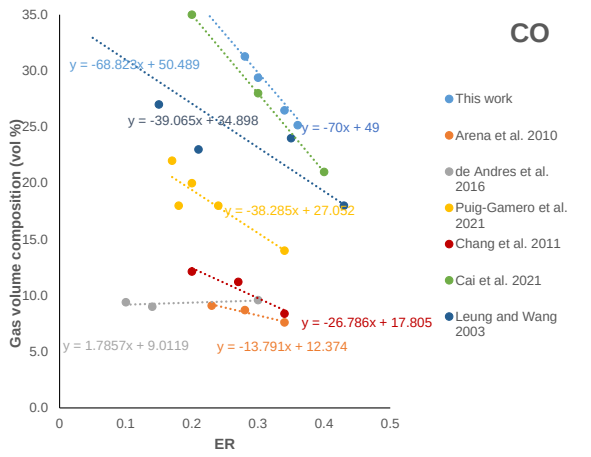

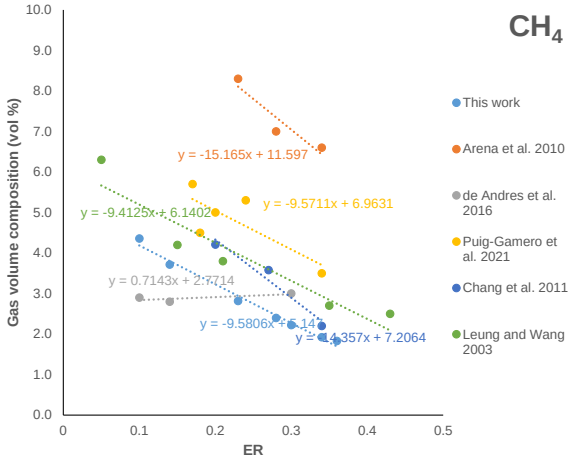

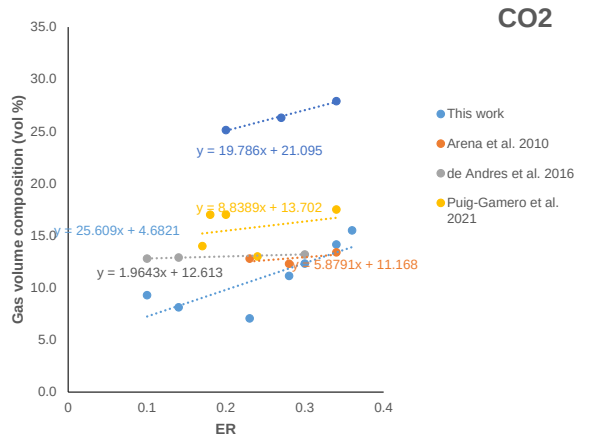

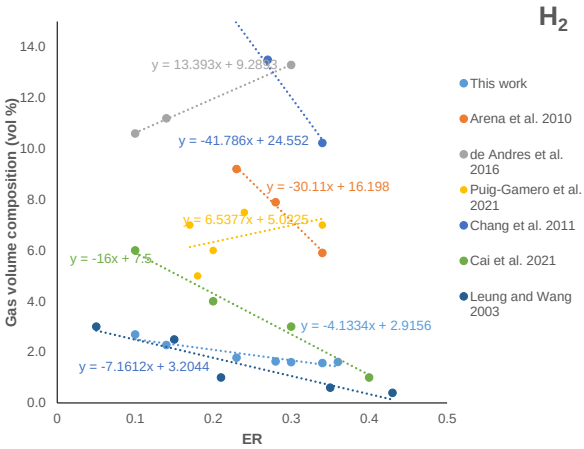

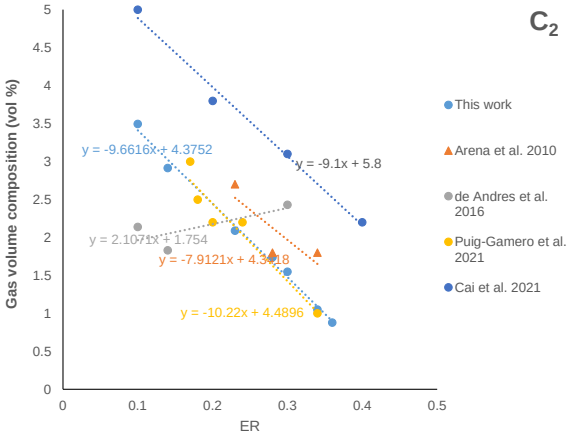

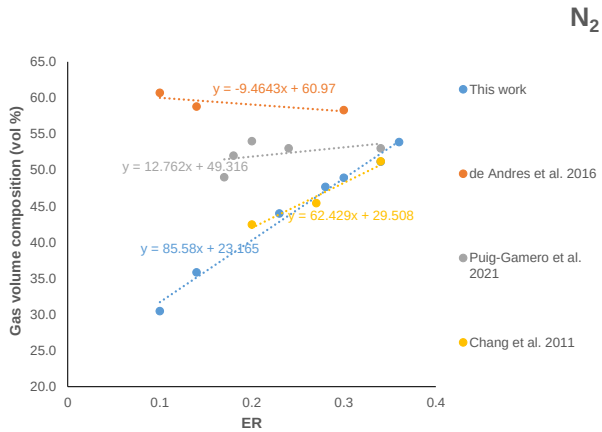

Appendix B.3 Summary of streams composition

Streams	**S-9**	**S-13**	**S-14**	**S-17**	**S-18**	**S-16**
product of	**Pyrolysis (R-1)**	**Decomposition (R-3)**	**Oxidation (R-5)**	**Crude syngas (SEP-10)**	**Clean Syngas (R-8)**	**Solid by-products (SEP-7)**
Temp (°C)	500.0	420.2	900.0	950.0	950.0	950.0
Mass flow (kg/h)	10.00	24.29	24.29	23.52	23.52	0.77
Syngas						
CO	1.99	1.99	7.60	6.91	9.91	-
CO_2	0.97	0.97	1.49	2.90	0.02	-
H_2	0.21	0.28	0.28	0.38	0.54	-
CH_4	0.50	0.50	0.56	0.52	0.01	-
O_2	-	3.80	-	-	-	-
H_2O	0.46	0.46	0.71	-	0.03	-
N_2	0.08	11.51	11.51	11.51	11.51	-
Hydrocarbon						
C_2H_4	0.23	0.23	0.18	0.18	-	-
C_2H_6	0.19	0.19	0.19	0.19	-	-
C_3H_8	0.19	0.19	-	-	-	-
C_4H_2	-	-	-	-	1.56	-
C_2H_2	-	-	-	-	0.66	-
C_3H_3	-	-	-	-	0.01	-
Tar						
C_6H_6O	0.27	0.27	0.27	0.26	3.36×10^{-06}	-
C_6H_6	0.29	0.29	0.29	0.30	2.73×10^{-03}	-
C_7H_8	0.38	0.38	0.38	0.38	1.06×10^{-05}	-
$C_{10}H_8$	0.08	0.08	0.06	0.00	8.12×10^{-04}	-
Solid						
Biochar	4.16	-	-	-	-	-
C	-	2.39	0.02	-	-	0.01
Ash	-	0.76	0.76	-	-	0.76
Waste	<0.00001	<0.00001	<0.00001	-	-	<0.00001

Appendix B.4 Tar Compositon Crude syngas

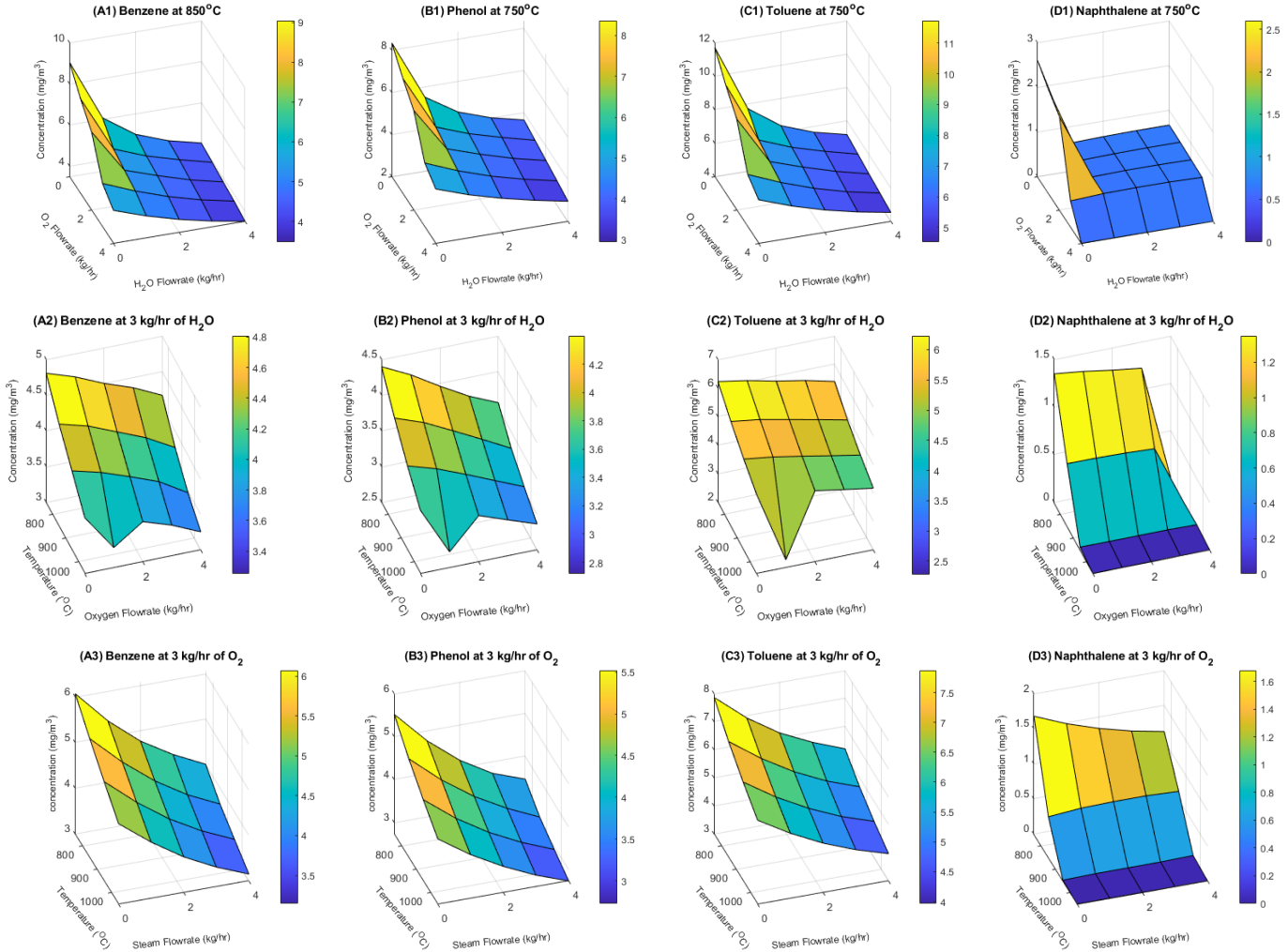

Appendix B.5 Hydrocarbon Compositon Crude syngas

Syngas mol fraction of (A) CH_4 and (B) C_2, at varying temperature, oxygen, and steam flow rates, where (1) constant temperature (2) Constant Steam flow rate and (3) Constant Oxygen flow rate.

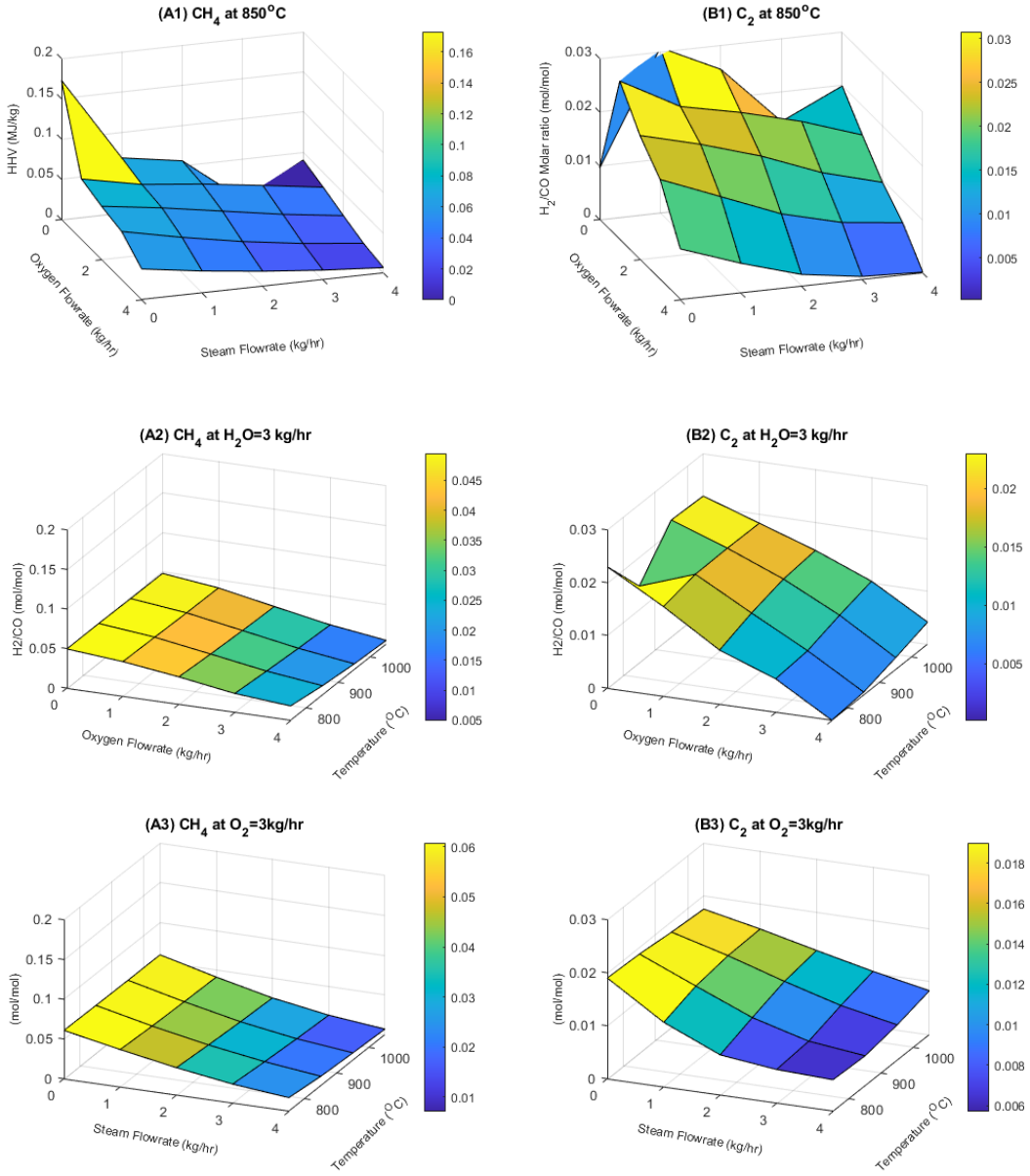

Appendix B.6 Sensitivity Analysis Range

For the sensitivity analysis to establish the deep tar cracking range, the highest and lowest operating range for tar concentrations are shown below, the data is simulated in Chemkin Ansys and the result is shown in the Appendix B.6.

Code Identification	**Composition-1 Lowest gas flow rate and Highest Tar concentration**	**Composition-2 Highest gas flow rate and lowest tar concertation**
Temperature (oC)	750	1050
Steam flow rate	0	4
Oxygen flow rate	1	4
Flow rate (L/min)	668.36	1621.91
Mol fraction composition		
CO	0.412	0.0781
CO2	0.065	0.3358
H2	0.377	0.5607
CH4	0.075	0.0020
C2H4	0.017	0.0001
C2H6	0.013	0.0025
C7H8	0.009	0.0046
C10H8	0.001	0.0001
N2	0.017	0.0089
C6H6O	0.006	0.0031
C6H6	0.008	0.0042

Appendix B.7 Sensitivity Analysis Result

Chemkin result of sensitivity analysis of two ranges based on the crude syngas part for their tar (A) and syngas conversion (B) and mol composition of Tar (C), Hydrocarbon (D) and Syngas (E) for condition 1 and 2 (According to the range).

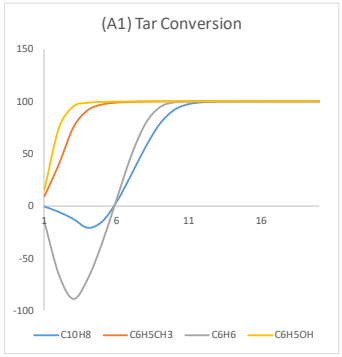

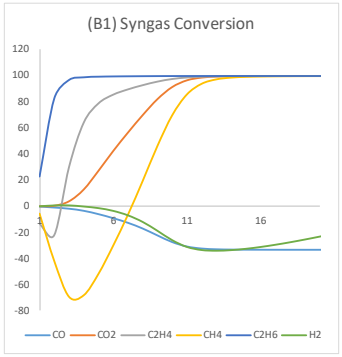

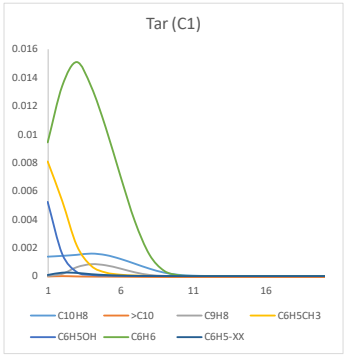

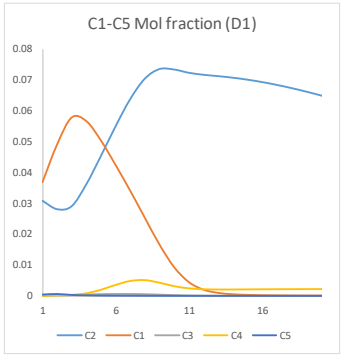

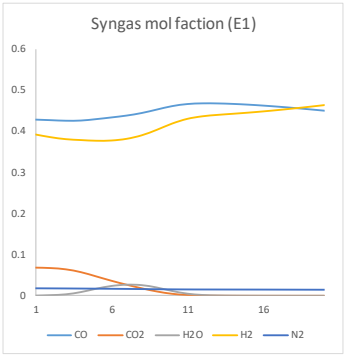

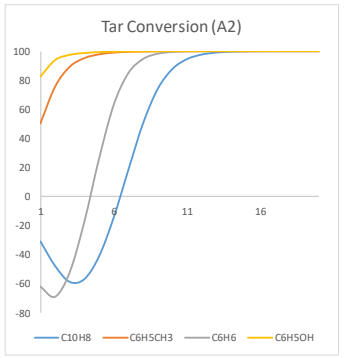

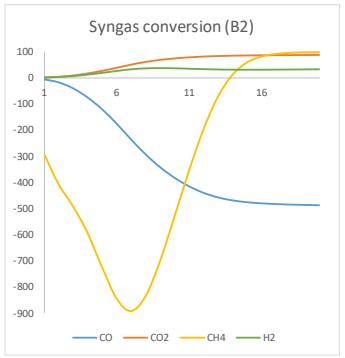

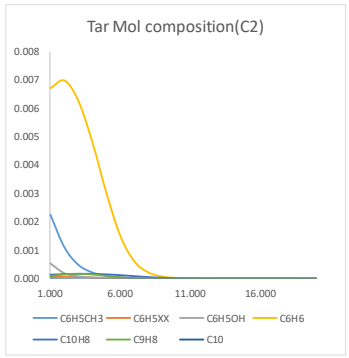

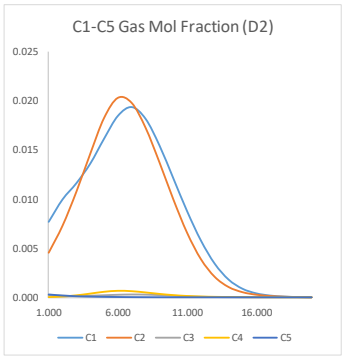

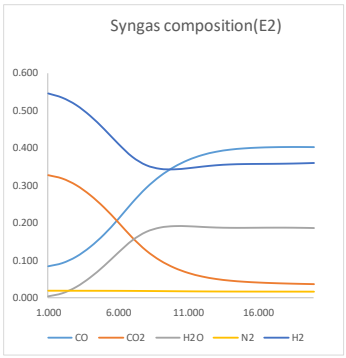

Appendix B.8 MLR Result

MLR Coefficients for each output prediction

Coeff	CO	Log (CO_2)	H_2	Log (C_1)	C2	Log (C_3)	Log (C_4)	N_2	Log (H_2O)	Log (tar)
T	-7.56E-04	-3.29E-03	-	-	-3.27E-05	1.42E-03	-5.73E-04	-3.53E-05	-3.19E-03	-2.41E-03
F	1.01E-01	2.85E-01	4.69E-03	4.40E-01	1.30E-02	3.26E-01	3.59E-01	3.75E-03	1.42E-01	3.42E-01
P	-8.54E-02	1.55E-01	4.97E-01	4.65E+00	-6.92E-03	-1.29E-01	-1.57E-01	-1.94E-04	9.59E-02	-1.97E-01
F-1	-9.36E+00	1.07E+01	-1.42E+00	-	-	-	-	-	-2.58E+01	-
P^{-1}	-4.34E+01	-	-5.31E-02	2.18E+01	-	-	-	-	1.33E+02	-
Log (1)	1.09E+00	-	-	-	-	-	-	-	-	-
Log (2)	1.21E+00	4.92E+00	-	-	-	-	-	-	-	-
(2)	-	-2.28E-01	-	-	-	-	-	-	-7.62E+00	-
(3)	-	-	2.27E-01	1.33E+01	-	-	-	-	-9.45E+01	-
(4)	-	-	-3.76E-01	-1.84E+01	-	-	-	-	-	-
(5)	-	-	-5.50E-02	3.24E+01	-	-	-	-	-	-
(6)	-	-	2.32E-03	-2.39E-01	-	-	-	-	-	-
(9)	-	-	-	-	-	-	-	7.75E+00	-	-
Log (4)	-	-	1.15E-02	3.77E-01	-	-	-	-	-	-
Log (5)	-	-	3.88E-03	1.09E-01	-	-	-	-	-	-
Log (6)	-	-	9.73E-03	4.71E-01	-	-	-	-	-	-
Log (9)	-	-	-	-	-	-	-	-2.39E-02	-	-
(2×2)	-	-	-	-	-	-	-	-	-	-3.21E+01
(3×3)	-	-	-	-	-	-	-	-	-4.91E+01	-
(3×2)	-	-	-	-	-	-	-	-	8.22E+01	-
(2x3)	-	-	-	-	-	-	-	-	7.29E+01	-
(2×2)	-	-	-	-	-	-	-	-	-	-3.21E+01
(2×9)	-	-	-	-	-	-	-	-	-	-3.10E+03
(2×11)	-	-	-	-	-	-	-	-	-	4.39E+03
(2×12)	-	-	-	-	-	-	-	-	-	-1.29E+03
(7×2)	-	-	-	-	-	-	-	-	-	-1.43E+03
(4×4)	-	-	-	-	4.25E+01	-3.11E+02	7.33E+00	-	-	-
(4×6)	-	-	-	-	-8.02E+01	-4.95E+02	-8.59E+02	-	-	-

Coeff	CO	Log (CO_2)	H_2	Log (C_1)	C2	Log (C_3)	Log (C_4)	N_2	Log (H_2O)	Log (tar)
(4×7)	-	-	-	-	2.08E+02	9.49E+02	3.65E+03	-	-	-
(4×8)	-	-	-	-	7.17E+02	1.87E+04	1.49E+03	-	-	-
(4×8)	-	-	-	-	1.59E+02	-9.42E+03	-3.07E+03	-	-	-
(4×10)	-	-	-	-	-5.50E+02	9.47E+03	1.79E+03	-	-	-
(4×11)	-	-	-	-	3.82E+00	1.87E+03	2.50E+02	-	-	-
(5×5)	-	-	-	-	6.26E+02	2.41E+03	7.28E+03	-	-	-
(5×6)	-	-	-	-	-2.40E+02	7.70E+03	-5.27E+03	-	-	-
(5×8)	-	-	-	-	-1.49E+04	-2.45E+04	4.95E+04	-	-	-
(5×11)	-	-	-	-	3.36E+03	-2.86E+04	1.56E+03	-	-	-
(6×6)	-	-	-	-	1.47E+03	7.91E+03	1.97E+04	-	-	-
(6×7)	-	-	-	-	-3.72E+03	-3.58E+04	-6.79E+04	-	-	-
(6×10)	-	-	-	-	4.75E+03	-1.34E+04	-6.52E+03	-	-	-
(6×11)	-	-	-	-	2.71E+02	4.80E+04	6.37E+04	-	-	-
(7×5)	-	-	-	-	1.87E+03	5.35E+04	5.66E+04	-	-	-
(7×7)	-	-	-	-	-2.24E+03	3.88E+04	2.18E+04	-	-	1.26E+03
(7×8)	-	-	-	-	-9.10E+03	-3.82E+05	-3.87E+05	-	-	-
(7×10)	-	-	-	-	2.61E+02	-1.75E+05	-1.44E+05	-	-	-
(7×11)	-	-	-	-	8.65E+03	8.71E+04	1.22E+05	-	-	1.53E+05
(8×6)	-	-	-	-	-4.19E+03	1.29E+05	1.33E+05	-	-	-
(8×7)	-	-	-	-	-	-	-	-	-	-3.79E+05
(8×8)	-	-	-	-	2.74E+05	4.05E+06	3.95E+06	-	-	2.29E+06
(8×10)	-	-	-	-	-1.15E+04	-8.64E+05	-1.09E+06	-	-	-
(8×11)	-	-	-	-	-7.66E+03	2.73E+05	4.88E+05	-	-	-4.98E+04
(10×5)	-	-	-	-	-6.46E+03	-6.20E+04	-9.52E+04	-	-	-
(10×7)	-	-	-	-				-	-	-5.10E+04
(10×10)	-	-	-	-	2.95E+03	-6.58E+03	2.49E+04	-	-	-1.19E+05
(10×11)	-	-	-	-	2.09E+02	4.17E+05	3.57E+05	-	-	-1.19E+05
(11×11)	-	-	-	-	-5.27E+03	-2.37E+05	-2.55E+05	-	-	9.74E+04
Ones	1.02E+01	6.86E+00	4.13E-02	-9.35E+00	-2.12E-01	-1.63E+01	-1.35E+01	-1.60E-01	1.52E+01	-9.71E+04

Coefficients = T: Temperature, F: Flow rate, P: Power, 1: CO concentration, 2: CO_2 concentration, 3: H_2 concentration, 4: CH_4 concentration, 5: C_2H_4 concentration, 6: C_2H_6 concentration, 7: Toluene concentration, 8: Naphthalene concentration, 9: N_2 concentration, 10: Phenol concentration, 11: Benzene concentration, and Ones: Intercept

Appendix B.9 MLR Comparison operating conditions.

Operating parameters for Comparison crude syngas scenario with MLR predicted result.

Scenario	**A**	**B**	**C**
Temperature (oC)	750	950	1050
Flow rate (L/s)	13.69391	18.73405386	18.89359
Power (kW)	20	20	20
C_2H_4 (mol/mol)	0.014	0.011	0.009
C_2H_6	0.011	0.009	0.010
C_7H_8	0.007	0.006	0.007
C_6H_6O	0.005	0.004	0.005
C_6H_6	0.006	0.006	0.006
CH_4	0.061	0.052	0.055
CO	0.430	0.372	0.410
CO_2	0.052	0.089	0.095
E	1.00E-08	1.00E-08	1.00E-08
H_2	0.399	0.439	0.390
N_2	0.014	0.012	0.013
$C_{10}H_8$	0.001	0.000	0.000

Appendix C: Thermal Plasma Analysis Studies Detailed LCA

Appendix C.1: Summary of LCA analysis

(Ref Appendix C.6)

Ref	FU; Model; Method: location	Impact categories	Boundary condition	Aim	Scenarios
[1]	1 Tonne of RDF derived from landfill. SimaPro; ReCiPe; Belgium	CCHH; CCE; OD; AP; WE; HTP; POCP; WE; IR ALC; ULC; NLT; MD; FFD; PM; TE	R/T/E/L	Comparing plasma gasification to incineration for enhance landfilling mining	Sc1 Plasma gasification and landfilling of slag Sc2 Incineration with landfilling bottom ash Sc3 Incineration with bottom ash aggregate production Sc4 Plasma gasification with aggregate production Sc5 Plasma gasification with polymer cement production from slag Sc6 Plasma gasification with polymer block production from slag Sc7 Plasma gasification with blended cement production from slag Sc8 Plasma gasification with blended cement block production
[2]	1 kg of MSW GaBi; method N/A:United Kingdom	GWP; AP; AD; EP; POCP; HTP	R/T/PT/E/L	Comparing landfilling, incineration, and gasification and pyrolysis	Sc1 Gasification + plasma cleaning Sc2 Fast pyrolysis + Combustion Sc3 Gasification + syngas oxidation Sc4: Landfill Sc5: Incineration 1 Sc6. Incineration 2
[3]	1 kg industrial organic hazardous waste GaBI; CML; Hungary	GWP; AP; HTP; OD	R/T/E	Comparing different EFW technology to process hazardous waste	Sc1 Plasma gasification and vitrification Sc2 Incineration without APC Sc3 Pyrolysis Sc4 Gasification Sc5 Incineration with APC
[4]	1 tonne of incineration fly ash	WE, MET, TE, HTP, ALC,	R/T/L	Comparing various pathway to dispose incineration ash	Sc1 Plasma vitrification Sc2 Furnace/Fuel vitrification

Ref	FU; Model; Method: location	Impact categories	Boundary condition	Aim	Scenarios
	OpenLCA- Ecoinvent; ReCiPe; location N/A	GWP, FFD, IR, MET, MD, NLT, ODP, PM, AD, ULC, Water depletion			Sc3 Thermal treatment in rotary kiln Sc4 Solidification and landfill
[5]	FU: N/A GaBi, CML, Location N/A	AP, GWP	R/T/PT	Comparing two technology to convert municipal sludge into hydrogen	Sc1 Plasma gasification Sc2 Plasma gasification with chemical looping
[6]	1 tonne of MSW GaBI, CML, based on global data	GWP, EP, AP, AD (fossil & elemental), OD, POCP, ME, WE, TE, HTP	R/T/PT/E/L	Comparing alternative EFW technology	Sc1 Incineration Sc2 Gasification Sc3 Plasma gasification
[7]	1 tonne of MSW GaBi, CML, Location N/A	GWP, EP, AP, ODP, ADP (element and fossil), WE, NET, TE, HTP, POCP	R/T/PT/E	To assess the environmental impact of low temperature gasification in comparison to other thermal conversion	Sc1 Low temperature gasification Sc2 Incineration Co3 Landfill (From Evangelisti 2015) Co4 Fast pyrolysis Co5 Plasma gasification
[8]	1 tonne of MSW GaBI, CML, based on global data	AD, AP, EP, GWP, WE, HTP, ME, OD, POCP, TE	R/T/PT/E/L	LCA for two stage plasma gasification	Sc1 Two stage plasma gasification Sc2 Incineration
[9]	1 MJ of energy SimaPro; Recipe: Location N/A	GWP, HTP, PM, AP, WE, MET, TE, FFD	R/T	Comparing two different energy sources for cement production	Sc1 Syngas-from-RDF combustion produced by plasma gasification Sc2 Hard coal combustion Sc3 Mixture of RDF and hard coal
[10]	80 ktpa of waste N/A	Energy consumption	C&T/R/T/PT	Conduct Energy LCA for different gasification technology	Sc1 Radiofrequency plasma gasification Sc2 Microwave induced system Sc3 Downdraft gasifier Sc4 Plasma torch system
[11]	1 kg of waste and 1 MJ of gas produced Simapro; CML; United Kingdom	GWP, AP, AD, EP, POCP, WE, TE, HTP, OD	R/S/T/PT/AD/E/L	Compare environmental burden of different conversion and whether separation creates an impact on methane production	Sc1 Separated organic into AD and other to recycling and incineration Sc2 Separated organic into AD and other to recycling and landfill Sc3 Separated organic into AD and other to incineration Sc4 Separated organic into AD and other to landfill Sc5 Advance thermal two stage plasma gasification

Ref	FU; Model; Method: location	Impact categories	Boundary condition	Aim	Scenarios
[12]	1 tonne medical waste OpenLCA- Ecoinvent; CML; China	PED, AD, GWP, ODP, AP, RI, POCP, EP	R/T/L	Compare different thermal conversion and sterilisation technology on medical waste	Sc1 Rotary kiln incineration Sc2 Pyrolysis-incineration Sc3 Plasma melting Sc3 Steam sterilisation Sc4 Microwave sterilisation
[13]	1 MJ of fuel Model method N/A; United State	GWP	R/T/PT/E/L	To assess different pathway to produce jet fuel from MSW	Sc1 Conventional gasification – Fischer Tropsch Sc2 Plasma gasification – Fischer Tropsch Sc3 Conventional gasification – Alcohol to
[14]	1 tonne of product gas GaBI; EDIP 2003; Singapore	GWP; AP; TE; POCP	R/T/L	Comparing various thermal pathway to produce gas-from-waste	Sc1 MSW Pyrolysis gasification Sc2 Pyrolysis of MSW Sc3 thermal cracking gasification Sc4 MSW pyrolysis-gasification Sc5 CFB gasification or organic waste Sc6 Steam gasification of shredded wood Sc7 Gasification of RDF Sc8 Gasification of Shredder tyres
[15]	1 tonne of MSW GaBi, EDIP Europe	GWP, AP, TE, POCP, HT (air and solid), ecotoxicity via solid	R/T/PT/E	Comparing three different EFW technology to process MSW	Sc1 Direct incineration Sc2 Pyrolysis with steam turbine Sc3 Pyrolysis gas turbine Sc4 Pyrolysis internal combustion engine Sc5 Gasification with steam turbine Sc6 Gasification gas turbine Sc7 Gasification internal combustion engine
[16]	297,200 tpa USES-LCA; method N/A, Italy	HTP	R/S/T/PT/AD/L/E	To assess impact of integrated waste management system	Sc1 Wet fraction is bio-dried, gasification, while organic goes to AD. Sc2 Wet fraction goes to AD, while mixed waste goes to gasification Sc3 Wet fraction goes into thermal drying provided from AD Sc4 organic to AD wet fraction into Incineration
[17]	1 tonne of solid waste SimaPro, Impact 2002+, Europe	HTP (carcinogens and non-carcinogens), RI, TE GWP, FFD, TE, AP, MET, ME,	R/T/PT	To assess the environmental impact of gasifier and incineration	Sc1 vertical shaft gasifier Sc2 incineration

Ref	FU; Model; Method: location	Impact categories	Boundary condition	Aim	Scenarios
		ULC, GWP, MD			
[18]	1 tonne of biomass Gemis. Method N/A, Japan	GWP, PM, AP, FFD	R/T/PT/ES/E	To assess a cleaner cost-effective technology	Sc1 Incineration Sc2 Gasification Sc3 Gasification and Fischer-Tropsch Sc4 Ethanol fermentation and incineration
[19]	1 tonne of waste SimaPro, Impact 2002+, Spain	HTP, RI, IR, OD, WE, TE, AP, ALC, EP, ME, FFD, MD	R/RE/AD/T/PT/L	To assess different integrated waste management technology	Sc1 Mechanical, biological recycling, and landfill Sc2 Mechanical, biological recycling, and landfill gas capture Sc3 Mechanical, biological recycling, AD, and landfill gas capture Sc4 Mechanical, biological recycling, RDF production, and landfill gas capture Sc5 Mechanical recycling, gasification, and ash landfill Sc6 Mechanical recycling, incineration, and ash landfill *Standalone unit* Sc7 Mechanical treatment Sc 8 Biological treatment Sc 9 Anaerobic digestion Sc 10 SRF production Sc11 Gasification Sc12 Incineration Sc13 Landfill Sc14 Landfill gas capture Sc15 Ash landfill disposal
[20]	1 tonne of MSW Model N/A, TRACI, USA	AP, GWP, EP, HTP, ODP, Photochemical smog	C&T/R/T/PT/L	To assess four different technology for MSW treatment in Austin Texas	Sc1 Landfill Sc2 Landfill gas capture Sc3 Incineration Sc4 Gasification
[21]	1 tonne of MSW Model and Method N/A, South Europe	GWP	R/T/PT/L	To assess alternative options from refuses produced from MBT plants	Sc1 Grate combustion – Steam Rankine cycle Sc2 fluidised bed gasification – Internal combustion engine Sc3 fluidised bed gasification – Organic Rankine cycle Sc4 fluidised bed gasification - Steam Rankine cycle Sc5 Landfilling

Ref	FU; Model; Method: location	Impact categories	Boundary condition	Aim	Scenarios
[22]	1 MJ of energy EcoInvent, ReCiPe, Spain	GWP, OD, AP, WE, MET, HTP, POCP, FFD, PM	R/T/PT/:	To compare two technologies to valorise olive by-products	Sc1 Combustion Sc2 Gasification
Assefa 2004 [23]	GWh of energy ORWARE, method N/A Sweden	GWP, AP, EP, PED	R/T/PT/E	To compare different MSW waste management	Sc1 Gasification with catalytic combustion Sc2 Gasification with flame combustion Sc3 Incineration Sc4 Landfilling with gas recovery
[24]	1 tonne of MSW Model method N/A, Indonesia	GWP, AP, EP, POCP	R/T/L	To compare various waste valorisation technology	Sc1 Landfilling Sc2 Landfilling with gas recovery Sc3 Incineration and AD Sc4 Gasification and AD Sc5 Incineration Sc6 Gasification
[25]	1000 tonnes of food waste GaBi, EcoInvent, CML, Singapore	AD (Element, fossil), AP, EP, WE, GWP, HTP, MET, OD, POCP, TE	R/T/L	To compare various technology to process eateries waste	Sc1 Incineration Sc2 AD – Composting Sc3 AD – Incineration Sc4 AD – Gasification
[26]	1 tonne of MSW GaBi, EDIP, China, France Finland	GWP, AP, TE, POCP, HTP (via air and solid), Ecotoxicity via solids	R/T/PT	To assess and compare for different waste conversion technology from three real plants across China and Europe	Sc1 Gasification Sc2 Mechanical-grate incineration Sc3 Fluidised bed incineration
[27]	1 MWh of energy SimaPro, EcoInvent; ReCiPe, Location N/A	GWP, AP, WE, ME, FFD, PED	R/T/PT	To assess different gasification technology for corkscrew waste	Sc1 Gasification without char valorisation Sc2 Gasification and char for black carbon production Sc3 Gasification and char for heavy metal absorbent Sc4 Gasification with energy recovery (heat and power)
[28]	1 tonne of MSW GaBI, EDIP, China	GWP, AP, POCP, Nutrient enrichment potential	R/T/PT/E	To assess four different technology for EFW	Sc1 Direction incineration Sc2 Gasification with steam turbine system Sc3 Gasification with gas turbine/ catalytic converter Sc4 Gasification with internal combustion engine

Ref	FU; Model; Method: location	Impact categories	Boundary condition	Aim	Scenarios
[29]	1 kg of mixed plastic and paper SimaPro, CML, Australia	GWP, AP, EP, POCP	R/T/PT/E/L	To assess different waste management strategy for common recyclate	Sc1 Landfill (mixed paper) Sc2 Incineration (mixed paper) Sc3 Gasification Pyrolysis (mixed paper) Sc4 Landfill (mixed plastic) Sc5 Incineration (mixed plastic) Sc6 Gasification Pyrolysis (mixed plastic)

Impact categories
GWP: Global warming impact
AP: Acidification potential
AD: Abiotic depletion
EP: eutrophication potential
POCP: Photochemical ozone creation potential
HTP: Human toxicity potential
CCHH: Climate change on human health
CCE: Climate change on ecosystem
OD: Ozone depletion
WE: freshwater ecotoxicity
IR: Ionising radiation
ALC: Agricultural land occupation
FFD: Fossil fuel depletion
MD: Metal depletion
ULC: Urban Land Occupation
TE: Terrestrial ecotoxicity
ME: Marine ecotoxicity
MET: Marine Eutrophication
PM: Particulate matter formation
PED: Primary Energy Demand
RI: Respiratory Inorganics
Boundary condition
C&T: Collection & Transport
S: Sorting
R: Receiving
T: Thermal conversion
PT: Post treatment
E: Energy recovery
AD: Anaerobic digestion
L: landfilling/Ash disposal
ES: Supplementary energy source
RE: Recycling
Others
MBT: Mechanical biological treatment
MRF: Material Recycling facility
AD: Anaerobic digestion
APC: Air Pollution Control

Appendix C.2 Numerical value for LCA comparison for thermal plasma gasification

Impact indicator collected from selected LCA studies (some studies are not included in relative differences analysis) (Ref Appendix C.6)

References	Data from	Scenario	Impact Indicator					
			CCHH	CCE	HTP	PM	MD	FFD
[1]	Figure 7	Sc1 Plasma gasification and landfilling of slag	3.09E-02	1.93E-02	3.62E-03	-2.15E-03	-7.01E-03	-5.99E-02
		Sc2 Incineration with landfilling bottom ash	4.35E-02	2.76E-02	9.60E-03	5.65E-04	-9.04E-04	-4.77E-02
		Sc3 Incineration with bottom ash aggregate production	4.04E-02	2.55E-02	3.28E-03	1.13E-03	-1.02E-03	-4.99E-02
		Sc4 Plasma gasification with aggregate production	2.69E-02	1.70E-02	-4.41E-03	-2.71E-03	-7.23E-03	-6.40E-02
		Sc5 Plasma gasification with polymer cement production from slag	1.80E-02	1.14E-02	-3.95E-03	-3.50E-03	-6.89E-03	-6.56E-02
		Sc6 Plasma gasification with polymer block production from slag	2.33E-02	1.52E-02	-4.18E-03	-3.16E-03	-8.59E-03	-6.33E-02
		Sc7 Plasma gasification with blended cement production from slag	2.31E-02	1.48E-02	-4.52E-03	-3.05E-03	-7.34E-03	-6.64E-02
		Sc8 Plasma gasification with blended cement block production	3.45E-02	2.19E-02	-5.54E-03	-3.62E-03	-1.68E-02	-6.63E-02
			GWP	AP	AD	POCP	EP	HTP
[2]	Figure 6	Landfill	1.79E+00	8.76E-04	-3.45E-01	3.00E-04	1.01E-03	-2.99E-02

References	Data from	Scenario	Impact Indicator								
		Incineration Sheffield	8.65E-01	-1.01E-03	-3.30E+00	-5.14E-05	4.33E-04	1.61E+00			
		Incineratin North Hykeham	5.81E-01	-1.02E-02	-3.54E+00	-1.53E-04	1.03E-04	3.74E-01			
		Fast-pyrolysis + combustion	6.61E-01	-7.42E-03	-4.36E+00	-7.23E-05	4.05E-05	1.54E-01			
		Gasification + syngas combustion	7.45E-01	-4.38E-03	-2.58E+00	-6.36E-05	1.93E-04	5.44E-01			
		Gasification + plasma cleaning	4.77E-01	-1.02E-02	-6.39E+00	-9.08E-05	7.51E-06	5.05E-02			
			GWP	AP	ODP						
[3]	Text and Figure 1-4	Sc1 Plasma gasification and vitrification	8.36E-01	4.48E-03	4.03E-08						
		Sc2 Incineration without APC	5.03E+00	2.59E-01	1.00E-03						
		Sc3 Pyrolysis	1.54E+01	3.76E-01	3.20E-03						
		Sc4 Gasification	9.89E-01	1.80E-01	4.09E-11						
		Sc5 Incineration with APC	6.98E-01	2.11E-01	9.68E-05						
			Human health	Ecosystem	GWP	CCHH	PMF	HTP			
[4]	Figure 3 and 4	Sc1 Plasma vitrification	1.20E+03	1.16E+01	1.01E+01	1.47E+01	9.03E+00	1.47E+01			
		Sc2 Furnace/Fuel vitrification	5.14E+02	1.87E+01	1.83E+01	3.05E+01	2.71E+00	1.47E+01			
		Sc3 Thermal treatment in rotary kiln	1.23E+04	1.04E+02	5.94E+01	9.11E+01	3.94E+01	2.27E+02			
		Sc4 Solidification and landfill	1.27E+03	-	-	8.00E+00	6.45E-01	1.87E+01			
			GWP	AP							
[5]	Figure9	Sc1 Plasma gasification	9.38E+03	3.15E+01							
		Sc2 Plasma gasification with chemical looping	3.93E+03	2.63E+01							
			GWP	EP	AP	OD	AD E	AD Fossil	WE	MET	TE
[6]	Table 3	Sc1 Incineration	-1.71E+02	-3.86E-02	-2.42E-01	-1.16E-10	-5.01E-05	-2.00E+03	-2.67E-01	-2.63E+04	-5.90E-02
		Sc2 Gasification	2.70E+01	-2.32E+03	-3.99E-01	2.08E-08	-9.35E-06	2.40E+02	1.86E-03	-3.12E+05	1.45E-02
		Sc3 Plasma gasification	-3.10E+01	-1.55E+03	-3.97E-01	-2.13E-08	-1.62E-05	-3.82E+02	-6.41E-02	-2.14E+05	-2.95E-02
			GWP	EP	AP	OD	AD E	AD Fossil	WE	MET	TE
[7]	Table 5	Sc1 Low temperature gasification	2.70E+01	-2.32E+03	-3.99E-01	2.08E-08	-9.35E-06	2.40E+02	1.86E-03	-3.12E+05	1.45E-02
		Sc2 Incineration	4.30E+02	-3.89E-02	-2.43E+00	-3.96E-05	-6.09E-03	-9.26E+02	-3.82E-01	-3.40E+05	-1.61E-02
		Co3 Landfill (FromEvangelisti 2015)	2.09E-12	3.72E-12	-5.49E-12	1.25E-10	-	1.37E-12	5.29E-11	-1.37E-11	1.40E-10
		Co4 Fast pyrolysis	2.19E-10	-4.16E-11	-1.19E-10	5.71E-09	-	-2.56E-12	9.61E-12	2.91E-10	-3.85E-11
		Co5 Plasma gasification	1.96E-11	-5.76E-11	-1.82E-10	4.45E-09	-	3.95E-11	-1.97E-12	-6.69E-11	-4.98E-11
			GWP	EP	AP	OD	ADElements	AD Fossil	WE	MET	TE
[8]	Table 3 and text	two stage plasma gasification	-3.10E+01	-1.55E+03	-3.97E-01	-2.13E-08	-1.62E-05	-3.82E+02	-6.41E-02	-2.14E+05	-2.95E-02
		Incineration	4.00E+02								
			GWP	HTP	PM	AP	WE	MET	TE	FFD	
[9]	Table 4	Sc1 Syngas-from-RDF combustion produced by plasma gasification	5.10E+01	3.01E+01	6.00E-02	2.00E-01	4.00E-02	1.00E-02	1.17E+00	1.27E+01	
		Sc2 Hard coal combustion	1.30E+02	3.83E+01	2.60E-01	8.40E-01	4.00E-02	2.00E-02	1.36E+00	2.98E+01	
		Sc3 Mixture of RDF and hard coal	1.07E+02	3.58E+01	2.00E-01	6.50E-01	4.00E-02	2.00E-02	1.30E+00	2.47E+01	

References	Data from	Scenario	Impact Indicator							
			GWP	AP	WE	EP	AD	OD		
[11]	from figure 11.8	Sc1 Separated organic into AD and other to recycling and incineration	4.86E-01	-5.63E-04	2.29E-02	3.69E-04	-2.34E+00	2.81E-09		
		Sc2 Separated organic into AD and other to recycling and landfill	9.19E-01	-2.70E-04	2.32E-02	9.30E-04	-9.48E-01	1.82E-09		
		Sc3 Separated organic into AD and other to incineration	5.46E-01	-1.63E-04	-2.23E-03	6.69E-04	-2.28E+00	3.01E-09		
		Sc4 Separated organic into AD and other to landfill	9.78E-01	2.20E-04	-1.97E-03	1.08E-03	-4.75E-01	4.24E-10		
		Sc5 Advance thermal two stage plasma gasification	7.24E-01	3.26E-04	4.87E-03	1.15E-04	-3.20E+00	9.18E-10		
			PED	AD	GWP	ODP	AP	RI	POFP	EP
[12]	From table 1	Sc1 Rotary kiln incineration	5.29E+03	1.02E-03	4.20E+02	2.69E-05	4.32E+00	1.36E+00	4.33E-01	5.69E-01
		Sc2 Pyrolysis-incineration	2.43E+03	3.60E-04	1.87E+02	8.84E-06	4.97E+00	8.50E-01	2.63E-01	5.49E-01
		Sc3 Plasma melting	1.29E+04	2.18E-03	6.86E+02	5.16E-05	5.32E+00	1.25E+00	6.55E-01	5.00E-01
		Sc3 Steam sterilisation	4.74E+03	1.22E-03	1.65E+02	2.96E-05	1.66E+01	6.94E-01	2.62E-01	1.38E+00
		Sc4 Microwave sterilisation	1.79E+03	7.85E-05	1.35E+02	2.47E-07	1.65E+01	6.61E-01	5.22E-02	1.31E+00
			GWP							
[13]	Table 1	Sc1 Conventional gasification - Fischer Tropsch	3.29E+01							
		Sc2 Plasma gasification - Fischer Tropsch	6.23E+01							
		Sc3 Conventional gasification - Alcohol synthesis	5.27E+01							
			GWP	AP	EP	POCP				
[14]	Figure 2-5	Sc1 MSW Pyrolysis gasification	1.92E+02	7.30E+00	6.33E+00	7.75E-06				
		Sc2 Pyrolysis of MSW	1.70E+02	1.40E+01	1.14E+01	5.52E-05				
		Sc3 thermal cracking gasification	2.66E+02	8.66E+00	1.20E+01	5.75E-05				
		Sc4 MSW pyrolysis-gasification	2.01E+02	9.64E+00	1.85E+01	8.92E-05				
		Sc5 CFB gasification or organic waste	1.84E+02	1.24E+01	2.08E+01	9.94E-05				
		Sc6 Steam gasification of shredded wood	1.94E+02	7.73E+00	4.70E+00	2.33E-05				
		Sc7 Gasification of RDF	2.14E+02	1.56E+01	1.65E+01	8.14E-05				
		Sc8 Gasification of Shredder tyres	2.41E+02	9.12E+00	5.84E+00	8.21E-06				
			GWP	AD	EP	POCP	HT air	HT Solid	TE -Solid	
		Sc1 Direct incineration	7.00E-03	-8.00E-03	6.00E-03	6.00E-03	2.10E-02	4.90E-01	1.54E-05	
[15]	Figure 3	Sc 2 Pyrolysis with steam turbine	1.60E-02	-6.00E-03	5.00E-03	4.00E-03	1.50E-02	5.22E-01	1.12E-05	
		Sc3 Pyrolysis gas turbine	8.00E-03	-6.00E-03	3.00E-03	-7.90E-05	1.80E-02	5.41E-01	1.22E-05	
		Sc4 Pyrolysis internal combustion engine	1.00E-02	-5.00E-03	3.00E-03	-1.03E-04	1.80E-02	5.41E-01	1.22E-05	
		Sc5 Gasification with steam turbine	1.20E-02	-8.00E-03	4.00E-03	3.00E-03	1.50E-02	5.20E-01	1.12E-05	
		Sc6 Gasification gas turbine	3.00E-03	-1.50E-01	-3.00E-03	-4.00E-03	6.00E-03	4.61E-01	9.12E-06	
		Sc7 Gasification internal combustion engine	1.50E-02	-9.00E-03	-1.00E-03	-2.00E-03	8.00E-03	4.66E-01	9.17E-06	
			HTP							
[16]	Based on fig 3	Sc1 Wet fraction is bio-dried, gasification, while organic goes to AD.	2.74E+07							
		Sc2 Wet fraction goes to AD, while mixed waste goes to gasification	2.08E+07							

References	Data from	Scenario	Impact Indicator								
		Sc3 Wet fraction goes into thermal drying provided from AD	1.90E+07								
		Sc4 organic to AD wet fraction into Incineration	2.00E+07								
			GWP								
[17]	Figure 5	Sc1 vertical shaft gasifier	1.48E+02								
		Sc2 incineration	3.52E+02								
			FFD	GWP	PM	AP					
[18]	Figure 5-8	Sc1 Incineration	-1.04E+04	-5.65E+02	-1.27E+00	-3.15E-01					
		Sc2 Gasification	-1.09E+04	-5.44E+02	-8.03E-01	-3.59E-01					
		Sc3 Gasification and Fischer-Tropsch	-1.20E+04	-2.38E+02	-2.01E+00	-6.80E-01					
		Sc4 Ethanol fermentation and incineration	-1.04E+04	-2.64E+02	-1.81E+00	-5.75E-01					
			IR	OD	HTP	TE	AP	MET	GWP	FFD	MD
[19]	Table 12 and 13	Sc1 Mechanical, biological recycling, and landfill	4.33E+03	3.60E-05	3.70E+01	5.10E+03	5.47E+00	4.00E-02	6.25E+02	3.92E+03	3.83E+00
		Sc2 Mechanical, biological recycling, and landfill gas capture	1.38E+03	2.70E-05	3.11E+01	4.60E+03	4.46E+00	4.00E-02	4.34E+02	2.77E+03	2.80E+00
		Sc3 Mechanical, biological recycling, AD, and landfill gas capture	-5.00E-02	3.20E-05	4.00E+01	6.13E+03	5.88E+00	5.00E-02	3.24E+02	3.13E+03	3.33E+00
		Sc4 Mechanical, biological recycling, RDF production, and landfill gas capture	5.97E+03	6.60E-05	7.14E+01	1.02E+04	1.04E+01	8.00E-02	5.99E+02	7.02E+03	6.95E+00
		Sc5 Mechanical recycling, gasification, and ash landfill	9.79E+02	3.80E-05	4.60E+01	6.96E+03	6.54E+00	6.00E-02	3.76E+02	3.86E+03	4.00E+00
		Sc6 Mechanical recycling, incineration, and ash landfill	-8.31E+03	-2.20E-05	6.69E+01	2.33E+03	7.44E+00	1.00E-02	3.72E+02	-2.46E+03	-4.20E-01
		Sc7 Mechanical treatemt	7.87E+02	0.00E+00	1.75E+00	1.34E+02	2.70E-01	0.00E+00	1.51E+01	3.06E+02	2.70E-01
		Sc8 Biological treatment	3.54E+03	0.00E+00	3.52E+01	4.97E+03	5.20E+00	4.00E-02	2.99E+02	3.61E+03	3.55E+00
		Sc9 Anareobic digestion	2.17E+03	0.00E+00	4.41E+01	6.50E+03	6.62E+00	5.00E-02	1.89E+02	3.97E+03	4.08E+00
		Sc10 SRF productin	4.59E+03	0.00E+00	4.03E+01	5.59E+03	5.97E+00	5.00E-02	1.66E+02	4.25E+03	4.15E+00
		Sc11 Gasification	7.10E+01	0.00E+00	4.36E+01	4.56E+03	5.48E+00	4.00E-02	2.71E+02	2.80E+03	3.28E+00
		Sc12 Incineration	-9.22E+03	0.00E+00	6.44E+01	-6.81E+01	6.38E+00	0.00E+00	2.66E+02	-3.52E+03	-1.15E+00
		Sc13 Landfill	0.00E+00	0.00E+00	7.00E-02	0.00E+00	0.00E+00	0.00E+00	3.11E+02	0.00E+00	0.00E+00
		Sc14 Landfill gas capture	-2.96E+03	0.00E+00	-5.83E+00	-5.03E+02	-1.02E+00	0.00E+00	1.20E+02	-1.15E+03	-1.03E+00
		Sc15 Ash landfill disposal	1.20E+02	0.00E+00	6.70E-01	2.26E+03	7.90E-01	1.00E-02	9.04E+01	7.53E+02	4.50E-01
			AP	EP	GWP	HTP	OD	POCP			
[20]	Figure 3	Sc1 Landfill	2.14E+02	1.84E-03	1.62E+03	3.76E-01	2.29E-08	8.83E+00			
		Sc2 Landfill gas capture	9.28E+01	-9.44E-03	1.36E+03	-9.94E-02	1.94E-08	-6.89E+00			
		Sc3 Incineration	-1.57E+02	4.56E-01	5.47E+02	-8.91E-02	1.00E-08	1.19E+01			
		Sc4 Gasification	-4.51E+02	-2.37E-01	-9.60E+01	-1.73E+00	8.49E-09	-6.18E+01			
			GWP								
[21]	Table 9	Sc1 Grate combustion – Steam Rankine cycle	3.31E+02								
		Sc2 fluidised bed gasification – Internal combustion engine	2.85E+02								
		Sc3 fluidised bed gasification – Organic Rankine cycle	2.75E+02								
		Sc4 fluidised bed gasification - Steam Rankine cycle	2.85E+02								

References	Data from	Scenario	Impact Indicator								
		Sc5 Landfilling	4.54E+02								
			CCHH	OD	HTP	POCP	PM	IR	CCE	AP	WE
[22]	Table 7 and 8	Sc1 Combustion	9.96E-07	1.69E-11	5.91E-08	9.43E-11	1.15E-07	8.22E-11	5.64E-09	1.22E-11	9.69E-14
		Sc2 Gasification	2.76E-06	3.59E-11	1.38E-07	5.92E-10	1.37E-06	1.70E-10	1.56E-08	2.31E-10	2.12E-13
			GWP	AP	EP	PED					
[23]	Figure 2-4	Sc1 Gasification with catalytic combustion	3.20E-02	6.37E-01	4.90E-02	1.00E+00					
		Sc2 Gasification with flame combustion	3.20E-02	1.74E+00	4.90E-02	1.00E+00					
		Sc3 Incineration	4.64E-01	1.84E+00	1.00E-01	2.21E+00					
		Sc4 Landfilling with gas recovery	5.31E+00	8.39E+00	9.80E-02	1.43E+01					
			GWP	AP	EP	POCP					
[24]	Table 3	Sc1 Landfilling	3.74E+02	2.21E-02	2.40E-03	4.10E-01					
		Sc2 Landfilling with gas recovery	1.88E+02	4.28E-02	5.00E-03	3.90E-01					
		Sc3 Incineration and AD	1.55E+02	-8.69E-01	-7.82E-02	-7.02E-02					
		Sc4 Gasification and AD	-4.90E+01	-2.81E+00	-1.47E-01	-1.53E-01					
		Sc5 Incineration	6.10E+01	-1.43E+00	-7.87E-02	-6.71E-02					
		Sc6 Gasification	-1.68E+02	-2.80E+00	-1.62E-01	-1.59E-01					
			AD El	AD F	AP	EP	WE	GWP	HTP	MET	OD
[25]	Table 3	Sc1 Incineration	1.21E-02	-6.56E+05	-8.64E+01	3.53E+01	-8.87E+02	1.07E+05	-1.31E+02	-3.97E+06	3.86E-04
		Sc2 AD – Composting	-1.95E-01	-1.49E+06	-1.69E+02	4.00E+01	-1.13E+04	9.41E+04	-2.55E+04	-4.09E+07	-4.17E-04
		Sc3 AD – Incineration	1.07E-02	-1.16E+06	-2.61E+01	7.31E+01	-1.96E+03	9.25E+04	-4.47E+03	-9.36E+06	1.98E-03
		Sc4 AD – Gasification	9.81E-03	-1.42E+06	-9.01E+01	6.86E+01	-2.75E+03	3.85E+04	-4.57E+03	-1.31E+07	1.12E-03
			AD	AP	EP	GWP	OD	HTP	WE	MET	TE
[30]	Figure 5	Sc1 Pyrolysis Gasification	-4.60E-02	2.48E-01	1.13E+00	4.12E+02	-1.40E-05	8.06E+02	2.15E+02	1.87E+05	2.51E+00
		Sc2 Incineration	-4.56E-02	5.85E-01	1.75E+00	4.24E+02	-1.90E-05	1.18E+03	3.23E+02	2.81E+05	7.03E-01
		Sc3 Landfill	-9.05E-02	2.44E-01	8.83E-02	7.46E+02	-9.60E-06	8.15E+00	-2.54E-01	8.36E+02	9.38E-03
			AP	GWP	EP	POP					
[31]	Figure 2-5	Sc1 landfill gas capture	4.57E+03	1.07E+07	1.26E+04	1.83E+03					
		Sc2 Incineration	1.01E+04	1.55E+07	2.39E+03	3.95E+02					
		Sc3 Gasification Pyrolysis	2.00E+04	2.30E+07	4.79E+03	4.39E+02					
			GWP	AP	TE	POCP	HTP Air	HTP Sol			
[26]	Table 7	Sc1 Gasification	-5.00E-04	-2.00E-02	-6.00E-04	-1.00E-03	-2.00E-03	-9.00E-04			
		Sc2 Mechanical-grate incineration	2.00E-03	-7.00E-03	7.00E-03	7.00E-03	2.00E-03	1.70E-02			
		Sc3 Fluidised bed incineration	1.10E-02	-4.00E-04	9.00E-03	1.50E-02	4.00E-03	1.60E-02			
			GWP	AP	WE	MET	FFD				
[27]	Table 6	Sc1 Gasification without char valorisation	1.22E+02	6.70E-01	5.00E-02	3.97E-03	3.70E+01				
		Sc2 Gasification and char for black carbon production	4.09E+01	3.00E-01	5.00E-02	3.58E-03	-3.93E+01				

References	Data from	Scenario	Impact Indicator				
		Sc3 Gasification and char for heavy metal absorbent	1.34E+02	7.00E-01	6.00E-02	4.21E-03	3.93E+01
		Sc4 Gasification with energy recovery (heat and power)	1.86E+02	1.53E+00	8.00E-02	1.00E-02	4.23E+01
			GWP	AP	POCP		
[28]	Figure 2	Sc1 Direction incineration	3.42E+01	-4.16E-01	5.80E-03		
		Sc2 Gasification with steam turbine system	6.60E+01	-1.01E+00	4.02E-03		
		Sc3 Gasification with gas turbine/ catalytic converter	2.17E+01	-1.80E+00	-4.11E-03		
		Sc4 Gasification with internal combustion engine	8.07E+01	-1.12E+00	-1.56E-03		
			AP	GWP	EP	POCP	
[29]	Figure 2	Sc1 Landfill (mixed paper)	-1.49E-04	1.56E+00	9.60E-04	4.63E-08	
		Sc2 Incineration (mixed paper)	-6.51E-05	1.03E+00	-3.34E-05	-1.61E-09	
		Sc3 Gasification Pyrolysis (mixed paper)	1.02E-04	1.03E+00	1.04E-05	5.04E-10	
		Sc4 Landfill (mixed plastic)	5.95E-05	5.14E-02	7.30E-05	3.53E-09	
		Sc5 Incineration (mixed plastic)	-6.62E-04	9.49E-01	-1.94E-04	-9.37E-09	
		Sc6 Gasification Pyrolysis (mixed plastic)	1.38E-04	1.91E+00	2.50E-05	1.21E-09	

Appendix C.3 Numerical value for LCA comparison for conventional gasification

(Ref Appendix C.6)

References	Code	Relative differences								
Plasma Gasification vs Landfilling		GWP	AP	AD	POCP	EP	HTP			
[2]	PGLF1	-73%	-1269%	1752%	-130%	-99%	-269%			
		Human health	Ecosystem	GWP	CCHH	PMF	HTP			
[4]	PGLF2	-5%			84%	1300%	-21%			
		GWP	EP	AP	OD	AD-E	AD Fossil	WE	MET	TE
[7]	PGLF3	838%	-1648%	-3215%	3460%		2783%	-104%	-388%	-136%
		GWP	AP	WE	EP	AD	OD			
[11]	PGLF4.1	-21%	221%	-79%	-88%	-238%	-49%			
	PGLF4.2	-26%	48%	348%	-89%	-574%	117%			
Plasma Gasification vs Incineration/Combustion										
		CCHH	CCE	HTP	PM	MD	FFD			
[1]	PGINC1.1	-29%	-30%	-62%	-480%	-675%	-26%			
	PGINC1.2	-23%	-24%	10%	-290%	-589%	-20%			
	PGINC1.3	-59%	-59%	-141%	-720%	-663%	-38%			
	PGINC1.4	-56%	-55%	-221%	-410%	-578%	-31%			
		GWP	AP	AD	POCP	EP	HTP			
[2]	PGINC2.1	-45%	-913%	-94%	-76%	-98%	-97%			
	PGINC2.2	-18%	0%	-80%	41%	-93%	-87%			
		GWP	AP	OD						
[3]	PGINC3.1	-83%	-98%	-100%						
	PGINC3.2	20%	-98%	-100%						
		Human health	Ecosystem	GWP	CCHH	PMF	HTP			
[4]	PGINC4	-90%	-89%	-83%	-84%	-77%	-94%			
		GWP	EP	AP	OD	ADElements	AD Fossil	WE	MET	TE
[27]	PGINC5	82%	-4015444%	-64%	-18262%	68%	81%	76%	-714%	50%
		GWP								
[8]	PGINC6	-108%								
		GWP	HTP	PM	AP	WE	MET	TE	FFD	
[9]	PGINC7.1	-61%	-21%	-77%	-76%	0%	-50%	-14%	-57%	
	PGINC7.2	-52%	-16%	-70%	-69%	0%	-50%	-10%	-48%	
		GWP	AP	WE	EP	AD	OD			
[11]	PGINC8.1	49%	158%	-79%	-69%	37%	-67%			
	PGINC8.2	33%	300%	319%	-83%	-41%	-70%			
		PED	AD	GWP	ODP	AP	RI	POFP	EP	
[12]	PGIN9	144%	114%	63%	92%	23%	-8%	51%	-12%	
Plasma Gasification vs Conventional Gasification										
		GWP	AP	AD	POCP	EP	HTP			
[2]	PGGAS1	-36%	-134%	-148%	-43%	-96%	-91%			
		GWP	AP	ODP						

References	Code	Relative differences								
[3]	PGGAS2	-15%	-98%	98433%						
		GWP	EP	AP	OD	ADElements	AD Fossil	WE	MET	TE
[27]	PGGAS3	-215%	33%	1%	-202%	-73%	-259%	-3546%	31%	-303%
		GWP								
[13]	PGGAS4.1	90%								
	PGGAS4.2	18%								
Plasma Gasification vs Pyrolysis										
		GWP	AP	AD	POCP	EP	HTP			
[456]	PGPYRO1	-28%	-38%	-47%	-26%	-81%	-67%			
		GWP	AP	ODP						
[457]	PGPYRO2	-95%	-99%	-100%						
		PED	AD	GWP	ODP	AP	RI	POFP	EP	
[464]	PGPYRO3	431%	506%	267%	484%	7%	47%	149%	-9%	
Plasma Gasification vs Plasma gasification										
		CCHH	CCE	HTP	PM	MD	FFD			
[2]	PGPG1.1	-13%	-12%	-222%	-26%	-3%	-7%			
	PGPG1.2	-42%	-41%	-209%	-63%	-2%	-10%			
[3]	PGPG1.3	-25%	-21%	-216%	-47%	-23%	-6%			
	PGPG1.4	-25%	-23%	-225%	-42%	-5%	-11%			
[12]	PGPG1.5	12%	14%	-253%	-68%	-140%	-11%			
		GWP	AP							
	PGPG2	-58%	-17%							
Gasification vs Landfilling										
		GWP	AP	AD	POCP	EP	HTP			
[2]	GASLF1	-58%	-600%	-648%	-121%	-81%	1923%			
		AP	EP	GWP	HTP	OD	POCP			
[20]	GASLF2.1	-311%	-12980%	-106%	-560%	-63%	-800%			
		GWP								
[21]	GASLF3.1	-39%								
	GASLF3.2	-37%								
		GWP	AP	EP	PED					
[23]	GASLF4.1	-99%	-92%	-50%	-93%					
	GASLF4.2	-99%	-79%	-50%	-93%					
		GWP	AP	EP	POCP					
[24]	GASLF5.1	-113%	-12831%	-6213%	-137%					
	GASLF5.2	-145%	-12755%	-6842%	-139%					
	GASLF5.3	-126%	-6674%	-3034%	-139%					
	GASLF5.4	-189%	-6635%	-3336%	-141%					
		AP	GWP	EP	POCP					
[29]	GASLF6.1	169%	-34%	-99%	-99%					
	GASLF6.2	131%	3615%	-66%	-66%					
		IR	OD	HTP	TE	AP	MET	GWP	FFD	MD
[19]	GASLF7.1	-77%	6%	24%	36%	20%	50%	-40%	-1%	0.044386
	GASLF7.2	-29%	41%	48%	51%	47%	50%	-13%	39%	0.428571
	GASLF7.3	710099900%	-100%	>100%	>100%	>100%	399900%	-13%	2804410%	31.8
	GASLF7.4	102%	-100%	847%	1006%	637%	-60%	126%	344%	418%
		AP	EP	GWP	HTP	OD	POCP			

References	Code	Relative differences								
[20]	GASLF2.2	-586%	-2411%	-107%	-1640%	-56%	-797%			
Gasification vs Incineration										
		GWP	AP	AD	POCP	EP	HTP			
[2]	GASINC1.1	-14%	-333%	22%	-24%	-55%	-66%			
	GASINC1.2	28%	57%	27%	58%	88%	45%			
		GWP	AP	ODP						
[3]	GASINC2.1	-80%	-31%	-100%						
	GASINC2.2	42%	-15%	-100%						
		GWP	EP	AP	OD	ADElements	AD Fossil	WE	MET	TE
[27]	GASINC3	116%	-6010263%	-65%	18031%	81%	112%	101%	-1086%	125%
		GWP	EP	AP	OD	ADElements	AD Fossil	WE	MET	TE
[7]	GASINC4	-94%	-5963910%	84%	100%	100%	126%	100%	8%	190%
		GWP								
[17]	GASINC5	-58%								
		FFD	GWP	PM	AP					
[18]	GASINC6.1	-4%	4%	37%	-14%					
	GASINC6.2	-15%	58%	-59%	-116%					
		IR	OD	HTP	TE	AP	MET	GWP	FFD	MD
[19]	GASINC7.1	112%	273%	-31%	199%	-12%	500%	1%	257%	1052%
	GASINC7.2	101%	-10%	-32%	6793%	-14%		2%	180%	385%
		HTP								
[16]	GASINC8	4%								
		AP	EP	GWP	HTP	OD	POCP			
[20]	GASINC9	-187%	-152%	-118%	-1842%	-15%	-619%			
		CCHH	OD	HTP	POCP	PM	IR	CCE	AP	WE
[22]	GASINC10	177%	112%	134%	528%	1091%	107%	177%	1793%	119%
		GWP	AP	EP	PED					
[23]	GASINC11.1	-93%	-65%	-51%	-55%					
	GASINC11.2	-93%	-5%	-51%	-55%					
		GWP	AP	EP	POCP					
[24]	GASINC12.1	-180%	-97%	-86%	-128%					
	GASINC12.2	-375%	-96%	-106%	-136%					
	GASINC12.3	-132%	-224%	-88%	-118%					
	GASINC12.4	-208%	-222%	-107%	-126%					
		AD El	AD F	AP	EP	WE	GWP	HTP	MET	OD
[25]	GASINC13	-19%	-116%	-4%	94%	-210%	-64%	-3389%	-230%	190%
		GWP	AP	TE	POCP	HTP Air	HTP Sol			
[26]	GASINC14.1	-125%	-186%	-109%	-114%	-200%	-105%			
	GASINC14.2	-105%	-4900%	-107%	-107%	-150%	-106%			
		GWP	AP	POCP						
[28]	GASINC15.1	93%	-143%	-31%						
	GASINC15.2	-36%	-334%	-171%						
	GASINC15.3	136%	-169%	-127%						
		AP	GWP		EP	POCP				
[29]	GASINC16.1	257%	0%		131%	131%				
	GASINC16.2	121%	101%		113%	113%				
Gasification vs Gasification										

References	Code	Relative differences						
		GWP	AD	EP	POCP	HT air	HT Solid	TE -Solid
[15]	GASGAS1.1	-20%	11%	500%	250%	88%	12%	22%
	GASGAS1.2	-80%	-1567%	-200%	-100%	-25%	-1%	0%
		FFD	GWP	PM	AP			
[18]	GASGAS2	-10%	56%	-150%	-90%			
		GWP						
[21]	GASGAS3.1	-14%						
	GASGAS3.2	-17%						
	GASGAS3.3	-14%						
		GWP	AP		EP	PED		
[23]	GASGAS4	0%	-63%		0%	0%		
		GWP	AP		EP	POCP		
[24]	GASGAS5	-243%	1%		-10%	-3%		
		GWP	AP	FFD	WE	MET		
[27]	GASGAS6.1	-66%	-55%	-206%	0%	-10%		
	GASGAS6.2	10%	4%	6%	20%	6%		
	GASGAS7.3	53%	128%	14%	60%	152%		
		GWP	AP			POCP		
[28]	GASGAS7.1	-18%	9%			357%		
	GASGAS7.2	-73%	-61%			-163%		

Appendix C.4 Comparison for various gasification scenarios

Case studies of different variation of plasma gasification and gasification technology (Ref Appendix C.6)

References	Plasma Gasification/Gasification	Base scenario	Code
Gasification vs Gasification			
[15]	Sc7 Gasification internal combustion engine	Sc5 Gasification with steam turbine	GASGAS1.1
	Sc7 Gasification internal combustion engine	Sc6 Gasification gas turbine	GASGAS1.2
[18]	Sc2 Gasification	Sc3 Gasification and Fischer-Tropsch	GASGAS2
[21]	Sc1 Grate combustion – Steam Rankine cycle	Sc2 fluidised bed gasification – Internal combustion engine	GASGAS3.1
	Sc1 Grate combustion – Steam Rankine cycle	Sc3 fluidised bed gasification – Organic Rankine cycle	GASGAS3.2
	Sc1 Grate combustion – Steam Rankine cycle	Sc4 fluidised bed gasification - Steam Rankine cycle	GASGAS3.3
[23]	Sc2 Gasification with flame combustion	Sc1 Gasification with catalytic combustion	GASGAS4
[24]	Sc4 Gasification and AD	Sc6 Gasification	GASGAS5
[27]	Sc1 Gasification without char valorisation	Sc2 Gasification and char for black carbon production	GASGAS6.1
	Sc1 Gasification without char valorisation	Sc3 Gasification and char for heavy metal absorbent	GASGAS6.2
	Sc1 Gasification without char valorisation	Sc4 Gasification with energy recovery (heat and power)	GASGAS6.3
[28]	Sc4 Gasification with internal combustion engine	Sc2 Gasification with steam turbine system	GASGAS7.1
	Sc4 Gasification with internal combustion engine	Sc3 Gasification with gas turbine/ catalytic converter	GASGAS7.2
Plasma Gasification vs Plasma Gasification			
[1]	Sc4 Plasma gasification with aggregate production	Sc1 Plasma gasification and landfilling of slag	PGPG1.1
	Sc5 Plasma gasification with polymer cement production from slag	Sc1 Plasma gasification and landfilling of slag	PGPG1.2
	Sc6 Plasma gasification with polymer block production from slag	Sc1 Plasma gasification and landfilling of slag	PGPG1.3
	Sc7 Plasma gasification with blended cement production from slag	Sc1 Plasma gasification and landfilling of slag	PGPG1.4
	Sc8 Plasma gasification with blended cement block production	Sc1 Plasma gasification and landfilling of slag	PGPG1.5
[5]	Sc2 Plasma gasification with chemical looping	Sc1 Plasma gasification	PGPG2
	Sc2 Plasma gasification with chemical looping	Sc1 Plasma gasification	PGPG2

Appendix C.5 Comparison for various gasification scenarios

Different scenarios' relative differences of gasification technology for selected impact indicators

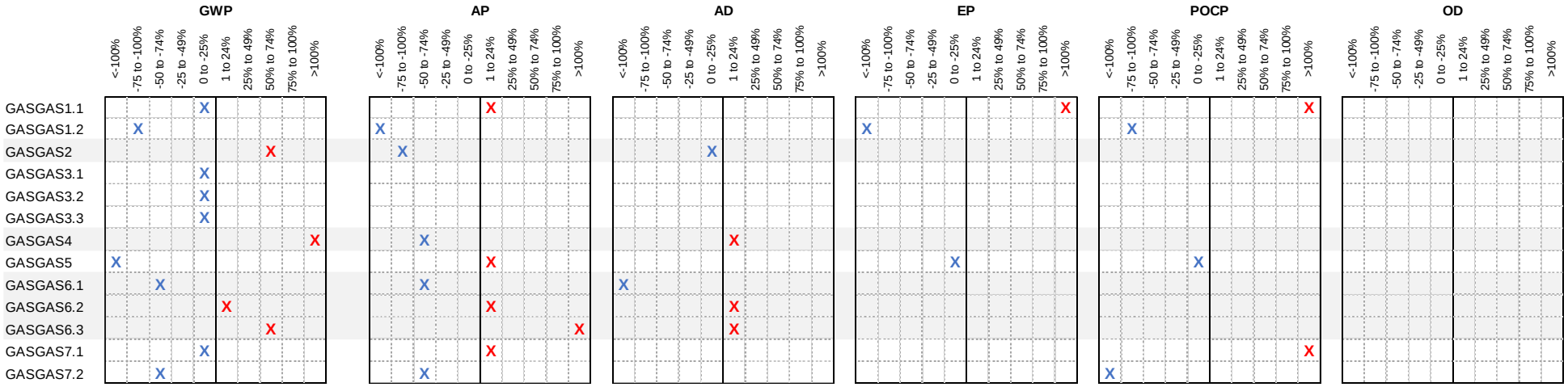

Different scenarios' relative differences of gasification technology for human health and environmental impact.

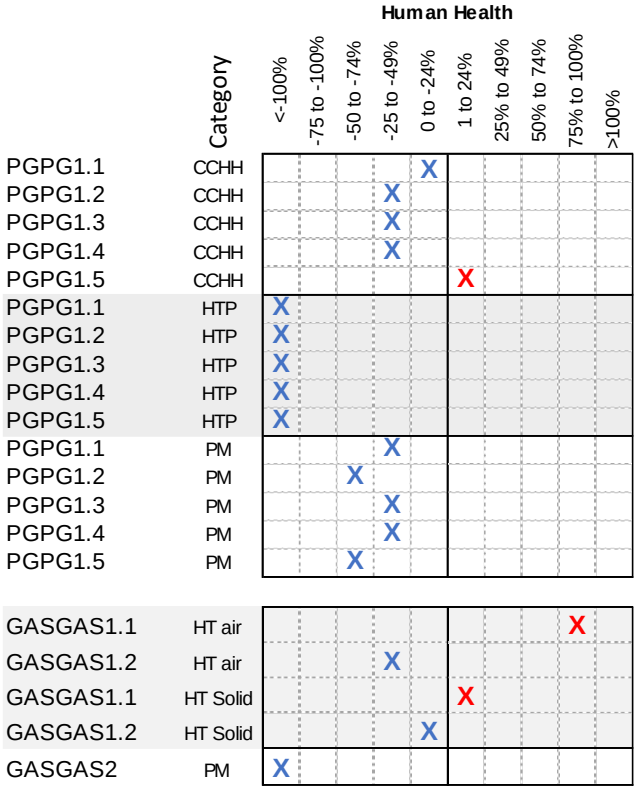

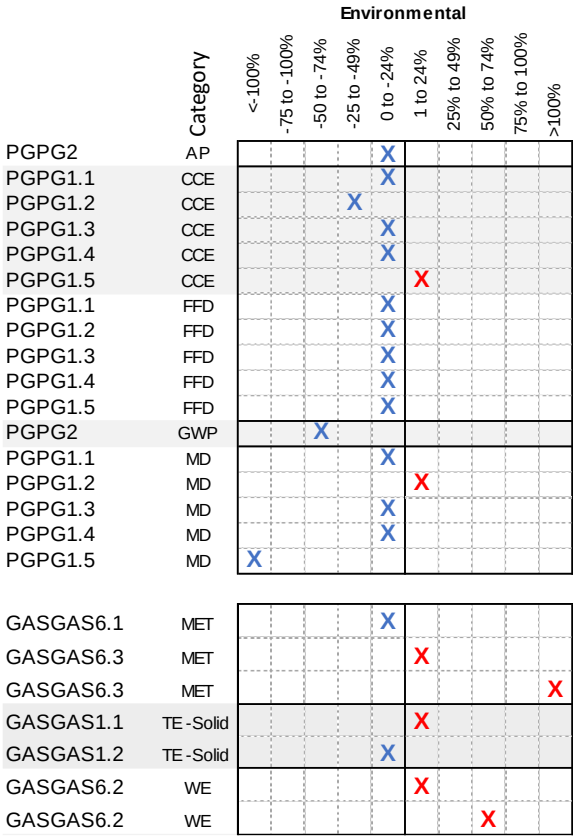

Appendix C.6 References for LCA studies

[1] M. Danthurebandara, S. Van Passel, I. Vanderreydt, K. Van Acker, Environmental and economic performance of plasma gasification in Enhanced Landfill Mining, Waste Management 45 (2015) 458-467.

[2] S. Evangelisti, C. Tagliaferri, R. Clift, P. Lettieri, R. Taylor, C. Chapman, Life cycle assessment of conventional and two-stage advanced energy-from-waste technologies for municipal solid waste treatment, J Journal of Cleaner Production 100 (2015) 212-223.

[3] V. Mannheim, I. Bodnár, Life Cycle Assessment for Thermic Treatments of Organic Industrial Waste, Enviro-management, 2012.

[4] S.-L. Pei, T.-L. Chen, S.-Y. Pan, Y.-L. Yang, Z.-H. Sun, Y.-J. Li, Addressing environmental sustainability of plasma vitrification technology for stabilization of municipal solid waste incineration fly ash, J Journal of Hazardous Materials 398 (2020) 122959.

[5] H. Qi, P. Cui, Z. Liu, Z. Xu, D. Yao, Y. Wang, Z. Zhu, S. Yang, Conceptual design and comprehensive analysis for novel municipal sludge gasification-based hydrogen production via plasma gasifier, J Energy Conversion Management 245 (2021) 114635.

[6] A. Ramos, A. Rouboa, Renewable energy from solid waste: Life cycle analysis and social welfare, J Environmental impact assessment review 85 (2020) 106469.

[7] A. Ramos, C.A. Teixeira, A. Rouboa, Assessment study of an advanced gasification strategy at low temperature for syngas generation, J International Journal of Hydrogen Energy 43(21) (2018) 10155-10166.

[8] A. Ramos, C.A. Teixeira, A. Rouboa, Environmental assessment of municipal solid waste by two-stage plasma gasification, J Energies 12(1) (2019) 137.

[9] A.M. López-Sabirón, K. Fleiger, S. Schäfer, J. Antoñanzas, A. Irazustabarrena, A. Aranda-Usón, G.A. Ferreira, Refuse derived fuel (RDF) plasma torch gasification as a feasible route to produce low environmental impact syngas for the cement industry, J Waste Management Research 33(8) (2015) 715-722.

[10] J.-L. Shie, C.-Y. Chang, C.-S. Chen, D.-G. Shaw, Y.-H. Chen, W.-H. Kuan, H.-K. Ma, Energy life cycle assessment of rice straw bio-energy derived from potential gasification technologies, J Bioresource technology 102(12) (2011) 6735-6741.

[11] C. Tagliaferri, P. Lettieri, Methane from waste: Thermal and biological technologies compared under a life cycle assessment perspective, Substitute Natural Gas from Waste, Elsevier2019, pp. 275-315.

[12] H.-L. Zhao, L. Wang, F. Liu, H.-Q. Liu, N. Zhang, Y.-W. Zhu, Energy, environment and economy assessment of medical waste disposal technologies in China, J Science of The Total Environment 796 (2021) 148964.

[13] P. Suresh, R. Malina, M.D. Staples, S. Lizin, H. Olcay, D. Blazy, M.N. Pearlson, S.R. Barrett, Life cycle greenhouse gas emissions and costs of production of diesel and jet fuel from municipal solid waste, J Environmental science technology 52(21) (2018) 12055-12065.

[14] H.H. Khoo, Life cycle impact assessment of various waste conversion technologies, J Waste management 29(6) (2009) 1892-1900.

[15] J. Dong, Y. Tang, A. Nzihou, Y. Chi, E. Weiss-Hortala, M. Ni, Life cycle assessment of pyrolysis, gasification and incineration waste-to-energy technologies: Theoretical analysis and case study of commercial plants, J Science of the Total Environment 626 (2018) 744-753.

[16] M. Schiavon, M. Ragazzi, E. Rada, G. Merler, Proposal for the correct management of the life cycle assessment results from integrated municipal solid waste treatment, J WIT Trans. Ecol. Environ 180 (2014) 163-173.

[17] U. Arena, F. Ardolino, F. Di Gregorio, A life cycle analysis of two combustion and gasification-based waste-to-energy units, J Proceedings Venice (2014).

[18] J. Portugal-Pereira, L. Lee, Economic and environmental benefits of waste-to-energy technologies for debris recovery in disaster-hit Northeast Japan, J Journal of Cleaner Production 112 (2016) 4419-4429.

[19] J.-M. Fernández-Gonzalez, A.L. Grindlay, F. Serrano-Bernardo, M.I. Rodríguez-Rojas, M. Zamorano, Economic and environmental review of Waste-to-Energy systems for municipal solid waste management in medium and small municipalities, J Waste Management 67 (2017) 360-374.

[20] Z.A. Coventry, R. Tize, A.T. Karunanithi, Comparative life cycle assessment of solid waste management strategies, J Clean Technologies Environmental Policy 18(5) (2016) 1515-1524.

[21] C. Aracil, P. Haro, D. Fuentes-Cano, A. Gómez-Barea, Implementation of waste-to-energy options in landfill-dominated countries: Economic evaluation and GHG impact, J Waste Management 76 (2018) 443-456.

[22] M. Parascanu, P. Sánchez, G. Soreanu, J. Valverde, L. Sanchez-Silva, Environmental assessment of olive pomace valorization through two different thermochemical processes for energy production, J Journal of Cleaner Production 186 (2018) 771-781.

[23] G. Assefa, O. Eriksson, B. Frostell, Technology assessment of thermal treatment technologies using ORWARE, J Energy conversion management 46(5) (2005) 797-819.

[24] M. Gunamantha, Life cycle assessment of municipal solid waste treatment to energy options: Case study of KARTAMANTUL region, Yogyakarta, J Renewable energy 41 (2012) 277-284.

[25] H. Tong, Y. Shen, J. Zhang, C.-H. Wang, T.S. Ge, Y.W. Tong, A comparative life cycle assessment on four waste-to-energy scenarios for food waste generated in eateries, J Applied Energy 225 (2018) 1143-1157.

[26] J. Dong, Y. Tang, A. Nzihou, Y. Chi, E. Weiss-Hortala, M. Ni, Z. Zhou, Comparison of waste-to-energy technologies of gasification and incineration using life cycle assessment: Case studies in Finland, France and China, Journal of Cleaner Production 203 (2018) 287-300.

[27] A. Ramos, J. Berzosa, F. Clarens, M. Marin, A. Rouboa, Environmental and socio-economic assessment of cork waste gasification: Life cycle and cost analysis, J Journal of Cleaner Production 249 (2020) 119316.

[28] Y. Tang, J. Dong, G. Li, Y. Zheng, Y. Chi, A. Nzihou, E. Weiss-Hortala, C. Ye, Environmental and exergetic life cycle assessment of incineration-and gasification-based waste to energy systems in China, J Energy conversion management 205 (2020) 118002.

[29] A. Demetrious, E.t. Crossin, Life cycle assessment of paper and plastic packaging waste in landfill, incineration, and gasification-pyrolysis, Journal of Material Cycles and Waste Management 21(4) (2019) 850-860.

[30] A.U. Zaman, Comparative study of municipal solid waste treatment technologies using life cycle assessment method, J International Journal of Environmental Science Technology 7(2) (2010) 225-234.

[31] A. Demetrious, K. Verghese, P. Stasinopoulos, E. Crossin, Comparison of alternative methods for managing the residual of material recovery facilities using life cycle assessment, J Resources, Conservation & Recycling 136 (2018) 33-45.

Appendix D: LCA Data Inventory and Result

Appendix D.1 LCA input data inventory

Process	Unit	PG	GAS	LF	INC-A	INC-B	NTP-E	NTP-M
Electricity	MJ	2.25	1.35	0.781	1.47	1.57	1.62	2.1
Aluminium	kg	1.40E-05	4.97E-06		1.78E-05	3.81E-06	1.40E-05	1.40E-05
Chromium	kg	1.00E-05	1.50E-06		5.73E-06	1.20E-06	1.00E-05	1.00E-05
Copper	kg	1.60E-05	3.09E-06		9.19E-06	2.48E-06	1.60E-05	1.60E-05
Iron	kg	1.78E-04	4.39E-05	1.09E-03	2.40E-04	3.82E-05	1.78E-04	2.00E-03
Manganese	kg	2.46E-06		1.63E-06	1.51E-06	6.30E-07	2.46E-06	2.46E-06
Nickel	kg	2.40E-05	2.67E-06		1.39E-05	2.14E-06	2.40E-05	2.40E-05
Zinc	kg	3.86E-06			2.06E-06	2.00E-09	3.86E-06	3.86E-06
Clay	kg	5.30E-04	1.23E-02	5.97E-02	3.74E-02	9.10E-03	1.23E-02	1.23E-02
Inert rock	kg	2.25E-01	1.05E-01	3.79E-02	5.88E-02	7.48E-02	1.05E-01	1.05E-01
Limestone (calcium carbonate)	kg	6.61E-03	5.30E-02	2.05E-03	1.17E-01	3.94E-02	5.30E-02	5.30E-02
Natural Aggregate	kg	3.36E-03	3.58E-02	4.22E-02	1.08E-01	2.65E-02	3.58E-02	3.58E-02
Pyrite	kg	1.90E-04			-			
Quartz sand	kg	4.90E-05	1.49E-02	3.33E-02	9.30E-06	1.28E-06	1.49E-02	1.49E-02
Sodium chloride (rock salt)	kg	1.10E-02	7.49E-02		3.90E-05	3.95E-04	7.49E-02	7.49E-02
Soil	kg	1.18E-03	1.85E-03	2.06E-02	1.49E-03	2.74E-04	1.85E-03	3.00E-03
Fuel cell production	item						5.5E-8	
Water	m^3	1.31E-01	8.78E-03	2.46E-02	6.28E-03	8.19E-03	8.78E-03	8.50E-02

Appendix D.2 LCA output data inventory

	PG	GAS	LF	INC-A	INC-B	NTP-E	NTP-M
Emissions to air							
Iron	1.34E-07	4.29E-08	9.40E-09	1.40E-07	3.91E-08	4.29E-08	4.29E-08
Lead	2.64E-08	9.06E-09	7.69E-09	2.00E-09	7.93E-09	9.06E-09	9.06E-09
Manganese	2.61E-08	8.53E-09	1.39E-08	7.91E-09	7.53E-09	8.53E-09	8.53E-09
Mercury	6.09E-09	3.39E-09	1.92E-08	4.71E-09	1.88E-09	3.39E-09	3.39E-09
Nickel	2.46E-08	4.18E-09	1.26E-09	2.10E-08	4.22E-09	4.18E-09	4.18E-09
Selenium	1.18E-08	6.21E-09	9.66E-10	3.80E-09	5.34E-09	6.21E-09	6.21E-09
Tin	9.13E-09	5.47E-09	5.10E-10	3.66E-09		5.47E-09	5.47E-09
Titanium	8.14E-09	2.54E-09	1.77E-10	8.17E-09	2.25E-09	2.54E-09	2.54E-09
Vanadium	6.18E-08	8.80E-09	2.55E-09	5.43E-09	9.49E-09	8.80E-09	8.80E-09
Zinc	4.93E-08	1.60E-08		3.18E-08	1.35E-08	1.60E-08	1.60E-08
Ammonia	-	-	-	1.42E-05	-	-	-
carbon dioxide (fossil)	9.90E-01	7.18E-03	1.00E-01	5.66E-03	7.11E-03	7.18E-03	7.18E-03
Carbon monoxide (fossil)	5.30E-04	1.46E-03	1.09E-03	1.31E-03	-	1.46E-03	9.49E-04
Hydrogen	-	2.25E-04	1.10E-04	1.93E-04	1.69E-04	2.25E-04	2.25E-04
Hydrogen sulphide	-	1.57E-05	-	-	-	1.57E-05	1.57E-05
Nitrogen (atmospheric nitrogen)	3.70	-	-	-	-	-	-

	PG	GAS	LF	INC-A	INC-B	NTP-E	NTP-M
Dinitrogen monoxide	-	-	-	1.50E-04	1.32E-04	-	-
Nitrogen oxides	4.65E-04	1.75E-04	2.32E-04	9.43E-04	1.04E-04	1.75E-04	1.75E-04
Sulphur	6.16E-04	-	-	-	-	-	-
Sulphur dioxide	4.31E-04	2.06E-04	-	2.56E-04	6.13E-04	2.06E-04	2.06E-04
Group NMVOC to air	2.04E-05	1.89E-05	5.62E-05	4.06E-05	2.47E-05	1.89E-05	1.89E-05
Hydrocarbons (unspecified)	8.34E-08	7.21E-08	-	-	5.00E-07	7.21E-08	7.21E-08
Methane	5.12E-04	1.38E-03	2.60E-04	1.21E-03	1.07E-03	1.38E-03	1.38E-03
Methane (biotic)	4.01E-07	7.80E-08	2.13E-02	2.73E-07	6.89E-08	7.80E-08	7.80E-08
Particles to air (Assume to be organic carbon)	3.80E-05	2.43E-05	2.88E-06	5.15E-05	1.10E-04	2.43E-05	2.43E-05
Emissions to fresh water							
Antimony	-	5.39E-05	-	1.63E-04	3.98E-05	5.39E-05	5.39E-05
BOD	2.01E-06	3.66E-03	-	1.11E-02	2.70E-03	3.66E-03	3.66E-03
Boron	2.27E-01	2.16E-01	-	4.43E-01	1.69E-01	2.16E-01	2.16E-01
Bromine	-	5.82	-	1.76E+01	4.30	5.82	5.82
Chloride	7.98E+03	4.98E+02	5.85E+01	1.05E+03	7.08E+02	4.98E+02	4.98E+02
Chromium	-	3.46E-05	-	1.05E-04	2.56E-05	3.46E-05	3.46E-05
Copper	-	3.05E-05	-	9.27E-05	2.26E-05	3.05E-05	3.05E-05
Dissolved organic carbon	2.51E-06	4.20E-03	-	1.34E-02	3.27E-03	4.20E-03	4.20E-03
Fluoride	6.69E+01	4.64E+01	7.28	3.79E+01	3.86E+01	4.64E+01	4.64E+01
Iron	-	3.30E-05	-	1.03E-04	2.47E-05	3.30E-05	3.30E-05
Lead	-	8.38E-03	-	2.68E-05	6.53E-06	8.38E-03	8.38E-03
Manganese	7.76E-06	2.93E-06	-	9.75E-06	2.24E-06	2.93E-06	2.93E-06
Nitrate	1.15E+01	2.23	6.31	1.47	1.96	2.23	2.23
Phosphate	4.31	1.00	1.30	4.46	1.04	1.00	1.00
Potassium	8.17	1.14E+03	3.69	3.47E+03	8.44E+02	1.14E+03	1.14E+03
Sodium	4.83E+02	9.84E+02	2.25E+01	3.00E+03	8.23E+02	9.84E+02	9.84E+02
Solids (suspended)	1.85E-04	1.05E-02	-	3.20E-02	7.78E-03	1.05E-02	1.05E-02
Strontium	2.77E-06	-	-	-	-	-	-
Sulphate	1.80E-02	9.37E+02	2.91E+01	2.73E+03	6.96E+02	9.37E+02	9.37E+02
Tin	-	3.22E-06	-	-	2.38E-06	3.22E-06	3.22E-06
TOC	2.51E-06	4.42E-03	-	1.34E-02	-	4.42E-03	4.42E-03
Vanadium	-	6.15E-06	-	-	4.54E-06	6.15E-06	6.15E-06
Zinc	1.73E-12	7.24E-05	-	-	5.35E-05	7.24E-05	7.24E-05
Aluminium	1.75E-05	2.30E-03	-	6.99E-03	1.70E-03	2.30E-03	2.30E-03
Ammonium / ammonia	3.32E-06	1.05E-07	1.55E-04	6.73E-07	2.15E-06	1.05E-07	1.05E-07
Barium	-	-	1.02E-07	2.58E-07	1.29E-07	-	-
Bromate	8.43E-07	-	-	-	-	-	-
Calcium	8.65E-04	2.05E-03	2.48E-05	6.20E-03	1.52E-03	2.05E-03	2.05E-03
Carbon disulphide	-	-	5.10E-06	-	-	-	-
Carbonate	1.28E-06	7.20E-07	-	4.05E-07	2.56E-06	7.20E-07	7.20E-07
Chlorate	6.44E-06	-	-	-	-	-	-
Chlorine (dissolved)	7.74E-07	4.51E-07	-	2.17E-07	3.86E-07	4.51E-07	4.51E-07
Magnesium	9.82E-05	1.54E-04	2.77E-06	4.69E-04	1.15E-04	1.54E-04	1.54E-04
Nitrogen	2.47E-07	-	-	-	-	-	-
Nitrogen organic bounded	4.63E-07	2.27E-07	8.74E-07	-	3.32E-07	2.27E-07	2.27E-07
Phosphorus	3.04E-07	-	1.56E-05	-	-	-	-
Sodium hypochlorite	9.63E-07	-	-	-	3.58E-07	-	-
Sodium sulphate (as sulphate)	7.22E-06	-	-	2.16E-07	2.55E-07	-	-
Sulphide	3.87E-07	-	3.22E-06	-	4.68E-07	-	-
Mercury	2.20E-05	6.11E-05	4.73E-06	1.79E-04	4.37E-05	6.11E-05	6.11E-05
Particles to fresh water (as dissolved solids)	2.15E-04	6.27E-05	1.22E-04	9.64E-05	5.60E-05	6.27E-05	6.27E-05

	PG	GAS	LF	INC-A	INC-B	NTP-E	NTP-M
Emission to sea water							
Inorganic (solids) emissions to sea water	9.89E-05	4.62E-05	1.35E-04	6.60E-05	5.07E-04	4.62E-05	4.62E-05
Total organic carbon	9.00E-07	1.07E-06	8.00E-09	3.62E-06	1.40E-06	1.07E-06	1.07E-06
Other emissions to sea water (unspecified)	2.55	2.01	5.40E-02	9.40E-01	1.72	2.01	2.01

Appendix D.3 LCA result

Direct and Indirect Burden	**PG**	**GAS**	**LF**	**INC-A**	**INC-B**	**NTP-E**	**NTP-M**
GWP	1.60E+00	4.40E-01	8.46E-01	4.93E-01	4.96E-01	5.16E-01	3.37E-01
AP	2.80E-03	1.63E-03	8.80E-04	2.25E-03	2.17E-03	1.93E-03	1.19E-03
EP	4.02E+00	8.35E-01	1.86E+00	1.81E+00	7.87E-01	8.35E-01	4.18E-01
POCP	1.88E-03	1.18E-03	1.03E-03	2.02E-03	1.14E-03	1.36E-03	8.50E-04
HTP	1.20E+00	5.24E+00	3.43E-01	5.60E+00	1.63E+00	5.32E+00	3.45E+00
PMFP	9.80E-04	5.70E-04	3.10E-04	7.70E-04	6.70E-04	6.80E-04	4.10E-04
Avoided Burden							
GWP	5.84E-01	3.48E-01	4.69E-02	2.98E-01	5.53E-01	5.64E-01	6.69E-01
AP	2.19E-03	1.35E-03	1.70E-04	1.07E-03	2.03E-03	2.12E-03	3.52E-03
EP	1.61E-03	9.40E-04	1.30E-04	8.20E-04	1.54E-03	1.55E-03	1.61E-03
POCP	1.38E-03	8.60E-04	1.00E-04	6.80E-04	1.28E-03	1.34E-03	3.73E-03
HTP	6.57E-01	4.11E-01	4.91E-02	3.34E-01	6.03E-01	6.37E-01	1.92E+00
PMFP	7.70E-04	5.00E-04	5.00E-05	3.70E-04	6.90E-04	7.50E-04	2.08E-03
Total							
GWP	1.01E+00	9.28E-02	7.99E-01	1.95E-01	-5.78E-02	-4.80E-02	-3.32E-01
AP	6.10E-04	2.80E-04	7.10E-04	1.18E-03	1.40E-04	-1.90E-04	-2.32E-03
EP	4.02E+00	8.34E-01	1.86E+00	1.80E+00	7.86E-01	8.34E-01	4.16E-01
POCP	5.00E-04	3.20E-04	9.30E-04	1.33E-03	-1.40E-04	2.00E-05	-2.88E-03
HTP	5.40E-01	4.83E+00	2.94E-01	5.27E+00	1.03E+00	4.69E+00	1.53E+00
PMFP	2.10E-04	8.00E-05	2.60E-04	4.00E-04	-2.00E-05	-7.00E-05	-1.67E-03